FACULTY OF SCIENCE, ENGINEERING AND COMPUTING

School of Life Sciences and

Pharmacy and Chemistry

Department of Chemistry and Pharmacy

Negeen KARGAR

BSc, MSc, AFHEA

K1455207

The use of polymers to enhance the delivery of antidiabetic drugs

Thesis

submitted for the degree of

DOCTOR OF PHILOSOPHY

September 2021

Supervisors

Dr Amr ElShaer, Dr Ian Beadham, Professor Fawaz Aldabbagh

and Professor Raid Alany

ACKNOWLEDGEMENT

Dedication

I want to dedicate this thesis to the Afghan girl, the girl who wants to rise and shine, walk proud as if she can reach the peak of Hindukush, with the noise of the Afghan jewelry she wore. However, the cruel war never let her fulfill her dreams, a dream of being a schoolgirl, wearing a white headscarf. Her books in hand, walking proudly to school, nevertheless she becomes the victim of child marriage. The deadly war never let her educate under a peaceful blue sky. She travels over the mountains and nearly drowns in the Mediterranean. From one country to another. The tradition never allowed her to be herself, but her irrepressible character never accepts confines. She breaks the boundaries; she strives for education and sees the world as a picturesque place once again. She thinks about the other passionate little and young girls she left behind, in dust and smoke of bombs, who fill the buckets of water from the rivers. The rivers were full of blood of their loved ones. All those little girls who could not come with her still cannot see the world is a beautiful place, as they are victims of one or another name.
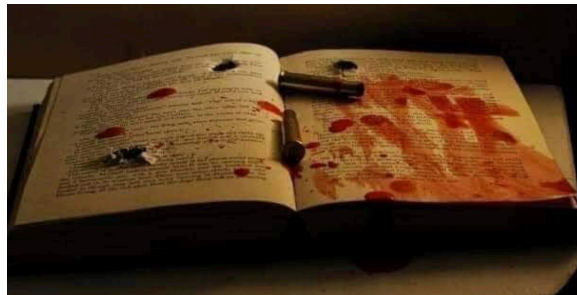

Photo curtesy social media Kabul university terrorist attack November 2020

Plagiarism Statement

I (Negeen Kargar), wrote this PhD dissertation in my own words, except for quotations from published and unpublished sources which are indicated, cited (using Endnotes) and acknowledged. I know the incorporation of material from other works or a paraphrase of such material without acknowledgement will be treated as plagiarism. Subject to the system and usage of the subject, according to the Kingston University of London's Regulations on Conduct of Examinations. The sources of any pictures, schemes, results in software or other illustration are cited in the text, apart from my experimentation, observation, or samples.

Negeen Kargar

Date: 30.11.2020

ABSTRACT

Background: Diabetes is one of the oldest and deadliest healthcare conditions to be reported in history. The currently available insulin delivery systems fail to maintain a basal insulin level in the blood. Closed-loop insulin delivery systems that intelligently release insulin according to the body's needs will enable better control of glucose levels. Over the last decade, biodegradable and biocompatible polymers have been widely investigated as micro and nanoparticle diabetic drug delivery systems. Self-regulated release of drugs by stimuli-responsive polymers has been a research area in recent years. In the event of diabetes, a self-regulated insulin-releasing system responding to variations in glucose concentration would be a major therapeutic breakthrough.

Aim: This project aims to synthesise a number of novel polymers to improve the delivery of antidiabetic drugs including a cosolvent approach and a smart glucose-sensitive delivery system that can release insulin only in response to high blood glucose levels.

Method: Polyglycerols were end-functionalised using phenylboronic acid. Initially, polyglycerol was synthesised by ring-opening copolymerisation of glycerol and glycidol under acidic conditions. A novel end functionalised polymer was developed using an in situ deprotection method. Liquid formulations of hydrochlorothiazide (HCTZ) were prepared using glycerol, polyethylene glycol (PEG-400), commercial polyglycerine and synthetic polyglycerol and were tested for their solubility and stability using HPLC. Subsequently, RAFT polymerisation of sugar sensitive polymers was carried out, and optimised conditions for further block polymer synthesis were established.

Results: A new efficient method was developed to synthesise end-functionalised polyglycerol using DL-1,2-isopropylideneglycerol,4-carboxyphenylboronic acid pinacol ester, with glycidol and glycerol polymerisation.

Liquid formulations of the hydrophobic drug (HCTZ) which were stable at 25 °C, relative humidity (RH-65 %) and 40 °C (RH-75 %) were developed. The dielectric constant of each polymer was calculated, and the solubility of HCTZ in those polymers was determined. PEG-400 had a solubilisation power (σ) of 1.83, while polyglycerine and glycerol had σ of 1.77 and 1.56 respectively. The corresponding dielectric constant (ϵ) for PEG-400 was 12.4 and for polyglycerine and glycerol, 30.5 and 42.5, respectively.

RAFT polymerisation of 3 and (4-(Acrylamido)phenylboronic acid pinacol ester (4-APBAPE) was carried out at varying degrees of polymerisation (DP), (DP $\approx$ 150, 100, 50, 25 and 13) giving high to very high monomer conversions and a low fraction of dead chains as indicated by the GPC and NMR analysis. With shorter block copolymer chains, a living polymer was obtained, and a higher degree of conversion was observed. For the RAFT polymerisation of 4-APBAPE (DP = 150), the polymer chain growth began within 30 min and ceased after 90 min. Nevertheless, polymerisation with 150 blocks leads to broadening of the molecular weight distribution and (PDI = 1.64) reflecting the lack of living polymer.

A polymer with DP= 150 at 30 min, Mn =1450 gmol^{-1} with 98 % livingness and 92 % AIBN remained, compared with (polymer 293), DP= 13, Mn = 2350 gmol^{-1} and a PDI = 1.08 gives 99.7 % livingness with AIBN (85 %) remained after the first hour. After 24 hours only 2.3% AIBN remained, demonstrating complete consumption of the initiator, giving a narrow polydispersity (PDI = 1.21) and a high monomer conversion.

Conclusions: In conclusion, in situ polymerisation of end functionalised polyglycerol was successfully developed using cationic ring-opening

polymerisation of glycerol and glycidol. Liquid formulations of HCTZ were developed using five different biodegradable polymers and tested for stability. RAFT polymerisation of block end functionalised sugar sensitive copolymers was optimised. This was the first time 4-APBAPE has been polymerised by RAFT, and a kinetic study was additionally conducted.

Keywords: Polymer, diabetic drug delivery, solubility, cosolvents, PEG 400, polyglycerine, glycerol, RAFT polymerisation, sugar sensing, end functionalised polymer

Abbreviations

ACN	acetonitrile
ACPBAPE	Acrylamide phenylboronic acid pinacol ester
(T1DM)	type 1 diabetes mellitus
(T2DM)	type 2 diabetes mellitus
BCS-	Biopharmaceutical Classification System
CS	Chitosan
(CRP)	Controlled Radical Polymerization
DM	Diabetes mellitus
DMAP	Dimethylamino pyridine
EDCI.HCl	1-(3-dimethyl aminopropyl)-3-ethyl carbodiimide hydrochloride
GIT	Gastrointestinal 'tract
HPLC	High-Performance Liquid Chromatography
ICH	International Council for Harmonisation
MALDI-TOF	Matrix-assisted laser desorption ionization time-of-flight mass spectrometry
mp	Melting point
MP	Maximum average molecular weight
MWDs	Molecular Weight Distribution
NM	Microneedles
PBA	Phenylboronic acid
PDI	Polydispersity index
PEG	Polyethylene glycol

PG	Polyglycerol
PG-4-PCPE	Polyglycerol-4-phynylcarboxy pinacol ester
RAFT	Reversible Addition Fragmentation Chain Transfer
RH	Relative Humidity
RSD	Relative Standard deviation
SGF	simulated gastric fluid
SIF	simulated intestinal fluid
TDD	Targeted Drug delivery
TFA	trifluoroacetic acid
WHO	World Health Organization

The structure of the thesis

According to the World Health Organization (WHO), almost half of all deaths before the age of 70 are attributable to high blood glucose in diabetes patients. It is estimated that diabetes was the seventh leading cause of death in the past ten years. There is a huge demand for improving the delivery of antidiabetic drugs to enhance the quality of life for diabetic patients.

The long-term aim was to design a nanoparticle system that can encapsulate insulin and release it into the blood if the blood glucose is high for diabetic patients. Both conventional and Reversible Addition Fragmentation Chain Transfer (RAFT) polymerisations were investigated to obtain a new polymer system for insulin incorporation into nanoparticles, which could be then tested for insulin release and sugar sensitivity as a smart delivery system. The intelligent system would ideally respond to high glucose levels in diabetic patients, releasing insulin accordingly.

Chapter 1 is the general literature review of the thesis, which covers the drug delivery aspects of antidiabetic drugs. Also, it reports the insulin delivery via different delivery routes, their advantages, and drawbacks. The polymeric insulin delivery, liposome, gene therapy, and current insulin pumps and artificial pancreas are addressed. Additional methods that use sugar sensitive materials such as protein binding sugar sensitive methods and enzyme-based sugar sensors were surveyed. Biodegradable natural and synthetic polymers for diabetic delivery were also discussed, with a focus on insulin delivery and the importance of polymers in insulin formulations.

Chapter 2 describes the synthesis of polyglycerols end-functionalized with phenylboronic acid. Phenylboronic acid has a unique property to sense sugars and bind to glucose or any other diols covalently at a specific pH.

Changes in boronic acid geometry can also occur when the equilibrium between the boronic acid and boronate ions is established. The acidity of boronic acid

depends on the neighbouring group. The interactions also occur through complexation, such as intermolecular coordination between the electron-deficient boron and an electron-rich ortho, meta or para side group.

vacant p orbital, electrophilic sp2   anionic form, nucleuphilic sp3

The scheme above shows boronic acid in aqueous equilibrium, when it is charged, it can bind to any sugar.

Polyglycerol was synthesised and was modified with phenylboronic acid. The reaction is carried out by cationic polymerisation. Incorporation of amide and ester-linked boronic acid resulted in the rapid and efficient synthesis of a potential glucose-sensing polymer. The end functionalised polymers were analysed using NMR, MALDI-TOF, and FTIR.

Chapter 3 describes the development of a hydrochlorothiazide (HCTZ) liquid formulation. According to the Biopharmaceutical Classification System (BCS), HCTZ is a class IV antidiabetic drug with low solubility and low intestinal permeability. HCTZ was used as a model drug in this study. The chapter looked at the use of the food additive polyglycerine (E476) and synthetic polyglycerol to develop liquid formulations using a cosolvent approach. Subsequently, the formulations were tested for their physical and chemical stabilities. Polyglycerine improved the solubility of HCTZ and hence could be used as a replacement for PEG-400. Glycerol also enhanced HCTZ solubility but to a limited extend. The synthetic high molecular weight polyglycerol did not improve the solubilities and promoted the degradation of HCTZ.

The interaction between the cosolvent and HCTZ was analysed using FTIR, and changes to the crystalline morphology of HCTZ were investigated under a Scanning

Electron Microscope (SEM). The SEM images showed that HCTZ had lost its crystalline structure and became more amorphous. The liquid formulation was successfully developed, and PEG-400, polyglycerine and glycerol showed good solubility but poor stability.

Chapter 4 describes the Reversible Addition-Fragmentation chain Transfer (RAFT) polymerisation method. The chapter starts with a literature review of RAFT polymerisation of the phenylboronic acid monomer and reproducing the synthesis of poly dimethyl acrylamide (polyDMA) as a model RAFT polymer as reported by Chalmers (2017). The experimental parts contain six sections, due to the amount of work carried out the data and different condition for the optimisation of these experiments, this chapter is represented in different sections.

Section 1 surveys the current literature concerning RAFT/ monomer/ initiator ratios, concentration of final polymer solution, the degree of polymerisation and molecular weight and sugar sensitive properties. Kinetic studies of RAFT polymerisation of phenylboronic acid and living block copolymer were also explored.

Section 2 describe our experimental work on conventional free radical polymerisation of DMA and DMA chain extension.

Section 3 explains our optimisation studies into radical initiator concentration for polymerisation of 4-ACPBAPE via RAFT Using VA-044. VA-044 is a water-soluble initiator the ideal condition would be to use the same condition of DMA macroRAFT (dioxane water 80:20) which dissolves VA-044. Attempts are made to use this condition and polymerise N-(3-(4,4,5,5-tetramethyl-1,3,2-dioxaborolan-2-yl)phenyl)acrylamide pinacol ester using Poly(DMA)macro-RAFT$_{50}$.

Section 4 studies the monomer solubility under acidic conditions designed to prevent degradation of the RAFT agent. However, it was found that the addition of acid (HCl) caused precipitation. The solvent system and initiator were changed, and three different concentrations of the initiator AIBN were investigated.

Section 5 investigated the effect of radical concentration, which is essential for the synthesis of well-defined block copolymers. Under the optimised conditions, size exclusion chromatography indicated a narrow molecular weight distribution.

In Section 6, experiments were carried out to optimise 150, 100, 50, 25, and 13 monomer blocks for novel 4-acrylamide phenylboronic acid RAFT polymer. At high to very high monomer conversions, a low fraction of dead chains was obtained. The polymerisation conditions were optimised using a constant amount of AIBN. Only the monomer and the RAFT agent concentrations were varied. Anisole was used to spike the ^{1}HNMR samples in order to calculate the reaction conversion therefore the polymer NMR spectra are not assigned as the conversion are calculated to obtain monomer conversion to polymer.

In summary, a novel monomer of glycerol which can be polymerised and deprotected in situ was developed. A liquid formulation of HCTZ was developed, which was stable, and the use of polyglycerine, a food additive improved the solubility of HCTZ. RAFT polymerisation conditions were optimised, and a kinetic study of the polymerisation was carried out.

Table of Contents

17

List of schemes

List of equations

List of figures

Table of tables

43

1.1 Diabetes mellitus

Diabetes mellitus (DM) was first documented in an Egyptian papyrus, dated back to 1550 BC (Ramirez-Dominguez, 2016). Presently, the World Health Organization (WHO) estimates the number of diabetic patients to be around 422 million worldwide; this number is likely to double in the next 20 years (Figure 1.1), shows the projection of population with diabetes from 2010 -2045. The high projected numbers are in the geographical regions of South Asia and Western Pacific. However, in the areas of Europe, Middle East, Caribbean and south and central America, the population that could be affected by diabetes in 2045 remain lower than in South Asian countries. Nevertheless, by 2045 it tends to rise in Africa, yet now it seems to be similar to other countries except for South Asia and Western Pacific. Diabetic patients' numbers projected to rise to 592 million by 2035. Diabetes UK states, one in ten people over 40 are now living with Type 2 diabetes, 3.8 million people were diabetes in the UK, and 90% of those with Type 2. Almost 1 million more people live with Type 2 diabetes who do not know they have it since they have not been diagnosed, bringing the total number up to 4.7 million. By 2030 it is predicted that this number will rise to 5.5 million. According to the international diabetes federation (IDF), approximately 463 million adults (20 - 79 years) live with diabetes; by 2045, diabetic patients will reach 700 million. People who live at a low level and middle-income countries tend to be more susceptible to Type 2 diabetes due to lack of awareness and an unhealthy diet.
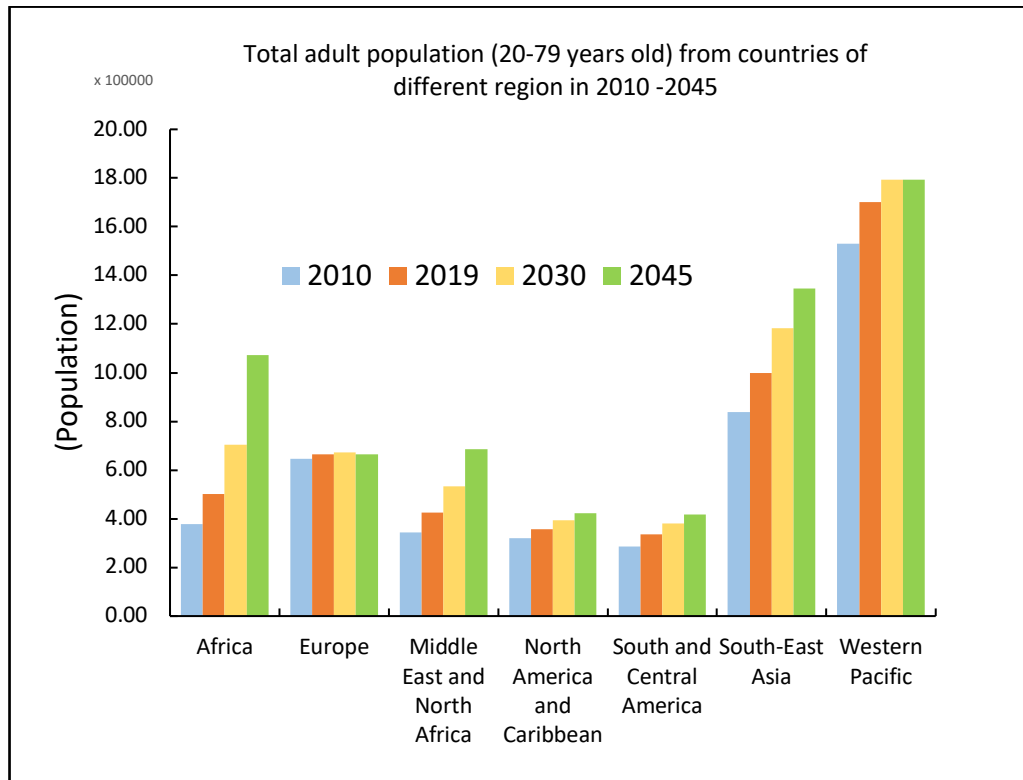
Figure 1. 1 Total adult population (20-79 years old) from countries of a different region in 2010 -2045 IDF.

1.2 Types of Diabetes mellitus

Diabetes is divided into main types; Type 1 (T1DM) and type 2 diabetes mellitus (T2DM). T1DM is caused by an autoimmune disorder that attacks and destroys β-cells in the pancreas resulting in a deficiency of insulin production. Many genetic and environmental factors cause such immune response in type 1 diabetic patients. T1DM is affecting around 10% of diabetic patients and known as juvenile-onset diabetes or Insulin-dependent diabetes.

T2DM affects around 90% of diabetic patients and is caused by the development of insulin resistance. The causes of T2DM are still unknown, but risk factors

include obesity, sedentary lifestyle, age, family history and ethnicity. For instance, Asians and South Americans ethnic are at high risk of getting T2DM.

The third type of diabetes affects pregnant females during the second and third trimester and is known as Gestational Diabetes mellitus (GDM). The production of several hormones in the placenta during pregnancy is believed to impair the actions of insulin. Idiopathic, immunogenic, and monogenic diabetic syndromes are other types of diabetes that affects around 5% of diabetic patients. This type develops in women during pregnancy. Gestational diabetes usually goes away after pregnancy. However, if a lady has gestational diabetes, she is at higher risk of developing type 2 diabetes later in life.

A stage of diabetes that happens before diabetes is called prediabetes, the stage before type 2 diabetes. In this type, the person's blood glucose levels are higher than average, but it is as high as diagnosed with type 2 diabetes.

Monogenic diabetes syndromes are rare inherited forms of diabetes accounting for up to four per cent of all cases, such as neonatal diabetes and maturity-onset diabetes of the young (MODY).

Cystic fibrosis-related diabetes is a form of diabetes-specific to people with this disease. Drug or chemical induced diabetes happen after organ transplant, following HIV/AIDS treatment or are associated with glucocorticoid steroid use.

Diabetes insipidus is one of the rare conditions that cause kidneys to produce a large amount of urine.

1.3 Management of Diabetes mellitus

Diabetes management includes strategies such as changing lifestyle by modifying diet and exercising more. Exercise and diet modification in diabetes results in a long-lasting effect on diabetes control (de Boer et al., 2020). Moreover, diabetes can be managed using a wide range of therapeutic agents depending on the stage and type of diabetes. Over the years, several therapeutic agents have been developed to control hyperglycaemia in diabetic patients (Table 1.1).

Table 1. 1 List of some medicines used in diabetes (Type 1 & Type 2), Maturity Onset Diabetes of the Young (MODY) and Gestational diabetes mellitus (GDM)

Type of antidiabetic drug	Generic name	Branded name	Medicinal forms	Diabetes
Biguanides	Metformin hydrochloride	RIOMET ® (500mg/5m)	Oral solution	Type 2 & GDM
		Glucophage ® (500mg)	Tablets	
Sulfonylureas	Glipalamides	Amglidia ® (0.6 mg/ml)	Oral suspension	Type 2, neonatal& GDM (second &third trimester)
	Gliclazide	Diamicron ® (80 mg)	Tablets	Type 2
	Glimepiride	Amaryl ® (1 mg)	Tablets	Type 2
	Tolbutamide	Tolbutamide ® (500mg)	Tablets	Type 2
	Glipizide	Minodiab® (5mg)	Tablets	Type 2 & MODY (1,3, & 4)
Thiazolidinediones	Pioglitazone	Actos ®	Tablets	Type 2, reduce the amount of glucose produced by liver
dipeptidyl peptidase-4 inhibitor	Vildagliptin	Galvus ®	Tablets	
	Sitagliptin	Januvia ®	Tablets	
	Saxagliptin	Onglyza ®	Tablets	
	Linagliptin	Trajenta ®	Tablets	Type 2
Sodium-glucose co-transporter 2 inhibitor	Canagliflozin	Invokana ®	Tablets	
	Dapagliflozin	Forxiga ®	Tablets	
	Empagliflozin	Jardiance ®	Tablets	Type 2, helping to lower glucose in kidney
Glucagon-like peptide-1 receptor agonist	Dulaglutide	Trulicity ®	Injection	Type 2

Exenatide	Bydureon ®	Injection
Liraglutide	Victoza ®	Injection
Lixisenatide	Lyxumia ®	Injection
Semaglutide	Ozempi ®	Injection

1.4 Insulin

In 1910 English physiologists known as Sir Edward Albert Sharpley Schafer he discovered a substance excreted by pancreatic cells that enables the body to use glucose to generate energy. This substance was later identified as insulin from the Latin name insula or island (Standl, 2019, Ziegler et al., 1991, Standl et al., 1981). Ten years then, Fredric Banting and his student Charles Best extracted insulin from dogs' pancreas for the first time in 1921. Insulin is first used for the treatment of diabetes in 1922, purified by James B Collip. Insulin is a hormone which is produced in the pancreas (Figure 1.2). The β-cells are the most numerous cell types and are located mainly in the islet's core, while α and δ cells are situated on the margin (Rudy Bilous, 2010). Human insulin has a molecular weight (Mw) of ~ 6000 Da that is negatively charged and is composed of two polypeptide chains joined by two disulfide bonds (Kalia et al., 2004).
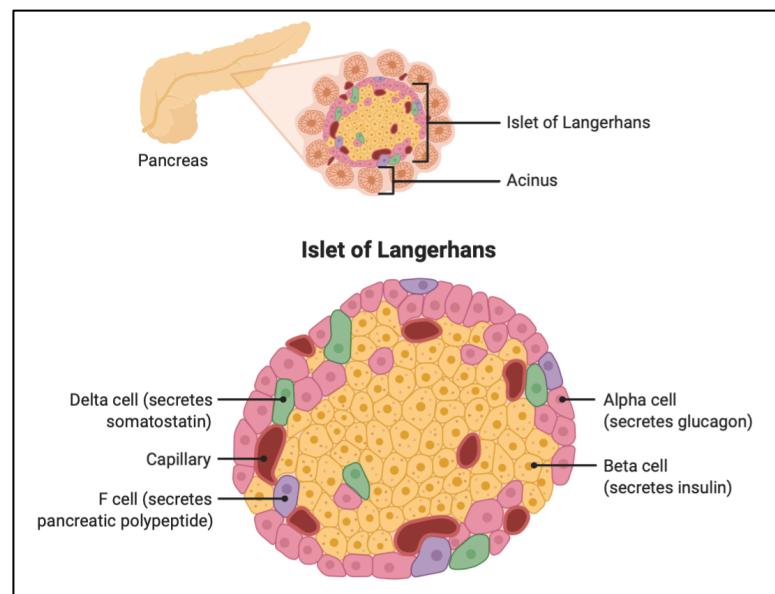
Figure 1. 2 Pancreatic cells and functions .

Insulin is a peptide hormone, a small biochemical protein responsible for transferring blood sugar into the body and cells through the cell walls' insulin receptor. Nowadays, insulin as medicine is synthesized by recombinant DNA

technology (Sanger, 1945). The biologically active insulin made of two chains; chain A which is composed of the antiparallel alpha-helix with A1 to A8 amino acid and a carboxy-terminal of A12 - A20, while the B chain has a single central helix B8 - B19 and Beta strand B21 - B30 (Figure 1.3). The 3D structure has a three-helix structure with three disulfide bridges (Weitai Wu, 2013).
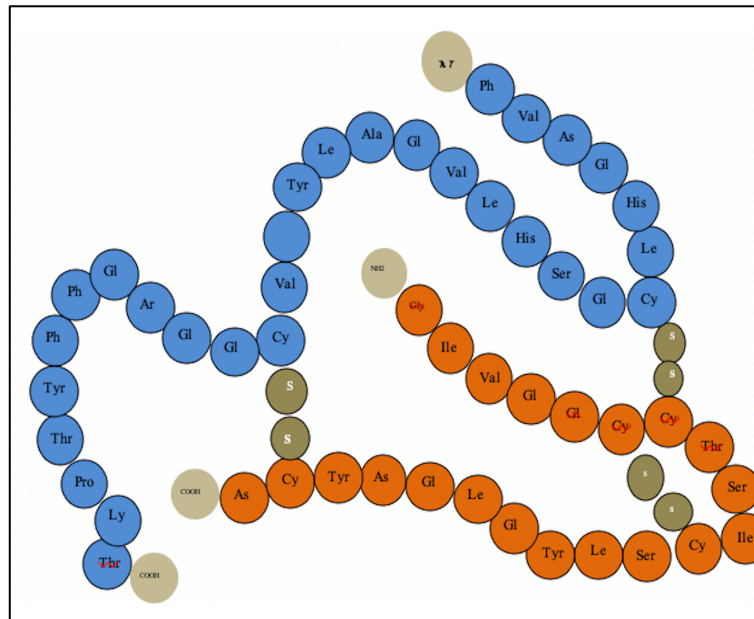
Figure 1. 3 Schematic structure of insulin, depicting disulfide bonds (image created in Microsoft word).

Subcutaneous injections of insulin make standard glycemic control hard to achieve. The intestinal concentration of glucose generated from the degradation of dietary carbohydrates, entering the Krebs cycle or Tricarboxylic acid cycle (*TCA cycle) which is the second stage of cellular respiration. TCA cycle is a three-stage process by which the living cells break down organic molecules in the presence of oxygen to convert to the energy for cell growth and division.

 Including starch or sucrose, leads to an increased blood glucose level, which stimulates the secretion of insulin from the pancreas into the bloodstream (Elena Matteucci, 2015). Insulin then promotes the transport, intake, consumption, and storage capacity of sugar from the blood to the cells in the target tissues, such as

liver, skeletal muscles, and adipose tissue (James D Gifford, 1984), (Guenther Boden, 2011).
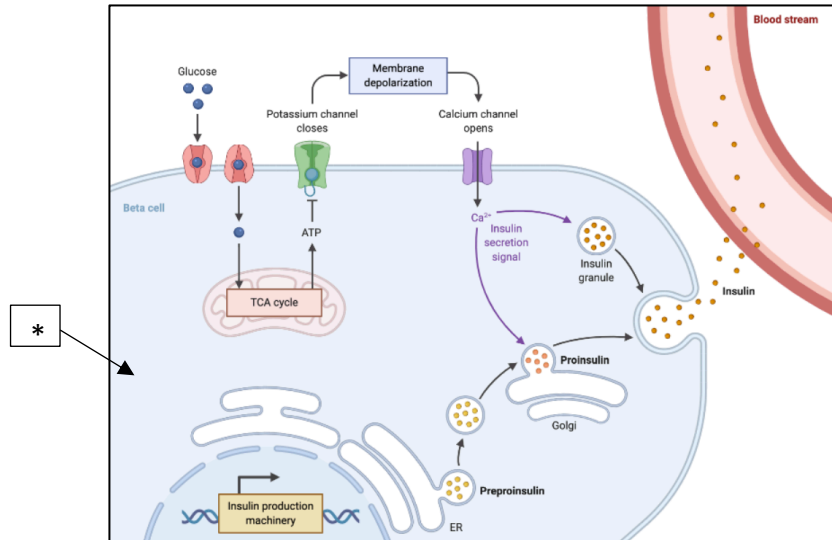
Figure 1. 4 Insulin production Pathway in pancreatic β-cells (Insulin Production Pathway"

1.5 Delivery of insulin

The current administration of insulin formulations for diabetes is entirely based on subcutaneous injection (Flavia Sousa and Bruno, 2015). Traditional syringes marked in insulin units or alternative pen-like devices and insulin-containing cartridges deliver the hormones subcutaneously; nevertheless, subcutaneous delivery is associated with numerous limitations. Diabetic patients have to suffer from multiple injections, for instance, before meals or before bedtime, to imitate the basal insulin secretion. The repeated subcutaneous infusion brings about pain, tissue invasion, infection, and nerve damage, which cause poor patient compliance and non-adherence towards medications (Chowdhury and Escudier, 2003). Insulin lipohypertrophy (Figure 1.5) is a tumour-like swelling of fatty tissue at the injection site, secondary to the lipogenic effect of insulin, or lipoatrophy is considered an adverse immunological side effect of insulin therapy (Mokta et al., 2013). Besides, other factors such as injection site depth and affect the absorption

rate of insulin (Flavia Sousa and Bruno, 2015). Since the discovery of insulin which, was initially extracted from the bovine or porcine pancreas, substantial developments were made.
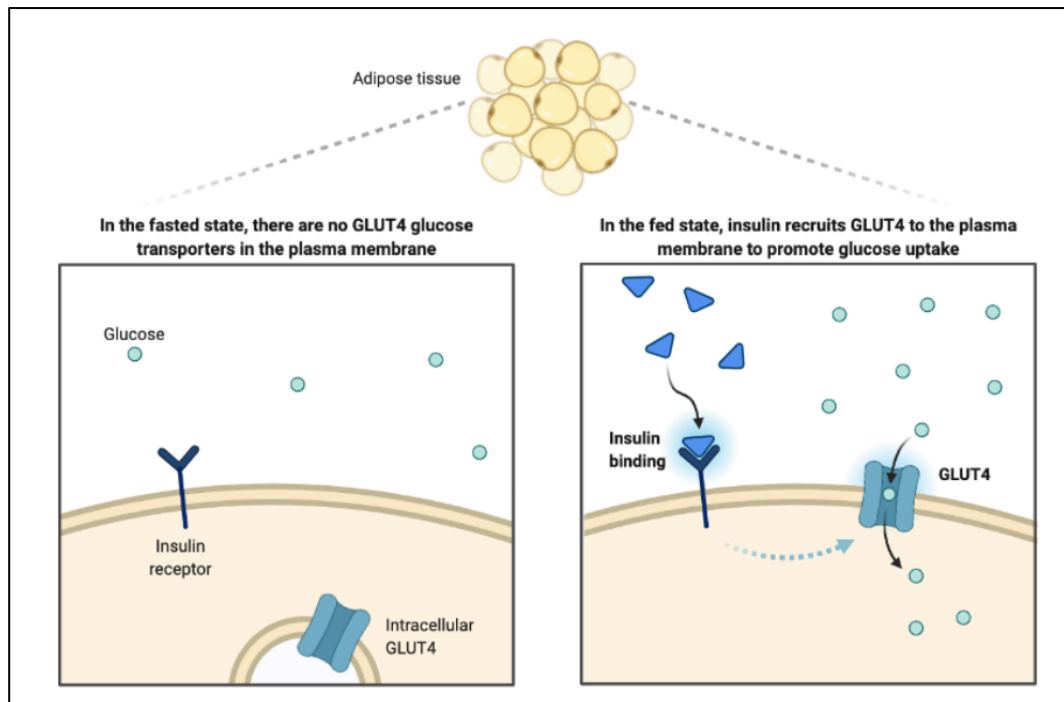
Figure 1. 5 Insulin receptor which exists on the cell surface, which opens up the intracellular channels for glucose to enter to the cells.

As depicted (Figure 1.5) in the fast state, this is no glucose transport available. However, in fed state insulin binding to the receptor creates a possible route to the intracellular glucose uptake to happen.

There are some insulin formulations for non-subcutaneous administration in preclinical or clinical trials. These formulations are designed for nasal, pulmonary, transdermal, and oral routes, as summarised in Table (1.2).

Table 1. 2 Different formulation of insulin in different phases of clinical trials.

Formulation	Manufacturer	Clinical trial phase	Effect	Reference
Oral-lyn spray ™	Generex	Approved in 2009	Rapid absorption reduces the number of required injections, treatment with buccal spray insulin is a simple therapy for lowering postprandial hyperglycemia in obese focuses on impaired glucose tolerance, or (IGT). Notably, this treatment is safe, and none of the study subjects experienced hypoglycemia.	(Palermo et al., 2011)
ORMD 0801	Oramed	phase 3	And disease development and delays late-stage complications. ORMD-0801 is oral insulin capsules used in conjunction with subcutaneous insulin injections, well-tolerated, and effectively reduces glycemia throughout the day.	(Eldor et al., 2013)
IN-105 Tablets	Biocon,	phase 3	These tablets are in phase III study in India with IN-105, which did not meet its primary endpoint. IN-105	(Khedkar et al., 2010)

			mimics the natural physiology of the body by targeting the liver	
EMISPHERE™	Emisphere Technolofies	phase 2	Emisphere is oral insulin, and it has the potential to mimic the natural physiology of insulin release by targeting the liver before being distributed to the peripheral circulation.	(Zijlstra et al., 2014)
APH-0907	Aphios Corporation	Preclinical patent	In an in vivo study of nano-encapsulated insulin conducted in diabetic mice, the advantages showed a significant decline in glucose levels after oral administration.	Aphios corporation
Nodlin is an oral formulation	Shanghai biolaxy	phase 1	Nodlin is a patented bio-adhesive nano-particle oral delivery technology to overcome the barriers of oral insulin. Oral enteric insulin capsules induced significant glucodynamic effects and exhibited a time-action profile. There is no detectable increases in serum insulin concentration were observed in any treatment group.	(Li et al., 2012)

1.6 Barriers to the delivery of insulin

1.6.1 Oral delivery of insulin

The first physical barrier to oral insulin delivery is glycocalyx and mucus on the epithelial layer's top. This layer is made of sulfated mucopolysaccharides, glycoproteins, enzymes, electrolytes, and water. These components are negatively charged and repulse with insulin preventing its absorption. Besides, the sizeable water-soluble molecule is poorly up taken via passive diffusion. The fatty acid bilayers only absorb the small lipophilic molecules into the cells.

Moreover, the tight junction between the cells prevents insulin absorption via paracellular transporter. Furthermore, the pore radius of the intestinal mucosa is between 7-15 A°. The intestinal barrier is a barrier for large molecules, including insulin. Insulin molecules aggregate at concentrations of over 100 nM. The insulin monomer's aggregation forms a larger molecular dimension 12-14 A° and changes insulin conformation to hexameric. This deteriorates insulin transport across the intestinal epithelium (Damge et al., 2007, Christiane Damgé, 1998, Damge et al., 2008).

Besides, the gastrointestinal tract (GIT) has a variety of enzymatic barriers for oral insulin delivery. Intracellular enzymes such as cathepsin can degrade insulin. Moreover, bacterial flora in the mucus layer and the epithelial cells of the intestine can degrade insulin. Proteolytic enzymes in the stomach and the intestinal lumen (pepsin, trypsin, and chymotrypsin) also affect insulin stability. In addition to the above enzymes, enzymes at the brush border membrane, such as endopeptidases, can also denature this hormone. Enzyme inhibitors have been used to prolong the insulin degradation rate and increase the insulin available for absorption (Herrero et al., 2012).

The extreme changes in pH and degradation by pepsin are amongst the chemical barriers for insulin delivery via GIT. The intestinal tract's pH is changing from highly

acidic conditions in the stomach (1.2 -3.0) to slightly alkaline in the intestine (6.5 – 8.0). The molecular weight of insulin is 6000 Da, and the structure is very prone to changes in pH. At physiological pH, the carboxylic and amino groups of insulin get ionized, resulting in a zwitterionic configuration. The charges on the surface of the macromolecules prevent its absorption from transcellular diffusion until neutralization with surrounding ion pairs (Damge et al., 2008). The physiologically active insulin group contains an asymmetric carbon atom, prone to degradation in an acid environment (Scott, 1931). Through hydrolysis, the protein would decay into two or more inactive parts.

Otherwise, the rapid loss of potency may be due to some peptide or amino acids cleavage responsible for insulin's hypoglycemic properties.

1.6.2 Nasal delivery of insulin

Nasal delivery of insulin can improve patient compliance compared to other delivery routes. The nasal route offers a lower dose of the drug, and there is no need for a complex formulation to cross the nasal path of drug delivery. The nasal space has a relatively large surface area (150-160 cm^2), and the nasal secretion is around 15 mL per day under normal physiological conditions (Illum, 2003). Nasal insulin delivery is an attractive focus for researchers since enzymatic activity within the nose is low, suggesting that insulin solutions are less likely to be destroyed by the body's natural defence systems.

Nonetheless, the primary obstacle to the nasal delivery of insulin is a procedure called mucociliary clearance, which is intended to remove foreign bodies from the nasal cavity. During this process, nasal cilia beat in a coordinated fashion to transport foreign entities captured in mucus away from the nose. The other factor affecting drug permeation is the pH of the drug formulation and the nasal cavity's pH. The pH of the nasal formulation should be at 4.5 - 6.5. Also, the nasal surface area's irritation

should avoid protecting the surface of the nasal cavity from growing bacteria, and nasal absorption depends highly on the degree of ionization of the formulation. Despite the low enzymatic activities in the nasal cavity, some of the peptides and proteins are unstable (Illum, 2003, Tolksdorf et al., 1992, Wu et al., 2005, Shiotsuka et al., 2010, McMartin et al., 1987).

The nasal cavity can facilitate drug permeation by an active or transcellular way or a passive paracellular way. Carrier-mediated endocytosis is also a possible transport route, and the effective permeability was studied mathematically articulated by Lang et al. (Lang et al., 1996). An additional barrier to nasal delivery is the tight junctions located between epithelial cells in the mucous membranes inside the nose, preventing the penetration of large molecules such as insulin. The nasal mucosa is a barrier for the passage of large molecules, particularly those above 1,000 Da in size. The nasal bioavailability of hydrophilic peptides and proteins is usually less than 1% (McMartin et al., 1987).

In addition, the nasal cavity is covered by mucus and has a pH of 5.5 to 6.5 and will exchange every hour. The mucus layer in the nasal cavity works as a physical barrier preventing the adhesion of insulin molecules that could attribute to the negative charge on the mucus generated by the sialic acid and sulfate groups mucus glycoproteins.
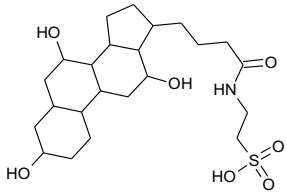
Therefore, excipients like bile salts, surfactants, fatty acids, and cyclodextrins (Table 1.3) have been evaluated for their permeation-enhancing efficacy and their effect on the sensitive nasal epithelium insulin (Marttin et al., 1999, Merkus et al., 1999, Seki, 2012).

The formulation strategy for nasal administration promotes adhesion of the formulation to the nasal mucosa, enabling the drug to permeate through the nasal membrane—liposome and lipid nanoparticles used nasal delivery of insulin. Polymer-based nanoparticles also developed for much-adhesiveness.

Polysaccharides such as chitosan were found to have mucoadhesive properties due to its high viscosity and ability to interact with negatively charged groups on mucosal surfaces electrostatically, thanks to the cationic amino group on the chitosan structure.

Yu et al. evaluated the effect of CS concentrations, osmolarity on the nasal delivery of insulin. The study shows that 1% chitosan and 0.1% ethylenediaminetetraacetic acid (EDTA), 5% polysorbate 80 (Tween 80), or 1.2% β-cyclodextrin (β-CD) did not lead to a higher relative fraction bioavailable compared to insulin formulated with 1% chitosan alone. The formulation containing both 5% hydroxypropyl-β-cyclodextrin (HP-β-CD) and 1% chitosan was more useful as they reduce blood glucose levels than the formulation comprising 5% HP-β-CD or 1% chitosan alone. The studies concluded that chitosan concentrations, osmolarity, medium, and absorption enhancers in chitosan solution significantly affect basal insulin delivery (Shaoyun Yu, 2004).

Table 1. 3 Permeation enhancers used for insulin drug delivery

Permeation enhancers	Structures	Properties and Reference
Bile salts		
Taurocholate		Bile salts comprise a large, rigid, and hydrophobic steroid moiety with attached hydrophilic groups (typically two or three hydroxyl groups) and an anionic carboxyl head group. Bile salts are known to be useful absorption promoters of insulin across mucosal barriers. Bile acids emulsify dietary fat droplets through the formation of mixed micelles (Hofmann, 2009).

Glycocholate
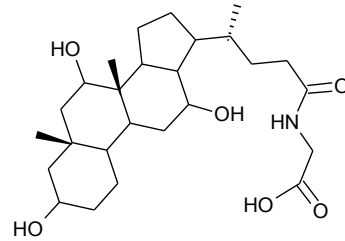
Cholate
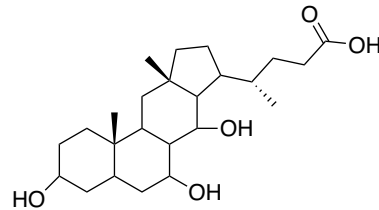
Surfactants

Sodium stearate
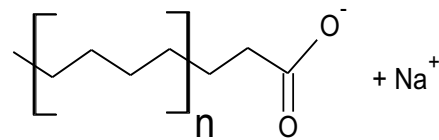
Ionic and nonionic surfactants could serve as intranasal absorption enhancers. However, taking ciliototoxicity into account, non- ionic surfactants are more famous for intranasal drug delivery. To consider the surfactant's ciliotoxicity, the concentration of the surfactant in the

formulation is vital for overcoming two main barriers to nasal delivery (Li et al., 2016b).

One is the low membrane permeability of polar drugs, and the other is the rapid clearance of administered formulation from the nasal cavity owing to mucociliary removal (Illum, 2003).

Anionic Surfactant

Sodium p-dodecylbenensulfonate

$+ Na^+$

$O=S=O$

O^-
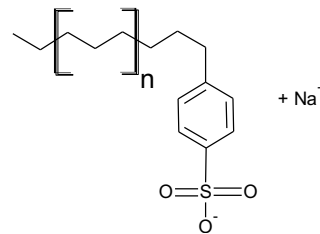
Cationic surfactant

Hexadecyltrimethylammoniumchloride

$+ Cl^-$
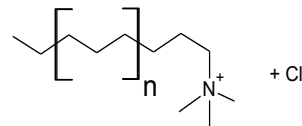
Nonionic surfactant

Di(ethylene glycol)dodecylether

diethylene glycoldodecylether
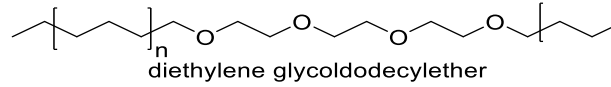
Fatty acids

Stearic acid (C18)

Stearic acid
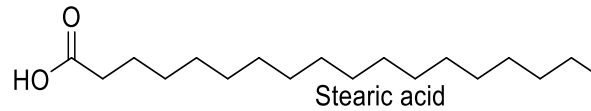
Fat or lipids are a large class of organic compounds that requires nutrition, growth, and development. Fatty acids are the main building blocks for these lipids, and their structural configuration defines their bioactive property in optimizing cell membrane structure and function. However, fatty acids and lysolipids are cytotoxic in micromolar concentrations and can induce cell lysis and apoptosis. Experiments with living cells have shown
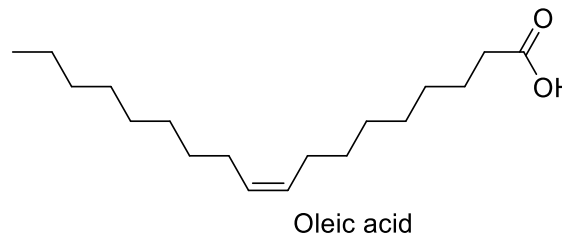
Oleic acid (c18:2)

Oleic acid

Linoleic acid (C18: 2)

Linoleic acid

Alpha-linoleic acid (C18:3)
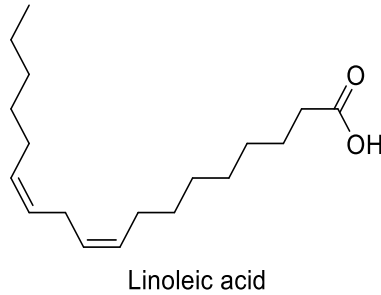
alpha-linolenic acid
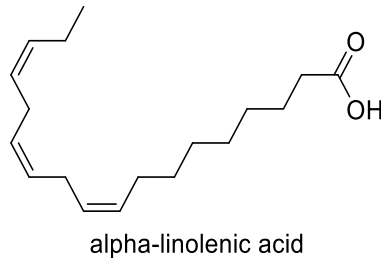
that fatty acids and lysolipids at levels below their cytotoxicity limit cannot render cell membranes more permeable by perturbing the layer's lipid-bilayer component. This implies that the development of liposomal drug-delivery systems, e.g., those using endogenous phospholipase activity as a trigger to unload drugs, are faced with the problem of overcoming the barrier for transferring active medications across the target membranes (Arouri and Mouritsen, 2013).

Cyclodextrins
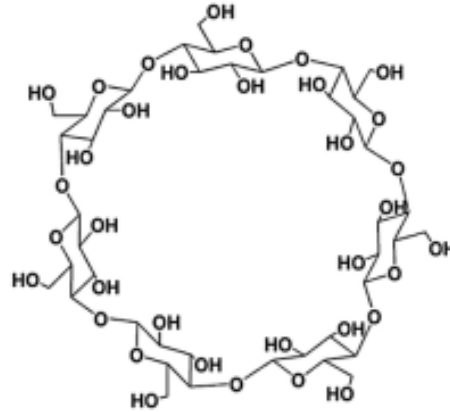
Cyclodextrins are relatively large molecules with a hydrated external surface, and under normal conditions, cyclodextrin molecules only permeate biological membranes with considerable difficulty. Cyclodextrins can enhance the permeation of poorly soluble drugs through biological membranes. Excess of cyclodextrins' concentration can decrease the permeability of drugs (a, β, and γ, Cyclodextrins) (Irie and Uekama, 1999).

Varshosaz and his co-workers studied the nasal delivery of insulin using bioadhesive chitosan gels. A nasal perfusion test was used to evaluate four absorption enhancers: saponin, sodium deoxycholate, ethylenediamine tetra-acetic Acid (EDTA), and lecithin. The gels contained 4,000 IU/dL insulin, 2 or 4% of low and medium molecular weight of chitosan, and lecithin or EDTA. In pharmaceutical protein formulation EDTA is used for chemical and physical stability.
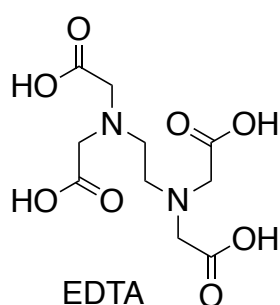
Figure 1. 6 Chemical structure of ethylenediamine Tetra-acetic (EDTA)

The gel was administered nasally in diabetic rats and upon analysis of the serum insulin levels. It was found that preparations which had 2% of low molecular weight of chitosan (LMWc) with EDTA had a better release of insulin and dissolution efficiency (DE) approximately (2.5%), lower T (50%) (T is the time required to release at least 50% of the drug), mean dissolution time, and adhesion than gels containing 4% of the molecular weight of chitosan with lecithin. The insulin release study at zero-order kinetic from the gels was carried out. The gel of 2% average molecular weight of chitosan with EDTA produced an increase in insulin absorption and reduced glucose level by as much as 46% of the intravenous route (Varshosaz et al., 2006). Varshosaz and co-workers found that the controlled delivery of insulin with this proposed study could be achieved through nasal route administration of insulin (Varshosaz et al., 2006).

Nazar and his co-workers formulated an in situ thermo-gelling, mucoadhesive formulation based on N-trimethyl chitosan chloride. The formulation assessed for its

potential to affect the transmucosal delivery of insulin via the nasal route. *In vitro* studies have shown that the formulation releases most of its insulin load (ca. 70%) in a non-concentration dependant manner during the timescale over which the sol-to-gel transition (ca. 8 min) takes place. Moreover, once gelation is obtained, the rest of the therapeutic subject matter's release follows first-order kinetics over at least sixty minutes. Calu-3 cell monolayer revealed that the formulation could induce tight junctions' transient opening (Nazar and Tsibouklis, 2012).

Flavia Laffleur (Flavia Laffleur, 2016) co-precipitated poly(vinyl pyrrolidone) (PVP) and thiolated or unmodified poly(acrylic acid) (PAA) using an air jet mill. Due to the mucoadhesion, the thiolated polymers interpenetrate the mucus gel layer resulting in intimate contact with the mucosa. Results could lead to a higher concentration on the mucosa and therefore facilitating the absorption (Flavia Laffleur, 2016).

Kurvetech technology studied the effect of intranasal insulin at phase II clinical trial. The insulin administration ViaNaseTM line studied cognition, function, cerebral glucose in adults with mild cognitive impairment or Alzheimer's (Craft et al., 2012). In this clinical trial, three groups participated; group one was placebo, group two used 20 IU insulin, and group three used 40 IU insulin. Intranasal insulin on cognition and function showed that participants receiving 20 IU insulin do compare to 40 IU insulin doses given via injection. The 40 IU insulin dose exceeded the optimal insulin dose for memory. Besides, on some measures, optimal performance derived with 20IU insulin and higher levels did now show such an impact on activity (Craft et al., 2012).

1.6.3 Pulmonary delivery of Insulin

Human airways possess a complicated structure and have a defence mechanism against air born particles. Nevertheless, particles can reach airways depending on their size and shape. With a surface area of 140 m^2, lungs can act as a perfect absorption site for therapeutic agents, besides its proximity to blood flow, avoiding first-pass hepatic metabolism (Koskela et al., 2015). Drug delivery to the action's

location, smaller doses are required than oral routes to achieve equivalent therapeutic effects. Medications and macromolecules can be targeted to several layers of the lung depending on their proposed use and their ability to be brought into or through specific layers. Insulin is the first macromolecules used for pulmonary delivery (Proud, 2008).

The pulmonary system's principal function is the blood's oxygenation and the removal of carbon dioxide from the body. The high capacity for solute exchange led the lung to serve as an ideal administration route for applying drugs to treat systemic disorders.

The respiratory tract starts with the nasal epithelium, followed by the tracheo-bronchiolar region, consisting of the trachea and bronchial tree. At the distal region is the alveolar-interstitium, constituted by respiratory bronchiole and alveoli. The pulmonary system functions by approximately 49 different cell types, different in morphology and roles (Proud, 2008). At the moment, these different epithelial cell types' identities rely mainly on the expression of secreted proteins (Cardoso and Lu, 2006). Almost all of the drug-metabolizing enzymes found in the liver are located in the lung's cells too. However, quantitively they are different from the kidney and liver.

The major xenobiotic's metabolizing enzymes, including phase I and phase II enzymes, have been detected in animal and human lung tissues.

The delivery device influences the drug's deposition via the emitted particle size and the aerosol's velocity (Neena Washington, 2001). Therefore, apart from the correct aerodynamic particle size (often expressed as the mass median aerodynamic diameter, MMAD), particles should have a relatively narrow particle size distribution (PSD) and should be aerosolized at relatively low aerodynamic distribution forces (Chow et al., 2007).

Inertial impaction, gravitational sedimentation, and Brownian diffusion are the primary mechanisms involved in particle deposition. The efficiency of particles depends on the particle's aerodynamic properties, the anatomy, and the flow pattern of the particles in each area of the respiratory tract (Lippmann et al., 1980). Ideally, an inhaled particle should possess an aerodynamic diameter between 1-3 µm to enable deposition at the alveoli or deep lung. In the lung, particles with aerodynamic diameters more than 10 µm get trapped at the tracheobronchial or oropharyngeal regions. Smaller particles tend to be exhaled in addition to mucus, which covers the lungs and acts as a physical barrier for insulin permeation (Proud, 2008).

The concept of inhaled insulin was first investigated in Germany in 1925, where a nebulizer is used to deliver insulin. Then, in 1971, Wigley and colleagues administered aerosolized insulin, via a nebulizer, to rabbits and showed a hypoglycemic effect. Delivery technology has since advanced. It is accepted that for inhaled insulin to be sufficient, the particle size entering the lungs should be small enough (1–3 µm) but large enough not to be exhaled. Inhaled insulin was not cost-effective. Higher doses were required to reach the therapeutic level due to the low bioavailability of pulmonary insulin. Some formulations of the pulmonary and nasal route of insulin delivery are in clinical trials and have shown a promising result up to this stage (Table 1.4).

Table 1. 4 Insulin formulation and phases in the clinical trial.

Formulation type	Route of delivery	Company	Phase in Clinical trials
Spray	Intranasal	Nastech	Phase II
Spray	Intranasal	MDRNA	Phase II
Dry Powder Technosphere, Afrezza	Pulmonary	Mannkind or Sanofi	Approved in 2014

Dry Powder AIR	Pulmonary	Mannkind Corp	Phase III
Liquid insulin (AERx)	Pulmonary	Novo Nordisk	Phase III
ViaNase™ line	Intranasal	Kurve Technology, Inc.	Phase II

Exubera™ or inhalable insulin (recombinant human insulin with particle diameters between 1 and 5 μm) was a massive achievement, involving stabilizing the insulin molecule to make in its bioavailable dry powder form. Exubera™ inhaled insulin has demonstrated efficacy regarding achieving significant reductions in HbA1c (Glycated haemoglobin) and facilitating treatment to recommended HbA1c targets in type 1 and type 2 diabetes. Furthermore, there may be some benefit regarding further reducing fasting blood glucose levels than subcutaneous (SC) insulin. The apparent advantage of this therapy lies in patient satisfaction and thus, potentially, treatment adherence. The impact of inhaled insulin on treatment adherence remains to be explained; however, it would be reasonable to speculate that in clinical practice, more patients achieve target HbA1c levels and that patients who were previously poorly controlled may improve because of improved, patient-tailored therapy (Gatto et al., 2019, Hompesch et al., 2009, Alabraba et al., 2009).

In a study by Ungaro and co-workers, large porous particles (LPP) of poly (lactide-co-glycolide) (PLGA) were prepared by the double emulsion solvent evaporation technique and insulin incorporated with optimal aerodynamic properties. *In vivo*, potential in pulmonary delivery was tested. The method for the sustained delivery of insulin to the lungs, the particle deposition characteristics, and insulin release in simulated lung fluids of PLGA/HPβCD/insulin LPP is studied. The study results revealed that the addition of appropriate amounts of insulin and HPβCD played a

crucial role in achieving PLGA/HPβCD/insulin LPP with the desired bulk and aerodynamic properties. Massive Porous Particle (LPP) with a porous structure, low density (0.1 g/ml) and MMAD ranging from 4 - 7 μm were obtained. Besides, the fine particle fraction (FPF) was estimated to be 27 - 90 % at the different airflow rates. The study suggested that particles reach alveoli and remain *in situ* after delivery (Ungaro et al., 2009). The pharmacological effect of PLGA/HPβCD/insulin LPP was confirmed by dose-response studies performed on normoglycaemic and streptozotocin-induced diabetic rats. While insulin solutions administered via the pulmonary route cannot cause a significant hypoglycaemic effect, insulin delivered through PLGA/HPβCD/insulin LPP at similar doses (0.5-4.0 IU / kg) reduced the blood glucose, a function of the administered dose in both animal models. The improved LPP, tested in hyperglycemic rats at visible pathological conditions, resulting in a vital and more prolonged hypoglycaemic effect level at insulin doses as low as 0.5 IU/kg compared to an insulin solution. These results supported the viability of a dry powder formulation based on biodegradable LPP for the controlled release of insulin to the lungs. *In vivo* data demonstrated that PLGA/HPβCD/insulin LPP can reach alveoli and release insulin absorbed in its bioactive form (Ungaro et al., 2009).

Bi et al worked on sustained-release formulations for pulmonary delivery. In their study, a novel dry powder inhalation (DPI) system of insulin-loaded solid lipid nanoparticles (Ins-SLNs) investigated the insulin release, stability, and active inhalation (Bi et al., 2009). Firstly, insulin was incorporated into the lipid carriers achieving a maximum entrapment efficiency as high as 69 ± 3 % (n = 3). Furthermore, DPI formulation was prepared by spray freeze drying of Ins-SLNs suspension, with optimized cryoprotectant and technique parameters. The *in vivo* analysis of intratracheal instillation of insulin solid lipid nanoparticle (Ins-SLNs) to diabetic rats showed a prolonged hypoglycemic effect. The relative pharmacological bioavailability of 44 % was achieved at a dose of 8 IU/kg dosage. These results indicated that (Ins-SLNs) had shown increasing potential as an effective and non-toxic

lipophilic colloidal drug carrier for enhanced pulmonary delivery of insulin (Bi et al., 2009).

SLN can protect insulin from degradation and leakage. However, the drawback of the SLN is that these particles bind to the lungs. Spray-dried insulin has good respirability of particles and capacity for low insulin aggregation. Besides, a moderate number of excipients used for spray dry insulin, and it does not require special storage requirements (Bi et al., 2009).

Insulin inhaler Exubera™ was large; new insulin inhalers are smaller and can be held in hand. In clinical trials, the latest inhaled insulin, Afrezza®, succeeded in lowering HbA1c by using multiple daily doses. On June 27, 2014, the US Food and Drug Administration approved Afrezza®, (MannKind) as an ultra-rapid-acting inhaled insulin to develop postprandial glycemic administration in adults with diabetes mellitus. This is the solely ultra-rapid-acting insulin on the market with more active pharmacokinetics and pharmacodynamics than the current commercially available three rapid-acting insulin; insulin aspart, insulin glulisine, and insulin lispro. Upon inhalation, approximately 60% of the released dose of insulin reaches the lungs. The remainder, 40%, is swallowed and enters the gastrointestinal tract. The technosphere particles dissolve rapidly at the lungs' physiological pH (7.38 - 7.42) (Mikhail, 2016). The efficiency of Afrezza®, usage can be monitored by BluHale® PRO, which is compatible with Android, iPhone, and Microsoft devices. It flashes a green light if Afrezza®, is appropriately inhaled and a red light if not. Doctors can view the tracked data and offer patients advice on how to use Afrezza®, best. BluHale® PRO will ultimately be able to track and share dosing data as well.

1.6.4 Subcutaneous insulin delivery

Until today, the main route to administrate insulin is subcutaneously using insulin syringes, insulin infusion pumps, jet injectors, and pens. Besides, to mimic the physiological secretion of basal and postprandial insulin, long-acting and short-acting analogues of insulin produced by recombinant DNA technology are respectively used (Abraham J. Domb, 2011). On the other hand, amino acid substitutions of insulin

analogues are useful strategies to reduce insulin self-association since these substitutions are crucial to the formation of insulin monomers. Despite the advantages of subcutaneous insulin administration in the treatment of diabetes and besides patient compliance problems, this administration route also presents other significant drawbacks. Such as hyperinsulinemia and consequently severe hypoglycemia, stimulation of smooth muscle cell proliferation, incorporation of glucose into the lipid of arterial walls (Radziuk, 2012) and lipohypertrophy (et.al., 2011). Therefore, the search for an alternative non-invasive route is crucial to improving patients' quality of life. Transdermal insulin delivery is an attractive alternative to subcutaneous insulin delivery because skin presents a large surface and enables the avoidance of first-pass liver effects, which may contribute to a bigger bio-potency (Weitai Wu, 2013). Moreover, compliance with treatment may be more significant compared to traditional subcutaneous insulin. However, the skin is relatively impermeable to insulin, a hydrophilic, and large polypeptide (Donna Zazworsky, 2005).

1.6.5 Transdermal insulin delivery

The skin has a vast surface area compared to the rest of the organs (Figure 1.7). Skin offers an excellent route to deliver the drug to the systemic circulation. The biological barrier is the outermost layer of the skin that is called the stratum corneum. This layer is made of dead keratinocytes and had a thickness of 10-15 μm. This lipophilic barrier is a suitable route to deliver small, potent drugs only. Below the stratum corneum, an epidermis layer, 50-100 μm, containing keratinocytes and enzymes. Skin also possesses the proteolytic enzyme that causes protein degradation. Under the epidermis, there is a layer called the dermis, which is 1-2 mm thick and is full of collagen and elastin fibbers. Also, there is a vascular part of the skin (Kim et al., 2008).

Besides, there are three essential lipids available in the skin making it more lipophilic. These are ceramides, cholesterol, and free fatty acids.
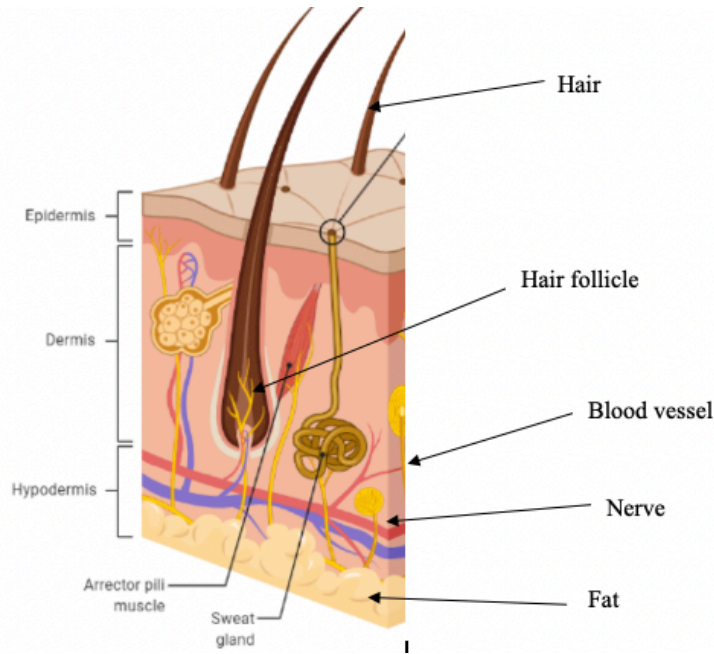
Figure 1. 7 Schematic representation of the skin. The skin comprises of three main layers which are the epidermis, dermis and hypodermis.

Different cell types and components are present throughout the skin, including multiple cell groups, allow for efficient barrier protection against water loss and microbial invasions. The blood and lymph vessels permit the migration of immune cells through the skin during the steady-state and under inflammatory diseases.

High molecular weight, low bioavailability, immunological adverse skin reactions, and little skin permeation capacity limit insulin delivery factors by the transdermal route to be considered valid and safe. Moreover, transdermal insulin administration may present some subcutaneous insulin administration problems since peripheral hypoglycemia may occur, leading to health complications.

Due to transdermal insulin delivery limitations, several strategies have developed to avoid the skin's lipid barrier and its associated complications. These strategies included the use of skin absorption enhancers (e.g., surfactants, fatty acids, fatty

esters), physical methods (e.g., iontophoresis, sonophoresis), or microneedles. Until today, several studies have been evaluated insulin delivery via the transdermal route, and a disposable device is already in the market, which combines one association of a transdermal patch and conventional ambulatory pumps. This system, known as V-Go ®, is a disposable insulin delivery device from Valeritas, Inc. and allows a controlled insulin delivery, even though this is not considered as an alternative yet. Therefore, more studies about insulin delivery by the transdermal route that continue to overcome the inherent limitations are needed.

Microneedles are <300 μm diameter, 50–900 μm long needle-shaped devices that are used for intradermal delivery of insulin. Microneedle-based delivery of insulin offers many advantages such as minimal training for use. Besides, the system is associated with no pain upon insertion, as well as there is the potential to combine microneedles with sensors and drug delivery devices to create an autonomous artificial pancreas (Narayan, 2014).

Liu et al. (Liu et al., 2012) have developed novel insulin-loaded microneedle arrays to study their applicability in the transdermal delivery of insulin. In another study by Liu, a novel insulin-loaded microneedle arrays (MNs) were fabricated from hyaluronic acid (HA), a significant component of skin and a common ingredient in cosmetics. They characterized their applicability in the transdermal delivery of insulin. (Liu et al., 2012). *In vitro*, the insulin release from insulin-loaded microneedles reached approximately 100% after 1 hour. They were suggesting that microneedles were wholly and rapidly absorbed as this system was based on self-dissolving properties.

There are three types of microneedles. Solid microneedles which work based on poke with patch approach and are used for pre-treatment of the skin. The second type is coated microneedles which works based on a coat and poke approach. A coating of drug solution is applied on the needle surface. Dissolving microneedles is the third type, which is made of biodegradable polymers. Hollow microneedles are filled with the drug solution and deposit the drug in the dermis layer of the skin.

Regarding transdermal absorption of insulin in diabetic rats, the results showed a significant and dose-dependent hypoglycemic effect for insulin-loaded microneedles. A decrease in plasma glucose of 11.9% for an insulin dose of 0.13 U/Kg and 57.4% for an insulin dose of 0.44 U/Kg. Thus, a hypoglycemic effect after treatment with insulin-loaded microneedles and a significant decrease in plasma glucose with these novel microneedles occurred. This study suggested that novel insulin-loaded microneedles fabricated from hyaluronic acid can be useful in transdermal insulin delivery to diabetic patients. Since there is already a system for transdermal insulin delivery in the market, it seems that this approach may be an alternative to subcutaneous insulin administration (Liu et al., 2012).

Mei-Chin Chen et al. (Chen et al., 2015a) used γ-PGA (high-molecular-weight polypeptide comprising a γ-linked glutamic acid) as a Micro Needles (MN) material as it is non-toxic, biodegradable, and has nonimmunogenic properties.

Mei and co-workers created a dissolving microneedle (MN) patch, comprising γ-PGA MNs and PVA/PVP supporting structures, by using a simple casting process. The drug-containing γ-PGA gel was first used to fill the mold cavities (Drug-Eluting Implantable Devices made from polymers such as Nylon (PA), Polycarbonate (PC), Polypropylene (PP)), and the residual gel on the mold surface was recycled to avoid wastage. A PVA/PVP solution without drugs was subsequently placed on the first layer and then centrifuged to form supporting structures and a backing layer (Chen et al., 2015a). Different concentrations of γ-PGA hydrogel into γ-PGA on the hygroscopicity and skin insertion ability of the prepared MNs was investigated. In the study by Chen, *in vitro* and *in vivo* transdermal drug delivery properties of the MNs were evaluated after optimizing the composition.

Moreover, the biological activity and long-term storage stability of insulin encapsulated in the MNs were also measured. The efficacy and reproducibility of using γ-PGA MNs for transdermal insulin delivery were studied. Insulin-loaded MNs were injected into streptozotocin (STZ)-induced diabetic rats once daily for two days (Table 1.5).

Pharmacokinetics and pharmacodynamics of MN-based insulin delivery with SC insulin administration were compared. In this study, insulin-loaded γ-PGA MNs to diabetic reduced the blood glucose level. Besides MN fabrication process used in this study does not alter the activity of encapsulated proteins . These results confirmed the efficacy and stability of using γ-PGA MNs for insulin delivery; this system may be an ideal candidate for treating T1DM. The study demonstrated that γ-PGA MNs with a supporting structure design enables complete and efficient insulin delivery into the skin (Chen et al., 2015a).

Table 1. 5 Transdermal delivery of insulin in the form of a hydrogel, or micelles.

Potential Polymer	Formulation	Delivery route	Reference
Poly (ethylene glycol)-b-poly(b-benzyl-L-aspartate) (PEG-b-PBLA)	Micelles	Not decided	(Hao Yang, 2013)
Poly (N isopropyl acrylamide co-acrylic acid) P(NIPAM-co-AA)	Nano gel	Not decided	(Shi, 2014)
Poly-γ-glutamic acid micro and nanoparticle (MNs) and polyvinyl alcohol (PVA)/polyvinyl pyrrolidone (PVP)	insulin-loaded microneedle	Transdermal	(Chen et al., 2015a)
Hyaluronic acid	insulin-loaded micro-needle	Transdermal	(Shu Liu, 2012)
4-(2-Acrylamidoethylcarbamoyl)-3-fluorophenylboronic acid (AMECFPBA)	Hydrogel	Subcutaneous	(A. Matsumoto , 2012)

1.6.7 Iontophoresis

Iontophoresis is a technique that was reported early in the 20th century to improve the drug permeation across the skin. This procedure uses an electric current for the delivery of large molecules such as proteins. It relies on a pair of electrodes positioned on the skin to produce an electrical potential between the skin surface

and the capillary's lower layers of skin. Positively charged therapeutic molecules are driven toward the capillaries from the skin surface at the positive electrode, while negatively charged particles transport through the skin toward the negative electrode—the transport of drug ions through the skin into blood supported by migration and osmosis. The amount of transported charge drugs depends on the intensity of the electric field and the treatment duration. Therefore, the transdermal delivery of insulin to give therapeutic levels is challenged by the negative charge of human insulin under physiological conditions. It shows that adjusting the aqueous solution of concentrated insulin to a pH of 3.7 was the most effective for regular insulin iontophoresis.

In contrast to chemical permeation enhancers, iontophoresis does not change the skin structure, affecting its barrier ability. Nonetheless, the low-level current of such a technique limits insulin transport efficiency through the stratum corneum. Although increasing current intensity can lead to a higher delivery rate, the potential risk of skin irritation and pain also limits the highest current intensity. (Banga AK, 1993).

Another electrically assisted transdermal drug delivery is electroporation. High-intensity electroporation leads to enhanced delivery of insulin compared to iontophoresis. The high-voltage pulses inevitably affect the deeper tissues, causing potential pain and muscle stimulation. Further studies on device design to minimize the side effect should facilitate clinical translation (Mohammad EA, 2016).

The jet injection is another needle-free administration for transdermal insulin delivery. Besides techniques such as ultrasound-mediated transdermal drug delivery, there are solid microneedles (MNs), hollow MNs, and multilayered MNs. Bioresponsive MNs that can respond to the physiological signals have been spotlighted as a promising approach for glucose-regulated insulin delivery. This platform generally, integrates glucose-responsive components with polymeric MN matrix.

1.7 Formulation of insulin

Different approaches such as liposome, lipid-based microemulsion, solid lipid (H.M. Patel, 1976)), polymeric materials such chitosan nanoparticles (Yeh et al., 2011), alginate-based micro/nanoparticles (P. Mukhopadhyay, 2015b),dextran-based nanoparticles (S. Sajeesh, 2010), Poly Lactic Glycolic Acid (PLGA) micro/nanoparticle, and inorganic micro/nanoparticles considered for oral delivery of insulin (Mansourpour et al., 2015, Cui et al., 2015, Agrawal, 2014, Mengmeng Niu, 2014b, Niu et al., 2014, Zhang et al., 2014, Mengmeng Niu, 2014a, Kisel M. A, 2011, Niu et al., 2011, Kisel MA1, 2011, Mohanraj et al., 2010, Ayogu, 2009, Jain et al., 2007, N. Zhang, 2005b, Zhang et al., 2005, N. Zhang, 2005a, Kisel et al., 2001, Iwanaga et al., 1999).

Liposomes (Kisel M. A, 2011) have shown encouraging potential in oral insulin delivery due to their facilitated absorption and ability to protect insulin from the harsh gastrointestinal (GI) environment.

Kisel et al. tried to deliver insulin using liposomes made of phosphatidyl ethanol phosphatidylcholine and phosphatidylinositol. The prepared liposomes associated with hyperinsulinemia; hence, it was believed that the insulin liposomal preparations could circumvent the gastrointestinal tract's harsh conditions. It is believed that the active insulin formed a lipid-protein complex with the liposomes to reach the insulin receptors. Additionally, Kisel et al. demonstrated that phosphatidyl ethanol-based liposomes mask the immune response to insulin when injected intraperitoneally into mice (Kisel M. A, 2011). However, standard phospholipids/cholesterol liposomes are sensitive to damage caused by gastric acid and enzymes, resulting in reduced oral bioavailability or the liposomes' decay. To prolong the stability of these lipid carriers' liposomes have been modified in several ways, such as the incorporation of bile salts, coating the liposomes with polymers, and the design of multi-layered or multi-vesicular transporter or liposome modified with plant-based sterols (Cui et al., 2015, Agrawal, 2014, Mengmeng Niu, 2014b).

In order to improve the performance of liposomes table 1.5 via the oral route, bilosomes, also called liposomes containing bile salts were developed by incorporating bile salts into the lipid bilayers (Mengmeng Niu, 2014b). Bilosomes were found to be more stable in the Gastro-Intestinal Tract (GIT) by showing prolonged residence time compared to conventional liposomes, which could attribute to the remarkable protective effect against damage by bile salts and protease. In Niu et al's study, sodium glycocholate bile salt was used as an enzyme inhibitor and permeation enhancer for oral insulin. Bilosomes of 154 ± 18 nm particles were successfully prepared by a reversed-phase evaporation method and managed to entrap around 30% of recombinant human insulin (rhINS). It was concluded that sodium glycocholate liposomes have superior protective characteristics compared to liposomes containing sodium taurocholate and sodium deoxycholate. The *in vitro* studies demonstrated that sodium glycocholate protected insulin against the enzymatic degradation of pepsin, trypsin, and α-chymotrypsin (Mengmeng Niu, 2014b).

Cui and co-workers (Cui et al., 2015) have used plant-based sterols such as beta-sitosterol, stigmasterol, ergosterol, and lanosterol in order to substitute cholesterol in the liposomal structure. Cui et al. demonstrated that the liposomal membrane could stabilize the four sterols used in the preparative process. However, liposomes containing ergosterol are deemed to have a more distinct capacity for protecting insulin against degradation in simulated gastrointestinal fluids than liposomes stabilized by the other three sterols (Cui et al., 2015). Also, this study showed that ergosterol-liposome exerted low toxicity to Caco-2 cells through a cell viability assay. The structure of ergosterol and cholesterol are similar. Meanwhile, insulin permeability significantly increased across Caco-2 monolayers by encapsulating in ergosterol -liposome (Cui et al., 2015).
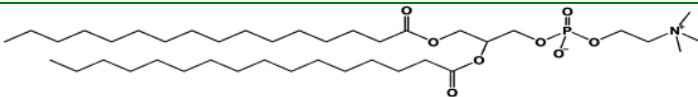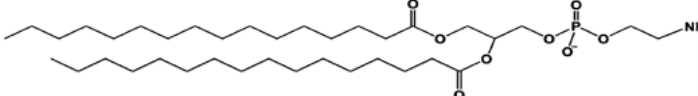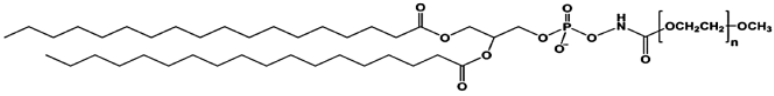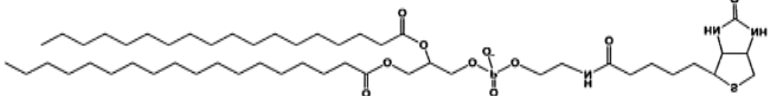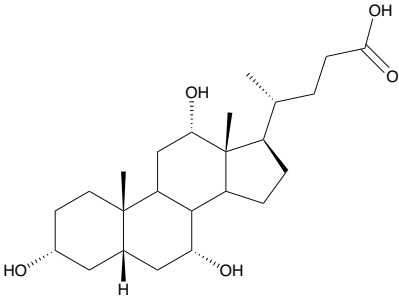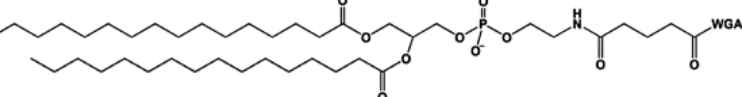
Another study by Agarwal and co-workers used folic acid (FA) functionalized insulin-loaded liposomes to improve the macromolecule's oral bioavailability. Liposomes stabilized by an irregular coating of negatively charged poly (acrylic acid) (PAA),

positively charged poly(allylamine) hydrochloride (PAH), and folic acid added as targeting ligand by synthesizing folic acid–poly(allylamine) hydrochloride conjugate (Agrawal, 2014). The *in vivo* pharmacodynamic and pharmacokinetic studies showed almost double hypoglycemic effect and approximately 20% relative bioavailability compared to subcutaneously administered insulin solution. Generally, this can help to design ligand-anchored polyelectrolyte-b—systems for drug delivery (Agrawal, 2014).

Saccharide derivatives such as Lectin were bound to N-glutaryl-phosphatidylethanolamine (N-glut-PE) to modify the pharmaceutical properties of liposome-based-insulin delivery. Wheat germ agglutinin-modified liposomes showed the highest hypoglycemic effect when administered orally to the diabetic mice and this was attributed to the affinity of Wheat germ agglutinin to glycoconjugates on the intestinal enterocytes and M cells hence higher insulin absorption across the intestinal epithelia (Zhang et al., 2005).

Coating liposomes (Table 1.6) with lipophilic materials as a protection layer was also investigated. Coating materials such as mucin and poly (ethylene glycol) 2000 (PEG) were reported in the literature (Iwanaga et al., 1999). Mucin and PEG-coated liposomes had higher insulin mean transit time (MTT) and deviation of transit time (DTT) than the uncoated liposomes. Besides, PEG-coated liposomes were found to interact with the intestinal mucus layer, which, in turn, slows the transit time of insulin (Iwanaga et al., 1999).

Table 1. 6 Liposome drug delivery of insulin. using different fatty acid

Lipid	Structure Oral insulin liposomal formulation	Reference
DPPC (Liposome)		(H.M. Patel, 1976)
DPPE (Liposome)		(Kisel MA1, 2011)
PEG-DSPE (Liposome)		(K. Iwanaga, 1997)
Biotin-DSPE (Liposome)		(N. Zhang, 2006)
bile salts (Liposome)		(Mengmeng Niu, 2014a)
Wheat germ agglutinin modified N-glutaryl-phosphatidyl (Solid lipid nanoparticles and microemulsion) (WGA-PE)		(N. Zhang, 2006) (N. Zhang, 2005a)

Ergosterol

Folic acid liposome
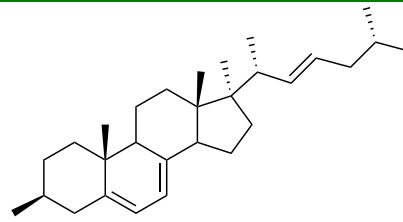
(Cui et al., 2015).

(Agrawal, 2014)
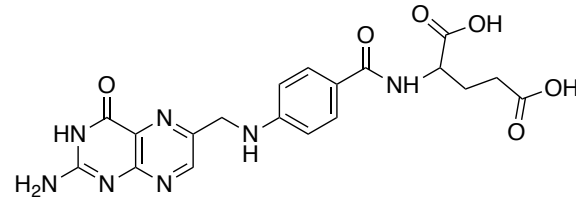
1.7.1 Insulin delivery using Inorganic molecules

There are inorganic molecule-based delivery systems of insulin. These inorganic materials are safe as their by-products such as calcium, phosphate, or carbonate ions are biocompatible and present in the bloodstream.

Inorganic molecules are used in tissue engineering since they are highly biocompatible, bioactive, non-immunogenic, and possess homology to natural inorganic material such as bones and teeth. Inorganic molecules used successfully in therapeutics for various applications in the form of macroscales such as cement and scaffolds, microscale as coatings, structures, and nanoscale colloidal particulate system, targeted therapy (Sharma et al., 2015).

Encapsulation of insulin with inorganic molecules can be achieved by infiltration, solvent evaporation, co-precipitation, and layer-by-layer methods (Kentaro Yoshida, 2015). A study noted that the pH threshold for insulin release was pH 5.0 - 6.0, which matches the isoelectric point of insulin, 5.4. The release of insulin from the microparticles with inorganic ions was rapid and was nearly complete within a few minutes. The polymer film disappeared as the charge on insulin changed from positive to negative. Therefore, the author claims that this polymeric system might be sufficient for the delivery of insulin; however, further studies are required (Hashide et al., 2014). Despite the considerable effort for using insulin inorganic nanoparticle, it is still not clear how insulin bind to these nanoparticles (Hashide et al., 2014).

1.7.2 Closed-loop system (Artificial Pancreas System)

Closed-loop system (Artificial Pancreas System) now referred to as AID (Automated Insulin Delivery) (Demirdjian et al., 1998, Selam et al., 1993, Slama and Selam, 1992, Forlenza et al., 2018). The only presently available implantable pump is the model 2007 from Medtronic-MiniMed (Northridge, CA, USA) is commercialized and up to now, Food and Drug Administration (FDA) has approved two initial commercial AID

systems, the Medtronic MiniMed 670G and Control-IQ from Tandem Diabetes Care (Table 1.6). Around 1200 implantable pumps have been used in diabetic humans worldwide. MiniMed niMed® 670G System is the first Closed Loop insulin delivery system approved anywhere in the world in January 2017 (Zhong et al., 2016).

Another system from Medtronic is MiniMed Paradigm® is a Veo™ System. This system combines insulin pump therapy and continuous glucose monitoring with a unique new capability to instinctively stop insulin delivery for up to two hours, if the glucose levels fall to a pre-determined level, unlike any other pump on the market. Paradigm® Veo actively protects the person against the risk of hypoglycemia, even while asleep. In a study by Zhong and co-workers in collaboration with Medtronic in which data from MiniMed 640G system users (n = 4818), MiniMed 530G system users, (n = 39,219) and MiniMed Paradigm® Veo™ system users (n = 43,193) were retrospectively analysed (Zhong et al., 2016). The results showed that the MiniMed 640G system could reduce the frequency of both high and low SG values and help maintain SG after the resumption of insulin delivery (Zhong et al., 2016). SmartGuard(TM) HCL is the system and the latest innovation in Medtronic's phased approach toward developing a fully automated, closed-loop system listed in table 1.7. SmartGuard(TM) HCL can automate basal insulin dosing 24 hours a day, and it is an anticipated advancement in diabetes. With this technology, managing diabetes by minimizing glucose, variability and maximizing time in the target range can be achieved (Selam, 2001). A fully automated closed-loop insulin delivery system is used in patients with insulin-treated type 2 diabetes (Thabit et al., 2017).

In this pilot study, 40 participants took part. Twenty patients were assigned to use the closed-loop insulin delivery system, and twenty patients were assigned to handle the conventional subcutaneous insulin injection as a control. In the closed-loop insulin delivery study group, contributors' natural insulin treatment with sulfonylurea medication, were discontinued on the day of closed-loop initiation. All other anti-diabetes medicines continued. In the conventional insulin therapy group,

participants' natural insulin and other antihyperglycaemic therapy continued throughout the 72h study period. A continuous glucose-monitoring receiver (Freestyle Navigator II) was modified to mask sensor glucose concentrations to the participant, investigators, and ward staff (Thabit et al., 2017).

The time needed to achieve the target glucose range was reduced by 60 % in the closed-loop group and 38 % in the control group (difference of 21 %). There were no episodes of severe hypoglycemia or hyperglycemia reported in either group (Thabit et al., 2017).

In another pilot study of the closed-loop system, 29 participants took part. Participants received insulin via the day-and-night closed-loop network (closed-loop period) for four weeks and via implanted pump therapy (control period). Participants used rapid-acting insulin analogue generally applied in their usual clinical care. The study was carried out under free-living conditions without direct or remote supervision by clinical investigators. Contributors were not limited in their dietary intake or daily activities. Standard local hypoglycemia and hyperglycemia treatment guidelines were followed. Compare with the control period for day-and-night, closed-loop insulin delivery lowered the glucose concentration by 50% in patient. Compared with standard pump therapy, closed-loop insulin delivery reduced time with glucose strength above the target range (for example,>10 mmol/L) by 69 %. Additionally, glycaemic variability was lower in the closed-loop period than in the control period (Bally et al., 2018, Bally et al., 2017b, Bally et al., 2017a, Bally and Thabit, 2017). The drawback of the closed-loop system is that aspect of metabolic modelling is not captured in the results related to the β-cell. Therefore, the optimized insulin dosing for every patient is not very accurate. Differences exist, of course, between the control problem faced by the β-cell and that of the artificial closed-loop system with even the most abbreviated list, including the delay in subcutaneous insulin absorption, lack of a direct portal effect of insulin to suppress hepatic glucose output. Besides, the β-cell potential benefits

from neural signals and incretin factors, signals that allow the β-cell to release insulin in advance of an increase in blood glucose and may potentiate the insulin response. There are two main issues with closed-loop insulin delivery systems, justifying the model controlled (glucose-metabolism/ insulin-action). Closed-loop systems or continuous glucose monitors demand an additional body site for insertion away from an insulin pump or injection site. In children and adults, closed-loop devices only have approval in particular sites. For paediatric bodies, this is in the abdomen or gluteus. However, patients often need to interchange between multiple insertion sites, most often in stomach, gluteus, or bilateral arms (Steil et al., 2006, Steil et al., 2004).

Table 1. 7 Comparative table of insulin pumps or closed-loop systems currently available.

Insulin Pump of closed-loopop system	Description of closed-loopp system	Reservoir/ cartridge and capacity of insulin (units)
Accu-Chek® Combo (Roche)	For users of the large daily volume of insulin	Provides up to 50U, 4 bolus options: quick/standard/extended bolus/multi wave
Accu-Chek® Insight (Roche)	For patient with low basal insulin	Standard, Extended and Multi wave Boluses, adjustable in increments of:0.05 U (up to 2.0 U)
MiniMedTM Paradigm VeoTM* (Medtronic)	Insulin Pump with low glucose suspend	Minimum: 0.025 Maximum: 75U
MiniMed 640G* (Medtronic)	Insulin Pump with Smart Guard algorithm that uses CGM data to predict and prevent hypos.	0.025 to 0.05 U increases -Maximum: 75U -3 personalized bolus settings: standard, dual, and square wave
mylife OmniPod (Ypsomed Ltd**)	Tubeless insulin pump with insulin filled pod with automatic insertion mechanism.	Max 30 U Maximum flow rate 1.5U/min, 0.05, 0.1, 0.5 or 1.0U bolus increments

mylife YpsoPump (Ypsomed Ltd)	Intuitive insulin pump having on ease-of- use and data connectivity.	0.1U, 0.5U, 1.0U, then 2.0U, bolus increases, 30U maximum
DANA Diabecare R (Advanced Therapeutics UK Ltd)	Insulin Pump and handset (Bluetooth connection) with a built-in blood test meter.	Dosage increases in 0.05, 0.1, 0.5 or 1.0 units up to 80U
DANA Diabecare RS (Advanced Therapeutics UK Ltd)	An insulin pump that communicates with the smartphone app via two-way Bluetooth	Bolus Increases in 0.05, 0.1, 0.5, 1.0 units, Up to 80 units
A6 TouchCare® (Medtrum)	Tubeless Insulin pump which is (reusable pump base and disposable reservoir patch)	Bolus increments: 0.05 U (maximum 25 U)
Cellnovo	Insulin pump and a handset with touch screen controls and built-in the blood glucose monitor	Delivers up to 30U bolus in increments of 0.05U

1.7.3 Exogenous cell therapy

Cell-based treatment for diabetes involves the regeneration of β cells, repairing of primary cells to secrete insulin, or transplanting insulin-producing cells to renovate insulin production in response to glucose level variations (Radziuk, 2012). Introducing new insulin-producing cells in the body can lead to an immune response. Long-term assurance against these responses is necessary to ensure the survival and function of transplanted insulin-producing cells. Nanoparticles can potentially help to address some of these challenges (Adams G, 2013).

Pancreatic islet transplantation or exogenous cell therapy, characteristically in the form of cells, was introduced as an approach to restore normal glycemia in patients with type 1 diabetes in the early 1970s. From the theoretical point of view, the exogenous cell therapy method of therapy could only be effective in patients with a short history of the diabetes. When there are at least a few β cells still working. As soon as the production stopped, pancreatic cells might be able to resume the secretion of sufficient amounts of insulin to maintain an average glucose level (Snarski et al., 2009). Nevertheless, due to host rejection of transplanted cells, reduced quantities of donor cells, and the immunosuppressive therapy that is required, the clinical submission of islet transplantation is regulated.

Over forty years, efforts have been made to develop an improved bio-artificial system. The studies also have suggested that adult bone harbour cells that can influence β-cell regeneration in diabetic animals (Nir et al., 2007). Nanotechnology managed to develop more advanced engineering of complex tissues. For example, nanotechnology can be applied to separate and protect relocated cells from the immune system while allowing adequate diffusion of oxygen, glucose, insulin, and other essential nutrients. Towards this goal, different coating approaches, including layer by layer polymer

deposition, complex formation, and chemical reactions of polymers, have been applied to islets to produce nano-thin coatings that may protect cell activity without inhibiting their function. One barrier in translating these technologies into the clinic remains the lack of encapsulating materials to avoid host recognition and following foreign body responses. Future improvement of islet encapsulation requires that documents and devices developed such that encapsulated cells can maintain function and viability while avoiding fibrosis (Veiseh et al., 2015).

1.7.4 Gene therapy

Gene therapy is an alternative strategy that circumvents the immune response to cell therapies (Ko et al., 2001). Gene therapy is used to expresses or silence individual genes involved in the immune reaction. Nanoparticles have been developed to protect and deliver nucleic acids to target cells (Figure 1.8).
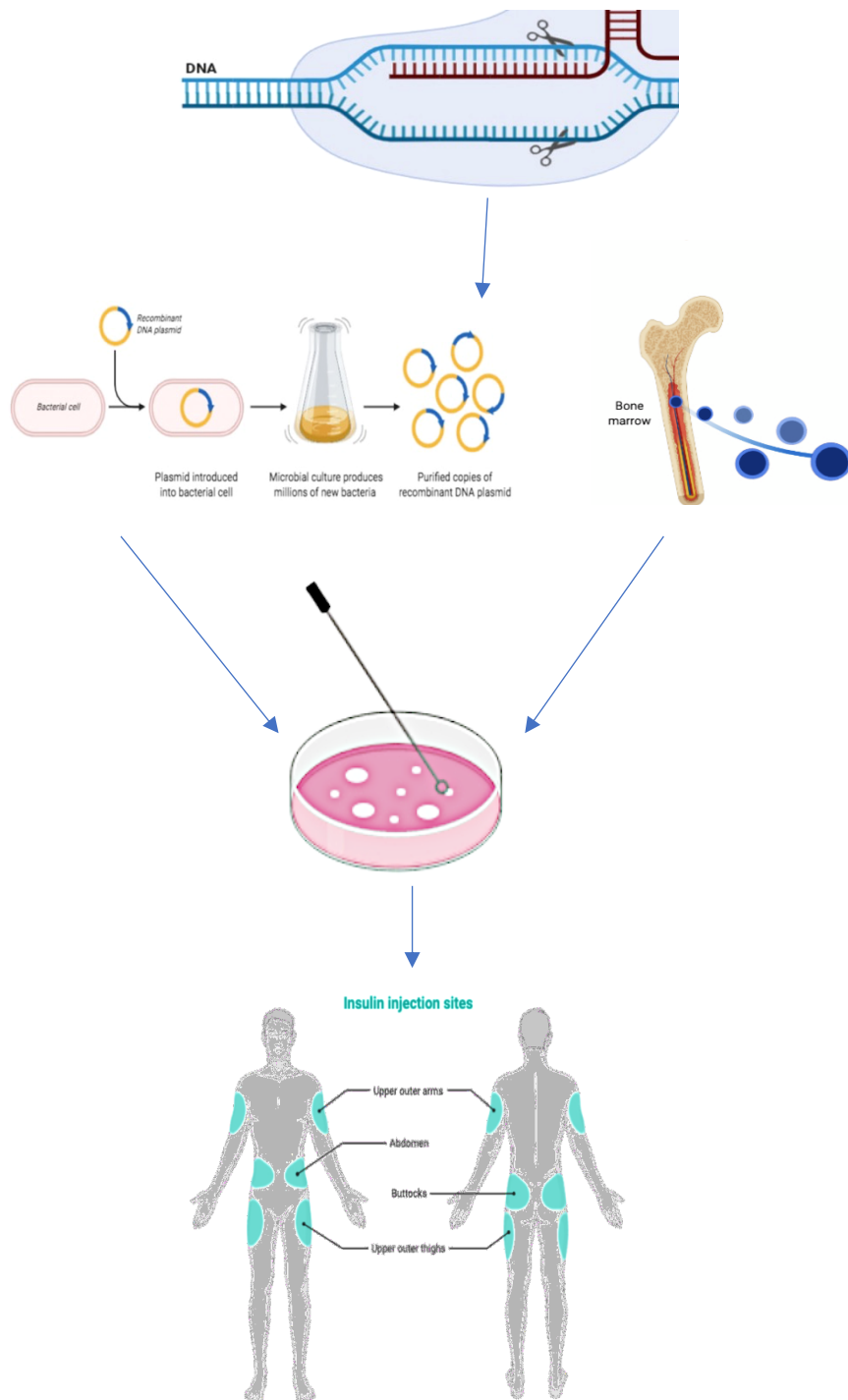
Figure 1. 8 Gene therapy for diabetes treatment, it express or silence individual genes involved in the immune reaction, which is an alternative strategy that circumvents the immune response to cell therapies

For example, a cationic polymeric carrier such as poly gamma-(4-aminobutyl)-L-glycolic acid (PAGA) nanoparticles have been used to deliver DNA encoding interleukin (Class of cytokines which are expressed by white blood cells and promote the improvement of T lymphocytes and B lymphocytes) to white blood cells to defeat the T cell reaction against residual innate islet cells in animal models of early diabetes. Therefore, preventing the development of diabetes in 75% of animals (Ko et al., 2001). In the study, Ko et al. examined the effect of specific cytokines on the suppression of insulitis, followed by diabetes development prevention. Glucose levels were measured weekly up to 32 weeks using blood collected from the mouse's tail vein. The results showed that the development of diabetes was prevented by the combined treatment of IL-4 and IL-10 plasmids. However, only a single plasmid (IL-4 or IL-10) injection did not show any difference with the control group (Ko et al., 2001).

Alternatively, the gene encoding glucagon-like peptide 1 (GLP-1) has been delivered via nanoparticles to boost insulin secretion and islet viability. In this study, a plasmid–polymer complex, GLP-1, was used. Gene delivery can decrease blood glucose concentration in type 2 diabetic animal model. The addition of GLP-1 level reduced plasma glucose concentration by increasing plasma insulin concentration (Oh et al., 2003).

A study by Keun (Tae Keun Oh, 2006) showed that intramuscular injection of lentiviral vectors containing human cytomegalovirus (CMV) (a common virus that belongs to the herpes family of viruses), with human proinsulin cDNA, modified furin (Furin is a protein that in humans is encoded by the FURIN gene) cleavage site could attenuate hyperglycemia, increase the survival rate of the treated rats and increase their body weight and prevent ketoacidosis in a type 1 DM rat model. These results suggest that the skeletal muscle tissue is an easy and productive target for insulin's ectopic

production. This method could be a potential treatment modality for the prevention of ketoacidosis in severe diabetes mellitus. The first gene therapy report to show the practical use of advanced lentiviral vectors to correct the hyperglycemia in an animal model of type 1 diabetes mellitus is by Keun (Tae Keun Oh, 2006). Studies on gene therapy are still conducted mainly in animal models, and the safety aspects of gene therapy are yet to be confirmed in humans. Little data are available, and a better knowledge of the biology of cytokines involved in diabetes is also necessary for the advancement of safe and effective immunotherapy. Adeno-associated viral (AAV) vector was studied in human gene therapy tests and could be delivered to the pancreas through a non-surgical endoscopic procedure. Investigators are examining gene therapy in non-human primates. If successful, work will begin with the Food and Drug Administration (FDA) to approve the first gene therapy that can go to phase 1 clinical trial in February 2020 (Muller et al., 2019, Handelsman et al., 2019, Blonde et al., 2019, Blonde et al., 2021).

Ultimately, vaccines have been considered as a long-term approach to prevent the autoimmune destruction of β cells for type 1 diabetes. Nanotechnology has been used to improve the development of vaccines for some diseases. It has shown to ease the need for antigen adjuvants and direct antigens to specific body sites. Nanotechnology can also improve antigens' potency, provide a reliable platform for the use of combinations of antigens, and enable the delivery of self-replicating and RNA-based antigens. Mainly, diabetes vaccine development efforts have focused on reducing the cytotoxic T cell immune response against β cells without compromising global immunity (Veiseh et al., 2015).

1.7.5 Dendrimers

The use of dendrimers to deliver insulin was also investigated. Dendrimers are highly branched, monodisperse macromolecules with a well-defined structure that significantly influences their physical and chemical properties. Moreover, their surface multifunctionality allows the chance for multivalent interactions with biological substrates. The highly branched, globular architecture of these molecules gives rise to some interesting properties compared to linear polymers of similar molecular weight (MW). For example, dendrimers increase solubility that can be readily adjusted by derivatizing the edge, and they show very low intrinsic viscosities. Another promising advantage of dendrimers is protein fibril formation inhibition, where aggregation and fibrillation of insulin occur in insulin-dependent diabetic patients after repeated administration. Polymaidoamine (PAMAM) dendrimers can exist as positively charged amine-terminated, neutral hydroxyl-terminated, or negatively charged carboxyl-terminated polymer.

In contrast to classical polymers, dendrimers have a high degree of molecular uniformity, narrow molecular weight distribution, specific size, shape characteristics, and a highly functionalized terminal surface. Lin and co-workers found that PAMAM dendrimers may loosen the tight junctions between cells of the epithelium to some extent. However, the paracellular pathway may not be enough to improve macromolecules' intestinal absorption, including insulin (Lin, 2011). A study was carried out for dendronized chitosan by grafting polyamidoamine (PAMAM) onto CS using Michael-type addition reaction. The grafted polymer formed sub-spherical nanoparticles of 85- 150 nm through coacervation and managed to encapsulate 95% of insulin. The dendritic system had more than 9% relative bioavailability and did not show any systemic toxicity (Piyasi Mukhopadhyay, 2014)

1.7.6 Hyaluronic acid

Another polymer that was investigated as a potential carrier for oral insulin is Hyaluronic acid (HA). HA was used in two novel formulations of insulin based on its fibrillar state (having a significant sequence of amino acid) and their use in the treatment of diabetic mice (Y. Dekel, 2009) (Li et al., 2016a).
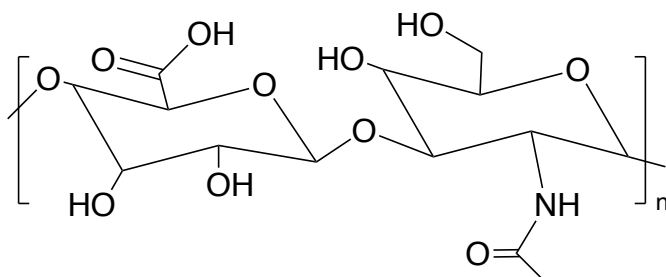
Figure 1. 9 Chemical structure of hyaluronic acid

Insulin fibrils are hydrophobic, with intensely packed conformation, and can restore full biological activity when dissociated. Insulin fibril is (Burke and Rougvie, 1972) a candidate for oral delivery. To protect the insulin from the severe GIT environments, and to target it to the intestinal mucosa, Dekel and his co-workers developed two types of fibrillar insulin particles. The first Hyaluronic acid-coated in a mixture of phospholipids and lipid-hyaluronan conjugates. While the second protein fibrils encapsulated within a particle named gagomer made of a hyaluronan shell and crosslinked via phospholipid. Gagomers can be generated as micro or nanoparticles and can encapsulate more significant protein with a molecular weight of 11000 KDa (Dekel et al., 2010).

The serum insulin levels of free insulin, insulin-loaded nanocarriers, and HA hydrogel system containing insulin-loaded nanocarriers were analysed in this study. The serum insulin concentration reaches the peak value at 95.7 (m IU/L) after oral administration of insulin solution in a short time (2 h) and then decreases quickly to a lower level. However, the serum insulin concentration increased with a lower rate at the initial stage (before four h) after oral administration of insulin-loaded nanocarriers (36.2 m

IU/L at four h) and HA hydrogel system containing insulin-loaded nanocarriers (61.0 m IU/L at four h), then decreased slowly. Both insulin-loaded nanocarriers and HA hydrogel system containing insulin-loaded nanocarriers showed significantly higher serum insulin concentration associated with insulin solution after post-administration for four h (Li et al., 2016a).

Biodegradable nanoparticles loaded with insulin–phospholipid complex formulated by reverse micelle–solvent evaporation method were also investigated. Soybean phosphatidylcholine (SPC) was used to improve the lipo-solubility of insulin, and to control drug release (Fude Cui, 2006). The study by Cui and his co-workers found that even though insulin was successfully formulated into the nanoparticles with the help of phospholipid complex, the pharmacological bioavailability in diabetic rats was still lower than that required in clinical situations (> 15%). Therefore, it is believed that further studies are necessary to prevent enzymatic degradation despite the high 90% drug entrapment efficiency. (Fude Cui, 2006).

In a study by Garcia-Diaz, Insulin was formulated with soybean phosphatidylcholine or sodium caprate by self-assembly and then loaded into PLGA nanoparticles using the double emulsion solvent evaporation technique (Garcia-Diaz et al., 2015). This study showed an improved appearance of insulin into the organic phase of the emulsion made from soybean fatty acids. It was eventually resulting in significantly better encapsulation efficiencies (90% compared to 24% in the absence of lipids). Significantly, the insulin loading capacity has increased by up to 20% by using fat–insulin complexes. Moreover, the results showed that the main fraction of lipid was incorporated into nanoparticles and remained associated with the polymer during release studies in buffers, whereas insulin release in a non-complexed form as a rupture of approximately 80% of the loaded insulin. In conclusion, the protein load in PLGA nanoparticles can significantly increase by employing self-assembled protein-lipid complexes (Garcia-Diaz et al., 2015).

1.7.6 Protein fibrillation

Although spontaneous fibrillation of endogenous proteins is usually detrimental and could lead to pathological situations, this study is an encouragement to consider protein fibrillation as a possible benefit for exogenous therapeutic proteins, especially if active monomers are released *in vivo* (Y. Dekel, 2009). The results confirm that both the coated insulin fibrils and the gagomeric insulin have a high potential for oral administration. Coated insulin and fibrils are useful for the reduction and control of basal glucose level (BGL). This study encourages us to consider protein fibrillation as a potential benefit for exogenous therapeutic proteins (Y. Dekel, 2009).

In another study (Li et al., 2016a). Calcium carbonate nanoparticles and hyaluronic acid (HA) for insulin delivery was designed. In the preparation process of nanoparticles, it was found that $CaCO_3$-HA nanoparticle had low toxicity in cell culture. The subsequent nanocarriers showed low comparative cytotoxicity against Caco-2 cells and evident stability against protein solution. Comparison between subcutaneous insulin injection, free insulin oral, and $CaCO_3$-HA nanoparticle oral administration to diabetic rats. The subcutaneous injection of free insulin showed a plasma decrease after 2 hours. Oral administration of free insulin did not alter blood glucose at all. At the same time, $CaCO_3$-HA nanoparticles lowered the blood glucose in rats after 3 hours and glucose declined slowly, the slow release of glucose shows that nanoparticles can maintain the high level of plasma insulin (Li et al., 2016a).

1.8 Glucose-responsive materials

The approaches for incorporating glucose sensing into formulations are called a smart delivery system, which can deliver an appropriate dose of insulin. There can be divide into three groups, enzymatic sensing, natural glucose-binding proteins, and synthetic molecular recognition. These classes include glucose oxidase (GOD), concanavalin A, and phenylboronic acid (scheme 1.1).

The enzymatic conversion which is frequently used in biosensors and uses glucose oxidase (GOx), an enzyme that catalyzes the transformation of glucose into hydrogen peroxide and helps glucose responsiveness for insulin delivery.
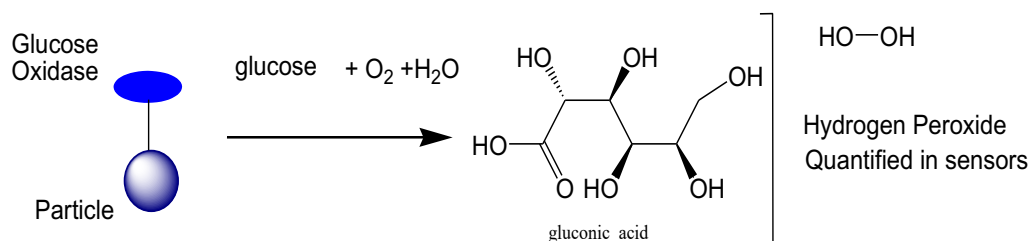
Scheme 1. 1 The enzymatic conversion is used in biosensors and uses glucose oxidase (GOx).

GOD (β-D-glucose: oxygen 1-oxidoreductase) this enzyme catalyzes the oxidation of β-D-glucose to gluconic acid using molecular oxygen as an electron acceptor immediate formation of hydrogen peroxide (H_2O_2).

Glucose-responsive materials are also used with lectins, carbohydrate-binding proteins, as a natural receptor for glucose-sensing. One of these lectins is concanavalin A (ConA) (scheme 1.2), a tetravalent binding protein. The first work was reported in 1979 and demonstrated the glucose-responsive release of a glycosylated insulin derivative from an insulin-ConA complex. The protein (ConA) is used in polymers or incorporation within microcapsules for controlled release of glycosylated insulin. Glycosylation of insulin, while maintaining the bioactivity of the protein, allows reversible binding to ConA, and glucose since an increase in local glucose concentration forces equilibrium toward the liberated modified insulin protein.

Sensor based on ConA a glucose binding protein
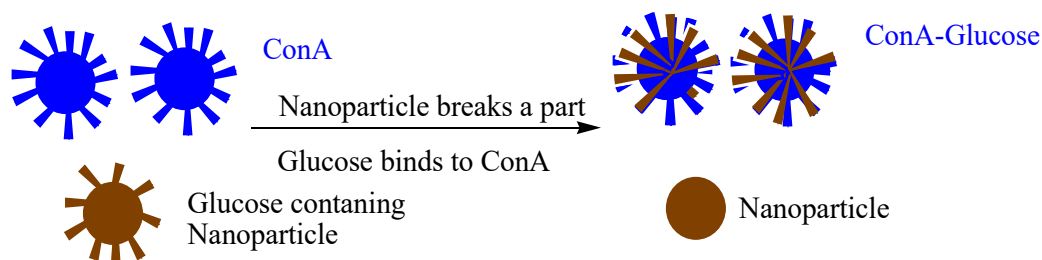
Scheme 1. 2 Glucose binding protein incorporated in nanoparticles binding to ConA.

Boronic acid and its derivatives react with 1,2-, 1,3- or 1,4-diol to create a stable cyclic ester (scheme 1.3). These are a unique class of stimuli-responsive molecules with potential applications as self-healing materials, self-regulated drug-delivery systems, and sensors to detect diols like dopamine, sugar, and glycoproteins (J.N. Cambre, 2011). In aqueous solution, boronic acid has a pKa of 8.70 at room temperature. Despite its weakly acidic nature, boronic acid can detect biologically active sugars such as glucose, fructose, and other sugar molecules (Lucia Babcock, 1980). This concept is essential for developing chemical sensors for sugar detection in drug delivery. This concept can be ideal for insulin delivery.
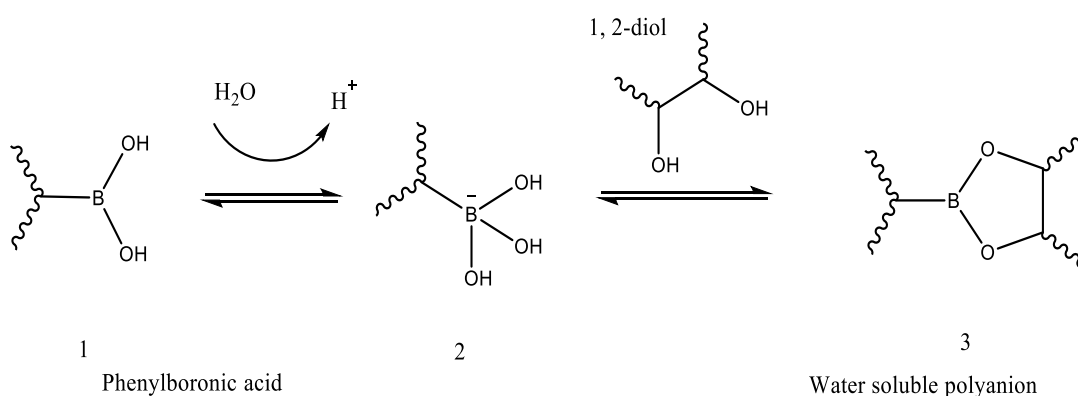
Scheme 1. 3 Mechanism of sugar sensing of phenylboronic acid incorporated in nanoparticles.

Loading insulin into a system and quantitatively releasing the hormone only when the blood sugar is high is still very challenging (Scheme 1.3). According to the human body's

needs, the challenge for insulin delivery is to deliver a precise dose of insulin. To control the treatment of insulin is another challenge.

Therefore, there must be a delivery system that can deliver insulin once an episode of hypoglycemia arises. Besides, a constant release profile with fast action when required is significant to achieve. It is challenging due to the nature of insulin itself, which is prone to degradation. Temperature and solvents disrupt the structure of insulin. Therefore, a pH-responsive system is required to achieve a high loading of insulin and release it when the blood sugar is high. A pH-responsive order for insulin delivery requires three main strategies.

Insulin has almost 60% bioavailability, but it is eliminated very fast from blood after subcutaneous injection, making standard glycemic control hard to achieve. The use of a polymeric material that releases insulin only in the presence of high blood glucose, remaining inactive in average blood glucose concentrations, is an ideal solution. The new challenge is to synthesize a stimuli-responsive polymer loaded with insulin. The insulin-loaded polymer would be studied against pH, temperature, ionic strength, and presence of glucose to quantify its stability and effectiveness for sensing glucose and release of insulin, once the polymeric system is optimised.

1.9 The role of polymers in delivery of antidiabetic drugs

Biodegradable polymers are classified, biopolymers and agropolymers. Biopolymers are then classified into synthetic and natural polymers (Figure 1.10). Then synthetic polymers are originated from natural or synthetic monomers, which are linked via ester groups and agropolymers, are connected via glycosidic and amide bonds (Scheme 1.4).

One example of these is poly(lactide-co-glycolide) (PLGA), polyglycolic acid, polylactide (PLA), and poly(caprolactone) (PCL) are the Food and Drug Administration (FDA) approved synthetic polyesters. They are generally classified into three groups based on the polymer degradation kinetics for example (PLGA, fast), (polyglycolic acid, medium), and slow (PLA and PCL slow) degradation time from 6 to 12 months.
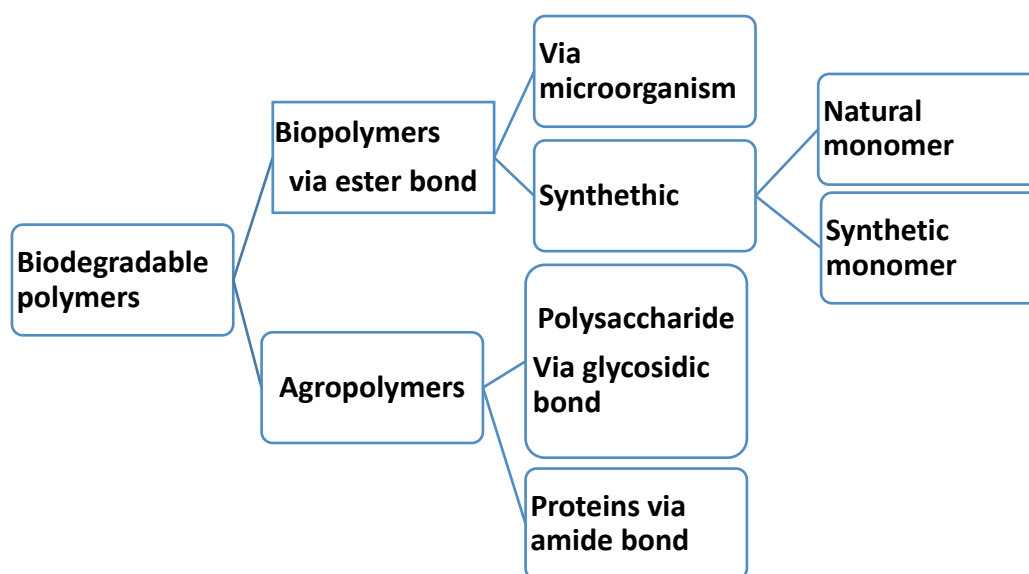
Figure 1. 10 Classification of biodegradable polymers, biopolymers are linked via ester, glycosidic and amide bonds.
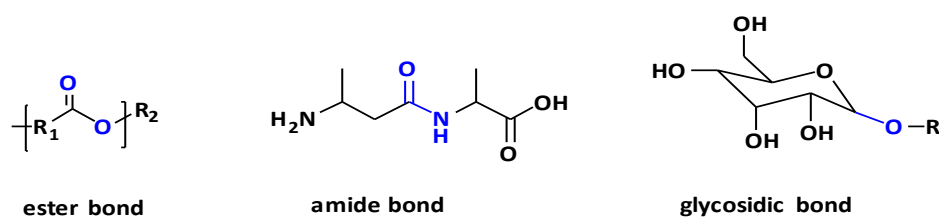
Scheme 1. 4 the bonds (blue) which natural and synthetic biodegradable polymers bond.

Polymeric material and advancement in micro and nanotechnology offer a new route to drug delivery in diabetes along with different courses of administration

The current development of insulin nanocarriers, smart-drug delivery systems (stimuli-responsive), pumps, nano sensors, micro and nano self-dissolving needles, liposome and micelles are numbers of advancement in this area. The use of nanoparticles (NPs) allows for improved bioavailability, controlled release, and targeted drug delivery (TDD).

To date, the advancement of nanomedicine has focused on the safe, effective, and accurate delivery of drugs for the treatment of many pathological conditions. Studies employing biodegradable natural/synthetic polymeric nanoparticles (PNPs) and manipulating the distinctive properties for diabetic drug delivery.

This mechanical strength reduces the degradation rate of the polymer, thereby providing the biomaterial with excellent durability. Some studies combine synthetic and non-synthetic polymers because synthetic polymers are hydrophobic and chemically and mechanically stronger in comparison to their non-synthetic counterparts. Researchers can control properties to achieve a superior insulin delivery system with enhanced therapeutic efficacy.

1.9.1 Polymer-based formulation of insulin

Polymeric micro/nanocarriers are widely used for insulin delivery. Polymeric carriers are used to protect insulin against degradation or instability due to pH changes across the GIT. Some of these polymers are modified in such a way that it can enhance mucoadhesion for oral absorption of insulin. Distinctive types of biodegradable polymers such as synthetic and natural that have been used to develop micro and nanoparticles-based formulations for antidiabetic drugs and how the numerous encapsulation approaches impact its therapeutic effect diabetic drugs, including pharmacokinetics studies, drug release profiles and efficacy of the encapsulated drugs.

1.9.2 Natural polymers

1.9.2.1 Chitosan

Chitosan (CS) is a natural cationic polysaccharide composed of glucose amine and N-acetyl-glucosamine units (Nagpal et al., 2010). Chitosan is biodegradable, biocompatible, and non-toxic. It is mucoadhesive and possesses penetration enhancing capacities (Yeh et al., 2011). The polymer cationic nature, together with its good solubility at physiological pHs, enables loading drugs of protein nature and making chitosan an ideal carrier for proteins such as insulin (Makhlof et al., 2011).

In the study, chitosan, multifunctional nanocarriers modified by L-valine and phenylboronic acid were designed and evaluated (Li et al., 2017). L-valine was used as a target ligand to facilitate the small intestine absorption. In contrast, phenylboronic acid was used as a glucose-responsive unit. The resultant nanocarriers exhibited relatively lower cytotoxicity and excellent stability against protein solution. pH and glucose changes *in vitro* triggered the insulin release from nanocarriers. The chemical stability of insulin against the digestive enzyme in conjunction with pepsin in simulated gastric fluid (SGF) and simulated intestinal fluid (SIF) containing pancreatin, respectively, was studied. The obtained chitosan-based multifunctional nanocarriers exhibited excellent protective properties for insulin against enzymatic degradation. The lower glycemic effect for oral insulin delivery was studied *in vivo* using STZ-induced diabetic SD rats as models. After the oral administration of insulin formulation to the diabetic rats, nanocarriers showed a significant hypoglycemic effect. They maintained a higher standard for a longer time (Li et al., 2017).

Chitosan is synthesized by partial deacetylation of chitin and is a copolymer of β-(1 → 4)-2-acetamido-D-glucose and β-(1 → 4)-2-amino-D-glucose units, with the latter

usually exceeding 80% (Bakshi et al., 2020). It is a biodegradable polymer very suitable for pharmaceutical applications due to its low toxicity, low immunogenicity, and good biocompatibility. Chitosan and its derivatives, such as glycol chitosan, succinyl chitosan, arginine-chitosan, and aminated chitosan, are efficient drug carriers for the oral route of administration (Tsai et al., 2019).

Many studies have used chitosan to design a system to deliver antidiabetic drugs. Eilleia et al. (Sarah Y.Eilleia, 2018) have concluded a study using microencapsulation technology to protect insulin from gastric and enzymatic degradation. Porous Microparticles were prepared using poly (d,l-lactide-co-glycolide) (PLGA) using w/o/w emulsion solvent evaporation method. The insulin solution 5 mg /ml in 0.01 M HCl (1 ml) was incubated with 10mg of porous PLGA microparticles and the surfaces of PLGA microparticles was coated with chitosan by double freeze-drying. Insulin released from microparticles examined with i*n vivo* trials by studying its effect on lowering blood glucose. Four formulations tested; insulin suspension, insulin loaded PLGA microparticles, insulin PLGA microparticles coated with chitosan, and SC insulin suspension. The results indicated that a significant reduction in blood glucose level (15.8% ± 4%) occurred for 2 hours with SC injection.

In contrast to the oral suspension of insulin, which did not affect the glucose level had failed due to the enzymatic degradation of insulin in the GIT. The blood glucose level rose to 70% after the first hour, then reduced to 50% and was maintained over 8 hours by using chitosan-coated microparticles. Chitosan believed to adhere to the upper intestinal part where insulin had minimum solubility resulting in low insulin absorption and sustained glucose reduction (Sarah Y.Eilleia, 2018). Zhang et al. concluded similar results of maintaining low blood glucose levels owing to the chitosan coating of insulin loaded PLGA nanoparticles (Zhang et al., 2012).

1.9.2.2 Chitosan and combination of Alginate

The confocal laser scanning microscopy showed hydroxypropyl methylcellulose phthalate chitosan (HPMCP-CS) nanoparticles had between 2- 4-fold higher mucoadhesive characteristics compared to CS-NPs. Besides, it has a more significant hypoglycemic effect. In addition to ionotropic gelation, self-assembly is another technique supposed successful in preparing insulin CS nanoparticles. Shrestha et al. managed to encapsulate up to 85% of insulin in the self-assembled nanoparticles of 200-550 nm in size. Self-assembled CS nanoparticles proved to be active and managed to reduce the glucose level within 4 hours of oral administration (Shrestha et al., 2014). Other CS insulin synthesis methods reported in the literature, are the microemulsion method coprecipitation and complicated coacervation method, and Emulsification solvent diffusion (Nagpal et al., 2010).

Modified chitosan as an insulin carrier was also investigated. Trimethylated chitosan (TMC) and poly(γ-glutamic acid) (γ-PGA, TMC/γ-PGA NPs) were used in Mi et al. (Fwu-Long Mi, 2008) studies to prepare self-assembled insulin nanoparticles (NPs). At pH 7.4, TMC/γ-PGA NPs significantly swelled, and insulin sustained release profile was observed for 2 hours. Besides, TMC/γ-PGA NPs were found to be more effective carriers for the transmucosal insulin delivery compared to Chitosan PG NPs, which were only active in the intestinal segment (Fwu-Long Mi, 2008). Krauland (Krauland, 2004) looked at utilizing thiolated chitosan to deliver insulin orally. CS molecules were covalently linked to 2-Iminothiolane together with a Bowman-Birk-Inhibitor as the enzyme inhibitor. The thiolation process improved the mucoadhesion of the prepared CS-insulin tablets by 60 folds and maintained a hypoglycemic effect. CS was used in Shrestha et al. (Shrestha et al., 2014) study to modify the surface of annealed thermally hydrocarbon-assisted Porous Silicon (AnnTHCPSi) microparticles. The surface

modification with CS had a significant impact on the insulin permeation across Caco-2/HT-29 cell co-culture monolayers. Insulin permeation increase by 20-fold; its apparent permeability went up by 7-fold, as CS interacted with the mucus layer putting the microparticles in close contact with the cell surface, hence a higher cellular uptake (Takenouchi et al., 2014).

Alginate (ALG) is another water-soluble natural linear polysaccharide. This polymer contains different amounts of 1,4-linked β-D-mannuronic acid and α-L-guluronic acid residues extracted from brown seaweed. It is a pH-responsive polymer due to its ability to shrink at low pHs, enabling encapsulated drug retention in the stomach while protecting it against enzymatic deactivation. Gelation is induced by cross-linking the guluronic acid units with di- or polyvalent cations such as calcium. Alginate's (ALG) biodegradability, biocompatibility, low toxicity, low immunogenicity, and good mucoadhesion facilitate its application in oral drug delivery. Micro or nanoparticles of ALG were used to sustain drug release (Reis et al., 2007) Reis and co-workers studied alginate dispersion containing insulin protein into an immiscible water phase. Gelation was triggered in situ by the immediate release of ionic calcium from the carbonate complex via gentle pH adjustment. Particle size was controlled through the emulsification parameters, yielding insulin-loaded microparticles (Reis et al., 2007). The RP-HPLC/HPLC- Mass and the Circular Dichroism Spectroscopy analysis revealed that the preparation method does not compromise insulin stability, and the protein maintained its secondary structure without any signs of damage.

A study conducted by Piyasi et al. demonstrated that nanoparticles made of Alginate (ALG) and chitosan (CS) might be a promising carrier for oral insulin and other therapeutic proteins such as insulin (P. Mukhopadhyay, 2015a). Ionic gelation prepared Core/shell nanoparticles with an average size ranging between 100- 200 nm. Despite

the high insulin encapsulation efficiency (85%), the insulin-relative bioavailability did not exceed 8.11%.

A similar approach was employed in Mansourpour et al's study where insulin nanoparticles were prepared using alginate, trimethyl chitosan, and cationic β-cyclodextrin polymers (CPβCDs). The design of the experimental approach was utilized to optimize the size, polydispersity, and entrapment efficiencies of the prepared insulin nanoparticles. The streamlined preparation managed to upload up to 93.2% ± 4.1 insulin and sustain the enzyme's release for 5 hours without showing any cytotoxicity effects on Caco-2 cell lines (Mansourpour et al., 2015).

Another group of researchers has prepared several microspheres composed of alginate, chitosan, and dextran sulfate by ionotropic gelation (Niederhofer and Muller, 2004). Dextran sulfate displayed higher protective properties of alginate microspheres, enhancing protein retention under gastric conditions compared to chitosan coating. The addition of the polyanionic dextran also increased the encapsulation parameter values. These outcomes indicate that dextran sulfate reinforced microspheres are good candidates for the oral delivery of insulin. Despite the suitability of this formulation and high release profile, this formulation required further optimization. Dextran was evaluated as a potential carrier for oral insulin (Sarmento et al., 2007a). In Chalasani et al. study, dextran was conjugated with vitamin-B12 to prepare insulin nanoparticles. Vitamin-B12 could mediate uptake of insulin, therefore maintain the hypoglycemic effect of insulin up to 54 h. Dextran/vitamin-B12 showed a relative pharmacological activity of 29.4% compared to SC insulin injection (Chalasani et al., 2007a, Chalasani et al., 2007b), table 1.9 lists the chitosan based formulation of insulin.

Table 1. 8 Polymeric nanoparticle of insulin and the further outcome details in review article (Nihad Al-Hashimi, 2020).

Polymeric nanoparticles	Drugs incorporate	Route of Administration	OUTCOME		Reference
			Pharmacokinetic	Therapeutic	
Chitosan NPs (300-400 nm) **Loading Efficiency ~55%**	Insulin	Intranasal	↑nasal absorption	Significant rapid *in vitro* release. ↑*In vivo* release in albino mice as compared to insulin solution.	(Fernández-Urrusuno, 1999)
Alginate/chitosan NPs (750 nm) **L.D > 70%**	Insulin	oral	↑oral absorption ↑oral bioactivity	↓basal glucose levels up to 40% for 18hours.	(Sarmento et al., 2007b)
Chitosan NP	Insulin	oral	↑Interaction between rat intestinal epithelium & CS NPs after 3hours.	↓ Serum glucose levels in streptozotocin-induced diabetic rats for 11hours.	(Sarmento et al., 2007a)
Chitosan-mucin NPs combined with poloxamer & PVA **EE ~88-92%**	Insulin	oral	Negligible release at pH 1.2 and >80% sustained release for 8hrs at pH 7.4	Fast onset of action in alloxan-induced diabetic rats. The NPs provided sustained release (12hrs) than subcutaneous insulin whose effect lasted for 4hrs.	(Momoh A.Mumuniam Franklin C.Kenechukwua, 2020)

Fatty acid conjugated Chitosan Nanoparticles LE and LC>98%	Insulin	Liver-targeted SC delivery	↑Hepatocyte absorption ↑antidiabetic efficacy. ↑↑ relative pharmacological availability than free insulin	↑↑ Relative pharmacological availability in liver than free insulin in diabetic mice.	(Hongxiang Li, 2018)

1.9.2.3 Gelatin

Gelatin is a natural polymer obtained from animal collagen and possess low antigenicity. It is isolated using acid or base hydrolysis of collagen by breaking the hydrogen bonds responsible for the stability of collagen (Courts, 1955). Gelatin has been classified as type A or types B, depending upon the type of hydrolysis method used in its preparation. Gelatin nanoparticles were first developed in 1978 by Marty et al. (Lai et al., 2014).

Inoo, Bando and Tabata conducted a study to assess the insulin secretion by transport subcutaneously insulinoma cells and gelatin hydrogel microspheres in the back of rats to assess the insulin secretion from both of them. Model β cells were prepared by mixing gelatin hydrogel microspheres with insulinoma cells groups to sustain the vitality of the cells through studying the pathway of oxygen and nutrients and the effect of the composite hydrogel microspheres on the function of cell aggregates. Chemical cross-linking of gelatin in w/o emulsion was used to prepare gelatin hydrogel microspheres. The insulinoma cells with or without gelatin hydrogel microspheres were loaded in a sac-like a tool and insulin secretion was evaluated before and after the subcutaneous transplantation on 3 and 7 days for all formulations. The results showed that insulin secretion was markedly higher from the sac-like tool containing insulin insulinoma cells aggregates with gelatin microspheres compared with those without the microspheres. However, the secreted insulin amount was less after transplantation, and it was similar between 3 and 7 days after transplantation by *in vivo* studies (Inoo et al., 2018b, Inoo et al., 2018a)

In another study Inoo, Bando and Tabat used the same obtained gelatin hydrogel microspheres previously for *in vivo* experiments on rat-derived insulinoma cells to compare between the effect of gelatin hydrogel microspheres and microspheres-free cell groups on the survival and glucose-induced insulin secretion. After 14 days of cultivation at the initial seeding density of cells the results showed an excellent cell survival and reductase action for the cells with gelatin microspheres and a significant

increment in insulin secretion with cell groups of large-sized microspheres compared to the middle-sized and the cell groups without microspheres. Hence, cell groups combined with large gelatin hydrogel microspheres can be considered to prepare the cells for the treatment of type 1 diabetes (Inoo et al., 2018a, Inoo et al., 2018b).

Gelatin was used by Wang, Tabata and Morimoto to prepare animated microspheres for nasal drug delivery system of peptide drugs. The *in vitro* drug release study was used to evaluate fluorescein-labelled insulin (RITC-insulin) and FITC-dextran as model drugs. The release of RITC-insulin from the animated gelatin microspheres was slower than from control gelatin microspheres, with 18.4% and 32.4% within 30 min, and 56.9% and 75.1% within 8 hours accordingly. However, the release of FITC-dextran from both gelatin formulations (animated and the native) was fast, and no significant difference observed between them. The *in vitro* study was used to test the hypoglycaemic effect after intranasal administration of the formulations in healthy rats. The outcomes showed a noteworthy reduction in glucose level with nasal administration of animated gelatin microspheres in powder form in contrast to the intranasal suspension which had no significant effect on glucose level after at insulin dose of 5 IU/Kg (Wang et al., 2006).

1.9.2.4 Albumin

Albumin is a biopolymer, and it is an emerging nanocarrier for protein-based drugs, including oral delivery of insulin. Albumin is the most abundant plasma protein having a molecular weight of 66.5 KDa. It possesses high stability at pH 4 to 9 and thermal stability up to 60 °C. Furthermore, it has been preferentially used as an oral drug delivery system for its biodegradable nature, low toxicity and non-immunogenicity making albumin an ideal material for drug delivery (Kratz, 2008).

Mahobia and co-workers prepared egg albumin nanoparticles to deliver insulin orally. The microemulsion method was employed to prepare egg albumin NPs in the presence

of glutaraldehyde as a crosslinker. The NPs were then placed in insulin PBS solution to load the drug. The NPs were subjected to swell up and absorb the drug until equilibrium was achieved. The size of these NPs was reported to be 10-30 nm under TEM, while the *in vitro* cytotoxicity was investigated in fibroblasts and the albumin NPs were deemed non-toxic. It was observed that an increase in albumin content up to a specific limit increased insulin release proportionally. Formulations with 68% drug loading showed a maximum cumulative release up to 5mg while formulations with 33% drug loading exhibited 4 mg cumulative release (Mahobia et al., 2016).

Another group of researchers prepared chitosan-albumin coated particles for oral insulin delivery using a complicated formulation based on emulsification gelation technique. Insulin was incorporated to be trapped between alginate-dextran sulphate pockets, and a dual coating was applied by dropwise addition of chitosan and albumin, sequentially. The particles possessed an average size of 300nm, PDI ≤ 0.30 and surface charge of -30.6 ± 0.8 mV. The encapsulation efficiency of NPs before the coating was 72.4 ± 3.3% while it was reduced to 21.9 ± 2.8 and 30.7 ± 3.4%, after coating with chitosan and albumin, respectively. Similarly, the loading degree of NPs also reduced from 10.1 ± 2.8% to 4.8 ± 0.4% and 6.2 ± 1.4% after chitosan and albumin coating, respectively. The *in vitro* studies showed complete insulin release at pH 5.5 after 2 hours for both chitosan and alginate coated NPs, but a sustained release at pH 7.4 was observed only with albumin coated NPs while in chitosan-coated NPs insulin release was halted due to insolubility of chitosan at that pH. *In vivo* permeability studies were carried out in a triple co-culture of Caco-2/HT29-MTX/Raji B model proved that dual-coated NPs had increase permeation across the intestinal cell and longer retention in mucus layer than non-coated NPs (Lopes et al., 2016).

Woitiski and co-workers developed a similar type of NPs formulation in 2010 where hypoglycemic effects of chitosan stabilized alginate-dextran NP coated with albumin

were investigated. These NPs were administered orally to Wistar diabetic rats. The NPs carried negative charge; therefore, the bioactivity of insulin was maintained bioactivity and pharmacological availability was improved by avoiding enzymatic degradation of insulin and via chemical and physical facilitation of permeation through the intestinal membrane. The NPs were 396 nm (PDI 0.6) in size with a ZP of -38mV. *In vivo* results indicated a drop of 40% in blood plasma levels with a sustained hypoglycemic effect maintained over 40hours. The oral bioavailability of 13% for a dose of 50 IU/Kg was three times higher than free insulin. Confocal microscopy confirmed internalization of insulin in the small intestinal mucosa (Woitiski et al., 2010)
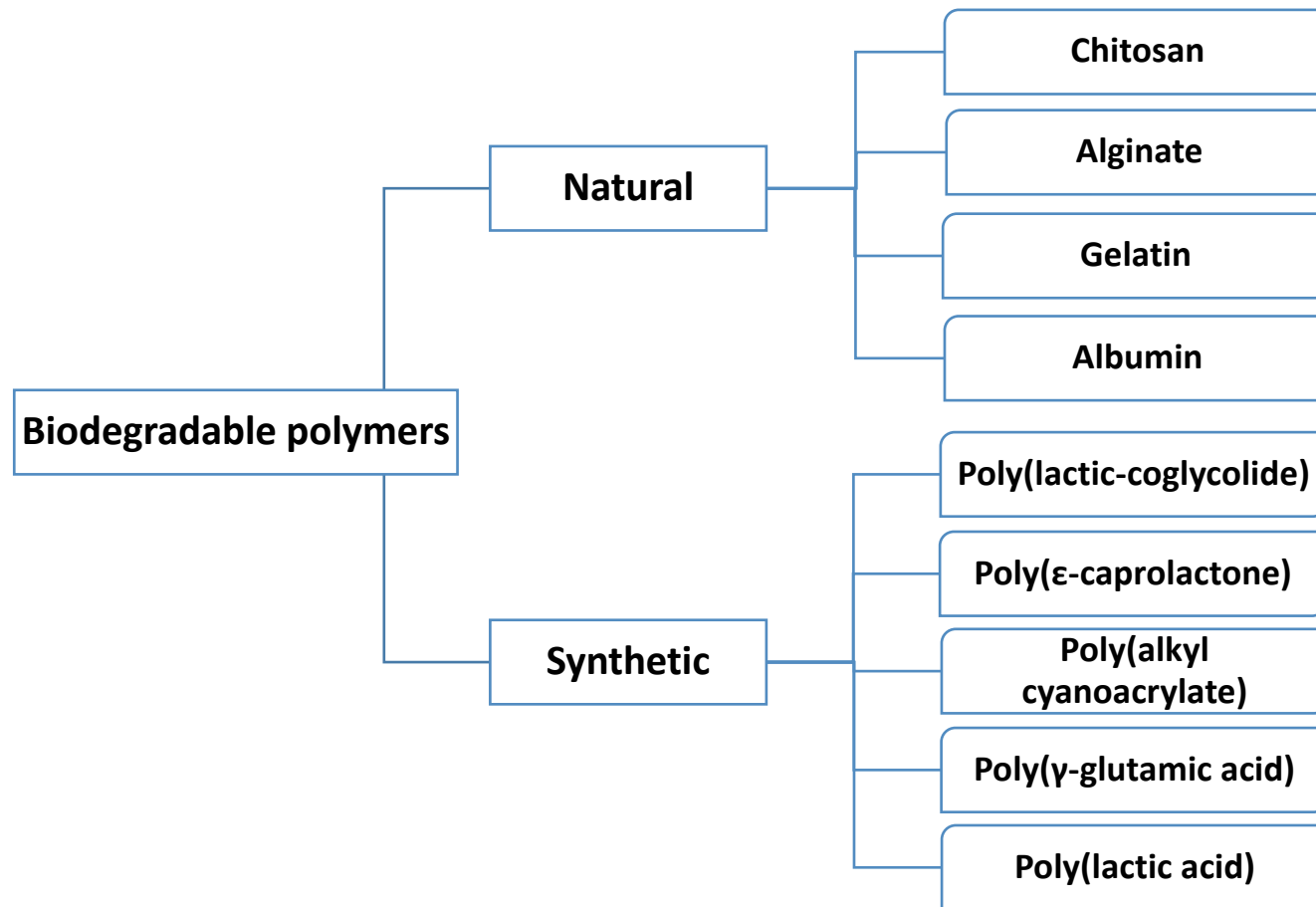
Figure 1. 11 A schematic presentation of natural and synthetic biodegradable polymers.

1.10 Synthetic polymers

1.10.1 Poly(lactic-co-glycolic acid)(PLGA)

PLGA based carriers have been studied for the development of the prolonged release of inhaled drugs in the lung in order to sustain the pharmacological effect and reduce the daily doses (Ungaro et al., 2012). Ungaro et al. investigated the potential of pulmonary delivery of insulin loaded in PLGA and cyclodextrin microparticles volume median diameter (VMD: 26.2±1.2 µm) by assessing the in vivo deposition pattern and hypoglycaemic activity of insulin loaded in PLGA and cyclodextrin. The delivery route is intratracheally in normoglycemic rats and induced diabetic rats, respectively. The *in vivo* deposition studies showed that insulin loaded PLGA reached alveoli surface and remained after administration. Upon testing the induced diabetic rats, insulin loaded PLGA showed a significant reduction in blood glucose level compared to the control group treated with insulin solution in the absence of PLGA (p< 0.0001) (Ungaro et al., 2009). Another study conducted by Hamishehkar et al. evaluated the feasibility of pulmonary delivery for the controlled insulin release by preparing a dry powder inhaler formulation (DPI) of insulin loaded PLGA microcapsules blended with mannitol as a carrier and tested the aerosolization performance of the formulations (Hamishehkar et al., 2010b, Hamishehkar et al., 2010a)Hamishehkar et al. designed a PLGA microsphere (VMD 4.04µm) dry powder system for sustained delivery of insulin via lungs and monitored serum insulin and glucose concentrations in diabetic rats. Pharmacokinetic analysis in diabetic rats showed that the insulin means residence time of insulin loaded PLGA microcapsules was 7 and 5 folds longer than spray dried insulin powders administered by intratracheal insufflation and NPH insulin administered by SC route respectively. The study demonstrated that insulin loaded PLGA microcapsules administered via intratracheal insufflation had longer sustained insulin profile in serum than NPH insulin via SC route. Insulin loaded in PLGA microcapsules showed

a prolonged insulin release from PLGA microcapsules. However, reaching the blood circulation from PLGA microcapsules was slower than the SC route. Moreover, the safety study assessed by lung histology for insulin loaded PLGA microcapsules showed mild to moderate local irritation in rat lungs treated with insulin loaded PLGA microcapsules. This could point to a decline in pH in the lung caused by the degradation of PLGA (Hamishehkar et al., 2010b, Hamishehkar et al., 2010a)

1.10.2 Polyalkyl cyanoacrylates

Poly(alkyl cyanoacrylate) (PACA) is one of a biocompatible and biodegradable synthetic polymer that is degraded in biological fluids by an enzyme called esterases. It produces certain toxic products that excite or harm the central nervous system (CNS). Consequently, PACA is not further recommended for human use. Recently, and it has been utilized in the transportation of insulin through intestinal epithelium polymeric insulin carrier for oral administration (Damge et al., 1997) Graf, Rades & Hook reported a study of oral delivery of insulin loaded into poly(alkyl cyanoacrylate) (i.e., poly(ethyl cyanoacrylate)) based nanoparticles prepared by using microemulsion as templates for polymerization with poly(alkyl cyanoacrylate). The results demonstrated a consistent reduction in blood glucose level for up to 36 hours after intragastric administration (a reduction to 68% of the initial blood glucose level achieved at nine h and 30-40% of the initial blood glucose level maintained for up to 36 hours) in induced diabetic rats. This result showed a significant difference as compared to the insulin solution that is not entrapped in nanoparticles and dispersed in the microemulsion (Graf et al., 2009).

1.10.3 Polycaprolactone (PCL)

Poly (caprolactone) (PCL) undergoes ester hydrolysis in physiological conditions. It is applied in medicine in long-term implantable systems as the rate of biological degradation is slow. This polymer has sufficient permeability to various drugs, and low toxicity properties make PCL suitable for colloidal drug delivery.

Poly (ε-caprolactone) (PCL)/Collagen (COLL) was used to produce a potential wound care dressing and coated with chitosan nanoparticle, which were prepared by ionic gelation for insulin delivery by making a PCL/COLL (1:1 (w/w)) solution. This nanofibrous hybrid wound dressing studied for surface microstructure and wettability, polymeric mechanical properties, and microbe penetration. Prolonged delivery of insulin into the wound bed achieved. It can determine that the PCL/COLL/Cs-Ins had a positive effect on the wound-healing progression. In this study, the data presented that after 14 days, the wounds covered with PCL/COLL/Cs-Ins nanoparticles wound dressing could reach nearly full wound healing compared with the sterile gauze, which demonstrated nearly 45% of wound size reduction. These results suggest that fictional scaffolds can potentially be applied in clinical practice for wound treatment and insulin delivery (Ehterami et al., 2018).

1.10.4 Poly-γ-glutamic acid (γ-PGA)

Poly-gamma-glutamic acid (γ-PGA) is a high-molecular-weight polypeptide comprising g-linked glutamic acid units and alpha-carboxylate side chains produced by certain strains of *Bacillus subtilis* (model for gram positive bacteria). It has non-toxic, biodegradable, and non-immunogenic properties. Besides, PGA has anti-inflammatory and antiangiogenic properties. It is a biodegradable polymer super absorbent polymer.

Sonaje et al. studied the oral delivery of insulin by preparing insulin loaded γ-PGA nanoparticles. Freeze-dried red insulin nanoparticles were filled into hard gelatine capsules. The *in vivo* study compared between the blood glucose level of SC injection of insulin solution (5IU/ Kg) and oral administration of the freeze-dried insulin loaded nanoparticles (30 IU/ Kg) in the induced diabetic rats. The study concluded that γ-PGA oral formulations were not accompanied by hypoglycaemic effects. SC insulin showed a decrease in blood glucose levels by 75% in 2 h and returned to the basal levels at ten h. The maximum plasma concentration was achieved at one h after subcutaneous administration. In contrast, γ-PGA nanoparticles maintained reduced blood glucose levels (about 50% in 10 h) and the maximum plasma concentration was achieved five h after administration (Sonaje et al., 2010). To improve the oral bioavailability of insulin, Su et al. prepared insulin loaded pH-responsive nanoparticles using chitosan in conjugation with γ-PGA and diethylenetriamine pentaacetic acid (DTPA), which was used as a protease inhibitor. The enzyme inhibitory activity of the γ-PGA and DTPA conjugate was studied using the small intestine isolated from rats. The study demonstrated that the prepared nanoparticles prevented enzymatic degradation of insulin, with only 30% of insulin was degraded from the nanoparticles in 2 hours against 90% degradation from non-protected insulin. Moreover, the pharmacodynamic and pharmacokinetic results in rats showed that insulin solution (5 IU/ Kg) in the absence of nanoparticles had a significant reduction in the blood glucose level within 2-3 hours and achieved the maximum plasma concentration (101.5±6.2 µIU/mL) at one h after SC administration. In contrast, oral administration of γ-PGA insulin nanoparticles (30 IU/ Kg) showed a slow and prolonged reduction in blood glucose level for 10 hours and achieved a maximum insulin concentration (39.2±2.8 µIU/mL) at four h after oral administration. The area under the plasma concentration-time curve (0-10h) for insulin solution was 156.3±29.7 and 197.7±32.5 µIUh/mL for γ-PGA insulin

nanoparticles. The relative oral bioavailability of γ-PGA insulin nanoparticles was 19.7±1.3% (Su et al., 2012).

Lin et al., 2007 used chitosan (CS) in combination with poly (ϒ-glutamic acid) (ϒ -PGA) to prepare insulin nanoparticles through ionic gelation. CS formed the nanoparticles' outer shell, and thanks to the positive charge on its surface, the paracellular permeation of insulin across Caco-2 cells increased through transiently losing the tight junctions between the epithelial cells. The study also proved that the glucose level in a diabetic rat model reduced the oral administration of the CS nanoparticles (Lin et al., 2007). A similar approach was used in (Sonaje et al., 2012, Sonaje et al., 2010) studies, where CS and (ϒ -PGA) were used to prepare pH-sensitive nanoparticles. The biodistribution studies in rats revealed that the NPs remained in the stomach for a long time when administered orally. This study leaves insulin susceptible for degradation. Sonaje et al. utilized enteric-coated capsules to bypass the acidic conditions of the stomach. At high pH, the tablet released the insulin nanoparticles, and gel electrophoresis analysis showed that the release of insulin remained intact with no fragmentation or aggregation. The pharmacodynamics and pharmacokinetics studies demonstrated a prolonged hypoglycemic content to 10 hours (Sonaje et al., 2012, Sonaje et al., 2010). Similar findings were reported earlier in (Makhlof et al., 2011) studies, where CS nanoparticles of 250–400 nm size managed to extend the hypoglycemic effect in alloxan-induced diabetic rats over 15 hours. CS-NPs showed a relative pharmacological bioavailability of 14.9% compared to subcutaneous injections of insulin. Hydroxypropyl methylcellulose phthalate (HPMCP) was used together with CS to improve the pH sensitivity of CS-NPs by (Makhlof et al., 2011).

1.10.5 Alginate based polyurethanes

Alginate-polyurethane was investigated as a potential insulin carrier. Sodium alginate was combined with the chemically synthesized polyurethane at a 7:3 ratio to prepare the pH-sensitive polymer. The *in vitro* release outcomes demonstrated that the prepared nanoparticles protected insulin against the acidic conditions. Furthermore, the insulin nanoparticles managed to limit the glucose to its basal state after 13 hours of diabetic mice (Sosale et al., 2016).

1.11 Conclusion

Studies over past 100 years shows that many attempts have been made by researchers to improve insulin delivery, prolong its affect and different delivery routes have been optimised. The existing progress of insulin nanocarriers, smart-drug delivery systems (stimuli-responsive), pumps, nano sensors, micro and nano self-dissolving needles, liposome, and micelles are numbers of advancement in this area which are demonstrating a promising future. The use of nanoparticles (NPs) which allows for improved bioavailability, controlled release, and targeted drug delivery (TDD) of insulin is a long-time achievement by researchers. Investment in this area of research could lead to highly effective treatment methods.

Chapter 2

Synthesis of end functionalised sugar sensitive polyglycerol

2.1 End functionalised sugar sensitive polyglycerol

The World Health Organisation (WHO) marked diabetes as the seventh leading cause of death globally in 2016. In the last 100 years insulin has emerged as one of the major medications for diabetes. The use of polymers, enzymes, proteins, and synthetic phenylboronic acid derivatives (Scheme 2.1) have shown great potential as sugar sensors for the management of diabetes. Insulin formulations in a delivery system must respond to high glucose levels in the blood but also are improve the dose accuracy and accelerate therapeutic response time.
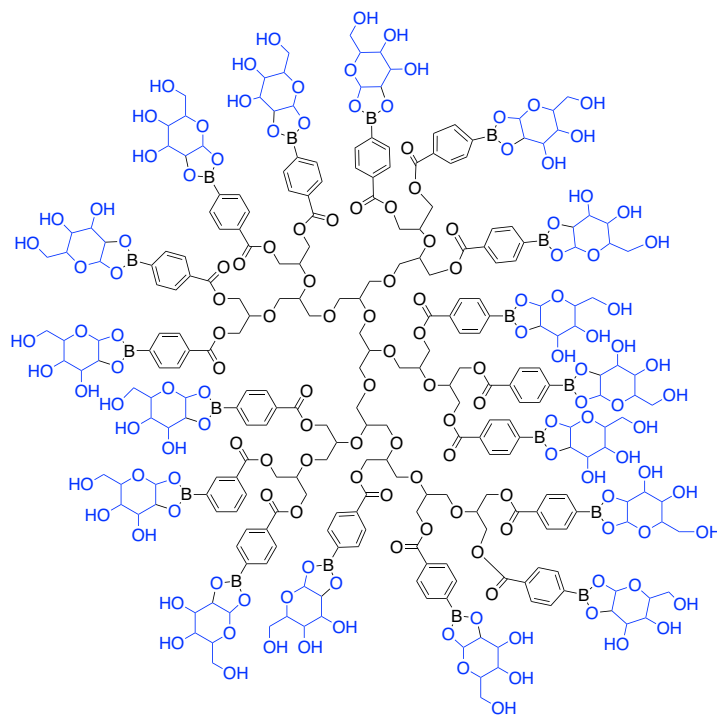
Scheme 2. 1 A depiction of polyglycerol phenylboronic acid sugar sensitive polymer, which shows sugar binding at the boronic acid end to the glucose molecules (blue).

Making such polymers called "smart insulin delivery systems" are, therefore, fascinating the scientists due to these unique properties, which are challenging but not impossible. Likewise, throughout the diabetes treatment, a milestone is expected; phenylboronic acid gives light to achieve such a system. Boronic acid

derivatives form a reversible covalent bond with glucose when it is dissolved in water (T.Aoki, 1996 , A. Matsumoto, 2012, Weith et al., 1970). They are amongst the most frequently used glucose-binding molecules used in technologies for blood glucose measurements.

The idea of a drug delivery system for diabetes treatment, which can work as a sugar sensor and release insulin when needed, has recently become the focus of many researchers (Li et al., 2019, Zhang et al., 2017, Brooks and Sumerlin, 2016, Zhou et al., 2015, Sugnaux and Klok, 2014, Maji et al., 2014, Ke Caoa, 2013).

One of the limitations of phenylboronic acid (PBA) is its poor water solubility. Using a hydrophilic, biocompatible polymer will facilitate the *in vivo* application of PBA. For this purpose, glycerol came out as a potential monomer candidate because its dimers and trimers are nontoxic, FDA approved, biocompatible and biodegradable.

2.1.1 Glycerol

Glycerol was first discovered in 1783 by the Swedish chemist Carl Wilhelm Scheele during his experiments on natural oils and alkaline materials. Scheele observed the formation of a liquid which he tasted, finding it very sweet in flavour. Scheele published his research results under the title ''Experiment about a special sugar material coming from squeezed oils and fats'' (Carl Wilhelm Scheele (1742–1786) (Lennartson, 2017). However, the discovery of ''Scheele's sweet'' had no impact on scientific research or industrial procedures for an extended period. The name ''glycerol'' was coined in 1811 by the chemist Michel Eugene Chevreul, who derived this name from the Greek word ''glykos'' which means sweet (Lennartson, 2017).

Glycerol is a nontoxic, edible, biodegradable compound. It is a convenient building block, and it is produced either produced by fat saponification or synthesised from propylene on an industrial scale. Glycerol assists various functions in the human

body, including being found in triglycerides and phospholipids, which are the main form of energy storage, and both are also essential elements of cell membranes. Glycerol has an oral median lethal dose (LD5$_0$) of 12 - 600 mg kg^{-1} in rats and is generally considered to be nontoxic. It is listed on the GRAS list by FDA as "generally regarded as safe." Glycerol is extensively used in pharmaceutical and cosmetic applications as an additive (e.g., a plasticiser, thickener, emollient, demulcent, humectant, bodying agent, lubricant) due to its physical characteristics. It is used in many drug delivery applications when polymerised. Glycerol polymers have gained recent attention due to their biocompatibility and ease of modification.

2.2.2 Polyglycerol

In our work, the hydrophilic highly functional polyglycerol structure was synthesized using glycidol and sulfuric acid (10%) (Carolina Ardila-Suárez, 2015). This polymer was further modified to increase lipophilicity using phthalic anhydride and end functional polymer with phenylboronic acid. The chemistry of polyether formation is significantly distinct from that of classical vinyl polymerization processes. Glycidol can undergo cationic polymerization via secondary and tertiary oxonium ion intermediate under acid catalysis as outlined in Scheme 2.2.

The ring-opening step in each case is nucleophilic substitution. When the stereochemistry was established, it showed that the carbon atom was undergoing nucleophilic attack. Epoxide polymerization can be described in three different mechanisms, such as anionic (base-catalyzed), cationic (acid-catalyzed), and

coordinate.
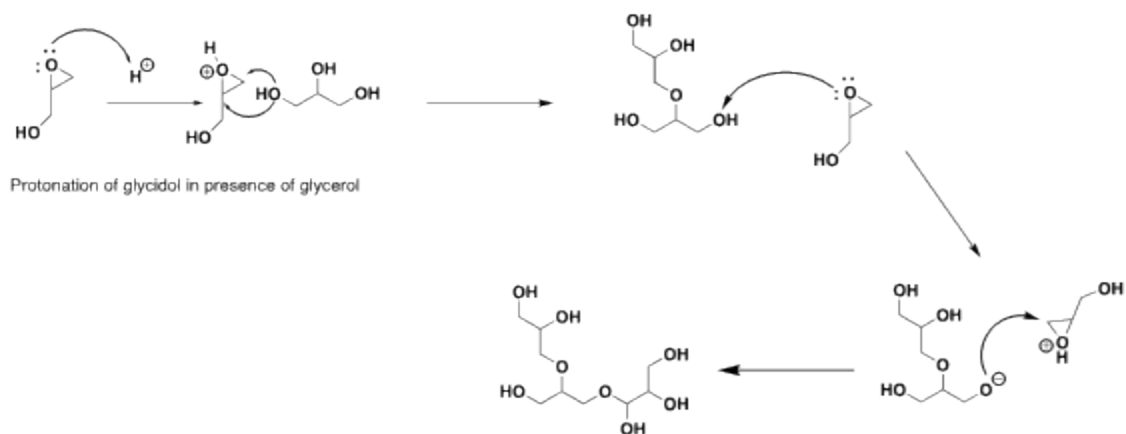
Scheme 2. 2 Cationic ring opening polymerization of glycidol by glycerol.

If the monomer itself, is a strong nucleophile, such as alkoxide ion, SN2 reaction takes place. However, when the epoxide is converted to an oxonium state, as in the cationic process, it becomes such a good "leaving" group that even the monomer's weakly nucleophilic oxygen can attack effectively (Su, 2013).

2.2 Aims and Objective of the polymerization

2.2.1 Aim

The design of a phenylboronic acid functionalised polymer with balanced hydrophilic and hydrophobic properties is described in this chapter. Polyglycerol was used as a matrix to synthesize a sugar-responsive water-soluble polymer that can potentially form micelles or nanoparticles to encapsulate insulin.

2.2.1 Objectives

- To develop an efficient approach to protect 4-carboxyphenylboronic acid (4-CPBA) as its pinacol ester prior to coupling.
- To synthesize of (2,2-dimethyl-1,3-dioxan-5-yl)methyl 4-(4,4,5,5-tetramethyl-1,3,2-dioxaborolan-2-yl)benzoate monomer.

4

- To Polymerize (2,2-dimethyl-1,3-dioxan-5-yl)methyl 4-(4,4,5,5-tetramethyl-1,3,2-dioxaborolan-2-yl)benzoate with *in situ* deprotection.

2.2.2 Materials

All chemicals were purchased and the purity of them were checked by NMR. Glycerol (propane-1,2,3-triol, Sigma), glycidol (2, 3-Epoxy-1-propanol, Sigma), 4-carboxyphenylboronic acid, 4-aminophenylboronicacid pinacol ester (4-(4,4,5,5-Tetramethyl-1,3,2-dioxaborolan-2-yl)pinacol ester, TCI chemicals), pentaerythritol (2, 2-Bis (hydroxymethyl)-1,3-propanediol from Sigma, sulfuric acid and coupling reagents DCC (*N,N'* Dicyclohexylcarbodiimide), 4-Dimethylaminopyridine (DMAP),) purchased from Sigma Aldrich; solvents were distilled or purchased as anhydrous in sealed bottles before use from Sigma.

2.3 Methods

Polymers were characterized with nuclear magnetic resonance spectroscopy (NMR), Fourier transform infrared spectroscopy (FTIR).

All polymerization reactions were carried out in a Schlenk flask sealed with septa and flushed with nitrogen gas (N_2) for 30 min. Some reactions were carried out in acidic solution, to minimize epoxide reactivity (oxidation) and used an ice bath at the start of the reaction for cooling. Solvents were either purchased anhydrous or distilled in the laboratory before use.

2.3.1 Nuclear Magnetic Resonance (NMR) Spectroscopy: ^{1}HNMR was recorded (400 MHz, CDCl$_3$) using standard parameter sets, on a Bruker Avance III 400MHz FT-NMR spectrometer equipped with a 5 mm PABBO BB-1H/D Z-GRD probe head. Using NMR, the chemical shift is reported in parts per million and referenced to the

solvent lock signal, a solvent such as d4-MeOH, d6-DMSO, D_2O, and $CDCl_3$ was used for NMR analysis. Also, the conversion of polyglycerol was measured gravimetrically by precipitation of polymer in cold acetone. Data were analysed using TopSpin (Bruker, Switzerland).

2.3.2 Mass spectrometry: Mass spectra were recorded with Waters LCT Premier (ES-ToF) / Acquity i-Class Ionisation mass spectrometry: Electrospray (ES), which provides low and high-resolution data in both positive and negative modes. Mass spectrometry was also carried out using Matrix assisted laser desorption/ ionization (MALDI). This method permits the generation of intact singly charged, high mass (m/z 103-104) ions of polar and non-polar samples. The ions generated by MALDI-TOF are calculated using the kinetic energy for characterization of polymers. The ion ranges are considered from 100 to 5000 and calculated using (E_{kin}= ½ m v^2). This method allows accurate determination of the monomer units. The mass spectra also confirmed the molecular weight of the polymer using number average equation 2.1 for the calculation. Equations 1 and 2 were used to analyse every peak in the MALDI-TOF spectrum to calculate the average molecular number and the average molecular weight, respectively.

$Mn = \Sigma niMi/\Sigma ni$

Equation 2. 1 Average molecular number of the polymer.

$M_w = \Sigma_{ni}M_i^2/\Sigma_{ni}M_i$

Equation 2.1 Average molecular weight of polymer.

n_i is the intensity of signals, M_i is the corresponding mass.

2.3.3 Fourier-transform infrared spectroscopy (FTIR): NICOLETiS5 (Thermos Scientific) FTIR was used to identify the functional groups of the synthetic polymers.

Each sample powder was placed in the instrument after the instrument was calibrated for a background collection.

2.4 Polymerization of glycerol and modification of polyglycerol for end functionalised sugar sensing

A general cationic ring-opening polymerization of glycerol and polyglycerol modification for end functionalised sugar sensing polymer was carried out. Solutions were left at room temperature overnight. Polymerizations were stopped by precipitating the polymer in cold acetone. Each polymer was modified in a separate step after analysis for end functionalisation. NMR and FTIR were carried out and the molecular average number (Mn) and molecular average weight (Mw) were measured using MALDI-TOF.

2.4.1 Synthesis of polyglycerol

Acid catalysed polymerization of glycerol as core unit and glycidol as initiator

Polymerisation of glycerol (7.3 mL, 0.1 mol) and glycidol (1,2-epoxypropane 6.6 mL, 0.1 mol) in sulfuric acid (50 mL), 10% was carried out in a Schlenk flask under nitrogen overnight at room temperature (although the reaction was in acidic solution but due to the reactivity of glycidol it was carried out under nitrogen).

The glycerol solution in acid was left stirring placed in an ice bath until fully mixed and then activated then carefully glycidol was added dropwise with a syringe pump over 3 hours, under nitrogen gas and stirring condition. The acid concentration was chosen in two ranges of (10%) and (50%) as previously reported by (C.Ma´rquez-Alvarez, 2004) that it affects the molecular weight of the polymer. The polymer solution was neutralised with NaOH 1 M to pH 7 then precipitated in acetone, for further refinement, the polymer was dissolved in methanol and precipitated in acetone, dried overnight under vacuum at room temperature. Although the

reaction was in acidic solution but due to the reactivity of glycidol it was filtered off and the filtrate evaporated down under vacuum. The remainder is taken up in CH_2Cl_2 and, filtered free of any further precipitated urea. The CH_2Cl_2 solution is washed 3x with HCl 2 M and the aqueous phase is precipitated in cold acetone. The ester isolates by precipitation, crystalline products can be obtained in pure form acetone after drying under vacuum modified from the method used by Hutton et al,. (A.Hutton, 2004).
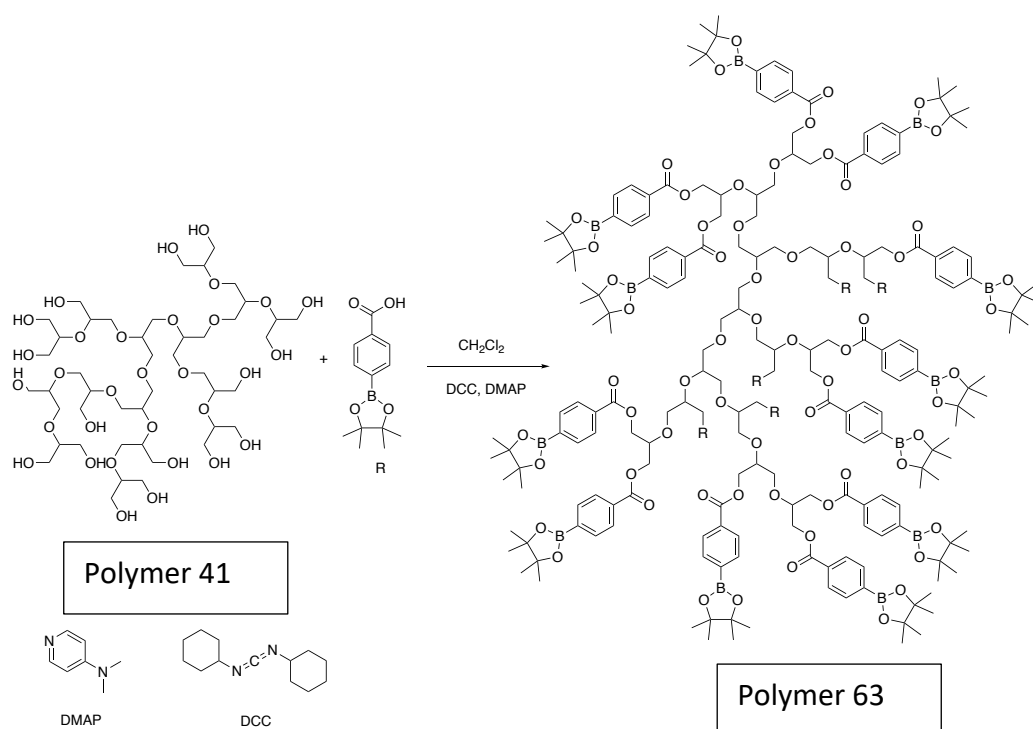
Scheme 2. 3 Steglich reaction, using polyglycerol, 4-carboxyphenylboronicacid pinacol ester, DCC and DMAP as catalyst.

The Steglich esterification is a well-known mild reaction that allows for the transformation of sterically demanding and acid-labile substrates. In the esterification mechanism, the DCC (dicyclohexylcarbodiimide) and the carboxylic acid can form an O-acylisourea intermediate, which has reactivity like the corresponding carboxylic acid anhydride (Scheme 2.4). Therefore, in the reaction

with phthalic anhydride, the DCC or DCI is not used as the anhydride has a similar function.

1- Proton transfer activation of C=N bond

2- Nu attack

3- formation of O-acylisourea

4- pyridine attck on carbonyl

8- ester formation and leaving of pyriding as catalyst

7- aclohol attck acyl dimethyl pyridinium ion

6- formation of urea as by product

5- formation of tetrahedral intermediate

acyl pyridinium ion resonance structure
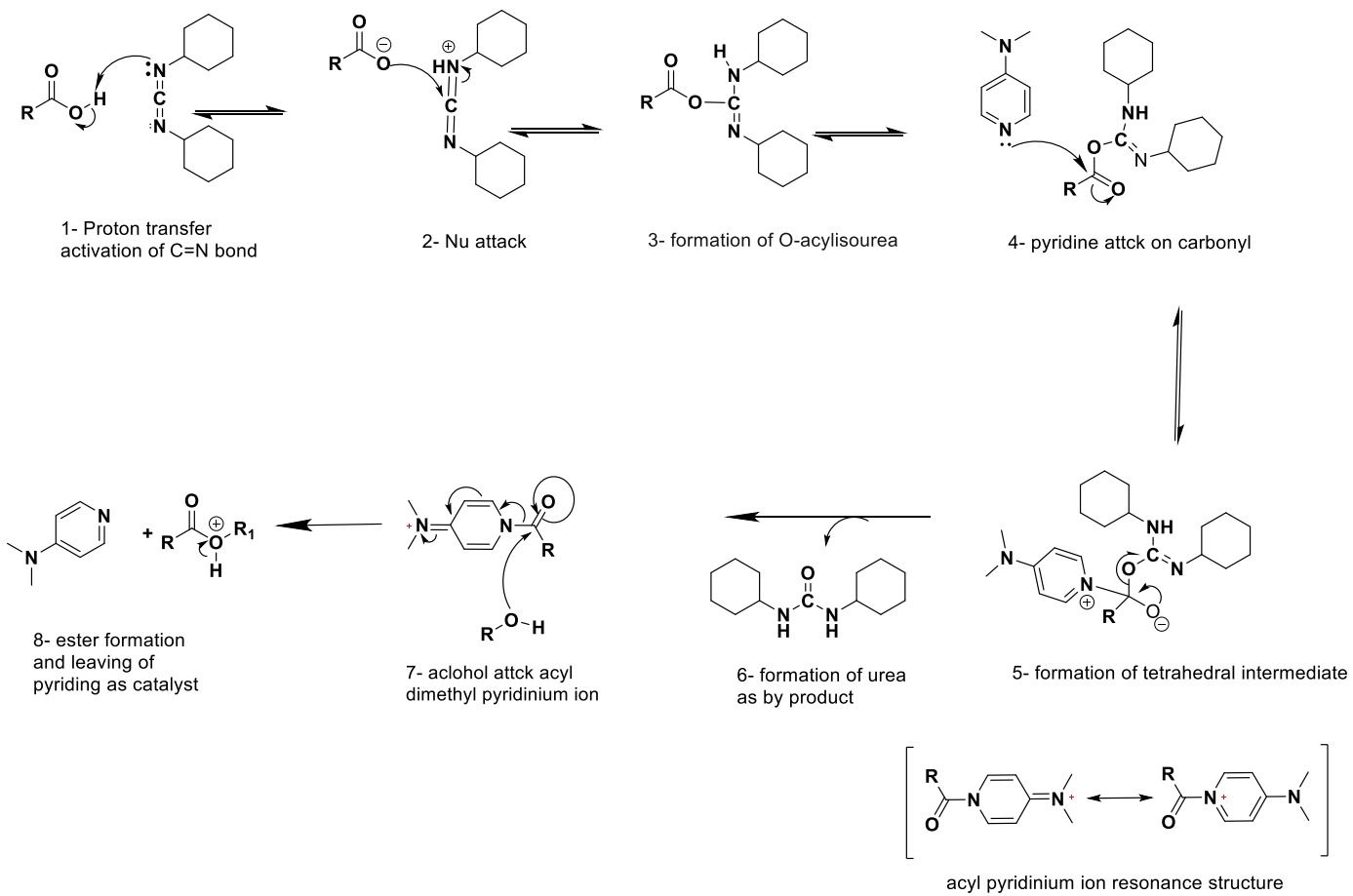
Scheme 2. 4 Reaction of phenylboronicacid with polyglycerol catalysed by DMAP.

The second step the alcohol may now add to the activated carboxylic acid to form the stable dicyclohexylurea (DHU) and the ester.

The mechanism of reaction is that DCC (dicyclohexylcarbodiimide) and the carboxylic acid can form an O-acylisourea intermediate, which offers reactivity the corresponding carboxylic acid anhydride. DMAP function as a catalyst is explained that it is a stronger nucleophile than the alcohol (Scheme 2.4) in which reacts with the O-acylisourea leading to a reactive O-asylpyredinuium ion. This intermediate cannot form intramolecular side products but reacts rapidly with alcohol. DMAP acts as an acyl transfer reagent in this way, and subsequent reaction with the alcohol gives the ester.

2.4.2 Carboxylic acid formation of boronic acid end functionalised polyglycerol

To a polyglycerol (6.76 g, 6.96 mmol), 3-carboxyphenylboronic acid (4.01 g, 24.17 mmol) was added, DMAP was added catalytic amount (0.50 g, 4.0 mmol) and coupling reagent EDC.HCl was added (0.4 g, 2.46 mmol). In dioxane and water (80: 20) due to water solubility of polyglycerol for 48 h. The polymer (167) was precipitated in cold diethyl ether and left to dry under vacuum. NMR, FTIR and MALDI TOF was carried out (Scheme 2.5 polymer 167).

Polymer 41

Polymer 167

DMAP, EDC-HCl , Dioxane

R =
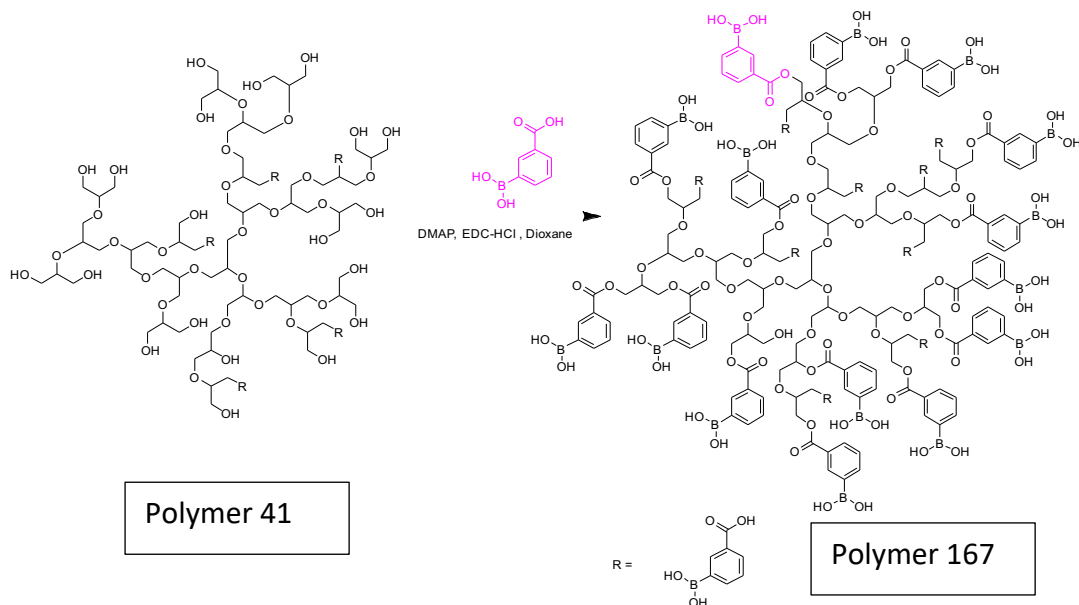
Scheme 2. 5 Ester bond formation of polyglycerol and carboxyphenylboronic acid using dioxane, DMAP and EDC to synthesis of polyglycerolester of phenylbornic acid.

2.4.3 Deprotection of pinacol from polyglycerol phenylboronic acid pinacol ester

To achieve a sugar sensitive property, the boronic acid end functional group must be deprotected. The deprotection procedure of modified polyglycerol with phenylboronic acid was carried out using different established litrature methods. The system comprised of water and hexane (1:1), table 2.1 summaries all the deprotection attempts and condition in which the reactions were carried out. A solid-phase process containing polystyrene boronic acid used for polyglycerol transesterification phenylboronic acid pinacol ester was used. Polystyrene suported resin in presence of 2 mL trifluoroacetic acid (TFA) and 13 mL acetonitrile (ACN) under the nitrogen gas left for 24 hours (Hutton. A, 2004). Amberlyst® 15 which is a strong acidic resin was also used for deprotection in methanol. The other deprotection method used is diethanolamine in ether. The deprotection of modified polyglycerol with 4-carboxyphenylboronic acid, with diethanolamine (DEA) to form

an sp3-hybridized boron is a two-step procedure for deprotection of alkylpinacolyl boronate esters via transesterification with diethanolamine $HN(CH_2CH_2OH)_2$ followed by hydrolysis using 0.1, 1 M HCl and acid adjusted to pH 3, in presence of ether and nitrogen was carried out (Sun et al., 2011). To confirm the full removal of diethanolamine from the reaction mix and product, a short test was carried out by forming a salt of diethanolamine was formed with TMS chloride and methanol. To a 10 mL methanol, 1 mol (105.14 $gmol^{-1}$) of diethanolamine and 2 mol (216.29 $gmol^{-1}$) TMS chloride was used to form the salt.

Deprotection was carried out using Amberlyst which is a sulfonic acid containing resin. In addition, the last attempt was made to deprotect pinacol was transesterification with phenylboronic acid using a biphasic system, which takes advantage of the solubility differences of starting material polyglycerol phenylboronic acid pinacol ester in an aqueous environment and phenylboronic acid in hexane.

Table 2. 1 attempts of deprotection methods

Polymer ID	Deprotection of pinacol	Solvent and reagents	PG-4-PBAPE	Deprotecting agent	Time	Outcome
63	polystyrene supported phenylboronic acid (PBA) resin	ACN: TFA (1: 0.15), 0.1 M HCl	polyglycerol modified with 4-carboxyphenylboronic acid pinacol ester(10 mmol)	polystyrene supported phenylboronic acid (PBA) resin (1.8 mmol with 10 mmol active sides)	24 h	☒
63 d	polystyrene supported phenylboronic acid (PBA) resin	ACN: TFA (1:3), 1M TFA	polyglycerol modified with 4-carboxyphenylboronic acid pinacol ester(10 mmol)	polystyrene supported phenylboronic acid (PBA) resin (1.8 mmol with 10 mmol active sides)	24h	☒
63 a	polystyrene supported phenylboronic acid (PBA) resin	Methanol: TFA (1: 0.15)	polyglycerol modified with 4-carboxyphenylboronic acid pinacol ester(10 mmol)	polystyrene supported phenylboronic acid (PBA) resin (1.8 mmol with 10 mmol active sides)	24	☒
94	Deprotection using diethanolamine	Diethyl ether	polyglycerol modified with 4-carboxyphenylboronic acid pinacol ester, 1g (1.7 mmol) in ether diethanolamine (0.5 g 5 mmol)	Diethanolamine $HN(CH_2CH_2OH)_2$, 1.0 mmol, 0.1 M HCl wash	20 min	☒
98	Deprotection using diethanolamine	Diethyl ether	polyglycerol modified with 4-carboxyphenylboronic acid pinacol ester, 1g (1.7 mmol) in ether	$HN(CH_2CH_2OH)_2$ 5 mmol (excess) 1 M HCl wash	1 h	☒

			diethanolamine (0.5 g 5 mmol)			
103	Deprotection using diethanolamine	Diethyl ether	polyglycerol modified with 4-carboxyphenylboronic acid pinacol ester, 1g (1.7 mmol) in ether diethanolamine (0.5 g 5 mmol)	$HN(CH_2CH_2OH)_2$, 1.1 mmol, 1 M HCl wash	24 h	☒
156	Amberlyst® 15 0.5 g (ion exchange resin with a strongly acidic sulfonic group)	Methanol	(Polyglycerol phenylboronic acid pinacol ester 0.5 g)	Amberlyst® 15	24 h	☒
158	Biphasic solvent system DI water and hexane	Hexane: water (1:1)	(Polyglycerol phenylboronic acid pinacol ester 1 g),	benzeneboronic acid	24 h	☒
158	Biphasic solvent system HCl and hexane	Hexane : HCl (1:1) (1 mM)	(Polyglycerol phenylboronic acid pinacol ester 1 g),	benzeneboronic acid	24 h	☒
151	Biphasic solvent system HCl and hexane	Hexane: HCl, (1:1) (1M HCl adjusted to pH 3)	(Polyglycerol phenylboronic acid pinacol ester 1 g),	benzeneboronic acid	24h	☑

Deprotection was obtained from polymer 151 at 24 h using biphasic system Hexane: HCl, (1:1) (1M HCl adjusted to pH 3).

2.4.4 Carboxylic acid formation from polyglycerol

Polyglycerol is water soluble polymer and in order to modify this and decrease the water solubility succinic anhydride was used to get terminal carboxylic acid group to modify with amino phenyl boronic acid. The water solubility reduction was not improved therefore phthalic anhydride was used in a separate reaction in order to increase lipophilicity.

Carboxylic acid formation of polyglycerol (PG) was following the procedure by S. Xu et al (Xu S, 2005), where 4-Dimethylaminopyridine (DMAP) catalysed acetylation of alcohols was carried out in the presence of acetic anhydride. The difference is that in this study succinic anhydride was used and polyglycerol was used as the alcohol. DMAP was the catalyst, triethylamine (TEA) (base) and dichloromethane used as the solvent (Scheme 2.6).
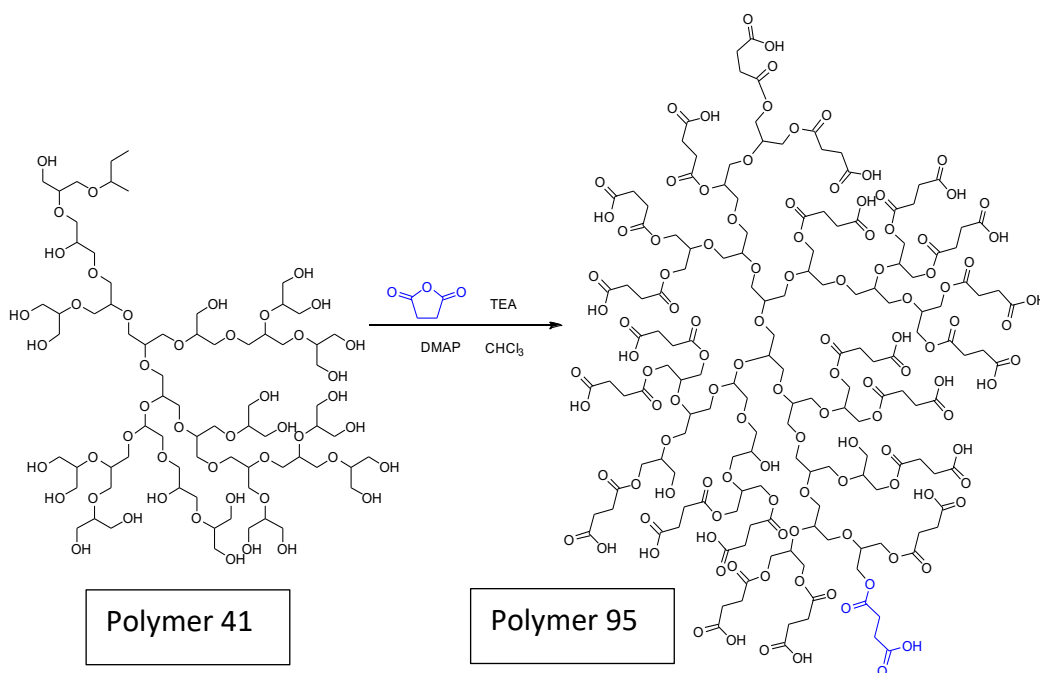
Scheme 2. 6 Carboxylic acid formation from polyglycerol (PG) .

Polyglycerol (PG) (2 g, 2191.24 g mol^{-1}) and succinic anhydride (0.91 g, 100.07 gmol^{-1}) was added to a 250 mL Schlenk flask equipped with a magnetic stirrer on a Schlenk line. After that DMAP (2.4 g. 2% catalytic amount) was added to the flask and cooled

under an ice bath whilst stirring under nitrogen. Then after 30 minutes dichloromethane (100 mL) was slowly added and then triethylamine (50 mL) was added to the solution. The reaction was left over night for 24 hours at room temperature. In another attempt Polyglycerol (2148 g mol^{-1}, 96 g) was added to anhydrous dichloromethane (100 mL DCM) under nitrogen, succinic anhydride (110.07 g mol^{-1}, 46 mg) was dried under vacuum overnight. Triethylamine (10119 g mol^{-1}, 45 mg, density = 0.73 g cm^{-3}), and DMAP (122.17 g mol^{-1}, 6 g) DMAP was added in the stoichiometric ration of polyglycerol: succinic anhydride: triethylamine: DMAP (1: 0.1: 0.1: 0.01) was added. The reaction was left stirring under nitrogen for 18 hours; proton NMR was carried out. The reaction was stopped with 30 mL of 2 mM HCl, DMAP was washed with HCl, and the sample was left on a rotary evaporator, then the polymer was precipitated in cold acetone and dried under vacuum as per the study by S. Xu et al (Xu S, 2005).

Hydrochloric acid (1M) was then added dropwise to neutralise the solution, the solution was then put on a rotary evaporator after removal of solvent, the compound was washed with cold acetone. Subsequently, the solution (aqueous) was put in a freeze drier for 4 days white powder obtained. Several attempts were carried out using for the reaction of polyglycerol and anhydride formation of terminal carboxylic acid using (succinic anhydride) and (phthalic anhydride).

This experiment was carried out to obtain functionalised polymer with terminal carboxylic acid. Further reaction (157) is with 3-carboxyphenylboronic acid final formation of ester bond. Dioxane was distilled under metallic sodium and benzophenone at 60   °C. To the fresh distilled dioxane polyglycerol (0.01 mol, 3488.62 gmol$^{-1,}$ 3.49 g) was added and stirred under nitrogen. Phthalic anhydride (0.5 mol) was added to the solution of polyglycerol, and dioxane. DMAP (0.01 mmol, 1.2 mg) was added, and the reaction mixture was heated under reflux for 6 hours and dried over night at room temperature (5.7 g compound obtained).

The solvent was evaporated the reaction was stopped using 2 mM HCl and washed with DCM, dried under vacuum confirmed by NMR and FTIR (results) by appearance of new carboxylic acid and carbonyl peak.

2.4.5 Carboxylic acid formation of polyglycerol (HMW)

Synthesis of terminal carboxylic acid group using phthalic anhydride from polyglycerol. Dioxane was distilled under metallic sodium and benzophenone at 60 °C. To the fresh distilled dioxane polyglycerol (sample 39.1) (0.01 mol, 3488.62 gmol^{-1}) was added and stirred under nitrogen. Phthalic anhydride (0.5 mol) was added to the solution of polyglycerol, and dioxane. DMAP (0.01 mmol) was added and the reaction mixture was heated under reflux for 6 hours and left-over night at room temperature (polymer 157).

The solvent was evaporated the reaction was stopped using 2 M HCl and washed with DCM, dried under vacuum confirmed by NMR and FTIR by appearance of new carboxylic acid and carbonyl peak (Scheme 2.7).

Polymer 39

DMAP, Dioxane

Polymer 147
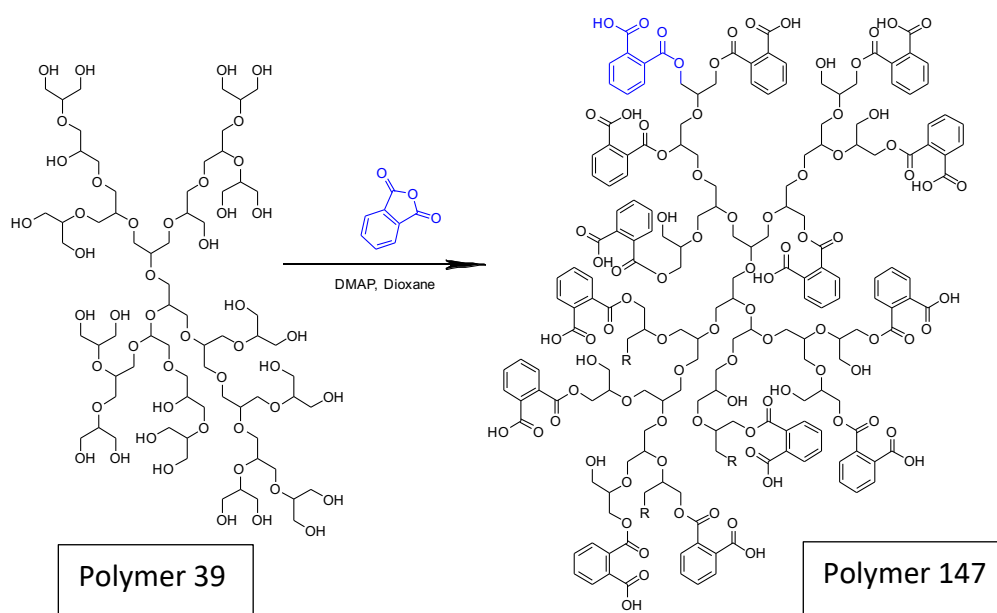
Scheme 2. 7 Carboxylic acid formation of polyglycerol (HMW)using Dioxane and DMAP, synthesis of terminal carboxylic acid group using phthalic anhydride.

2.4.6 Polyglycerol carboxylic acid phthalic anhydride reaction with 3-aminophenylboronic acid

Polymer (147) polyglycerol phthalic anhydride (1.69 g, 10 mol, 1692.57 g mol^{-1}) was added into 50 mL DCM, 3-amniophenylboronic acid monohydrate (1.55 g, 100 mmol) was added in presence of (1.92 g, 0.5 mol) 1-(3-Dimethylaminopropyl)-3-

ethylcarbodiimide hydrochloride (EDCI.HCl) coupling reagent for amide bond formation. Polyglycerol phthalic anhydride was stirred in DMC and 3-aminophenylabornic acid was added while stirring then EDCI.HCl was added, and the reaction was left stirring over night at room temperature. The compound was stopped with water and extracted with DCM, dried over Na₂SO₄ and after removal of solvent under rotary evaporator it was dried in vacuum (polymer 160, scheme 2.8).
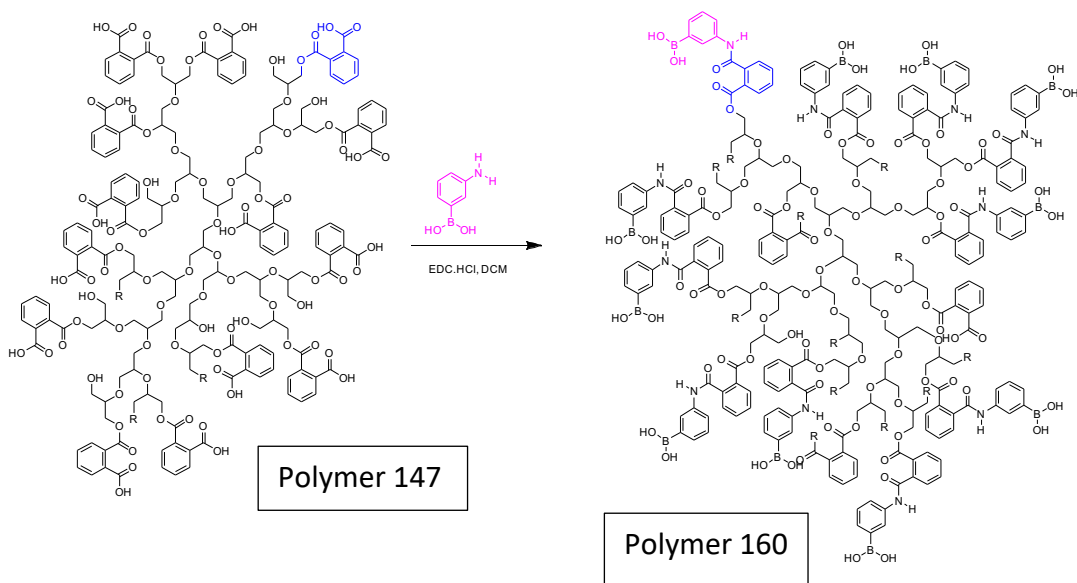
Scheme 2. 8 Amide formation using EDCI.HCl coupling reagent for addition of 3-aminophenylboronic acid from polyglycerol modified with phthalic anhydride.

2.5 Synthesis of novel monomer (2,2-dimethyl-1,3-dioxolan-4-yl)methyl 4-(4,4,5-trimethyl-1,3,2-dioxaborolan-2-yl)benzoate

2.5.1 End functionalized glycerol monomer for polymerization

4-Carboxyphenylboronic acid pinacol ester (4.96 g, 1 mol) and 1 DL-1,2-isopropylideneglycerol (10.57 mL, 4.0 mol) were weighed and added to a Schlenk flask under nitrogen stirred for 30 min. After catalyst, DMAP (dimethylamino pyridine) (1.22 g, 0.50 mol) was added with 1-ethyl 3-(3-dimethyl aminopropyl) carbodiimide hydrochloride (1.92 g, 0.5 mol). The reaction was left under reflux for 3 hours at 60 ºC and 18 hours at room temperature. TLC was performed using

petroleum ether and ethyl acetate (4:1) for checking the presence of starting material. NMR, GCMS, and FTIR confirmed the product formation (Xu et al., 2005).

.
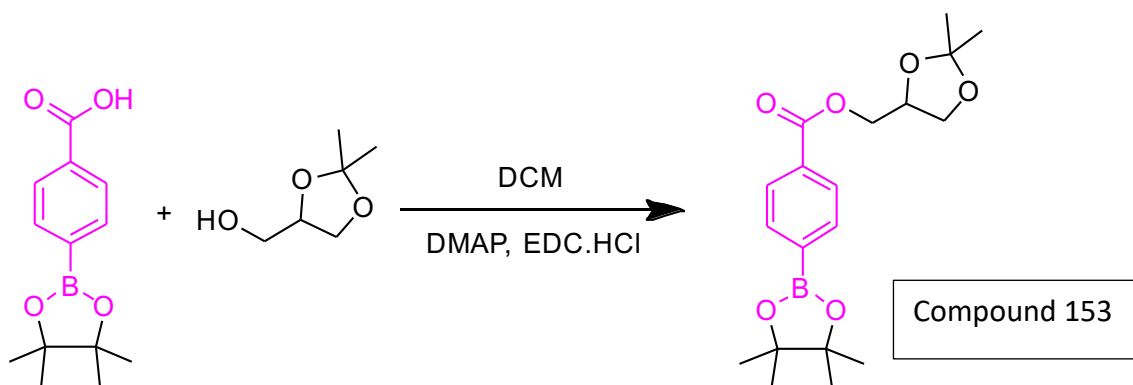
Scheme 2. 9 reaction of 4-carboxyphenylboronic acid with DL-1,2-isopropylideneglycerol.

Table 2. 2 Attempts for preparation of DL-1,2-isopropylideneglycerol with 4-carboxyphenylboronic acid pinacol ester

Reaction ID	DL-1,2-Isopropyliden eglycerol	4-CPBAPE	Coupling reagent	DMAP	Solvent	Success
	Mmol	mmol	mmol	mmol	mL	
127	2	2	DCC (2 mmol)	0.01	CH_2Cl_2	☒
135	4	4	DCC (2 mmol)	0.02	Dry CH_2Cl_2 under nitrogen	☒
137	4	4	EDC.HCl (4 mmol)	0.03	THF: water (9:1)	☒
139	1	1	Triphenylphosphine (1mmol)	0	$CHCl_3$	☒
142	50	10	EDC.HCl (2.6mmol)	0.16	DMF	☒
143	25	5	EDC.HCl (0.4mmol)	0.2	Excess of DL-1,2-Isopropylideneglycerol	☒
146	20	5	EDC.HCl (0.2 mmol)	0.2	Dry CH_2Cl_2	☑
153	1	4	EDC.HCl (10 mmol)	10	Dry CH_2Cl_2	☑

Mechanism of EDCl.HCl is removed was repeating

These experiments were carried out to synthesis a novel compound (Monomer) for polymerisation of polyglycerol by acid deprotection of isopropyl from glycerol group. Polymer 153 confirmed the formation of product confirmed by NMR, GC-MS and FTIR (result). Polymerisation of Isopropyl glycerol carboxylic acid pinacol ester was carried out successfully.

The solvents were evaporated, and the reaction was quenched with 2 M HCl to remove the DMAP. The sample was extracted from DCM, the DCM was then washed 3 times with 2 mM HCl. The organic layer was then dried over magnesium sulphate (MgSO$_4$) and the solvent was removed under reduced pressure. NMR of crude sample was obtained; therefore, the impurities were removed by washing with saturated solution of NaHCO$_3$, ^{1}H, and ^{13}CNMR was performed. The analysis by NMR confirmed formation of the product with presence of starting material, which was then followed by further wash up of the starting material with a base.
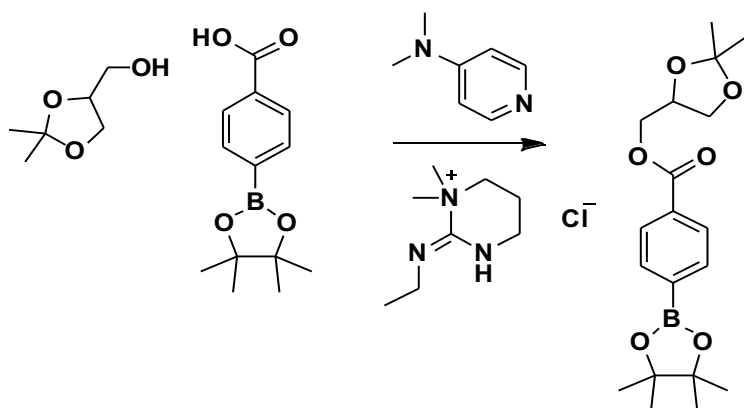
Scheme 2. 10 Synthesis of (2,2-dimethyl-1,3-dioxolan-4-yl)methyl 4-(4,4,5,5-tetramethyl-1,3,2-dioxaborolan-2-yl)benzoate using DMAP, EDC.HCl.

The reaction was successfully completed, and the desired product was obtained confirmed and GC-MS (giving a peak of m/z = 347 g mol^{-1}), (1.4 g, 50 %) mp =108.

1- Proton transfer activation of C=N bond

2- Nu attack

3- formation of O-acylisourea

4- pyridine attck on carbonyl

Proton abstract

5- formation of tetrahedral intermediate

8- ester formation and leaving of pyriding as catalyst

7- aclohol attck acyl dimethyl pyridinium ion

6- formation of urea as by product (salt)

acyl pyridinium ion resonance structure
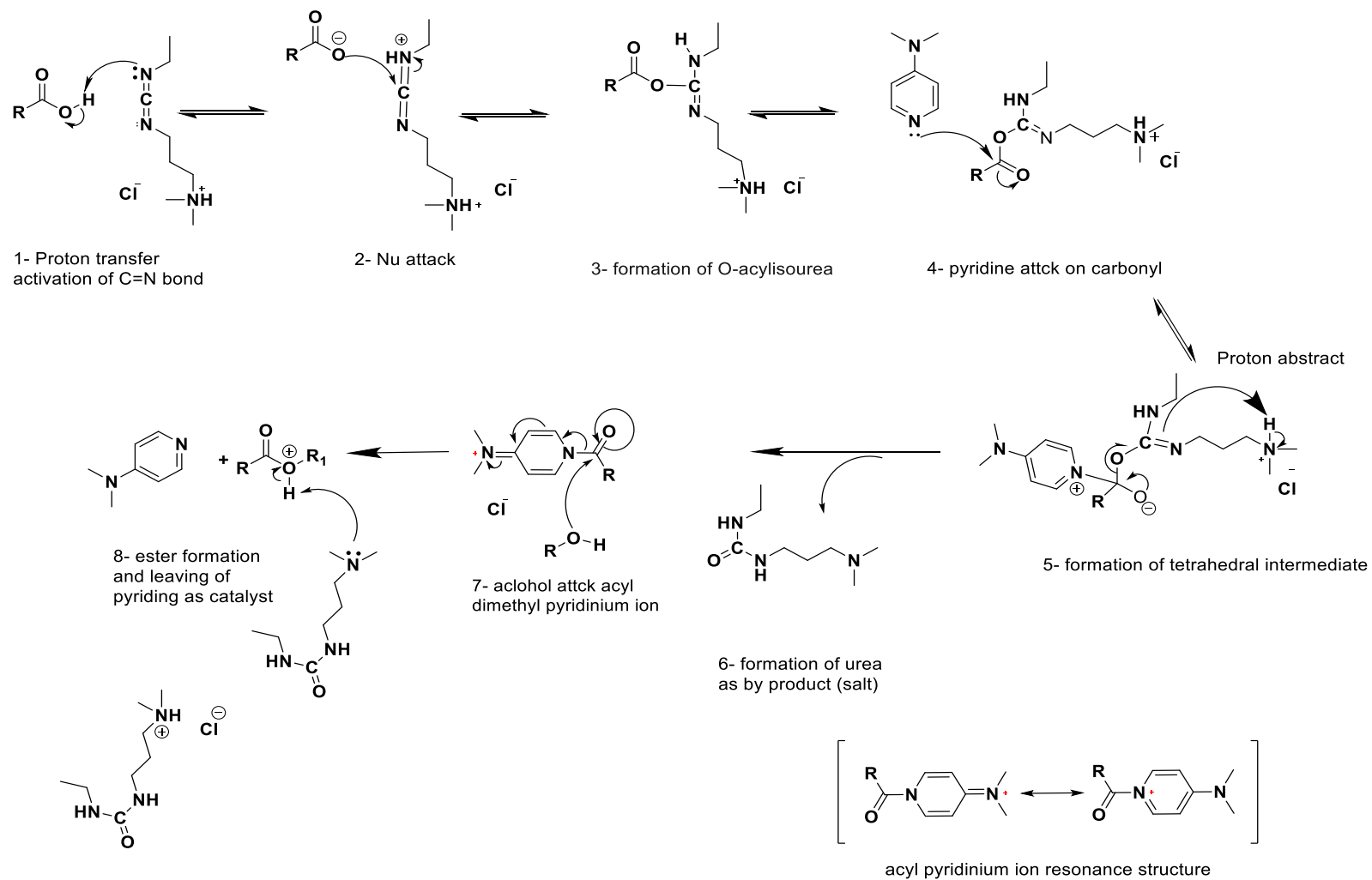
Scheme 2. 11 Ionization of EDC.HCl in aqueous solution. The structure of 1-ethyl-3-(3-dimethylaminopropyl) carbodiimide hydrochloric acid EDC.HCl. Once in aqueous media it ionizes in cyclic form and the reaction of EDC.HCl forming urea.

23

2.6 Polymerisation of (2,2-dimethyl-1,3-dioxolan-4-yl)methyl 4-(4,4,5-trimethyl-1,3,2-dioxaborolan-2-yl)benzoate

2.6.1 Polymerization in presence of glycerol and glycidol

These experiments were carried out to synthesis novel compound for polymerisation of polyglycerol by acid deprotection of isopropyl from glycerol group. Sample153 confirm the formation of the product confirmed by NMR, GC-MS and FTIR. The polymerisation of Isopropyl glycerol carboxylic acid pinacol ester was carried out successfully.
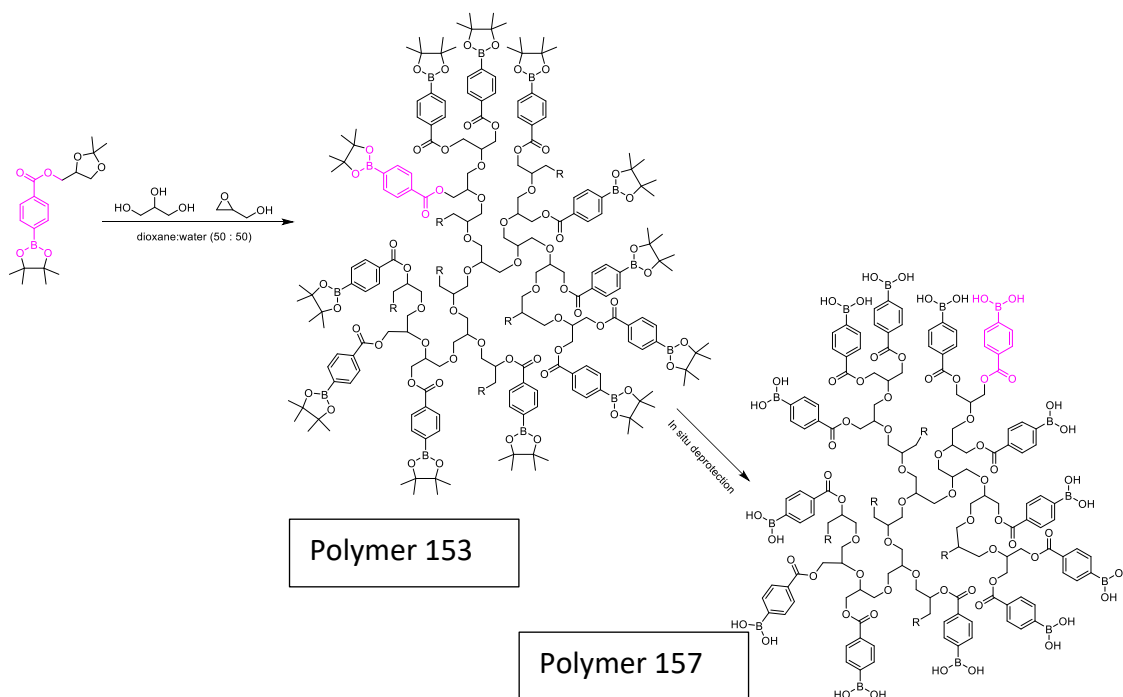
Scheme 2. 12 polymerisation of DL-1,2-Isopropylideneglycerol 4-carboxyphenylboronic acid pinacol ester with glycerol and glycidol deprotection happening In situ.

4-Carboxyphenylboronic acid pinacol ester (153) (347 mg, 1mol) was weighed and added to a 50:50 dioxane sulfuric acid (10 %) solution and left for 30 min to a round bottomed flask stirred for 30 min, slowly glycerol (92 mg , 1 mol) was added

and afterwards glycidol (222.12 mL, 3 mol) was added dropwise with pump under ice bath. The reaction was then left at room temperature.

2.7 Efficient methods for pinacol protection of boronic acid

1 - Pinacol was protected (Qiu D, 2012) by adding 0.54 g (3.25 mmol) 3-carboxyphenylboronic acid and 0.68 g (5.04 mmol) pinacol (1:1.75) in chloroform, stirred for 72 h, most of the boronic acid dissolved in the solvent after 4 h, water droplets formed. The reaction mixture was poured into a separating funnel, and the lower layer extracted and dried over Na_2SO_4, filtered evaporated, and the pure compound was obtained, but an excess of pinacol was visible in NMR. For recrystallization, the crude compound was dissolved in hot ethyl acetate and placed on an ice bath for crystals to form. Once the crystals wholly formed, the liquid solution carefully removed using a glass pipette.
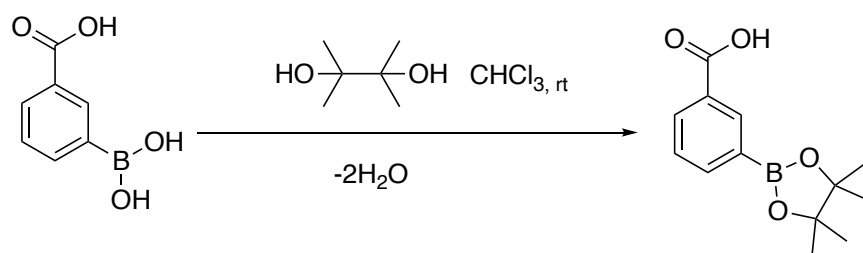
Scheme 2. 13 synthesis of 3-carboxyphenylboronic acid pinacol ester (3-CPBAE) using chloroform.

2 - A household microwave was used to activate 3Å molecular sieves were activated by the microwave (Toshiba ER-7620 650W) 3 x 2 min medium power (Villemin, 1991). Molecular sieves 8 g were stirred for 72 hours with 3-ACPBA 0.5 g (0.03 mmol), pinacol 0.46 g (3.95 mmol) (1:1.3) ratio under nitrogen, dichloromethane (DCM), and 3-carboxyphenylboronic acid (3-ACPBA) solution placed on a magnetic stirrer. The suspension was then filtered, and extracted from the chloroform. Therefore, the solution was dried more by the addition of Na_2SO_4. The solution was then re-filtered into a round bottom flask and dried under the vacuum. For recrystallization, the crude compound dissolved in hot ethyl acetate and placed on

an ice bath for crystals to form. Once the crystals completely formed, the liquid solution was carefully removed using a glass pipette. Proton and carbon NMR spectra of the product were obtained before and after crystallization. IR was also obtained after crystallisation and the melting point (mp) of the product was determined (François D'Hooge 2008) (see results section).

3 - 3Å molecular sieves were activated by microwave (Toshiba ER-7620 650W) 3 x 2 min medium power, 3-CPBA 1.66 g (10 mmol), pinacol 1.12 g (9.5 mmol) (1:0.95) equivalent, and 20 mL chloroform in a 50 mL Schlenk flask under nitrogen were stirred with approximately 4 g activated molecular sieves for 24 h on a magnetic stirrer. The solution was then dried under the vacuum. The proton and carbon NMRs obtained were clean, therefore, recrystallisation was not required (Table2.3).

Table 2. 3 Experiments are showing the ratio, time, amount of solvent, giving a yield of 97 %.

Entry	Ratio of CPBA: pinacol	Time (h)	CHCl$_3$ (mL)	CPBA (mmol)	Pinacol (mmol)	Theoretical yield (g)	Actual yield (g)	Yield %
1a	1:1	4	20	10	10	2.48	0.56	23
2a	1:1.3	24	60	12	16	2.98	1.64	55
3a	1:1.1	24	60	12	13	2.98	1.98	66
4a	1:1.3	48	60	12	16	2.98	2.07	70
5a	1:1.1	72	60	12	13	2.98	2.20	74
6a	1:0.9	24	60	12	11	2.73	2.27	83
7b	1:0.95	24	20	10	9.5	2.49	2.27	91
8b	1:0.95	24	20	10	9.5	2.35	2.24	95
9b	1:0.95	24	20	10	9.5	2.36	2.29	97

Note: a ~ 8 g and b~ 4 g of molecular sieves were used. MP for all compounds confirmed (241 – 243)

The yield of the product with a different time, the volume of the solvent, and the ratio of (1: 0.95) pinacol to carboxyphenylboronic acid presented a promising modification. The formation of carboxyphenylboronic acid pinacol ester performed via simple dehydration reaction between 3-carboxyphenylboronic acid and pinacol. The protection of boronic acid with pinacol is the most popular method. The formation of pinacol ester gives the molecule stability and reactivity that it requires and also provided ease of preparation compared to other boronic acid esters. If needed, the boronic acid ester can simply be deprotected after polymerization with either glycerol or via RAFT polymerization.

2.8 Synthesis of additional monomers

(Z)-2-(3-(4,4,5,5-tetramethyl-1,3,2-dioxaborolan-2yl) phenyl carbamoyl) acrylic acid

Acylation of aminophenylboronic acid pinacol ester (ortho, meta and para) was carried out using maleic anhydride (89 mg, 0.912 mmol). To the maleic anhydride amino phenylboronic solution acid pinacol ester (200 mg, 0.912 mmol) in 20 mL of dry CH_2Cl_2 was added. The resulting compound was stirred, under nitrogen, for 12 h. The reaction mixture was concentrated under vacuum using a rotary evaporator, the product obtained, yield (82.1 mg, 28 %) after precipitation in hexane (Andrea Temperini 2009). The outcome showed traces of starting material. This compound is not soluble in hexane. Therefore, by precipitating the compound in hexane twice, a pure compound is obtained. This can be used as a derivative of carboxy methyl chitosan (Weith et al., 1970) for nanoparticle formation and insulin incorporation.
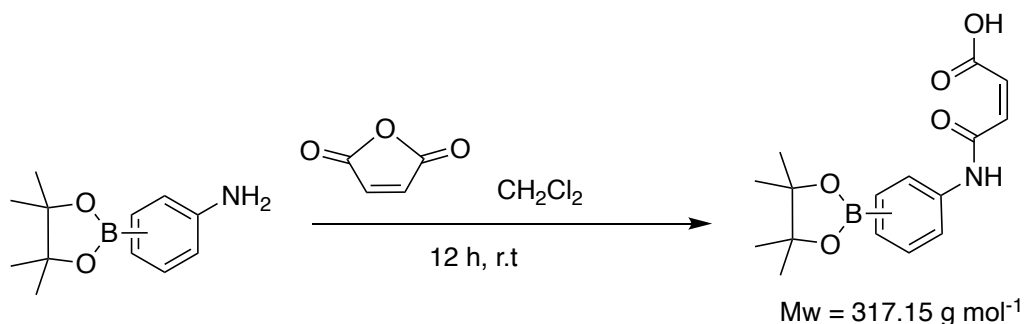
Scheme 2. 14 Formation of (Z)-x-3-(4,4,5,5 Tetramethyl-1,3,2dioxaborolan 2yl) phenylcarbamoyl) acrylic acid (x = ortho , meta para).

The same condition were used for all three substituted monomers (Andrea Temperini 2009). In the analysis of the binding of various sugars and other polyols, it has become apparent that the most critical factor is the availability in the polyol of a glycol group containing the required configuration and conformation. Upon binding these monomers with the amine group of chitosan, it can be possible to form nanoparticles followed by deprotection and study of the sugar-binding property, which is already established in the research group (Weith et al., 1970).

2.9 Results and discussion

2.9.1 Acid catalysed polymerization of glycerol and glycidol

Polymerization of glycerol and glycidol in sulfuric acid was carried. ^{1}HNMR (400 MHz, D$_2$O) indicated the formation of product the peaks at 3.2 - 4.5 ppm correspond to the polymer backbone, which is exhibits significant overlapping peaks, A D$_2$O peak at 4.8 ppm overlapping with the OH groups of the polymer (al., 2000).
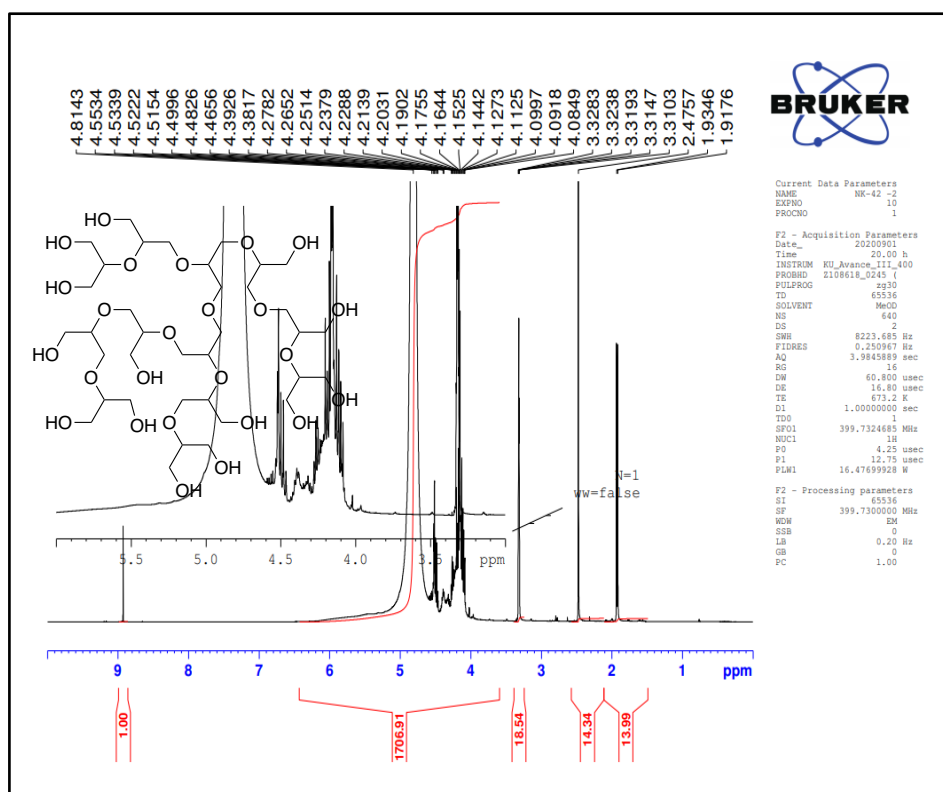
Figure 2. 1 ^{1}HNMR of polyglycerol reaction using core unit glycerol and active monomer (glycidol) with sulfuric acid as catalyst.

δ_H (400 MHz) (D$_2$O), the NMR result shows peaks of polyglycerol at δ = 3.49 -3.63 (2H, (C-CH$_2$)) ppm, δ = 4.61 ppm (s, OH) of glycerol.

2.9.2 Acid-catalyzed polymerization of pentaerythritol with glycidol

Using the general acid catalysed method above, the reaction of pentaerythritol was carried out with glycidol under a similar condition to glycerol. Lower molecular weight polymer was (MALDI-TOF result) obtained for this combination than the glycerol and glycidol.
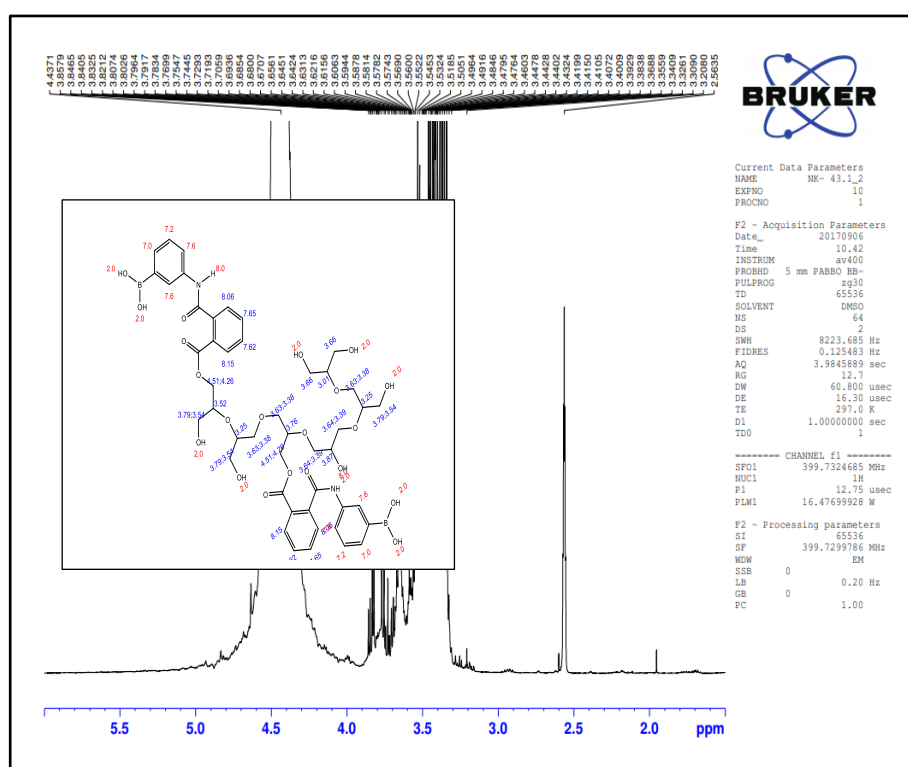
Figure 2. 2 ^{1}HNMR of polyglycerol reaction using core unit pentaerythritol and active monomer (Glycidol) sulfuric acid as a catalyst.

The peaks correspond to the polymer backbone, which shows significant overlapping.

Peaks, at 3.2 – 4.5 and DMSO peak at 2.5 ppm, at 4.9 ppm broad OH groups of the polymer.

δ_H (400 MHz) (DMSO), the NMR result shows peaks of polyglycerol at δ = 3.01 (CH), 3.63 – 3.79 (CH$_2$) ppm, δ = 4.61 ppm broad peak shows the sample is moist and 2.5 ppm (s, OH) of glycerol.

2.9.3 Modification of polyglycerol using 4-(4,4,5,5-Tetramethyl-1,3,2-dioxaborolan-2-yl) benzoic acid

The ester isolates by precipitation, crystalline products can be obtained in pure form acetone after drying under vacuum (A.Hutton, 2004). NMR, FTIR, and MALDI-TOF analysis confirmed the outcome.
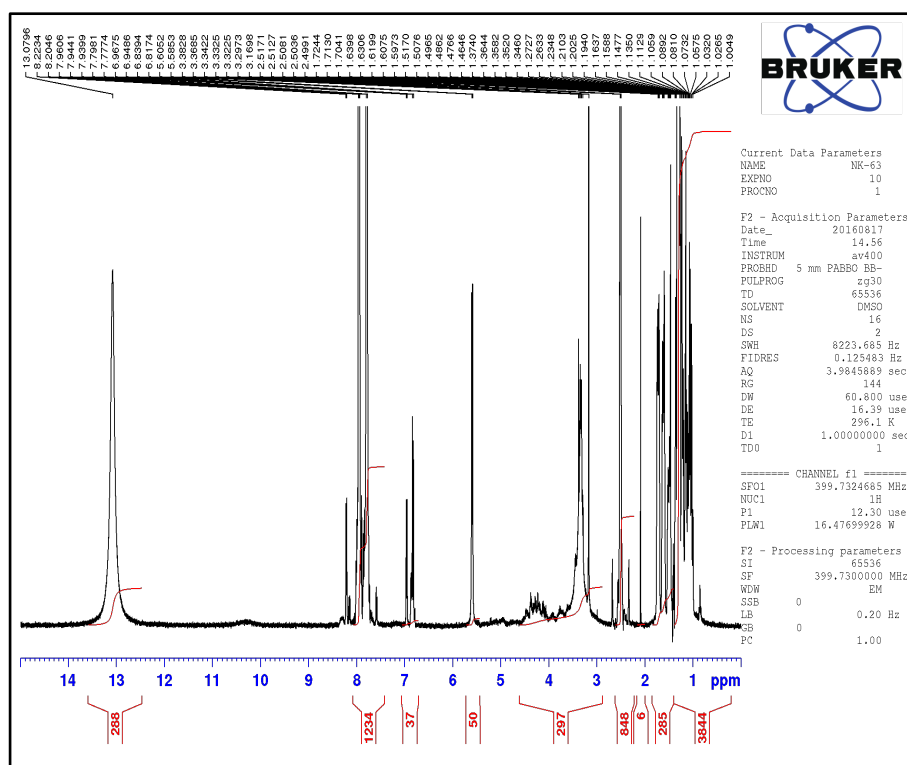
Figure 2. 3 ^{1}HNMR of polyglycerol for the formation of ester bond via Steglich reaction using 4-carboxyphenylboronic acid and polyglycerol.

δH (400 MHz) (DMSO), the spectra of the reaction product show the polymer peaks and addition pinacol peaks at δ =1.3 ppm, the polyglycerol peaks from δ =

31

3.2 -3.4 ppm, the benzene ring at δ =7.5 ppm and δ = 8.2 ppm. FTIR data is listed in table 2.11.
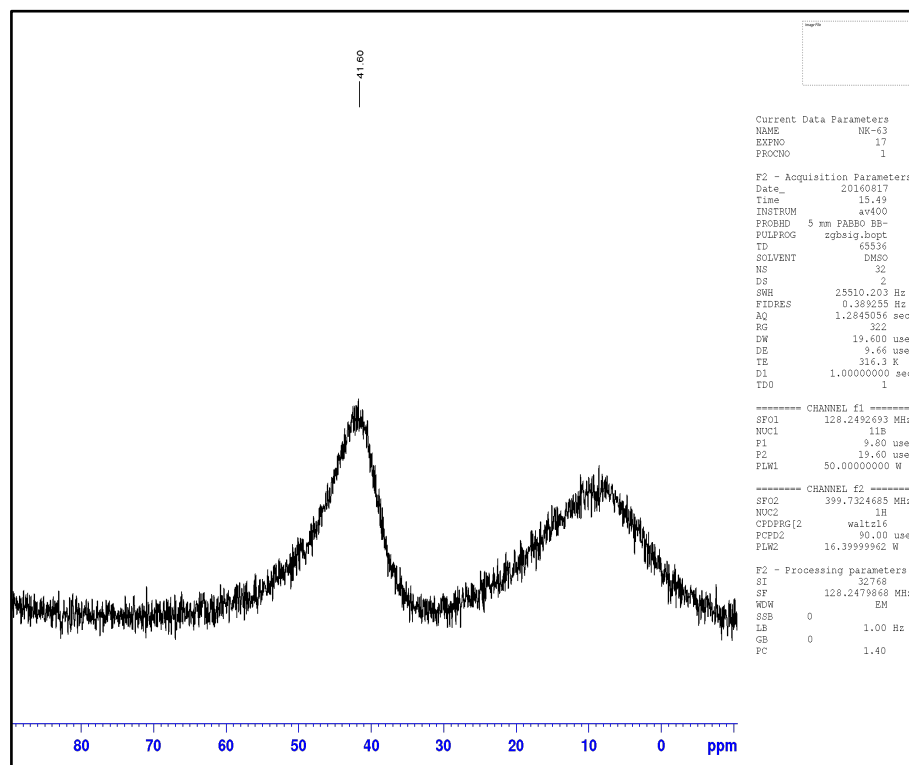
Figure 2. 4 ^{11}BNMR of the compound is the product from the Steglich reaction.

The ^{11}BNMR spectra show a peak at δ = 41.50 ppm, which shows trigonal planar boron. The ^{11}BNMR resonance of boron esters allow distinction between five-six, seven-membered cyclic and acyclic boronate.

^{11}B spectra from approximately (-100 to 100) ppm correspond to the NMR tube and spectrometer probe background signal.

2.9.4 Deprotection of Polyglycerol phenylboronic acid pinacol ester

Attempted deprotection using polystyrene supported phenylboronic acid (PBA) resin using acetonitrile (ACN) and TFA.

In this reaction, which is carried out using polystyrene boronic acid supported resin, the deprotection did not take place under these conditions and starting material was obtained. The repeat NMR experiment has slightly shown improvement in pinacol ester's deprotection by lowering the methyl shifts integrals from the ^{1}HNMR spectra in DMSO (2.50 ppm). However, improvement is still required (Hutton. A, 2004).

Attempted deprotection of pinacol from polyglycerol phenylboronic acid. The deprotection of modified polyglycerol with 4-carboxyphenylboronic acid, using diethanolamine was carried out. The transesterification procedure with diethanolamine (DEA) to form sp3-hybridized boron· It is a two-step procedure for deprotection of alkyl pinacolyl boronate esters via transesterification with diethanolamine $HN(CH_2CH_2OH)_2$ followed by hydrolysis using HCl 1M, in the presence of ether and nitrogen was carried out (Sun et al., 2011).
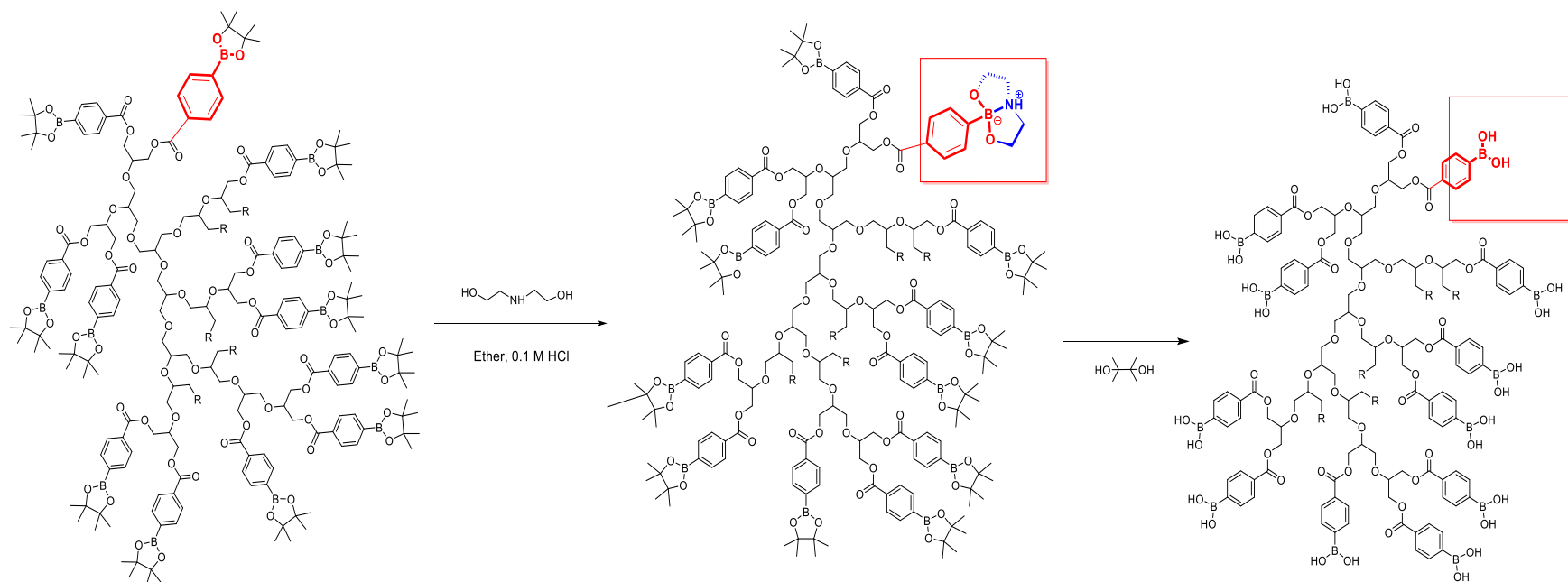
Scheme 2. 15 Highlight shows two-step deprotection protocol for alkyl pinacolyl boronic esters via diethanolamine DEA-protected boronate, which is purified by filtration.

This experiment was carried out in using different ratios of reagents. To a solution of compound (0.85 mmol) phenylboronic acrylamide pinacol ester in ether, diethanolamine (DEA) (0.95 mmol, 0.09 g) was added and stirred for a few minutes. The white precipitates formed, and the reaction was monitored by TLC and was continued until the starting material was consumed entirely. The precipitate was filtered, washed with ether, and dried off. In the next step, 10 m of 1 mM hydrochloric acid from (37%) and ether were added to the DEA-boronate complex in a 1:1 ratio. The reaction was extracted three times with ether, washed with brine, dried with magnesium sulphate, and concentrated under reduced pressure to obtain the pure product.

Six other reactions were also carried out under the same conditions along with the reaction, as mentioned above, using 1 mM and 2 mM hydrochloric acid with and without diethanolamine (DEA), with and without PBA and PB-acrylamide monomer as the controls. These are summarized as in Table 2.4. The symbol ☑ and ☒ indicate the presence or absence of the specified ingredient, respectively.

Table 2. 4 Deprotection of Pinacol group from PBA and PB-Acrylamide *(solvent) and **(aqueous).

Reaction ID	Acid + diethyl ether (10 mL)	DEA	4-APBA	4-ACPBAPE
1s	1 mM HCl	☒	☑	☒
1a				
2s	2 mM HCl	☒	☑	☒
2a				
3s	1 mM HCl	☑	☑	☒
3a				
4s	2 mM HCl	☑	☑	☒
4a				
5s	1 mM HCl	☑	☒	☑
5a				

6s	2 mM HCl	☑	☒	☑
6a				
7s	2 mM HCl	☒	☒	☑
7a				

The deprotection was carried out in 1mM HCl and 2 mM HCl to confirm that the pinacolyl ester is entirely removed. The experiment was designed first to see if the compound 4 amino-phenylboronic acid pinacol ester (PBA) results from the removal of pinacol. The NMR analysis was carried out for both aqueous and solvent phases after purification of the sample.

In order to confirm the deprotection, a control experiment was run in which the 4-carboxyphenylboronic acid pinacol and the same reaction condition was used as an experiment.

To confirm the deprotection takes place, the first monomer was deprotected using diethanolamine. This experiment was carried out to deprotect the monomer first in order to confirm the removal of pinacol and diethanolamine. To confirm the deprotection takes place, the first monomer was deprotected using diethanolamine. Therefore, the NMR spectra have given the idea that using diethanolamine for deprotection of pinacol is not suitable for deprotection of such compound.

δH (400 MHz) (D$_2$O), shows δ = 2.74 (CH$_2$), δ = 4.72pmm solvent proton which the δ = 2.74 ppm corresponds to the CH$_2$ of diethanol amine, between the 4.6 and 5.6 ppm vinyl regions of the acrylamide (4-ACPBA).

δH (400 MHz) (DMSO), corresponds to DMSO and δ= (s, CH$_2$ 2.95), next to OH appears δ= (s, CH$_2$ 3.63), and CH2 near NH appears downfield at 5.10 and OH broad peak appears at 8.84 ppm.
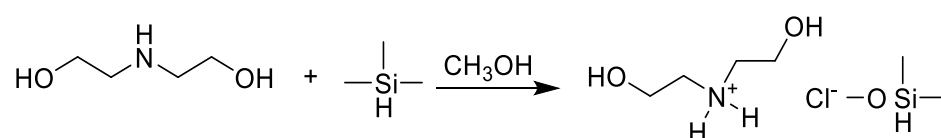
Scheme 2. 16 Salt formation of diethanolamine with Tetramethylsilane (TMS)

Salt formation of diethanolamine with Tetramethylsilane (TMS) is the organosilicon compound with the formula $Si(CH_3)$ chloride in methanol to confirm the NMR peaks in the final product.

Deprotection of pinacol ester using Amberlyst® 15 and methanol NMR of polymer 156.

Previously synthesized (polyglycerol phenylboronic acid pinacol ester) and Amberlyst® 15 was added and left stirring overnight in Methanol. The mixture was filtered, dried under vacuum and pure deprotected compound should be obtained. However, this technique was not successful as the product was as the desired polymer was not o btained.

2.10 Deprotection of pinacol ester using a biphasic system from (4-ACPBAPE)

2.10.1 Biphasic solvent (1 M HCl and hexane)

Deprotection of previously synthesised (polyglycerol phenylboronic acid pinacol ester 83) is carried out. The 1 HCl is adjusted to pH 3, and 100 mL hexane (Hexane :HCl, 1:1) in a round-bottomed flask 1 g benzyl of phenylboronic acid was added and left stirring for 30 min. The mixture was filtered, and dried under vacuum. The polymer (83) deprotected to polymer (158) precipitated in cold acetone dried over vacuum overnight an NMR of both dried hexane layer (158s) and the aqueous layer (158a) was carried out. The NMR showed traces of pinacol ester impurities in the aqueous polymer phase, which further purified by precipitating in cold acetone for three times.

δ_H (400 MHz) (MeOH), corresponds δ = (3.29 -3.54, CH_2) δ = (3.79, 3.52 CH), δ =(4.03 OH) δ = (2.00 CH) and δ = (7.4 – 8.0 of Aromatic region) in addition δ = (4.79 CH_2) and δ = (1.26 CH_3) of pinacol. ^{1}HNMR of deprotection of pinacol ester from polyglycerol phenylboronic acid pinacol ester using biphasic system (2 M HCl and Hexane) for aqueous layer (158a), shows the compound is not deprotected fully and both polymer pinacol present.

δ_H (400 MHz) (MeOH), corresponds δ = (3.29 -3.54 .3.79 , CH$_2$) δ = (3.79, 3.54 CH), δ =(4.03 OH) δ = (2.00 CH) and δ = (7.4 – 8.0 of Aromatic region) in addition δ = (4.79 CH$_2$) and δ = (1.26 CH$_3$) of pinacol. ^{1}HNMR of deprotection of pinacol ester from polyglycerol phenylboronic acid pinacol ester using biphasic system (2 M HCl and Hexane) for aqueous layer (158s), shows the compound is not deprotected entirely and together polymer and pinacol is existing.

2.11 Carboxylic acid formation of polyglycerol

Carboxylic acid formation from polyglycerol in the presence of succinic anhydride. Carboxylic acid formation of polyglycerol (PG) was followed by catalysed acetylation of alcohols in the presence of acetic anhydride. The difference is that in this study, succinic anhydride was used, and polyglycerol was used as the alcohol (polymer 89).

δ_H (400 MHz) (DMSO), corresponds δ = (3.78 - 3.98 , CH$_2$) δ = (4.55 - 4.45 CH), δ =(5.43 OH) δ = (8.10, H of COOH), In addition it also shows the NMR spectrum some methyl peaks of DMAP.

Carboxylic acid formation of polyglycerol (LMW) using Dioxane and DMAP, Synthesis of the terminal carboxylic acid group using phthalic anhydride polymer (158) polyglycerol is very water-soluble, and in order to make it suitable for work up at organic layer, an attempt was made to bind phthalic anhydride to alcohol bonds of polyglycerol. Polyglycerol reacted with phthalic anhydride giving end carboxylic acid functional group for further modification.

Dioxane was distilled under metallic sodium and benzophenone at 60 ˚C. To the freshly distilled dioxane polyglycerol (42) was added and stirred under nitrogen. Phthalic anhydride was added to the solution of polyglycerol, and dioxane. DMAP and the reaction mixture was heated under reflux for 6 hours and left-over night at room temperature.
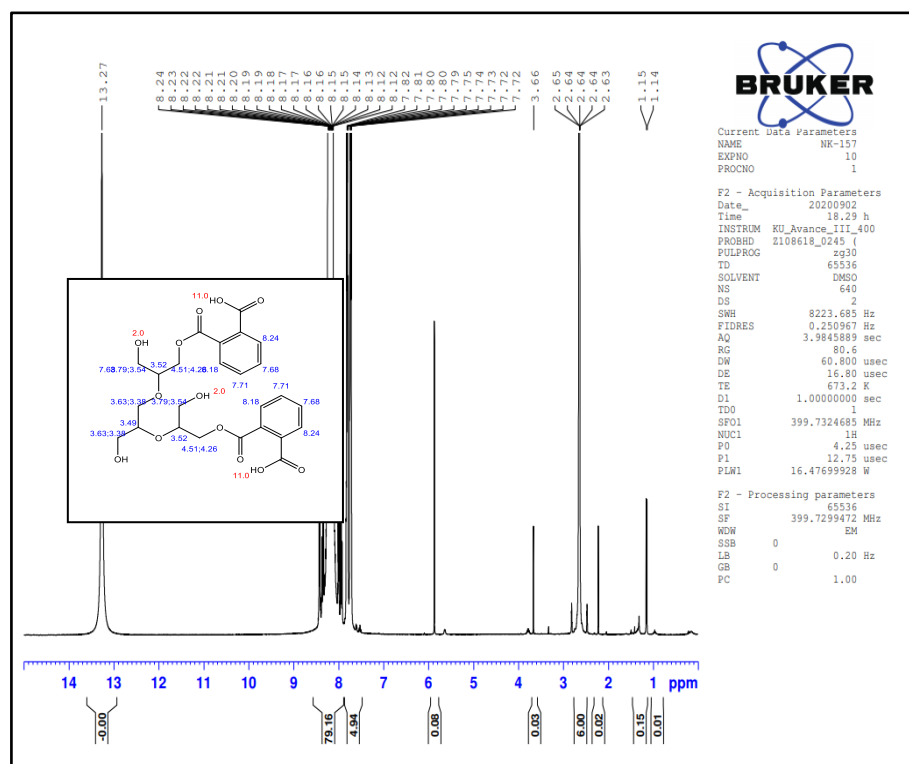
Figure 2. 5 ^{1}HNMR of the modification of polyglycerol with phthalic anhydride experiment.

δ_H (400 MHz) (DMSO), the ^{1}HNMR result shows peaks of polyglycerol at δ = 3.49 - 3.63 (2H) ppm, δ = 4.61 ppm I H of glycerol, and the phthalic anhydride benzine ring peaks at δ =8.18 ppm (2H) and δ =7.6 ppm (1H) and δ =11.00 ppm for OH of carboxylic acid end group. δ (CH$_3$ of DMAP is visible at 1.3 ppm), δ (CH$_2$ = 3.66, 3.91 4.38 ppm), δ (CH = 4.03 4.6 3.52 ppm of glycerol, and OH peaks at 2.00 ppm the phthalic anhydride benzine ring peaks at δ (8.23 ppm, 2H) and δ (7.71, 7.68 ppm) δ (1H) and δ (11.00 ppm) for OH of carboxylic acid end group. Polyglycerol Carboxylic acid Phthalic anhydride reaction with 3 phenylboronic amino acid (160).

2.12 Formation of amide bond

Polyglycerol phthalic anhydride (sample ID 160) was added into 50 mL DCM, 3-Amniophenylbornic acid added in the presence of 1-(3-Dimethylaminopropyl)-3-ethyl carbodiimide Hydrochloride coupling reagent for amide bond formation.
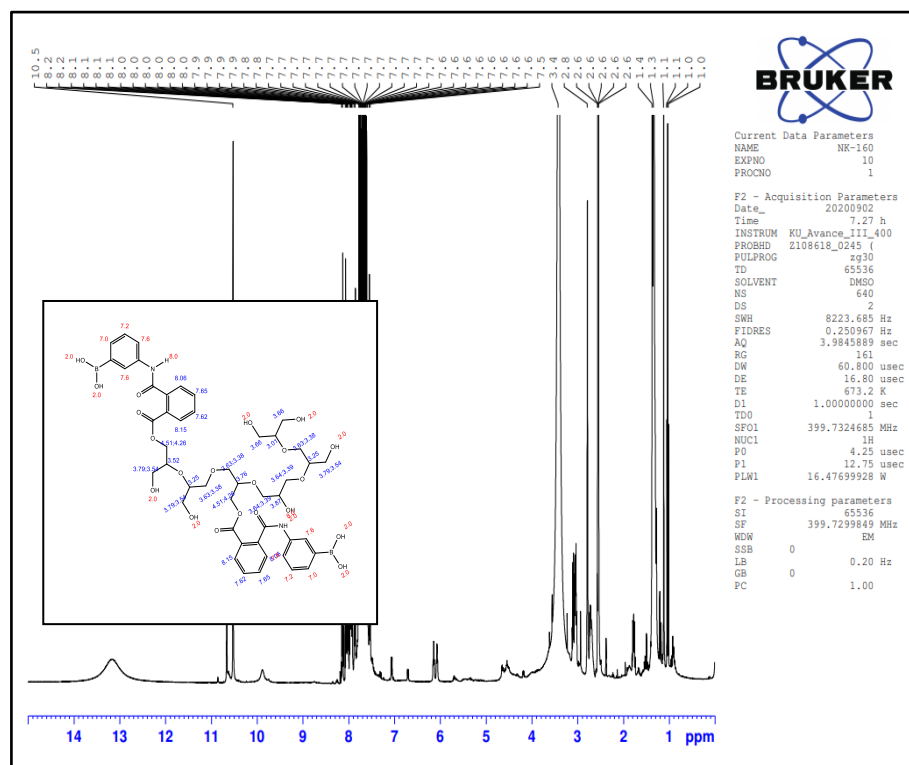
Figure 2. 6 ^{1}HNMR of the modification of polyglycerol phthalic anhydride with amino boronic acid experiment.

δ_H (400 MHz) (DMSO), the NMR, the NMR result shows peaks of polyglycerol modified with phthalic anhydride and aminoboronic acid confirms the compound that at δ= 3.20 -3.83 (2H) ppm, δ =4.51 ppm I H of glycerol, and the phthalic anhydride benzine ring peaks at δ= 8.18 ppm amide proton, and δ =7.6 ppm (1H) and δ =7.0 – 7.6 ppm for the benzene ring if amino boronic acid and δ =13 ppm a broad peak ppm for OH of carboxylic acid end group.

2.13 Synthesis of monomer

2,2-dimethyl-1,3-dioxolan-4-yl)methyl 4-(4,4,5-trimethyl-1,3,2-dioxaborolan-2-yl)benzoate

The reaction was successfully completed, and the desired product was obtained confirmed and GC-MS (giving a peak of m/z = 347 g mol^{-1}) and 1.4 g, 54 % yield .
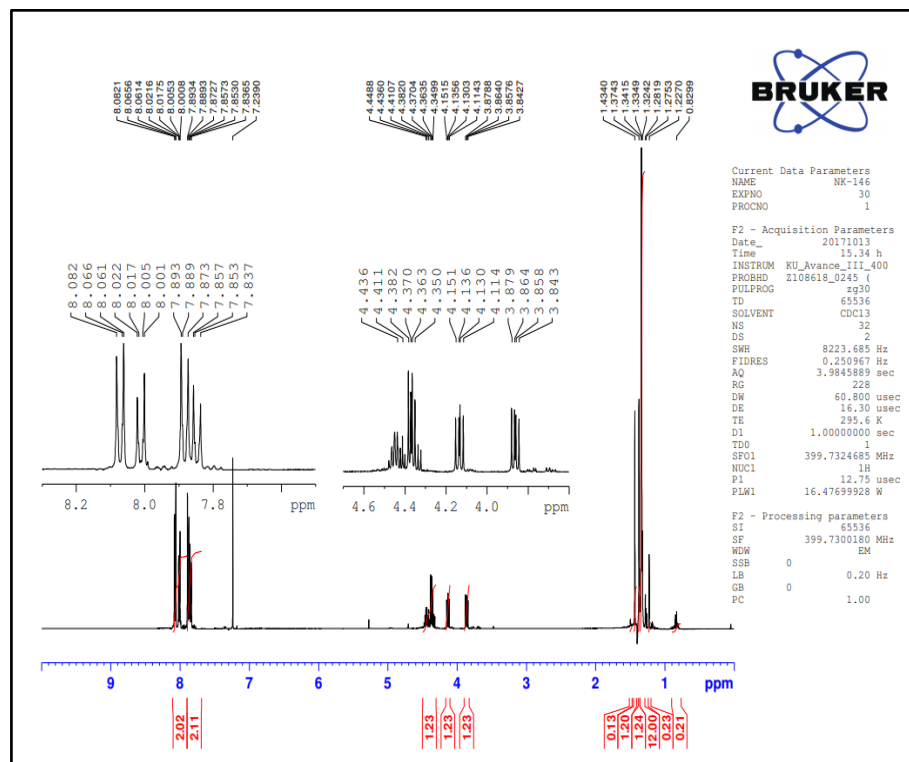
Figure 2. 7 ^{1}HNMR of 2,2-dimethyl-1,3-dioxolan-4-yl)methyl 4-(4,4,5-trimethyl-1,3,2-dioxaborolan-2-yl)benzoate.

δ_H (400 MHz) (CDCl$_3$), 1.26 (s, 12H, CH$_3$), 1.33 (s, 6H, CH$_3$), 3.87 (q, J = 6.0 Hz, 2H),(q, J = 6.4 Hz, 2H), 4.43 – 4.36 (m, 1H), 7.83 – 7.89 (m, 2H), 8.00 - 8.08 (2-H).
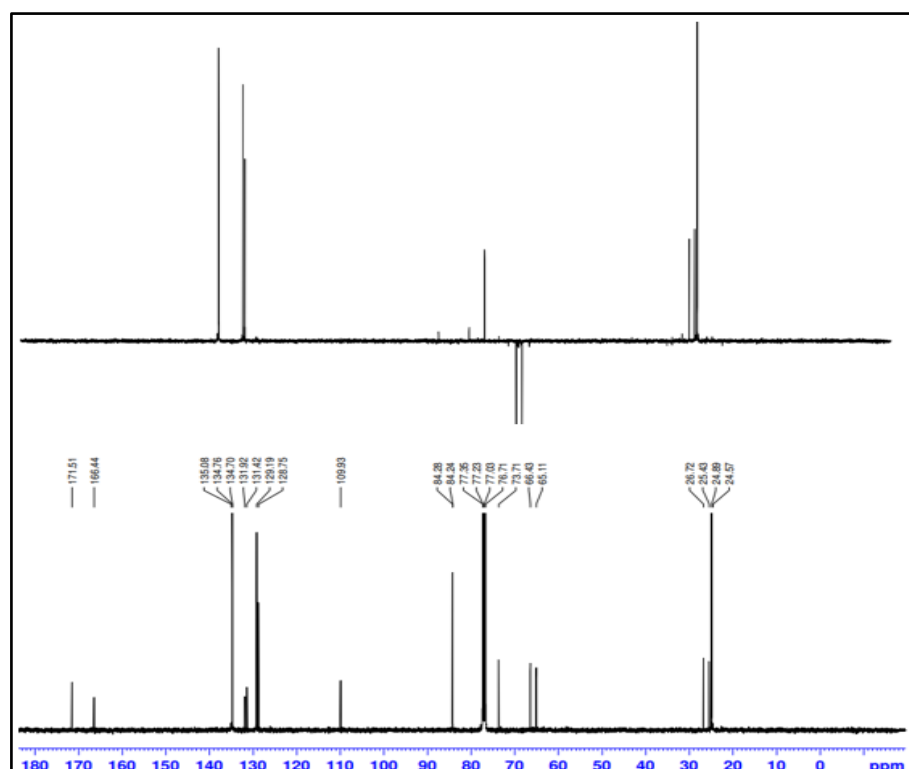
Figure 2. 8 ^{13}CNMR of (2,2-dimethyl-1,3-dioxolan-4-yl)methyl 4-(4,4,5-trimethyl-1,3,2-dioxaborolan-2-yl)benzoate

^{13}C (100 MHz) (CDCl$_3$) δ_C = 24.71 (4 x CH$_3$), 84.28 and 84.24(C), 65.11 and 65.43 (CH$_2$) 128.75., 129.19, 131.42, 131.02, 134.70, 135.08 (all CH) and 166.44, and 172.51 (COOH), 109.93 (C).

IR: 2980, 1709 (C=O), 1052, 1335, 813 cm^{-1}.

2.14 Polymerisation of (2,2-dimethyl-1,3-dioxolan-4-yl)methyl 4-(4,4,5-trimethyl-1,3,2-dioxaborolan-2-yl)benzoate

2.14.1 Deprotection of polyglycerol isopropyl phenylboronic acid

Deprotection (polymer 161) was carried out using biphasic system of hexane and hydrochloric acid 1mM consequently freeze drying. This is a transesterification with phenylboronic acid and removals of the pinacol as the phenyl boronate ester. The procedure uses a biphasic system that takes advantage of the solubility difference in the pinanediol ester, the free boronic acid (both soluble in the aqueous phase), and the pinacol phenyl boronate ester (soluble only in the organic phase) (Coutts, 1994) (polymer 164).

2.15 Preparation of DL-1,2-isopropylideneglycerol with 4-carboxyphenylboronic acid pinacol ester

2.15.1 Glycerol based Phenyboronic acid monomer for polymerization

These experiments were carried out to synthesis novel compound for polymerisation of polyglycerol by acid deprotection of isopropyl from glycerol group. Samples 146 confirmed the formation of the product by NMR, GC-MS and FTIR. The polymerisation of isopropyl glycerol carboxylic acid pinacol ester was carried out successfully polymer 160.
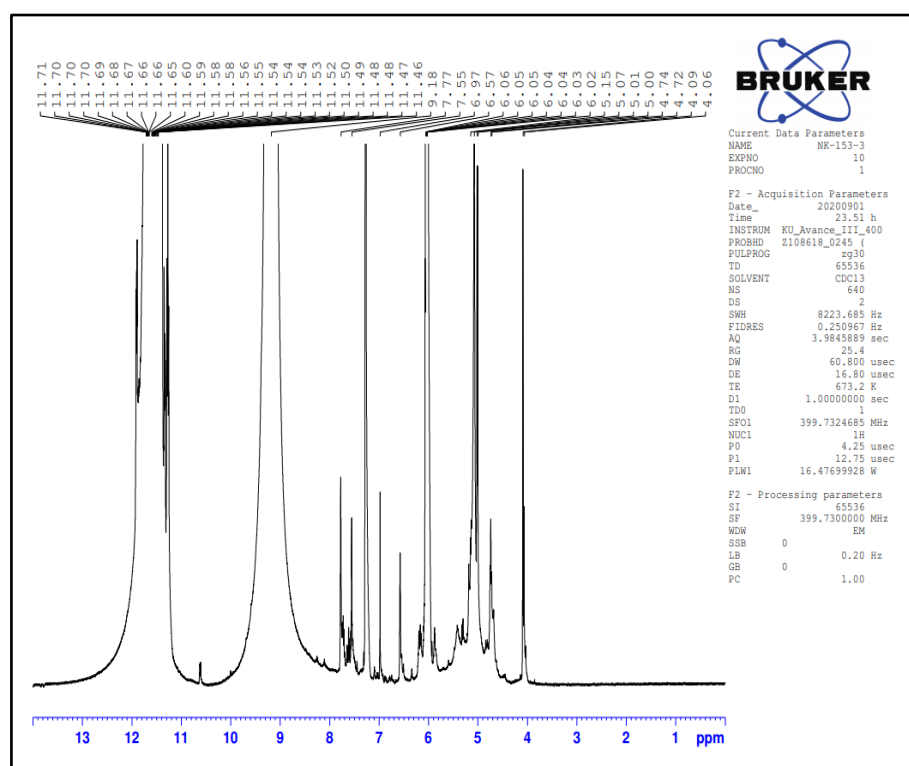
Figure 2. 9 ^{1}HNMR of polymerisation of isopropyl glycerol carboxylic acid pinacol ester in the presence of glycerol and glycidol. glycerol end functionalised DL-1,2-isopropylideneglycerol with 4-carboxyphenylboronic acid pinacol ester in dioxane.

δH (400 MHz) (CDCl$_3$), δ (4.03, s, CH, CH$_3$), δ (4.35 – 4.38), δ = (CH$_2$), 7.4 - 7.77 Aromatic H, 9.18 (OH) 11.46 – 11.71 ppm) corresponds to COOH peak. Intramolecular hydrogen bonding in polymer causes substantial downfield shifts. Therefore, the value must come at downfield. NMR of the product was obtained and analyzed to determine/confirm the resulting product with an easy method

compared to the method above where polymerization was done first and then modified. This method is much more efficient as the deprotection takes place during work up.

2.16 An efficient method for protection of pinacol

2.16.1 Protection of 3-carboxyphenylboronic acid using chloroform in absence of molecular sieves

After the dry compound attained, the yield was calculated as well as by NMR the percentage of product and starting material pinacol. The presence of triplets at 7.49 ppm in the NMR spectrum before crystallization was possibly due to the emergence of doublet peaks, which appeared as triplet because of overlapping. There were also two *tert*-butyl peaks at 1.25 -1.27 ppm, which were presumed to be due to the unreacted pinacol. Therefore, recrystallization carried out in ethyl acetate, and after recrystallization, the peak at 1.25 disappeared. The calculation was carried out using the sum of integrals.

% product by NMR = $\dfrac{Integrals\ of\ pinacol\ in\ product}{Integrals\ of\ pinacol\ in\ product+integrals\ of\ residual\ pinacol}$ *x 100*

Percentage of the product by NMR: $\dfrac{11.370}{11.370+6.70}$ *x 100 = 63%*

Percentage of pinacol by NMR: $\dfrac{6.70}{11.370+6.70}$ *x 100 = 37%*

Actual yield of the product = 0.05 g

Theoretical Yield = 0.8 g

Percentage yield = $\dfrac{0.049g}{0.821g}$ *x 100 = 6%*

The product also confirmed by ^{13}CNMR and DEPT, the melting point (mp) of the 3-CPBA pinacol ester (product) was determined to be 229 -230 $^{\circ}$C literature value reported 228 - 231 ° C, light brown compound.

NMR of the product was obtained and analyzed to confirm the resulting product
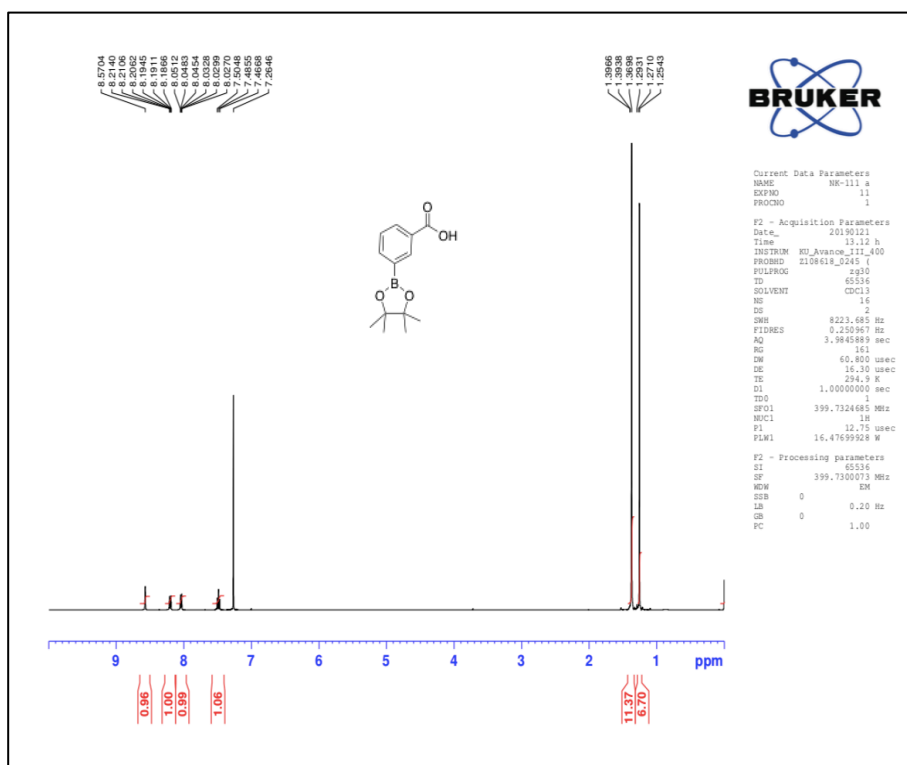
Figure 2. 10 ^{1}HNMRof preliminary experiment 1 before recrystallisation.

δ_H (400 MHz) (CDCl$_3$), 1.27 (s, 6H, CH$_3$), 1.39 (s, 6H, CH$_3$), 7.49 (t, 1H), 8.03-8.05 (m, 1H), 8.19-8.21 (m, 1H), 8.57 (s,1H, 2-H).

To purify the product recrystallisation was carried out using warm ethyl acetate and scratching technique was used to speed up the crystallization process. The resulting product was then dried under a vacuum. Proton and Carbon NMR of the product were obtained after recrystallization using ethyl acetate.
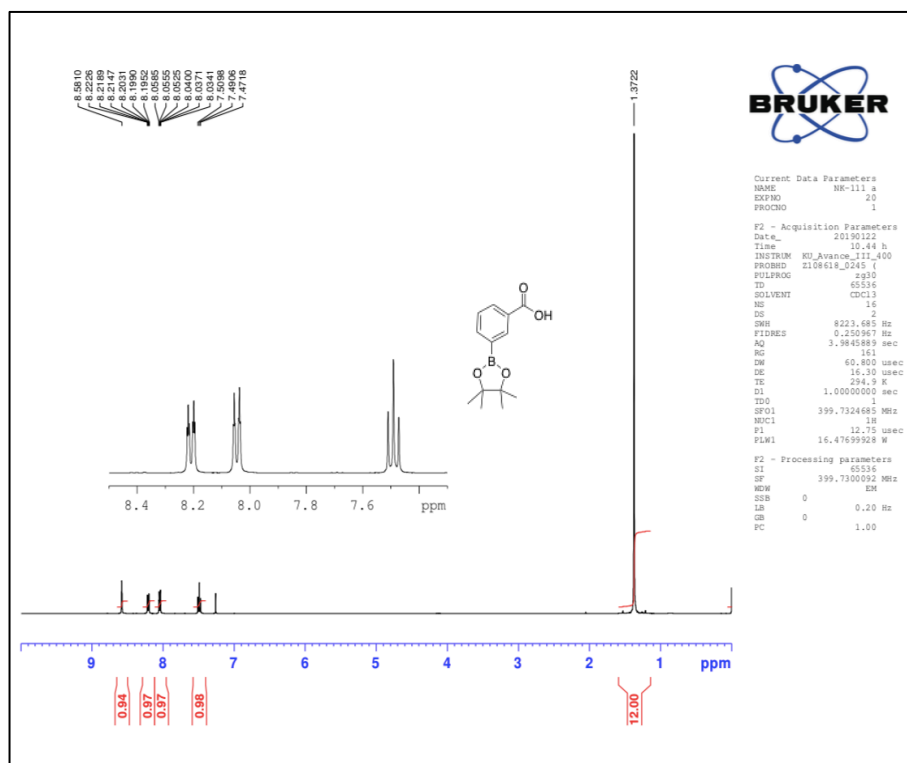
Figure 2. 11 ^{1}HNMR δ_H (400 MHz) (CDCl$_3$) of preliminary experiment 1 after recrystallisation.

δ_H (400 MHz) (CDCl$_3$), 1.37 (s, 12H, CH$_3$), 7.49 (t, J = 7.6 Hz, 1H, 5-H), 8.03 - 8.06 (m, 1H), 8.20 - 8.22 (m, 1H), 8.58 (s, 1H, 2-H). COOH peak did not appear.
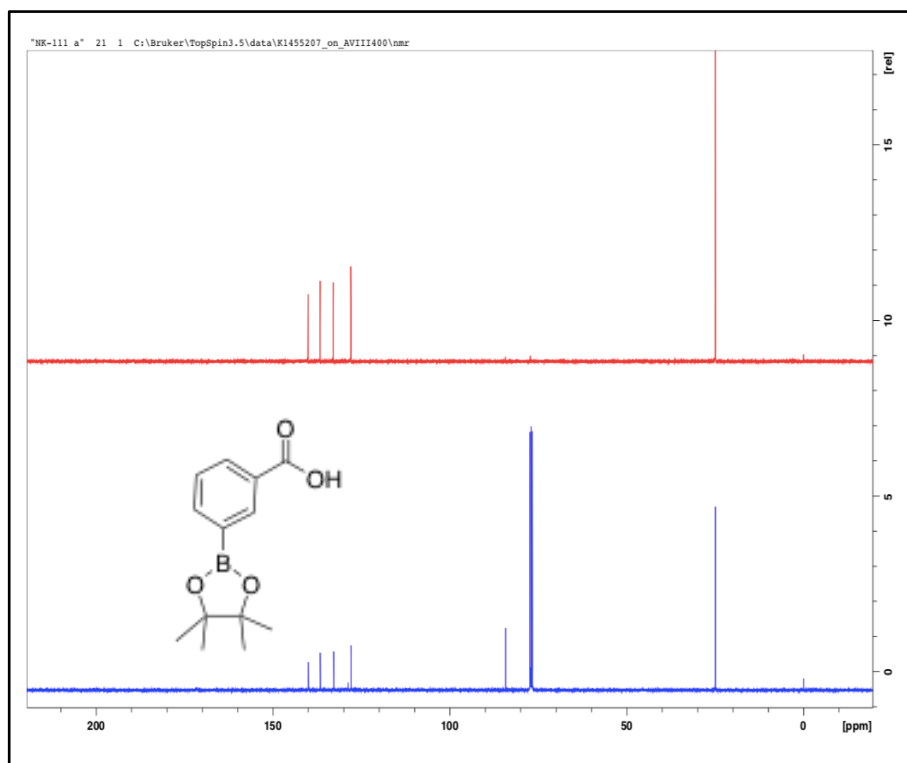
Figure 2. 12 ^{13}C (100 MHz) (CDCl$_3$) and dept of preliminary experiment 1.

^{13}C (100 MHz) (CDCl$_3$) δ$_C$ = 24.91 (4 x CH$_3$), 84.22 (C), 127.88, 132.83, 136.63, 139.94, 140.00 (all CH) and 172.10 (COOH) not showing.

IR: 2977, 1682 (C=O), 1604, 1485, 1409, 1205,1164 cm^{-1}.

Protection of 3-carboxyphenylboronic acid using DCM

2.16.2 Protection using activated 3Å molecular sieves

Molecular sieves 8 g were activated in domestic microwave, they were then stirred for 72 hours with pinacol, DCM and 3-CPBA solution on a magnetic stirrer. The solution was then filtered into a conical flask. The extraction of the chloroform layer from the water layer was not needed as water layers got adsorbed by molecular sieves. Therefore, the solution was dried further by the addition of Na$_2$SO$_4$, a drying agent, until it was free floating in the solution. The solution was then re-filtered into a round bottom flask and dried under the vacuum. Recrystallization was done for purification of the product. The product was dissolved in hot ethyl acetate and put in ice for crystals to form. Scratching technique was used to aid the process. Once the crystals were formed entirely,

the liquid solution was carefully extracted using a glass pipette. Hydrogen and carbon NMR of the product were obtained before and after crystallization. IR was also obtained after crystallisation, and the MP of the product was determined.

Percentage of the product by NMR: $\dfrac{12.32}{12.32+2.50}$ x 100 = 83%

Percentage of pinacol by NMR: $\dfrac{2.50}{12.32+2.50}$ x 100 = 17%

Actual yield of the product = 0.12g

Theoretical Yield = 0.75 g

Percentage yield = $\dfrac{0.1239g}{0.7517g}$ x 100 = 16.5%
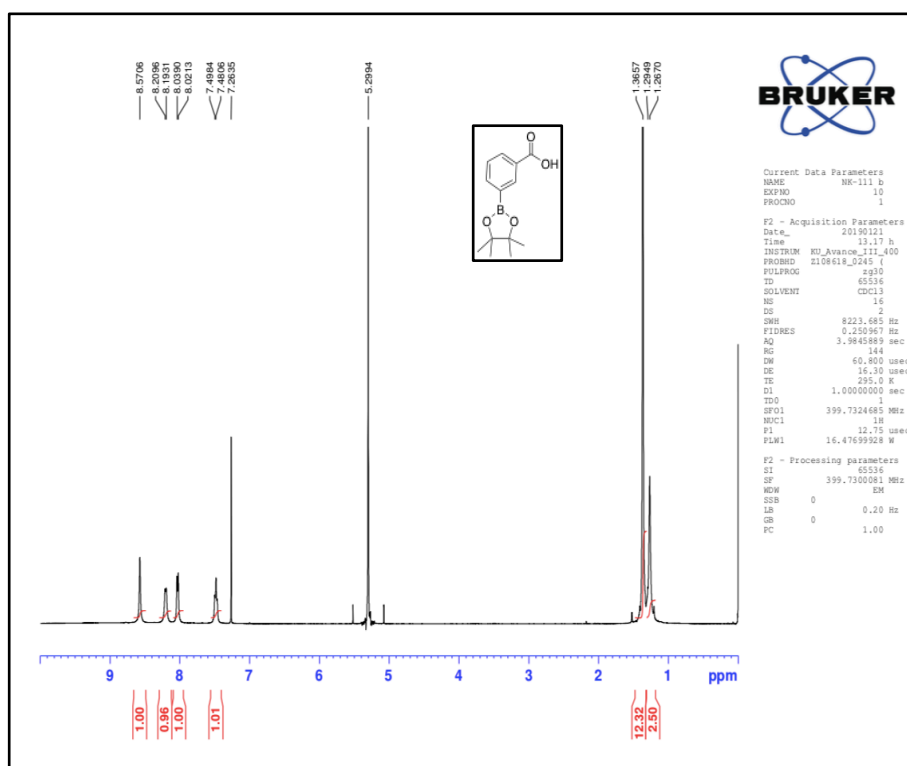
Figure 2. 13 ^{1}HNMR δ_H (400 MHz) (CDCl$_3$), of preliminary experiment 2 after recrystallisation

δ_H (400 MHz) (CDCl$_3$), 1.37 (s, 12H, CH$_3$), 7.49 (t, J = 7.5 Hz, 1H, 5-H), 8.02-8.03 (d, 1H, 4-H) and 8.19-8.21 (d, 1H, 6-H), 8.57 (s, 1H, 2-H). COOH peak did not appear.

After recrystallisation δ_H (400 MHz) (CDCl$_3$), 1.37 (s, 12H, CH$_3$), 7.49 (t, J = 7.5 Hz, 1H, 5-H), 8.02-8.03 (d, 1H, 4-H) and 8.19-8.21 (d, 1H, 6-H), 8.57 (s, 1H, 2-H)11.11 (s, 1H, COOH).
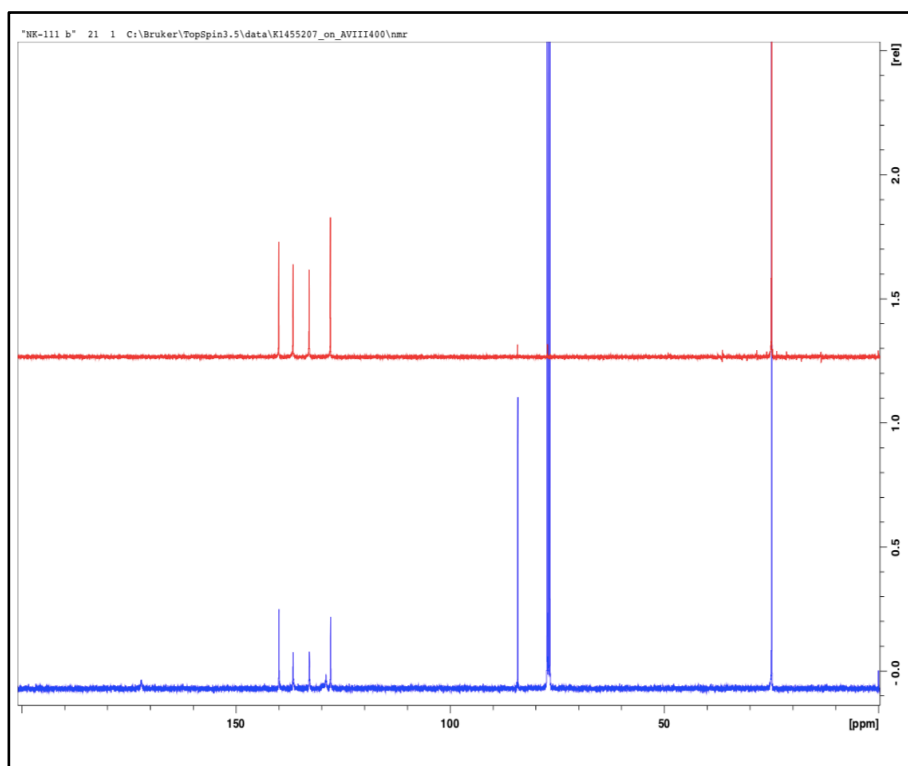
Figure 2. 14 carbon dept ^{13}C (100 MHz) (CDCl$_3$) of preliminary experiment.

^{13}C (100 MHz) (CDCl$_3$) δ = 24.87 (4 x CH$_3$), 84.18 (C), 127.88 (CH), 128.96 (C), 132.83, 136.63, 139.94 (all CH) and 172.10 (COOH).

IR: 2977, 1682 (C=O), 1605, 1583, 1486, 1387, 1132,1078 cm^{-1}.

2.16.3 Modification of the above 2 protection methods of

As the results of the initial experimentations, it was decided to combine the two methods. Chloroform was chosen as the final solvent due to its high boiling point (61.2 °C) compared to DCM (40 °C). Chloroform used with careful handling to avoid inhalation chloroform handled within fume cupboard throughout the time. As, rubber gets dissolved in chloroform, so glass equipment was used to avoid contamination.
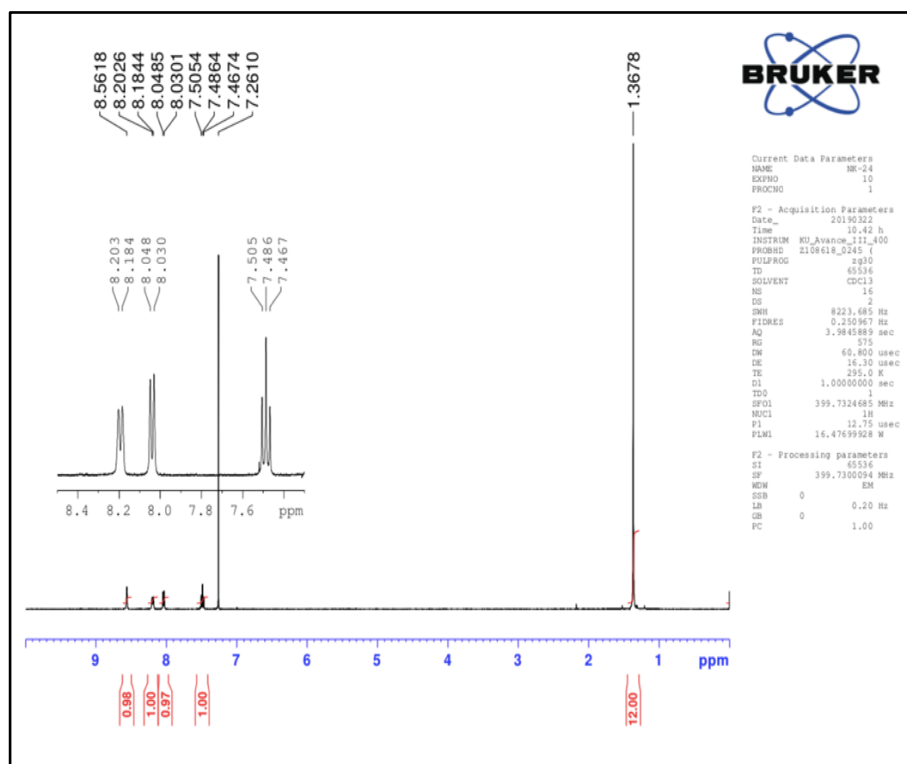
Figure 2. 15 ^{1}HNMR of 3-CPBA pinacol ester from method 3.

The yield of the product was still low, but it was better than what was obtained with preliminary experiment 1. The two *tert*-butyl (pinacol) peaks at 1.25 -1.27 also appeared indicating unreacted pinacol, which then disappeared after recrystallization. There was also a peak in ^{1}HNMR at 5.29, which could be due to some impurity and disappeared after recrystallization. The melting point of this compound (mp) of the 3-CPBA pinacol ester (product) was determined to be 229-230 ^{o}C literature value reported 228- 231 °C.

The carbon dept also confirmed the carbon groups the upwards dept of the peak at 24.89 confirmed CH$_3$ group, no dept for a peak at 76.68 -77.31 and 84.21 confirmed presence of C only group and the upward depts for the peaks at 127.93, 132.89, 136.64 and 139.99 confirmed the presence of CH group.
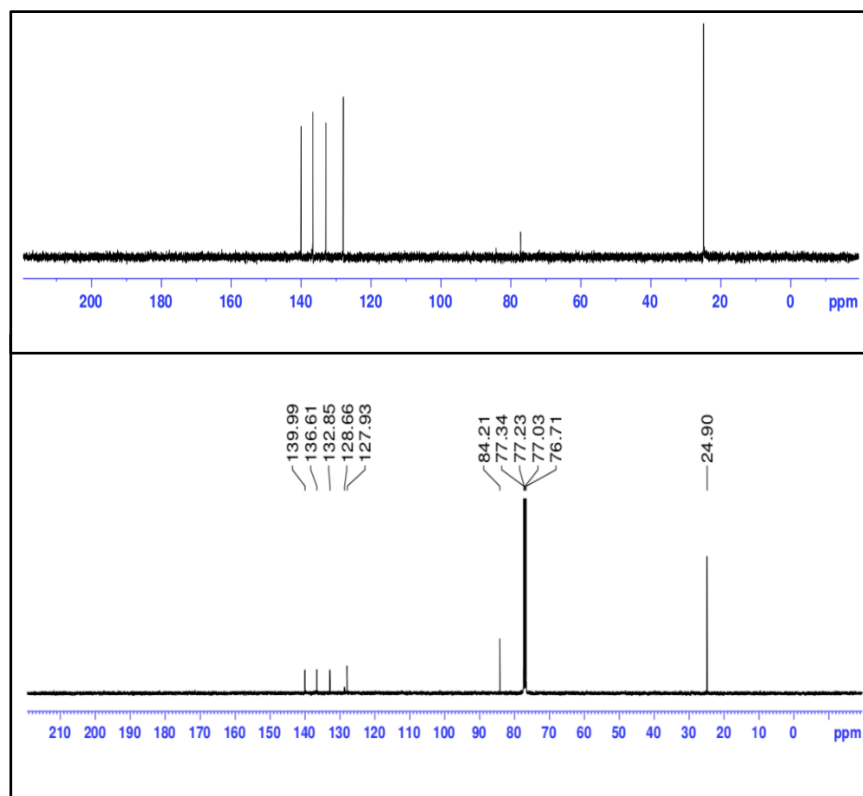
Figure 2. 16 ^{13}C NMR of 3-CPBA pinacol ester from method 3..

The preliminary experiments were carried out with 3-CPBA to determine which one of the methods were best for the protection of boronic acid. It was also to determine which solvent to use for the reaction. The yield of the preliminary works was significantly low. For preliminary experiment 1, the literature reported a 22% yield, whereas we got a 6% yield. For preliminary experiment 2, the literature reported a 48% yield, though it is a 13% yield. The yield was lower than expected, which could be attributed to the fact that for drying purposes, MgSO$_4$ was added to the solution instead of Na$_2$SO$_4$. There was a possibility that the product might have reacted to magnesium sulphate, thus, resulting in low yield. MgSO$_4$ was, therefore, proved to be incorrect drying agent, and this error could have been

avoided by adding the right drying agent, Na$_2$SO$_4$. Later, when Na$_2$SO$_4$ was added to dry the solution further, it did not affect the yield, thus, proving that the low yield was a result of the error made by adding MgSO$_4$. Although, the final compound obtained was pure, but due to the low yield of the product drying agents and recrystallization needed modification to improve yield.

2.17 Results of synthesis of additional monomers

2.17.1 (Z)-2-(3-(4,4,5,5-tetramethyl-1,3,2-dioxaborolan-2yl) phenyl carbamoyl) acrylic acid

The NMR of the starting material from TCL (Tokyo Chemical Limited) showed impurities of pinacol at 1.12 ppm. This has affected the reaction. Therefore, the product was recrystallized. However, it did not purify, so I have purified first the 2-APBAPE using column chromatography, (Petrol ether: ethyl acetate, 1:1).
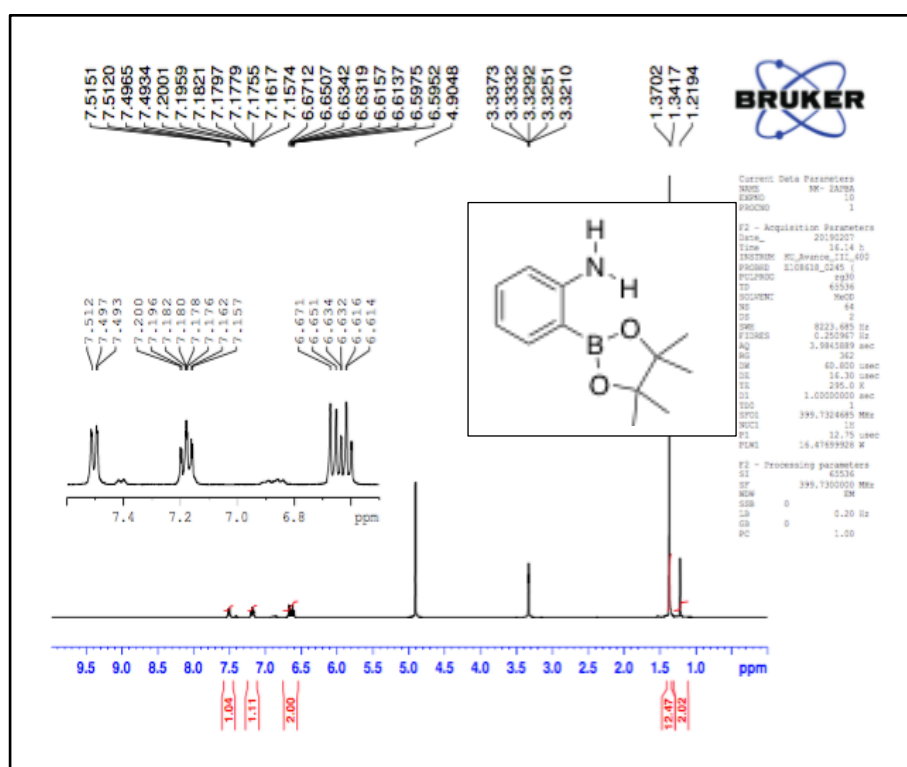
Figure 2. 17 ^{1}HNMR of starting material checked for purity, showed some impurity. Therefore it was purified before reaction.
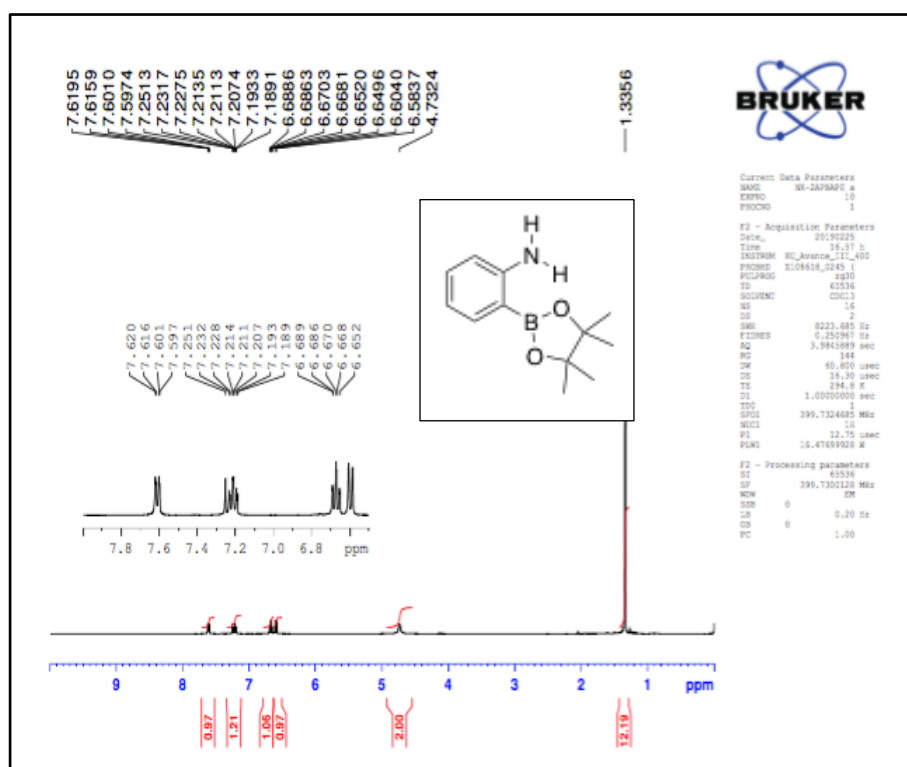
Figure 2. 18 ^{1}HNMR of starting material purified using column chromatography.

δ_H (400 MHz) (CD$_3$OD),1.34 (s,12H,CH$_3$), 4.7 (s,br, 2H) for 6.59(d, J = 8.3 Hz,1H), 6.68 (t, J = 7.31, 7.19 Hz, 1H), 7.19 − 7.251(m, 1H),7.61 and 7.56 (dd, J = 1.44, J =1.44, 1H).

^{1}HNMR after precipitation of product in hexane:(Z)-methyl2-(4-(4,4,5,5-tetramethyl-1,3,2-dioxaborolan-2 yl)phenylcarbamoyl)acrylate.
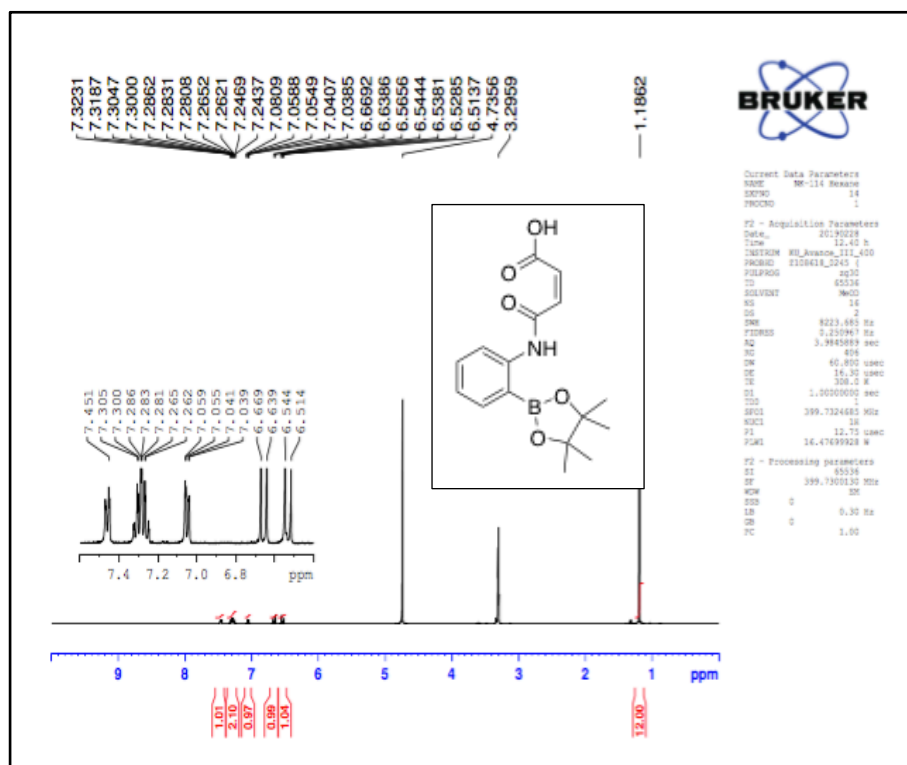
Figure 2. 19 ^{1}HNMR after precipitation of product in hexane: (Z)-methyl 2-(4-(4,4,5,5-tetramethyl-1,3,2-dioxaborolan-2 yl)phenyl carbamoyl)acrylate

δ_H (400 MHz) (CD$_3$OD),1.86 (s,12H,CH$_3$), 3.29 solvent, 4.76 water in MeOH, 6.66 (d, 1H, J = 12.23 Hz), 6.54 (d, 1H, J = 12.27 Hz), 7.07 (d, 1H, J = 1.55 Hz), 7.73 (d, 1H, J = 0.88 Hz), 7.25 − 7.31 (m, 2H), 7.47 (d, 1H, J = 1.55Hz), 7.46 (d, 1H J= 1.79 Hz)
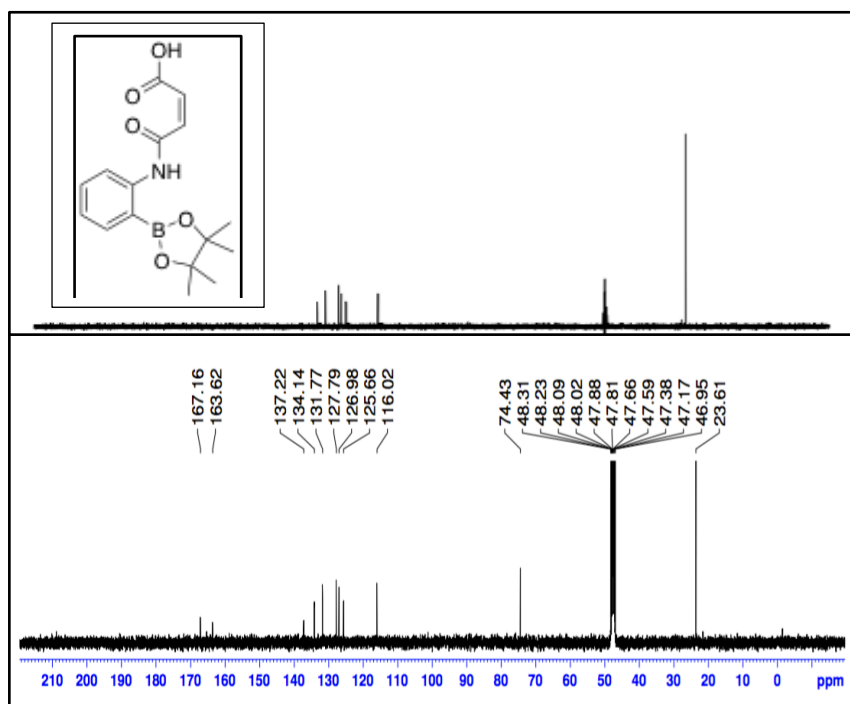
Figure 2. 20 ^{13}C NMR after precipitation of product in hexane: (Z)-methyl 2-(4-(4,4,5,5tetramethyl-1,3,2-dioxaborolan-2 yl)phenylcarbamoyl)acrylate

[13]C δc (100 MHz) (CDCl$_3$) δ = 23.61 (4 x CH$_3$), 74.43 (C-(C=O)-R), 116.02 (C), 125.66, 126.98, 127.79,131.77 all (CH), 134.14, 137.22 (C=C), 163.62, 167.16 (C=O.)

^{1}HNMR result of: (Z)-3-(3-(4,4,5,5 tetramethyl-1,3,2dioxaborolan-2yl) phenyl carbamoyl) acrylic acid.
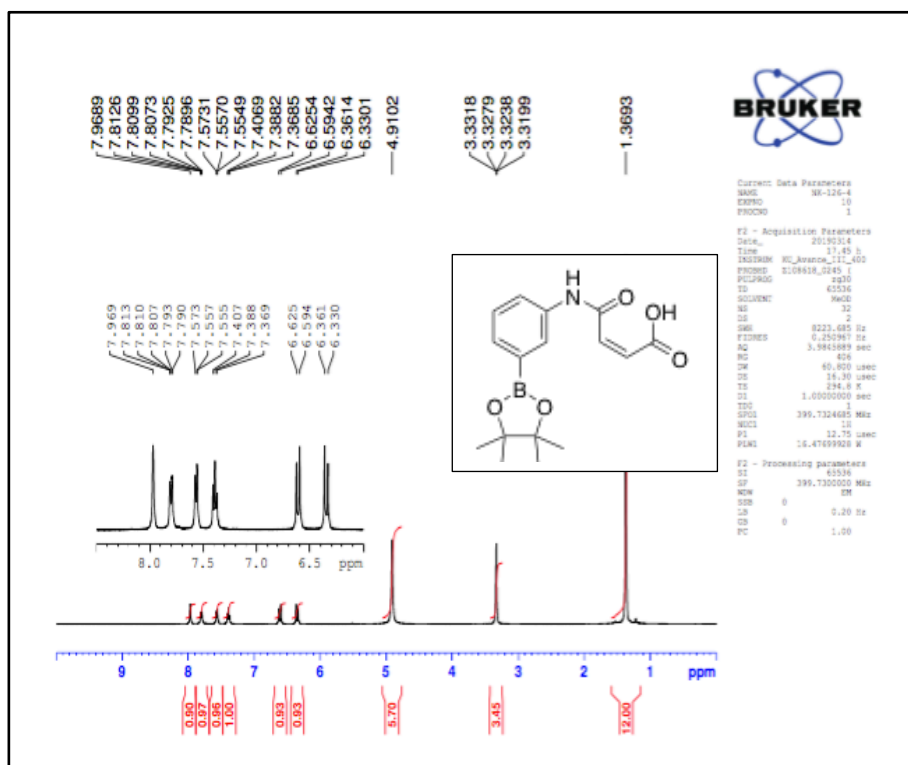
Figure 2. 21 ^{1}HNMR of: (Z)-3-(3-(4,4,5,5 tetramethyl-1,3,2dioxaborolan-2yl)phenylcarbamoyl)acrylic acid

^{1}HNMR δ_H (400 MHz) (CD$_3$OD),1.37 (s,12H, CH$_3$), 6.32 (d, 1H, J = 12.5 Hz), 6.61 (d, 1H, J = 12.5 Hz), 7.39 (t, 1H J = 15.3, 7.9 HZ), 7.57 (d 1H, J = 6.9 Hz), 7.80 (d, J = 8 Hz, 1H), 7.96 (s, 1H).
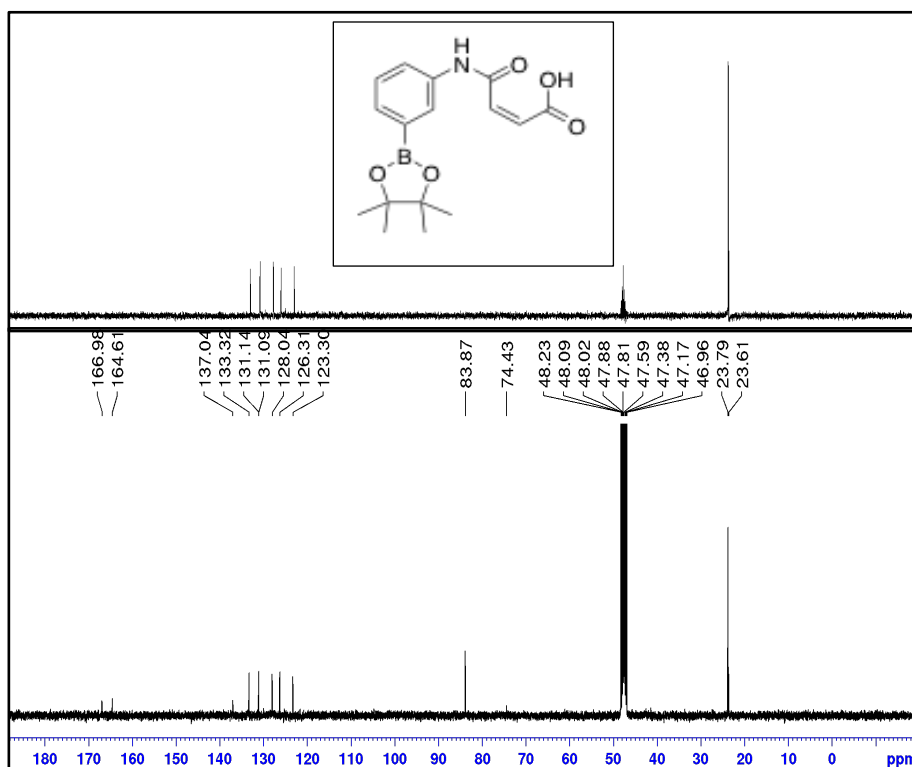
Figure 2. 22 ^{13}C NMR of: (Z)-3-(3-(4,4,5,5-tetramethyl-1,3,2-dioxaborolan-2-yl)phenylcarbamoyl)acrylic acid

^{13}C (100 MHz) (CDCl$_3$) δ = 23.70 (4 x CH$_3$), 74.43 (C-(C=O)-R), 83.87 (C), 123.30, 126.31, 128.04, 131.11 all (CH), 133,32, 137.04 (C=C), 164.61, 166.98 (C=O.)

^{1}HNMR result of (Z)-4-(4-(4,4,5,5-tetramethyl-1,3,2-dioxaborolan-2-yl) phenyl carbamoyl) acrylic acid
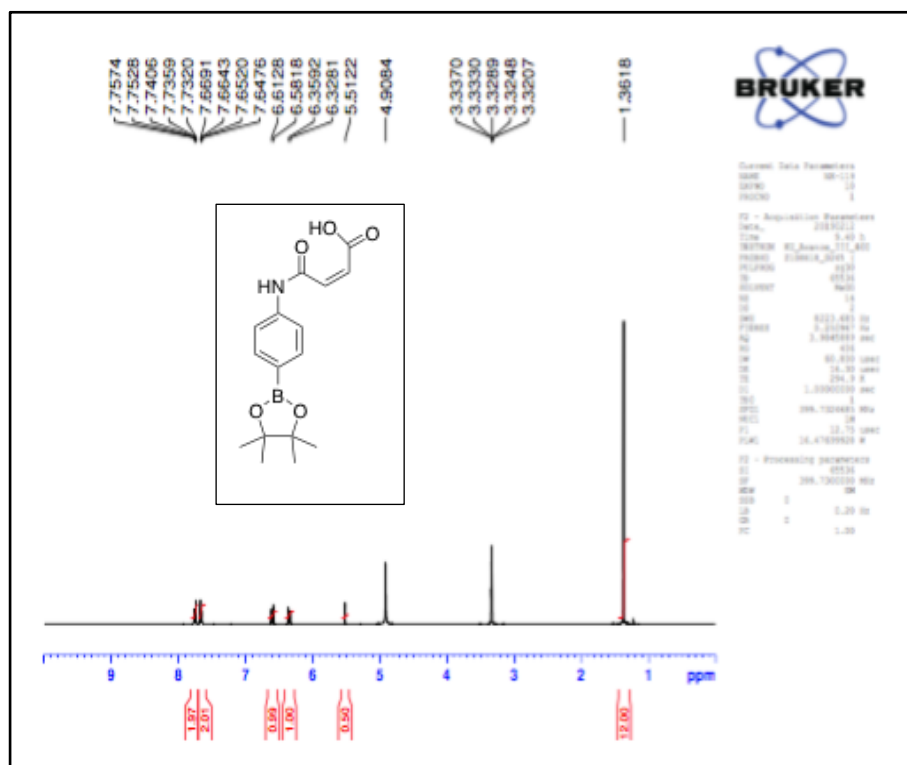
Figure 2. 23 ^{1}HNMR after 48 h: (Z)-3-(4-(4,4,5,5-tetramethyl-1,3,2-dioxaborolan-2-yl) phenyl carbamoyl) acrylic acid.

Shifts δ_H (400 MHz) (CD$_3$OD),1.36 (s,12H,CH$_3$), 3.33 solvent peak, 4.90 water content in NMR solvent, 5.51 (s,1H) for H-N, 6.34 (d, J= 12.4 Hz,1H), 6.59 (d, J =12.4 Hz, 1H), 7.65 (d, J= 6.8, 6.8 Hz, 2H), 7.74 (d, J= 6.7, 3.4 Hz, 2H). OH of carboxylic acid did not appeared.
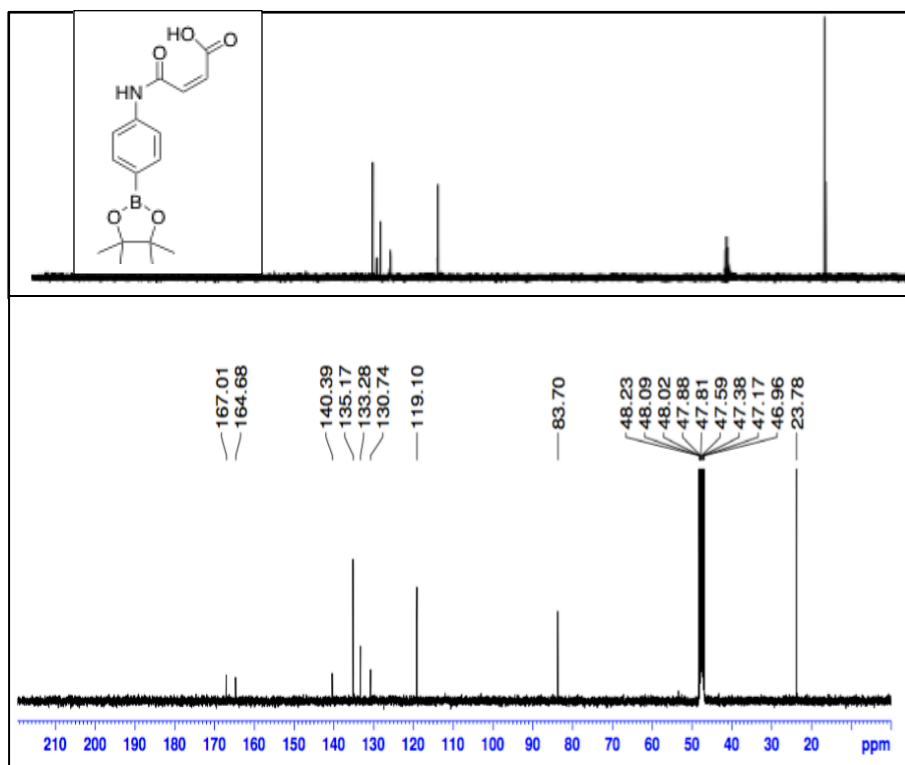
Figure 2. 24 ^{13}C NMR: (Z)-4-(4-(4,4,5,5-tetramethyl-1,3,2-dioxaborolan-2-yl) phenyl carbamoyl) acrylic acid.

^{13}C (100 MHz) (CDCl$_3$) δ = 23.78 (4 x CH3), 83.70 (C), 119.14, 130.74, 133.28 all (CH), 135.17 (2 x CH of double bond), 140.39 (C), 164.68 (C=O), 167.02 (COOH).

Maleic anhydride is used for polymerization. The synthesis of the monomer is sensitive to time. 48 h reaction requires crystallization, and 12 h reaction is neat.

A second step can be added if the monomer is used for polymerization; otherwise, this can be crosslinked with chitosan for sugar sensitivity. The yield of the second step reaction requires improvement. May be useful to carry out the reaction at a lower T.

2.18 MALDI-TOF and FTIR Results

MALDI-TOF mass spectrometry was developed in 1988 by Hillen kamp and Karas for the analysis of large biomolecules, but it did not demonstrate until 1992 that synthetic polymers can also analyse molecular weight above 100 000 Da. The main

reasons for this delay are; first, the methods of sample preparation for biopolymers with water-based solvents did not apply to most synthetic polymers, and second synthetic polymers are always polydisperse (Hillenkamp et al., 1991). MALDI-TOF demonstrated the formation of a new oligomer and dendrimer as new peaks appeared. Obtained spectra are similar to previously reported.

Mass spectra were recorded by external supplier with Waters LCT Premier (ES-ToF) / Acquity i-Class Ionisation: Electrospray (ES), which provides both low- and high-resolution data in both positive and negative modes by MEDAC ltd.

The mass spectra also confirmed the molecular weight of the polymer, for number ordinary equation 2.2 is used in the calculation

$M_n = \Sigma n_i M_i / \Sigma n_i$.

Equation 2. 2 Average molecular number of the polymer.

For the weight, average equation two is used

$M_w = \Sigma n_i M_i^2 / \Sigma n_i M_i$

Equation 2. 3 Average molecular weight of the polymer.

The average number of the polymer is calculated by using the (n_i) the intensities of signals, and (M_i) is the corresponding mass. The average molecular weight (Mw) is also calculated according to the formula 2 considering the n_i and M_i values. High-resolution Mass spectrometry allows accurate determination of monomers unites and the isotopic pattern of the oligomers. The measured mass for this synthesis of polyglycerol was 3118.01 g mol^{-1}.
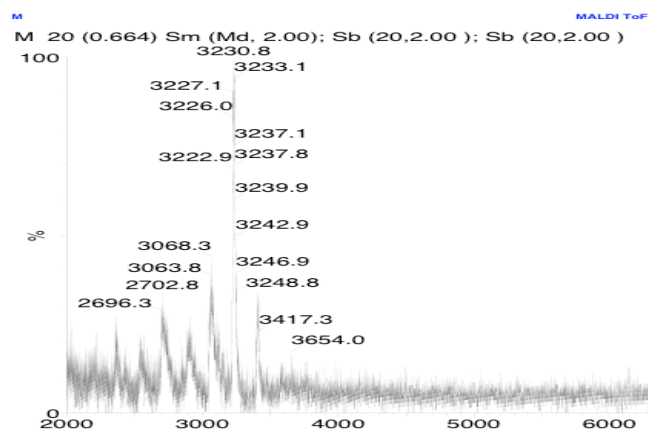
Figure 2. 25 MALDI-TOF map of each m/z represents a point in the raw spectral data or a point in the signal which is taken in the calculation for the average molecular weight of the polymer.

Table 2. 5 polymer Mass spectrometryresult and polydispersity (PD).

Synthesized polyglycerol Sample ID	Core unit	Active monomer	Acid % used	MALDI TOF	PD
	Glycerol	Glycidol			
39.1	1	1	10	3488.62	1.08
43.1	1	4	50	2466.74	1.82
44.1	1	1	50	1657.31	1.27
32.1	1	1	10	3118.01	1.01
32.2	1	1	10	3178.69	1.02

Table 2. 6 Polymers Mass spectrometryresult and polydispersity (PD).

Synthesized polyglycerol Sample ID	Core unit	Active monomer	Acid % used	MALDI-TOF	PD
	Pentaerythritol	Glycidol			
40.1	1	1	10	846.88	1.04
41.1	1	1	50	655.57	1.02
45.1	1	4	10	570.78	1.03
42.1	1	4	50	971.52	1.02

Mass spectrometry result shows that glycerol and glycidol give a higher mass over charge ratio (m/z) than pentaerythritol. However, gives similar polydispersity index (PDI) for both 10% acid and 50% acid. That shows the catalyst has not much effect than the structure of core unit is more obvious to have impact on the molecular weight of the polymer.

(A)

(B)
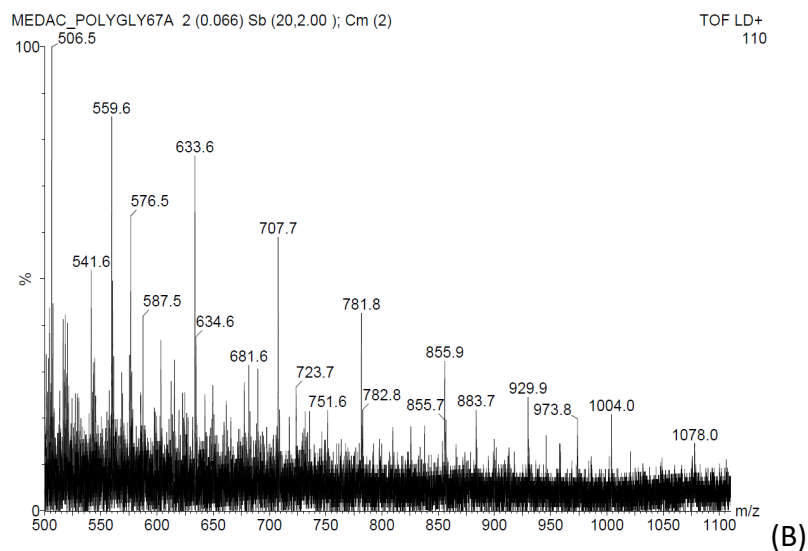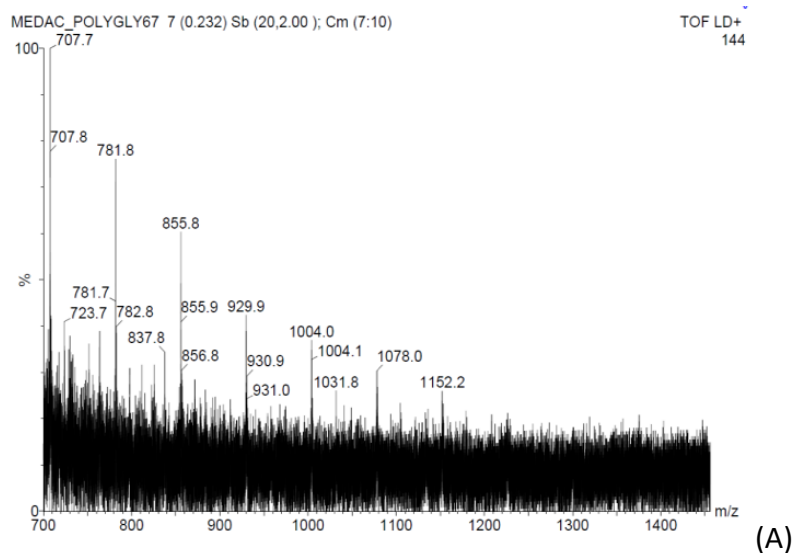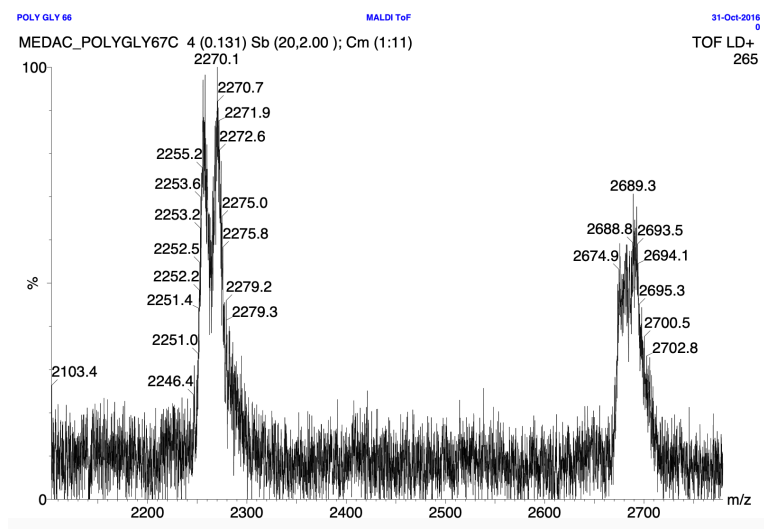
Figure 2. 26 MALDI-TOF spectrum of (Polyglycerol) (A), (B) and (C). Each m/z signifies a point in the raw spectral data or a point in the signal which is carried in the calculation for the average molecular weight of the polymer.

The number and weight average molecular weight of the synthesized polymer was calculated considering each peak.

The mass spectra also confirmed the molecular weight of the polymer the polydispersity index (PDI) was also calculated from the weighted average over number average molecular weight.

Fourier-Transform Infrared (FTIR) spectroscopy was performed with the help of Thermo-Scientific Nicolet iS5 with iD5 ATR by taking a small amount of all the reactants and products formed during each procedure carried out.

The FTIR spectrum attained gives an indication of the functional groups which were desired for PG. The OH group is evident at $3373.91 cm^{-1}$, which characterises the OH group. The sharp peak at 1085.43 implicates the CO bond.

2.18.1 Acid-catalyzed polymerization of glycerol

Significant bands corresponding to polyglycerol were observed, such as -OH stretching at 3377.43 cm^{-1}, asymmetric C-H stretching at $2994.52–2887.79$ cm^{-1}, -CH at 1416.08 cm^{-1}, C-O-C stretching at 1107.29 cm^{-1}. FTIR investigations indicate

that the resultant adhesive is composed of polyglycerol. A detailed FTIR peak is in the table below.

Table 2. 7 significant bands are corresponding to polyglycerol by FTIR

Functional group	Wavenumbers (cm^{-1})	Literature values (cm^{-1})
OH	3330.26	2500-3300
C-H stretching	2941.38	2500-3300
C-H (CH$_2$, CH$_3$)	1404.71	1480-1575
C-O-C	1037.93	1250-1050
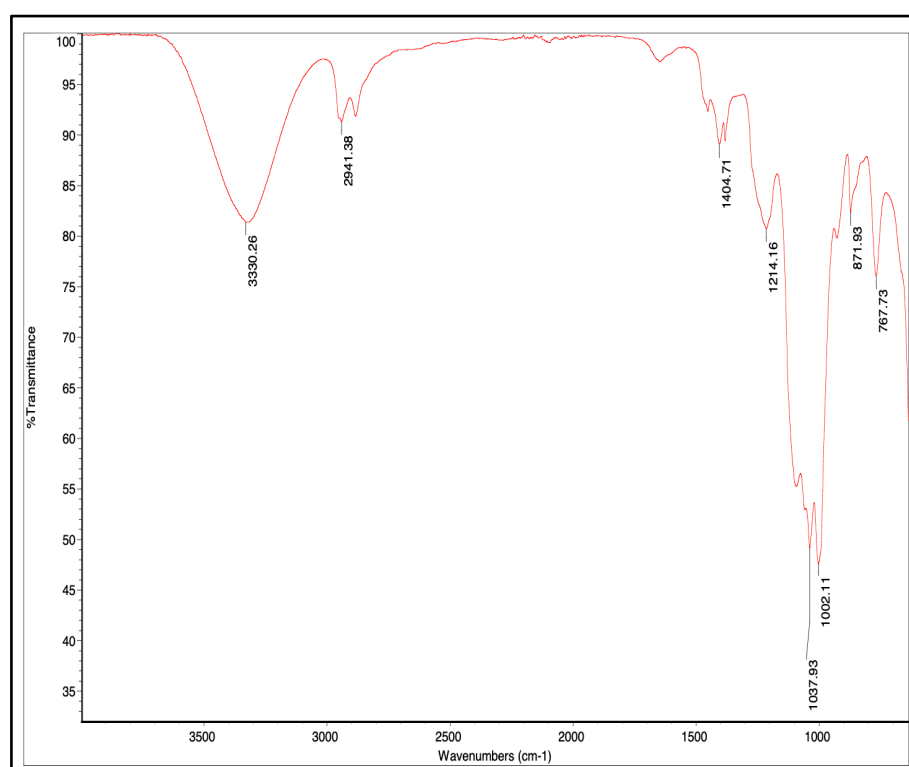
Figure 2. 27 Acid-catalyzed polymerization of glycerol in glycerol as core unit and glycidol.

FTIR frequencies of acid-catalysed polymerization of glycerol in glycerol as core unit and glycidol.

Table 2. 8 FTIR frequencies of polymerisation of pentaerythritol and glycidol

Functional group	Wavenumbers (cm^{-1})	Literature values (cm^{-1})
OH	3296.54, 3287.59	2500-3300
C-H stretching	2934.41, 2878.17	2500-3300
C-H (CH$_2$, CH$_3$)	1416.78	1480-1575
C-O-C	1107.01, 1030.29	1250-1050
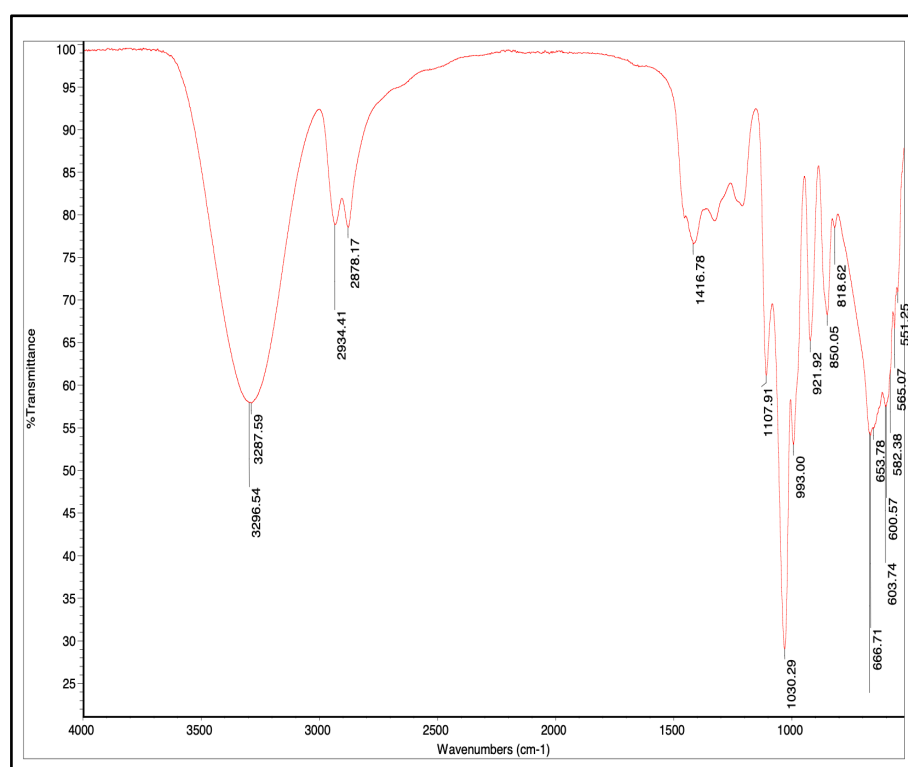
Figure 2. 28 FTIR spectra of polymerization of pentaerythritol and glycidol

Table 2. 9 FTIR signals of ester bond formation of polyglycerol and phenylboronic acid pinacol ester.

Functional group	Wavenumbers (cm^{-1})	Literature values (cm^{-1})
OH, of COOH	2980.31, 2929.07	2500-3300
C-H stretching	2539.07	2500-3300
C-H (CH$_2$, CH$_3$)	1682.51,1560.72	1480-1575
C-O-C	1267.89	1250-1050

C=O	1682.51	1600-1700
Aromatic Group	943.05, 827.22	800-900
B-OH plane	1213.31, 1312.83	1230-1330
B-OH bending	1086.47	1000
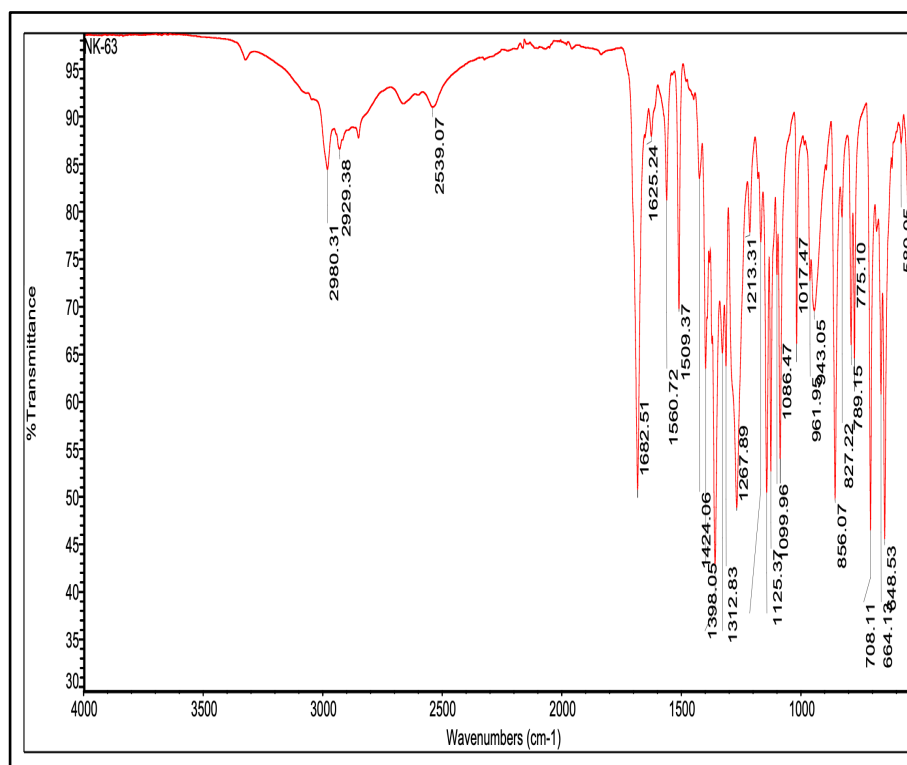
Figure 2. 29 FTIR of ester bond formation of polyglycerol and phenylboronic acid pinacol ester.

Transesterification with Polystyrene supported PBA resin (Deprotection of pinacol ester)

Table 2. 10 FTIR analysis of deprotection with diethanolamine and phenylboronic acid (PBA).

Functional group	Wavenumbers (cm^{-1})	Literature values (cm^{-1})
OH of COOH	2934.56	2500-3300
C-H (CH2, CH3)	1560.33	1480-1575
C=O	1644.33 -1704.56	1600-1700
Aromatic Group	801.12 - 857.32	800-900

B-OH plane	1313.37 -1399.12	1230-1330
B-OH bending	1017.17	1000

To confirm the deprotection, an NMR of a blank sample was made from

4-carboxyphenylboronic pinacol ester and diethanolamine in ether, and to confirm the removal of diethanolamine, a salt of diethanolamine was made by mixing it with TMS chloride.

Table 2. 11 Deprotection of pinacol ester with diethanolamine after extraction FTIR of the aqueous part

Functional group	Wavenumbers (cm^{-1})	Literature values (cm^{-1})
OH, of COOH	3303.70,2956.13, 2783.16	2500-3300
C-H (CH_2)	1444.24	1480-1575
C=O	1645.24	1600-1700
Aromatic Group	803.68, 939.45	800-900
B-OH plane	1213.56	1230-1330
B-OH bending	1029.24	1000
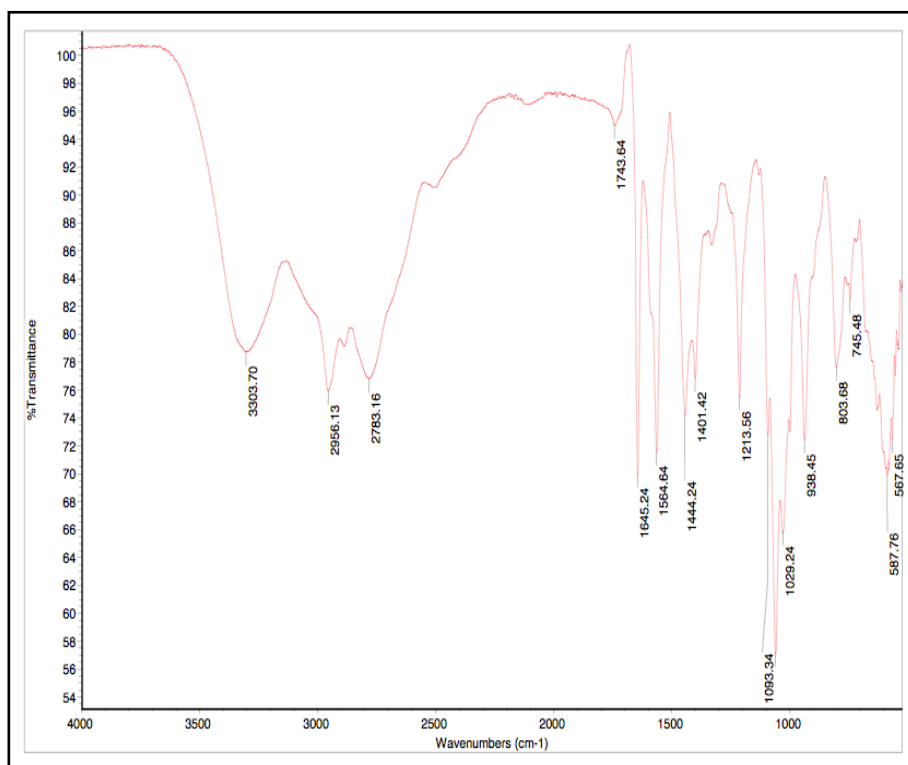
Figure 2. 30 deprotection of pinacol ester with diethanolamine after aqueous extraction part.

Table 2. 12 FTIR signals of different functional groups for deprotection of pinacol ester with diethanolamine after aqueous extraction part.

Functional group	Wavenumbers (cm^{-1})	Literature values (cm^{-1})
OH, of COOH	2980.44, 2926.67, 2849.39	2500-3300
C-H (CH2, CH3)	1509.06, 1560.79	1480-1575
C=O	1682.68	1600-1700
Aromatic Group	892.15, 962.40	800-900
B-OH plane	1268.60, 1314.88	1230-1330
B-OH bending	1016.44	1000
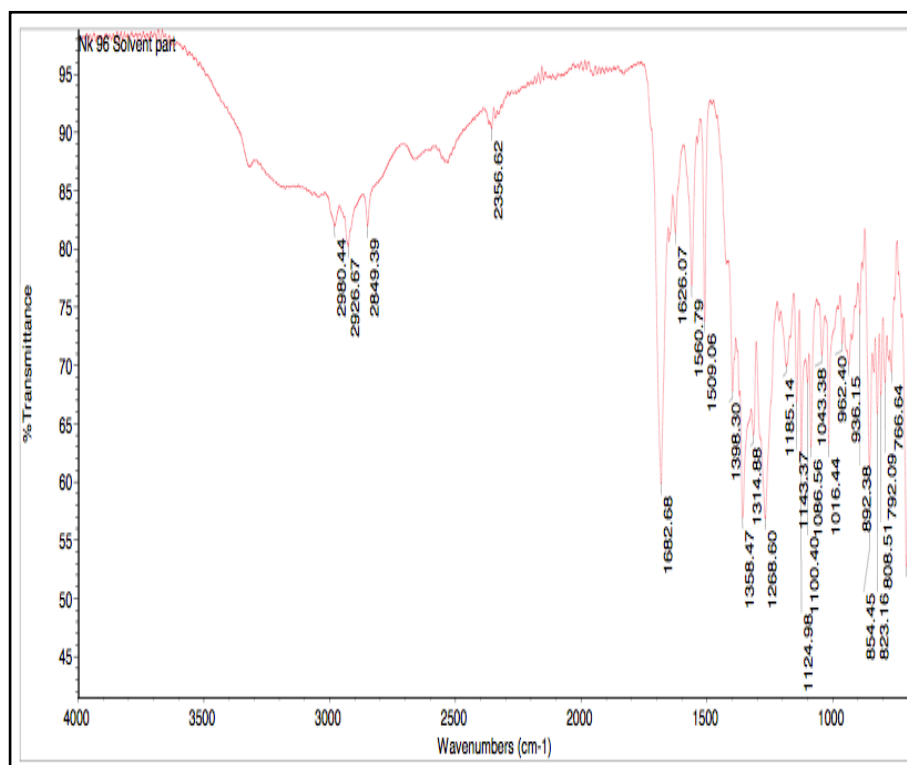
Figure 2. 31 deprotection of pinacol ester with diethanolamine after extraction solvent part.

From FTIR and NMR data, it looks that the deprotection with diethanolamine (Sun et al., 2011) is not successful; therefore, other methods of deprotection were carried out. The other method for deprotection of pinacol used is to pursue the reaction with phenylboronic acid supported resin (A.Hutton, 2004) and to use of the biphasic system (Simon J.Coutts, 1994). However, there is still the using of LiOH (Alexander K L Yuena, 2005). still to be carried out. Although various trials were made to deprotect the pinacol for the end functional boronic acid polymer, finally using a different deprotection method was successful. The polymerisation of end functional polyglycerol and deprotection was carried out using of DL-1,2-isopropylidene glycerol with 4-carboxyphenylboronic acid pinacol ester formation resulting in polyglycerol-based Phenyboronic acid followed by deprotection of pinacol.

2.18.2 Deprotection of pinacol ester using biphasic solvent method 2 mM HCl and hexane

The deprotected polymer 83 precipitated in cold acetone dried over vacuum overnight an NMR of both dried hexane layer (158s) and the aqueous layer (158a) was carried out (Simon J.Coutts, 1994). The NMR showed traces of pinacol ester impurities in the aqueous polymer phase, which further purified by precipitating in cold acetone for three times. The FTIR was conducted for both the aqueous layer and solvents layer.

Table 2. 13 deprotection of pinacol ester using biphasic solvent method 2 mM HCl and hexane aqueous part.

Functional group **158 a**	Wavenumbers (cm^{-1})	Literature values (cm^{-1})
OH, of COOH	3071.41, 2361.21	2500-3300
C-H (CH_2)	1493.48, 1574.42	1480-1575
C=O	1694.19, 1601.96	1600-1700
Aromatic Group		800-900
B-OH plane		1230-1330
B-OH bending		1000
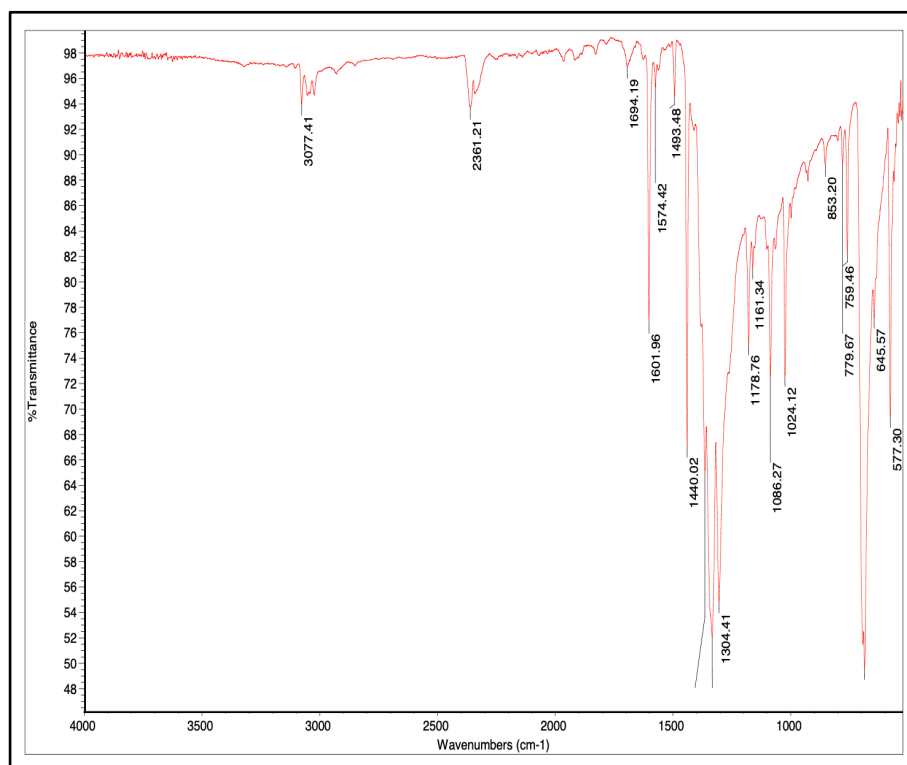
Figure 2. 32 FTIR of deprotection of pinacol ester using biphasic solvent method 2 mM HCl and hexane aqueous part.

Table 2. 14 Deprotection of pinacol ester using biphasic solvent method 2 mM HCl and hexane solvent part.

Functional group 158 s	Wavenumbers (cm^{-1})	Literature values (cm^{-1})
OH, of COOH	2980.62, 2929.47	2500-3300
C-H (CH2)	1509.71, 1561.54	1480-1575
C=O	1682.54	1600-1700
Aromatic	855.55, 962.08	800-900
B-OH plane	1226.62, 1313.44	1230-1330
B-OH bending	1016.86	1000
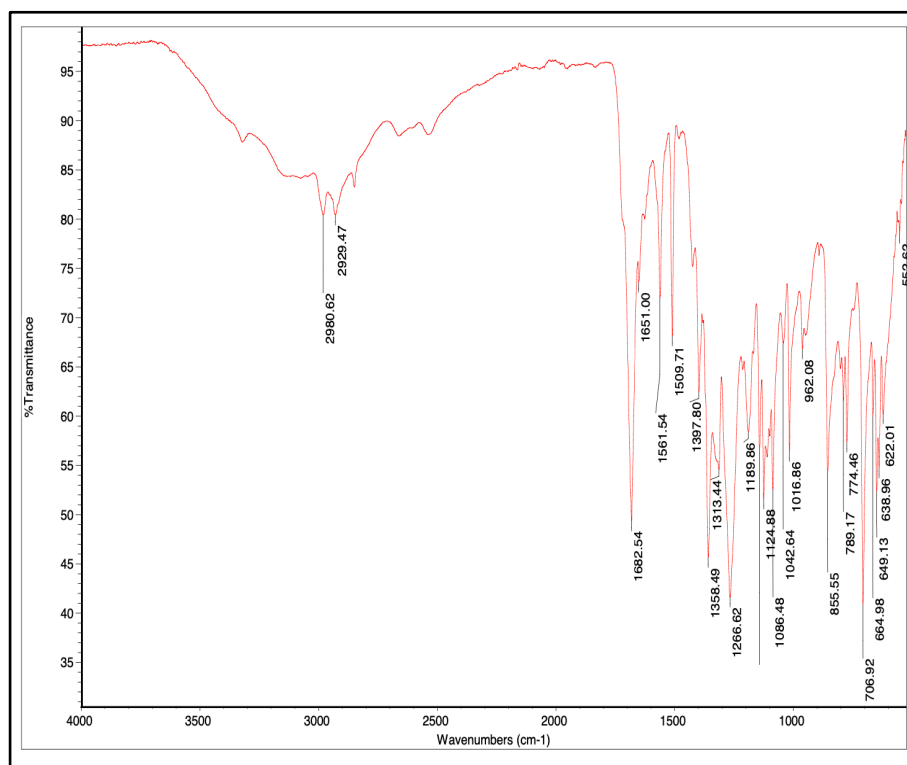
Figure 2. 33 deprotection of pinacol ester using biphasic solvent method 2 mM HCl and hexane solvent part.

2.18.3 Carboxylic acid formation of polyglycerol (LMW)

Using Dioxane and DMAP, Synthesis of terminal carboxylic acid group using phthalic anhydride

FTIR result of (polymer 157) are listed in the (table 2.15)compared with literature values.

Table 2. 15 FTIR signals of carboxylic acid formation of polyglycerol (LMW)using Dioxane and DMAP, synthesis of a terminal carboxylic acid group using phthalic anhydride.

Functional group 157	Wavenumbers (cm^{-1})	Literature values (cm^{-1})
OH, of COOH	3071.80, 2650.14	2500-3300
C-H (CH$_2$)	1496.46, 1403.65, 1470.42	1480-1575
C=O	1848.27, 1790.06, 1758.96	1600-1700

| Aromatic Group | 973.42, 838.16 | 800-900 |
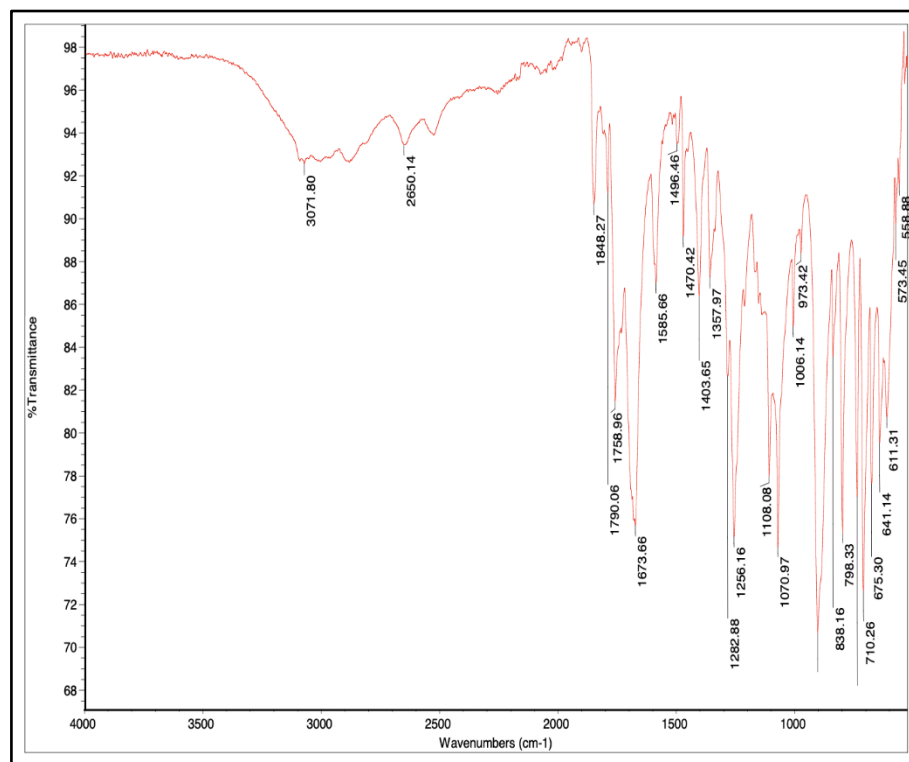
Figure 2. 34 FTIR spectra of carboxylic acid formation of polyglycerol (LMW)using Dioxane and DMAP, Synthesis of a terminal carboxylic acid group using phthalic anhydride (157).

2.18.4 Polyglycerol Carboxylic acid Phthalic anhydride reaction, formation of amide bond.

Polyglycerol phthalic anhydride was added into 50 mL DCM, 3-Amniophenylbornic acid added in the presence of 1-(3-Dimethylaminopropyl)-3-ethyl carbodiimide Hydrochloride coupling reagent for amide bond formation (160).

Table 2. 16 FTIR signals of polyglycerol carboxylic acid, phthalic anhydride reaction with 3 amino phenylboronic acid formation of an amide bond.

Functional group 160	Wavenumbers (cm^{-1})	Literature values (cm^{-1})
OH, of COOH	2975.79	2500-3300
C-H (CH2)	1469.40	1480-1575
C=O	1785.1, 1715.92	1600-1700

73

N-H	1591.52	1600
C-O	1018.94	1000
Aromatic Group	962.81, 858.14	800-900
Ar-N	1256.40	1200
B-OH plane	1226.62, 1313.44	1230-1330
B-O bending	1016.86	1000
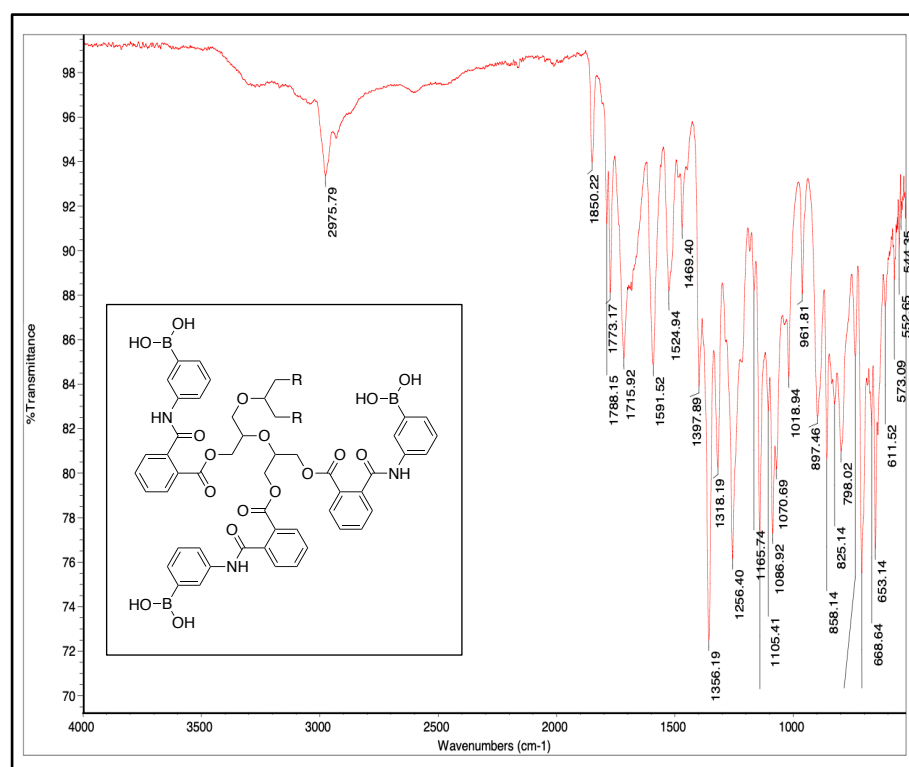
Figure 2. 35 FTIR spectra of polyglycerol carboxylic acid phthalic anhydride reaction with 3 amino phenylboronic acid formation of an amide bond.

2.18.5 Preparation of DL-1,2-isopropylideneglycerol with 4-carboxyphenylboronic acid pinacol ester

These experiments were carried out to synthesis novel compound for polymerisation of polyglycerol by acid deprotection of isopropyl from glycerol group. Polymer (153) confirms the formation of the product confirmed by NMR, GC-MS and FTIR. The polymerisation of Isopropyl glycerol carboxylic acid pinacol ester was carried out successfully.

Table 2. 17 FTIR signals (cm^{-1}) of DL-1,2-isopropylideneglycerol with 4-carboxyphenylboronic acid pinacol ester

Functional group (polymer 153)	Wavenumbers (cm^{-1})	Literature values (cm^{-1})
OH, of COOH	2980.47	2500-3300
C-H (CH2)	1561.84, 1450.80	1480-1575
C=O	1709.97	1600-1700
Aromatic Group	973.58, 930.87	800-900
C-O	1052	1050-1150
CH3 (bending)	1335.49, 1399.83	1350-1480
B-C	1309.75	1300
Aromatic Group	813.46, 973.58	800-900
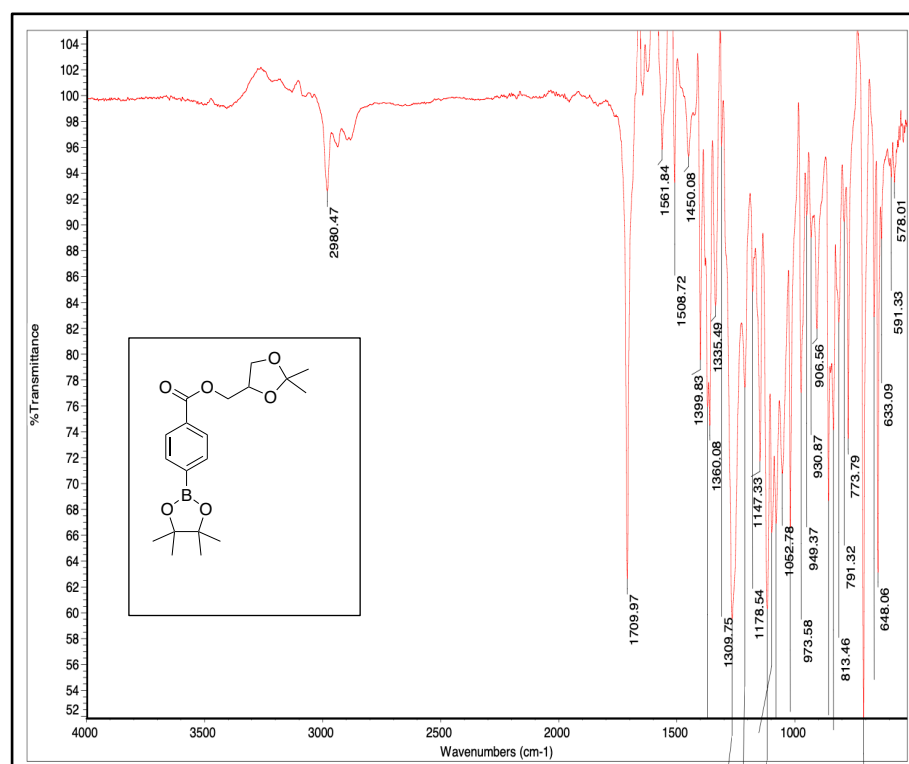
Figure 2. 36 FTIR spectra of DL-1,2-isopropylideneglycerol with 4-carboxyphenylboronic acid pinacol ester.

2.18.6 Deprotection of isopropyl phylphynylboronate

Deprotection (polymer 161) was carried out using a biphasic system of hexane and hydrochloric acid 1 M consequently freeze-drying. This is a transesterification with

phenylboronic acid and removals of the pinacol as the phenyl boronate ester. The procedure uses a biphasic system that takes advantage of the solubility difference in the pinanediol ester, the free boronic acid (both soluble in the aqueous phase), and the pinacol phenyl boronate ester (soluble only in the organic phase) (Coutts, 1994).

Table 2. 18 Deprotection was carried out using a biphasic system of hexane and hydrochloric acid 1 M consequently freeze-drying.

Functional group (Polymer 164)	Wavenumbers (cm^{-1})	Literature values (cm^{-1})
OH, of COOH	3023.46	2500-3300
C-H (CH2)	1580.92	1480-1575
C=O	1600	1600-1700
Aromatic Group	863.89	800-900
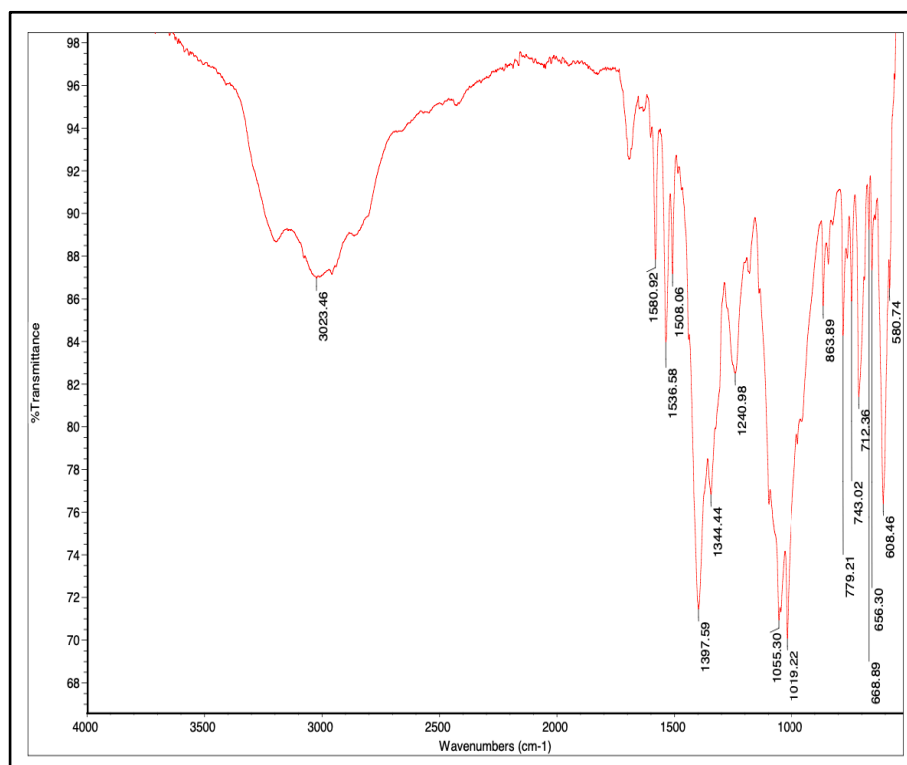
Figure 2. 37 FTIR spectra of deprotection of 161 polyglycerol isopropyl phenylboronic acid deprotection was carried out using biphasic system of hexane and hydrochloric acid 1 mM consequently freezedrying.

2.19 Conclusion

Polyglycerol was synthesized and end functionalized with sugar sensitive boronic acid group. Characterization of the sugar sensitive polymer was carried out using NMR, MADLI-TOF and FTIR. Methods for deprotection of pinacol required to obtain end functionalized polyglycerol for sugar sensing purpose. Deprotection methods were investigated, such as using phenylboronic acid supported resin, diethanolamine and a biphasic method using hexane and water (1:1) or hexane and HCl (1:1). However, there is still the using of LiOH to be carried out (Alexander K L Yuena, 2005). Although various trials were made to deprotect the pinacol for the end, functional boronic acid group, on polyglycerol, finally using a different deprotection method was successful. This method was the polymerization of DL-1,2-isopropylidene glycerol with 4-carboxyphenylboronic acid pinacol ester and in situ deprotection using glycerol and glycidol. The resulting compound was

77

polyglycerol-based Phenyboronic acid followed by deprotection of pinacol. The successful modification of the protection method is cost-effective and comfortable, with more than 90 % yield without further purification. This method applies to different amine and carboxylic acid boronic acid to find an efficient way of protecting carboxyphenylboronic acid (CPBA), amino boronic acid and giving phenylboronic acid to protect with pinacol ester. In this experiment, a universal method for the protection of boronic acid has been productively developed. The yield suggests the ideal conditions for the reaction and the number of molecular sieves for reaction time and solvent volume. The purity of the product confirmed by the melting point range suggests that the experiment for the formation of carboxyphenylboronic acid pinacol ester proceeded successfully. Therefore, it can be implied that the experiment with the ideal conditions can be repeated with ortho, meta, and para-substituted carboxyphenylboronic acid and is applicable for the protection of any boronic acid.

The synthesis of phenylboronic acid acrylamide monomer was successfully obtained via a green method using water and acetone, which is the main component of a smart glucose-sensitive system with a sugar-sensing functional end. The monomer obtained is chemically stable and reproducible. The removal of pinacol esters from the polymer is challenging, making the $B(OH)_2$ bonds available for sugar-binding. Using diethanolamine and acid-assisted hydrolysis, deprotected boronic acid from pinacol moiety showed a low yield. Considering other possible deprotection methods. Polyglycerol is modified with phthalic anhydride to make the PG more organic soluble and then modified with amino phenylboronic acid pinacol ester.

Efficient protection method for ortho, meta and para boronic acid monomers were developed with high yield.

Amino phenylboronic acid pinacol ester (ortho, meta and para) reaction was carried out using maleic anhydride (Andrea Temperini 2009). These can be incorporated with a derivative of carboxymethyl chitosan (Weith et al., 1970) for nanoparticle formation and insulin incorporation. The same condition was used

for all three substituted monomers. Upon binding these monomers with the amine group of chitosan, it can be possible form nanoparticles followed by deprotection and study of the boronic acid for the sugar-binding property.

2.20 Future work

End functionalized polyglycerol will be incorporated to form nano or microparticles depends on the size (100 - 1000 nm), or polymeric micelles (20 -200 nm), depends on the size measurement by Zita sizer.

In this chapter, after all, attempts of polymerisation, the polymer formed from the monomer (DL-1,2-isopropylideneglycerol with 4-carboxyphenylboronic acid pinacol ester) is the novel method. This particular experiment resulted in the formation of glycerol-based phenyboronic acid polymer followed by deprotection of pinacol *In situ*. Therefore, this can be further tested first for elemental analysis, then for toxicity, nano or microparticle formation and consequently release profile with insulin followed by analysis and sugar sensitivity.

Chapter 3

The development of Hydrochlorothiazide oral solution using cosolvent systems: Solubility and stability studies

3.0 The development of Hydrochlorothiazide oral solution using cosolvent systems: Solubility and stability studies

In this study, solutions of Hydrochlorothiazide (HCTZ) with adequate physical and chemical stability were developed. The solubility of HCTZ was the biggest challenge in formulating it as an oral liquid formulation due to its extremely low water solubility. This study evaluated the solubility enhancement of HCTZ in PEG 400, polyglycerine and glycerol, the two polymers with high molecular weight polyglycerol and low molecular weight polyglycerol synthesised in the laboratory.

HCTZ is known as a BCS class IV drug with low solubility and low permeability (BNF, 2020). Possible environments which could enhance HCTZ solubility can have a negative influence on its stability. HCTZ is a diuretic drug, frequently used for the treatment of hypertension in combination with other medications. HCTZ is ideal for fixed combination formulations in hypertension treatment (Kenneth A. Connors, 1996). HCTZ is slightly soluble in water and has therefore poor gastrointestinal absorption. Its solubility is potentially improved by the addition of weak organic solvents.

Modification of drugs is also used for solubility, such as prodrug design and salt formation. Physical and inorganic bases that increase pH of solution can also be used. On the other hand, HCTZ undergoes alkaline hydrolysis in the presence of heat and moisture (Kenneth A. Connors, 1996).

In this chapter a cosolvent approach is used to overcome the poor water solubility of HCTZ. The non-polar hydrocarbon region in the cosolvent can reduce the aqueous system's ability to press out non-polar solutes by reducing the intermolecular hydrogen bonding network water. The solubilization effectiveness of a cosolvent depends upon the degree to which it weakens the surface tension of water by reducing the distance of water molecules than water in its pure form (Marta Rodriguez-Aller, 2015).

3.1 Introduction

A drug substance's solubility is the amount that is passed into the solution until equilibrium is established, and no further drug molecules can dissolve. According to the Food and Drug Administration (FDA), and the biopharmaceutical classification guidelines (BCS), a drug substance is considered highly soluble when its highest dose is entirely soluble in 250 mL (Equation 3.1)or less of aqueous media over a pH range of 1.0 - 7.5 (Kim, 1984).

The improvement of drug solubility remains one of the most challenging aspects of poorly soluble drugs and the drug development process. There are different approaches available in the literature to improve the solubility of poorly water-soluble drugs. These techniques are selected based on specific aspects of the drug under development, the nature of excipients in the formulation, and the drug's ideal dosage form. Water-soluble, biodegradable, and approved polymers are used in the cosolvent method for drug solubility.

3.1.1 Barriers to orally administered drugs

3.3.1.1 Physiochemical barrier (Permeability):

This parameter is for drug absorption permeability measurement, the rate of mass transfer across a biological membrane. When 85% of the drug is permeated, then the drug is highly permeable based on mass balance or compare to IV dose. In biopharmaceutical classification, some numbers are used, such as Absorption number (An), dissolution number (Dn) and dose number (Do) (Equation 3.3).

$$An = \frac{mean\ residence\ time}{mean\ absorption\ time}$$

Equation 3. 1 Absorption number (An)

If a drug is rapidly absorbed. The absorption time will be low and absorption number will be high and this is governed by equation (3.1).

3

$$Dn = \frac{mean\ residence\ time}{mean\ dissolution\ time}$$

Equation 3. 2 Dissolution number (Dn)

If a drug rapidly dissolves the dissolution time will be low and dissolution number will be high as per equation (3.2) Of drug.

$$Do = \frac{mass\ of\ a\ drug}{uptake\ volume\ V0\ x\ Cs}$$

Equation 3. 3 Dose number (Do)

Dose number is equal to mass divided by product of uptake volume (V_0) *250 mL and solubility of drug (Cs) saturation solubility.

(250 mL*) is the volume for maximum solubility of drug in water.

Class I			Class II		
High permeability	High An		High permeability	High An	
High solubility	High Dn		Low solubility	Low Dn	
	Low Do			High Do	
Class III			**Class IV**		
Low permeability	Low An		Low permeability		
High solubility	High Dn		Low solubility		
			All parameters are case		
	Low Do		dependent		

Figure 3. 1 Biopharmaceutical Classification System showing the effect of permeability and solubility on the absorption, dissolution and dose parameters.

3.3.2 Ionisation

The solubility of a drug depends on how much drug is ionized usually calculated as percentage (%) ionisation. Drugs are weak acids or bases. However, when they are

soluble, they undergo ionization. To understand the ionization, drug absorption can be predicted by calculation of percentage unionized drugs. The degree of ionization at a precise pH can be determined from its pKa value; also, it is given by the Henderson-Hasselbalch equation (Equation 3.4 and 3.5).

$$pH = pKa + \log(\frac{A^-}{HA})$$

Equation 3. 4 The Henderson–Hasselbalch equation relates the pH of a solution containing a mixture of the two components to the acid dissociation constant, Ka, and the concentrations of the species in solution.

$$\frac{A^-}{HA} = \frac{10^{\,pH-pKa}}{1}$$

$$\% \, ionised \; = \frac{10^{\,pH-pKa}}{10^{\,pH-pKa} + 1} \; x \; 100$$

Equation 3. 5 Calculation of percentage ionised drug using the pKa and pH values.

The drug pKa give information about how ionisable the drug is and the percentage ionisation can be predicted from the equations above. One of the physiological barriers in the digestive system is pH, as it varies across the gastrointestinal tract (GIT) track making ionization state changes according to the pH of the GIT site, there are different methods for overcoming poor aqueous solubility of drugs. These methods are chemical modification it is also possible for example, to get modification at solid-state, particle size modification, use at a cosolvent, using surfactant and lipids, and cryogenic methods can be used. Poorly water-soluble drugs can be improved by the techniques mentioned in (Figure 3.1).

Changes in particle size might modify the correlated characteristics, such as crystallinity, surface area, and porosity. This, in turn, can influence bulk features, product performance, processability, stability, and features of the end product (Gilbert S. Banker, 2007). Particles move across the membrane via diffusion.

Diffusion is the movement of any substance from high concentration to low concentration through a selectively permeable membrane (Figure 3.2). Facilitated diffusion is the same as passive diffusion; however, it works with the help of transport proteins, when the ions are polar, the support moves them. This is for the diffusion of polar molecules. Beside solution drugs must be able to diffuse across the intestinal membrane. Transcellular diffusion can either take place by passive or active diffusion. The latter is facilitated by active carriers.
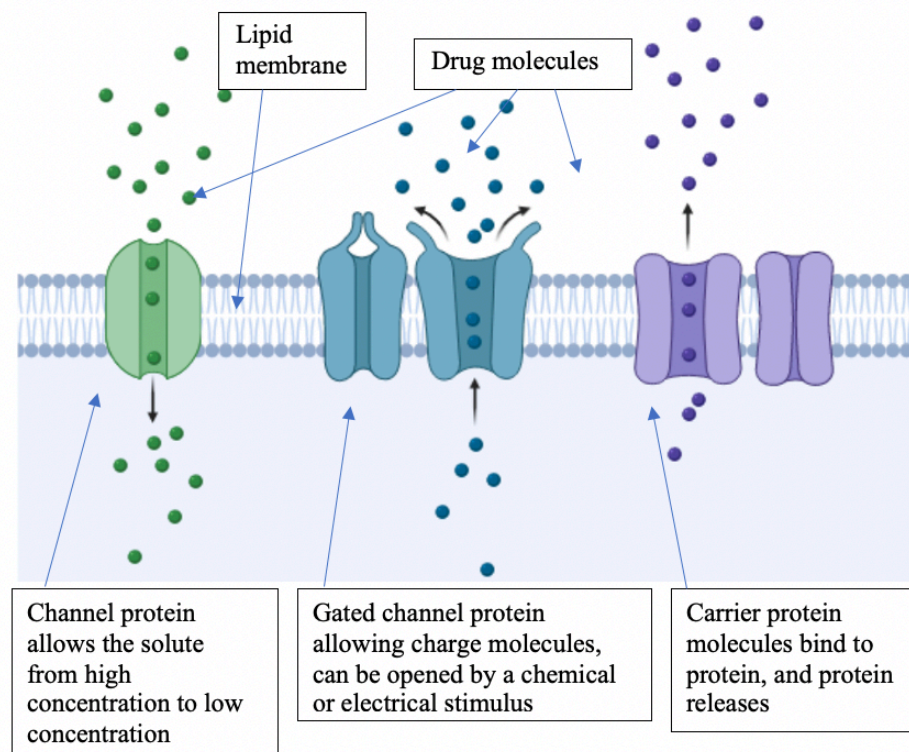
Figure 3. 2 A depiction of the lipid bilayer, which shows particle diffusion with the help of channel proteins (image assembled using dynamic BioRender).

3.2 Physiological barriers

Different physiological barriers hinder the absorption of oral drugs delivery such as pH, the effect of food and gastric emptying, and the cellular level.

3.2.1 The pH of the Gastrointestinal Tract (GIT):

The first barrier in the gastrointestinal tract is the extreme pH of stomach (1 -2) and its aqueous environment; this makes the absorption of basic drugs challenging. Besides, the extreme pH in the stomach affects the stability of drugs which can cause hydrolysis or degradation of drugs, therefore reducing the activity of drugs. If a drug passes as the pH of the stomach (1- 2), it enters the small intestine, which has a pH (5 - 7) and this affects the ionisation state of the drug (Figure 3.3). For further digestion and absorption, the content of the stomach will be emptied.
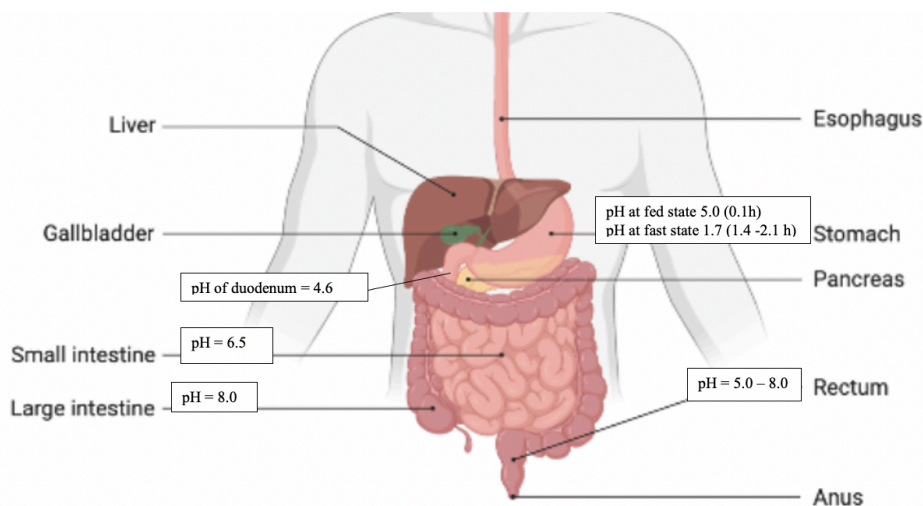
Figure 3. 3 Physical characteristics of the Gastrointestinal tract (GIT), with estimated values and representation of the GIT system, mostly result in the pH values referring to middle quantities. (Image assembled using dynamic BioRender software).

The viscosity of the lumen fluid will be increased, which then affects the absorption of the drug. However, some drugs are not compatible with dairy products, and other drug molecules are better to be taken with food. For instance, lipophilic drugs will dissolve better with heavy meals because of the secretion of bile salts that enable micelle formation. Besides, there are many enzymatic

activities in GIT that can metabolize the drug and reduce its bioavailability (Avdeef, 2012).

3.2.2 Mucus layer (hydrophobic and hydrophilic layer):

There are different mucus cells and layers with a thickness of 50 – 450 μm in the intestine. This layer protects the intestine from acid and microbes and inhibits diffusion of some material depending on the thickness of the mucus layer. There is a layer of water, glycoprotein, ions and other proteins which is called the unstirred water layer with a thickness of 40 μm. Drugs have to partition across the unstirred water layer and lipophilic molecules with poor water solubility will not diffuse. The mucus layer is composed of a high-molecular-weight (2 × 106 KDa) glycoprotein, which is 90% oligosaccharide, rich in sialic acid residues imparting a negative charge to the Intestine epithelium layer. Hence, it is permeable to hydrophilic compounds.

The tight junction (Figure 3.4) hinders paracellular diffusion and only enables drugs with low molecular weight (less than 200 Da) to be permeated. When the drug passes all the gastrointestinal barriers, it will enter the liver and can be removed by phase I and phase II metabolism.

3.4 Methods of improving the solubility of poorly soluble drugs

Solubility, by definition of IUPAC, is the analytical composition of a saturated solution shown as a proportion of a selected solute in a chosen solvent. Solubility is the drug concentration in a specific solvent and can be expressed in molality, mole fraction, mole ratio, and w/v % ratio. In drug discovery and formulation, drug solubility in water and organic solvent plays an important role. It affects many pharmaceutical processes, including design, synthesis, extraction, purification, formulation, absorption, and distribution in body fluids. The drug solubilisation is a dynamic process, which results from the simultaneous and opposing processes of dissolution and phase joining, for example, precipitation of solids.

Equilibrium in the solute and cosolvent happens when both processes are proceeding at a constant rate. Under specific conditions, the equilibrium and solubility may be exceeded to give a supersaturated solution, which is metastable (Yihong Qiu, 2009)

3.5 Solubility Enhancement Techniques

Solubility enhancement techniques are categorized in to physical or chemical modifications of the drug and other methods such as co-administration with soluble excipients. Physical modification such as particle size reduction or solid-state polymorphism can be considered. Chemical modification, such as salt formation or prodrug formulation can be used. Cyclodextrin (CD) inclusion complexes, Lipid-based drug delivery system Polymeric nanoparticles. Modification of pH, use of a different buffer, derivatization, complexation, and salt formation come under chemical modification (Figure 3.5).
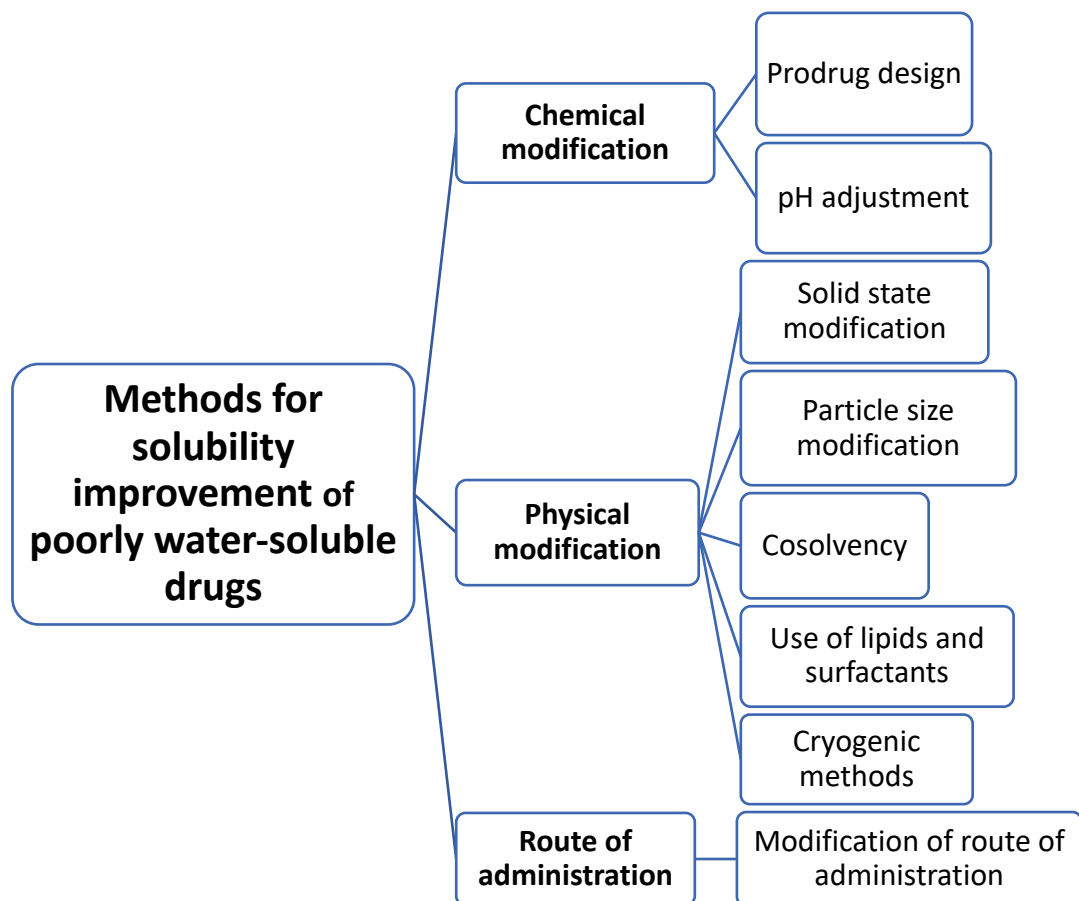
Figure 3. 5 A diagram illustrating the distinctive approaches of drug solubility.

Other methods such as supercritical fluid process, use of surfactant, solubilizers, cosolvency, hydrotrophy, and novel excipients are also studied in the literature. Each technique has advantages and drawbacks, which are summarised in table 3.1.

Table 3. 1 A list of solubility enhancement techniques included in the table below. In addition to examples, the advantages and disadvantages of these methods.

Modification	Example	Advantages	Disadvantages
Physical modification	Particle size reduction	Reduction of particle size increases surface area, therefore improved solubility, and absorption.	Degradation during grinding, reduction in drug shelf life
	Solid-state polymorphs	A drug in the amorphous state is highly soluble due to its thermodynamic properties.	Can revert to a crystalline form, short shelf life.
Chemical modification	Salt formation	Converting the insoluble form to a salt form of drug which can be ionized subsequently improve solubility and absorption.	It requires a drug with an ionizable functional group, and the salt should be ionizable at physiological pH
	Prodrug in which a drug will be activated by metabolic enzymes once in the digestive system.	A soluble inactive form of the drug is made, which is made active by enzymes once enter metabolism. Pro-drug administration is also a choice of interest to improve the bioavailability.	New chemical entity is required, which should be feasible with the drug is the active compound.

Cyclodextrin inclusion complexes	Incorporation of drug with cyclodextrins which has a hydrophilic cavity and hydrophobic surface and can form a complex with a hydrophobic drug.	It is only suitable for drugs which can fit the hydrophilic cavity of cyclodextrin cavity, therefore limited for specific drug molecules.
Cosolvent	Co-administration of drug with soluble excipients such as surfactants, water soluble polymers and solvents to improve solubility.	Can cause toxicity or precipitation upon adding solvents
Lipid based solubility methods	Formulation of microsome, liposome, noisome, and other lipid-based incorporation of drugs for solubility	Lipids drug interaction causes safety and efficacy issues.
Polymeric Nanoparticles	Drug molecule formulation into polymeric Nanoparticles.	To develop a comprehensive drug carrier, it depends on the Physicochemical property of the drug. Therefore, it is very challenging.
Cryogenic methods	Cryogenic techniques enhance the dissolution rate of drugs by creating nanostructured amorphous drug particles with a high degree of porosity at very low temperature.	Requires sophisticated instruments.

3.6 Physical modification

3.6.1 Particle size reduction:

Particle size modification is a physical process in which the size reduction of drugs particle increases the surface area, which improves the drug dissolution. Particle size reduction permits an efficient, reproducible, and economical means of solubility enhancement.

Other particle size reduction methods, such as spray drying, rely upon mechanical stress to disaggregate the active compound. Mechanical forces such as milling and often grinding significantly impact the drug product, which may induce degradation. The thermal stress which may occur during spray drying and grinding also is an issue when processing thermosensitive or unstable active compounds. In a study by Chu et al, looked at the particle size reduction of HCTZ . Particles were divided into different size groups. Group one from 600 to 250μm reduction of the particle group two $250 - 150$ μm, group three from $150 - 45$ μm and group four particles smaller than 45 μm, the surface area of HCTZ increased (Chu et al., 2012). This study suggested that with increasing specific surface area, even though there is an issue with the particle shape, the mean dissolution time showed a good correlation with each fraction's mean particle size (Chu et al., 2012)

3.6.2 Micronization

Micronization is another conventional technique for particle size reduction used in pharmaceutics. Micronization enhances the dissolution rate of drugs through the increased surface area. Micronization of drugs is carried out by jet mill, rotor-stator, and colloid mills. This method is not suitable for a formulation that has a high dose as it does not change the saturated solubility of the drug.

Okafor et al micronized partially pregelatinized maize starch (Starch 1500®) and microcrystalline cellulose (MCC) and their mixtures with HCTZ. It was noticed that drug particle size affects the blend segregation especially with low dose

formulations of micronized (HCTZ). It was reported that micronization of HCTZ significantly improved the dissolution rate from tablets due to particle size reduction and increased surface area. Nonetheless, further particle size reduction (<55 µm) of HCTZ did not increase dissolution rate (Okafor et al., 2001).

3.6.3 Particle size reduction (supercritical fluid (SCF)

Particle size reduction can also be achieved using supercritical fluid (SCF). This is a novel nanosizing and solubilization technology. Once the drug particles are solubilized within the Supercritical fluid (SCF) (usually carbon dioxide), they may recrystallize at a reduced particle size. At near-critical temperatures, SCFs are highly compressible and allow moderate changes in pressure to significantly alter their density and other fluid characteristics that largely determine their solvating power. The SCF processes are flexible and allow micronization of drug particles at the submicron level, with a reduced particle size range, often to submicron levels. Currently, SCF processes have demonstrated the ability to create nanoparticulate suspensions of particles with diameter between 5–2,000 nm.

3.6.4 Solid Dispersions (SD)

Solid dispersion (SD) applies to a group of solid products containing at least two different components, generally a hydrophilic matrix and a hydrophobic drug. This is a useful pharmaceutical technique for increasing the dissolution, absorption, and therapeutic efficacy of drugs in dosage forms. The common hydrophilic carriers for solid dispersion methods are polyvinylpyrrolidone (Povidone, PVP), polyethylene glycol (PEG), and surfactants like Tween-80, docusate sodium, Pluronic-F68, and sodium lauryl sulphate (SLS).

The solid dispersion method uses a group of solid products having a hydrophobic drug for example class IV, dispersed in at least one hydrophilic carrier, improving

surface area and enhancing drug solubility and dissolution rate. SDs are classified as into 3 generations as outlined in Figure 3.6.

1st classification	• Cryslaine carrier such as manittol, Fructose and glucose
2nd classification	• polymeric carrier • Synthetic polymers include povidone (PVP), PEG , and polymethacrylates • nd natural polymers include hydroxypropylmethylcellulose (HPMC), ethyl cellulose, and starch derivatives such as cyclodextrins (CDs).
3rd classification	• mix of surfactant and poymer • polymers • surfactsnts

Figure 3. 6 Classification of The solid dispersion (SD) method and materials used.

Solid dispersions with carriers that are dispersible in water such as polyethylene glycol (PEG 1500) and polyvinylpyrrolidone (PVP k30) are currently one of the most used strategies to overcome the limitations of water solubility. In a study by de Souza study, a specific ratio of (HCTZ/ PVP K30, 1:1 or 1:2 or 2:1) presented the best HCTZ dissolution increase, which contributed to greater bioavailability of HCTZ (Cinthya Maria Pereira de Souza, 2017).

3.6.5 Polymorphic behaviours:

A drug in the amorphous state is highly soluble compared to its crystalline state due to its thermodynamic properties. However, amorphous forms can go back to a crystalline form, reducing shelf life due to thermodynamic instability. Some

drugs have more than one crystalline structure called polymorphs. Polymorphic forms have different physical properties, such as solubility and melting points.

Previously four polymorphic forms (I, II, III and IV) of HCTZ had been characterized (Kim, 1984, Guillaume Binson, 2019). Based on X-ray diffractometry and differential thermal analysis, form I was obtained by crystallization from N,N-dimethylformamide and form II was crystallized from hot methanol. Form III was precipitated from sodium hydroxide aqueous solution by treatment with hydrochloric acid, and Form IV was crystallized from 50% methanol. Recently, analytical techniques identified the HCTZ IA polymorphic form and it was found to be the most soluble form (Saini, 2015, Kim, 1984, Guillaume Binson, 2019).

3.7 Chemical modification

3.7.1 Salt formation

Drugs are made either as a weak acid or a weak base. However, the salt form of the drug is not continuously optimal for dissolution or absorption into the body. Without absorption into the systemic circulation, a drug cannot have a therapeutic effect. Therefore, the salt formation of some drugs can help in improving the overall drug bioavailability. More than 50% of all drug molecules used in medicine are hydrochloride, sodium, or sulphate salts of that drug. According to the Food and Drug Administration (FDA), all drug products in salt forms are considered pharmaceutical alternatives and not pharmaceutical equivalents. Suppose these drugs contain the same active ingredient but are in the salt form. Salts are more stable forms of the drug as they usually have few amorphous forms, as well salt formation increases the stability and prolongs shelf life. The principal purpose of forming a salt is to enhance the amount of drug in solution

3.7.2 Prodrug:

A prodrug is a drug substance that is inactive and is converted into the pharmacologically active agent by a metabolic or physicochemical process that takes place *in vivo*. Prodrugs that exist naturally or were produced accidentally through drug development include aspirin, codeine, heroin, and L-dopa. Other prodrugs were prepared as part of the pharmaceutical processes to reach a specific target such as nonsteroidal anti-inflammatory drugs or penicillin-related agents (bacampicillin, amoxicillin). Prodrugs are classified either based on the therapeutic category such as anticancer prodrugs, antiviral prodrugs, antibacterial prodrugs, nonsteroidal anti-inflammatory prodrugs, cardiovascular prodrugs, or based on synthetic linkages that attach to the active drug. For instance, ester prodrugs, glycosidic, bipartite, tripartite, and antibody, gene, virus-directed enzyme prodrugs. Also, based on operative categories using strategic approaches to avoid insufficiencies inherent to the active drug, for example, prodrugs for improving site-specificity, prodrugs to bypass high first-pass metabolism, prodrugs for improving absorption, for reducing the adverse effect. There is no prodrug of HCTZ in the market. However, there are potential sites for HCTZ to be developed as a prodrug, HCTZ is used as a mixture of some other drug which is available in the market, for example, Telmisartan, Amlodipine & Hydrochlorothiazide Tablets.

3.7.3 Solvent Evaporation

The solvent Evaporation Method developed by Tachibana and Nakamura in which they dissolve both the carrier and the drug in a universal solvent and then evaporate the solvent under vacuum to produce a reliable solution (Nakamura, 1965). Many groups studied solid dispersion, which suggests that the solvent evaporation technique can be employed successfully to improve and stabilize the solid dispersions of poorly water-soluble drugs. The main benefit of the solvent evaporation method is that thermal breakdown of drugs or carriers can be

stopped because of the low temperature needed for the evaporation of solvents. However, the drawbacks associated with this method are the high cost of preparation, the trouble in completely removing the solvent, the possible adverse effect of the supposedly negligible amount of the solvent on the chemical stability of the drug, the selection of a universal organic solvent, and the difficulty in reproducing crystal forms. A delivery system for an increased dissolution rate of HCTZ was developed suggesting an overall prospective to increase the availability of HCTZ at the absorption site when used *in vivo* (Chikukwa et al., 2020). The size of the microparticles may reduce the difficulty in swallowing medicines reported in this target population. Microparticles produced by the solvent evaporation method with an encapsulation efficiency > 75% hydrochlorothiazide. Therefore, the microparticulate technology can offer a potential resolution to the half-life mediated dosing frequency, and a release of hydrochlorothiazide of > 80% suggests an improvement in limited solubility dissolution (Chikukwa et al., 2020).

3.8 Inclusion Complex Formation Technique

Inclusion Complex with cyclodextrin: This is a solubility enhancement technique that has been employed more precisely to improve the hydrophilic solubility, dissolution rate, and bioavailability of poorly water-soluble drugs dosage forms. There are three naturally occurring cyclodextrins (CDs) are α-Cyclodextrin, β-Cyclodextrin, and γ-Cyclodextrin that are used in this method and have been studied extensively for safety.
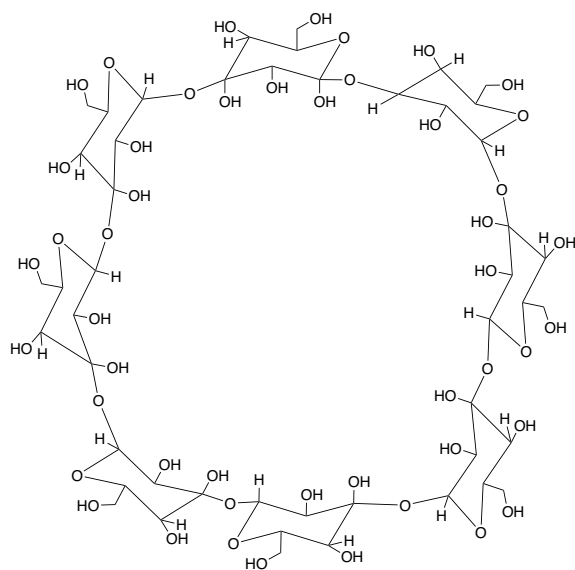
Scheme 3. 1 α- cyclodextrin (* Cyclodextrine are named α, β, and γ by order of a 6, 7 or 8 for the number of glucose molecules).

Cyclodextrins are relatively large molecules with a hydrated external surface. Under the usual conditions, cyclodextrin molecules only permeate biological membranes with considerable difficulty. Cyclodextrins can enhance the permeation of poorly soluble drugs through biological membranes. Excess of the concentration of cyclodextrins can decrease the permeability of drugs (a, β, and γ, Cyclodextrins) (Irie and Uekama, 1999).

When a nonpolar molecule or the nonpolar region of one molecule (known as a guest) inserted into the space of another molecule or group of molecules (host), inclusion complexes formed. Cyclodextrins are the most common host molecules. Cyclodextrins molecules are non-reducing, crystalline, water-soluble, and cyclic oligosaccharides consisting of glucose monomers arranged in a doughnut-shaped ring having a hydrophobic cavity and hydrophilic outer surface. The effect of β-cyclodextrin and different surfactants on solubility, stability, and permeability of HCTZ was studied. According to the solubility data, the composition complex with HCTZ provides the best improvement of solubility 28 folds compared to 3 folds using tween 80. Besides, the formation of a 1:1 complex ratio was found based on the applied calculation. Degradation half-life for HCTZ in water was found to be

9.5 h compared to > 260 h at the higher selected collections of β-CD (Altamimi, 2018).

3.9 Media Milling

When using the media milling technique, a nanosuspensions are prepared using high shear. Dry media mills are used for the finest powders. However, wet media mills are used for making slurries which then can be processed by cryogenic or spray during techniques to form powders.

In practice, milling is carried out to facilitate the extraction of crude drugs or improve their bulk processing properties. Milling is a procedure where mechanical energy is applied to the drugs molecules to break down the coarse drug particles into fine particles. Hence, it is regarded as a "top down" approach in the production of fine particles. Products that are possessed through milling have specific physical attributes that contribute to improved drug dissolution and solubility. Milling reduces the size and alters the size distribution of the drug particles. There are different milling procedures, such as tumbling ball mill, agitated ball mill, planetary mill, vibrational mill, and centrifugal mill, which works on different mechanisms. The mechanism is ball-ball impact, ball-ball pressure, ball-ball sheer, or a combination of these mechanisms above.

The milling chamber is filled with milling media, water, drug, and a stabilizer is rotated at a high-shear rate under controlled temperatures for several days. The milling medium is made of glass, Zirconium oxide, or cross-linked polystyrene resin. Shear forces generated because of the impaction of the milling media with the drug results in the breaking of the microparticulate drug to nanosized particles. A high-pressure homogenization technique is used to prepare nanosuspension of many poorly water-soluble drugs. The drug suspension and surfactant come under pressure through a nanosized aperture valve of a high-pressure homogenizer. This method is based on cavitation in the aqueous phase.

The cavitation forces within the particles must be high to change the drug microparticles into nanoparticles. The problem with this method is the need for small sample particles before loading. Therefore, many cycles of homogenization are required.

3.10 Combined Precipitation and Homogenization

The precipitated drug nanoparticles tend to continue crystal growth to the size of microcrystals. They need to be processed with high-energy forces (homogenization). The particle is either amorphous, semi-amorphous, or crystalline. This method can create problems in long-term stability and bioavailability, so the precipitated particle suspension requires homogenization to preserve the particle size obtained after the precipitation step.

3.11 Cryogenic techniques

Spray freezing onto the Cryogenic Fluids method is when the drug formulation and the carriers such as mannitol, maltose, lactose, inositol, or dextran are dissolved in water are used. Cryogenic techniques are developed to enhance the dissolution rate of drugs by creating nanostructured and amorphous drug particles with a high porosity level at very low-temperature requirements. Cryogenic methods such as Spray Freezing into Cryogenic Liquids (SFL), Spray Freezing onto Cryogenic Fluids (SFCF), Ultra-Rapid Freezing (URF), Spray Freezing into Vapor over Liquid (SFV/L), would be defined by the type of device (capillary, rotary, pneumatic, and ultrasonic nozzle), location of the nozzle.

After cryogenic processing, dry powder amorphous form of the drug can be obtained by various drying processes like spray freeze drying, atmospheric freeze-drying, vacuum freeze-drying, and lyophilization.

3.12 Physical and physiochemical properties of hydrochlorothiazide

HCTZ is available in capsule and tablet dosage forms. HCTZ is a thiazide diuretic also called a (water pill). It is used to help reduce the amount of water in the body by increasing the flow of urine. It is used only or composed with other medicines to treat high blood pressure, fluid retention alone that is caused by congestive heart failure, severe liver disease (cirrhosis), kidney disease, or treatment with a steroid or hormone medicine. Thiazides have been linked with hyperlipidaemia, hyperglycaemia, new-onset diabetes, hypokalaemia, and hyperuricemia and stimulation kidney. (Deppeler, 1981)
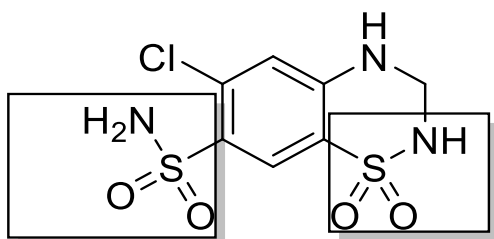
Scheme 3. 2 The chemical structure of HCTZ pKa = 9.7, 6.8

Moreover, according **to** MHRA all patients treated with hydrochlorothiazide-containing products may face increased risk of non-melanoma skin cancer.
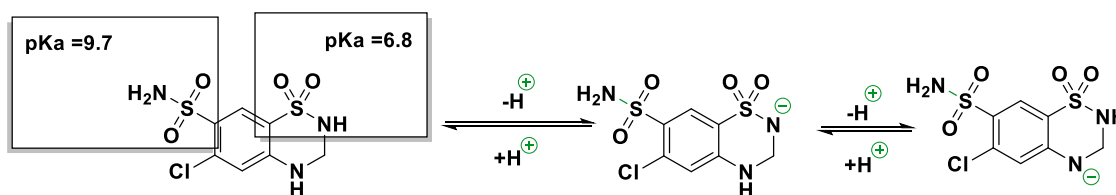
Scheme 3. 3 Ionisation of hydrochlothiazide in presence of water.

3.12.1 Pharmacokinetic and Pharmacodynamic properties

HCTZ affects the distal renal tubular mechanism of electrolyte reabsorption. HCTZ blocks the reabsorption of Na^+ and Cl^- ions in the body. Approximately 55% - 77% of the orally administered HCTZ appears in the urine, and it subsequently raises the amount of sodium crossing the kidney and the quantity of water discharged.

After oral use, HCTZ begins to act within 2 hours, peaks in about 4 hours and lasts about 6 to 12 hours. HCTZ is not metabolized but is eliminated rapidly by the kidney. The plasma half-life for HCTZ was reported to be between 5.6 and 14.8 hours and the drug binds to 40- 68 % of body proteins. At least 61% of HCTZ oral dose is eliminated unchanged within 24 hours. HCTZ crosses the placental but not the blood-brain barrier and is excreted in breast milk.

Long term consumption of HCTZ is associated with depletion of sodium, and may produce an excessive loss of potassium, hydrogen, and chloride ions. HCTZ also lowers the secretion of calcium and uric acid, which may enhance the excretion of iodide and reduce the glomerular filtration rate.

3.13 Materials and methods

Hydrochlorothiazide, known as microzide or hydrodiuril, (1, 2, 4 benzothiadiazine-1, 1-dioxide, Mw – 297.72 g mol-1). 97.0 % CAS 58-93-5 purchased from Tokyo Chemical industry CO (TCI) Ltd. Glycerol 1, 2, 3- Trihydroxypropane 99 %, Mw = 92.09 g mol^{-1} purchased from Sigma Aldrich. Polyglycerine-polyglycerol-2,3.4 purchased from carbosynth Ltd (100.0 g) containing H335. Polyglycerol high molecular weight and polyglycerol low molecular weight synthesised in the laboratory. Methanol and acetonitrile HPLC grade from laboratory reagents purchased from VWR.

3.13.1 Methods

3.13.1.1 Quantification of HCTZ using HPLC

A stock solution of 0.1 mg ml^{-1} was prepared by transferring 10 mg of HCTZ into a 100 mL volumetric flask, topped up with acetonitrile until dissolved. A serial dilution of 200, 300, 400, 500 and 600 ng ml^{-1} were prepared using the mobile phase (methanol: acetonitrile at ratio of 60:90) as a solvent.

HCTZ sample at concentration of 40 mgml^{-1} was placed in a cuvette and wavelength scan between 200 nm to 350 nm was done using a UV, Agilent technology, UV-Vis compact spectrophotometer. The software used is CaryUV workstation. The maximum absorbance wavelength for the HCTZ sample was found to be 270 nm, the UV detector of the HPLC machine used was set at 270 nm.

3.13.1.2 HPLC Conditions

A reverse phase HPLC method was used to quantify HCTZ. The HPLC Agilent Technologies parameters were a run time of 5 minutes, 1 mL /min flow rate, 10 µL injection volume. Wavelength was set at 270 nm. The HPLC machine was used on each day, the mobile phase was left to run for 30 minutes – 1 hour. The stationary phase used was Phenomenex 5µ 150 x 4.60 mm 5 micron, SphereClone 5u ODS (2), serial number 546388-14.

Methanol: acetonitrile at ratio of 60:90 was used as a mobile phase and was pumped into the column at a flow rate of 1 mL /min. The column was conditioned by running the mobile phase for 30 minutes before starting the experiment.

3.13.1.3 HPLC Method validation

The HPLC method developed was validated following the ICH guidelines. The ICH guideline demonstrates that the analytical method is suitable for its purpose by testing several validation characteristics of the analytical procedure and the procedure should meet the accepted criteria.

Linearity- This is the ability of the analytical procedure (within a given range) to obtain test results which are directly proportional to the concentration of the analyte in the sample. Accepted criteria: linear regression coefficient of determination $R^2 = 1$

Accuracy- This expresses the closeness between the accepted value and the value found is 98 – 100 % recovery which is in the range of accepted criteria.

Accepted criteria: 97%- 103% recovery for active pharmaceutical ingredients.

Precision- This is the closeness between a series of measurements obtained from multiple sampling of the same homogenous sample. The three types of precision are repeatability (intra-day precision), intermediate precision (inter-day precision) and reproducibility (inter-day).

Precision was conducted with three quality control (QC's) reference standards of 150. 350 and 550 ngml^{-1}. Sample were prepared on the day of analysis and run-in triplicate nice injection for each QC.

Repeatability is the precision under the same operating conditions over a short interval of time.

Intra-day precision (repeatability) was evaluated by running QC of sample concentration (n=3) under the same operating condition.

Intermediate precision is the precision with laboratory variations such as different days. This was carried out by running same QC concentration in triplicate nine injection for three consecutive days (inter-day).

Accepted criteria: Percentage relative standard deviation (percentage RSD) ≤ 5%.
Accepted criteria: There should be no significant change in peak area.

Selectivity: This refers to the extent to which the method can determine a particular analyte in a complex mixture without interference from the other components in the mixture.

Robustness: This is the ability of the method to remain unchanged by small but deliberate variations in method parameters such as injection volume, mobile phase flow rate.

3.14 Stability studies

The purpose of stability testing is to provide evidence on how the quality of an active substance (drug) or finished product varies with time under the influence of a variety of environmental factors such as temperature, humidity, and light, and to establish a re-test period for the active substance or a shelf life for the finished product and recommended storage conditions. The choice of test conditions defined in this guideline refers to the Note for Guidance on Stability testing of New Drug Substances and Products (CPMP/ICH/2736/99 corr).

A set of each HCTZ formulation was stored at 25 °C (64 % relative humidity, RH) and 40 °C (75% RH) for 30 days. At day 0, 1, 3, 14 and 30 aliquots were withdrawn and tested for assay using HPLC. The samples were also visually observed on each of above-mentioned days and the pH was measured (pH meter EIL 7015, Fisher pH electrode pre calibrated with buffers at pH 4, 7 and 10). The humidity for the stability studies were controlled by preparing saturated salt solutions. A saturated salt solution of sodium chloride and sodium nitrate were prepared to obtain 75% RH and 64% RH respectively (Hong et al., 2005).

3.15 Solubility study

The solubility of HCTZ was studied using the shaking flask method. Excess amount of HCTZ was added to 5 mL of deionised water and was stirred for 24 hours at ambient temperature to achieve equilibrium. After the 24 hours the solution was filtered, using a 0.2 mg syringe filter MILLEX filter unit 0.22 μm, single use Carrigwohhill, Co, Cork, Ireland Ref.12/02 PF07857, and the solution was analysed using the HPLC. Solubility was measured three times and the mean solubility was calculated. The solubility study of a liquid formulation of hydrochlorothiazide is carried out following ICH guidelines.

3.15.1 Solubility study in cosolvents

A solubility study of a liquid formulation of hydrochlorothiazide using five different cosolvent was carried out using HPLC. The cosolvent solubility studies was carried out at ambient temperature by dissolving excess amount of HCTZ in 5 mL of water as control and total volume (5mL) and fractions (0 - 100%) of cosolvent PEG-400, polyglycerol, glycerine, low and high molecular weight polyglycerol (Table 3.2). The samples were stirred for 24 hours to reach equilibrium. Then, samples were filtered through sterile micro filter MILLEX®GP 0.22μm PES membrane and 20 μL was dissolved in a 1000 μL mobile phase (50 x dilution). Distilled water and the cosolvents (PEG 400, polyglycerol and glycerol, polyglycerol low molecular weight (1000 g mol^{-1}) and polyglycerol high molecular weight 4000 g mol^{-1}) were mixed together using a magnetic stirrer to form mixtures containing 0 - 100% cosolvent concentrations. solubility studies were done in triplicate and data was presented as mean ± SD.

Table 3. 2 The volume of water and cosolvents that were mixed together to form each of these concentrations (the total volume was 5mL).

cosolvent (%v/v)	Volume of water (mL)	Volume of Cosolvent (mL)
0	5	0
10	4.5	0.5
20	4	1
20	3.5	1.5
40	3	2
50	2.5	2.5
60	2	3
70	1.5	3.5
80	1	4
90	0.5	4.5
100	*0*	*5*

3.16 pH measurements

The pH of the formulation of HCTZ with cosolvent (n =3) was measured using pH meter EIL 7015, Fisher pH electrode pre calibrated with buffers at pH 4, 7 and 10. Each sample was measured.

HCTZ(2H-1,2,4-Benzothiadiazine-7-sulfonamide,6-chloro3,4-dihydro-,1,1-dioxide) is class IV biopharmaceutical classification which is characterized by poor water solubility and low permeability; this means it has low oral bioavailability. HCTZ is a polyfunctional molecule with pKa values of 6.8 and 9.7. That is at pH < 6, HCTZ is uncharged, while at pH > 10 it exists as di-anion. While, in the pH range from 6–10, a mixture of uncharged, monoanionic and dianionic forms of HCTZ co-exist. Therefore, at pH = 7, HCTZ molecules are solubilized. The PolyglyLMw and PolyglyHMw had no solubility after 50 % amount of cosolvent was added.

3.16.1 Dielectric constant calculations

Dielectric constant (ε)* is a measure of the polarity of a solvent. The higher the ε of a co-solvent, the higher its polarity. The polarity of a cosolvent is one of the factors that affects solubility. The dielectric constant of solvent mixtures can be calculated using the equation below:

$$\varepsilon_{mix} = \varepsilon_{ws} f_{ws} + \varepsilon_{ss} f_{ss}$$

Equation 3. 6 Equation for calculation of Dielectric constant (ε)* which is a measure of the polarity of a solvent.

Where ε and f are the dielectric constant and volume fraction respectively; and subscripts mix, ws and ss represents values for the mixture, weaker solvent and stronger solvent respectively.

3.17 Fourier Transformer Infra-Red (FTIR) Study

Further experiments were performed by FT-IR spectroscopy using the freeze-dried formulation of HCTZ and cosolvent after solubility at 24 h. The FTIR spectra were carried out to observe the change in the vibration of specific functional groups. This could not be obtained using liquid formulation; therefore, the formulation was first cryoprotected using liquid nitrogen and freeze drying. The IR spectrum of the formulation significantly in the N–H stretch region of sulphonamide groups shows shifts.

3.18 Scanning Electron Microscopy study (SEM) study

Scanning electron microscopy (SEM) ZEISS EVO Scanning Electron Microscope for Materials Analysis from Carl Zeiss Microscopy with a resolution capacity 1.9nm @ 30kV SE with HD and 5x to 1,000,000x with largest chamber size. The freeze-dried formulations were sprinkled onto carbon, double sided, sticky tabs which were affixed to aluminium pin stubs. The samples were then sputter coated with gold / palladium alloy via a POLARON SC 7640 SPUTTER COATER. The samples were examined in the secondary electron mode at 20 KV accelerating voltage.

Images of HCTZ in water post freeze drying after 24h were analysed. HCTZ + PEG 400, glycerol, polyglycerol, PolyglyLMw and PolyglyHMw are all treated the same for analysis. The images of formulation after solubility clearly shows a scale of 1 µm the rigid surface of HCTZ.

3.19 Results and discussion

3.19.1 HPLC validation, Linearity and Range

A calibration curve was constructed by plotting the mean peak areas of HCTZ against corresponding concentrations of standard solutions. Standard solutions of

200 – 600 ng ml^{-1} were used to establish the calibration curve (Table 3.3). Good linearity was achieved as the calculated r^2 values ranged between 0.9983 and 0.9979. The linear regression coefficient was within the ICH guidelines acceptable range (r^2 > 0.99), according to ICH guidelines. Moreover, the relative standard deviations (%RSD) at each different concentration (< 5%) met the ICH guidelines.

Table 3. 3Analytical performances of HCTZstandards used in calibration graphs.

Standards	HCTZ
Regression equation	y = 4.0749 x + 43.2250
r^2	0.9983
Linear range	200 – 600 ng ml^{-1}
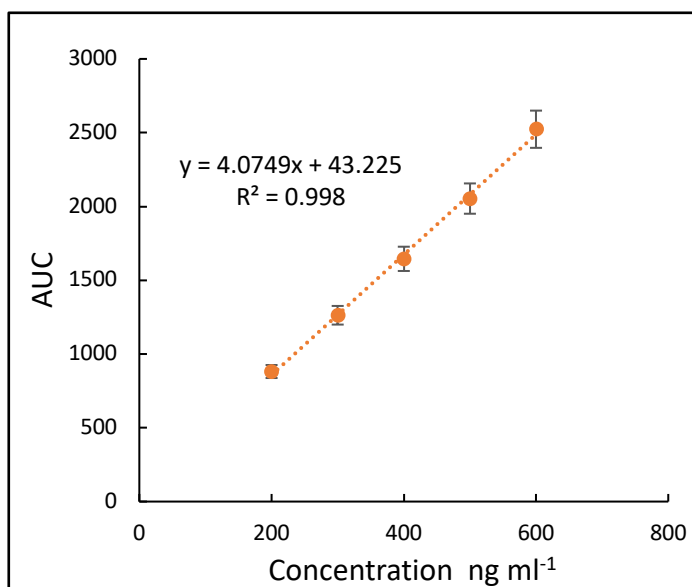
Figure 3. 7 Calibration graph of HCTZ standard solution, the calibration curve was constructed using HCTZ concentrations between 200 – 600 ng mL-1   (n = 3).

3.19.2 Selectivity

Selectivity of the method is the ability to measure and differentiate the analytes in the presence of components that may be expected to be present. These could, impurities, degradants, or matrix components.

The selectivity of the method was determined by injecting the blank mobile phase and diluted cosolvents into the HPLC system. The dilutions were as follows: 0.5 mL of PEG 400 made up to 100mL with the mobile phase, 0.5mL of glycerol and polyglycerine made up to 50 mL with the mobile phase, and polyGlyLMw and polyGlyHMw 50 mg in 50 mL dissolved in mobile phase and injected in HPLC instrument.

The selectivity of method was studied and there was no peak interference of the cosolvents (PEG 400, Polyglycerine and glycerol, polyglycerol LMw and polyglycerol HMw) and the blank mobile phase (ACN: MeOH) at the retention time of HCTZ1.42 min (Figure 3.8).
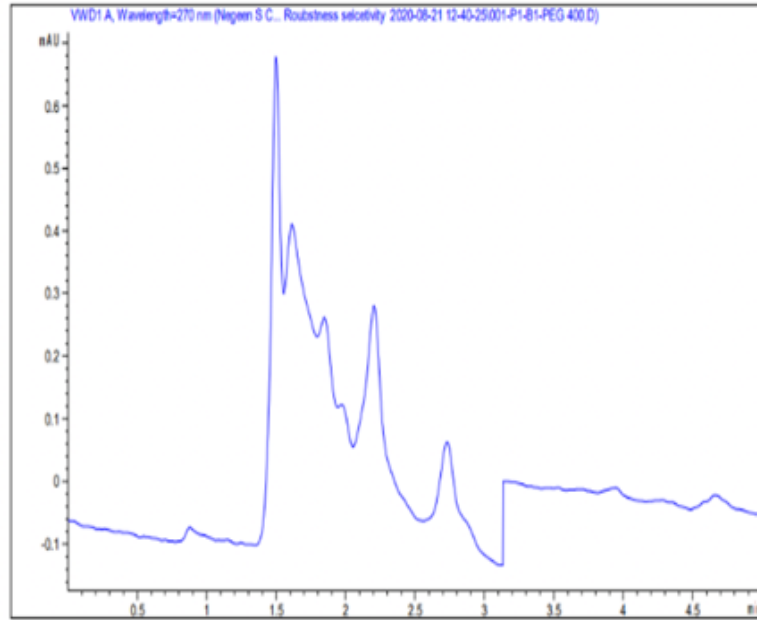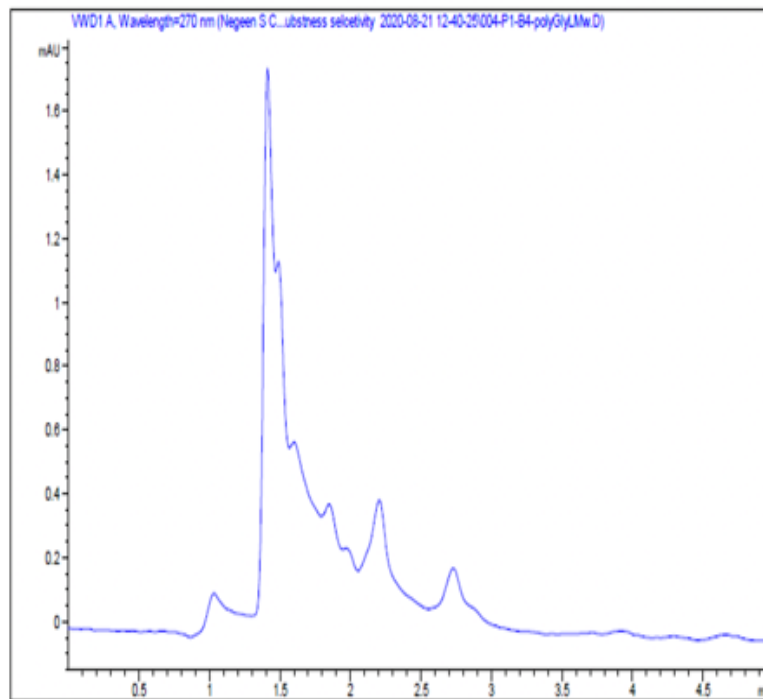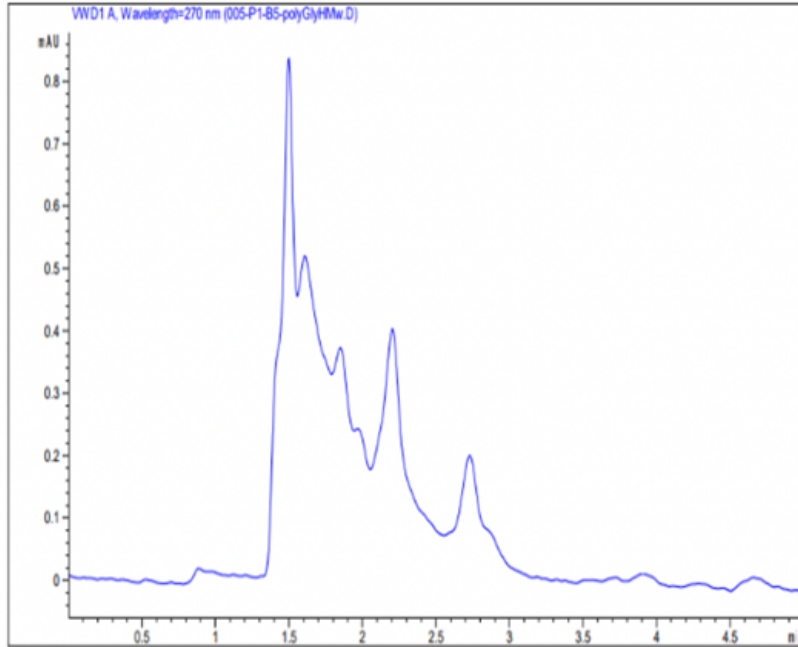
VWD1 A, Wavelength=270 nm (Negeen S C... Roubstness selcetivity 2020-08-21 12-40-25\001-P1-B1-PEG 400.D)

a

VWD1 A, Wavelength=270 nm (Negeen S C...ubstness selcetivity 2020-08-21 12-40-25\004-P1-B4-polyGlyLMw.D)

b

c

d

34
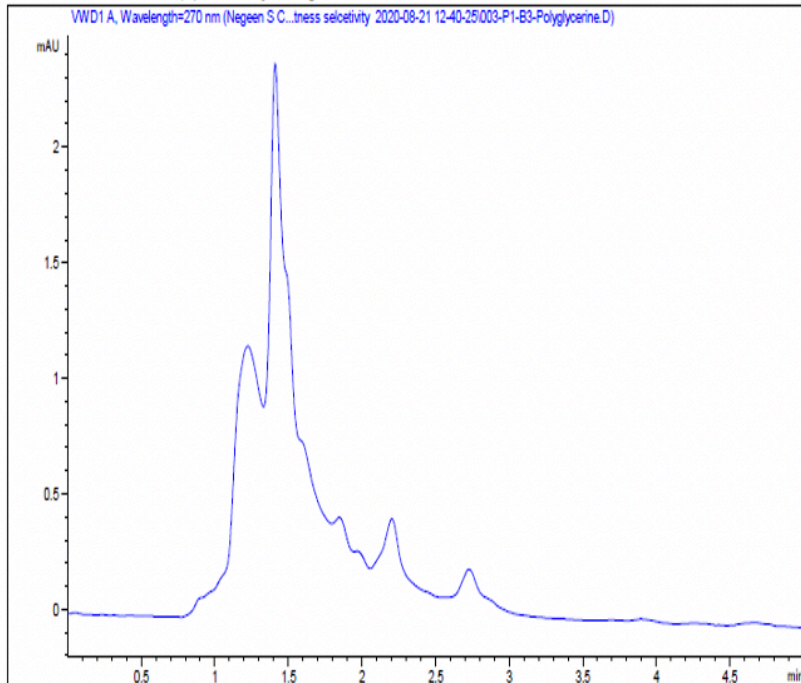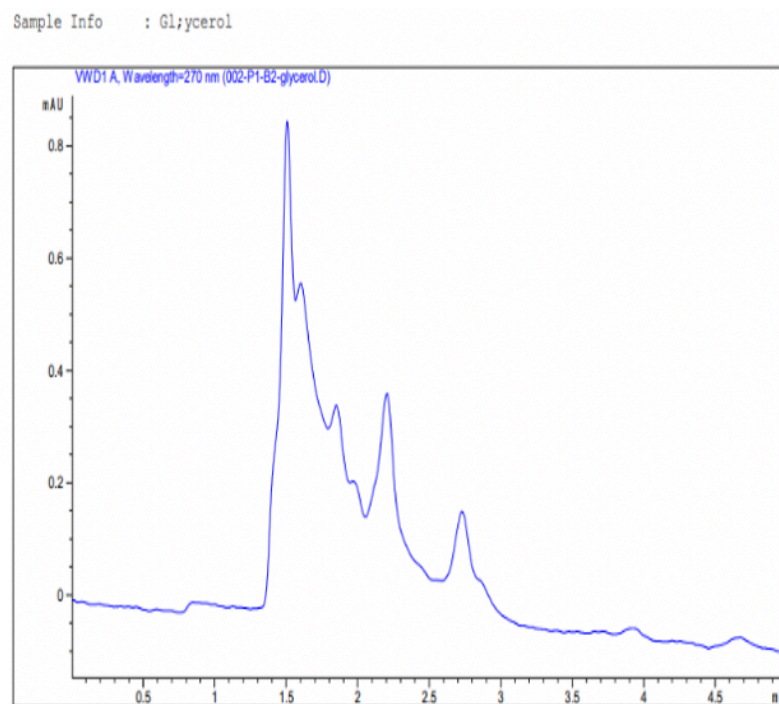
Figure 3. 8 Selectivity runs of the HPLC method development for each polymer a) PEG 400, b) polyglyLMw, c) polyglyHMw, d) polyglycerine and e) glycerol used in solubility study of HCTZ, shows no peaks at 1.42 min, using (Acetonitrile: MEOH) mobile phase at 270 nm.

e

3.19.3 Intra-Assay Variation of HCTZ

The determination of the intra-assay variation of the HCTZ was assessed by injecting three levels of HCTZ concentrations (low (150 ng ml^{-1}), moderate (350 ng ml^{-1}), high (550 ng ml^{-1})) into a HPLC three times in a single batch (n = 3). Mean concentration was calculated using the calibration curve linear equation: y = 4.0749 x + 43.2250 (r^2 = 0.9983). The outcomes are summarized in Table (3.4) and demonstrated that the % RSD was < 5 % for HCTZ. Hence, there is no large variation in the intra-assay experiment.

Table 3. 4 Determination of intra-assay variation of the HCTZ was assessed by injecting three levels of HCTZ concentrations (low (150 ng ml^{-1}), moderate (350 ng ml^{-1}), high (550 ng ml^{-1}) in same day am and pm (n = 3).

HCTZ (ng ml^{-1})	Mean (ng ml^{-1}) of intra-assay variation	Standard deviation	(RSD %)	% Recovery
150	149.9325	1.4288	0.9530	99.9550
350	349.7316	3.5514	1.0155	99.9233
550	544.4628	2.9384	0.5397	98.9932

3.19.4 Inter-Assay Variation of HCTZ

The determination of inter-assay variation of the HCTZ was assessed by injecting three levels of HCTZ concentrations (low (150 ng ml^{-1}), moderate (350 ng ml^{-1}), high (550 ng ml^{-1})) into a HPLC instrument three times in a single batch (n = 3) over 3 consecutive days. Mean concentration was calculated using the calibration curve linear equations over the 3 days.

Table 3. 5 Determination of inter day assay variation of the HCTZ was assessed by injecting three levels of HCTZ concentrations (low (150 ng ml^{-1}), moderate (350 ng ml^{-1}), high (550 ng ml^{-1}) over three days (n = 3).

HCTZ (ng ml^{-1})	Mean (ng ml^{-1}) of inter-assay variation	Standard deviation	*% RSD	**% Recovery
150	156.9806	5.5960	2.9110	104.654
350	362.6815	31.5750	7.1080	103.623
550	563.3831	18.3700	8.4570	102.433

The % RSD over the three days was found to be less than 5 % for the lowest concentration. However, it was > 5% for HCTZ at medium and high concentration (Table 3.5). The experiment revealed that there is no large variation in the inter-assay experiment. The % recovery is within the range.

% RSD (*) represents precision, and % recovery (**) represents accuracy.

3.19.5 Limit of Detection (LOD) and Limit of Quantitation (LOQ)

The LOD and LOQ of the planned method were calculated mathematically by the association among the slope of the calibration curve and the standard deviation of the HPLC response using equations (3.8 and 3.9).

$$LOD = 3.3\sigma / S$$

Equation 3. 7 Limit of Detection (LOD)

$$LOQ = 10\sigma / S$$

Equation 3. 8 Limit of Quantitation (LOQ) where σ is the standard deviation of the response; S is the slope of the calibration curve.

Table 3. 6 Limit of detection (LOD) and limit of quantitation (LOQ) for (HCTZ) HCTZ standards.

Standards	HCTZ (ng ml^{-1})	r^2
Limit of Detection (LOD	47.5527	0.9962
Limit of Quantitation (LOQ)	144.0939	

Accuracy The accuracy of the analytical method was determined by measuring the percentage recovery of both the intraday and inter-day variations.

The % recovery = (concentration of HCTZ 24 h/standard concentration of HCTZ) × 100 and the accuracy = 100 − ((calculated concentration − actual concentration)/actual concentration) × 100 is calculated

Robustness: The robustness of the method was determined by making minor variations to the mobile phase ratio and the flow rate (table 3.7). The mobile phase ratio was changed from 60:40 to 58:42 and 62:32 while the mobile phase flow rate was changed from 1.0mL/min to 1.1mL/min and 0.9mL/min. HCTZ standard

concentrations 150 and 350 and 550 ng ml-1 were analysed when these variations were made, and the percentage RSD was calculated.

Table 3. 7 Robustness of the HPLC method.

Variable range		AUC	Mean AUC	RSD %	AUC	Mean AUC	RSD %	AUC	Mean AUC	RSD %
		150 ng ml^{-1}			350 ng ml^{-1}			550 ng ml^{-1}		
	58:42	653.22632	652.916	0.04 %	1423.86926	1423.394	0.05%	2171.76709	2172.334	0.08%
		652.69446			1422.64209			2174.30200		
		652.82574			1423.66919			2170.93311		
	60:40	652.10345	651.919	0.10 %	1421.86182	1421.417	0.04%	2170.88403	2170.974	0.6%
		651.19946			1420.87524			2169.62061		
Mobile phase ratio changes		652.45361			1421.51331			2172.40967		
	62:38	593.55878	593.259	0.04 %	1293.40491	1293.649	0.04 %	1973.77539	1972.369	0.06%
		593.20044			1294.22449			1971.91028		
		593.01642			1293.31873			1971.42126		
Flow rate changes	0.9 1.0 1.1		632.6976	4 %	1379.4868		4 %	2105.2248		4%

3.20 Cosolvents used for solubility of HCTZ

3.20.1 PEG 400

Polyethylene glycol (PEG) is repeated ethylene glycol units (Scheme 3.5), composed of polyether compounds. Most PEGs are obtainable commercially as mixtures of different oligomer sizes with broad or narrow defined molecular weight (MW) ranges. Polyethylene glycol (PEG-400) is cost-effective, non-toxic, and efficient medium for many applications. Eco-friendliness, low cost, high yields, and recyclability of the PEG-400 are the main advantages of this polymer. PEGs are used in cosmetics as their terminal primary hydroxyl groups can create mono-, di- and polyesters, amines, ethers, and acetals. Furthermore, PEGs can create additional compounds and complexes through a reaction in their ether bridges.
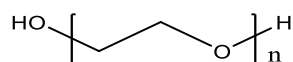
Scheme 3. 4 Polyethylene glycol used in formulation with HCTZ as cosolvent.

3.20.2 Glycerol

Glycerol is commonly used as a food preservative (scheme 3.6). It is a non-toxic, biodegradable, and recyclable liquid made from fossil fuel sources that have a high potential to serve as an alternative green solvent to improve the solubility of poorly soluble drugs. In its pure form, glycerol is a clear, colourless, odourless, and viscous liquid with a sweet taste. Because it is a trihydric alcohol, glycerol is a polar protic solvent with a dielectric constant of 42.5 (at 25 °C). At low temperatures, glycerol forms crystals. Its specific density is 1.26, and its molecular weight is 92.09 g mol^{-1} (Wolfson, 2007).
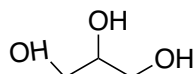
Scheme 3. 5 Glycerol (monomer)

3.20.3 Polyglycerine / polyglycerol (liquid) polyricinoleate (E 476)

Polyglycerol is used as a food additive. In 1978, the Scientific Committee for Food (SCF) established an acceptable daily intake (ADI) of 7.5 mg/Kg body weight per day for polyglycerol. PGPR hydrolyse in the gut forms free polyglycerols, polyricinoleic acid, and ricinoleic acid. Di- and triglycerol are absorbed and eliminated unchanged in the urine; whilst long-chain polyglycerols present lower absorption and are mainly excreted unchanged in faeces. The safety of polyglycerols (maximum use 5g /Kg, food) has been assessed, and no adverse effects were identified even at the highest doses tested. The accessible database on polyglycerol did not indicate adverse effects in short-term, sub chronic, chronic, or toxicity ranges (Additives et al., 2017).
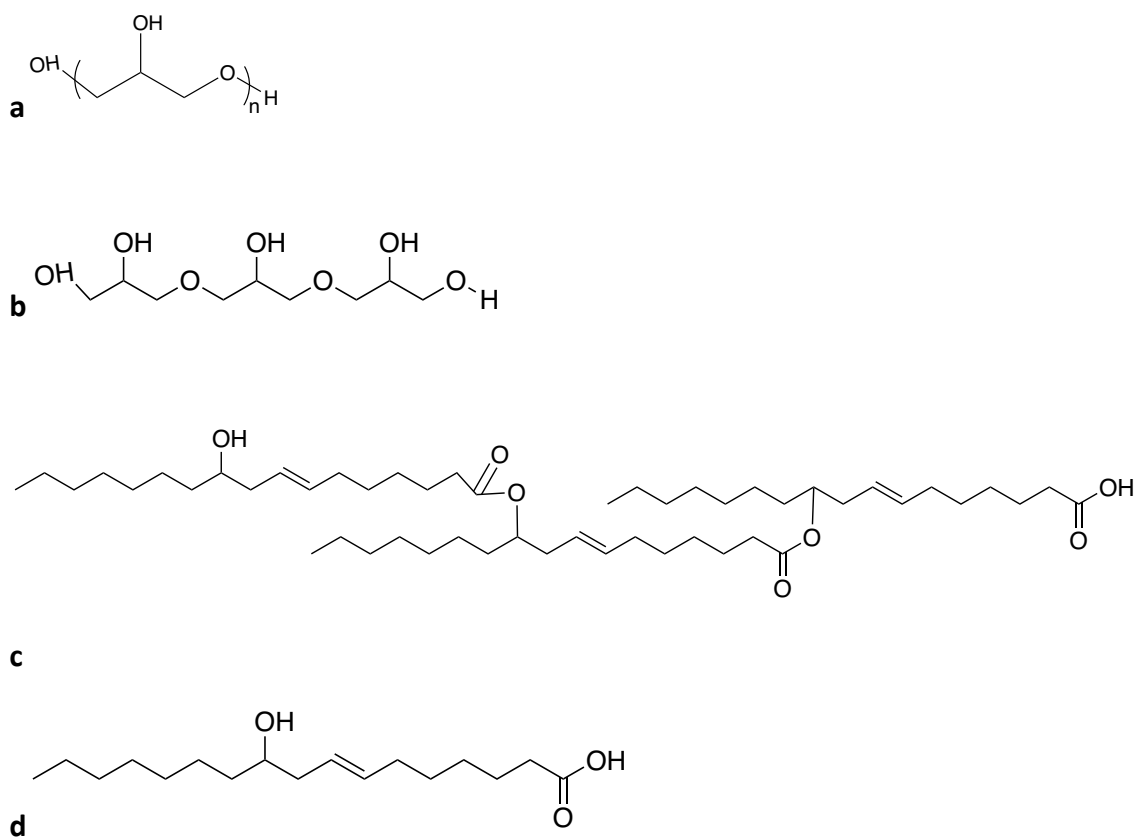
Scheme 3. 6 a Polyglycerol, b triglyceride, c polyricinoloeic acid, d recinoloic acid (polyglycerine).

3.20.4 Low and high molecular weight hyperbranched polyglycerol

Low molecular weight hyperbranched polyglycerol (Chapter 2) was prepared by polymerisation of pentaerythritol and glycidol in presence of sulfuric acid as. While high molecular weight hyperbranched polyglycerol was synthesized by polymerizing of glycerol and glycidol in sulfuric acid (Schemes 3.8, 3.9).
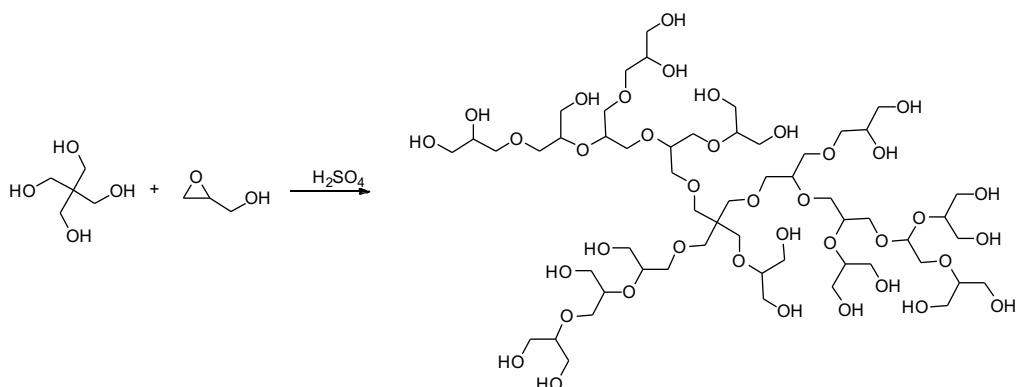
Scheme 3. 7 Acid catalysed polymerisation of pentaerythritol and glycidol in presence of sulfuric acid.
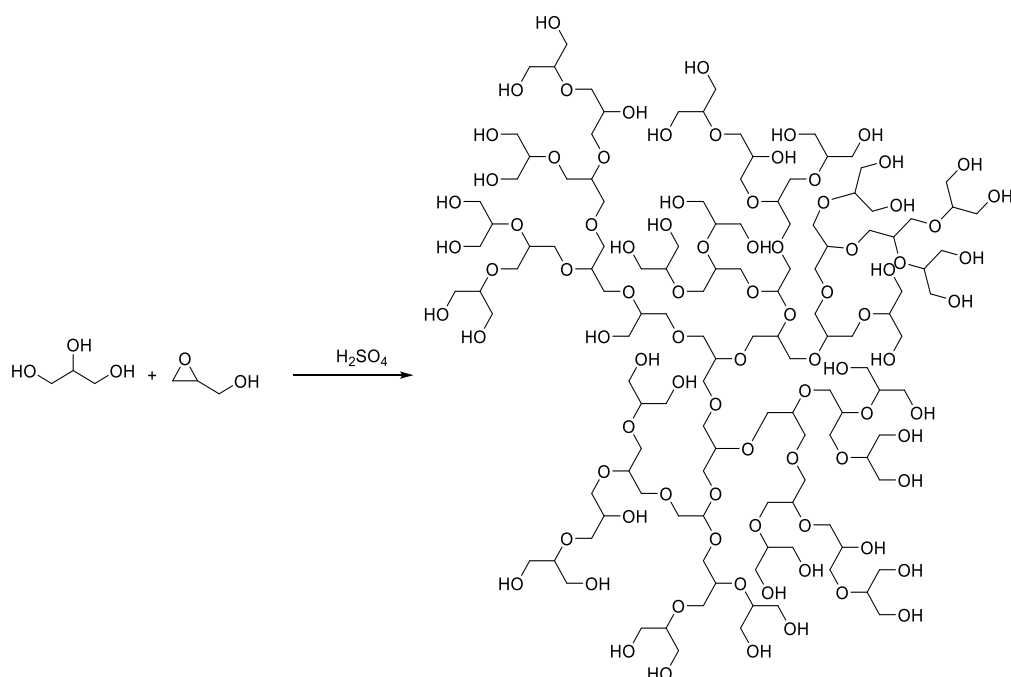
Scheme 3. 8 Acid catalysed polymerisation of glycerol and glycidol in presence of sulfuric acid.

3.21 Solubility of HCTZ in pure solvents

The solubility of HCTZ in water, polyglycerine, glycerol, PEG, Polyglycerol LMw and Polyglycerol HMw was investigated (table 3.8). HCTZ solubility in water was very poor as only 8.06 ± 6.69 µgml-1 was solubilized. This could be attributed to the high dielectric constant of water (high polarity) and the high lipophilicity of HCTZ. The

structure of HCTZ contains two sulphonamide and one aromatic amine group. The possible hydrogen bonding can form between N-H...O sulphonamide. The drug is quite lipophilic.
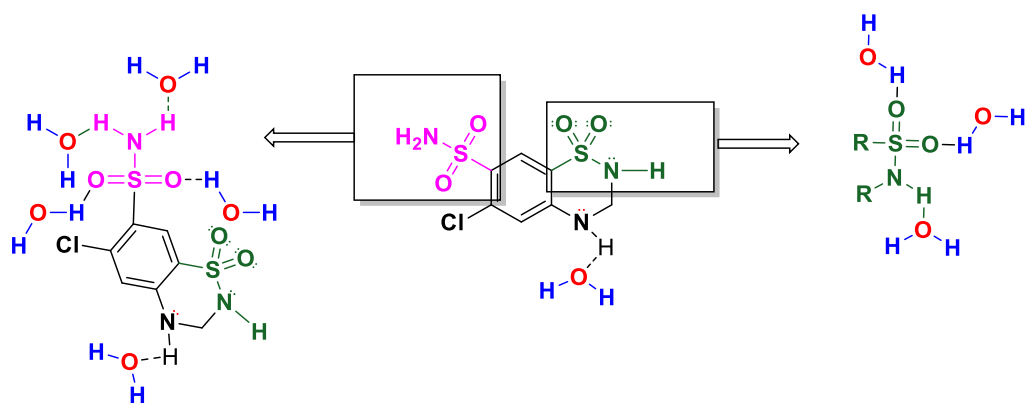
Scheme 3. 9 Hydrogen bonding of HCTZ in water.

On the other hand, the solubility in PEG 400 and glycerol and polyglycerine were 473.46 ± 8.47 µgml^{-1}, 102 ± 35.96 µgml^{-1} and 382.23 ± 35.96 µgml^{-1} respectively.

Understanding pH–solubility relationships is essential in predicting the response of ionic drugs in pharmaceutical formulations and the body. Cosolvents are an efficient method over using additives, such as surfactants and cyclodextrins (CDs), as it does not reach the maximum level most of the time. The cosolvent approach is more convenient, inexpensive (as no need for expensive pharmaceutical equipment for compounding). Moreover, it avoids the need for solvent mixing before administration, hence avoid dosing errors and contamination (Panigrahi, 2012).

Table 3. 8 Solubility of HCTZ in water, PEG 400, glycerol Polyglcerine, polyGlyLMw* and polyGlyHMw** are in solid form. (n = 9)

Solvent	Dielectric constant	Solubility of HCTZ (µgml$^{-1)}$)
Water	78.36	8.06 ± 6.69
PEG 400	12.40	473.46 ± 8.47
Glycerol	57.51	91.65 ± 30.02
Polyglycerine	30.50	382.23 ± 35.96

PolyglyLMw*	-	28.83 ± 0.23
PolyglyHMw**	-	11.63

3.21.1 Solubility results of HCTZ in PEG 400.

Solubility results of HCTZ in PEG 400 was studied by using 10 – 100 % v/v PEG 400. The solubility data are summarized in Figure (3.9). Increasing the concentration of PEG 400 has helped in increasing the solubility of HCTZ. HCTZ solubility increased from PEG-400 v/v 10% (20.06 ± 5 μgml^{-1}, n = 9) to (473.46 ± 8.47 μgml^{-1}, n=9) at 100%. The trend below shows that solubility increased with the increased fraction of PEG-400 at v/v50 % it is gone up to (121.58 ± 5 μgml^{-1} n = 9) and remained fairly steady on average of (320 ± 5 μgml^{-1} n = 9), from v/v 60 – 90 %. The highest solubility value for PEG reached 100 % cosolvent. This can attribute to the steady pH values at the cosolvent, as mentioned earlier fractions, as it shows a similar trend (Figure 3.9).
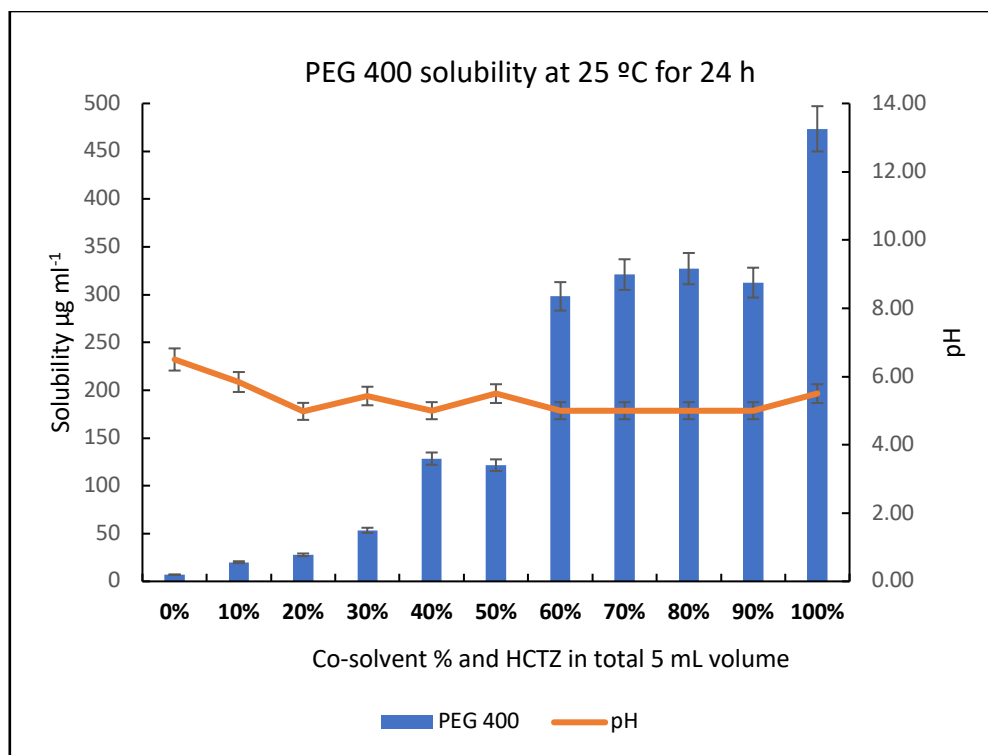
Figure 3. 9 Solubility and pH results of HCTZ in PEG 400 using 10 – 100 % v/v. Each sample was prepared in triplicate and run 9 times.

While the use of volatile organic solvents, for example, methanol, dichloromethane, and combinations of these to dissolve the drug are not suitable for human use. However, the use of aqueous solutions or dispersions remains the preferred manufacturing procedure due to the lack of solvent toxicity, increased method safety and lower manufacturing expenses.

HCTZ has some degree of solubility in water and, and its solubility was measured in this study during solubility. (6 µg mL^{-1}), the solute (HCTZ) molecule is moved from its crystal lattice, and a cavity for the drug molecule is created in the solvent. The analyte molecule is inserted into this cavity (Alexander T Florence and David Attwood, 2016)

.
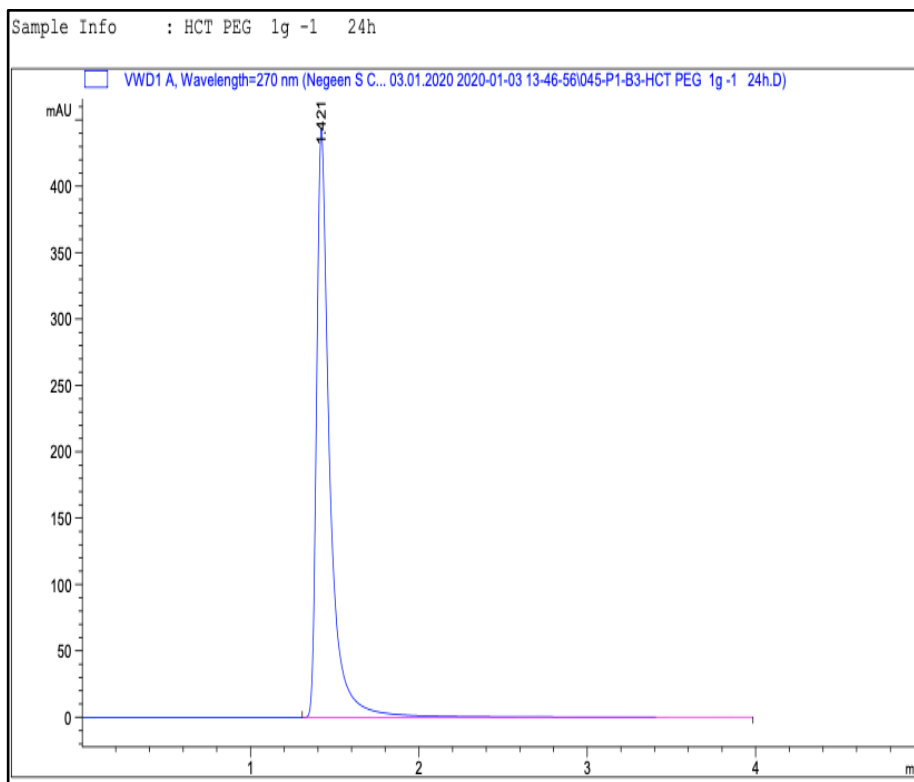
Figure 3. 10 Chromatogram of an example of HCTZ PEG-400, 20% v/v formulation after solubility at time 0.

Upon monitoring the changes of the pH of PEG 400 solutions, minimal changes were observed. Ionizable molecules that are surface-active or that have strong acid-base hydrogen potentials form hydrogen bonds.
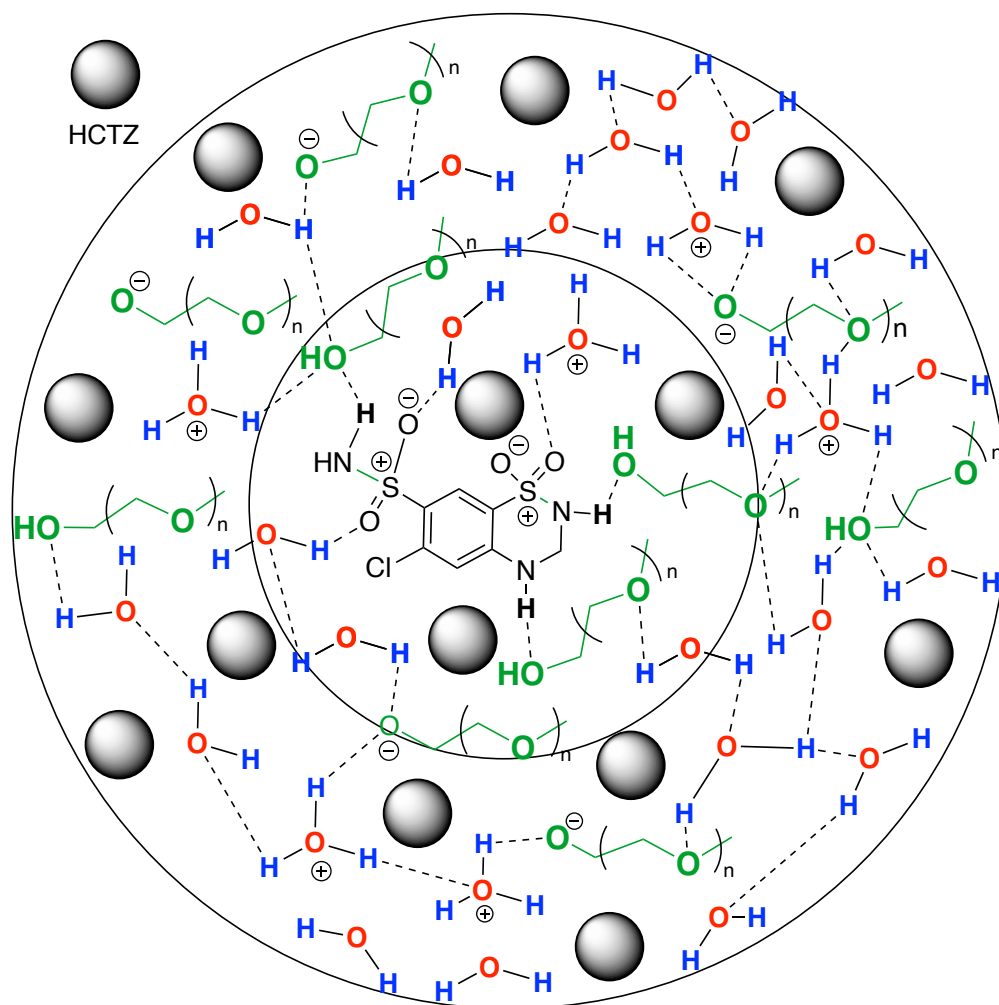
Figure 3. 11 A schematic diagram indicates that in the regions between the cosolvent ion (PEG 400) and bulk water ion.

The image shows the orientation of the 'in-between' water molecules which must have an arrangement between the oxygen-facing ion and that which suits the bulk water hydrogen-facing ion. The solubility of a drug for example HCTZ means the estimation of solubility from the surface area of molecules. This is affected by molecular shape factors and substituents on molecules that affect solubility and is one of the critical parameters of a drug molecule. The effects of solubility or hydration in aqueous media and the effects of co-solvents on a drug's solubility are the same, but most importantly, pH has a significant role on the solubility of an

ionizable drug. The pH of PEG 400 formulation starts at pH = 5 and after being fluctuating from v/v 10 -50 % fraction of PEG remains stable.

3.22.2 Solubility results of HCTZ in Glycerol.

Solubility results of HCTZ in Glycerol were studied by using 10 – 100 % v/v Glycerol in total 5 ml sample volume. Each sample was prepared in triplicate and each run 3 times using the HPLC method developed. The solubility is high at v/v 80 % glycerol and the pH remains similar from v/v 60 -80 % glycerol and increases as the fraction of water decreases (Figure 3.12) .
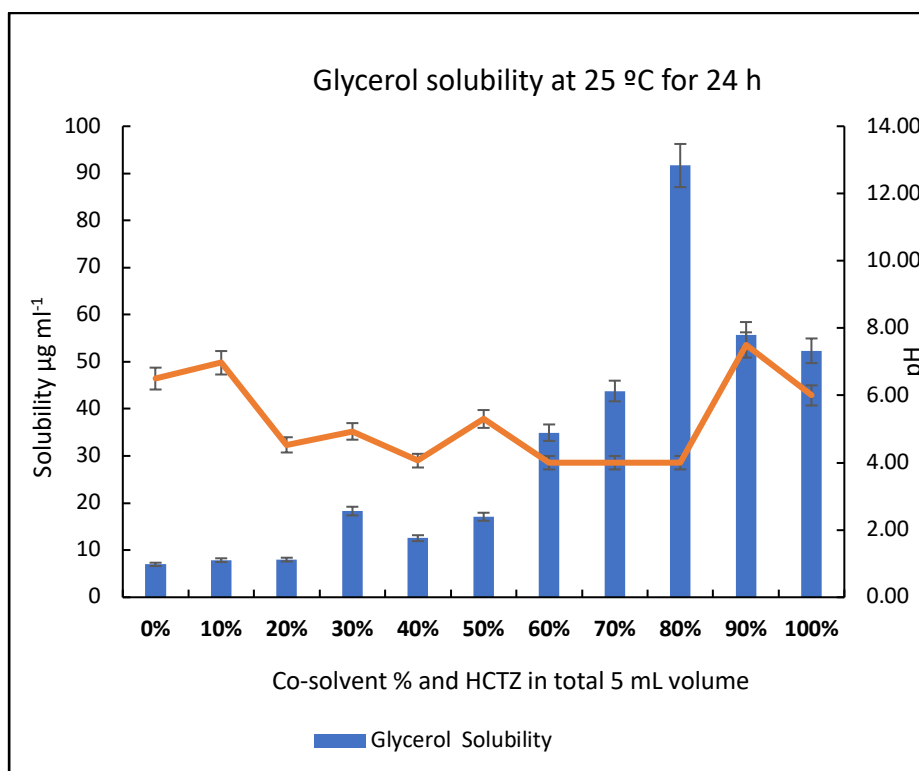
Figure 3. 12 Solubility and pH results of HCTZ in Glycerol using 10 – 100 % v/v in total 5 ml sample volume (w/v %). Each sample was prepared in triplicate.

The solubility of HCTZ in glycerol (small molecule) remains very low from 10 % to 50 % and increases at 60 % but more significantly it increases at 80 % that is due to the interaction of glycerol and water which facilitates the solubility, however at higher glycerol concentration the solubility decreases. HCTZ solubility increased from glycerol v/v 10% (7.88 ± 5 μgml^{-1}, n = 9) to (91.65 ± 30.02 μgml^{-1}, n=9) at 80%. The

trend below shows that solubility increased only with glycerol at v/v 80 % and remained fairly low on average, and from v/v 90 – 100 % the solubility decreases to an average of (50 ± 5 µgml^{-1}, n=9). This can be characteristic due to the unstable pH values as glycerol is a small molecule and at high solubility, pH is in acidic range (pH = 4, n = 3). at the cosolvent, as mentioned early fractions, as it shows a similar trend.
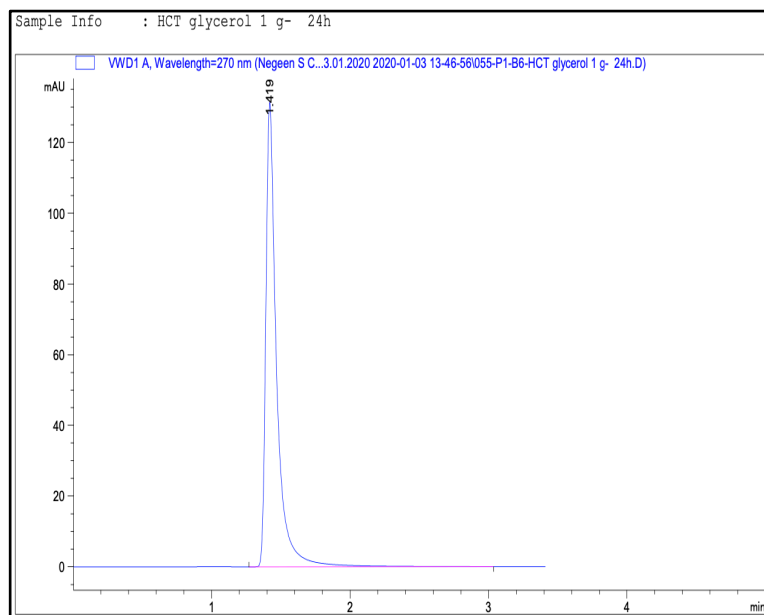
Figure 3. 13 HPLC chromatogram of HCTZ and glycerol formualtion. Mobile phase (ACN: MeOH).
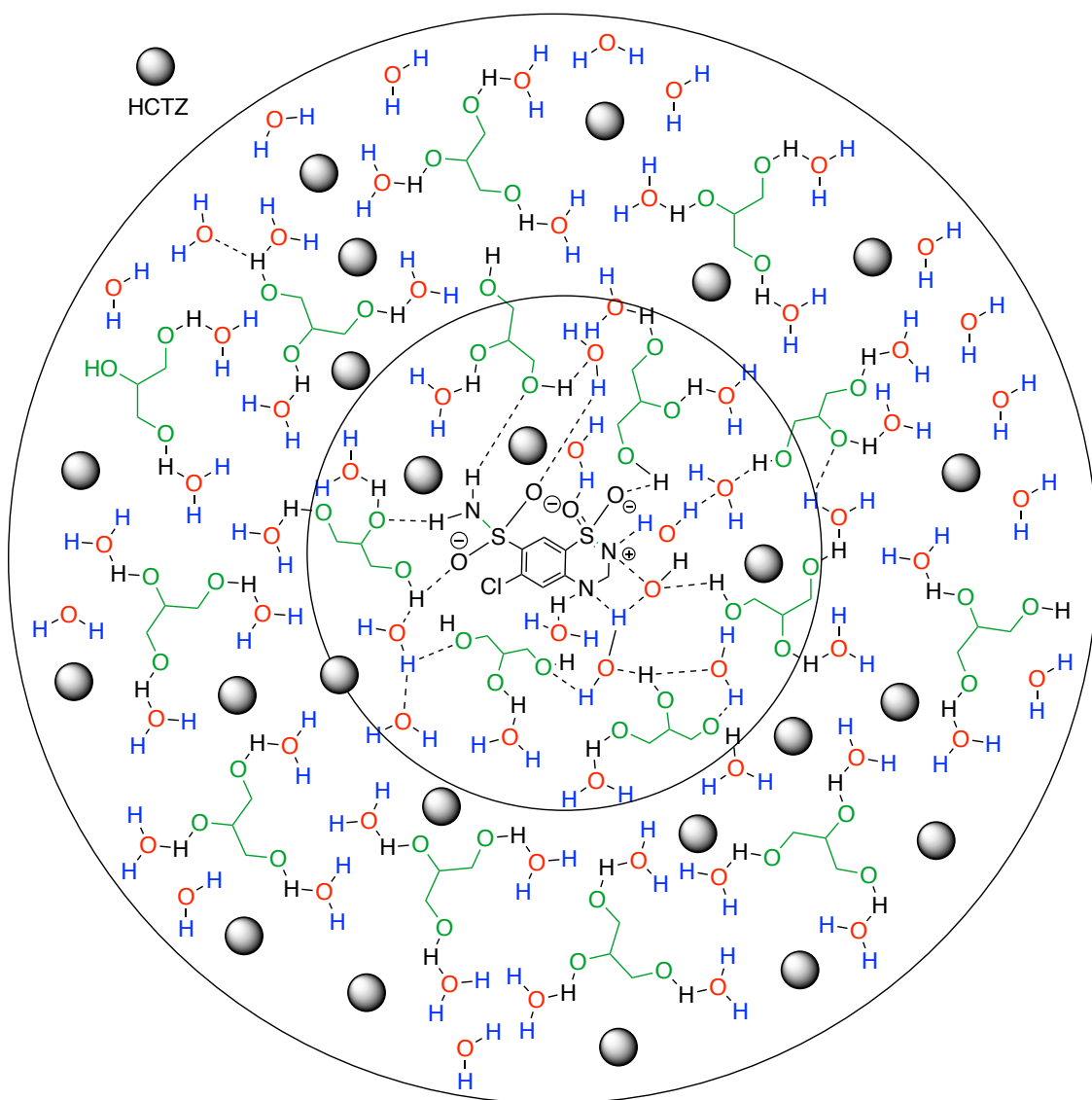
Figure 3. 14 A schematic representation of HCTZ and glycerol , water solubility and hydrogen bonding.

At the high concentrations (v/v, 100%), glycerol does not significantly increase the solubility of the drug the solubility increases to only (91.65 ± 30.02 µg ml^{-1} n= 9) in 80% glycerol and dielectric constant 57.51 and pH 4.00). This can be attributed to the fact the glycerol can only form hydrogen bond in three position which makes the drug solubility low at v/v 100 % solubility. However, in presence of 20 % water the solubility is at its maximum value. The reason for low solubility at a higher fraction of

glycerol could be attributed that glycerol is miscible with water and therefore the solubility of HCTZ low throughout all the range of cosolvent fraction (Figure 3.12).

3.22.3 Solubility results of HCTZ in polyglycerine and pH

Solubility results of HCTZ in Polyglycerine was studied by using 10 – 100 % Polyglycerine in total 5 ml sample volume. The solubility of HCTZ over 24 h was calculated using mean value of each sample using regression equation slope and intercept and area under the curve (AUC) from instrument response value. The pH of each batch was measured in triplicate and mean value is plotted against the percentage cosolvent in sample (Figure 3.15).
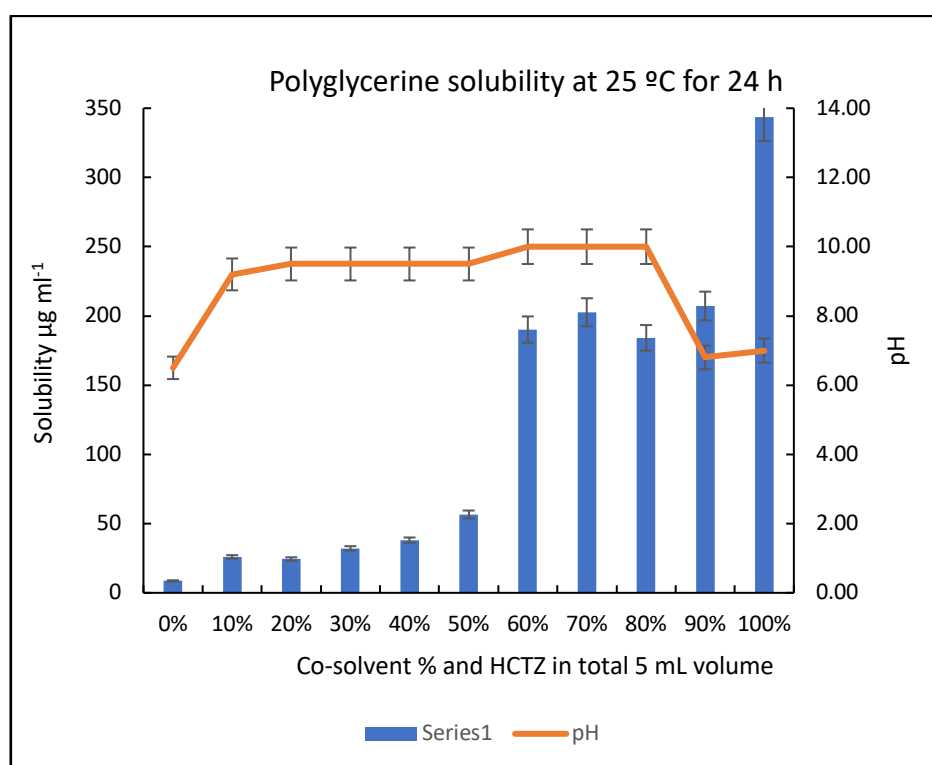
Figure 3. 15 Solubility and pH results of HCTZ in Polyglycerine using 10 – 100 % in total 5 ml sample volume (w/v %). Each sample was prepared in triplicate.

The maximum solubility at 100 % co solvent is 382.23 ± 35.96 µgml^{-1} at pH 7, at lower cosolvent fraction the pH remains in the basic range. At the high concentrations (v/v, 100%), polyglycerine significantly increase the solubility of the drug (343.47 ± 35.96

μg ml^{-1} n= 9), having pH = 7.0. This can be attributed to the fact the polyglycerine contains more components and fatty acids and ease the solubility at v/v 100 % cosolvent. The solubility remains low from v/v 10 – 50 % cosolvent however the pH is in the at v/v 10 – 80 % cosolvent fraction is around pH = 10, throughout the rest of cosolvent fraction. Solubility of HCTZ in polyglycerine (Figure 3.16) is high at using v/v 100 % cosolvent. This is since polyglycerine is a blend of di, tri glycerol and some other auditive therefore the scope of forming hydrogen bonds with drug and organic molecules is high. The solubility changes as the fraction of water increases and remains on average (200 μg ml^{-1} n= 9) from v/v 60 – 90 % cosolvent this is showing that polyglycerine is more polar and can increase the solubility of HCTZ with no added water similar to PEG -400.
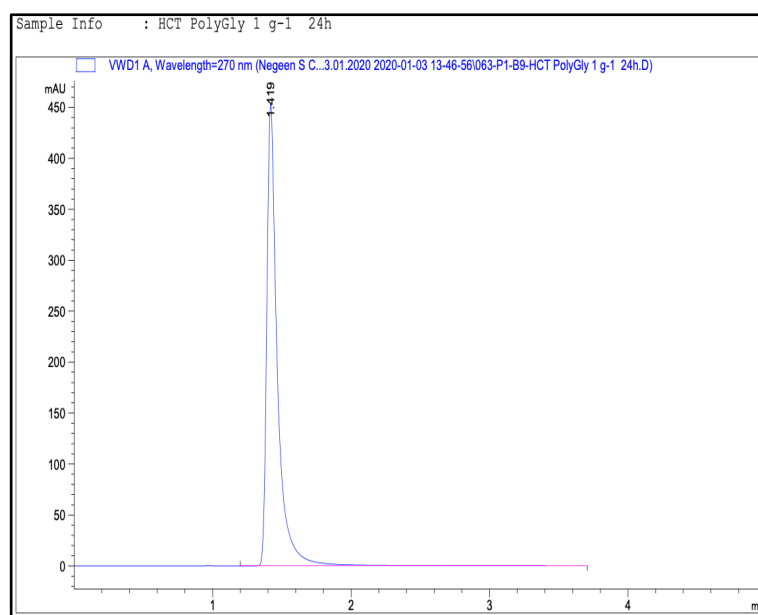
Figure 3. 16 HPLC chromatogram of HCTZ and polyglycerinel formualtion. Mobile phase (ACN: MeOH).
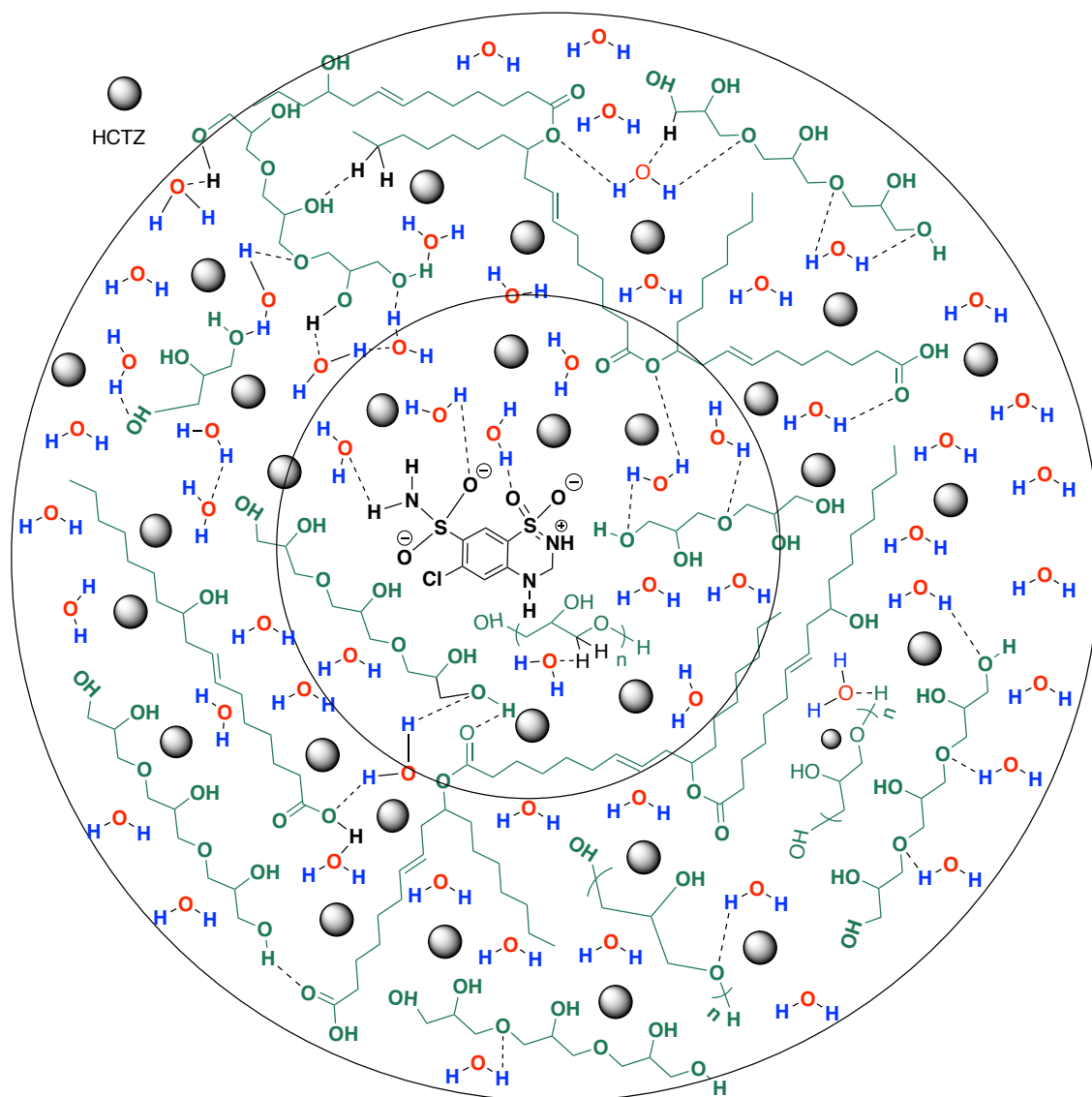
Figure 3. 17 schemiatic repesentation of polyglycerine , HCTZ and water.

Polyglycerine is a m uch more efficient cosolvent than glycerol and less toxic than PEG 400. However, the solubility reaches at v/v 100% polyglycerine mixtures, the

solubility increases to 382.2362 ± 35.96 μg ml^{-1} with a dielectric constant of 30 and pH 7.00.

3.22.4 Solubility results of HCTZ in Polyglycerol low molecular weight (polyGlyLMw) hyperbranched synthesised (see chapter 2)

Solubility results of HCTZ in polyGlyLMw was studied by using 10 – 100 % polyGlyLMw in total 5 ml sample volume. Each sample was prepared in triplicate and analysed 3 times using the HPLC method previously addressed. The solubility of HCTZ over 24 h was calculated using the mean value of each sample using regression equation slope and intercept and the area under the curve (AUC) from instrument response value. The pH of each batch was measured in triplicate and mean value was plotted against the percentage cosolvent in sample (Figure 3.18).
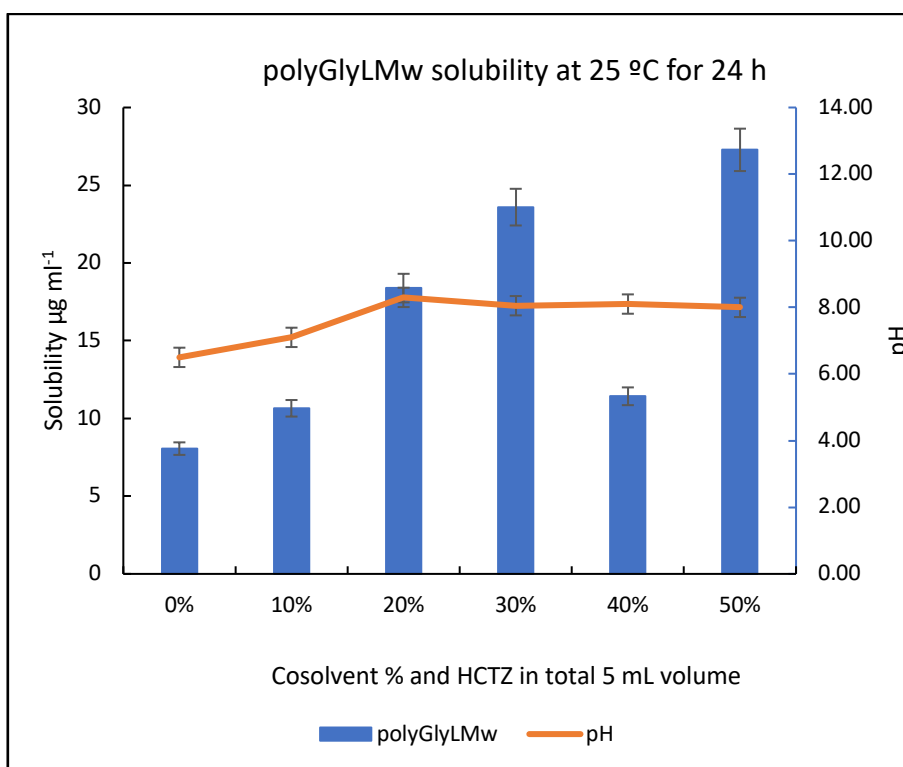
Figure 3. 18 Solubility and pH results of HCTZ in polyGlyLMw using 10 – 50 % in total 5 ml sample volume (w/v %). Each sample was prepared in triplicate.

Using polyGlyLMw as cosolvent did not significantly improve the solubility of HCTZ. The maximum solubility is 27.27 ± 0.23 μg ml^{-1} at pH = 8.00 and after 50 % cosolvent fraction there is no solubility results due to the nature of polymer which is solid. The low solubility of HCTZ using polyglycerol indicates that the higher the molecular

weight of these polymer the denser and therefore the lower the solubility. As per schematic representation there is a lot more hindrances for formation of hydrogen bond between the polyGlyLMw polymer water and HCTZ.
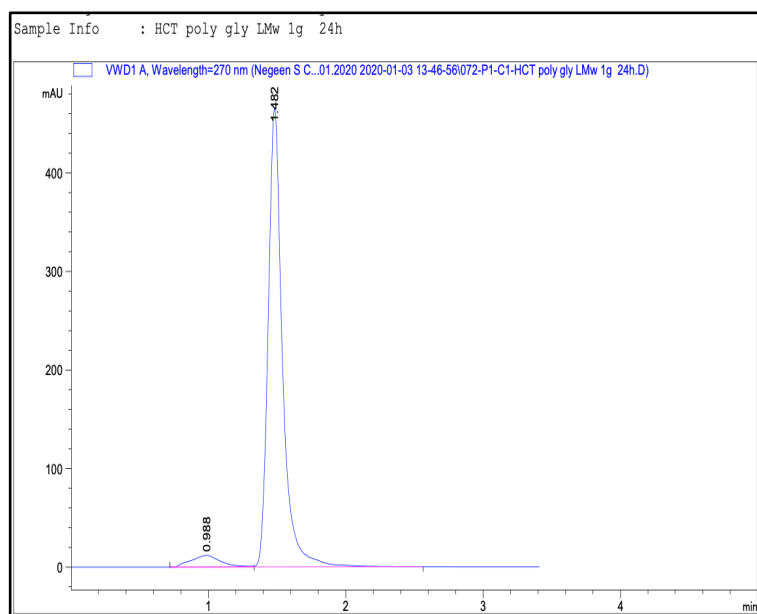
Figure 3. 19 HPLC chromatogram of HCTZ and polyGlyLMw formualtion. Mobile phase (ACN: MeOH).

The branched or high molecular weight (solid) polyglycerol are both located at the same distance from the core units such as the polyGlyLMw. This study suggests that due to the control over both molecular weights and degree of branching, the resulting current structures of polyglycerol can be used to prepare well-defined, complex surface modified polymer architectures. The solubility study of HCTZ with polyGlyLMw and polyGlyHMw polyglycerol shows this trend. that this polymer is not suitable without surface modification for drug solubility (et.al., 1999, al., 2000, Daniel Wilims 2010).
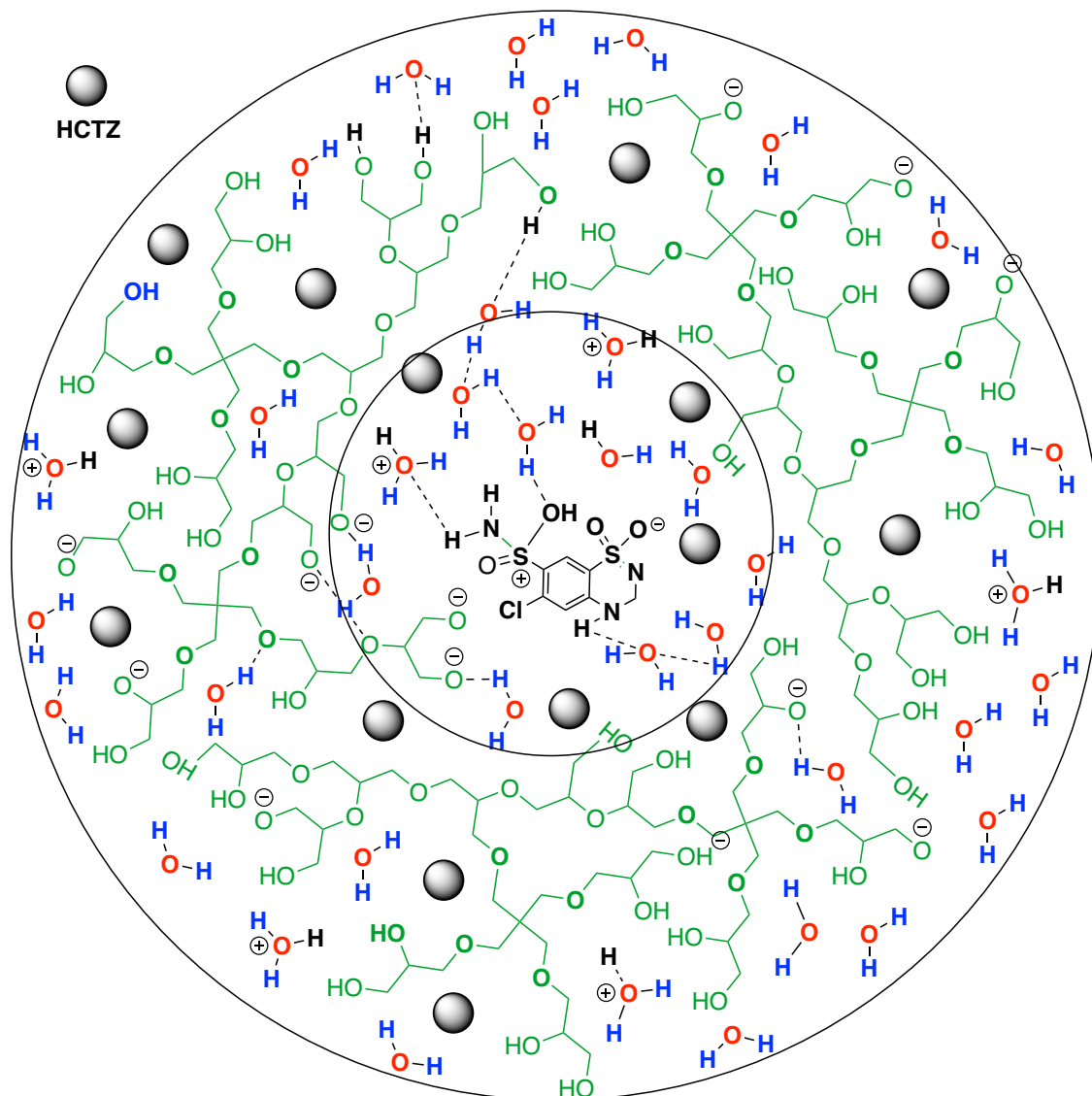
Figure 3. 20 schematic repesentation of low molecular weight polyglycerol , HCTZ and water.

3.22.5 Solubility results of HCTZ in Polyglycerol high molecular weight (polyGlyHMw) hyperbranched synthesised

Solubility results of HCTZ in polyGlyHMw was studied by using 10 – 100 % polyGlyHMw in total 5 ml sample volume. Each sample was prepared in triplicate and analysed 3 times using HPLC method. The solubility of HCTZ over 24 h was calculated using mean value of each sample using regression equation slope and intercept and area under the curve (AUC) from the instrument response value. The pH of each batch

was measured in triplicate and mean value was plotted against the percentage cosolvent in sample (Figure 3.21).
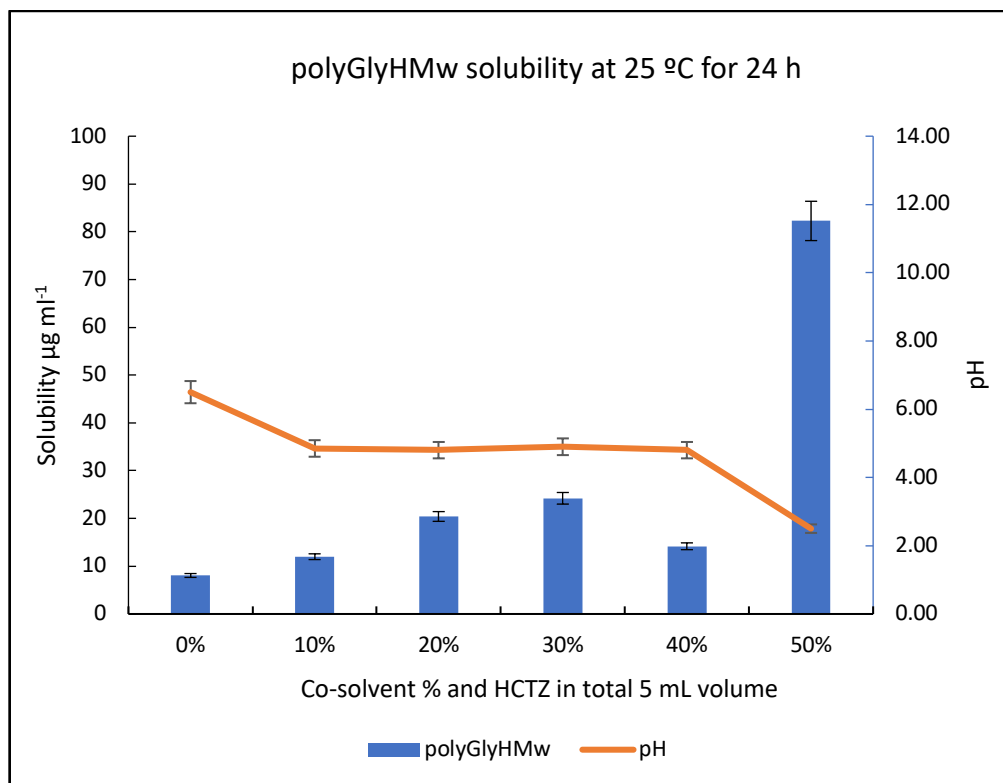
Figure 3. 21 Solubility and pH results of HCTZ in polyGlyHMw using 10 – 50 % in total 5 ml sample volume (w/v %). Each sample was prepared in triplicate.

Using polyGlyHMw as cosolvent did not significantly improve the solubility of HCTZ compare the PEG 400 glycerol and polyglycerine, however it is higher than polyGlyLMw, and it 82.26 ± 11.63 µg ml^{-1} at w/v 50 % cosolvent, at pH = 2.00 and after 50 % cosolvent fraction there is no solubility results due to the solid nature of polymer. The low solubility of HCTZ using polyglycerol synthesised in the lab indicates that the higher the molecular weight of these polymer the denser with higher viscosity and therefore lower solubility, compared with other cosolvents. As per schematic depiction there is a lot more interferences for establishment of hydrogen bond between the polyGlyHMw polymer, water and HCTZ. Also, the formulation precipitated after solubility and crystalised during stability.
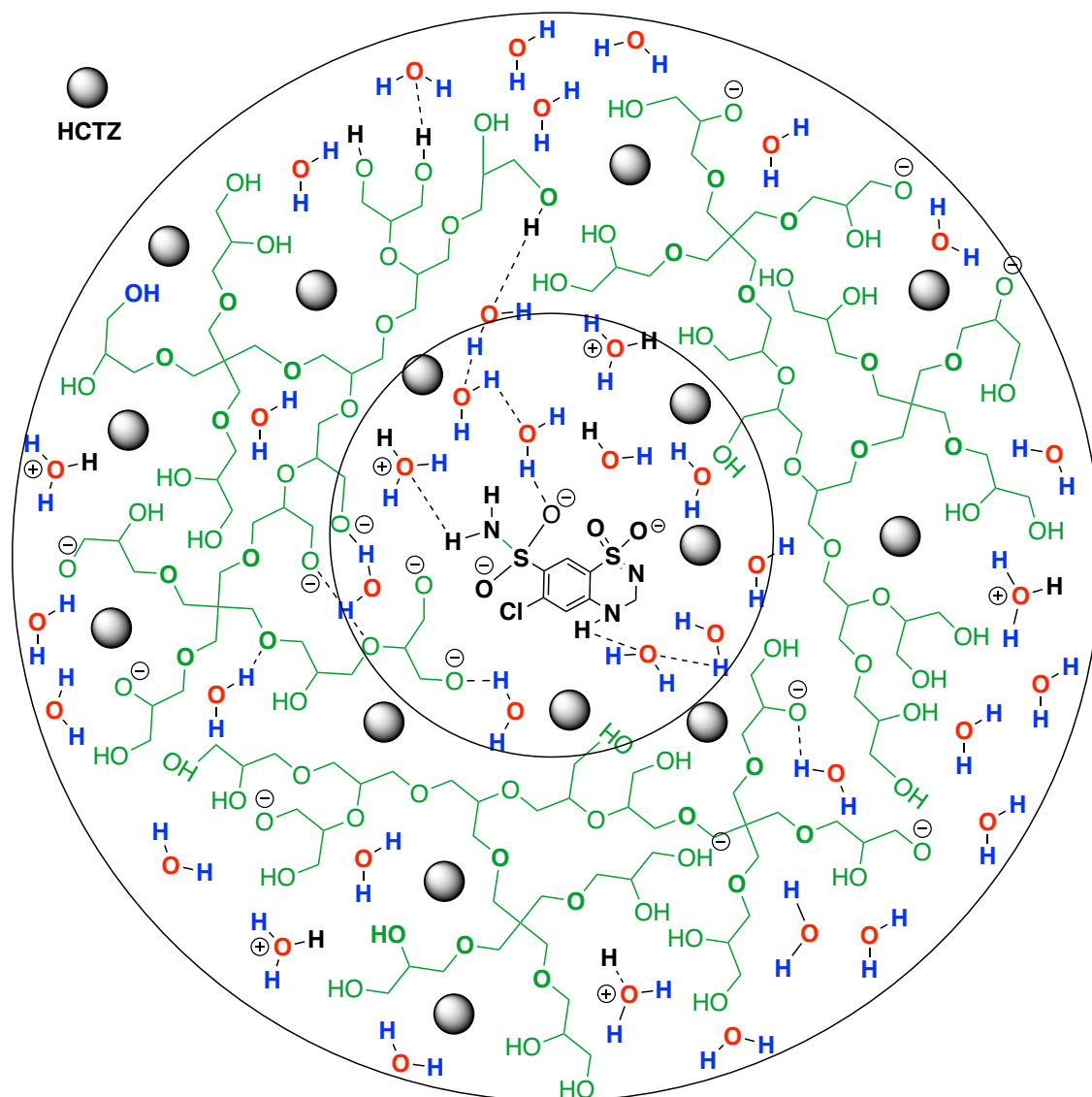
Figure 3. 22 A schemiatic representation of PGHMw cosolvent with HCTZ and water.

The solubility of HCTZ in polyGlyLMw was 2.88 µg ml^{-1} in 50% at pH 8.00. The solubility of HCTZ in polyGlyHMw was 82.26 µg ml^{-1} in 50% at pH 2.50.

The results show that the more favourable solubility cosolvents for a hydrophobic drug such as HCTZ are the mixture that matches the polarity of the hydrophobic drug. Besides, aqueous solutions HCTZ undergoes hydrolysis, giving formaldehyde and 4-amino-6-chloro-1,3-benzenesulfonamide. Hydrolysis of HCTZ is complete at pH

higher than 12 (Brittain, 2001), our experiments indicates that the solution are stable and have not reached the pH at 12 which can cause hydrolysis at 24 hour at room temperature. However, stability tests were carried out over period for day 1, day 3, week 2, week 4 and 6 months at 25°C and 40°C.

The high molecular weight (solid) polyglycerol suggests that the stability is due to the control over both molecular weights and degree of branching. The current polyglycerol can be used to prepare well-defined, complex surface modified polymer structures. The solubility study of HCTZ with polyGlyHMw shows this at the low solubility profile. This indicates that the above polymer is not suitable without surface alteration for drug solubility (Daniel Wilims 2010, et.al., 1999, al., 2000).

Table 3. 9 Solubility of HCTZ in PEG-400, polyglycerine and glycerol mixture at different cosolvent concentrations and their respective dielectric constant. Solubility is calculated from the regression equation slope and intercept obtained from calibration graph prior to each analysis (n = 3)

Cosolvent	PEG 400		Glycerol		Polyglycerine	
(% v/v)	Solubility ($\mu g \ ml^{-1}$)	$(\varepsilon)^*$	Solubility ($\mu g \ ml^{-1}$)	$(\varepsilon)^*$	Solubility ($\mu g \ ml^{-1}$)	$(\varepsilon)^*$
0	6.986	78.36	6.986	78.36	8.640	78.36
10	20.063	71.76	7.879	74.77	25.924	73.52
20	27.792	65.17	7.998	71.19	24.432	68.69
30	53.429	58.57	18.301	67.60	32.103	63.85
40	128.410	51.98	12.547	64.02	38.072	59.02
50	121.583	45.38	17.090	60.43	56.621	54.18
60	298.160	38.78	34.943	56.84	190.127	49.34
70	320.944	32.19	43.795	53.26	202.634	44.51
80	327.196	33.43	91.659	57.51	184.181	47.51
90	312.544	19.00	55.650	46.09	207.182	34.84
100	473.459	12.40	52.331	42.50	343.472	30.00

3.23 Log-linear solubilisation plot

This part of the solubility study's design is to develop constants for the log-linear cosolvent model, thereby allowing accurate prediction of solubilization of the cosolvents used are polyethylene glycol 400 and glycerol, and polyglycerine. The solubilization power (σ) of each cosolvent was determined for HCTZ from the slope of their log–solubility vs cosolvent volume fraction plots. The solubilization data are studied at room temperature. The log-linear solubilization plot compares the solubility profile of HCTZ in the different water-cosolvent mixtures. To obtain this plot, the log of the HCTZ solubility, S_{mix}, is calculated. The log-linear model describes an exponential increase in non-polar drug solubility with a linear increase in cosolvent concentration. The equation below describes this relationship.

$$\log S_{mix} = \log S_w + \sigma f_c$$

Equation 3. 9 Equation for calculation of log S mx from log Solubility of water and solubilization power (σ) which is calculated from logs and cosolvent fraction.

In this equation, S_{mix} is the total solute solubilities in the cosolvent- water mix and S_w is the solubility in water, respectively, is the cosolvent solubilization power for the particular cosolvent, and f is the volume fraction of the cosolvent in the aqueous media. Therefore, to determine the degree of solubilization of a specific compound by a particular cosolvent, the cosolvents solubilization power is calculated.

One way to obtain this value is by experimentation where individual sigma (σ) terms calculated from the slope of the log Smix vs. cosolvent volume fraction (f) profile of each concentration of drug and cosolvent. Figure 3.23 demonstrates that all the cosolvents showed an exponential increase in solubility with an increase in cosolvent volume fraction. Water-PEG 400 mixture showed the highest increase in solubility while water-glycerol mixture showed the lowest increase in solubility. The solubility

of HCTZ in polyglycerine increased in 80 and 100% v/v cosolvent concentration and then it plateaued (Figure 3.23).
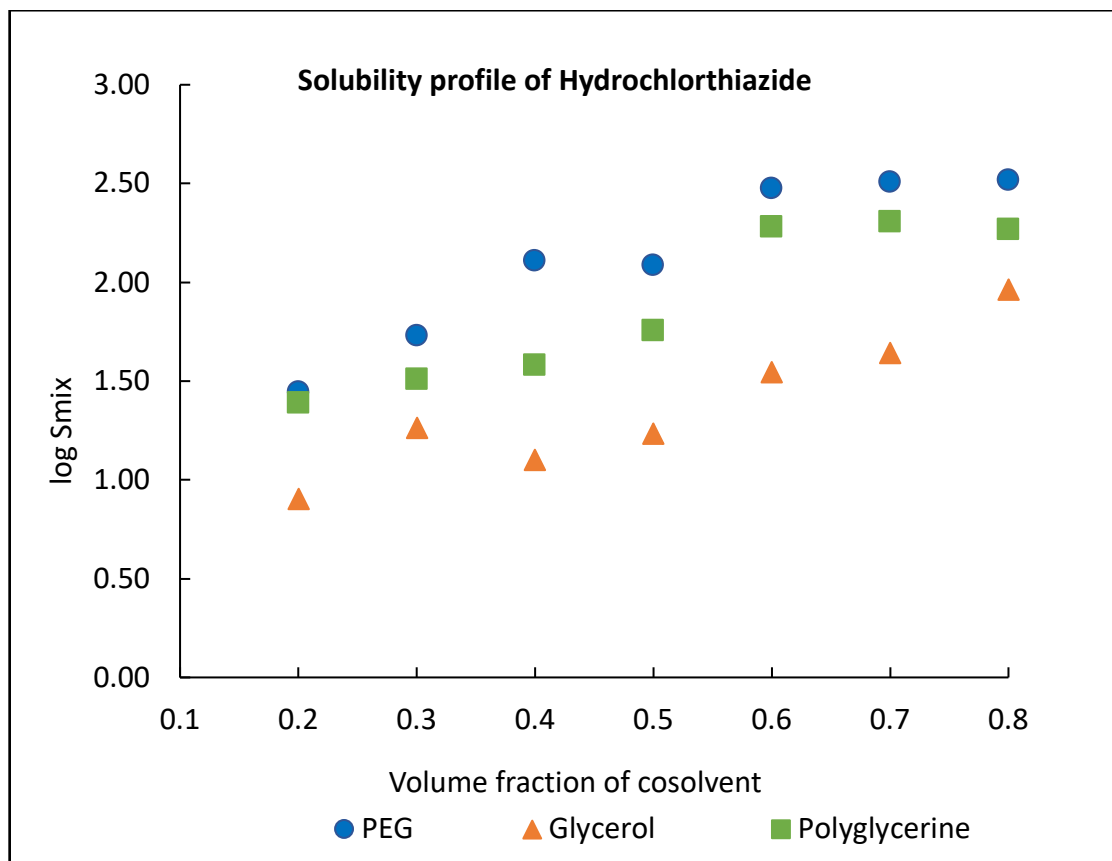
Figure 3. 23 The solubilization power (σ) of cosolvents PEG 400, glycerol and polyglycerine in the solubility study of HCTZ. When cosolvents and water are mixed, they form a homogeneous mixture.

Comparative solubility profile of HCTZ in various water-cosolvent blends by log-linear solubilisation plot. cosolvents were PEG 400, polyglycerine and glycerol.

The solubilisation powers of all the cosolvents (acquired from the slope of the graph) are provided in table 3.10 The order of solubilizing power of the cosolvents is PEG 400> polyglycerine> glycerol.

There is a noticeable inverse correlation between the solubilization powers of the cosolvents used and their dielectric constant. This suggests that HCTZ preferably

solubilizes in a non-polar environment rather than a polar environment. PEG 400, the least polar cosolvent used, provides a less polar environment for the drug to dissolve; hence, it has the highest solubilization power (Table 3.10). Glycerol, the most polar cosolvent used, and has the lowest solubilisation powers.

Table 3. 10 Solubilisation power (σ) of different cosolvents.

Cosolvent	Slope Solubilization power (σ)	Intercept	R^2	Dielectric constant
PEG 400	1.83	1.21	0.9031	12.4
Polyglycerine	1.77	0.98	0.8895	30.5
Glycerol	1.56	0.56	0.8828	42.5

Solubilisation powers of PEG 400, polyglycerine and glycerol calculated from the log-linear solubilisation plot and their respective dielectric constant. Hydrophobicity of the cosolvents is also another important factor involved in the solubility of drugs. Solubility typically increases with increase in hydrophobicity of the cosolvents Figure 3.23 shows that PEG 400 is the most hydrophobic cosolvent with lowest dielectric constant and high solubilisation power calculated from solubility data. In addition, PEG 400 may assist in reducing the dipole moment of water and allowing hydrophobic compounds to fit in. Nevertheless, polyglycerine, which is nontoxic, and biodegradable and edible shows a similar solubility profile for HCTZ.

The effect of added solute to PEG was studied to measure the solubility of PEG in water finding the polymer solution's intrinsic viscosity. PEG (polyethylene glycol, [–CH_2–CH_2–O–$]_n$) dissolves remarkably well in water. The origin of the different solubilities is commonly explained by assuming that the O atoms' distances in various polyether affect their solubility in water. As early as 1969, Blandamer et al. (Blandamer, 1969) recommended that water molecules solubilizing PEG can form a hydrogen-bond network analogous to that of bulk water based on O atoms' distances trans-gauche-trans conformation of the O-C-C-O backbone (Scheme 3.11). The

resulting good fit of the solvation hydrogen-bond network into that of the surrounding water would then explain PEG's high solubility.
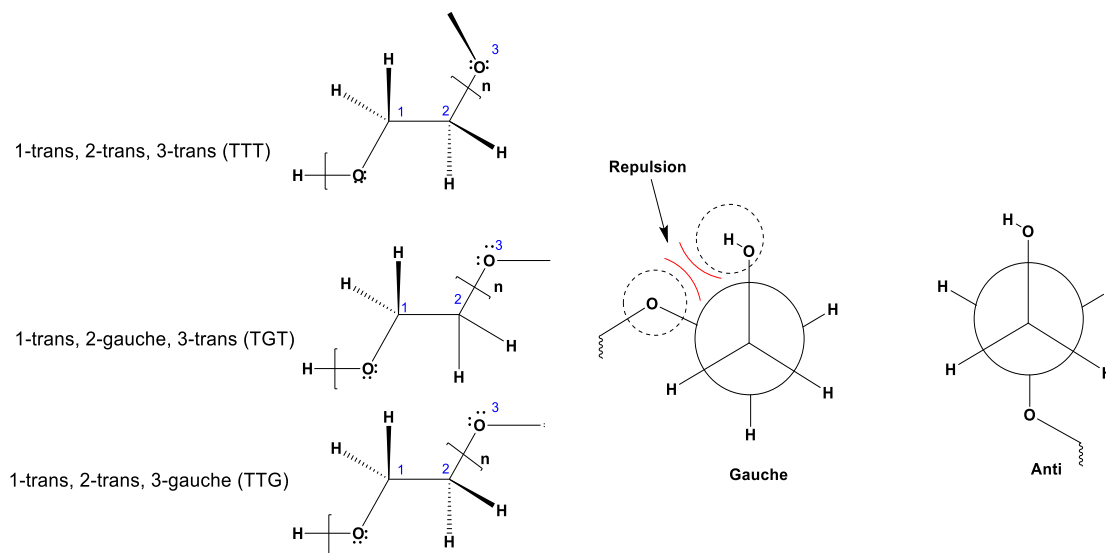
Scheme 3. 10 Three possible poly(ethylene glycol) (PEG) conformations.

Gauche conformation should not be favoured due to Van der Walls repulsion and dipole-dipole repulsion. However, it is more favoured due to empty orbital interaction.

In water, PEG has rigid gauche coordination. This means molecules are arranged similarly as oxygen atoms are arranged in ice. The oxygen molecules are 4.7Å apart. This is almost identical or double the size of the next nearest neighbour oxygen spacing in ice (2.76 Å). Therefore, it shows unlimited solubility in water compared to another polyether. The conformation of TGT relating to a helical polymer with a gauche confirmation about the C-C bond and a trans conformation about C-O bonds lead to infrared marker absorptions at approximately 1350 and 1288cm^{-1}. Elevated temperatures result in less helical ordering, thus affecting solubility and associated properties (Bernd Ensing, 2019).

Fourier Transform infrared spectroscopy (FTIR) using Thermo Fisher scientific Nicolet, Is5, ID transmission instrument and data were analysed using Omnic Spectra software. The experiment of the mixture of HCTZ and cosolvents (formulation) was

carried out to evaluate any hydrogen bond formation between the HCTZ and the cosolvent used. IR is a powerful tool to evaluate the existence of hydrogen bonding between functional groups. A shift in OH band was observed when OH group interact with C=O due to stretching in vibration of OH group at 3000 cm^{-1}. FTIR experiment was carried out for each formulation in powder form.

FTIR of PEG 400 showed a OH stretching peak at 3456 cm^{-1} and an aliphatic (C-H) stretching at 2865 cm^{-1}, similar results were reported by (Kamyar Shameli, 2012) (Figure 3.24). HCTZ characteristic peaks were recorded in the FTIR spectrum as NH stretching was observed at 3359, 3260 and 3161 cm^{-1}. The characteristic peak for SO$_2$ asymmetric stretching appeared at 1316 cm^{-1} and the SO$_2$ symmetric vibrations appeared at 1147 and 1120 cm^{-1}. For the HCTZ PEG mixture the vibration of the OH was shifted slightly to 3445 cm^{-1}. This reflects the involvement (Figure 3.24) of OH informing H bonds with HCTZ S=O groups (Panigrahi, 2012).
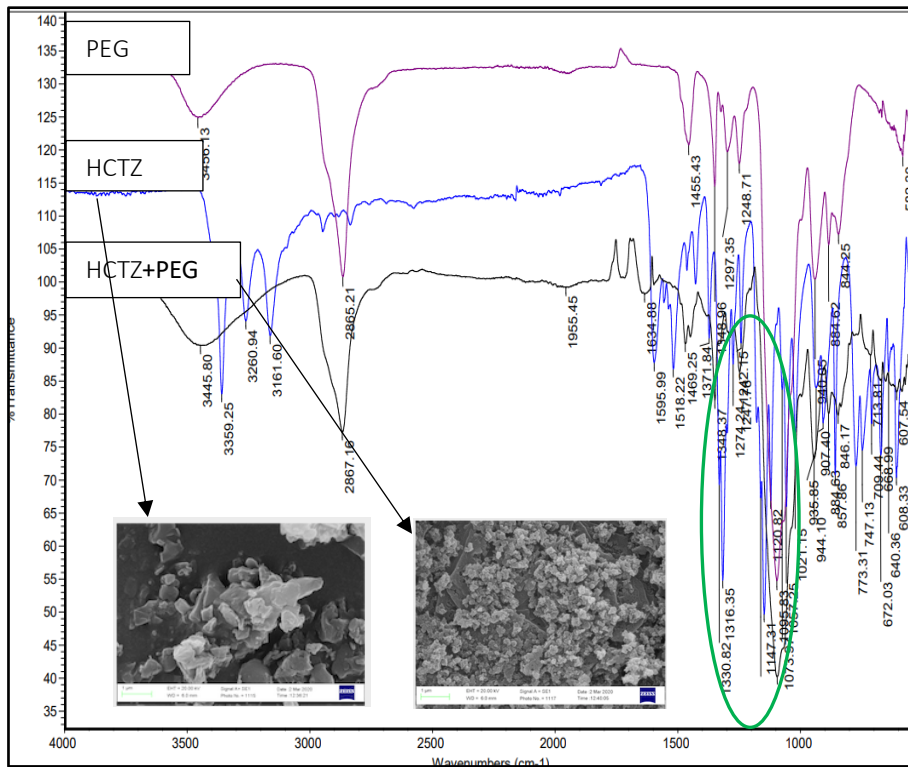
Figure 3. 24 FTIR vibration of PEG and PEG+ HCTZ and HCTZ formulation.(Scanning electron microscope images.

Scanning electron microscopy (SEM) images of HCTZ in water post freeze drying after 24h and HCTZ + PEG 400 formulation after solubility shows clear that at scale of 1 μm the rigid surface of HCTZ in water changes morphology from more rigid powder to soft clusters demonstrating that HCTZ has lost its crystalline structure because of the solvation power of PEG 400. The solubility of HCTZ in PEG-400 v/v 100 % (473.46 ± 8.47 μml^{-1}) is significantly higher than water (8.06 ± 6.69 μml^{-1}).

Glycerol is a liquid, very soluble (in water), and a very weakly acidic compound (based on its pKa). The three-dimensional hydrogen bond network of H_2O molecules plays a crucial role in the behaviour of water (Rosaria Grasso, 2018). The molecular movements in water demand constant breaking and rearranging each hydrogen bond on a picosecond time scale. At any moment, the degree of hydrogen bonding is very high. Using glycerol shows a dynamic equilibrium among changing percentages of

66

assemblages of different oligomers and polymer species at room temperature (temperature dependant). The study by Rosaria and co-workers (Rosaria Grasso, 2018) used neutron diffraction experiments and computational modelling for hydrogen-bond networks to study glycerol-water solutions at different concentrations. It was reported that glycerol and water can cause micro segregation to form hydrogen-bonded water-rich and glycerol-rich regions. The study above shows this is the formation of nanoclusters of water surrounded by the solute molecules' matrix. Besides, the many physical and chemical characteristics of water that have a significant and unprecedented role it is related to such low-density structuring molecules. In the glycerol molecule, all bonds between atoms are single, and there is considerable rotational freedom. The traditional classification of this molecule's molecular structure is based on the backbone conformation concept, defined by the heavy atoms (carbon and oxygen) irrespective of the hydrogen atoms' position. Each terminal CH_2OH group can rotate about the other backbone carbon-carbon bond (Towey, 2011).

The FTIR spectrum of glycerol (Figure 3.25) is showing an OH stretching at 3330 cm^{-1}. This is in line with the previous published data by (Fernando D.Pitt 2019).
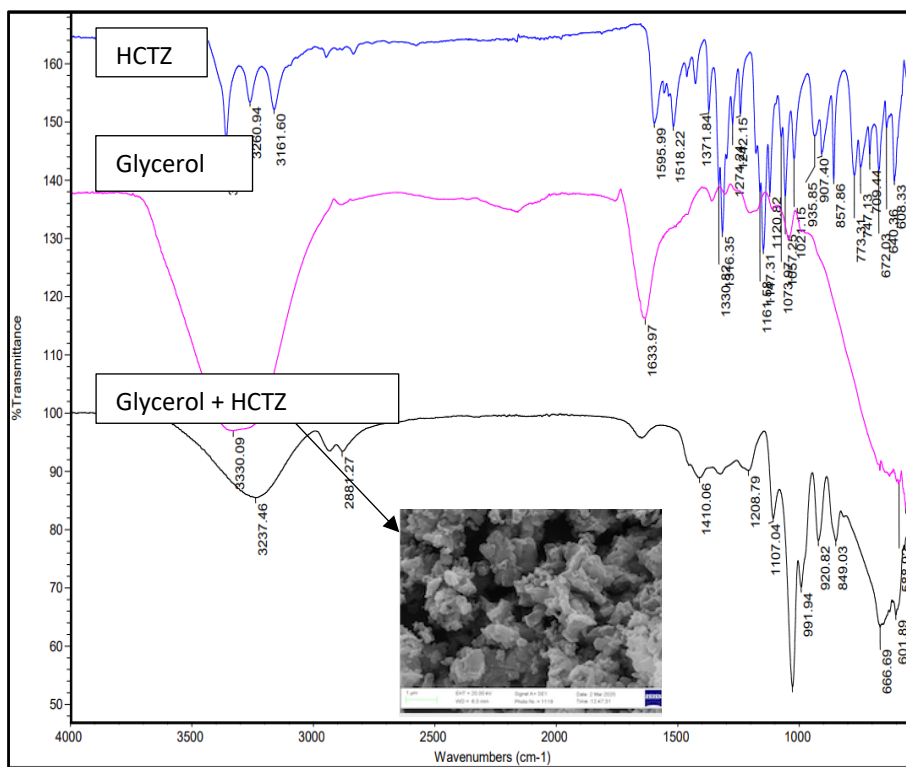
Figure 3. 25 FTIR vibration of glycerol and glycerol+ HCTZ and HCTZ formulation.

FTIR result of freeze dried HCTZ formulation with glycerol shows a strong H bond formation as the OH vibration has shifted from 3330 to 3237 cm^{-1} in the HCTZ glycerol mixture. Nonetheless, the solubility profile was lower than PEG-400 and polyglycerine. This can be since glycerol has a limited H bonding sites compared to the other 2 cosolvents. In addition, glycerol FTIR shows the distinct peaks of, in the formulation of glycerol HCTZ the CH stretching can be observed at 2882.27 cm-1, and C=O peaks at 1633.97 cm-1, and C-O-H and C-O-C of alcohol and ether can be seen at 991.94 cm^{-1}. Carbonyl can be also observed in 1597.36 cm^{-1}. In the formulation spectra the OH stretching at 3330.09 cm^{-1} in which is disappeared in the formulation due to the hydrogen bonding with HCTZ and water. The SEM images at 1 µm scale shows soft amorphous powder. In addition, the peaks of HCTZ in the regions from 1300- 700 cm^{-1} reduces due to the hydrogen bonding. Another significant change was observed in SO_2 stretch of sulphonamide moiety in the ring, that shifted from 1073 cm^{-1} in form I to 1032 cm^{-1} (Fernando D.Pitt 2019).

The freeze dried FTIR result of HCTZ formulation with cosolvent poly glycerine shows considerable solubility like PEG-400 and higher than glycerol and other cosolvents. Polyglycerine's good solubility profile can be because polyglycerine having a combination of fatty acids (Figure 3.26).
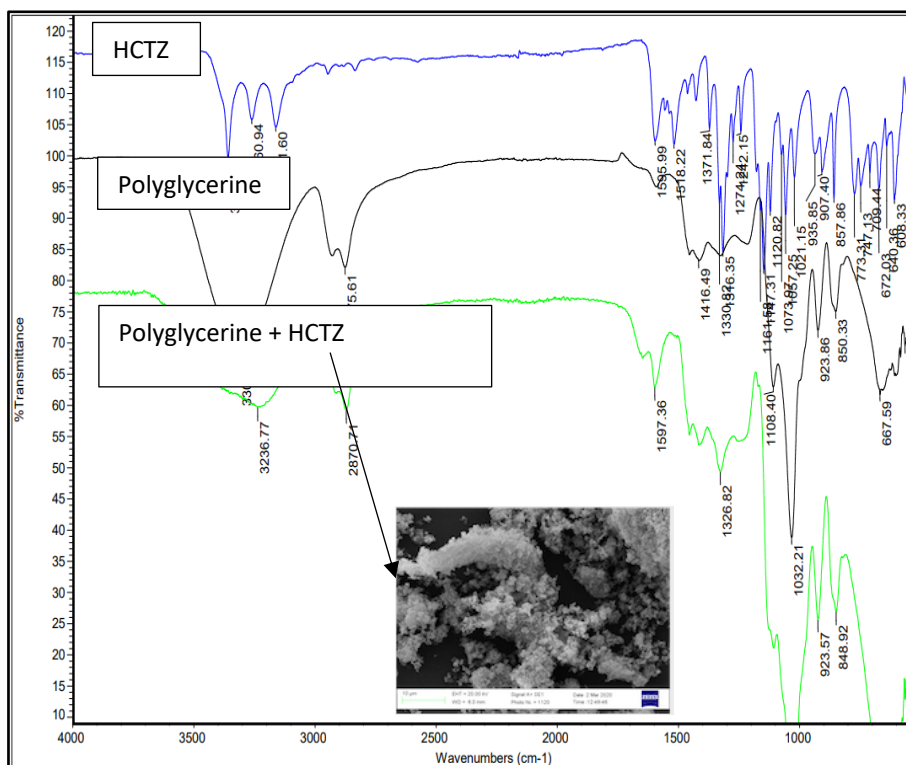
Figure 3. 26 FTIR vibration of polyglycerine, polyglycerine HCTZ and HCTZ alone.

The HCTZ molecule can form better hydrogen bonds with polyglycerine (OH vibration shifted from 3309 cm^{-1} in pure polyglycerine to 3231 cm^{-1} in the polyglycerine HCTZ mixture), which also indicated why the solubility of HCTZ is high at v/v 90 % cosolvent ratio (382.23 ± 35.96 µgml^{-1}). SEM results of HCTZ and polyglycerine solubility formulation shows soft, porous powder. The OH is shifted from 3309.46 to 3236.71 cm^{-1}. The CHO stretch can be observed at 2875.61 for polyglycerine and in the formulation at 2870.71 cm^{-1} slightly shifted. The C=O stretch can be observed in the formulation at 1597.36 cm^{-1} and the significant change was observed in SO stretch of sulphonamide moiety in the ring, that shifted from 1032.20 cm^{-1} in form I to 1000 cm^{-1}.

FTIR result for the HCTZ formulation freeze-dried for better FTIR visualization with co-existent polyGlyLMw shows low solubility. There is no significant changes observed in SO stretch of sulphonamide moiety in the ring, that shifted from 1073 cm^{-1} in form I to 1069 cm^{-1} (Figure 3.27).
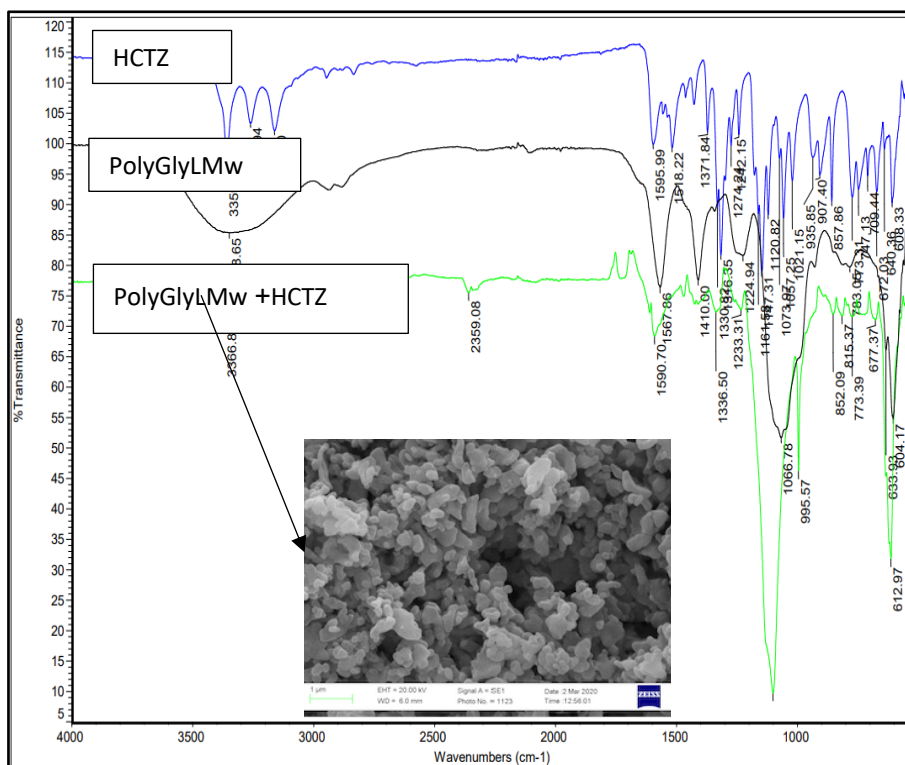
Figure 3. 27 FTIR vibration of PolyGlyLMw and PolyGlyLMw + HCTZ and HCTZ formulation.

The SEM images of the HCTZ cosolvent formulation using more water and less cosolvent can form better hydrogen bonds, which also indicated why the solubility of HCTZ is not high at w/v 50 % cosolvent ratio (27.27 ± 0.23 μml^{-1}). SEM image shows small uniform colloid like uniform structure, and this can be connected to the low solubility of this cosolvent.

FTIR visualization with the cosolvent polyGlyHMw (Figure 3.28) shows little higher than polyGlyLMw but lower solubility to all other cosolvents. The SEM images of the HCTZ cosolvent formulation at 1 μm can form better hydrogen bonds, which also

indicated why the solubility of HCTZ is highest at w/v 50 % cosolvent ratio (82.26 ± 11.63 µml^{-1}). However, compared to other cosolvent very low solubility.
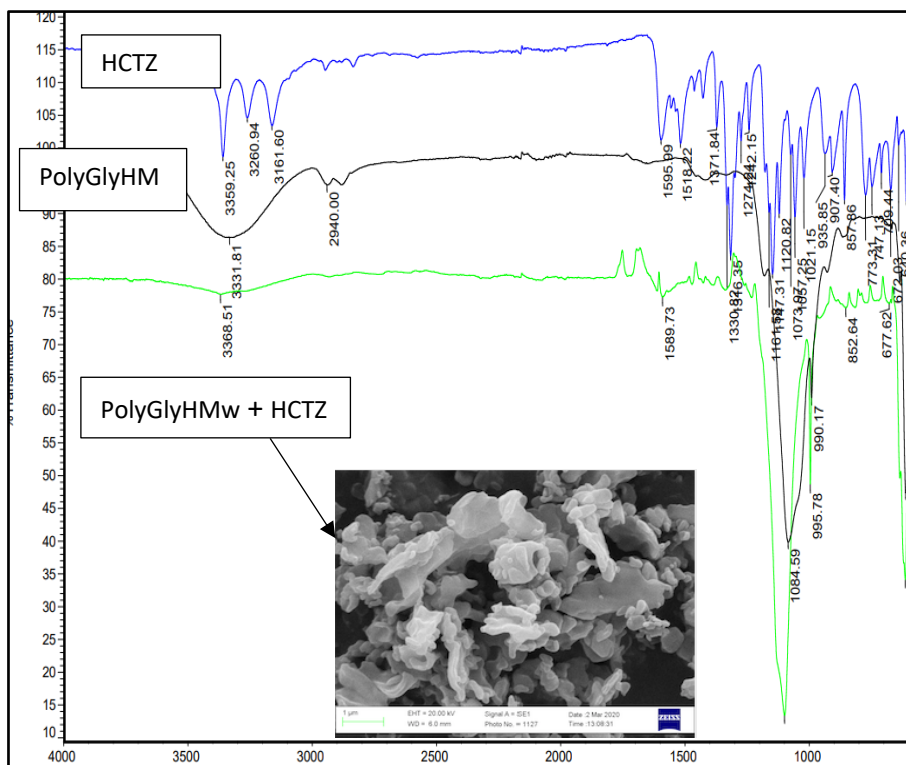
Figure 3. 28 FTIR vibration of PolyGlyHMw and PolyGlyHMw + HCTZ and HCTZ formulation.

The OH stretch at 3369 cm^{-1} is not shifted significantly as well the C=O peak of drug still visible, and no significant change was observed in SO stretch of sulphonamide moiety in the ring, that shifted from 1073 cm^{-1}.

SEM images of polyGlyHMw and polyGlyLMw shows similar profile which can be attributed to the low solubility of each cosolvent. SEM provided information about this formulation's ultrastructure and indicated that the freeze-dried particles could be easily dissolved back in an aqueous solution. For storage and stability, these formulations can be cryoprotected. The FTIR and SEM data give an insight into the more profound composition of such formulation using different cosolvents. They could provide a full detailed study for stability comparisons to the liquid formulation.

3.24 Stability study

In solid form, the drug HCTZ is stable at room temperature for five years. The old literature (Mollica, 1969) reports that the bell-shaped pH-dependent hydrolysis of HCTZ proceeds irreversibly to a ring-opened product (4-amino 6-chloro-1,3-benzenedisulphonamide, DSA) (Mollica, 1969).
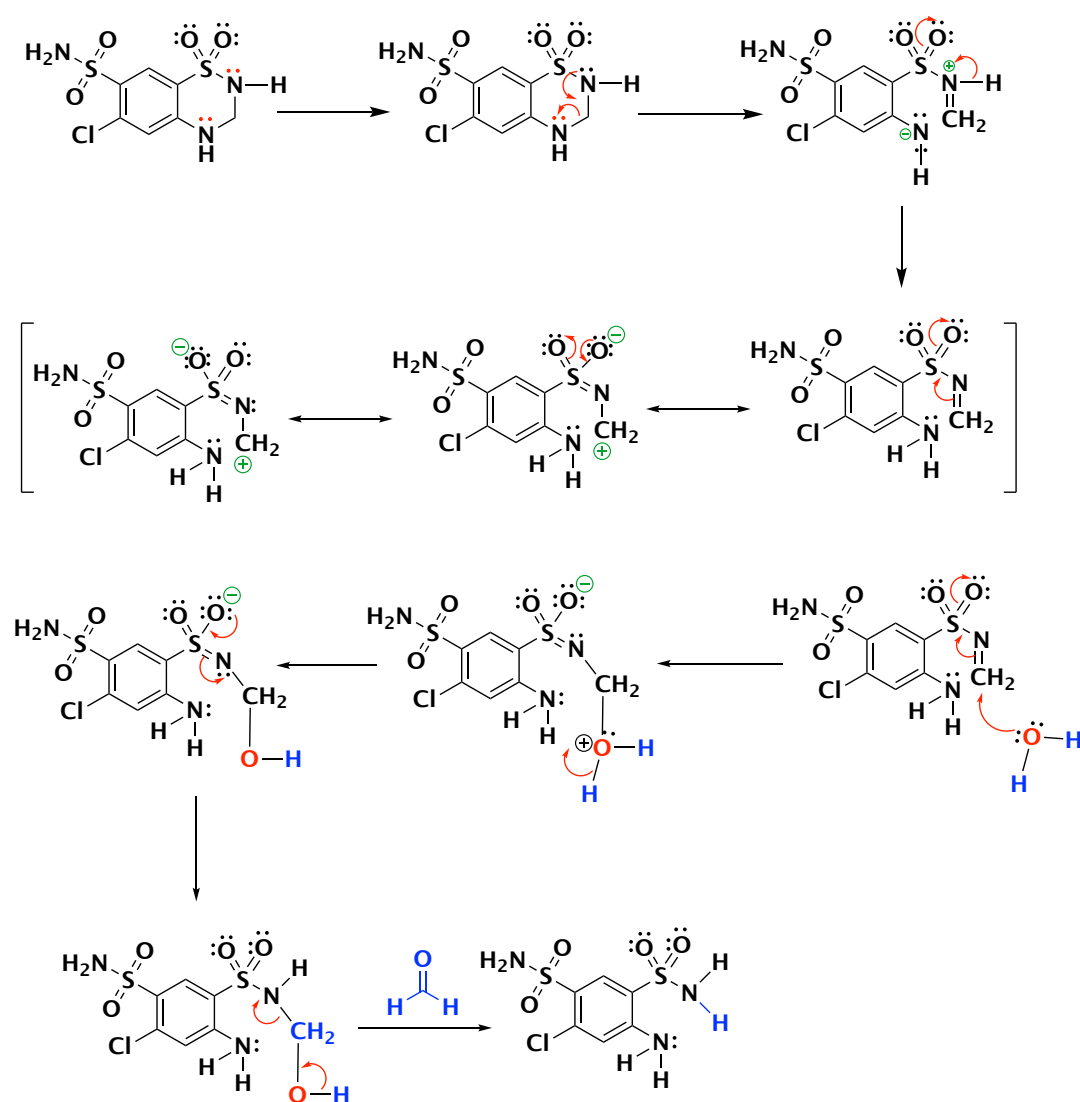
Scheme 3. 11 Hydrolysis of HCTZ formation of 4-amino 6-chloro-1,3-benzenedisulphonamide and formaldehyde.

A set of each HCTZ formulation (HCTZ+PEG400, HCTZ + polyglycerine, HCTZ + glycerol, HCTZ + HMwPolygly and HCTZ+LMwPolygly) was stored at 25° C / 64 % relative

humidity (RH), and the second set of formulations was stored at 40°C / 75% RH. The stability study was conducted at day 0, 1, 3, 7 and 14 and 30 days. The pH of the sample was tested using a calibrated pH meter, and aliquots were withdrawn and tested using HPLC, MeOH: ACN (60:40) mobile phase. The samples were also visually observed on each of those days.

3.24.1 PEG Stability

In principle, the properties of polyether impose significant constraints on their enzymatic degradation. When dissolved in water, PEG adopts a random coil formation due to its geometry in monomer units, with the alcohol groups at the termini distributed within the macromolecular space. This conformation causes problems when an enzymatic attack is targeted at the termini (Kawai, 2005). PEG 400 is a polyethylene glycol polymer which contains a mixture of ethylene oxides ranging from 3-15 molecules, and molecular weight varies from $242 - 594$ g mol^{-1}, which makes average molecular weight 400 g mol^{-1} PEG 400. During metabolism, PEG is converted by alcohol dehydrogenase to monoacids and diacids of diethylene and triethylene glycol ($n = 1–8$). These are components of low molecular weight PEGs, which are formed by oxidation. This oxidation decreases with increasing chain length.

3.24.2 Glycerol and polyglycerol stability

The acceptable daily intake for polyglycerine set by the Joint Expert Committee on Food Additive (JECFA) for the World health organization (WHO) in 1974 is 7.5 mg/Kg body weight/day. The United Kingdom Food additive committee (UK FAC) in 1992 estimated that the maximum daily intake of polyglycerine is 2.64 mg/kg body weight/day.

The metabolism of polyricinolic acid was studied by condensing stearic acid (1-14C) with ricinoleic acid and esterifying the resulting polyricinoleic acids incorporating the

73

14 carbon (14C) labelled marker fatty acid with polyglycerol to form 14C-stearic polyglycerine. The 14C stearic acid can be absorbed and metabolize similarly to standard fatty acids. Analysis of gut contents revealed a mixture of ricinoleic acid and polyricinoleic acid (Kawai, 2005, R. Wilson, 1998).
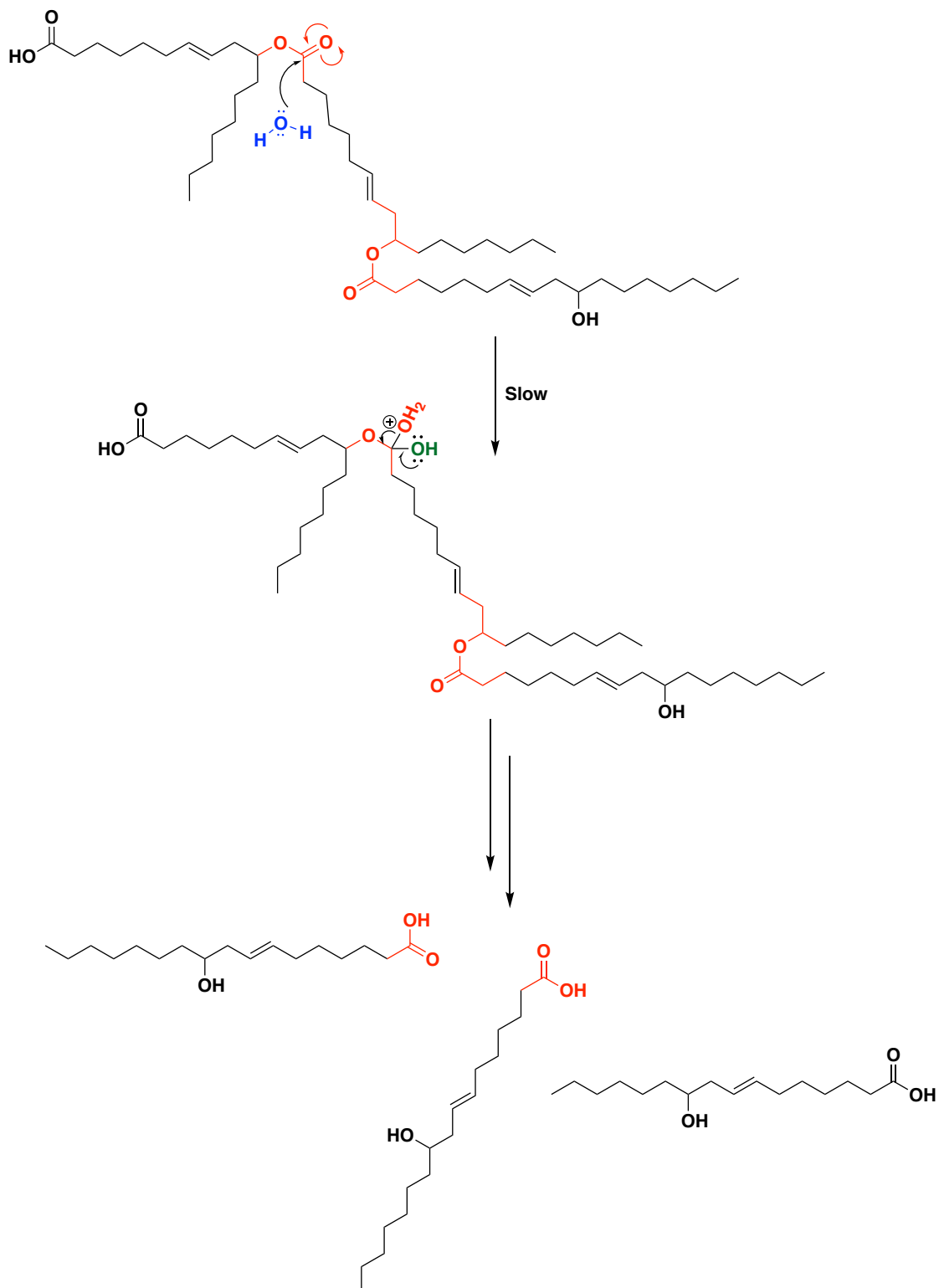
Scheme 3. 12 Hydrolysis of fatty acid ester in polyglycerine in presence of water.

Metabolic studies have shown that polyglycerine is digested in the rat's gut to give free polyglycerols, polyricinoleic acid, and free ricinoleic acid. Lower polyglycerols (up to three glycerol units) are absorbed and excreted unchanged in the urine, while higher polyglycerols are excreted in the faeces. Up to 90% of the fatty acid material is absorbed and metabolized. Acute toxicity tests involving the single oral intubation of polyglycerine in several species showed that polyglycerine was pharmacologically inactive. No deaths related to polyglycerine were seen in dosed rats (20 ml/kg body weight). The only observation noted was slight diarrhoea in some animals. Furthermore, there was no evidence of direct toxic action from the repeated oral administration of PGPR to rats at a dose of 10 ml/Kg body weight daily for five days. (R. Wilson, 1998).

3.25 Stability results

The stability assay results obtained for HCTZ are calculated as percentages remaining in 30, 50, and 70 % cosolvent compared to solubility result with HCTZ in water. The pH of each sample was also measured in triplicate. The liquid preparations are usually considered stable if the active ingredient remains ± 10% of the original amount. The stability over time indicates that storage conditions 25 °C (64% RH) and 25 °C (75% RH). The results obtained from using (30, 50 and 70 % v/v) cosolvents for solubility and stability of HCTZ are calculated as percentage remaining in, 30, 50 and 70 % cosolvent. The results are compared to solubility result with control, kept at (25 °C RH 64 %) and (40 °Cat RH 75 %). The samples were withdrawn from the solubility vials 5 ml total volume for HPLC analysis on day 1, 3, 14 and 30. On each sampling day, all the formulations were injected into the HPLC machine using mobile phase (Methanol: Acetonitrile, 60:40) three times using validated method and the average peak area was calculated. Each analysis day a fresh calibration was carried out prior to analysis. The regression equation was then used to calculate concentration of HCTZ in the formulations and then the percentage HCTZ in the amount of cosolvent was

calculated. The formulation chosen for stability were 30, 50 and 70% from a range of 10 – 100 %.

3.25.1 HPLC analysis of HCTZ stability (30 % v/v cosolvent)

Formulations of HCTZ (v/v 30 %) with different cosolvents were stored at 25 °C (64% RH) and 40 °C (75% RH). The formulation at 40 °C (75% RH) degraded faster than those stored at the room temperature. The HCTZ formulations in PEG-400 stored at different conditions had degraded to below 20%. The formulation of HCTZ, PEG 400 changed from day 0 to day 30 from 87 % to 66 % at 25 °C (64% RH). This is above 10 % of the original amount (Figure 3.29 and 3.30).

For the formulation of glycerol which has relatively low solubility still, the HCTZ remain from 18 – 16 % at 25 °C (64% RH) over 30 days.

At 30 % cosolvent fraction, the formulation of polyglycerine remains relatively stable over 30 days from 47 – 43 % at 25 °C (64% RH). However, the formulation of polyGlyLMw (38 – 29 %) remaining and polyGlyHMw (45 – 28 %) remaining, showed higher amount of HCTZ up to 78 % from day 1 – 3 this can be related to the degradation product having same elution time as the active compound at 25 °C (64% RH).

It was the excellent formulation in which the active ingredient remained within ±10% of the original amount. The changes can also be observed in table 3.11 overtime at 25 °C (64% RH), which tends to be more acidic over time and can indicate the hydrolysis of the HCTZ in the solvent formulation.

Table 3. 11 pH values of HCTZ in 30%v/v PEG, Polyglycerine and glycerol PolyglyLMw and PolyglyHMw liquid at 25°C (64% RH) and at 40°C (75% RH) over 30 days (n = 3).

Time	30 % PEG (HCTZ% pH)		30 % Glycerol (HCTZ %) pH		30 % Polyglycerine (HCTZ %) pH		30 % PolyGlyLMw (HCTZ %) pH		30 % PolyGlyHMw (HCTZ %) pH	
Days	25 °C (64% RH)	40 °C (75%RH)	25 °C (64% RH)	40 °C (75% RH)	25 °C (64%RH)	40 °C (75%RH)	25 °C (64%RH)	40 °C (75% RH)	25 °C (64%RH)	40 °C (75%RH)
Water	6.50	7.00	6.50	7.00	6.50	7.00	6.50	7.00	6.50	7.00
0	6.50	7.00	6.50	5.00	7.00	4.50	7.00	4.50	7.00	4.50
1	5.52	4.30	5.10	5.10	9.54	9.50	7.00	7.00	4.90	2.00
3	5.00	4.50	5.50	5.20	9.20	9.50	7.90	7.90	2.45	2.46
14	5.23	3.61	5.13	5.13	9.13	9.00	7.13	7.23	1.55	2.00
30	5.20	3.20	5.10	5.15	9.15	9.00	7.50	7.25	1.55	2.00
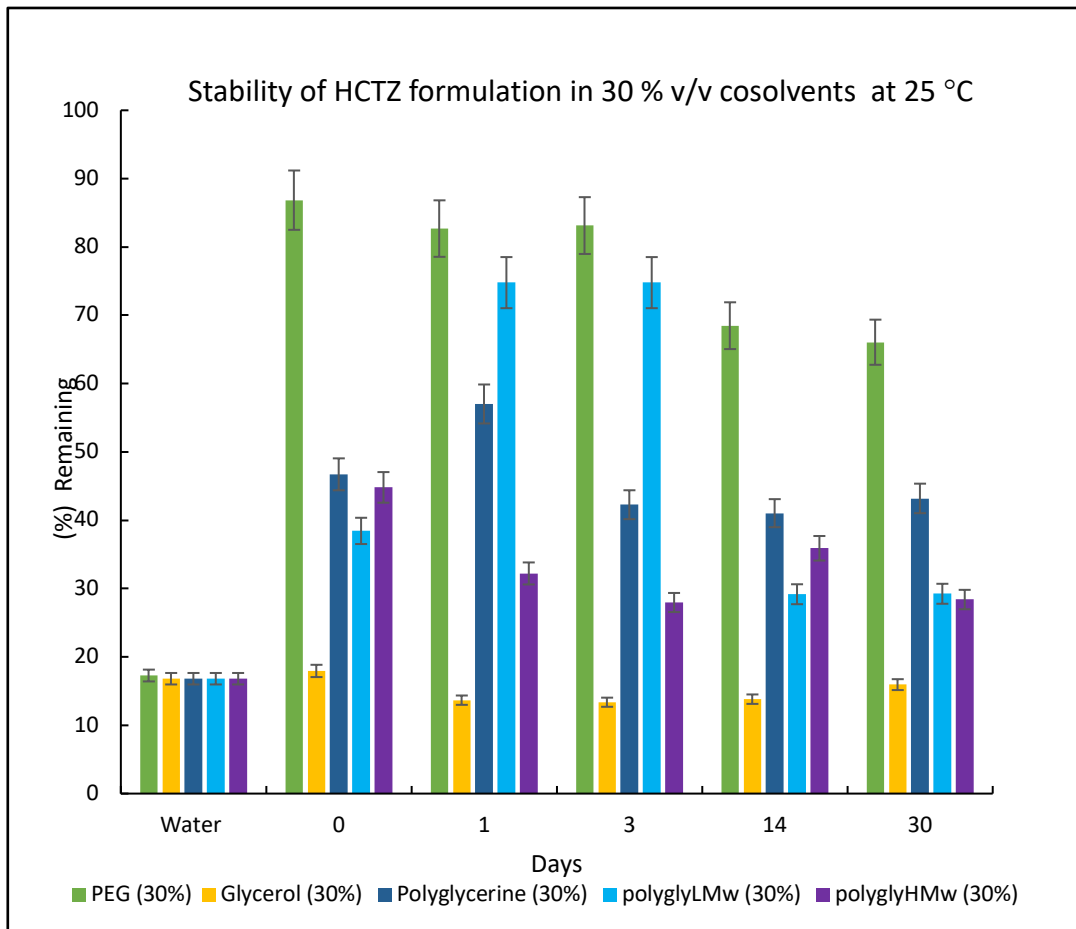
Figure 3. 29 Percentage of HCTZremaining in 30% PEG, polyglycerine and glycerol, PolyglyLMw and PolyglyHMw liquid at 25 °C (64% RH) over 30 days (n = 3).
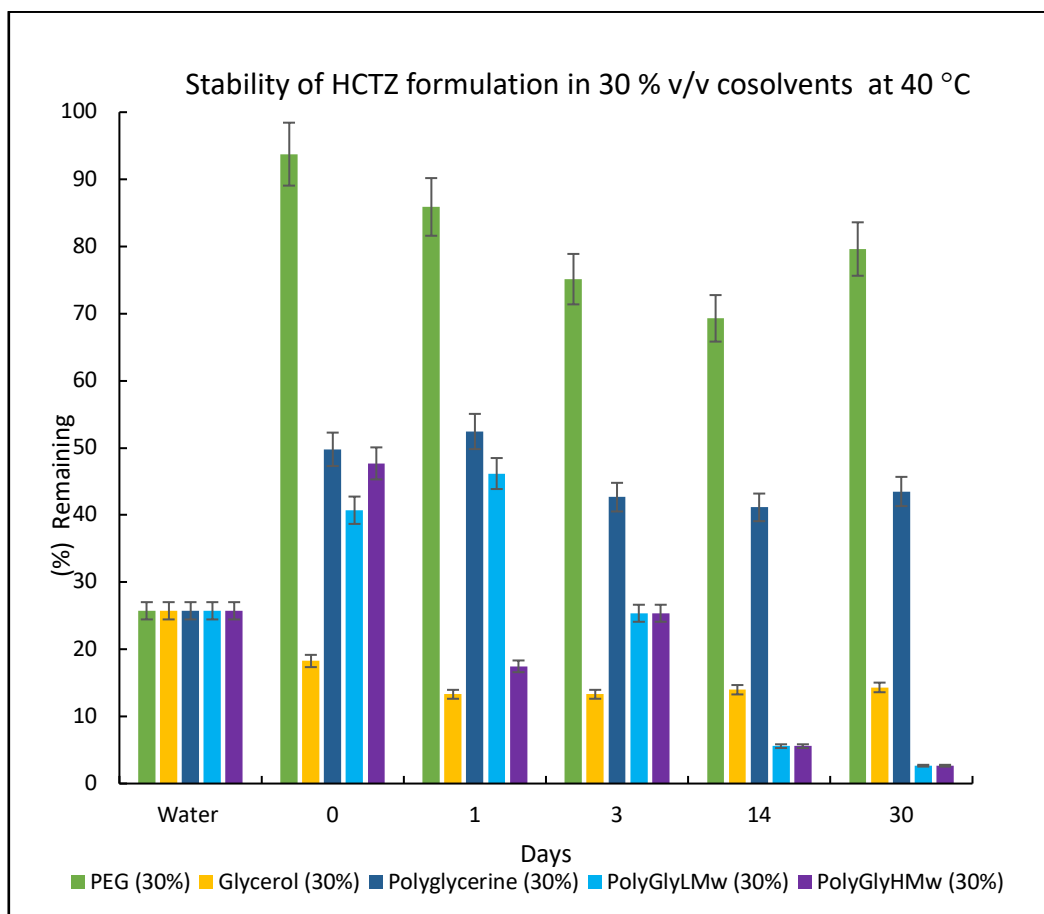
Figure 3. 30 Percentage of HCTZremaining in 30% PEG, polyglycerine and glycerol, PolyglyLMw and PolyglyHMw liquid at 40 °C (75% RH) over 30 days (n = 3).

The solubility results at 25 °C (64% RH) and 40 °C (75% RH) indicates that the storage condition affects the stability of the liquid formulation of hydrochlorothiazide. Formulations of HCTZ (v/v 30 % cosolvent) with different cosolvents were stored at 40 °C (75% RH) degraded faster than those held at the room temperature. The HCTZ formulations in PEG-400 stored at different conditions had degraded to below 20 % (Figure 3.30). The formulation of HCTZ, PEG 400 changed from day 0 to day 14 from 86 - 69 % at 40 °C (75% RH) with a gradual decrease. Nevertheless, at day 30, the % remaining increases to 80 %, which can attribute to the degradation product as a result of hydrolysis and same co-elution time with an active compound. Another factor which can accelerate the degradation is the high temperature, the percentage

drug remaining over 1-14 days is still above the accepted limits of 10 % of the original amount.

For the formulation of glycerol which has relatively low solubility still, the HCTZ remain from 18 – 14 % 40 °C (75% RH) compared to formulation stored at room temperature not considerable changes instability is observed (18 – 16 % at 25 °C (64% RH) over 30 days.

At 30 % cosolvent portion, the formulation of polyglycerine remains relatively stable over 30 days from 50 – 44 % at 40 °C (75% RH). This formulation showed a trend of gradual decrease of an active compound.

The formulation of polyGlyLMw (41 – 3 %) remaining and polyGlyHMw (48 – 3 %) remaining 40 °C (75% RH), showed the amount of HCTZ degrades over time. As the HCTZ remaining is below the accepted range, the acidic pH can support this. The changes can also be observed in table 3.11 overtime at 40 °C (75 % RH), which tends to be more acidic over time and can indicate the hydrolysis of the HCTZ in the cosolvent formulation.

When comparing the pH values of the different formulations, there was a significant difference in the pH value of PEG and glycerol and polyglycerine, PolyGlyLMw and PolyGlyHMw formulations stored at both storage conditions. The pH value for the PEG formulation stored at 25 °C (64% RH) and 40 °C (75% RH) at day 3 was 0.5 while the pH value for glycerol formulation stored at 25 °C (64% RH) and 40 °C (75% RH) was 0.3 Polyglycerine increase at higher temperature by 0.3 for PolyGlyLMw and PolyGlyHMw remain the same at for the last 2 polymers the pH changed drastically at day 1. However, there was no significant difference in the pH values of Polyglycerine when stored at both storage conditions 25 °C (64% RH) and 40 °C (75% RH).

The pH of the formulation (table 3.11) over time tends to change more towards basic pH apart from PEG 400 and PolyGlyHMw formulation.

3.25.2 HPLC analysis of HCTZ stability (50 % v/v cosolvent)

Formulations of HCTZ (v/v 50 %) with different cosolvents (PEG 400, Polyglycerine, glycerol, PolyGlyLMw, PolyGlyHMw) were stored at 25 °C (64% RH) and 40 °C (75% RH). The formulation at 40 °C (75% RH) degraded faster than those stored at the room temperature. The HCTZ formulations in PEG-400 stored at specific storage conditions show some stability profile, especially at room temperature. The formulation of HCTZ, PEG 400 changed from day 0 to day 30 and was showing to increase the percentage remaining. This could be because of the high amount of cosolvent and the formation of degradation product at 25 °C (64% RH). The percentage remaining of HCTZ shows 100 % (figure 3.30).

For the formulation with glycerol which has relatively low solubility, the HCTZ increases from (14 – 39 %) at 25 °C (64% RH) over 30 days, a similar trend to PEG-400.

At 50 % cosolvent fraction, the formulation of polyglycerine shows relatively similar profile over 14 days from 45 – 66 % at 25 °C (64% RH) and at 30 days the %ge remaining HCTZ decreased own to 19 %. However, the formulation of polyGlyLMw (66 – 19 %) remaining and polyGlyHMw (66 – 27 %) remaining, showed similar trend which can be related to the degradation product having same elution time as the active compound at 25 °C (64% RH).

PEG-400 was the better formulation in which the active ingredient remained within ±10% of the original amount. The changes can also be observed at 25 °C (64% RH), which tends to be more acidic for polyGlyLMw (pH = 2.00), and neutral (pH = 7.00 for polyglyHMw over time and can indicate the hydrolysis of the HCTZ in the solvent formulation (Table3.12).

Table 3. 12 pH values of HCTZ in 50%v/v PEG, Polyglcerine and glycerol PolyGlyLMw and PolyGlyHMw liquid at 25 °C(64% RH) and at 40 °C(75% RH) over 30 days (n = 3).

Time	50 % PEG (HCTZ%)		50 % Glycerol (HCTZ %)		50 % Polyglycerine (HCTZ %)		50 % PolyGlyLMw (HCTZ %)		50 % PolyGlyHMw (HCTZ %)	
Days	25 °C (64% RH)	40 °C (75%RH)	25 °C (64%RH)	40 °C (75% RH)	25 °C (64%RH)	40 °C (75%RH)	25 °C (64%RH)	40 °C (75% RH)	25 °C (64%RH)	40 °C (75%RH)
Water	6.50	7.00	6.50	7.00	6.50	7.00	6.50	7.00	6.50	7.00
0	5.00	5.00	5.10	5.00	11.00	11.00	7.00	7.00	3.00	3.00
1	6.00	6.00	5.50	5.30	9.50	9.80	8.00	8.55	2.50	3.00
3	5.00	5.50	5.20	4.50	10.10	9.00	7.00	7.00	1.00	2.00
14	4.00	4.00	4.00	4.20	10.10	10.20	7.50	7.00	1.00	2.00
30	4.15	2.50	8.30	3.55	9.00	9.00	7.00	7.00	2.00	2.00

Figure 3. 31 Percentage of HCTZ remaining in 50% PEG, Polyglcerine and glycerol, PolyGlyLMw and PolyGlyHMw liquid at 25 °C(64% RH) over 30 days (n = 3).
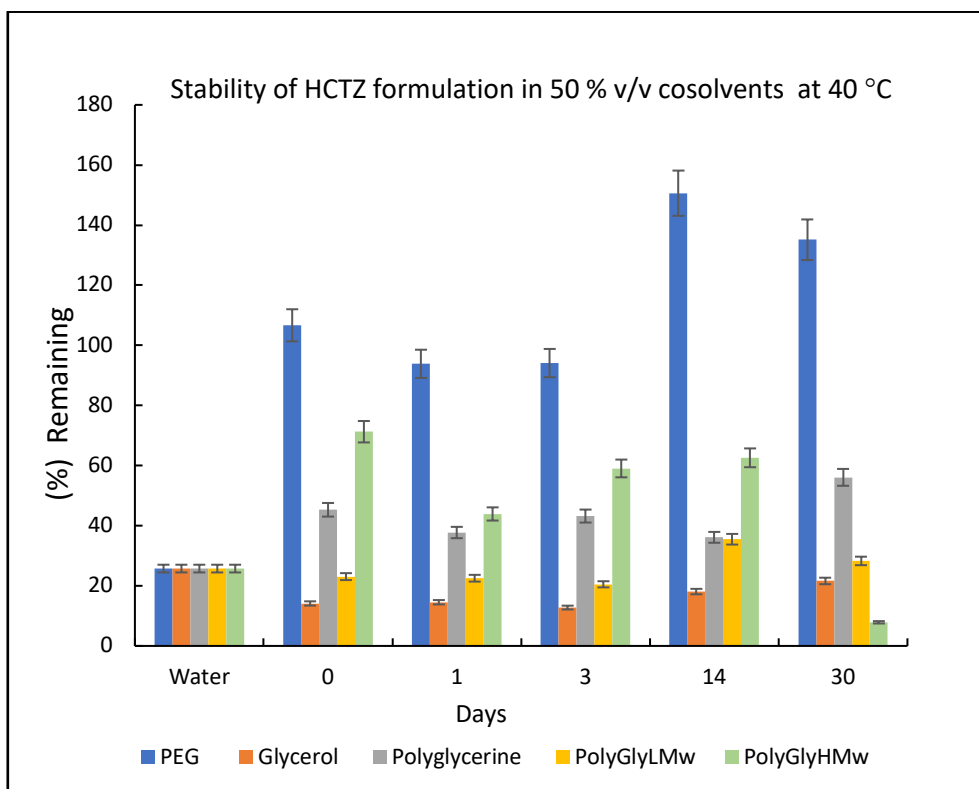
Figure 3. 32 Percentage of HCTZremaining in 50% PEG, Polyglcerine and glycerol, PolyGlyLMw and PolyGlyHMw liquid at 40 °C(75% RH) over 30 days.

The HCTZ formulations in PEG-400 stored at specific storage conditions show some stability profile, especially at room temperature. The formulation of HCTZ, PEG 400 changed from day 0 to day 30 shows an increase in the % remaining. This could be due to the effect of the high amount of cosolvent and the formation of degradation product at 40 °C (75% RH). The percentage remaining of HCTZ shows 107 to 151 % at day 14 and then decrease of 135 % on day 30 (Figure 3.32).

For the formulation of glycerol which has relatively low solubility still, the HCTZ increases from 14 – 22 % at 40 °C (75% RH) over 30 days, pH = 3.55.

At 50 % cosolvent fraction, the formulation of polyglycerine, pH = 9.00, shows relatively similar profile over 30 days from 45 – 56 % at 40 °C (75% RH). However, the formulation of polyGlyLMw (23– 28 %) remaining and polyGlyHMw (71 – 8 %)

remaining, showed similar trend which can be related to the degradation product having same elution time as the active compound at 40 °C (75% RH).

The formulation in which the active ingredient remained within ±10% of the original amount can be marked as stable. The changes can also be observed overtime at 40 °C (75% RH), which tends to be more acidic for polyGlyLMw (pH = 2.00), and neutral (pH = 7.00 for polyglyHMw over time and can indicate the hydrolysis of the HCTZ in the solvent formulation.

In these batches of HCTZ (50 % v/v) the batch PEG 400 shows higher solubility and stability for three days. However, the concentration of HCTZ starts changing over time. It fluctuates in solution, which is an indication of degradation as the degradation product may have similar elution time at the active compound. However, this requires more in dept study.

Glycerol is a small molecule compound with 3 OH groups which generally showed lower solubility of HCTZ apart from using at (70% v/v and 80 % v/v). The reason can be having a large quantity of OH ionisable group which facilitates the solubility of HCTZ. Besides, the concentration of HCTZ at 50 % v/v glycerol remain stable for up to three days at room temperature (Larissa Sakis Bernardi, 2020). However, the HCTZ concentration is low for solubility and change in concentration of HCTZ occurs at week 2 and 4 and the pH changes indicate that at day one there was a slight change in pH of the glycerol containing a liquid formulation of HCTZ. A similar trend for glycerol is observed at 40°C.

Polyglycerine shows to be only stable at 24 hours and shows variable concentration which is again an indication of the co-elution of degradation compounds of HCTZ in a liquid formulation.

From the physical appearance of PolyGlyLMw, it is evident that this is the compound with low solubility and low stability. However, the polymer with higher molecular

weight shows better solubility; however, the stability is not very promising after 24 hours at 25°C (64% RH).

3.25.3 pH measurements of HCTZ stability (50 % v/v cosolvent)

The pH of each formulation at 50 % v/v cosolvent from the solubility and stability result which were kept at (25 °C RH 64 %) and (40 °C, RH 74 %) were measured in triplicated using a pre calibrated pH meter with buffers of pH 4, 7 and 10.

In addition, from pH observation and stability data it can be concluded that the solution became acidic for both hyperbranched polymers (PolyGlyLMw and polyGlyHMw) at 25°C (64% RH) and 40°C (75% RH). For PEG 400 glycerol the, pH tended at both condition towards acidic however, Polyglycerine showed to remain at basic pH over time as the initial pH of Polyglycerine is pH = 11.

Table 3. 13 pH values of HCTZ in 50%v/v PEG, Polyglcerine and glycerol PolyGlyLMw and PolyGlyHMw liquid at 25 °C(64% RH) and at 40 °C(75% RH) over 30 days (n = 3).

Time	50 % PEG (HCTZ%)		50 % Glycerol (HCTZ %)		50 % Polyglycerine (HCTZ %)		50 % PolyGlyLMw (HCTZ %)		50 % PolyGlyHMw (HCTZ %)	
Days	25 °C (64% RH)	40 °C (75%RH)	25 °C (64%RH)	40 °C (75% RH)	25 °C (64%RH)	40 °C (75%RH)	25 °C (64%RH)	40 °C (75% RH)	25 °C (64%RH)	40 °C (75%RH)
Water	6.50	7.00	6.50	7.00	6.50	7.00	6.50	7.00	6.50	7.00
0	5.00	5.00	5.10	5.00	11.00	11.00	7.00	7.00	3.00	3.00
1	6.00	6.00	5.50	5.30	9.50	9.80	8.00	8.55	2.50	3.00
3	5.00	5.50	5.20	4.50	10.10	9.00	7.00	7.00	1.00	2.00
14	4.00	4.00	4.00	4.20	10.10	10.20	7.50	7.00	1.00	2.00
30	4.15	2.50	8.30	3.55	9.00	9.00	7.00	7.00	2.00	2.00

3.25.4 HPLC analysis of HCTZ stability (70 % v/v) cosolvent

The results obtained from using (70 % v/v) cosolvents for solubility and stability of HCTZ were calculated as percentage remaining in, 70 % cosolvent. The results are compared to solubility result with control, kept at 25 °C RH 64 % and 40 °C, RH 75 %. The samples from PEG, glycerol and Polyglycerol were withdrawn from the solubility vials 5 ml total volume for HPLC analysis on day 0, 1, 3, 7, 14 and 30. Samples for PolyGlyLMw* and polyGlyHMw** were not included as at 60 % cosolvent upwards there was no solubility of polymer possible. Therefore for 70% stability these are withdrawn. On each sampling day, all the formulations were injected into the HPLC machine using mobile phase Methanol: Acetonitrile, 60:40 three times using validated the previously method and the average peak area was calculated. Each analysis day a fresh calibration was carried out prior to analysis. The regression equation was then used to calculate concentration of HCTZ in the formulations and then the percentage HCTZ in the amount of cosolvent was calculated (Figure 3.33).

Table 3.13 pH values of HCTZ in 70%v/v PEG, Polyglcerine and glycerol PolyGlyLMw* and PolyGlyHMw** (*,** No data at 70 % v/v cosolvent) liquid at 25 °C(64% RH) and at 40 °C(75% RH) over 30 days (n = 3).

Time	70 % PEG (HCTZ%)		70 % Glycerol (HCTZ %)		70 % Polyglycerine (HCTZ %)	
Days	25 °C (64%RH)	40 ° C (75%RH)	25 °C (64%RH)	40 °C (75% RH)	25 °C (64%RH)	40°C (75%RH)
Control	6.50	7.00	6.50	7.00	6.50	7.00
0	5.00	5.00	4.00	4.00	10.00	10.00
1	6.00	5.50	4.50	4.00	9.50	7.00
3	5.50	5.00	4.15	4.00	9.50	7.50
14	5.25	4.00	4.00	4.00	10.00	8.00
30	5.50	6.40	3.80	3.90	6.86	6.00
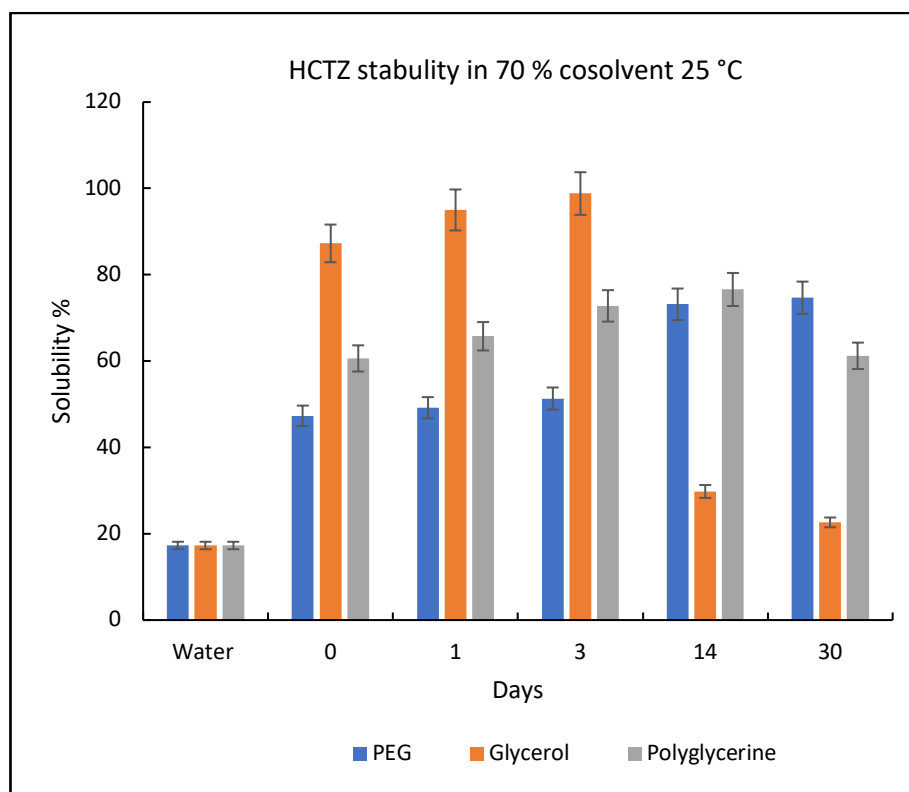
Figure 3. 33 Percentage of HCTZremaining in 70% PEG, Polyglcerine and glycerol, PolyGlyLMw* and PolyGlyHMw** liquid at 25 °C(64% RH) over 30 days (n = 3) (*, ** no solubility).

In this stability batch of HCTZ (70 % v/v) 25 °C (64% RH) only 3 compounds PEG 400, glycerol and polyglycerine were used as the remaining two hyperbranched polymers did not show solubility after 50 % cosolvent. Glycerol is a small molecule compound with 3 OH groups which generally showed lower solubility of HCTZ apart from being used at 70% v/v and 80 % v/v. The reason can be having large quantity of OH ionisable group which facilitates the solubility of HCTZ. In addition, the concentration of HCTZ at 70 % v/v 25 °C (64% RH) glycerol increases for up to three days at room temperature 25 °C (64% RH) (87 -99 %). However, the HCTZ concentration shows reduction at week 2 and week 4 (30- 23 %) and the pH changes table 3.13 indicated that at day one there was slight change in pH= 5.30

of the glycerol containing liquid formulation of HCTZ which then changes over 4 weeks to pH = 8.30.

Polyglycerine from day 0 to 3 shows the percentage remaining of the drug (61 – 99%) and after day 3 to 30 days shows reduction of (99 – 23 %) at 25 °C (64% RH) (Figure 3.34).
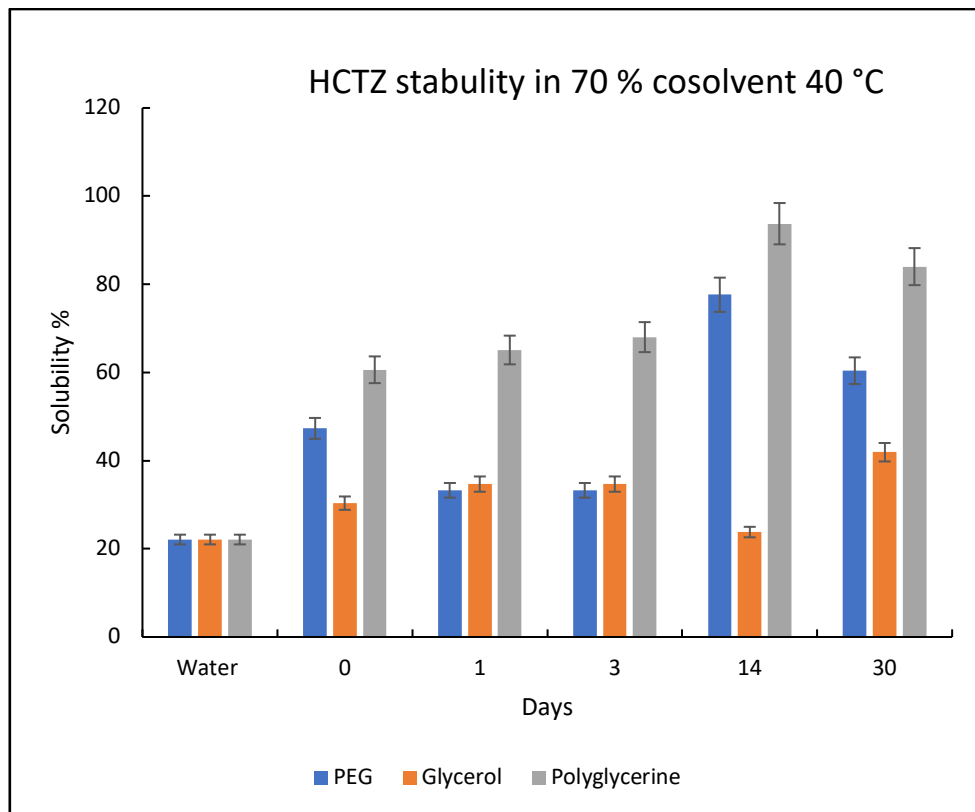
Figure 3. 34 Percentage of HCTZremaining in 70% PEG, Polyglcerine and glycerol, PolyGlyLMw* and PolyGlyHMw** liquid at 40 °C(75% RH) over 30 days (n = 3) (*, ** no solubility).

The formulation of HCTZ, PEG 400 40 °C (75 % RH) changed from day 0 to day 3 showing a reduction in the % remaining (47 – 33). The percentage remain of HCTZ shows at day 14 to 30 shows degradation by a decrease in the HCTZ amount may be due to co elution of degradation product (78 – 60%) at 40 °C (75% RH).

For the formulation of glycerol which has relatively low solubility still, the HCTZ increases from 61 - 63 % at 40 °C (75% RH) over 3 days, pH = 9.00

At 70 % cosolvent fraction, the formulation of polyglycerine, pH = 9.00, shows relatively similar profile from 14 days (81%) HCTZ remaining to 84 % at day 30 at 40 °C (75% RH).

The literature is not very clear regarding the identification of the chromatographic peaks of its two major related substances. However, a recent publication has validated and established a HPLC method for degradation products and impurities related to HCTZ. The products are chlorothiazide and 4-amino-6-chloro-1,3-benzenedisulfonamide (DSA) (Larissa Sakis Bernardi, 2020) (Scheme 3.15).

4-amino-6-chloro-1,3-benzenedisulfonamide (DSA)
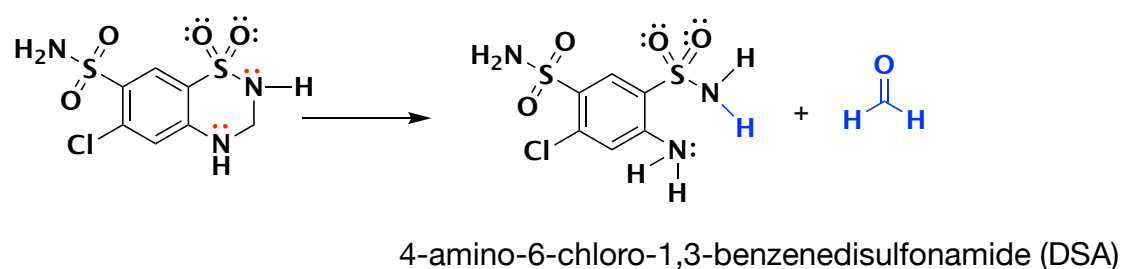
Scheme 3. 13 formation of aldehyde from HCTZand DSA.
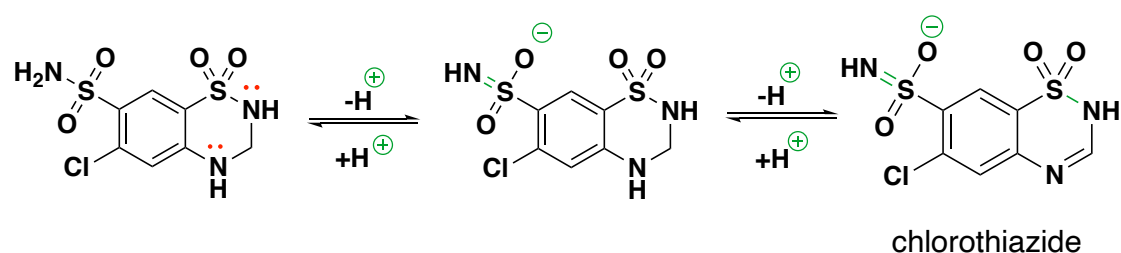
chlorothiazide

Scheme 3. 14 Reversible reaction of HCTZ in the presence of water and formation of chlorothiazide.

The recent literature (Fang et al., 2001) about the degradation products of HCTZ states that the formation of 4-amino-6-chloro-1,3-benzenesulfonamide. (DSA) (Scheme 3.15) was detected which was linked to a decrease of HCTZ

concentration in basic hydrolysis (16.4%). The acid hydrolysis caused a decrease of (15.8%), and after neutral/thermal hydrolysis (51.1%) of HCTZ was present.
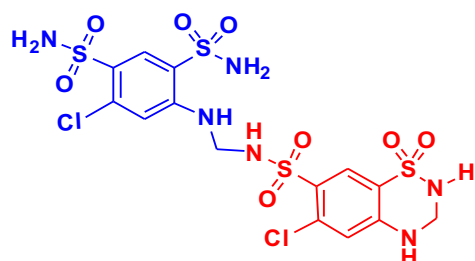
5-chloro-1-{[6-chloro-3,4-dihydro-2H-1,2,4-ben-zothiadizine-7-sulfonamide-1,1-dioxide(methyl)]-amino}-benzene-2,4-disulfonamide
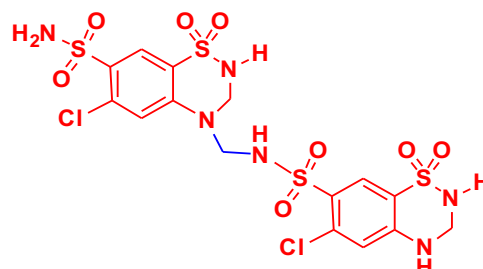
(4-[{6-chloro-3,4-dihydro-2H-1, 2,4-benzothiadiazine-7-sulfonamide-1,1-dioxide}-methyl]-6-chloro-3-hydro-H-1,2,4-benzothiadia-zine-7-sulfonamide-1,1,dioxide)

Scheme 3. 15 Common degredation compound identified in the existing litrature.

The authors (Fang et al., 2001) stated that their results confirmed that the formation of DSA occurs by irreversible hydrolysis, which is also an indication of the change in pH of our formulation over time, and this happens both in acid and in the basic atmosphere (Scheme 3.17).
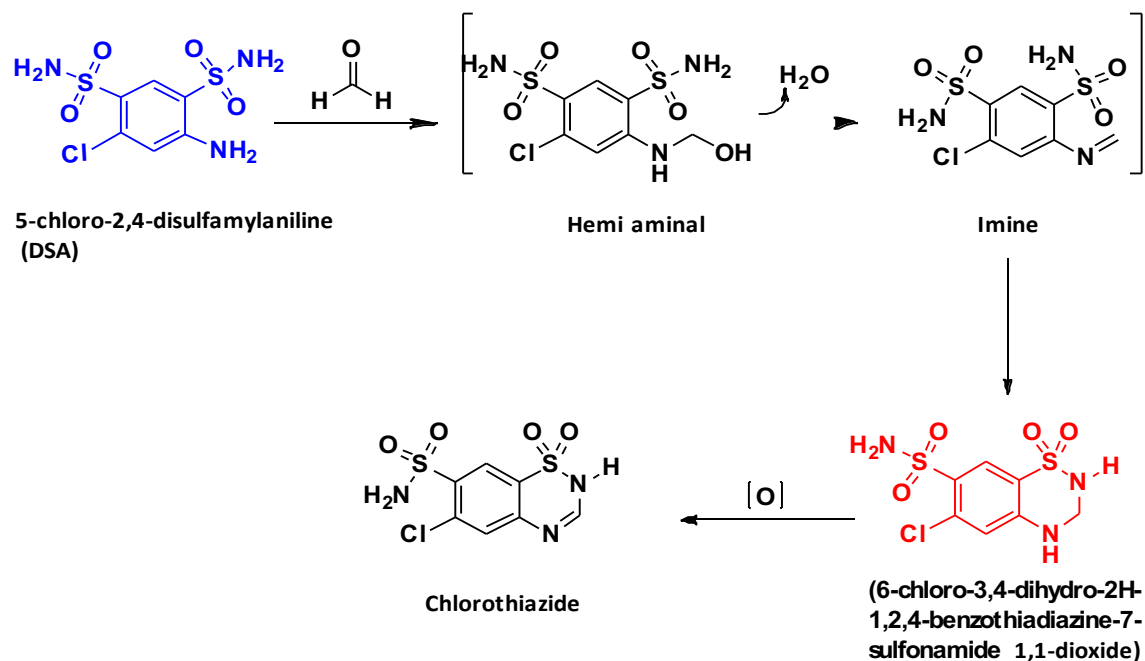
Scheme 3. 16 degradation products of HCTZ states that the formation of 4-amino-6-chloro-1,3-benzenesulfonamide. (DSA)

Hydrochlorothiazide (HCTZ) liquid formulation was stored at 25 °C (64% RH) and 40 °C (75% RH). The formulation of HCTZ degraded faster at 40 °C (75% RH) than the formulation stored at 25 °C (64% RH). By day 7, the HCTZ formulations stored at different conditions had degraded. NMR studies (Fang et al., 2001) had previously been conducted the degradation products of HCTZ, which can form dimers of HCTZ-CH2-HCTZ or DSA-CH2-HCTZ products. In this study (Fang et al., 2001), the impurity was concentrated and purified using a combination of solid-phase extraction and reverse-phase high-pressure liquid chromatography. Subsequently, the contaminant has been identified with different analytical techniques such as, ultraviolet spectroscopy, liquid chromatography/mass spectrometry, and NMR spectroscopy. Therefore, when the compounds were tested over six months shows an apparent degradation. A similar peak was observed in our stability assay.
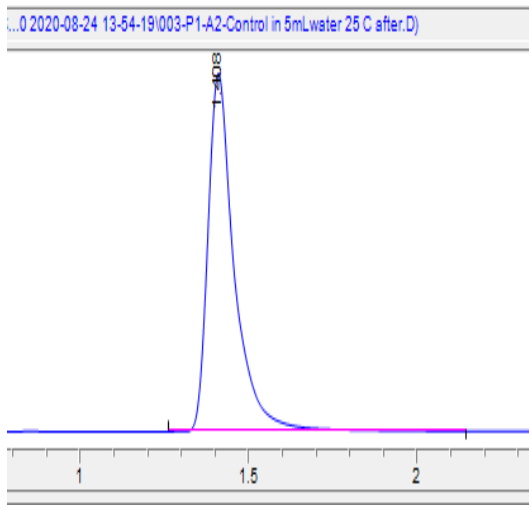
A
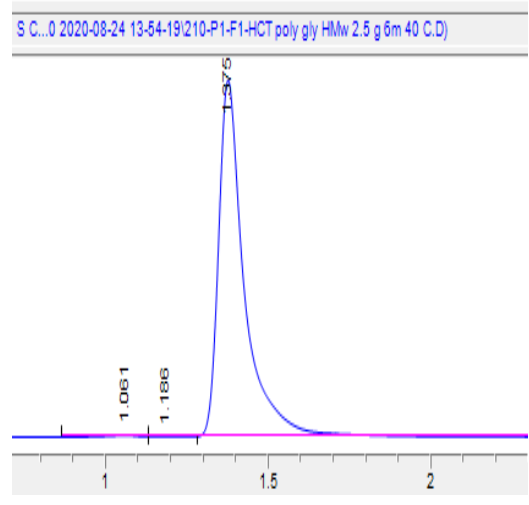
B

Figure 3. 35 A – HCTZ in DI water at 25 °C after 6 months and B – HCTZ formulation of PolyGlyHMw (50 % v/v) at 25 C (64 % RH) after 6 months.
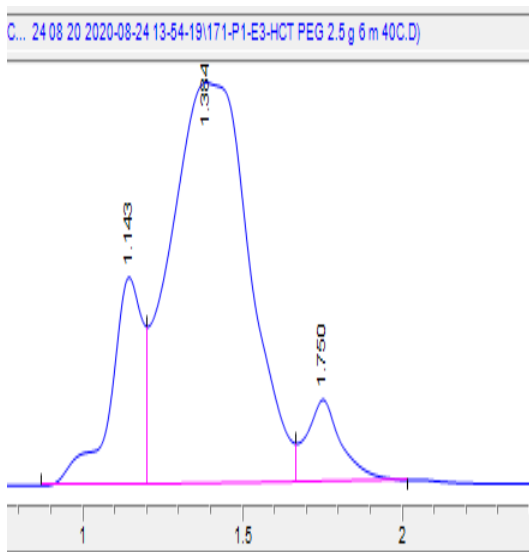
C
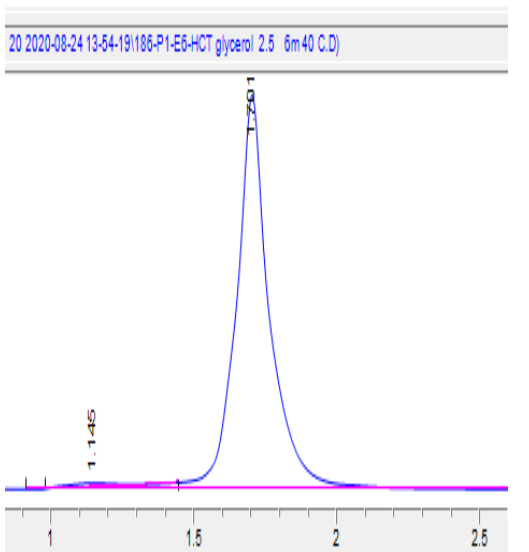
D

Figure 3. 36 C - HCTZ in PEG 400 (50 % v/v) at 40 °C (75 %RH) after 6 months and D – HCTZ formulation of Polyglcerine (50 % v/v) at 25 °C (64 %RH) after 6 months.
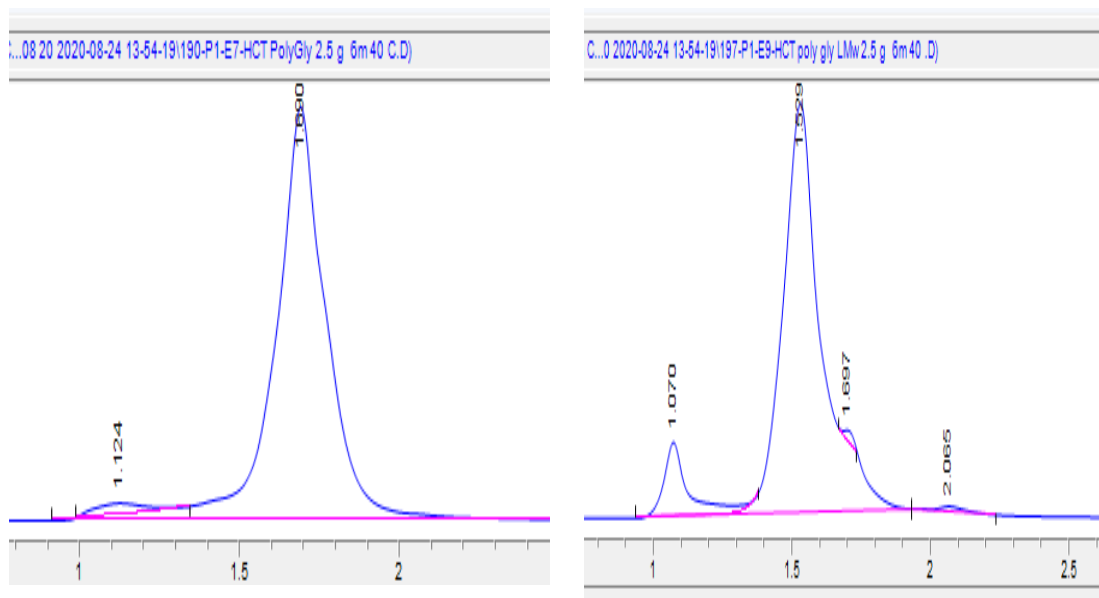
E

F

Figure 3. 37 E - HCTZ formulation of Polyglcerine (50 % v/v) at 40 C (75 %RH) after 6 months F - A fraction of polyGlyLMw formulation of HCTZ (50% v/v) at 40 C (75 % RH) over 6 months.

To compare the HPLC method, a preliminary 1H NMR study of the formulation solubility after 24 h (day 0) was carried out in the presence of standard internal anisole. The results suggested that the active compound is stable when formulated with these polymers.

3.26 Conclusion

Formulation of insoluble drugs using cosolvents is one of the oldest and most widely used techniques, especially for liquid formulation intended for oral and intravenous administration. The reduction of the dielectric constant is possible by

adding cosolvents, which facilitates increased solubilization of non-polar drug molecules.

All the cosolvents used in this study confirmed an increase in HCTZ solubility. The highest general increase in HCTZ solubility was seen using PEG 400 as a cosolvent succeeded by poly glycerine and glycerol. The dielectric constant was calculated and decreased by a rise in cosolvent fraction in the formulation.

In this study, hydrochlorothiazide's oral solution with sufficient physical and chemical stability for 14 days and six months is developed. The solubility of HCTZ was the biggest challenge in formulating it as an oral liquid as it has low water solubility.

This study evaluated the solubility enhancement of HCTZ in PEG 400, polyglycerine, and glycerol. PEG 400, which has been an acceptable cosolvent used in pharmaceutical liquid formulations, was shown to be the best cosolvent for improving hydrochlorothiazide's solubility. Polyglycerine, which is a food additive and is not commonly used as a co-solvent, shows a considerable increase in hydrochlorothiazide's solubility, which proves that it could be used to enhance the solubility of a drug with low solubility.

3.27 Limitation and Future work

The solubility study of HCTZ was carried out using four polymers (polyether) and one small molecule monomer (glycerol).

In the solubility study, it was found that the solubility of HCTZ was increased the highest by the cosolvent that was the least polar and most hydrophobic. Therefore, further studies should be done to test hydrochlorothiazide's solubility

using cosolvents with low polarity or high hydrophobicity (e.g., propylene glycol, ethanol).

ICH guideline indicates that accelerated stability studies should be carried out for six months. The accelerated stability study for 30 days six months after lockdown due to the Covid-19 pandemic was carried out. The most stable formulation was at 90 % cosolvent polyglycerine and PEG 400 stored at 25 °C (64% RH).

Stability studies in the fridge were not carried out. It will be essential to observe an accelerated stability study for the period recommended by the ICH guideline at fridge temperature to determine prepared formulations' shelf life. Alternatively, for better performance of the solubility and storage at room temperature to spray dry these formulations as a powder for use by cryogenic methods. A preliminary test was carried out using freeze-dried samples. Observing them under SEM shows that drug morphology changes as solid particles and shows a more amorphous structure that requires further analysis.

Besides analysing the stability of liquid formulations, other physiochemical parameters such as viscosity, sedimentation volume, ease of dispersibility, particle size analysis and microbiological studies can be measured. Measuring such parameters will give further information about the product's stability and help determine if excipients are needed for the liquid formulation. Such parameters were not measured in this study but should be measured in future studies.

Furthermore, to improve HCTZ stability, hydrolysis of the liquid formulations can be prevented by removing water from the formulations (that is, only use non-aqueous solvents), storing the formulations at room temperature, or by using a suitable buffer.

Chapter 4

Reversible addition Fragmentation chain Transfer (RAFT) towards Sugar-responsive polymer

4.1 Introduction

A polymer is a synthetic building block of a molecule built up by the repetition of small monomer-derived units. Polymers may sound like complicated large molecules, but humans have been using them during their lives. People have used wool, silk, wood, starch, rubber, and other natural polymers for long periods. The word polymer (polys) meaning many, and meros meaning parts. A macromolecule or polymer may consist of hundreds, thousands, tens of thousands, or more monomer molecules (Jenkins A, 1996). Polymers are many molecules built up by covalent linking of a large number of small units. Natural polymers, also called biopolymers, bring genetic information such as deoxyribonucleic acid (DNA). Besides, amino acid building blocks such as polypeptides and sugar building blocks such as polysaccharides are the making of the living organism.

In today's world, currently, existing technology material is used in different aspects of life, one of which is using the material for drug delivery. Since the invention of the first human-made synthetic plastic by Baekeland in 1907 and the investigations of Staudinger in the 1920s that form the basis for modern macromolecular science, synthetic polymers have revolutionized our way of life. Initially, there were two types of polymerization reaction, condensation (step-growth) polymerization and addition polymerization (chain growth). Condensation polymerizations use bond-forming reactions that produce a small molecule condensate, such as acid or water, which needs to be continuously removed to enable the polymer formation. Condensation polymerizations are also called step-growth polymerization. The other type of polymerization is the addition polymerization (chain growth), including radical, anionic, cationic, and Ziegler-Natta.

Controlled Radical Polymerization (CRP) is a method to develop polymers with narrowly defined structures, accurate molecular weights, and very low residual monomers concentrations. This includes Reversible Addition-Fragmentation chain Transfer (RAFT) polymerization, Nitroxide-Mediated Polymerization (NMP), and Atom Transfer Radical Polymerization (ATRP) (Per B. Zetterlund, 2009).

RAFT is one of the most popular polymerization methods for controlled radical polymerization, and it achieves controlled/living character by reversible deactivation of propagating radicals using degenerative chain transfer of the trithiocarbonate end-group. RAFT polymerization is a multipurpose method that allows the synthesis of polymers with sophisticated architecture, narrow molecular weight distribution, pre-calculated molecular weight, and high degrees of chain-end functionalized polymeric networks (John Chiefari, 1998). Well defined living-controlled polymerization (Scheme 4.1) forms when the maximum number of polymer chains initiated from the RAFT agent. Termination minimizes using an excess of RAFT agents compared to initiating (initiator, e.g., AIBN derived) radicals (Graeme Moad, 2017, Moad et al., 2008, Graeme Moad, 2003, John Chiefari, 1998).
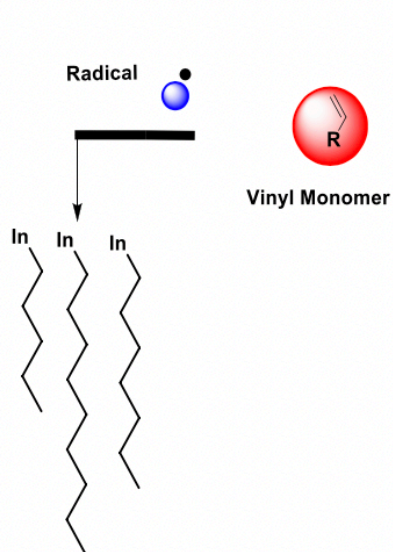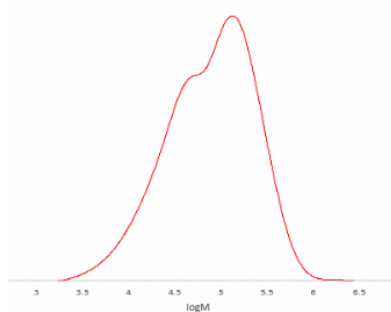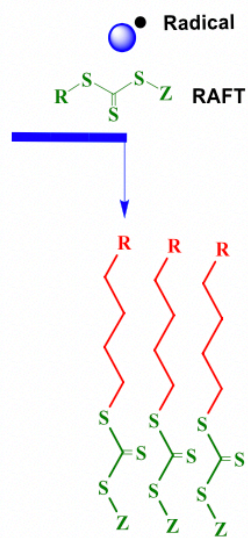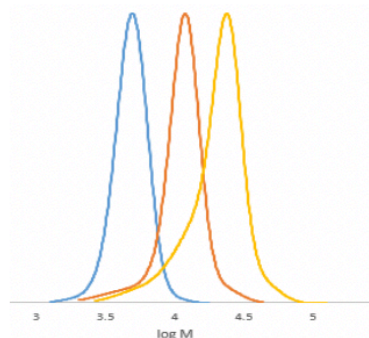
Scheme 4. 1 Comparison of conventional (left) and RAFT polymerization (right). The conventional polymerization, GPC /SEC traces show broad polydispersity and high molecular weight, right RAFT polymerization as the GPC/SEC traces show a three-block copolymer with narrow molecular weight distribution and controlled molecular weight.

4.1.1 Conventional (Free) Radical polymerization

In 1935 Staudinger and Frost suggested the vinyl polymerization process's arrangement as consisting of the three steps: chain initiation, chain propagation, and chain termination. The following measure, whereby an "active" polymer molecule is "deactivated," is incorporated as one of the main reactions. They suggested that the degree of polymerization remained unchanged with the monomer conversion to the polymer. However, Flory introduced the fourth step into the polymerization scheme, namely chain transfer, initiation, propagation, and termination.

These facts suggest that the reaction which determines the molecular weight and the reaction and destroys the active centers are not the same but are entirely independent processes. This concept has been embodied in the following scheme 4.2 for the mechanism of vinyl polymerizations that experience a similar chain reaction mechanism into the polymerization scheme, a fourth step, namely chain transfer, and the initiation, propagation, and termination.
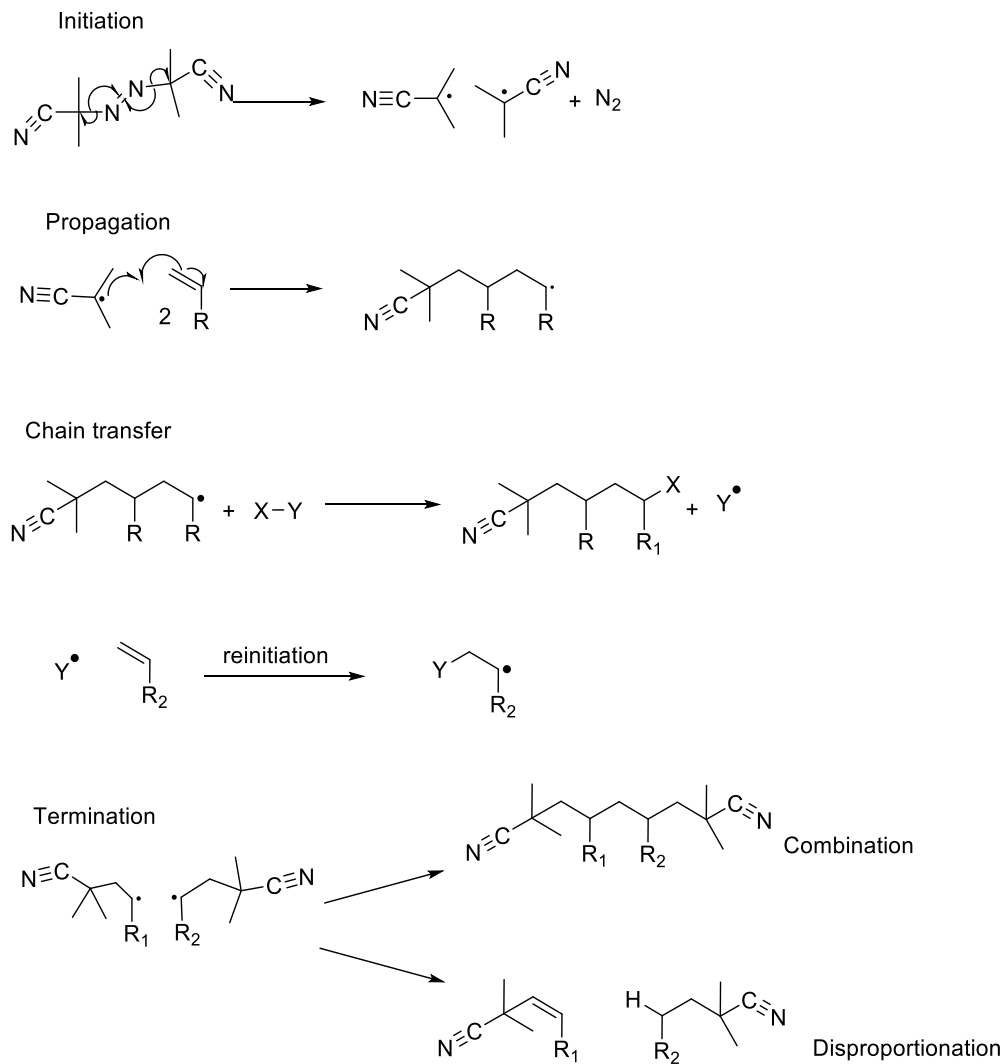
Scheme 4. 2 Mechanism of vinyl polymerizations via conventional polymerization.

In scheme 4.2, the reaction 1 Initiation starts, and two radicals are generated from one initiator molecule. The radical reacts with vinyl bonds and forms a propagating radical. The chain transfer step occurs when the propagating radical reacts with a new species in the reaction (X-Y), where A reacts with propagating radical, leaving a new radical species Y, which can re-initiate a radical with a new monomer. Termination occurs when two active centres react together, by disproportionation or combination reaction. Free radical polymerization, which proceeds via a chain reaction mechanism, generates high molecular weight polymer while propagating radicals are adding to the polymer chain. The

mechanism of free radical polymerization includes initiation, propagation, chain transfer, and termination steps. The initiation is a two-step procedure, first initiator decomposition than the formation of two radicals (I•). The rate of radical's formation from the initiator can calculate from the constant rate equation.

$R_{pr} = 2\,f\,kd[I]$

Equation 4. 1 Mechanism of vinyl polymerizations via conventional polymerization.

The rate of radical production (R_{Pr}) is equal 2 factor of initiator decomposition, f is the initiator efficiency and [I] is the initiator concentration and *the decomposition rate constant is k_d*

Initiation: In the first step (scheme 4.3), the rate of radicals produced is equal to 2 radicals produced from the initiator, where the efficacy of radical is 1 or less than 1 as the radicals can also cause side reaction, for example, initiator derived radicals.
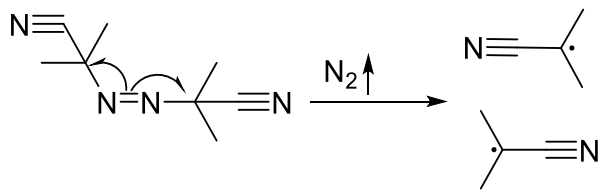
Scheme 4. 3 AIBN decomposition into 2 radicals
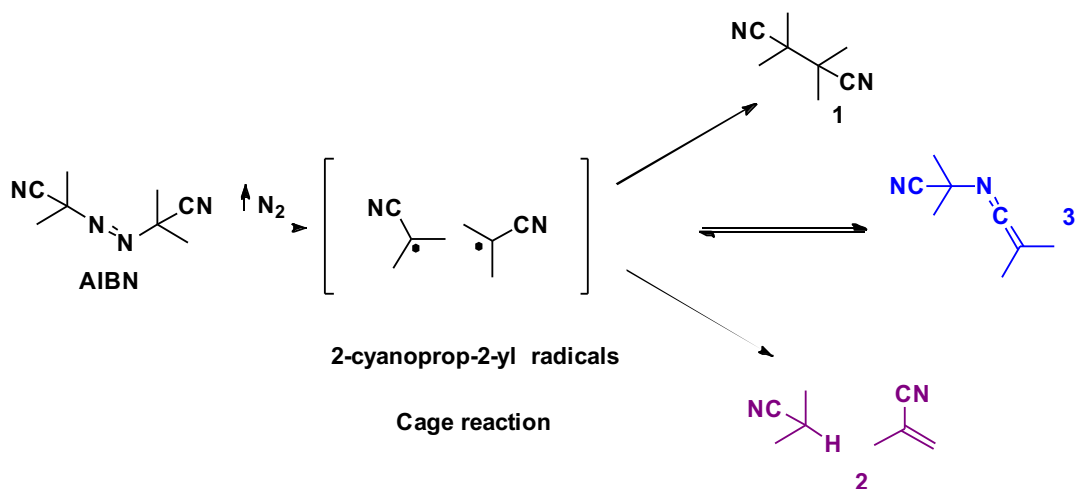
Scheme 4. 4 AIBN cage reaction.

AIBN decomposition to two isobutyronitrile radicals which then decompose to 1 (2,2,3,3-tetramethylsuccinonitrile) , 2 (methacrylonitrile and pivalonitrile (Trimethylacetonitrile)) and product 3 (2-methyl-2-(propan-2 ylideneamino) propanenitrile). Products 1 and 2 are inert and 3 is undergoing further reaction with a single radical.

Propagation: In the second step, the initiating radicals add to monomer forming propagating radicals (P•), many monomers form propagating radicals because of

forming a growing polymer chain. Every different type of monomer would form propagating radical at a different rate.

The rate of polymerization (Rp) is equal to the product of rate (kp) of propagating radical (P•), and monomer concentration [M].

$$\text{R}_p = k_p[P\bullet][M]$$

Equation 4. 2 The rate of polymerization

Chain transfer: It happens when radical reacts with a nonradical molecule to produce a dead chain and a new radical, which adds to the monomer and form a new propagating radical.

Termination: It happens when two propagating radical chains react or combine propagating radicals with hydrogen to produce a dead chain.

Conventional radical polymerization usually results in high-molecular-weight macromolecules. However, slow initiation and immediate termination steps are typically giving limited access to precalculated molecular weights, narrow molecular-weight distributions (MWDs), hold chain-end functionality, and block copolymer synthesis. Therefore, conventional radical polymerization, which can be initiated at a higher temperature, can be taken by the RAFT method, which requires low temperature and predetermined molecular weight.

4.1.2 Reversible addition-fragmentation chain transfer or RAFT

Michael Szwarc contributed in 1956 to polymer chemistry by the discovery of the living anionic polymerization of styrene and related vinyl monomers (Szwarc, 1956). Living polymers are polymers that can keep their ability to grow and grow to the desired size, while their degree of termination or chain transfer is insignificant (scheme 4.5). The living polymerization method provides access to uniform polymers of controllable size, block copolymers, functional polymers, star, and comb-shaped macromolecules. In 1998 Rizzardo and co-workers invented Reversible Addition-Fragmentation chain transfer polymerization (RAFT) (John Chiefari, 1998). Different types of controlled living polymerization, such as nitroxide-mediated polymerization (NMP) and atom transfer radical polymerization and RAFT. However, Reversible addition-fragmentation chain transfer (RAFT) is the most adaptable method to bring living comportment for a wide range of vinyl monomers via a range of initiation methods, for example, thermal or photo-induced. The RAFT polymerization reaction is possible in solution and emulsion at low temperatures. Improved controlled/living polymer vinyl monomer using the RAFT polymerization using different amount of RAFT agent is possible, with monomer and initiator to optimize the condition. A general RAFT polymerization mechanism is in scheme 4.5.

Initiation and propagation

Initiator $\longrightarrow$ I$^{\bullet}$

I$^{\bullet}$ + Monomer $\longrightarrow$ $^{\bullet}$P$_n$

Addition to RAFT

P$_n^{\bullet}$ + S=C(Z)-S-R $\underset{}{\overset{k_{add}}{\rightleftharpoons}}$ P$_n$-S-C$^{\bullet}$(Z)-S-R $\underset{}{\overset{k_{frag}}{\rightleftharpoons}}$ P$_n$-S-C(Z)=S + R$^{\bullet}$

Re-initioation

R$^{\bullet}$ $\xrightarrow[k_{re-in}]{\text{Monomer}}$ P$_1^{\bullet}$ $\xrightarrow[k_p]{\text{Monomer}}$ P$_m^{\bullet}$

Chain equilibration

P$_m^{\bullet}$ + P$_n$-S-C(Z)=S $\rightleftharpoons$ P$_n$-S-C$^{\bullet}$(Z)-S-P$_m$ $\rightleftharpoons$ S=C(Z)-S-P$_m$ + P$_n$

Active   Dormant state   Active

Over all

Initiator + Monomer + S=C(Z)-S-R $\longrightarrow$ S=C(Z)-S-P$_m$ + R

Termination P$_n$ + P$_m$ $\xrightarrow{k_t}$ Dead Polymer
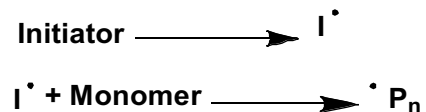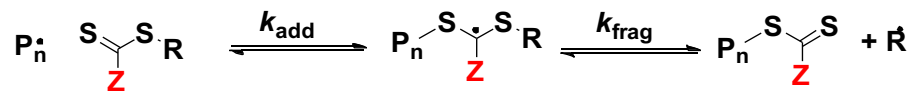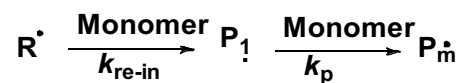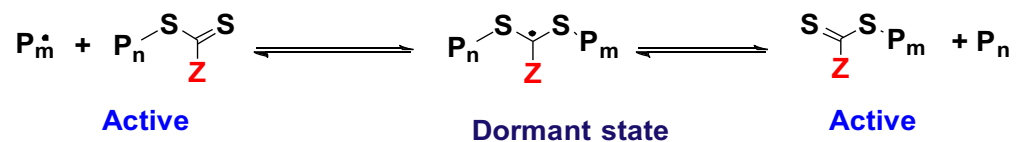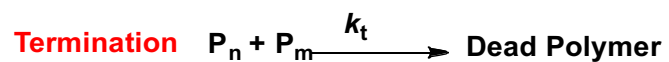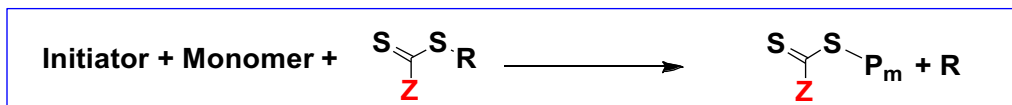
General Structure S=C(Z)-S-R
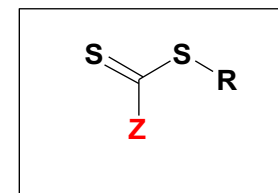
Z = Activating / Deactivating group
R = Leaving group, reinitiating group

Scheme 4. 5 General mechanism of Reversible addition-fragmentation chain transfer (RAFT).

4.1.3 Mechanism of RAFT polymerization

The RAFT process is different from nitroxide-mediate polymerization (NMP) and Atom Transfer polymerization (ATRP). RAFT relies on degenerative chain transfer, in which the rate of polymerization is the same throughout the polymerization. The initiator will introduce the radical and kept at minimum concentration due to obtaining more living polymer; the higher the initiator's strength, the less living chains can achieve therefore, to reduce the chances of termination, the minimum concentration of initiator is used. The initiator is essential because the RAFT agent does not generate radicals at the beginning (scheme 4.5).

Initiation: The initiator with low concentration will initiate radicals and generate some small amount of polymer radicals.

Addition to RAFT or pre-equilibrium stage: One of the first polymer chains with active radical species will react with RAFT agent and form an intermediate RAFT adduct. The reason why the Z group in the RAFT agent is significant to give a stabilized radical. The middle radical reacts with the R group radical and form thiocarbonyl carbonate again and R radical.

Re-initiation: The R group of RAFT agents with the first polymer will form a dormant radical of thiocarbonyl carbonate, which has a polymer chain end both sides.

Chain equilibrium or RAFT primary equilibrium step: In this step growing polymer chain is reversibly attached and detached with the RAFT agent when the polymer is not connected to the RAFT agent with can react with another RAFT agent. It can also be attached to the RAFT agent and form dormant radical species. This is an essential step as it shows how the radicals are distributed and keeps the reaction uniform in terms of radicals and can go further and avoid premature termination.

Termination: Also, termination can happen when two dormant species respond, or two growing radicals react with each other or reaction.

The main product of the RFAT reaction shall be the R-polymer-Thiocarbonate group, or the side products can be initiator-polymer -thiocarbonate group, or R-polymer -Dead or R group.

Theoretical number-average molecular weights (Mn,*th*) calculated according to equation 4.3. Theoretically, Mn (Mn,*th)* is calculated as a function of the initial amount of monomer [M]0 and RAFT agent [DDMAT]0 multiplying by the Mw of monomer and conversion by NMR or gravimetry and addition of the molecular weight of DDMAT (RAFT compound).

$$Mn, th = \left[\left(\frac{[M]_0}{[DDMAT]_0} \right) \times MW_M \times conversion \right] + MW_{[DDMAT]}$$

Equation 4. 3 Theoretical number-average molecular weights (Mn,th, a fraction of monomer initial concentration and initial concentration of RAFT and the molecular weight of monomer plus the molecular weight of RAFT agent.

Compatibility table 4.1 with different classes of the monomer listed indicates the appropriate choice of RAFT for the preferred monomer. The right RAFT agent for the selection of the monomer to polymerize by the RAFT method is crucial. To choose the appropriate R and Z group functional groups is to have a generous leaving radical than the incoming propagating radicals, which then initiates a new propagating radical chain, due to the reason that most propagating radicals must initiate from the RAFT agent.

In RAFT polymerization, the concentration of the initiator is low, this assumes that all growing chains are initiated from the RAFT agent. Therefore, living chains and the amount of radical initiator remaining can be calculated.

4.1.4 Living polymer character

Performing RAFT polymerization enables the production of "living" chains (equation 4.4), this means chains of polymer can be extended by further

monomer addition and minimum addition of initiator (table 1, different RAFT agents).
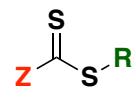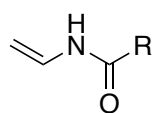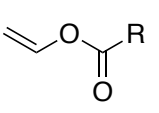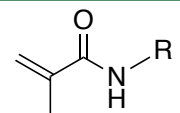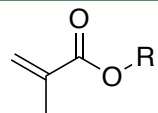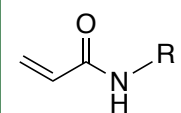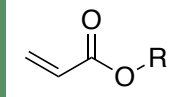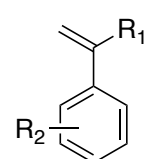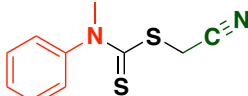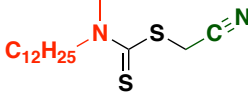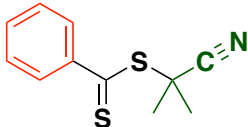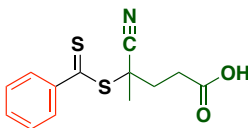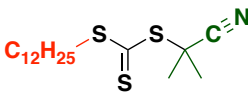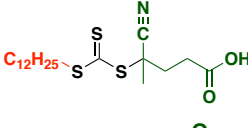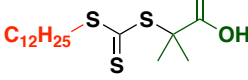
$$L = \left(\frac{[\text{CTA}]_0}{[\text{CTA}]_0 + 2 \, x \, f \, x[\text{I}]_0 \, x \, (1 - e^{-kdt}) \, x \, \left(1 - \frac{fc}{2}\right)} \right)$$

Equation 4. 4 Theoretical fraction of living chain is livingness (L) and it is calculated from the fraction of RAFT agent concentration and initiator half-life.

The factor "2" accounts for one molecule of azo initiator which gives two primary radicals with the efficiency f (assumed to be equal to 0.5). The decomposition rate constant is k_d. The decomposition rate k_d varies according to solvent and temperature, which for AIBN in DMF at 70 °C is 4.3x10^{-5} S^{-1}.

The quantity represents the number of chains produced in a radical–radical termination event with the coupling factor fc supposed to be zero.

Table 4. 1 RAFT agents' compatibility list, from vinyl amide compatible with one type of RAFT agent to styrene which is compatible with a variety of RAFT agents.

RAFT agent	Vinyl amides	Vinyl esters	Methacrylamides	Methacrylates	Acrylamides	Acrylates	Styrenes
	+++	+++	-	-	-	-	-
	-	-	-	-	+++	+++	+++
	-	-	+++	+++	_	+	++
	-	-	+++	+++	+	+	++
	-	-	+++	+++	++	++	+++
	-	-	+++	+++	++	++	+++
	-	-	+	+	+++	+++	+++

15

In table 4.1 the Z group modifies the rate of the addition of propagation of radicals to the thiocarbonyl. The Z-group is governing the stability of the intermediate radical. Therefore, CTA is chosen to control the polymerization, and the R group must be a good homolytic leaving group concerning propagating radical. The RAFT agent must be selected carefully in order to be compatible with the monomer of choice. The RAFT agents are commercially available for different types of vinyl monomers, such as acrylamides, styrenes, vinyl amides vinyl ester, acrylates, or methyl acrylates.
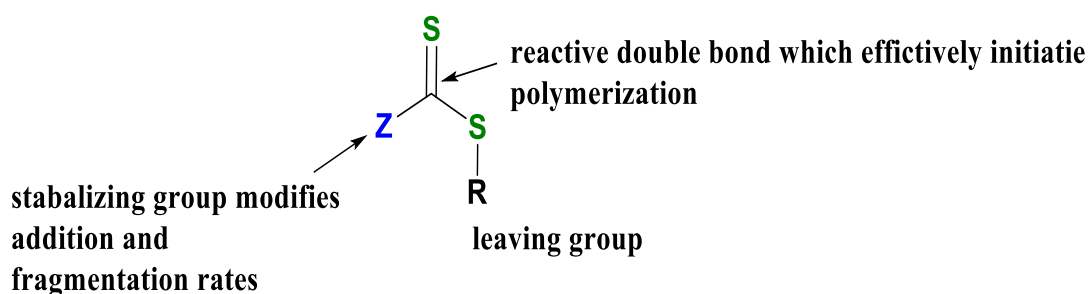
To activate the di-thiocarbonyl or tri-thiocarbonyl group directed by the Z group (Z usually is an alkyl group ($C_{12}H_{25}$, or other.) RAFT agents, as a result, affect the stability of the intermediate radicals in the reaction. The sulphur- carbon double bond affects the stability of the intermediate radical.
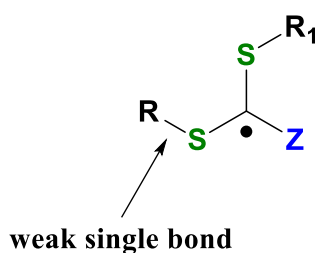
The Z group controls the reactivity of the week C=S which affects the rate of radical addition and fragmentation steps. R-S bond also is a weak bond and the free radical from R must reinitiate radical polymerisation when the radial from an initiator (for example AIBN, or VA-044) is consumed as the concentration of radical in RAFT polymerisation is minimum due to the fact that all propagating

chains must initiate from the RAFT agent and the reason for low concentration of initiator is to start the reaction.

The differences between dithiocarbamates, xanthones, thioesters and trithiocarbonate (table 1) is the z groups. Dicarbamates Z_1 group is usually methyl or alkyl and Z_2 is aromatic group. Xanthanes Z group is usually alkyl chain (scheme 4.6) .
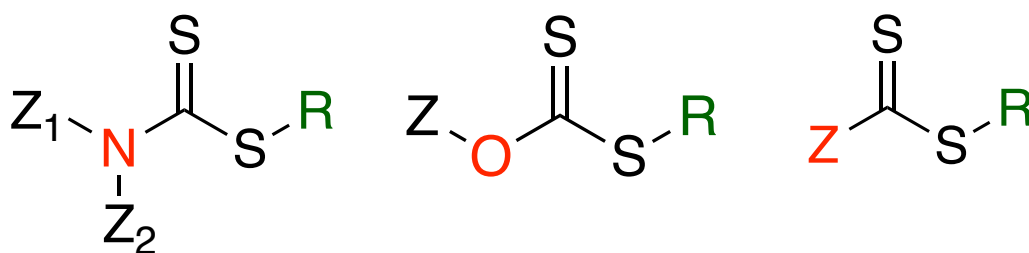
Dicarbamates   b.Xanthanes   c. trithiocarbonate

Scheme 4. 6 a. dicarbamates Z1 group is usually methyl or alkyl and Z2 is aromatic group, b. xanthanes Z group is usually alkyl chain and thioesters and c. trithiocarbonate z group are aromatic or aliphatic.

Resonance structure of RAFT agents

Z can vary widely but is typically an aromatic group.
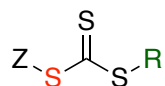
In most trithiocarbonates, Z is typically an alkyl group ($C_{12}H_{25}$, etc.)
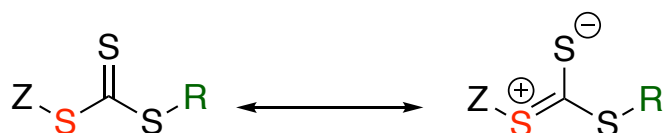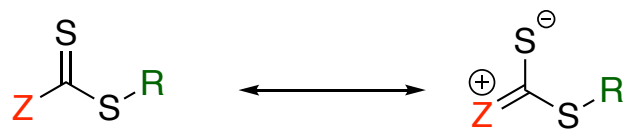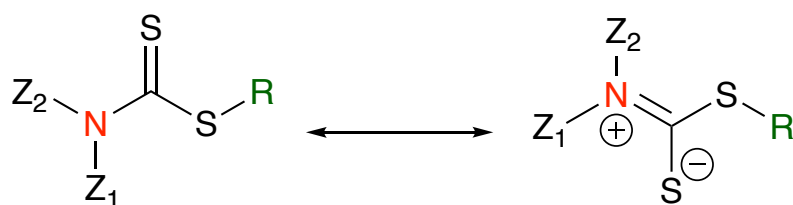
Scheme 4. 7 RAFT agent resonance structure

From the resonance structure of the RAFT agents, the lone pair of electrons on oxygen (xanthates) and nitrogen (dithiocarbamates) is delocalized in the thiocarbonyl group and consequently deactivates the C=S bond regarding radical addition and weaken the radical intermediate. This effect, thus, promotes propagation and intermediate fragmentation, hence enabling control over polymerization of Less Activated Monomers (LAMs) but poor control over polymerization of More Activated Monomers (MAMs).

Trithiocarbonates are the most popular RAFT agents for polymerization of MAMs, such as acrylates or methacrylates, as they equalize activity and stability. The most versatile trithiocarbonates in terms of monomer range are those with a tertiary R such as the commercially available 2-cyano-2-propyldodecyl trithiocarbonate or 2-(Dodecylthicarbonothio)-2-methylpropionic acid.

The choice of R group depends on the addition of propagating radical to the RAFT C=S bond. The propagating radical originated from the initiator add on to the C=S double bond to give an intermediate radical, which then fragments and replaces the R group. The leaving ability of the R group must be as good or better than the propagating radical. Therefore, bulky molecules require a large leaving group.

4.1.5 Temperature range of RAFT polymerization

RAFT polymerizations can efficiently be carried out in an aqueous medium, hence enabling the polymerization of anionic, cationic, zwitterionic, and neutral monomers leading to hydrophilic and functional polymers. RAFT polymerization in an organic medium can be carried out over a temperature range from room temperature to 140 °C. Performing RAFT reaction at higher temperatures due to yield of a better results is less recommended. Additionally, in homogenous aqueous polymerization, the RAFT agents that have shown higher versatility are the dithioesters and trithiocarbonates.
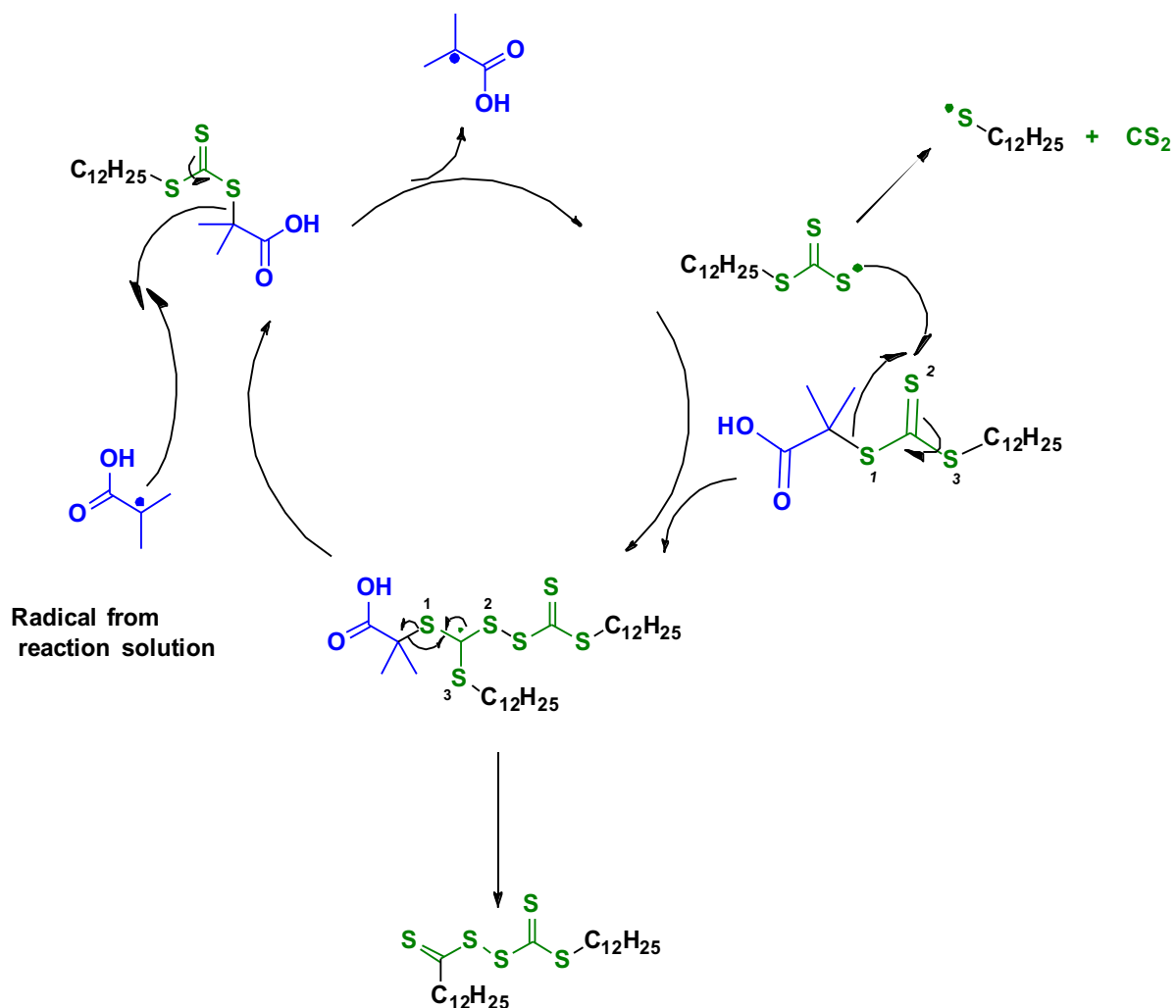
Scheme 4. 8 Decomposition of DDMAT.

In presence of a radical from the solution it is possible to cleave the carboxylic acid leaving group from RAFT agent which leaves a radical that can react with another RAFT agent causing degradation of RAFT.

4.2.1 RAFT polymerization and Molecular weight control

One of the unique properties of RAFT polymerization is that molecular weight is predetermined, which is calculated from the ratio of monomer concentration and RAFT agent [M] / [Z−C(=S)−S−R]. The ratio of monomer and RAFT agent is called the degree of polymerization since all chains have an equal opportunity to grow at the same rate. The resulting polymer obtained has a small molecular weight, which is shown by polydispersity (a ratio of average molecular weight, and average

molecular number (Mw / Mn). An ideal polydispersity (PD) value for RAFT polymerization shall be 1.05 – 1.20. Usually, the molecular weight of the polymer is lower in the RAFT method than conventional polymerization, therefore, the polymer obtained will have narrow polydispersity (PD).

4.2.2 Choice of Initiator for RAFT polymerization

Initiator type is also essential, thermal initiation choice depends on the choice of RAFT polymerization, whether it is the solution or emulsion polymerization. The polymerization reaction requires a thermal initiator to start the reaction. The initiator of choice must have a very short half-life to initiate the reaction and can be fully consumed in the shortest time possible since all the propagating chains must come from the RAFT propagating radical. Therefore, knowing the half-life of the initiator over time is crucial, which can be calculated from the Arrhenius equation. Traditionally thermal initiators used at a temperature between 70 – 100 °C with trithiocarbonates and dithiocarbamates.

Initiator efficiency: Initiator efficiency usually is dependent on the solvent and temperature of polymerization. The two factors define the efficiency of the radical, radical generation, and the efficiency of radical initiation. The efficiency of radical generation (fg) rate is a fraction of radical generation and number of radical disappearances as per equation (4.5).

$$f_g = \frac{rate\ of\ radical\ production}{n\ (rate\ of\ radical\ dissaperance)}$$

Equation 4. 5 The efficiency of radical generation (fg) rate is fraction of radical generation and number of radical disappearances.

The efficiency of radical initiation (fi) is fraction of initiation of propagating radical over number of initiator disappearance.

$$f_i = \frac{rate\ of\ initiation\ of\ propagating\ chains}{n(rate\ of\ intiator\ diassapearance)}$$

The rate expressed as half lifetime (t $_{1/2}$) where t $_{½}$ equals ln 2 / k_d = 0.693 / k_d. The rate constant K_d changes with temperature according to the Arrhenius equation.

$$\mathbf{K}d= (\mathbf{Ae})^{-\mathbf{Ea/RT}}$$

T is the absolute temperature (in Kelvins),   A is the pre-exponential factor, a constant for each chemical reaction, Ea is the activation energy for the reaction (in the same units as RT), R is the universal gas constant. The rate of polymerization R_p is equal to the rate (k_p) of product of propagating radical ($P^•$), and monomer concentration [M].

Efficiency factor f is employed to show the fraction of capable free radicals produced as for AIBN efficiency is not 100 % due to the bimolecular termination and recombination of radicals.

4.2.3 Chain transfer step and solvent effect

A transfer agent in polymerization reaction can be initiator, monomer, polymer, solvent, or an extraneous compound, for example, RAFT agent. Chain transfer is a process in which the growing chain loses its capacity for further growth, and the transfer agent becomes capable of starting a new chain. Chain transfer reaction has subjected to extensive studies for interpreting the polymerization mechanism and relevant to monomer and solvent in the literature, besides, for its practical importance as a method for controlling the molecular weight of the polymer.

One aspect of the chain transfer steps that the molecular weight of the polymer obtained by radical polymerization is intensely affected by the presence of a solvent. This effect, which cannot merely explain in terms of reagent dilution. Chain transfer involves a reaction or a series of reactions, by which the active centre of polymerization is transferred from a growing chain to another molecule. The result

is the disruption of the growth of the chain, with subsequent limitation of the molecular weight, without affecting the termination reaction. A sharp chain transfer reaction does not markedly affect the polymerization rate, as the new activity centre is supposed to form rapidly and to have the same reactivity as the preceding one. Other reactions, similar to chain transfer, which alter the overall polymerization rate fall within the retardation or inhibition reactions.

In 1943 Mayo proposed a simple equation that accounts for the effect of chain transfer on the polymerization degree.

$$\frac{1}{DP} = \frac{1}{Dp_0} + Cs\,\frac{[S]}{[M]} \quad \text{Equation 4.8}$$

Equation 4. 8 Mayo proposed equation that accounts for the effect of chain transfer on the polymerization degree.

C = (ktr / kp)

DP and DP_0 are the average number degrees of polymerization in the presence, and in the absence of the chain transfer agent(S) or RAFT. C is the chain transfer constant; C is defined as the ratio of the chain transfer (K_{tr}) and propagation rate constants (K_p). The concentrations of the chain transfer agent and monomer are [S] and [M].

4.3 Boronic acid

Boronic acid has been the choice since 1860 and has appeared in many literature studies, due to its distinctive reactivity and stability. A boronic acid is an alkyl or aryl substituted boric acid containing a carbon boron bond belonging to the larger class of organoboranes. Boronic acids act as Lewis acids. The unique feature of boronic acid is that they can form reversible covalent complexes with sugars, amino acids, or occasionally substituted Lewis base donors. Boronic acid (electrophilic, SP^2 hybridised) has a pKa of ~9 and can form tetrahedral boronate (nucleophilic, Sp^3) complexes with compounds having a pKa ~7. Boronic acid is used as a fluorescent detector in the area of molecular recognition to bind to saccharides for fluorescent detection or selective transport of saccharides across membranes.

Boronic acid mainly exists as negative ions in alkaline media. Therefore, it is making it more reactive towards diols. Upon interaction with diols, boronic acid can result in two forms of esters; a neutral ester or charged boronate ester. The neutral form is very unstable; therefore, the charged acid-based form forms readily. This pH-dependent chemistry of boronic acid makes it a means of interest to be used in applications such as self-assembly and sensing (Vancoillie and Hoogenboom, 2016) (Kim K, 2009).

Unlike carboxylic acid, boronic acid does not exist in nature. The boron molecule has an empty p-orbital, which makes it a Lewis acid and allows interaction with a Lewis base. This interaction causes the hybridization of boronic acid to change from sp^2 to sp^3. The conversion of neutral trigonal planar boron to anionic tetrahedral makes boronic acid-responsive to saccharides. The formation of cyclic boronic acid causes the bond angle of trigonal planar configuration (sp^2 hybridization) to change from 120° to 113°. The tetrahedral shape has a bond angle of tetrahedral structure (sp^3 hybridisation) is ~ 109°. This bond angle of the tetrahedral configuration moderates the angle strain, which is required to overcome the cyclization procedure. Boronic acid can make complexes with electron-donating groups such as an amine.

Early analyses into boronic acid saccharide interactions studied in 1959 when Lorand and Edwards (LORAND, 1959) found the saccharide binding constants of boronic acid and phenyl boronic acid using a pH-depression method.

The tetrahedral configuration reduces the angle tension, which is required for boron to overcome for the cyclization process. Boronic acid can make complexes with electron-donating groups such as an amine (Roy et al., 2008a). The neutral form is very unstable; therefore, the charged acid-based form forms readily. The pH-dependent chemistry of boronic acid makes it a mean of interest to be used in applications such as self-assembly and sensing. There are three principal methods

of controlling the acidity of boronic acid. The first approach is electronically, meaning incorporation of electron withdrawing/ donating groups.

Second approach is sterically to lower the pKa of phenyl boronic acid by bringing geometric changes. The equilibrium between the boronic acid and the boronate acid.

The third approach is through complexation via intramolecular coordination between the electron deficient boron and an electron rich ortho side group. Therefore, allowing easier formation of stable boronate esters at lower pH.

pH-sensitive polymers prepared using either acid-containing or base- containing monomers and are very appealing for drug delivery because the human organism holds many pH inclines that could be utilized for a beneficial result. The acid or base containing polymers commonly exhibit pH-responsiveness in a pH range near the pK_a or pK_b of the polymer (Hisamitsu et al., 1997).

Boronic acid is physiologically nontoxic and stable for formulation. Nevertheless, the sugar-responsive property of boronic acid containing polymers require relatively high pH ~8.8 - 9; which is a disadvantage to its medical use as ideally, glucose responding must take place at physiological pH (7.4). Therefore, the sugar binding at neutral pH ~7 is achieved via Wulff-type boronic acid.
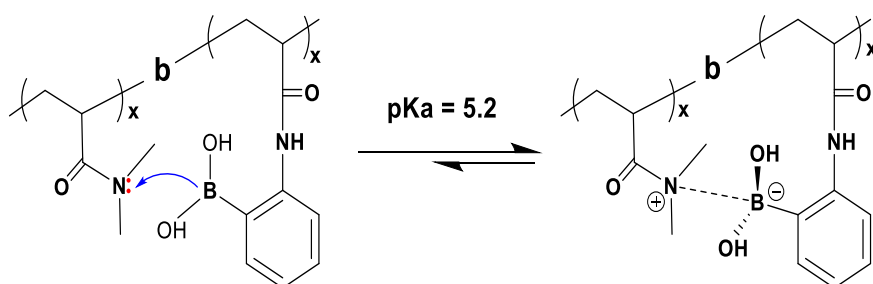
Scheme 4. 9 Wulff type Bornic acid inter molecular polymeric complex

Boronic acid (electrophilic, sp2 hybridized) has a pKa of ~9 and can form tetrahedral boronate (nucleophilic, sp3) complexes with compounds having a pKa ~7.

Boronic acid also can form cyclic esters (five-or six-membered) with cis-diol compounds in an aqueous medium, which dissociates in acidic solution. Different approaches in the literature discussed recognition of the saccharides by a boronic acid-based system. One of the principle states that it usually relies on the changes occur in conductivity (Lamping et al., 2018). This change occurs when the sugar binds to boronic acid moiety. Another principle states that the Lewis acid- Lewis base interaction between boronic acid and amine (Cambre et al., 2013) is enhanced upon saccharide binding to boronic acid. At the same time, some have reported that the hydrophilicity change is the primary strategy of the drug delivery system. This hydrophilicity change occurs when boronic acid reacts to a diol (glucose). This change in hydrophilicity is caused due to the conversion of boronic acid moieties from neutral to an anionic boronate ester. As most closed-ring carbohydrates, including glucose, have a cis-diol fraction in their structure, they can form a relatively strong complex with borate. Borate interacts with α-D glucose C1 - C2 and C4 - C6 diol units. It is to be noted that reversible exchange of borate/diol complexes takes place by competing for diol molecules which can form complexes more tightly. Based on this characteristic of borate - diol complex (Kataoka et al., 1995).

Boronate ester binding to *cis* 1, 2 diol
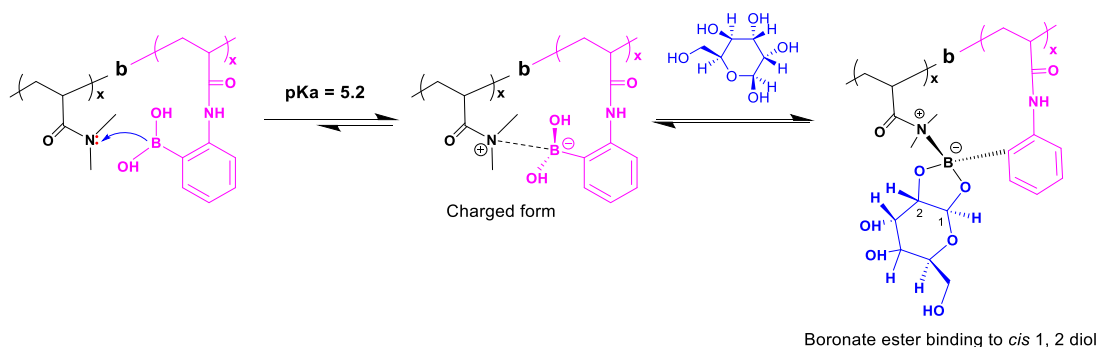
Scheme 4. 10 Glucose binding to Wulff type inter molecular polymeric complex, illustration of equilibria of boronic acid-based sugar sensing polymer.

Consequently, glucose can diffuse through the polymer complex, exchanging with the boronate dimethylacrylamide complex to form a boronate-glucose complex, which may facilitate the diffusion of macromolecular compounds, including insulin, through the polymer complex, to realize a glucose-dependent release of insulin. This

was the development of a novel drug delivery system for insulin based on the chemically modified glucose sensor containing the RAFT polymerization method (Cambre et al., 2012).

For the polymer to work and release insulin at physiological pH, the Wulff type complex should be used, which allows for sugar sensing at a pH of 5.2 in the physiological environment. The Wulff type complex has many functions for boronic acid-based polymers. However, the delivery tool of these polymers relies on supramolecular self-assembly of polymers. Therefore, accurate size, molecular weight, and structure are essential for their suitable function, and it can be synthesize by the radical addition-fragmentation chain transfer (RAFT) method (Li H, 2011).

4.4 Aims and Objective of the RAFT polymerization

This chapter aimed at developing a polymer that contains an active sugar sensing molecule of phenylboronic acid. At the end of my first year, respected Professor Fawaz Aldabbagh kindly suggested working on the RAFT polymerisation method and make block copolymers with sugar responsive phenylboronic acid, which was welcomed by our team as we have managed some polymerisation of polyglycerol with sugar sensitive end and monomer (chapter 2). Initially, for this project, a detailed literature search was carried out using phenylboronic acid and RAFT polymerisation; therefore, the critical and relevant data were collected from the initial literature search.

The Aldabbagh group has many years of involvement and interest in controlled living thermoresponsive and pH-responsive block copolymers. Previous to this thesis, the polymerisation of dimethyl acrylamide (DMA) was successfully published (Chalmers, 2017). This polymerisation strategy was based upon that of Zetterlund and Perrier (Gody et al., 2013). They confirmed the use of the RAFT procedure to yield well-defined multi-component polyacrylamide block copolymers in one pot without discontinuous purification by use of the water-soluble azo-initiator, VA-044, where each block was prepared in ~99% conversion in 2 h at 70 °C. My assignment to work on such a project was to initially synthesise the previously developed DMA polymer extended with a phenylboronic acid monomer resulting in an amphiphilic block copolymer via Reversible Addition Fragmentation Transfer (RAFT) polymerisation. In addition to this synthesis, macroRAFT of phenylboronic acid monomer and chain extend with dimethylacrylamide, DMA macroRAFT synthesis was attempted.

Gody et al. synthesised as one-pot copolymer using two different initiators (AIBN and VA0-44) via the RAFT method (Gody et al., 2013). This procedure is based on using a degenerative transfer mechanism in a radical polymerisation regulating the reaction conditions in a way that the polymerisation continues to full conversion in a reasonable time while keeping an exceptional level of control and providing large quantities of product. Thermal decomposition of VA-044 and AIBN were compared

to find a suitable radical initiator. The first attempt was to use VA-044 in Dioxane: water 80:20 as VA-044 is water-soluble and has a shorter half-life compared to AIBN. Nonetheless, there was the issue of boronic acid monomer solubility and full conversion. Therefore, AIBN was used.

4.5 Introduction

There are three kinds of glucose-responsive systems available in literature and practice, such as measuring sugar glucose. One of them is glucose oxidase (GOD), an enzyme-based technology. The second is concanavalin A, a sugar-binding protein, and a chemical sensor phenylboronic acid. Our groups' primary focus is on boronic acid building blocks for sugar sensing using RAFT polymerization.

Boronic acid and its derivatives react with 1,2, 1,3, or 1,4-diol and create a stable cyclic ester. Boronic acids are a distinctive class of stimuli-responsive molecules with possible functions as self-healing materials, self-regulated drug-delivery systems, and sensors to detect diols like dopamine, sugar, and glycoproteins. (J.N. Cambre, 2011). In aqueous solution, boronic acid has a pKa of 8.70 at room temperature. Despite the weakly acidic nature, boronic acid can detect biologically active sugars such as glucose, fructose, and other sugar molecules. This concept is essential for developing chemical sensors for sugar detection in drug delivery. This concept can be ideal for insulin delivery.

Lorand and Edwards confirmed the tetrahedral nature of the phenyl boronate anion in 1959 (Taylor et al., 2017, Lorand and Edwards, 1959). The tetrahedral nature of boronic acid demonstrates that the boronic acid group is highly useful and versatile in chemical sensors that sense biological species. The Lewis acid nature of boronic acid dominates boron compounds' nucleophile properties, the same as Florine, or Nitrogen, or the hydroxyl group (OH). The boron atom of tri-substituted boron species possesses sp2 trigonal planar geometry with an empty p orbital perpendicular to the plane of the molecule (Taylor et al., 2017, Lorand and Edwards, 1959). The acidic feature of boronic acid dominates both the synthetic and receptor

chemistry of boron compounds. Nucleophiles can interact with or donate to the boron molecule's vacant site, causing a subsequent change in geometry and hybridization. Jin and his co-workers studied the copolymerization of melamine with 3-acryl amino phenylboronic acid in methanol. They used the nanoprecipitation method, NPs with a narrow size distribution were successfully generated (Jin et al., 2009). The analysis of cell proliferation suggested that the glycopolymer, nanoparticles (NPs) had good biocompatibility. The glycopolymers that responded to changes in the glucose concentration of the surrounding environment were aimed for use in self-regulated insulin delivery (Jin et al., 2009).

Section 1 of chapter 4

This is the literature search. This comprises a consideration of RAFT, monomer, and initiator ratios and concentration of final polymer solution carried out previously by researchers. The results of each study are tabulated (table4.2).

4.6 Literature review on RAFT polymerization of phenylboronic acid

The equilibrium of aqueous boronate ion with some polyols has been studied, and the calculated equilibrium constants were compared with those of borate in 1959 by Lorand and Edwards (Dandegaonker, 1959). The favourable geometry of the 1,2-diol ends typically have a higher affinity for the boronic acid. Under the physiological pH 7.4, only a small amount of phenylboronic acid ionizes, which results in reduced water solubility. Therefore, it results in the low binding affinity of the diols. The literature search included consideration of RAFT, monomer, and initiator ratios and concentration of final polymer solution, the degree of polymerization and molecular weight, sugar sensitive properties, kinetic studies of RAFT polymerization of phenylboronic acid and living block copolymer were searched. In 2007 Cambre *et al.* published a strategy to produce a well-defined water-soluble boronic acid copolymer (Cambre et al., 2007b). This reaction was carried out using a styrene monomer of phenylboronic acid with RAFT agent, and then the block of PBA protected with pinacol was extended with *N, N*-Dimethylacetamide (*N, N* DMA). Results obtained from this study were that the block copolymer was successfully made. In this research paper, two different monomers and RAFT ratios were investigated, as per table 4.2, 70 -90 % conversion was obtained over 5 – 7 hours with small molecular weight (PD = 1.13 and 1.09).
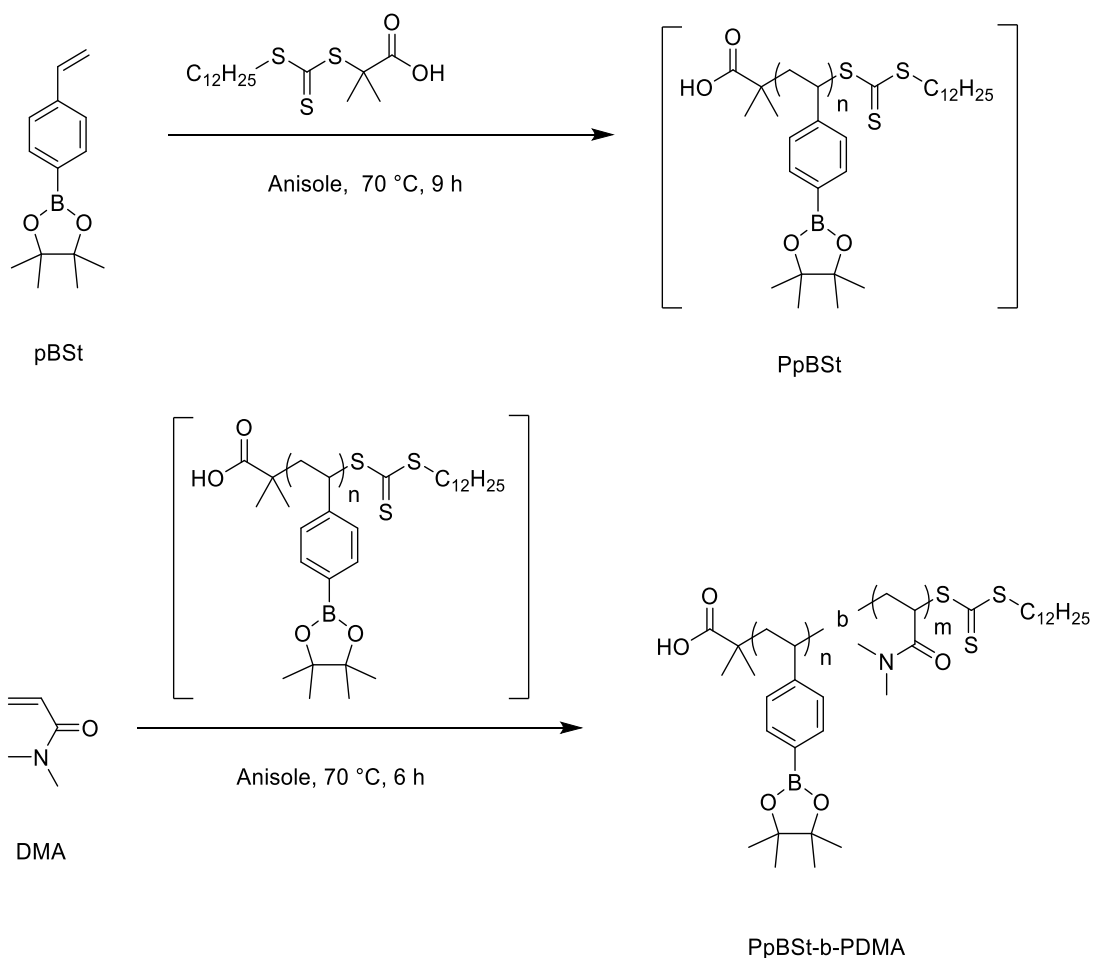
A styrene monomer of phenylboronic acid with the RAFT agent and then the block of PBA protected with pinacol extended with N, N-Dimethylacetamide (*N, N* DMA) was synthesized by Cambre *et al.*, (Cambre et al., 2007a). However, low PDI = 1.09 -1.13 obtained for 100, and 250 blocks PBA macroRAFT was obtained. There is no evidence of livingness and AIBN remaining in the reaction during chain extension. The boronic acid-containing macroRAFT was polymerized with DMA to make a block copolymer further deprotected with polymer-bound resins for sugar sensitivity experiments.

The vinyl monomer of boronic acid, 4-pinacolatoborylstyrene (pBSt) was polymerized by RAFT method using 2-(Dodecylthiocarbonothioylthio)-2-methylpropionic acid (DDMAT). The boronic acid-containing macroRAFT was polymerized with DMA to make

block copolymer that was further deprotected with polymer-bound resins for sugar sensitivity experiments.

In 2008 Roy and his group published a delivery system comprising an unprotected phenylboronic acid chain extended by Dimethyllacrylamide (DMA). Sugar-responsive block copolymers by direct RAFT polymerization of unprotected boronic acid monomer were synthesized by the same group in 2008 (Roy et al., 2008b).
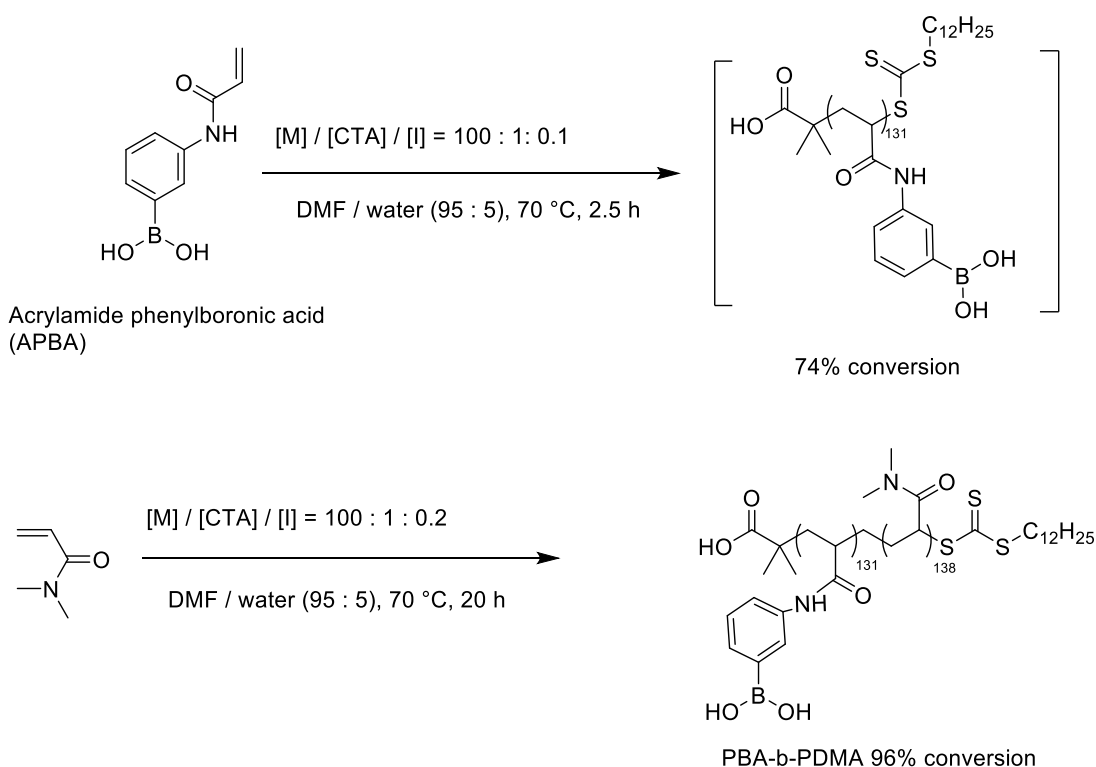
Scheme 4. 12 RAFT polymerization of 3-acrylamidophenyl boronic acid marcoRAFT extended with DMA.

Block copolymers of 3-acrylamido phenylboronic acid and *N, N*-DMA were obtained with good conversion values (table 4.2). In this study the macro-RAFT chain was a boronic acid polymer that was extended with *N, N*-DMA.

One of the drawbacks of using the unprotected boronic acid monomer is that it cannot be analyzed with GPC. Therefore, the boronic acid copolymer and macro-RAFT should be protected with pinacol for molecular weight analysis (Roy et al., 2008). Roy and his group published a delivery system comprising an unprotected phenylboronic acid chain

of 100 and 200 blocks extended by N, N Dimethylacrylamide (DMA). The drawback of unprotected phenylboronic acid lies in the not accurate analysis by GPC for molecular weight determination (Roy et al., 2008b).

A MacroRAFT of phenylboronic acid were synthesised temperature-responsive block, and the pH-responsive block synthesized. The aim was to obtain triply-responsive boronic acid block copolymers in a solution that could self-assemble by variations in temperature, pH, or sugar concentration (Roy et al., 2009). In this study, the block copolymer made with NIPAM did not lead to thermal responsive property. However, it was planned to be triply responsive. The NIPAM led to dehydration and interchain aggregation, as the boronic acid units are only pH-sensitive in the presence of diols. Therefore, a thermoresponsive polymer was not obtained and, at a comprehensive range of temperature, investigated the NIPAM blocks aggregated were carried out (Roy et al., 2009).
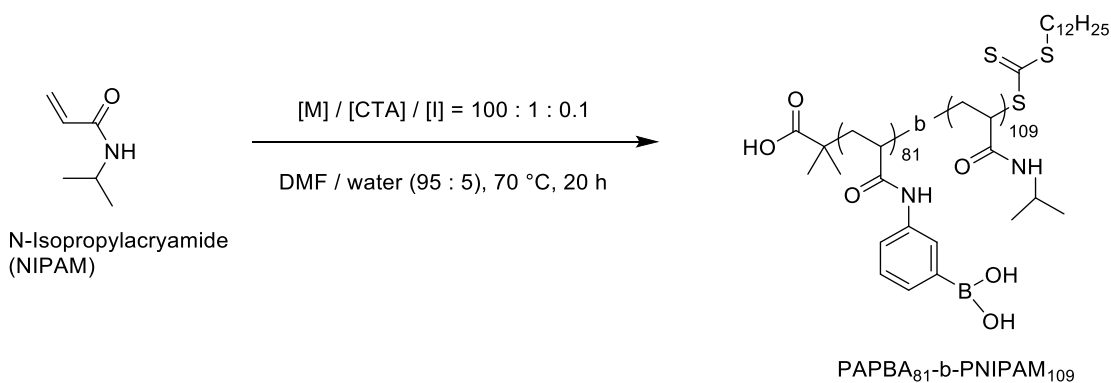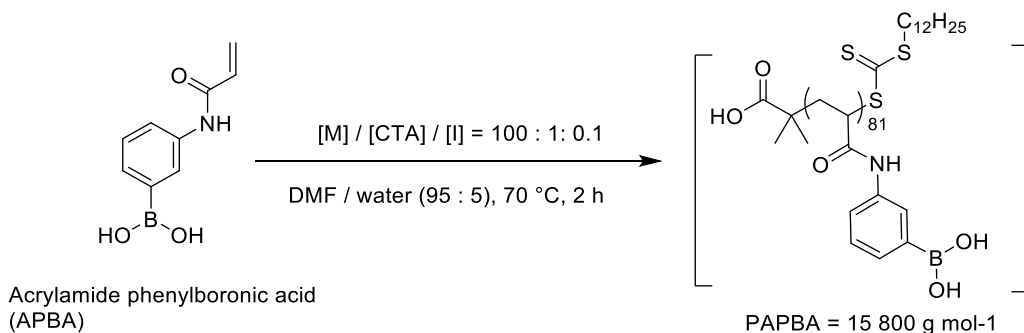
Scheme 4. 13 RAFT polymerization of NIPAM, and phenylboronic acid macroRAFT.

A glucose-Sensitive of Boronic acid Block Copolymer at Physiological pH was investigated by the RAFT polymerization method using *N*-(2-acryloylamino-ethyl)-4-(4,4,5,5,-tetramethyl-[1,3,2]dioxoborolan-2-yl-benzamide (Roy and Sumerlin, 2012).
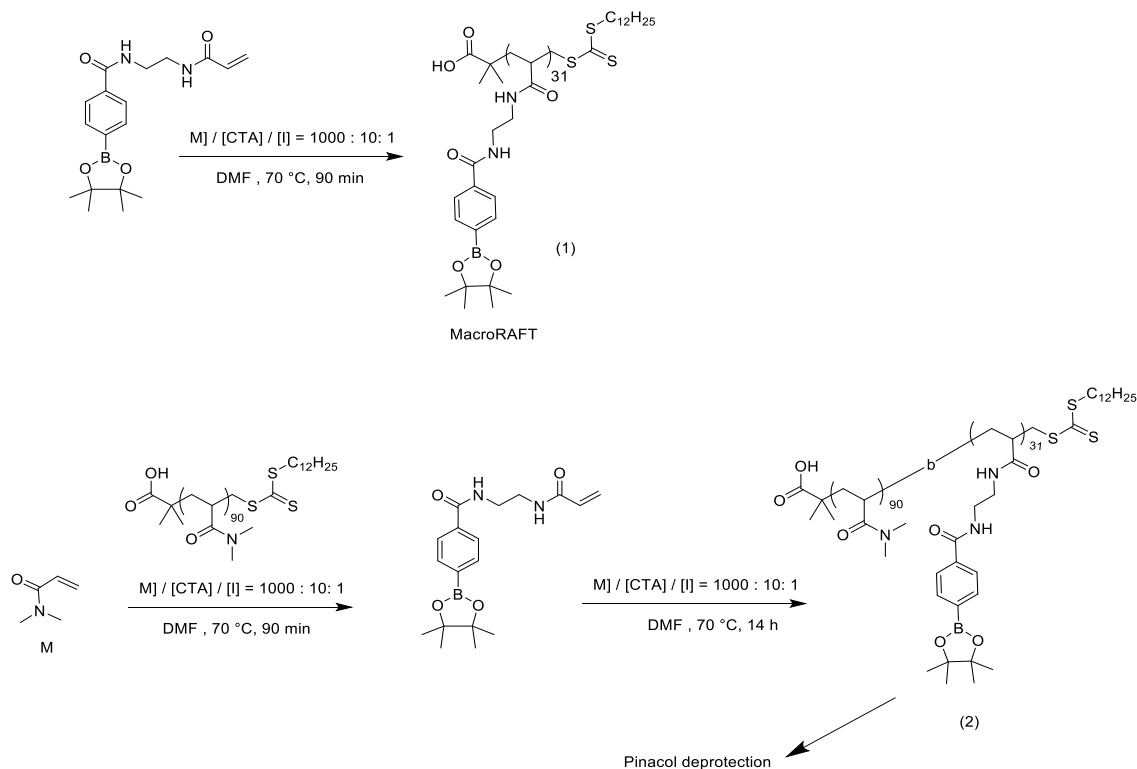
Scheme 4. 14 Reaction of boronic acid containing polymer and DMA macro-RAFT extended with phenylboronic acid group obtained from deprotection of pinacol.

In this work Poly(*N*-(2acrylolamino-ethyl)-4-(4,4,5,5-tetramethyl [1,3,2] dioxoborolane-2-yl)-4-brono-benzamide) (1) and Poly (*N, N* dimethylacrylamide-b-poly(*N*-2acryloylamino-ethyl)-4-brono-benzamide) (2) was synthesized.

Boronic acid-containing polymer and DMA macro-RAFT extended with a phenylboronic acid group obtained from the deprotection of pinacol (Roy and Sumerlin, 2012). The blocks of the polymer obtained were 100 and 200 with narrow PDI = 1.20 -1.28 and molecular weight near to theoretical values. This paper shows promising macro-RAFT of phenylboronic acid monomer; however, the chain extension was only carried out with DMA, and not multi blocks of phenylboronic acid macro-RAFT.

Thermo responsive properties of sugar sensitive Copolymer of *N*-Isopropylacrylamide and 3-(Acrylamido) phenylboronic acid was obtained by free radical polymerisation in dioxane for 6 hours at 70 °C. The polymer obtained show thermal and sugar sensitive properties with a 67% yield (et.al, 2004).
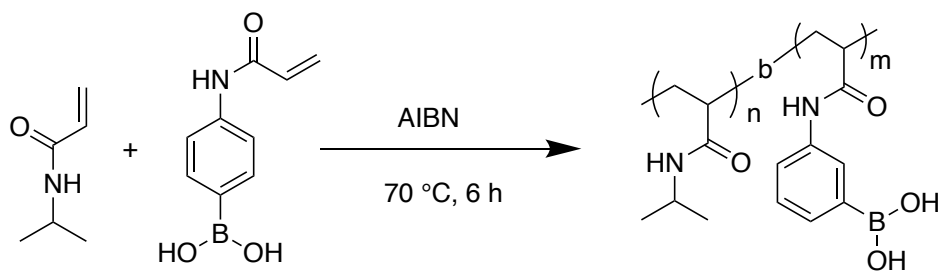
Scheme 4. 15 Free radical polymerization of 3-ACPBA with NIPAM in dioxane.

Mattiasson carried out free radical polymerization of 3-APBA with NIPAM for temperature-responsive polymer, there is not sufficient information in this paper (et.al, 2004).

Boronic acid linear homopolymers are effective emulsifiers and gelators were synthesized by RAFT polymerisation of styrene boronic acid and short chain RAFT agent in the presence of DMF and AIBN with 80% conversion (Chen et al., 2015b).

[M] / [CTA] / [I] = 100 : 1 : 0.5
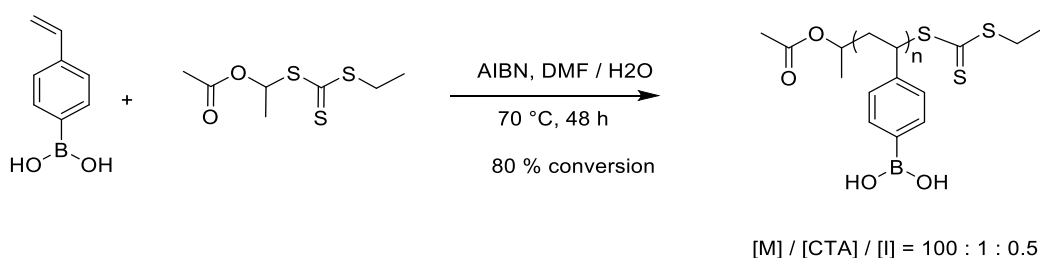
Scheme 4. 16 RAFT polymerization of boronic acid containing homo polymer.

Emulsifying phenylboronic acid gels were prepared using RAFT polymerization, which responded over a range of pH. Another styrene-based boronic acid linear homopolymer synthesized by RAFT polymerization using a short-chain RAFT agent in the presence of DMF and AIBN with 80% conversion. The conversion was reported as 80%, however, the non-protected boronic acid causes a drawback for this study (Chen et al., 2015b)

Development of phenylboronic acid-functionalized nanoparticles for emodin delivery were synthesised by RAFT polymerisation which was further used for nanoparticle formation for drug delivery (Wang et al., 2015).
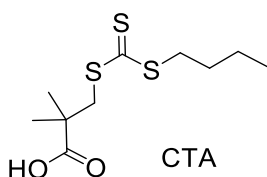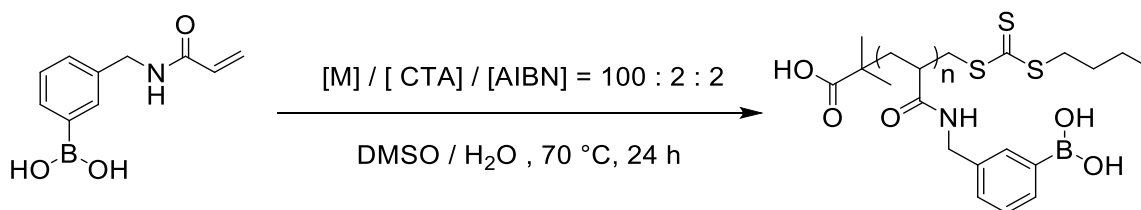
Scheme 4. 17 Development of phenylboronic acid-functionalized synthesized by RAFT polymerization which was further used for nanoparticle formation for drug delivery.

Most of crucial information, such as the number of blocks of the polymer is not mentioned in the article. Phenylboronic acid-functionalized nanoparticles for emodin delivery were synthesized by RAFT polymerization, which were further used for nanoparticle formation for drug delivery. In this study, more focus was on the drug delivery and formation of nanoparticle, not the RAFT polymerization, as the RAFT procedure was just a small part of the study and not much emphasis was given to the RAFT blocks and livingness (Wang et al., 2015).

Boronic acid containing surface RAFT agent was synthesized for glucose-sensitive quartz crystal microbalance (QCM-sensors) via direct surface RAFT polymerization (Kemal Arda Günay, 2012), (Sugnaux and Klok, 2014). PBA polymers were immobilized over silicon wafer that allows controlled growth of PBA polymers as brushes. These brushes could be applied for glucoses sensor, which can detect glucose in diluted samples.
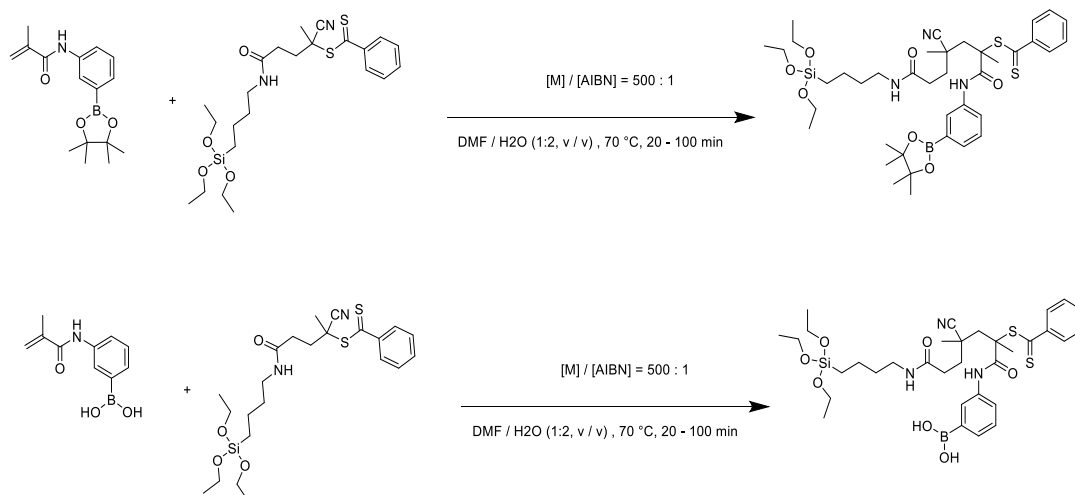
Scheme 4. 18 Synthetic strategy can be useful for glucose sensor and also glucose sensitive thin film preparations.

Phenylboronic acid-containing brushes that could be applied as a glucose sensor, and detect glucose in diluted samples were synthesized (Kemal Arda Günay, 2012). PBA polymers were immobilized over silicon, a wafer that allows the controlled growth of PBA polymers as brushes. This method was suggested for glucose sensor thin films (Sugnaux and Klok, 2014).

RAFT polymerization of 4-vinylphenylboronic acid was carried out in presence of PEGylated CTA as the basis for micellar sugar sensors (Maji et al., 2014). In this experiment 97% conversion of the polymer was obtained mPEG$_{114}$-b-P(4-VPBA)$_{30}$.
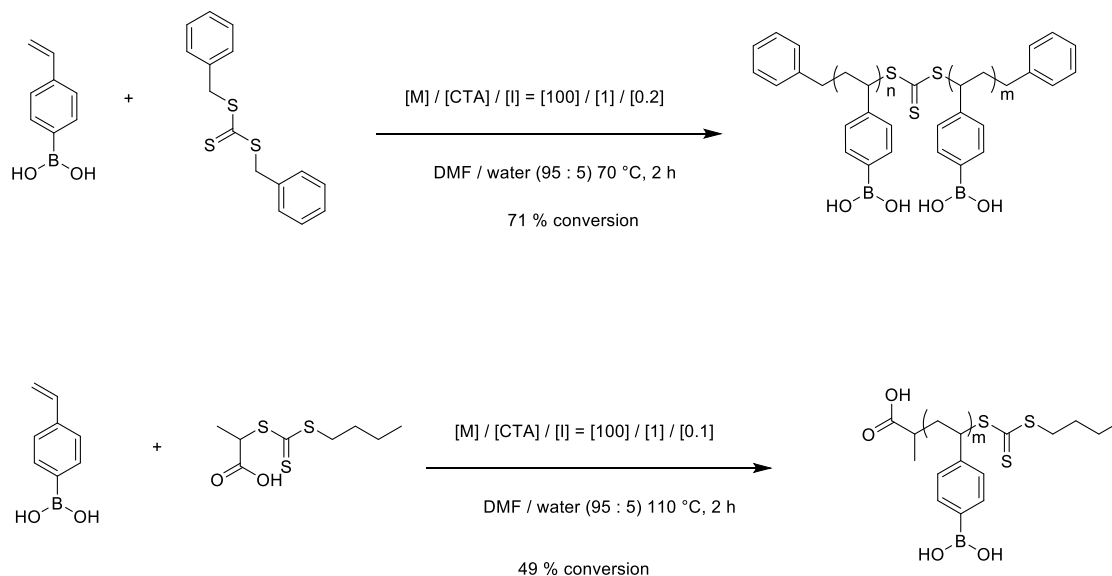
An amphiphilic random glycopolymers based on phenylboronic acid was synthesized, characterized as potential as a glucose-sensitive matrix (Jin et al., 2009). In this study, insulin, consolidated with the nanoparticle of this glycopolymers and the nanoparticle's swelling performance with the *in vitro* release profiles of insulin at different glucose concentrations, revealed the glucose sensitivity of the glycopolymers.

Unprotected homopolymer was synthesized by a RAFT polymerization method for a pH and sugar responsive polymer.

Glucose-Sensitive lower critical solution temperature changes of copolymers composed of *N*-Isopropylacrylamide and Phenylboronic Acid Moieties were studied (T.Aoki, 1996). In this study a glucose-sensitive ternary polymer was obtained by copolymerizing Poly(N-isopropylacrylamide) (PIP AAm), PBA, and *N,N*-dimethylacrylamide (DMA- PAA) and 3-acrylamidophenylboronic acid (PBA).
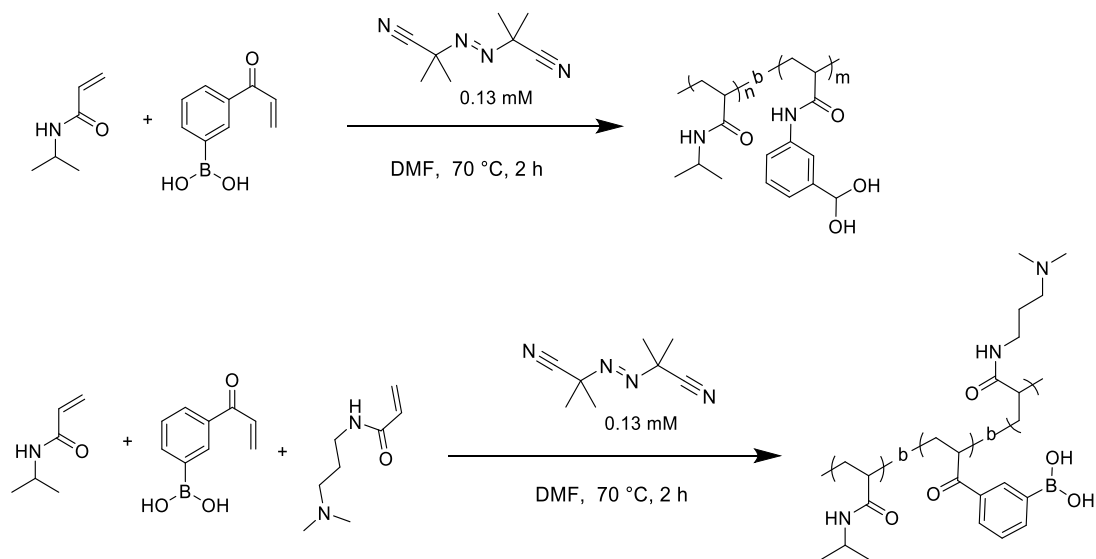
The RAFT polymerization of the commercially available unprotected 4-vinyl boronic acid (4-VBA) was optimized with two different CTAs, namely dibenzyl trithiocarbonate (DBTTC) (CTA-1) and 2-(butylthiocarbonothioylthio) propanoic acid (BTTCP) (CTA-2) to get well-defined poly(4-VBA). At higher conversion, a slight deviation of the Mn observed from the theoretical value. In this study, the higher Mn at higher conversion with higher dispersity (Đ) is not fully understood, and it might be due to the formation of stable side products formed by side reactions onto the trithiocarbonate, and using unprotected PBA which does not give entirely accurate GPC measurement due to interaction of PBA with the column.

An older study from 1996 shows glucose-Sensitive lower critical solution temperature changes of copolymers composed of N-Isopropylacrylamide and Phenylboronic Acid Moieties (T.Aoki, 1996) which was a radical polymerization using AIBN at 70 ºC and also using three monomers of N, N-DMA, phenylboronic acid and NIPAM (T.Aoki, 1996).

Glucose-responsive polymer gel bearing phenylborate derivative as a glucose-sensing moiety operating at the physiological pH (Matsumoto et al., 2004). A totally synthetic glucose responsive gel operating in physiological aqueous conditions (Kazunori Kataoka, 1998), (A. Matsumoto, 2010), (Matsumoto et al., 2003), (Matsumoto et al., 2004) was

synthesised using three vinyl monomers in the presence of DMSO and AIBN by free radical polymerisation method.
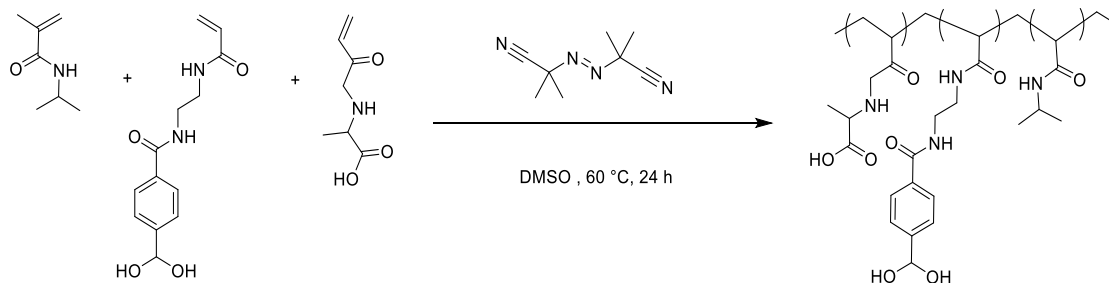
Scheme 4. 21 Glucose-responsive polymer gel bearing phenylborate derivative as a glucose-sensing moiety operating at the physiological pH.

This is a totally synthetic system that operates as glucose sensitive system at physiological pH. Previously glucose sensitive such systems were incorporated with enzymes and proteins that caused degradation of protein and enzyme. The toxicity of such system requires further investigation.

The literature suggests (table 4.2) that the studies were using conventional radical polymerization and RAFT polymerization methods for boronic acid glucose sensing systems. However, many of these studies used unprotected phenylboronic acid, which is problematic during GPC/SEC analysis. Table 4.2 summarises the main outcome of these studies and the block co polymers based of RAFT polymerisation of phenylboronic acid.

43
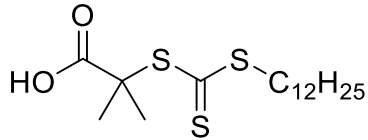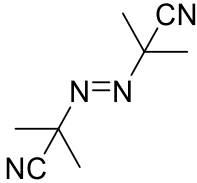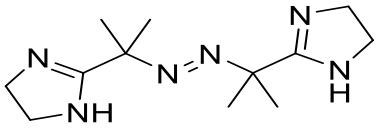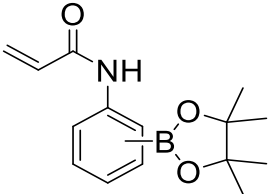
Table 4. 2 The results of RAFT polymerization of acrylamide phenylboronic acid previously obtained and the condition of the reactions.

RAFT polymerization	Polymer	[M] / [CTA] / [I]	T, Time (h),	Solvent	MW /mmol-1	PDI	Reference
Polystyrineboronic acid pinacol ester	PpBSt	1000 / 10 / 2	7h	Anisole	16300	1.13	(Cambre et al., 2007a)
	PpBSt-b-PDMA	2500 / 10 / 4	5h		60 800	1.09	
3-acrylamidophenyl boronic acid marcoRAFT extended with DMA.	PAPBA	100 / 1 /0.1	70 °C, 2.5 h	DMF / Water	19 700	1.16	(Roy et al., 2008a)
	PAPBA	200 / 1 /0.1	70 °C, 2.5 h	DMF / Water	37 800	1.16	
	PAPBA131-b-pDMA138	100 / 1 / 0.1	70 °C, 2.5 h	DMF / Water	38 700	1.17	
RAFT polymerization of NIPAM, and phenylboronic acid macroRAFT	PAPBA	1000 / 10 / 1	70 °C, 2.0 h	DMF / Water	15 800	1.02	(Roy et al., 2009).
	PAPBA81-b-pDMA109	1000 / 10 / 1	70 °C, 20.0 h	DMF / Water	28 100	1.15	
RAFT polymerization with a boronic acid terminated RAFT agent	PDMA	100: 1: 0.5	70 °C, 4.0 h	DMF	7700	1.11	(De et al., 2009)
	PDMA74-b-pPBA18	200: 1: 0.05	70 °C, 4.0 h	DMF	11 200	1.35	
	(HO)2-b-PDMA	100: 1: 0.025	70 °C, 7.0 h	DMF	12 500	1.16	
	(HO)2-b-PDMA-b-PNIPAM	100: 1: 0.07	70 °C, 1.5 h	DMF	15 900	1.28	
Boronic acid containing polymer and DMA macro-RAFT	1	1000: 10: 1	70 °C, 90. Min	DMF	28200	1.20	(Roy and Sumerlin, 2012)
	2	1000: 10: 1	70 °C, 14.0 h	DMF	22300	1.28	

4.7 Materials

VA-044 2,2'-Azobis[2-(2-imidazolin-2-yl)propane]Dihydrochloride, water soluble Azo Initiator, 25g purchased from Wako chemicals (VA-044, Wako) and 2-(Dodecylthiocarbonothioylthio)-2-methylpropionic Acid (DDMAT, TCI chemical Ltd, > 98%) were used as received. 2,2'-Azobis(2-methylpropionitrile) (AIBN, 98% Sigma). 1,4-Dioxane (Sigma-Aldrich, ≥99.0%) and DI water were used directly as solvents for polymerization. *N, N*-dimethylacrylamide (DMA, TCI, 98%) was distilled in vacuo to remove radical inhibitor, in presence of benzophenone and metal sodium available from the lab (Sigma Aldrich) and CH_2Cl_2 (Sigma-Aldrich, ≥ 99%), *N,N*-dimethylformamide (DMF (solvent), Sigma-Aldrich, HPLC-grade, ≥ 99.9%) used for GPC as 0.1 M solution of LiBr filtered with THF filter before use, diethyl ether (Et_2O, Sigma-Aldrich, ≥ 99.5%) for precipitation of DMA, hydrochloric acid (Sigma-Aldrich, 36.5-38%), $CDCl_3$ (Sigma-Aldrich, 99.8 atom%), , and LiBr (Sigma-Aldrich, 99%) were used as received. 2-(3-Aminophenyl)-4,4,5,5-tetramethyl-1,3,2-dioxaborolane > 98.0% and 2-(4-Aminophenyl)-4,4,5,5-tetramethyl-1,3,2-dioxaborolane > 98.0% were purchased from TCI, acrylamide from (Sigma). Acetone fisher scientific laboratory reagent, potassium carbonate purchased from Fischer Scientific.

Table 4. 3 Reagents used in RAFT polymerization of DMA and 4 or 3-ACPBAPE.

Chemical used	Structure	Name
RAFT agent		2-Dodecylthiocarbonothioylthio-2-methylpropanoic acid (DDMAT or DMP)
Initiator		2,2'-Azobis-isobutyronitrile (AIBN)
		VA-044 2,2'-Azobis[2-(2-imidazolin-2-yl) propane] Dihydrochloride (VA-044)
Monomer		N-((*ortho, meta, or para*)-(4,4,5,5-tetramethyl-1,3,2-dioxaborolan-2 yl)phenyl)acrylamide

4.8 Monomer synthesis
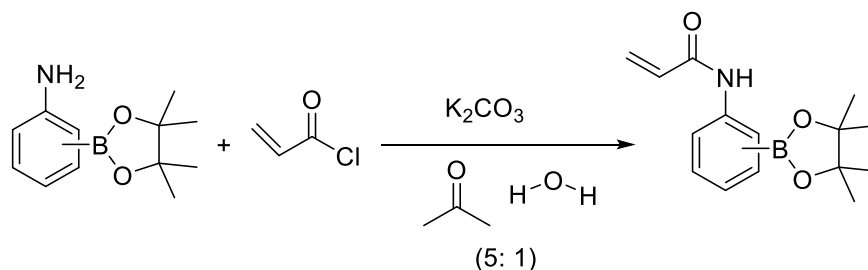
Scheme 4. 22 Synthesis of acrylamide monomer N-(4-(4,4,5,5-tetramethyl-1,3,2-dioxaborolan-2 yl)phenyl)acrylamide pinacol ester (4-ACPBAPE)

A stirred suspension of potassium carbonate (6.30 g, 45.64 mmol) in distilled water (13.4 mL) and acetone (53.6 mL) (1:5) was prepared. 4-Amino phenylboronic acid pinacol ester (5.01 g, 22.82 mmol) was added slowly to the mixture and stirred for 3 hours at 0 °C. Acryloyl chloride (3.69 mL 45.64 mmol) was added dropwise.

Thin layer chromatography was performed using petroleum ether: ethyl acetate (70:30) mixture after 1 and 3 hours to check the presence of any free amines. No free amines observed by staining the TLC plate with ninhydrin (2,2-dihydroxyindane-1,3-dione). K_2CO_3 was filtered; the mixture was concentrated under reduced pressure and extracted three times with dichloromethane (3 x 30 mL). Washed with saturated NaCl solution. The organic layer was dried over Na_2SO_4, filtered, and concentrated under reduced pressure to give the product 5.69 g, 91%.

The residue was purified dissolving in $CHCl_3$ and addition of hexane drop wise to give corresponding product as off white solid, 5.03g, 81 % yield (Chanthamath et al., 2013).
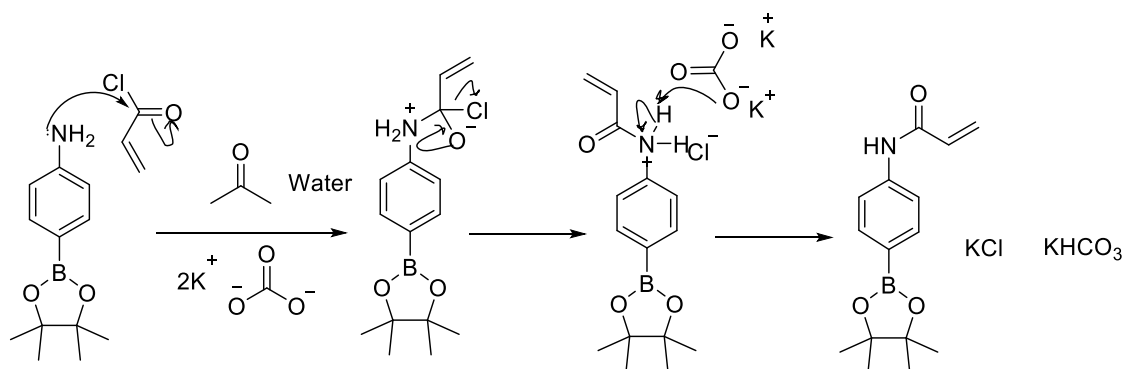
Scheme 4. 23 Mechanism of the formation of 4-ACPBAPE

^{1}H and ^{13}CNMR and correlation spectra were recorded in DMSO, CDCl$_3$, MeOD using standard parameter sets, on a Bruker Avance III 400MHz FT-NMR spectrometer equipped with a 5 mm PABBO BB-1H/D Z-GRD probehead. The chemical shift is reported in parts per million and are referenced to the solvent lock signal.
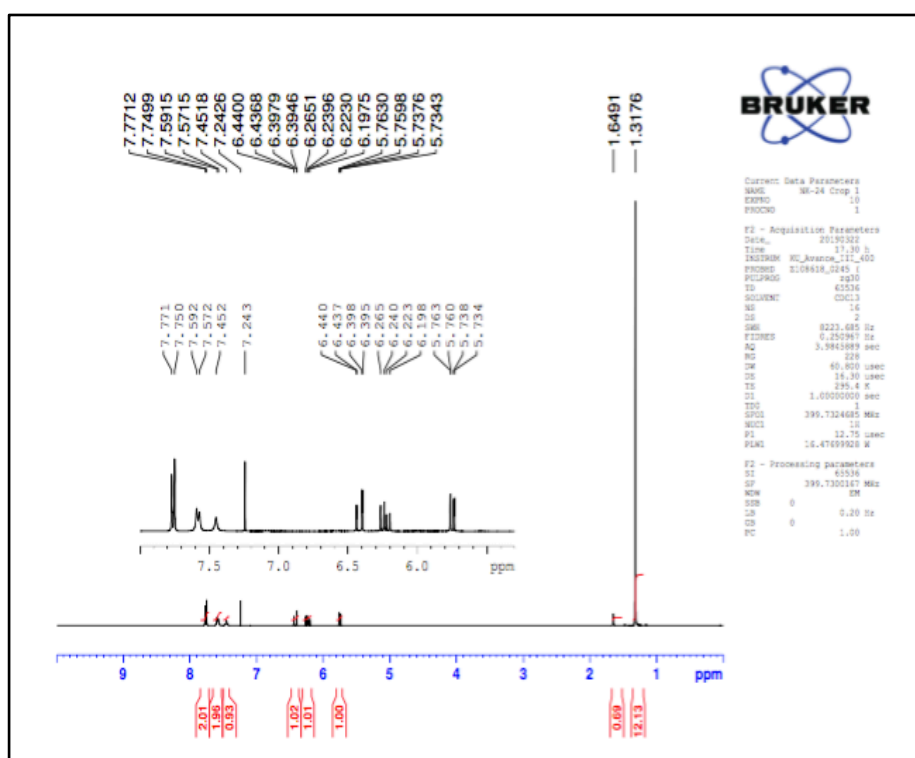
Figure 4. 1[1]HNMR of N-(4-(4,4,5,5-tetramethyl-1,3,2-dioxaborolan-2-yl)phenyl)acrylamide after crystallization with chloroform and precipitation in hexane.

Shift [1]H (400MHz), (CDCl$_3$) , δ = 1.32 (s, 12H), 1.64 water in CHCl$_3$, 5.75 (d, J = 10.2, 1.3 Hz, 1H), 6.23 (dd, J = 16.8, 10.2 Hz, 1H), 6.42 (d, J = 16.8 Hz, 1.3 1H), 7.45 (NH, br, disappeared D$_2$O shake), 7.76 (d,1H, J = 8.5 Hz), 7.65 (d, J = 8.0 Hz, 1H).
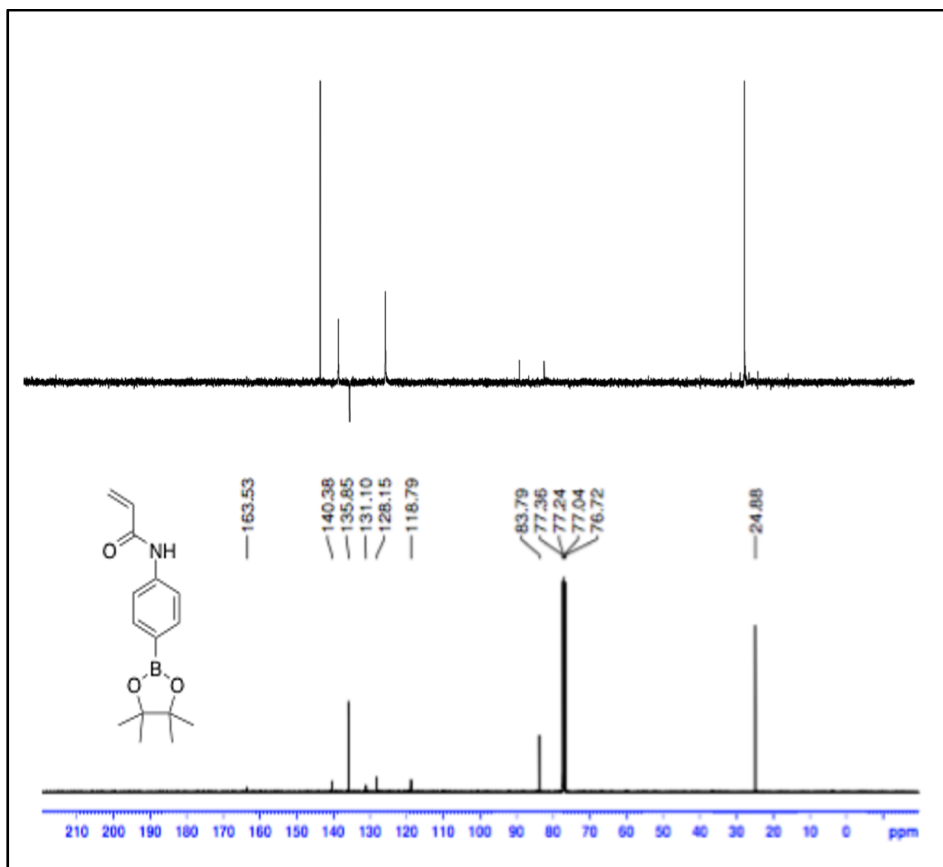
Figure 4. 2 ^{13}CNMR of *N*-(4-(4,4,5,5-tetramethyl-1,3,2-dioxaborolan-2-yl)phenyl)acrylamide after crystallization with chloroform and precipitation in hexane.

Shift [13]C (100 MHz), (CDCl$_3$) δ = 24.88 (4 x CH$_3$), 83.79 (2 x C), 118.72 (2 x CH aromatic), 128.15 (CH$_2$), 131.10 (CH alkene), 135.85 (2 x CH aromatic), 140.38 (C), 163.53 (C=O).

4.8.1 Optimizing suitable condition for monomer crystallization and solubility

The monomer was tested with different solvents to find ideal condition for recrystallization. The monomer was dissolved in chloroform and precipitated slowly in cold hexane filtered and left to dry.

4.9 Polymer characterization

4.9.1 Nuclear Magnetic Resonance Spectroscopy

The purity was determined using NMR. ^{1}HNMR and correlation spectra were recorded in CDCl$_3$, using standard parameter sets, on a Bruker Avance III 400MHz

FT-NMR spectrometer equipped with a 5 mm PABBO BB-1H/D Z-GRD probehead. All NMR experiments were carried out in CDCl$_3$ or other solvent indicated in the relevant section, and all the NMR data was processed using TopSpin 3.5 (Bruker BioSpin GmbH, Rheinstetten, Germany) by applying a fast Fourier transform. The spectra were automatically referenced to internal Trimethylsilyl propanoic acid (TMSP or TSP), automatically phase-corrected with manual correction of the phase as required, and automatically baseline corrected.

4.9.2 Gel permeation chromatography (GPC)

Gel permeation chromatography (GPC) or Size Exclusion Chromatography (SEC) is a chromatographic system that separates the molecules based on their size. GPC /SEC is the most usual method used to determine average MWs and polydispersity of polymers. A GPC system is divided into the injection, column, and detectors. A polymer sample is prepared as a dilute solution in the mobile phase. It is then pumped through the column, which is packed with porous beads that have controlled porosity and size. The most widely used detector is a differential refractometer, which measures the refractive index's difference between the eluent and the sample. Higher MW polymers, or hydrodynamic radius polymers, cannot permeate through the pores and have a shorter residence time in the column, while lower MW polymers are delayed by going through the pores of the beads and thus have longer residence time. Light scattering detector also allows more accurate MW detection by measuring incident beam light scattered by samples in the eluent.

4.9.2.1 Number average molecular weight

The number average MW, Mn, gives a value through the statistical average MW of all the chains in a batch. Mi is the MW of a chain, and Ni is the number of the chain with Mi. Mn has equal numbers of molecules on either side of Mn distribution, and it can be predicted with the DP of a polymer.

$$M_n = \frac{\sum \text{NiMi}}{\sum Ni}$$

Equation 4. 9 Weight average molecular weight

The weight average MW, Mw, studies the weight of a chain in determining the MW average. The larger the chain, the more it would contribute to Mw. Mw is more sensitive to the actual molecular size than their molecular number. There is also equal weight of molecules on either side of Mw distribution.

$$Mw = \frac{\Sigma NiMi^2}{\Sigma NiM^i}$$

Equation 4. 10 Number average molecular weight

A parameter used to measure the MW distribution is polydispersity. This value is defined by the fraction of Mw and Mn of the polymer batch.

$$Đ = \frac{Mw}{Mn}$$

Equation 4. 11 Polydispersity is the ratio of average molecular weight and average molecular number.

Mn and polydispersity (Mw /Mn) were measured by GPC, Agilent technology, using GPC/SEC Columns advancing polymer solution Polar GelM, 1200 infinity Series, PL-GPC 50, Serial No 0006367060-46, particle size 8 micon, pore type mixed, length / I.D. (mm) 300 x 7.5.

Theoretical number-average molecular weight (Mn, *th*) was calculated according to the equation.

$$M_{n,th} = \left[\left(\frac{[M]_0}{[DDMAT]_0}\right) \times MW_M \times conversion\right] + MW_{[DDMAT]}$$

Equation 4. 12 calculation of Theoretical, Mn (M, *nth*).

Theoretically, Mn (M, nth) is calculated as a function of the initial amount of monomer $[M]_0$ and $[DDMAT]_0$ multiplying by the Mw of monomer and addition of the molecular weight of DDMAT. Mn is calculated as a product of M, nth and percent conversion.

Section 2 of chapter 4

This section starts with conventional free radical polymerisation of DMA followed by RAFT polymerisation of *N, N*-Dimethylacrylamide$_{50}$ the subscript 50 means the formation of 50 blocks. This is reproduced from literature for reproducibility purpose and learning the technique. This was followed by extension of polyDMA macroRAFT chain to 50-b-50 and 50-b-50-b-50, Poly(N,N Dimethylacrylamide)$_{50-b-50}$, Poly(N,N Dimethylacrylamide)$_{50-b-50-b-50}$, RAFT polymerization of *N,N*-Dimethylacrylamide$_{100}$. The results are discussed under each GPC curved, NMR, and the calculation are tabulated.

4.10 Conventional free radical polymerization of DMA

For control of DMA Polymerization, the conventional free radical polymerization of DMA was also reproduced (Scheme 4.24).
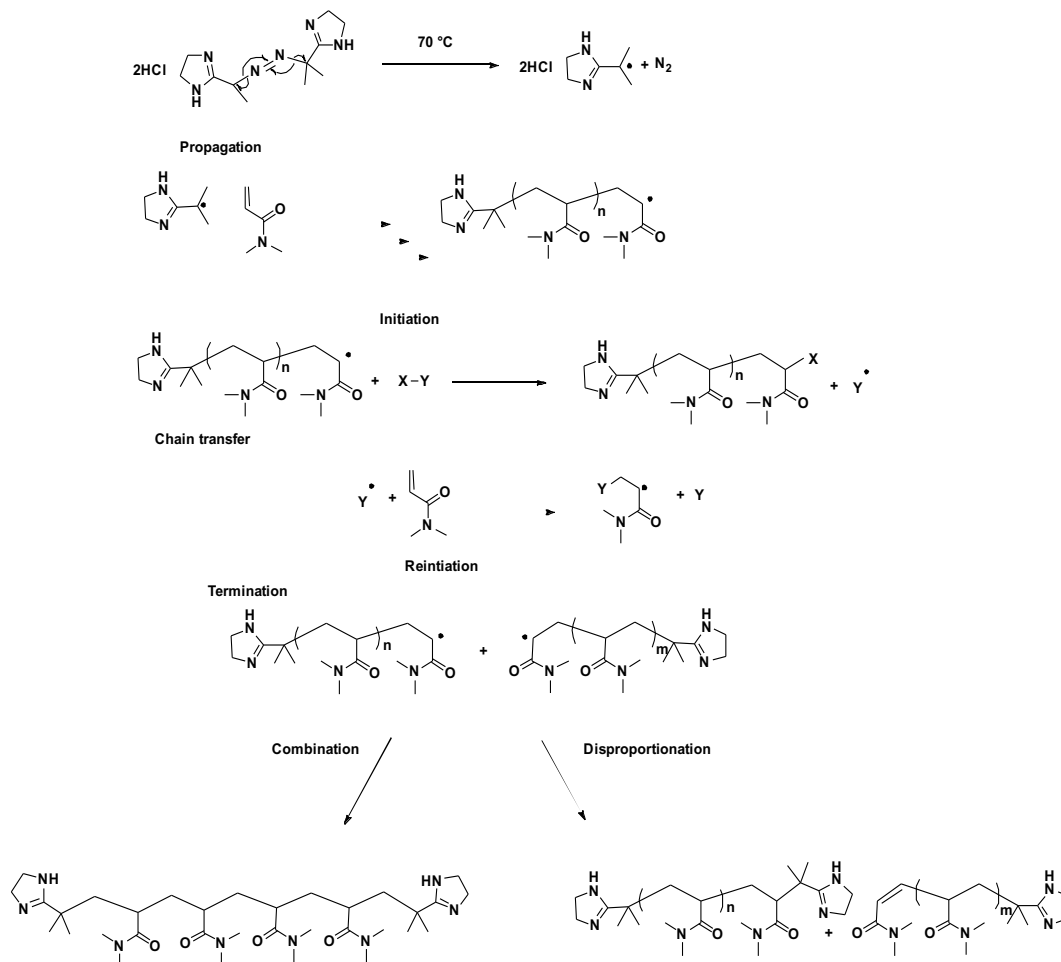
Scheme 4. 24 Conventional polymerization of DMA in presence of VA-044 reproduced from litrature(Chalmers, 2017).

4.11 RAFT polymerization of N,N-Dimethylacrylamide

General one-pot sequential polymerization procedure solutions were heated at 70 °C in a paraffin oil bath for 2 h. Polymerizations were stopped by placing test tubes in an ice-water bath. Conversion, Mn, and Mw/Mn were measured as described above. Sequential chain extension reactions were performed directly on the macroRAFT reaction solution with the amount of initiator remaining after each cycle taken into account (Chalmers, 2017) (Scheme4.25).
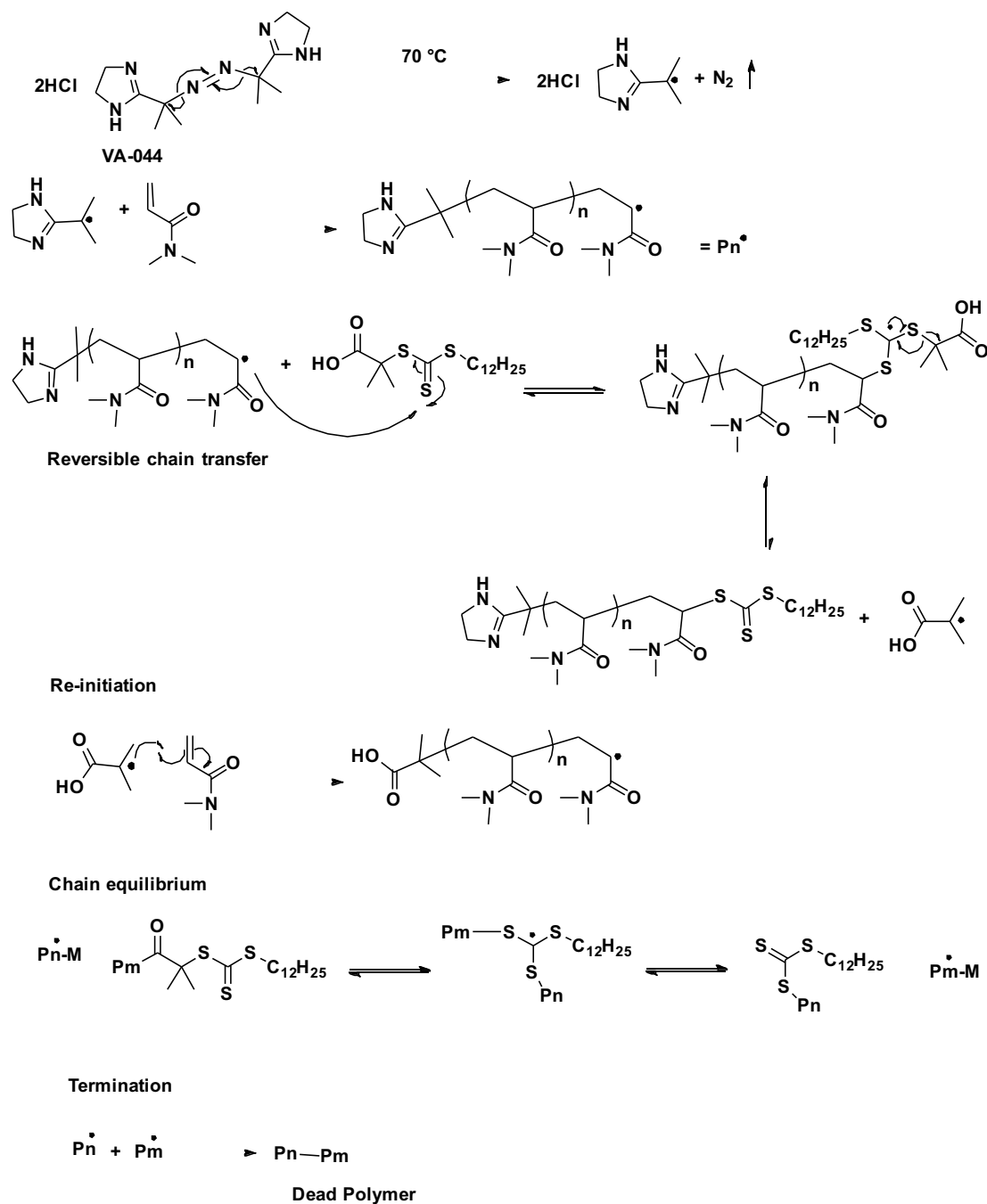
Scheme 4. 25 From litrature a RAFT polymerization of *N,N*-dimethylacrylamide (Monomer), RAFT agent 2-(dodecylthiocarbonothioylthio)-2-methylproppionic acid (DDMAT), and azo-initiator 2,2'–azobis[2-(2-imidazolin-2yl)propane]dihydrochloride (VA-044). RAFT polymerization of DMA in presence of VA-044.

4.12 Polymerization of polyDMA macro-RAFT

4.12.1 Preparation of MacroRAFT Agent Poly(N,N Dimethylacrylamide)50

This method is adopted from the Aldabbagh group, previously published (Chalmers, 2017). (DDMAT (163.0 mg, 0.45 mmol) and DMA (221.0 mg, 0.022 mol) were added

to VA-044 (4.5 x 10^{-3} mmol from a stock solution) in 5 mL dioxane/water (80/20) and heated at 70 °C for 2 h. The polymer was precipitated in diethyl ether (Et$_2$O), filtered, and dried at room temperature under vacuum for 24 h to give poly(DMA)$_{50}$ macro-RAFT, Mn = 4850 g .mol^{-1}, Mw/Mn = 1.11, 98% conversion, isolated = 2.20g.

4.12.1 RAFT preparation of Poly(N,N-Dimethylacrylamide)50-b-50 polymerization

4.12.1.1 Extension of Poly *N,N*-Dimethylacrylamide (DMA)50 macroRAFT

DMA (450.0 mg, 4.5394 mmol) and polyDMA macro-RAFT (500 mg, 0.1021 mmol) were added to VA-044 (30 mg, 0.092 mmol made into a 10 mL (1/100) stock solution) added in 5 mL dioxane : water (80: 20) and heated at 70 °C for 2 h. The polymer was precipitated in diethyl ether (Et2O), filtered, and dried at room temperature under vacuum for 24 h to give poly(DMA)50-b-50 macro-RAFT, Mn = 12457 g.mol-^{1}, Mw/Mn = 1.17, 98% conversion., isolated = 430 mg.

4.13.1 RAFT preparation of Poly(N,N Dimethylacrylamide)50-b-50-b-50 polymerization

4.13.1.1 Extension of Poly *N,N*-Dimethylacrylamide (DMA)$_{50}$ macro-RAFT

VA-044 (30 mg, 0.083mmol) was dissolved in 2 mL of water and topped with dioxane up to the mark of the 10 mL volumetric flask to give VA-044 9.0 x10^{-3}mmol) in 60:40 dioxane: water.

PolyDMA$_{50}$ macro-RAFT$_{50-b-50}$ (450 mg, 0.04 mmol) was added to 1 mL VA-044 stock solution in a test tube.

DMA (225 mg, 2.58 mmol) was added to the VA-044 and polyDMA macro-RAFT.

The reaction tube was purged with nitrogen and sealed, left in an oil bath at 70 °C for 2 hours. After 2 h the reaction was stopped by placing the test tube on ice.

The polymer was precipitated in Et$_2$O, filtered, and dried at room temperature under vacuum for 24 h. Yield = 410 mg, 61 %. Mn 1715, and PDI = 1.28.

4.14 RAFT polymerization of N-(4-(4,4,5,5-tetramethyl-1,3,2-dioxaborolan-2-yl) phenyl)acrylamide pinacol ester with PolyDMA macroRAFT28

Water soluble (171) polyDMA macro-RAFT (144.40 mg, 0.045 mmol and VA-044 (36.80 mg, 4.5 x10-3 mmol) was dissolved in 2 mL of water and topped with dioxane up to the mark of the 10 mL volumetric flask in 80:20 dioxane: water.

4-ACPBAPh (400.80 mg, 1.46mmol) was added to 1.0 mL VA-044 stock solution in a test tube. The reaction tube was purged with nitrogen and sealed, and left in oil bath at 70 °C for 2 h.

After 2 h the reaction was stopped by placing the test tube on ice. The polymer was precipitated in cold hexane, filtered, and dried at room temperature under vacuum for 24 h. Yield = 500.0 mg.

The list of polyDMA macroRAFT prepared at similar condition with 50 and 100 blocks as well as extension of the 50 blocks are in table 4.5. The result was consistent and in line with literature from the Aldabbagh group is previously published data.

Table 4. 4 The quantities used for polyDMA macro-RAFT extension with 4-ACPBAPE

Experiment [VA-044]$_0$ / [DDMAT]$_0$ /[DMA]$_0$		[VA-044]$_0$ in Dioxane: water (80 :20)		[DDMAT] in Dioxane: water (80 :20)		[DMA]$_0$ in Dioxane: water (80 :20)		Reaction T
Entry	Number of blocks	mg mmol^{-1}	Molarity	mg mmol^{-1}	Molarity	mg mmol^{-1}	Molarity	°C
84	45	14.61 / 323.27	0.0045	163.50 / 364.63	0.4470	2120 / 99.13	21.3861	70
87	50 – b -50	30.00 / 323.27	0.0093	500.00 / 4896	0.1021	450.0 / 99.13	4.5394	70
89	48	14.61 / 323.27	0.0045	163.50 / 364.63	0.4470	2120 / 99.13	21.3861	70
90	48	14.61 / 323.27	0.0045	163.50 / 364.63	0.4470	2120 / 99.13	21.3861	70
91	50-b-50-b-50	30.00 / 323.27	0.0093	450 / 9163.33	0.0491	225.00 / 99.13	2.2697	70
94	50	14.61 / 323.27	0.0045	163.50 / 364.63	0.4470	2120 / 99.13	21.3861	70
93	50 – b -50	30.00 / 323.27	0.0093	500.00 / 4896	0.1021	450.0 / 99.13	4.5394	70
170	50	35.50 / 323.27	0.0022	164.20 / 364.63	0.04503	2266 / 99.13	4.3942	70
171	50	35.50 / 323.27	0.0022	164.10 / 364.63	0.04500	2179 / 99.13	4.3962	70
175	100	36.80 / 323.27	0.00452	164.7 / 364.63	0.04516	470.00 / 99.13	4.5500	70

Table 4. 5 List of extension of polyDMA macroRAFT with 4-ACPBAPE carried out in dioxane water and VA-044 used as initiator.

Experiment $[VA\text{-}044]_0$ / $[pDMA\ macro\text{-}RAFT]_0$ /$[4\text{-}ACPBAPE]_0$		$[VA\text{-}044]_0$ in Dioxane: water (80 :20)		$[pDMA\ macro\text{-}RAFT]$ in Dioxane: water (80 :20)		$[4\text{-}ACPBAPE\ ]_0$ in Dioxane: water (80 :20)		Reaction T
Entry	Number of blocks	mg mmol^{-1}	Molarity	mg mmol^{-1}	Molarity	mg mmol^{-1}	Molarity	°C
173	40-b-30	36.80 / 323.27	0.0045	144.40 / 3199	0.0450	400 / 273.15	1.4643	70
174	50-b-35	35.90 / 323.27	0.0045	249.00 / 5895	0.0424	400.70 / 273.15	1.4669	70
170 - 182	50-b-50	35.80/ 323.27	0.0044	114.00 / 5208	0.0276	408.10 / 273.5	1.4941	70
170 - 183	50-b-50	36.70/ 323.27	0.0045	144.60 /5208	0.0270	400.00 / 273.15	1.4643	70
103*	50-b-50	30.00 / 323.27	0.0009	48.97 / 4784	0.0100	136.58 / 273.15	0.5000	70

* $[VA\text{-}044]_0$ / $[pDMA\ macro\text{-}RAFT]_0$ /$[3\text{-}ACPBAPE]_0$

4.15 RAFT polymerization of 4-ACPBAPE Using AIBN

RAFT polymerization of boronic acid monomer was carried out in dioxane and water in presence of VA-044. However, it showed some solubility issue therefore, the solvent system was changed from dioxane / water (80: 20) to DMF as AIBN is soluble in organic solvent. in addition, DMF is more aprotic solvent which can facilitate the polymerization reaction. Conventional polymerisation was carried out to test the reaction conditions required for RAFT polymerization of acrylamide phenylboronic acid. Initial experiments revealed that an optimal monomer concentration of 1 M.

A 10 mL stock solution of initiator and RAFT agent in DMF was made by diluting AIBN (59.2 mg, 0.36 mmol), DDMAT (25.5 mg, 0.07 mmol), and anisole (0.1242 g, 1.15 mmol) 250, 10, and 10 times respectively. The latter stock solution (1 mL) was transferred to 4-APBAE (0.2732 g, 1.0 mmol). The 1 M monomer solution was heated at 70 °C, and periodic sampling allowed conversion and molecular weight measurements. The anisole was used as an internal standard for conversion measurements using 1H NMR (400 MHz, CDCl3) by comparing the anisole peak at 3.81 ppm (3 H) with the monomer vinyl peaks.

Scheme 4.26 is the reaction mechanism of boronic acid monomer with RAFT agent in presence of VA-044.
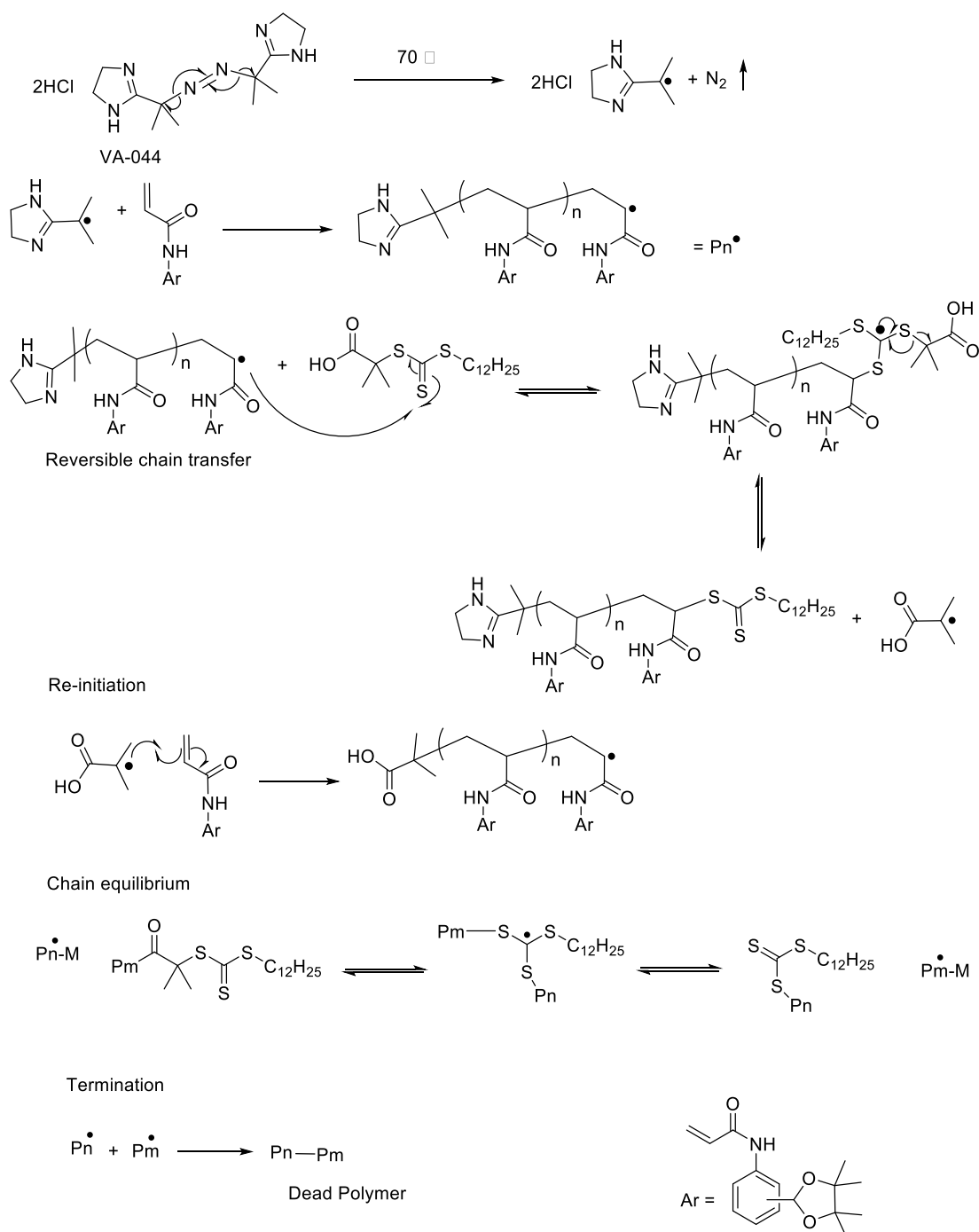
Scheme 4. 26 RAFT polymerization of N-(3 or 4-(4,4,5,5-tetramethyl-1,3,2-dioxaborolan-2-yl) phenyl) acrylamide pinacol ester in presence of VA-044 as initiator.

The reaction (scheme 4.26) would have been ideal to have same condition and the monomer could be extended with DMA (Chalmers, 2017). However due to solubility and reaction condition this was not proceeded further in section 4.15.1.

4.15.1 Optimization for synthesis of 4-APBAPE MacroRAFT

A 10 mL stock solution of initiator and RAFT agent in DMF was made by diluting AIBN (59.2 mg, 0.36 mmol), DDMAT (25.5 mg, 0.07 mmol), and anisole (0.1242 g, 1.15 mmol) 250, 10, and 10 times respectively. The latter stock solution (1 mL) was transferred to 4-APBAE (0.2732 g, 1.0 mmol). The 1 M monomer solution was heated at 80 °C and periodic sampling allowed conversion and molecular weight measurements. The anisole was used as internal standard for conversion measurements using 1HNMR (400 MHz, CDCl3) by comparing the anisole peak at 3.81 ppm (3 H) with the monomer vinyl peaks. Ideal condition would have been to extend the acrylamide phenylboronic acid monomer with DMA macro-RAFT previously established in Aldabbagh group (scheme 4.27). However, due to solubility and conversion limitation, our group has decided to change the reaction's condition for the boronic acid monomer. Using VA-044 a: water (80:20), therefore, was replaced using another solvent such as DMF was for the reaction in further experiments. (4-ACPBAPE solubility was determined in DMF which is 0.46 mg mL-1) This solubility was determined in the lab qualitatively.

p = **4-APBAE**
m = **3-APBAE**
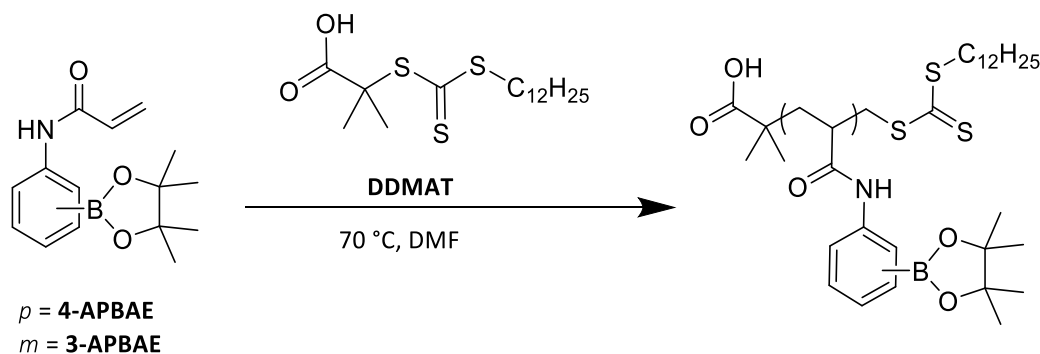
Scheme 4. 27 Reaction scheme for RAFT polymerization of N-(3 or 4-(4,4,5,5-tetramethyl-1,3,2-dioxaborolan-2-yl) phenyl) acrylamide pinacol ester.

4.16 Optimization of radical initiator concentration for conventional polymerization of 4-ACPBAPE

4.16.1 Selection of experimental conditions

Initial conventional experiments were designed to test the reaction conditions required for RAFT polymerization of DMA macro-RAFT adapted from literature (Chalmers, 2017).
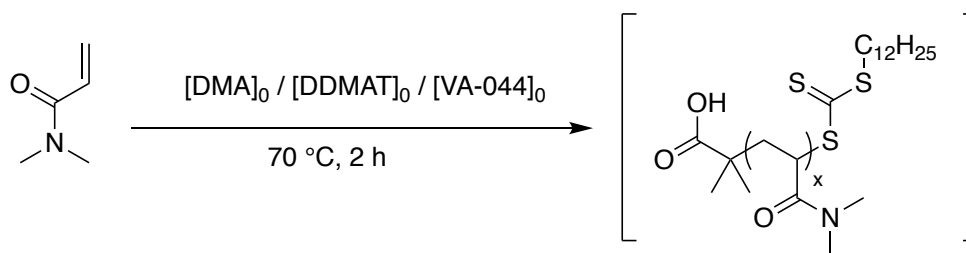
Scheme 4. 28 RAFT polymerization of Poly N,N-Dimethylacrylamide (DMA)$_{50}$ macro-RAFT to Poly(N,N Dimethylacrylamide)$_{50}$
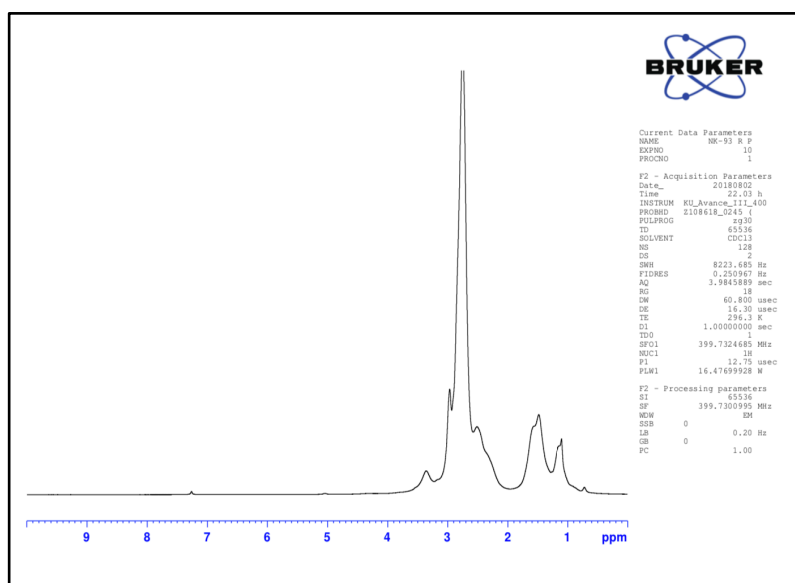
Figure 4. 3 ^{1}HNMR (CDCl$_3$) for poly (DMA)$_{28}$ macro-RAFT one pot 2-hour RAFT polymerization at 70 °C reproduced from litrature.

Attempted RAFT preparation of Poly(N,N Dimethylacrylamide)50-b-50

polymerization of Poly N,N-Dimethylacrylamide (DMA)50 macro-RAFT

VA-044 (30 mg, 1 x10^{-5} mmol) was dissolved in 2 mL of water and topped with dioxane up to the mark of the 10 mL volumetric flask to give VA-044 1x10^{-6}) in 60:40 dioxane / water.

PolyDMA$_{50}$macro-RAFT (500 mg, 0.0001 mmol) was added to 1 mL VA-044 stock solution in a test tube.

DMA (0.45 mL, 5.0 mmol) was added to the VA-044 and polyDMA macro-RAFT.

The reaction tube was purged with nitrogen and sealed with septa, left in oil bath at 70 °C for 2 h.

After 2 h the reaction was stopped by placing the test tube on ice.

The polymer was precipitated in Et2O, filtered, and dried at room temperature under vacuum for 24 h. Yield = 430 mg.
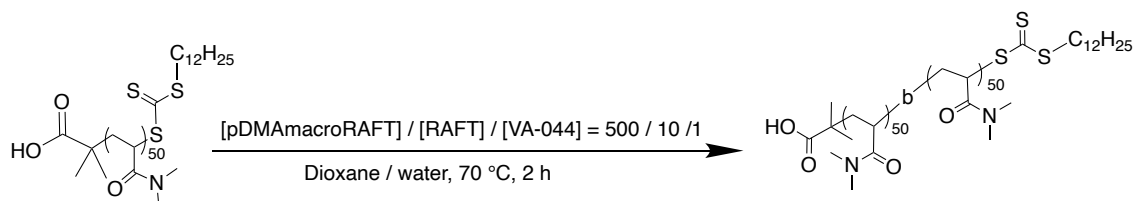
Scheme 4. 29 Polymerization of Poly N,N-Dimethylacrylamide (DMA)$_{50}$ macro-RAFT to Poly(N,N Dimethylacrylamide)$_{50-b-50}$.

4.17 Attempted RAFT preparation of Poly(N,N Dimethylacrylamide)$_{50-b-50-b-50}$ polymerization of Poly N,N-Dimethylacrylamide (DMA)$_{50}$-b-$_{50}$ macro-RAFT

VA-044 (30 mg, 0.083mmol) was dissolved in 2 mL of water and topped with dioxane up to the mark of the 10 mL volumetric flask to give VA-044 9.0 x10^{-3}) in 60:40 dioxane / water.

PolyDMA$_{50}$ macroRAFT$_{50-b50}$ (450 mg, 0.04 mmol) was added to 1 mL VA-044 stock solution in a test tube.

DMA (225 mg, 2.58 mmol) was added to the VA-044 and polyDMA macro-RAFT.

The reaction tube was purged with nitrogen and sealed, left in oil bath at 70 °C for 2 hours. After 2 h the reaction was stopped by placing the test tube on ice.

The polymer was precipitated in Et$_2$O, filtered, and dried at room temperature under vacuum for 24 h. Yield = 410 mg, 98 %.
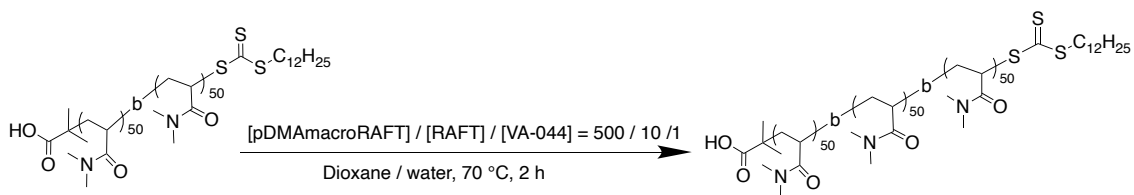
Scheme 4. 30 Attempted RAFT preparation of Poly(N,N Dimethylacrylamide)$_{50\text{-}b\text{-}50\text{-}b\text{-}50}$ polymerization of Poly N,N-Dimethylacrylamide (DMA)$_{50\text{-}b\text{-}50}$ macro-RAFT

Table 4.3 represents the results obtained by gravimetrical precipitation of polymer in cold diethyl ether (figure 4.4 MWD curve and figure 4.5 ^{1}HNMR)of (polymer 131), therefore the conversion of polyDMA macroRAFT is confirmed 98 % by weight, and the molecular weight for 50 blocks is 4574 gmol^{-1} by GPC with a polydispersity index PDI = 1.09 for 50 blocks (actual 42) blocks.

Polymer (87) table 4.6 is the chain extension of polyDMA macroRAFT from 50 blocks to 100 blocks (50-b-50) (figure 4.4 for GPC and 4.5 for NMR). This gives an average Mw of 12457 gmol-1 with a PDI =1.17, meaning that the molecular weight is nearly doubled, however the conversion by weight is slow (45 %).

Like the above polymer (90) table 4.7 is the chain extension of polyDMA macroRAFT from (50-b-50) to (50-b-50-b-50). This gives an average Mw of Mn = 9805 gmol^{-1} with a PDI =1.16 , meaning that the molecular weight is low but the conversion is 61 % which is visible with in the molecular weight distribution (MWDs) curve figure 4.4 with long tailing meaning dead chains.
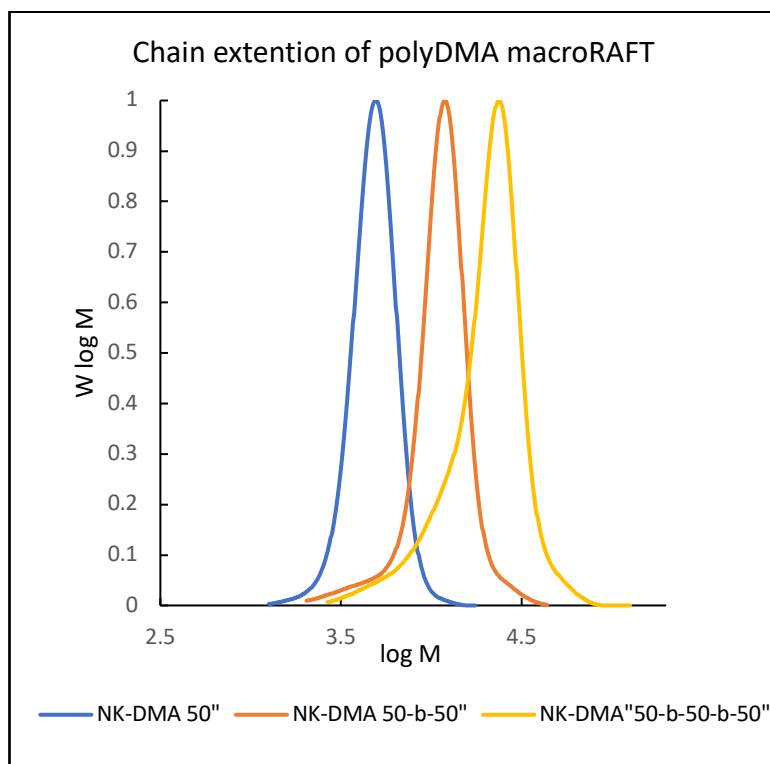
Figure 4. 4 MWDs curves of polyDMA macro-RAFT chain extension with 50 blocks in presence of VA-044 (blue line).
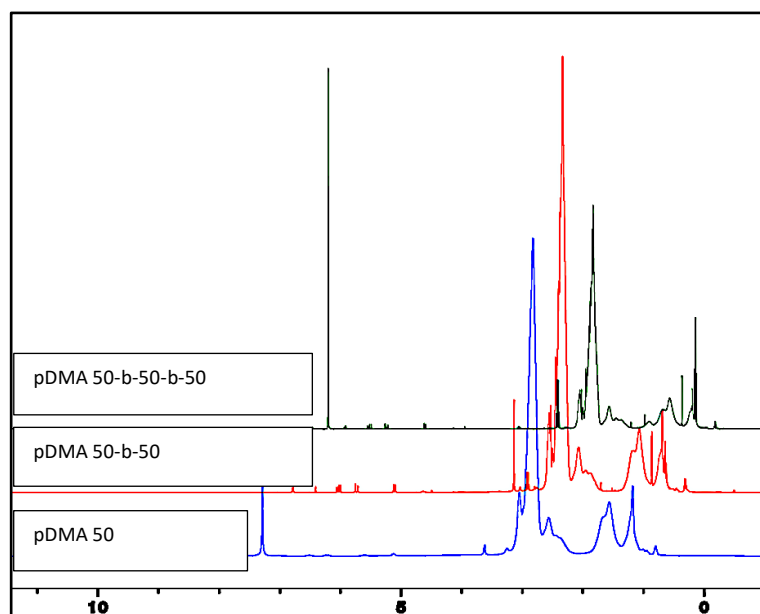
Figure 4. 5 ^{1}HNMR of polyDMA macro-RAFT. PolyDMA macro-RAFT chain extension with 50 blocks in presence of VA-044.

The blue line shows complete removal of vinyl peaks in the region of 4-5 ppm. However due to the low molecular weight tailing from GPC curve we see there are some vinyl peaks visible in red and black line for 100 and 150 blocks, respectively.

The results show (Table 4.6) that the molecular weight has increased from 50 blocks Mn = 4574 to 12457 with PD = 1.09 and 1.17 respectively, however for 150 blocks the Mn = 9850 and PDI = 1.16 which shows that the chains become shorter with higher degree of polymerisation.

Table 4. 6 Conversion result of pDMA macro-RAFT.

Entry	Polymer	Mass (g)	Conversion by weight %	Mn,th at 100 conversion	Mn by GPC	Mw/Mn	DP by GPC
131	50 blocks pDMA	2.18	98	5308	4574	1.09	42
87	50-b-50 pDMA	430	45	9304	12457	1.17	45
90	50-b-50-b-50 pDMA	410	61	13744	9850	1.16	47

4.18 RAFT polymerization of *N,N*-Dimethylacrylamide$_{100}$

Polymerisation polyDMA macroRAFT was carried out using 100 blocks.
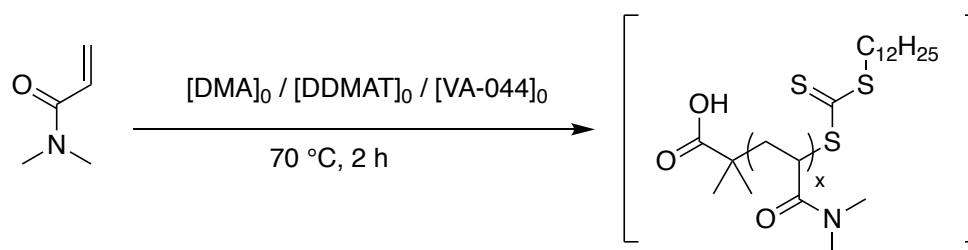
Scheme 4. 31 Attempt RAFT polymerization of N,N-Dimethylacrylamide to obtain polyDMA$_{100}$

MWDs curve shows (figure 4.6) that the calculated polyDMA macroRAFT for 100 blocks only gave 61 blocks, with Mw = 6444 g mol^{-1} and PDI = 1.13. Same condition gives living macroRAFT of polyDMA with a narrow polydispersity.

Attempt RAFT polymerization of *N,N-Dimethylacrylamide* to obtain polyDMA$_{100}$
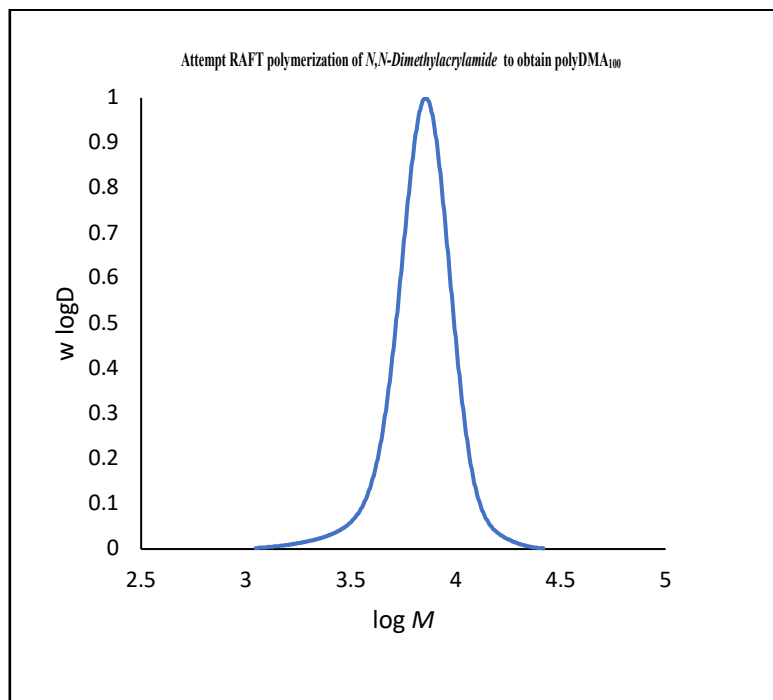
Figure 4. 6 MWDs curve of attempt RAFT polymerization of N,N-Dimethylacrylamide to obtain polyDMA$_{100}$

From Attempted 100 blocks of polyDMA macroRAFT 61 blocks was obtained but with a narrow PDI = 1.13 (Table 4.7) with 77 % conversion by gravity. However, MEDs curve (Figure 4.6) shows clean and narrow molecular weight.
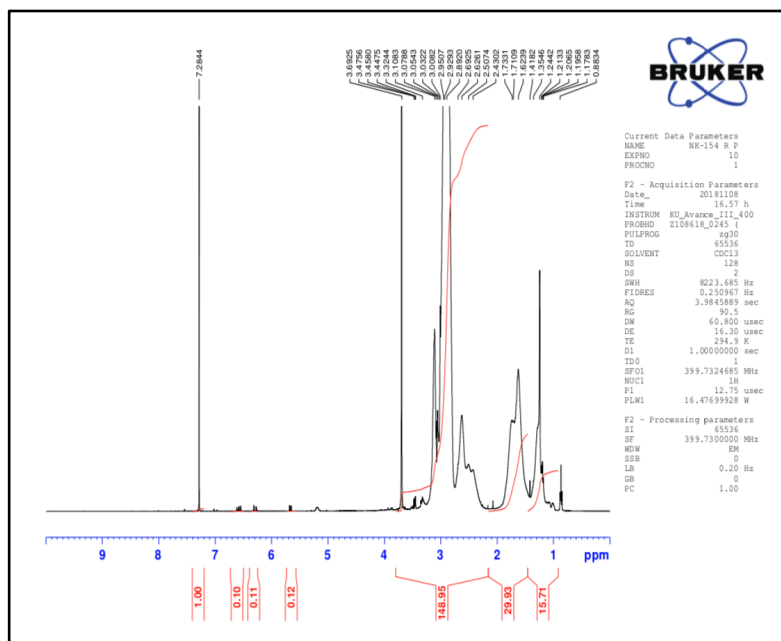
Figure 4. 7 ^{1}HNMR of attempt RAFT polymerization of N,N-Dimethylacrylamide to obtain polyDMA$_{100}$

From the results table 4.4 it is observed that higher numbers of blocks (100) only gives 61 blocks per GPC analaysis and NMR shows remaining vinyl peaks at 5.5 -7 ppm. In addition the conversion by gravity 77 % is in agreement with GPC results considering experimtal error.

Table 4. 7 GPC and NMR coversion results of RAFT polymerization of N,N-Dimethylacrylamide to obtain polyDMA$_{100}$

Polymer	Mass (g)	Conversion by weight %	$M_{n,th}$ at 100% conversion	$M_{n,th}$ by gravimetry	M_n by GPC	M_w/M_n	DP by GPC
154	2.9149	77	8424	6562	6444	1.13	61

4.19 Results discussion section 2

DMA macro-RAFT was successfully reproduced followed existing literature and chain extended in polyDMA macro-RAFT$_{50-b-50}$ and polyDMA macro-RAFT $_{50-b-50-b-50}$ blocks, a copolymer of polyDMA containing three blocks of 50. The MWDs curves of the polyDMA macro RFT block copolymer show that chain extensions were successfully achieved. However, the optimization of their block would be beneficial to reduce the dead chain and side reactions by reducing blocks of polymer.

The critical factor in one pot polymerization and chain extension is to select conditions that such high polymerization rate is achieved despite the low initiator concentration, in arrangement with high RAFT agent concentration. In the literature (Per B. Zetterlund, 2014a), experimental work showed that the livingness can decrease considerably at high conversion, but this is not the case. However, shorter blocks of chain extension can be achieved fully. Due to side reaction, the MWDs of the third block become broader, and to reduce the side reaction, the literature suggests extension of shorter chains of polymer. In RAFT polymerization, the RAFT agent is not taking part in the side reactions, which is calculated from the livingness of the polymer. Consequently, we have also attempted to make 100 blocks of polyDMA macroRAFT to observed this. When boronic acid is added as second block there will be blocks of hydrophilic and hydrophobic chains which can form micelles.

Section 3 of chapter 4

This section looks at the optimisation of radical initiator concentration for polymerisation of 4-ACPBAPE via RAFT Using VA-044. VA-044 is water-soluble initiator the ideal condition would be to use the same condition of DMA macroRAFT (dioxane water 80:20) which dissolves VA-044. Attempts are made to use this condition and polymerise N-(3-(4,4,5,5-tetramethyl-1,3,2-dioxaborolan-2-yl)phenyl)acrylamide pinacol ester using Poly(DMA)macro RAFT$_{50}$. Besides, attempts have been made to chain extend the boronic acid monomer with 50 and 100 blocks and RAFT polymerisation of N-(4-(4,4,5,5-tetramethyl-1,3,2-dioxaborolan-2-yl) phenyl) acrylamide pinacol ester with PolyDMA macroRAFT$_{28}$.

4.20 Optimization of radical initiator concentration for polymerization of 4-ACPBAPE via RAFT Using VA-044

4.20.1 Attempted RAFT polymerization of N-(4-(4,4,5,5-tetramethyl-1,3,2-dioxaborolan-2-yl)phenyl)acrylamide pinacol ester

Reaction of 4-ACPBAPE was carried out using VA-044 an attempt was made for RAFT reaction of 4-ACPBAPE, this reaction was carried out using VA-044 and dioxane water added to VA044 (36.50, 0.0045 mmol) solution.
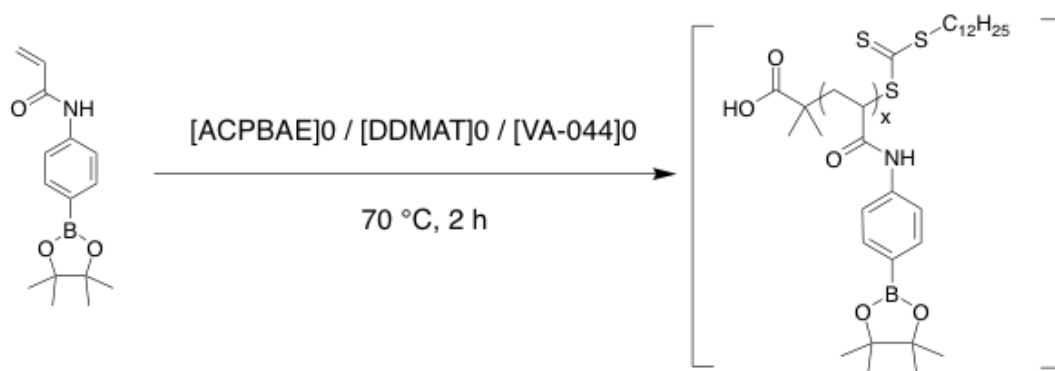
Scheme 4. 32 RAFT polymerization of N-(4-(4,4,5,5-tetramethyl-1,3,2-dioxaborolan-2-yl)phenyl)acrylamide pinacol ester.

VA-044 was dissolved in dioxane: water (25mL, 8:2) and was added to DDMAT (RAFT) (0.0302 mmol) and 4-ACPBAPE (400 mg, 1.46 mmol) was added to 1mL VA-044 stock solution at 70 °C for 2 h, the sample was fully in solution. The reaction carried out in 1 mL using 80:20 dioxane / water at 70 °C for 2 h, Solubility of 4-APBAPE (40 mg / 0.1 mL) in dioxane water (80:20). The polymerization is carried out in the presence of water-soluble initiator VA-044 in dioxane and water (80 :20). The MWDs curves figure 4.8 shows that the RAFT polymer is not formed and the PDI =2.90 is very broad. In addition, the Mw by GPC in solution is 30926 gmol-1 and after precipitation it is around 20040 gmol-1 probable short chains are removed during precipitation. This shows a unsuccessful RAFT attempt of formation of macroRAFT for 4-ACPBAPE (Table 4.9).
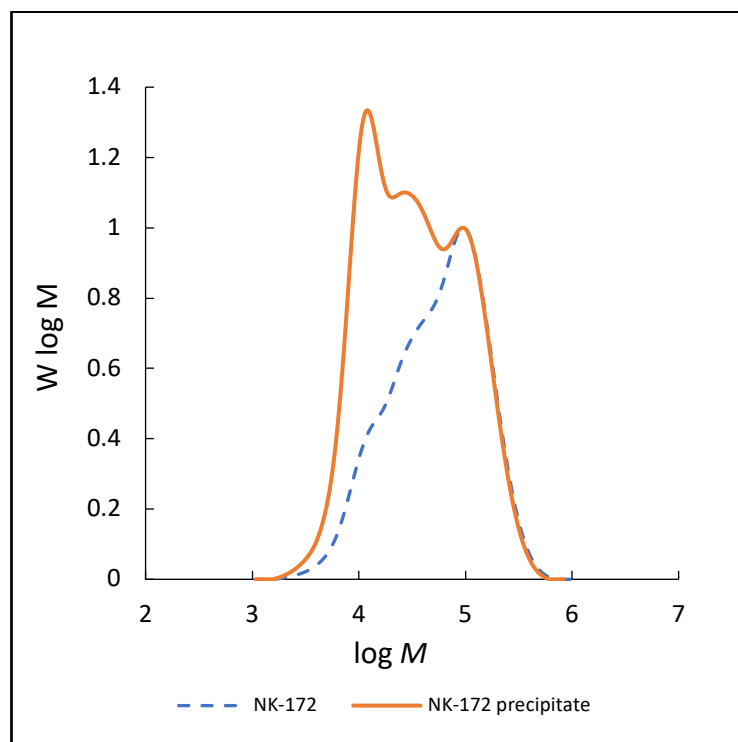
Figure 4. 8 MWDs curves of RAFT polymerization of N-(4-(4,4,5,5-tetramethyl-1,3,2-dioxaborolan-2-yl)phenyl)acrylamide pinacol ester (dashed blue line in solution) and (red solid) line precipitated.

Conversion was measured by ^{1}HNMR (DMSO) (Figure 4.0) comparing the integral of 1H of monomer with the integral of 1H of polymer at δ = 1.07 − 1.28 ppm for (19 Hydrogens)) by deducting (20 Hydrogens) of monomer using the integral of vinyl peak at δ = 5.55 ppm for (1 Hydrogen).
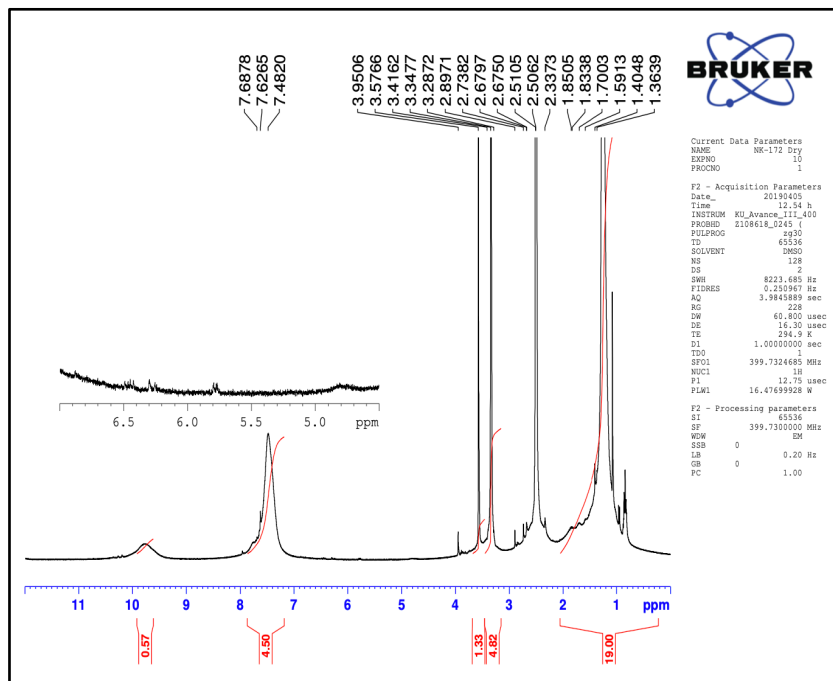
Figure 4. 9 ^{1}HNMR of poly (4-amino ACPBAE) = 98 % conversion.

Table 4. 8 GPC results of poly (4-ACPBAE) in polymer reaction solution and once precipitated shows a much high molecular weight than predicated, clearly a conventional reaction at this particular condition.

Polymer ID	Mass (mg)	Conversion by weight %	Mn, th at 100% conversion	Mn by GP C	Mw/ Mn	DP by GPC
172-in solution	-	-	13627	30926	11.65	113
172 dry	1.009	-	13627	20040	2.90	55

The polymer was precipitated in the reaction solution therefore, we decided to change the solvent and type of initiator. Initially then optimise a macro-RAFT of 4-ACPBAPE and then chain extend with water soluble DMA.

4.21 RAFT polymerization of N-(3-(4,4,5,5-tetramethyl-1,3,2-dioxaborolan-2-yl)phenyl)acrylamide pinacol ester using Poly(DMA)macro-RAFT$_{50}$

VA-044 (30 mg was dissolved in 100 mL, and 1 mL reaction using 80:20 dioxane: water was added to polyDMA macro-RAFT (478.97 mg 4784 mmol) and 3-ACPBAPE (136.58 mg, 0.45 mmol) was added to 1mL VA-044 stock solution at 70 °C for 2 h, the sample was fully in solution (Scheme 4.33).
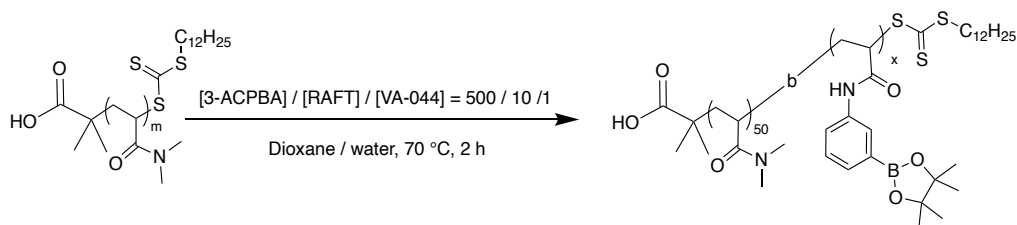
Scheme 4. 33 RAFT polymerization of N-(3-(4,4,5,5-tetramethyl-1,3,2-dioxaborolan-2-yl)phenyl)acrylamide pinacol ester using Poly(DMA)macro-RAFT50

The result did not come as expected and the polymer molecular was much higher than predicted. PolyDMA macroRAFT (Mn = 4783 gmol^{-1}) is chain extended with 3-ACPBAPE (scheme 4.33). The MWDs of polymer 103 (table 4.9) shows (green solid line) that the polymer has grown separately and not extended with polyDMA macroRAFT. This is maximum point (MP) of polymer is (Mp= 21061 gmol^{-1}) and the degree of Polymerization indicates that the polymer has turned out to be conventional. The Mn value by GPC is higher than predicted value (Mn,*th* at 100 %). Maximum average molecular weight (MP) is (21061 g mol^{-1}) the degree of Polymerization indicates that the polymer has turned out to be conventional.
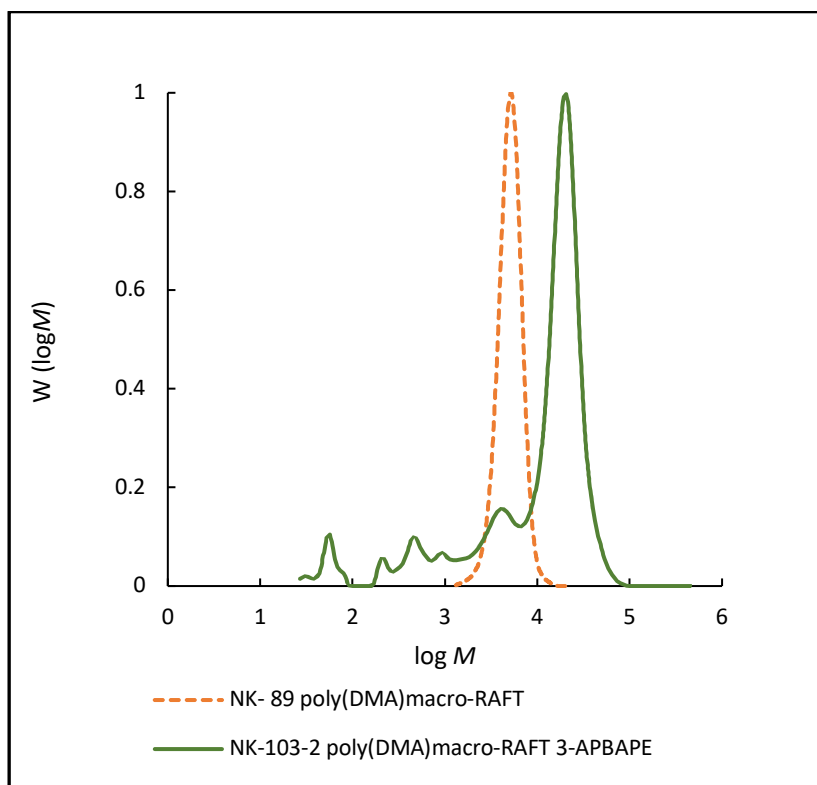
Figure 4. 10 Attempts to chain extend poly(DMA)macro-RAFT47 (red dashed line) with 3-aminophenylboronic acid pinacol ester at 70 °C for 2 hours using (80/20) dioxane / water, (green solid line).

MP is (21061 g mol^{-1}) the degree of Polymerization indicates that the polymer has turned out conventional.

Table 4. 9 GPC and ^{1}HNMR result of chain extend poly(DMA)macro-RAFT$_{47}$ with 3-aminophenylboronic acid pinacol ester at 70 °C for 2 hours using (80/20) dioxane / water and VA-044.

Entry	Polymer	Mass (mg)	Conversion by weight %	Mn, th at 100% conversion	Mn by GPC	Mw/Mn	DP by GPC
89	pDMA	1840	81	5091	4783	1.09	47
103	3-ACPBAPE	140	75	18166	19827	1.11	55

4.22 Attempts to chain extend poly (DMA)macro-RAFT$_{47}$ with 4-aminophenylboronic acid pinacol ester $_{(100)}$

4.22.1 RAFT polymerization of N-(4-(4,4,5,5-tetramethyl-1,3,2-dioxaborolan-2 yl) phenyl) acrylamide pinacol ester using Poly(DMA)macro-RAFT

Attempt was made to synthesis the block copolymer of 4-ACPBAPE using VA-044, with reduced concentration in order to achieve more living polymer. VA-044 (11.18 mg, 0.0345 mmol was dissolved in 100 mL, and 10 mL reaction using 80:20 dioxane: water was added to polyDMA macro-RAFT (175.73 mg 0.041 mmol) and 4-ACPBAPE (1000 mg, 3.66 mmol) was added to 10 mL VA-044 stock solution at 70 °C for 2 h, the sample was fully in solution.
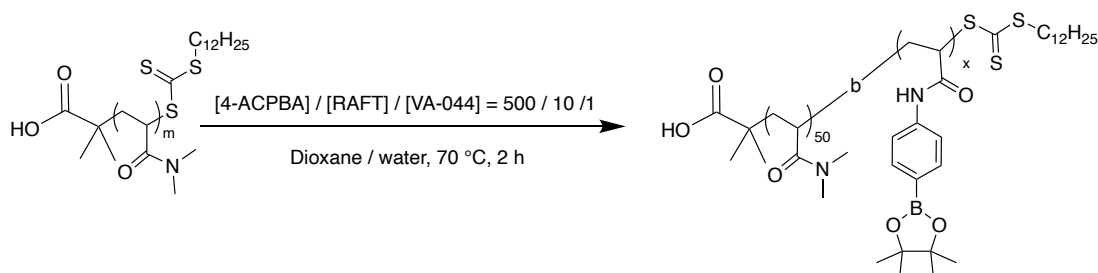
Scheme 4. 34 Reaction of polyDMA macroRAFT with 4-ACPBAPE in presence of Dioxane: water 80 :20 at 70° C for 2 h.
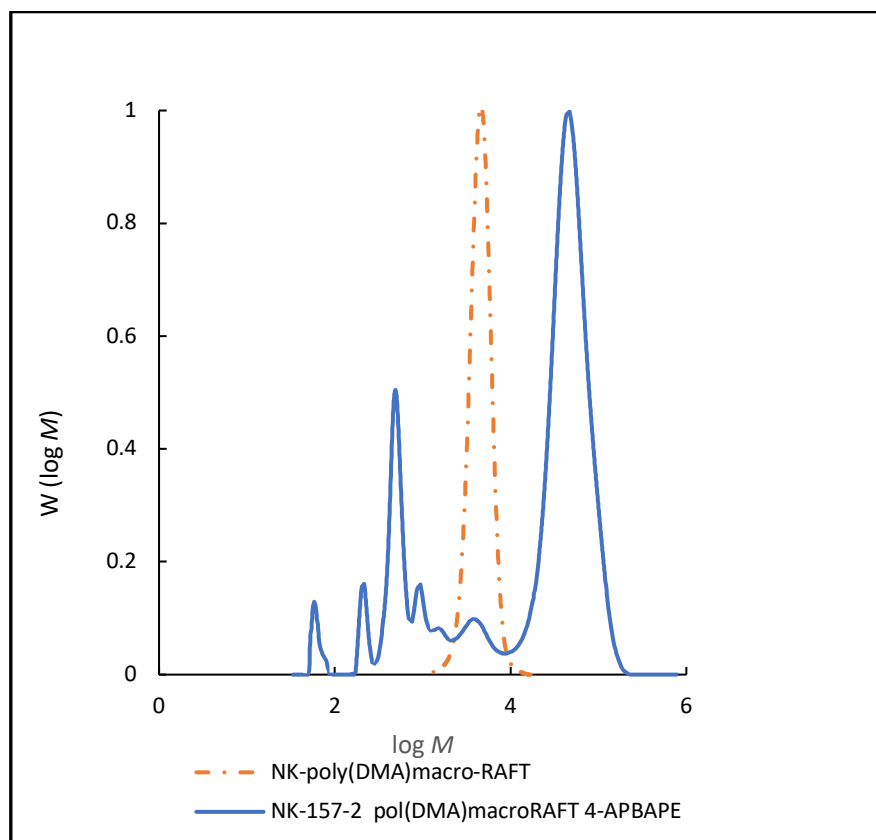
Figure 4. 11 Attempts to chain extend poly(DMA)macro-RAFT$_{42}$ (red dashed line) with 4-aminophenylboronic acid pinacol ester at 70 °C for 2 hours using (80/20) dioxane / water, (blue solid line).

The reaction undergoes conventional polymerisation as the maximum point (MP) (47208 g mol^{-1}), GPC /SEC shows only small fraction overlaps the polyDMA macroRAFT. The GPC MWDs shows that the polymerisation proceeded independently resulting in a conventional polymer giving double the calculated molecular weight.

When the polymer precipitated from the two different solvents it become clear of impurities and showed a conventional polymerisation. The extended polymer was precipitated in diethyl ether which give the red dashed line and in water which give green solid line.
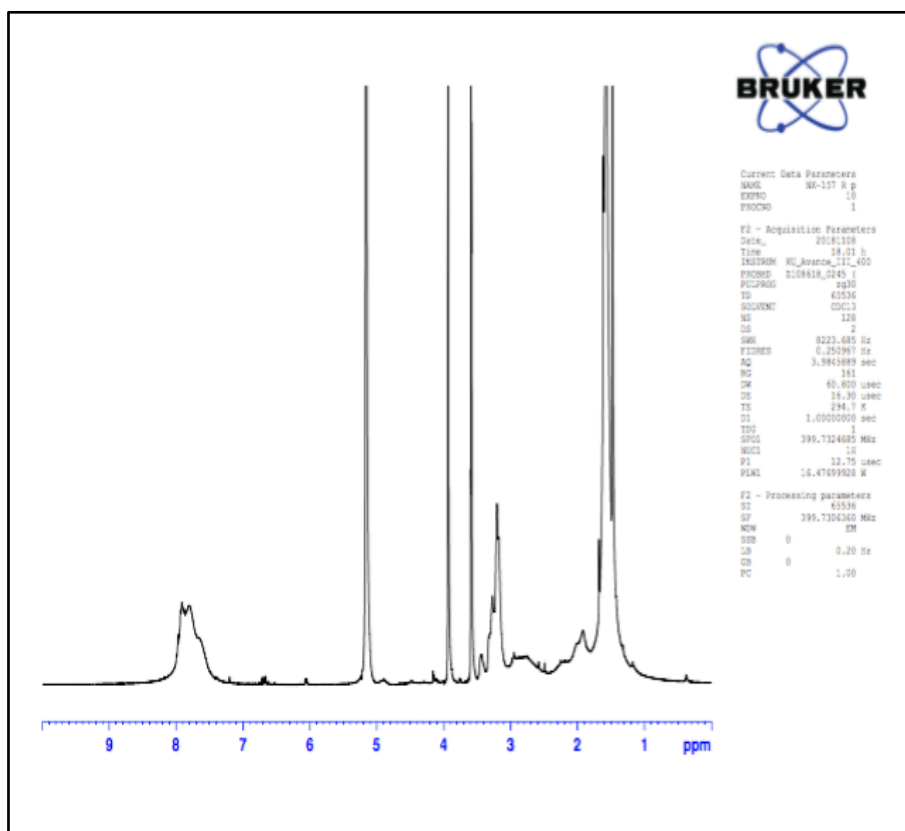
Figure 4. 12 ^{1}HNMR spectra of attempts to chain extend poly(DMA)macro-RAFT$_{42}$ with 4-aminophenylboronic acid pinacol ester at 70 °C for 2 hours using (80/20) dioxane / water, and VA-044. (from 1-3.5 ppm polyDMA with the polyphynylbornic acid where the vinyl bonds show that they are disapred).

Table 4. 10 NMR and GPC result of spectra of attempts to chain extend (157) poly(DMA)macro-RAFT$_{42}$ (97)with 4-aminophenylboronic acid pinacol ester at 70 °C for 2 hours using (80/20) dioxane / water, and VA-044.

Polymer ID	Polymer	Mass (mg)	Conversion by weight %	*Mn,th* at 100% conversion	Mn by GPC	Mw/Mn	DP by GPC
97	pDMA	20	91	5276	4295	1.09	42
157	4-ACPBAPE	-	-	28738	44382	1.24	147

The above results (figure 4.13) show that the polymer did not extend with pDMA macroRAFT and extended individually. This requires further attempts in order to find the best ratio of component to achieve a living polymer
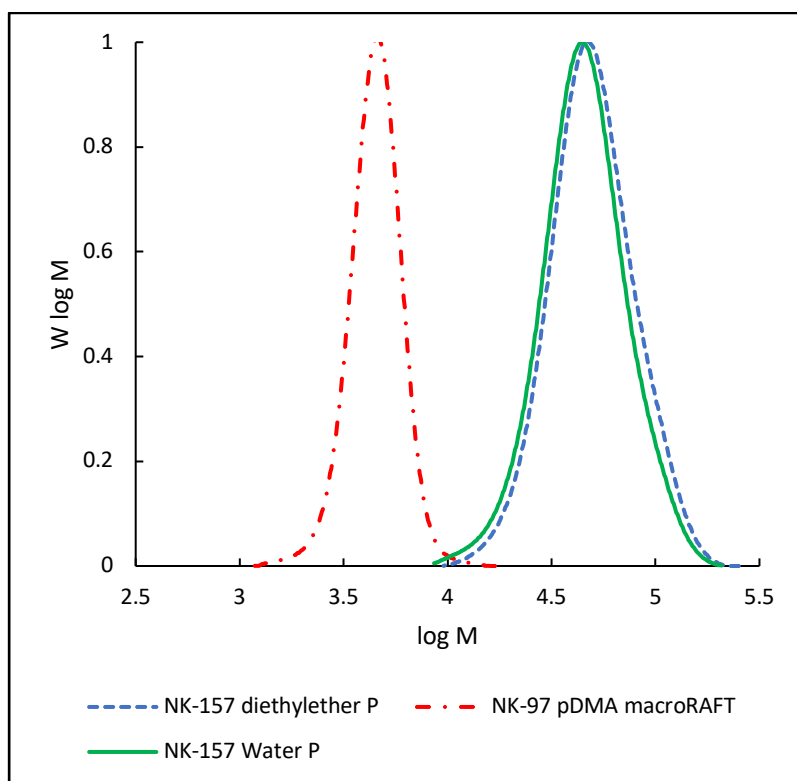
Figure 4. 13 Attempts to chain extend poly(DMA)macro-RAFT$_{42}$ (red dashed line) with 4-aminophenylboronic acid pinacol ester at 70 °C for 2 hours using (80/20) dioxane / water, and VA-044, (blue dashed line, and green solid line).

The GPC results (table 4.11) of polymer precipitated in diethyl ether and also in water shows a much high molecular weight than predicted values, which is clear indication of the fact that the polymer is conventional (Mw = 60609 gmol^{-1}) after precipitation in diethyl ether and water. In other words, the monomer is undergone polymerization individually without attaching to macroRAFT.

Table 4. 11 A comparison of GPC MWDs result to theoretical results shows clearly that the polymerization is conventional, and RAFT has not occurred.

Polymer ID	M, nth at 100% conversion	Mn by GPC	Conversion by GPC %	DP by GPC
PolyDMA-157 Diethyl-ether	28738	66192	Conventional	1.24

PolyDMA-157 Water	28738	60609	1.25

4.23 RAFT polymerization of N-(4-(4,4,5,5-tetramethyl-1,3,2-dioxaborolan-2-yl) phenyl) acrylamide pinacol ester with PolyDMA macroRAFT$_{28}$

Water soluble polyDMA macro-RAFT$_{171}$ (144.40 mg, 0.045 mmol, VA-044 (36.80 mg, 4.5 x10^{-3} mmol) was dissolved in 2 mL of water and topped with dioxane up to the mark of the 10 mL volumetric flask) in 80:20 dioxane / water.

4-ACPBAPE (400.80 mg, 1.46mmol) was added to 1.0 mL VA-044 stock solution in a test tube. The reaction tube was purged with nitrogen and sealed, left in oil bath at 70 °C for 2 h.

After 2 h the reaction was stopped by placing the test tube on ice.

The polymer was precipitated in cold hexane, filtered and dried at room temperature under vacuum for 24 h. Yield = 500.0 mg.

The GPC traces (figure 4.14) of RAFT polymerization of PolyDMA macroRAFT, N-(4-(4,4,5,5-tetramethyl-1,3,2-dioxaborolan-2-yl) phenyl) acrylamide pinacol ester with PolyDMA macroRAFT and 4-APBAPE, shows that the polymerization.
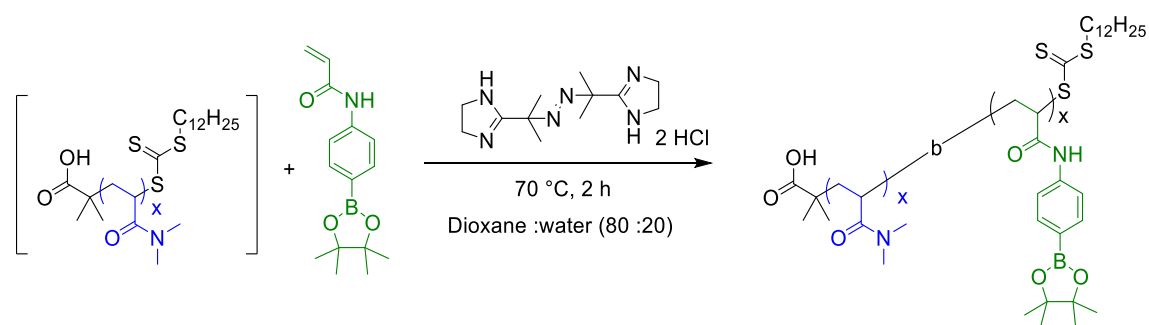
Scheme 4. 35 RAFT polymerization of N-(4-(4,4,5,5-tetramethyl-1,3,2-dioxaborolan-2-yl) phenyl) acrylamide pinacol ester with PolyDMA macroRAFT$_{28}$
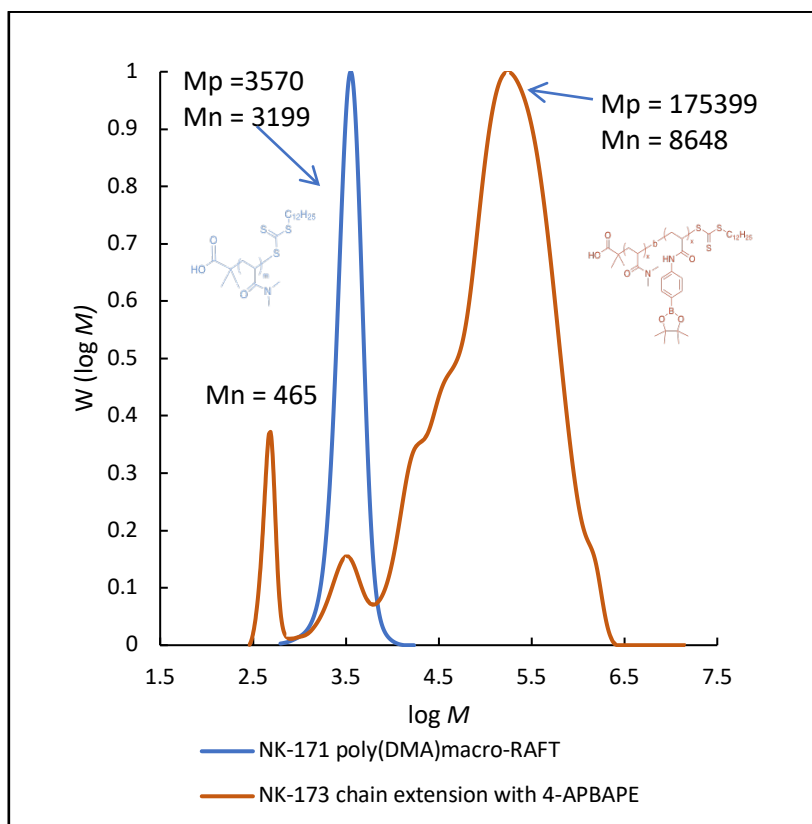
Figure 4. 14 Attempts to chain extend poly(DMA)macro-RAFT$_{28}$ (blue solid line) with 4-aminophenylboronic acid pinacol ester at 70 °C for 2 hours in 80: 20 dioxane / water, (red solid line).

The GPC MWDs curves for polyDMA macroRAFT (171) and attempted chain extension shows that the phenylboronic acid monomer polymerized individually and chain extension was unsuccessful.
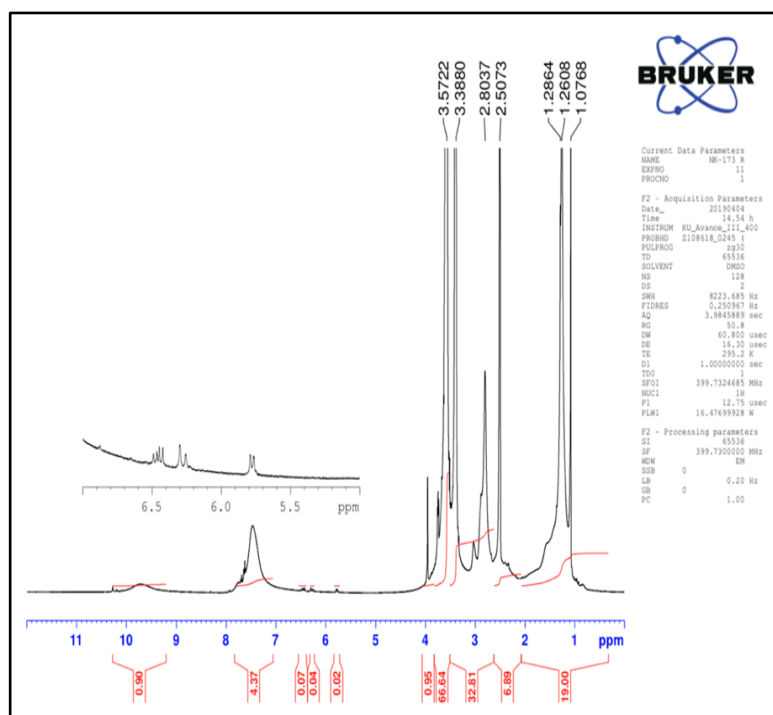
Figure 4. 15 ^{1}HNMR of attempts to chain extend poly(DMA)macro-RAFT$_{28}$ with 4-aminophenylboronic acid pinacol ester at 70 °C for 2 hours in 80/20 dioxane / water.

Table 4. 12 ^{1}HNMR and GPC results of chain extend poly(DMA)macro-RAFT$_{28}$ with 4-aminophenylboronic acid pinacol ester at 70 °C for 2 hours in 80 : 20, dioxane : water.

Polymer ID	Mass (g)	Conversion by weight %	M, *nth* at 100% conversion	Mn by gravimetry	Mn by GPC	Mw/Mn	Conversion by GPC%	DP by GPC
pDMA171	2.229	95	5205	4963	3177	1.13	64	28
pDMA$_{171}$-b-4-ACPBAPE$_{173}$	-	-	12074	-	8648	-	-	-

4.24 Discussion

The low molecular weight peaks of sample 171 (blue solid line) and 173 (red solid line) (figure 4.14) indicate that there is an inhibition of the time of polymerization when the conversion is supposed to be driven by RAFT or radical initiator (VA-044) (table 4.12), Mn by GPC = 8648 gmol^{-1}.

The inhibition is caused by the low concentration propagating radical and building up intermediate radicals from the monomer (4-APBAPE), which then produces conventional radical polymerization.

The activity of the RAFT group plays an essential role in controlling the polymerization process. RAFT agent (DDMAT sample 172) might be unable to form stable radicals of monomer / RAFT combination, therefore larger polyDMA macroRAFT may solve this polymer formation.

From the reaction procedure, there are no solubility problems and it shows a high conversion. For an ideal block of RAFT copolymer, the reaction must be stopped at intermediate conversion to preserve the polymer's livingness.

This can be done by: Running a conventional polymerization reaction of the same concentration of monomer and initiator to minimize initiator derived chains, analyze by GPC.

Run a sample for GPC at the start of the RAFT reaction, remove aliquots of the sample from the reaction tube via syringe in specific time intervals, and dilute them for GPC analysis. Due to the polymer's high conversion and viscosity, it might be useful to carry out the same reaction (diluted) using 2 or 3 mL of solvent instead of a 1 mL reaction.

Section 4 of chapter 4

Monomer solubility and addition of acid to the reaction media to prevent the degradation of the RAFT agent. In this section the experiments evaluated RAFT polymerization of N-(4-(4,4,5,5-tetramethyl-1,3,2-dioxaborolan-2-yl) phenyl) acrylamide pinacol ester with PolyDMA macroRAFT in presence of 1.15 equivalent HCl in 80/20 dioxane / water and HCl (3.28 M, 1.15 eq. HCl: Monomer).

4.25 Attempts to improve livingness of the polymer using acid

To improve the livingness of polymerization were carried out with RAFT polymerization of acrylamide monomer by addition acid into reaction solution in order to prevent the degradation of thiocarbonate end group.

The degradation mechanism shows the RAFT end group eliminating due to nucleophilic reaction of N group of terminal acrylamides (Scheme 4.36).
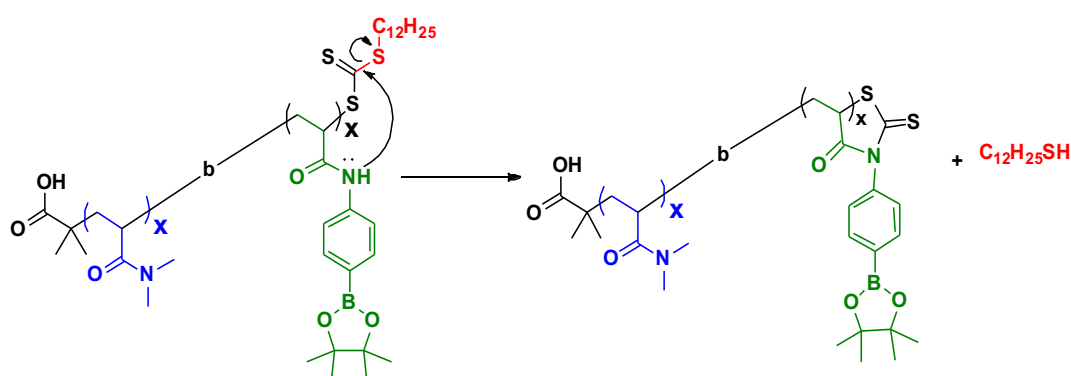
Scheme 4. 36 Proposed degradation mechanism of thiocarbonate end group, the terminal acrylamide group undergo nucleophilic attack on the thiocarbonate end-group.

Further attempts were made to improve the chain extension of 4-ACPBAPE, HCl 3.28 M was added to Dioxane and water which was 1 :1.15 equivalent to the 4-ACPBAPE. Dioxane and HCl ratio was 1:1 as the VA-044 was prepared in 25 mL stock solution of Dioxane: HCl (1:1).

RAFT polymerization of 4-ACPBAPE with PolyDMA macroRAFT in presence of 1.15 equivalent HCl in 80/20 dioxane / water and HCl (3.28 M, 1.15 eq. HCl: Monomer)

The reaction was carried out in 8:20 Dioxane: HCl as solvent, attempts to chain extend poly (DMA)macro-RAFT (blue solid line) with 4-aminophenylboronic acid pinacol ester at 70 °C for 2 hours in 80/20 dioxane / water and HCl (3.28 M, 1.15 eq. HCl: Monomer) (red solid line).

The GPC MWDs curves (figure 4.16) of extension shows similar profile as previous section 4. The GPC shows (red solid line) that the polymer is not attaching pDMA macroRAFT and grows individually. This means the addition of acid does not affect

the polymerisation. Polymer 182 (table 4.13) shows much lower Mw than expected at 100 %.

Table 4. 13 List of chemicals and ratios used in this reaction.

Chemical	mg	MW	mmol	Volume	Concentration	Ratio
VA-044	35.80	323.27	0.1107	4	0.0044	1
RAFT 170	144.00	3630	0.0397	4	0.0099	2.3
4-ACAPBAPE	408.10	273.15	1.4941	4	0.3735	85
4-ACPBAPE: HCl (1: 1.15)					3.28	1.15
4-ACPBAPE: HCl (1.4941: 1.6956)						
Dioxane: HCl (50 / 50)						
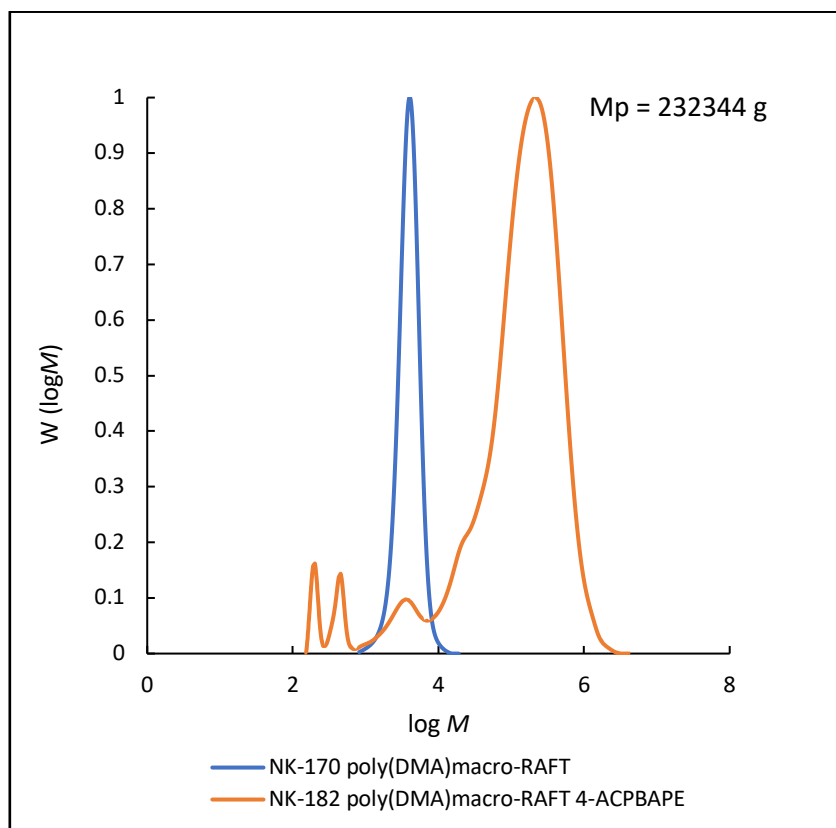
Figure 4. 16 Attempts to chain extend poly(DMA)macro-RAFT (blue solid line) with 4-aminophenylboronic acid pinacol ester at 70 °C for 2 hours in 80/20 dioxane / water and HCl (3.28 M, 1.15 eq. HCl: Monomer) (red solid line).

The result of polymerisation by GPC shows that there is no chain extension has occurred as the molecular weight did not increase as expected and the PDI is broad (Table 4.14).

From the theoretical calculation of Mn,th the polymer should have given a GPC value 14000 (Table 4.14), However the GPC Mn = 4353 with a broad PDI, which is also visible on MWDs curved (Figure 4.16) (orange solid line that the polymerisation chain extension was unsuccessful.

Table 4. 14 ^{1}HNMR and GPC results of attempts to chain extend poly(DMA)macro-RAFT (blue solid line) with 4-aminophenylboronic acid pinacol ester at 70 °C for 2 hours in 80/20 dioxane / water and HCl (3.28 M, 1.15 eq. HCl: Monomer) (red solid line).

Polymer	Mass (g)	Conversion by weight %	Mn,th at 100% conversion	Mn,th by gravimetry	Mn by GPC	Mw/Mn by GPC	Conversion by %	DP by GPC

pDMA171	2.229	95	5205	4963	3177	1.13	64	28
pDMA171-b-4-ACPBAPE182	-	-	13935	-	4353	56.01	-	-

4.26 RAFT polymerization of 4-ACPBAPE with PolyDMA macroRAFT$_{28}$ in presence of 1.15 equivalent HCl Dioxane: HCl (50 /50)
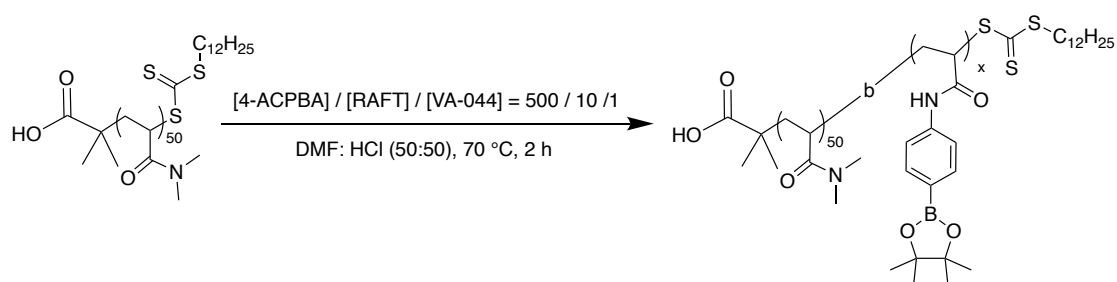
Scheme 4. 37 RAFT polymerization of 4-ACPBAPE with PolyDMA macroRAFT28 in presence of 1.15 equivalent HCl DMF: HCl (50 /50).

Attempts to chain extend poly(DMA)macro-RAFT with 4-acrylamide phenylboronic acid pinacol ester at 70 °C for 2 hours in 50/ 50 DMF /HCl (3.28 M, 1.15 eq. HCl: Monomer).

PolyDMA macroRAFT 50 block (144.6 mg, 0.0398 mmol), and VA-044 (36.70, 0.1135) added in 5 mL DMF / HCl, 50 /50, and the monomer 4-ACPBAPE (400 mg, 1.4644 mmol) at 70 °C for 2 hours, the reaction was stopped by placing the test-tube in ice.

Table 4. 15 Quantities used for the chain extension of poly(DMA)macroRAFT with 4-ACPBAPE in presence of hydrochloric acid.

Chemical NK-183	mg	Mw	mmol	Reaction volume	Concentration	Ratio
VA-044	36.70	323.27	0.1135	5	0.0045	1
RAFT 170	144.60	3630	0.0398	5	0.0079	2
4-ACPBAPE	400.00	273.15	1.4643	5	0.2928	65
4-ACPBAPE: HCl (1:1.15)						
DMF: HCl (50 /50)						

Attempts to chain extend poly(DMA)macro-RAFT (blue solid line) (figure 4.17) with 4-acrylamide phenylboronic acid pinacol ester at 70 °C for 2 hours in 50/50 DMF / water and HCl (3.28 M, 1.15 eq. HCl: Monomer) (red solid line).
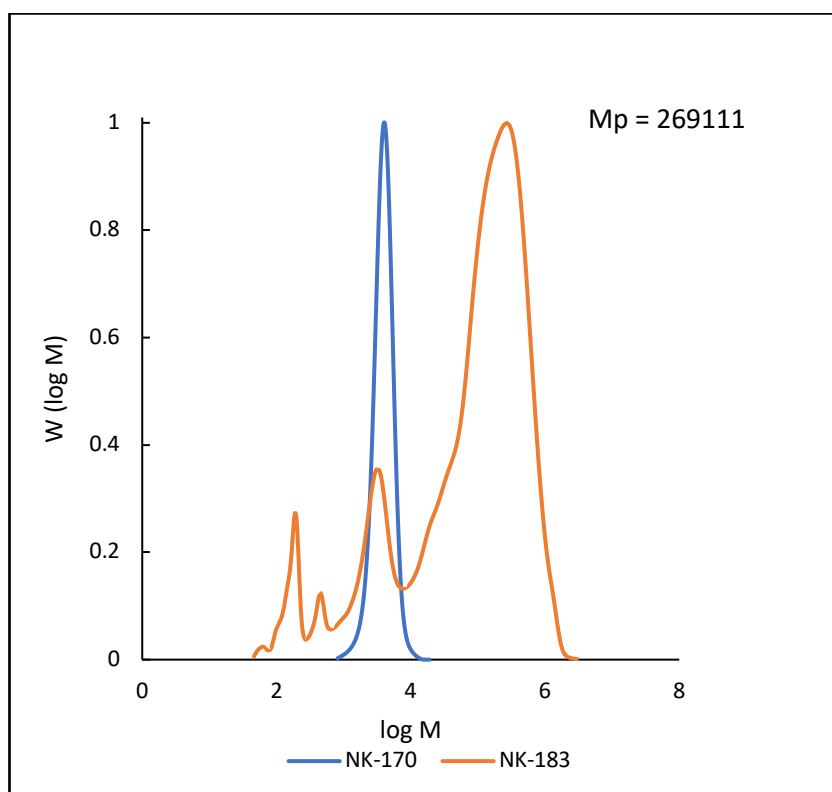
Figure 4. 17 Attempts to chain extend poly(DMA)macro-RAFT (blue solid line) with 4-aminophenylboronic acid pinacol ester at 70 °C for 2 hours in 50/50 DMF / water and HCl (3.28 M, 1.15 eq. HCl: Monomer) (red solid line).

MWDs (Figure 4.17) shows that polymer 183 is slightly improved by addition of acid which, however in all it shows a very high maximum peaks (MP), MP= 269111 which is showing that polymer 189 is proceeded in a conventional and the attachment of macroRAFT s failed.

Protecting the majority of propagating radicals and avoiding bimolecular termination through their reversible trapping in a dormant thiocarbonyl compound RAFT control is achieved. Reasonable stabilization of thiocarbonyl compounds and the radical's chemical nature affect the kinetics and thermodynamics of the addition and

fragmentation reaction. In RAFT polymerization, the oligomeric radicals formed in the early stages of the process can either initiate with the internal or inter molecular leaving group of RAFT end groups modify the reactions of attacking groups, and the main chain length comes from tertiary radicals (the most stable radical). The N group of acrylamides can deprotonate by the addition of acids, and the degradation of thiocarbonate end-group prevented. Acids can be HCl, benzoic acid, formic acid, or trifluoroacetic acid (TFA).
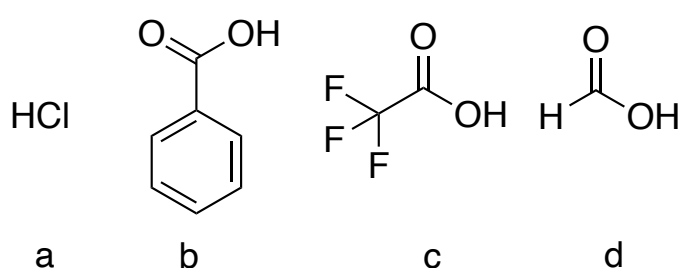
Scheme 4. 38 a) Hydrochloric acid, b) benzoic acid, c) trifluoroacetic acid (TFA), and d) formic acid, potential acids for improving the RAFT polymerization.

Addition of HCl improves the polymerisation. However, more efforts are required to avoid the precipitation of the polymer in solution. To observe this effect why the polymer precipitates, a RAFT polymerisation of 4-ACPBAPE was carried under similar condition.

Appearance of the sample in solution and after heating for 2 hours. The sample was not soluble in 1 mL of solvent, after 15 min the sample starts precipitating, and is not suitable for solution RAFT polymerization therefore DMF was considered instead of dioxane used previously (figure 4.17). The choice of RAFT agent depends on the monomer properties which is discussed in introduction.
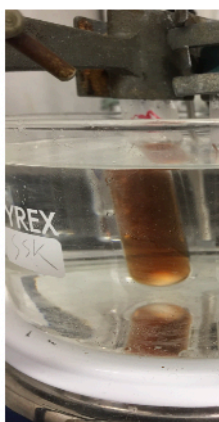
After adding solvent brown solution   After 15 min   After 30 min and up to 2 hours
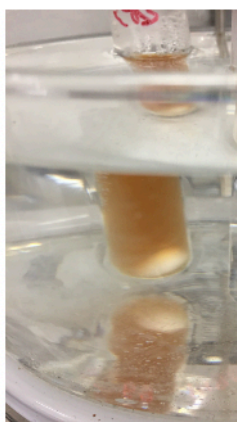
Figure 4. 18 Sample appearance after addition of solvent and heting in first 15 min and 30 min up to 2 hours 4-ACPBAPE over time in dioxane water (80 /20) using VA-044.

Observation of the reaction visually gave a clear idea that (Figure 4.17) the monomers precipitated after 15 min, and there was a solubility issue first which required full attention before using any organic soluble acid.

4.27 Discussion of section 4 results

Chain extension of poly DMA macro-RAFT with 4-ACPBAPE was attempted with radical polymerization. Optimization of the solubility, the chain extension, and degradation was checked with hydrochloric acid. However, due to the polymerization precipitation, this requires additional optimization, as the polymerization must run in fully solubilized components. It is essential to study the rate of polymerization in the RAFT agent's presence, the same as observed in the absence of the RAFT agent. Besides, observation should be carried out to find the optimum polymerization solution, so the polymer form should not precipitate or forms gel. Occasionally retardation can also relate to the R group of RAFT agents, the rate is reduced, but it is consistent with that expected in the absence of a gel effect. Various studies have investigated factors that may affect gelation by changing the primary chain length or

inter- vs. intramolecular reactions. The limitations comprise the monomer concentration $[M] \equiv [M_1] + [M_x]$, where $[M_1]$ denotes the strength of the monofunctional monomer and $[M_x]$ that of a crosslinker species with more than one polymerizable vinyl group; the amount of chain transfer agent (CTA). Various studies have investigated parameters that may affect gelation by changing the primary chain length or the level of inter- vs. intramolecular reactions (Yan, 2016) (Graeme Moad, 2003).

Section 5 of chapter 4

This is the RAFT polymerisation of 4-ACPBAPE using AIBN (solvent soluble) initiator in DMF due to the solubility of the monomer for optimisation of the synthesis of 4-APBAPE MacroRAFT.

Initially 3 different concentrations (high=0.0029 M, medium = 0.0015 M, low = 0.0007M) of AIBN were used.

The experiments were conducted using two different concentrations for a kinetic study at three different temperatures (90, 82, and 70 °C). For each of the AIBN concentration, the time vs conversion measurements were carried out using NMR. The outcome was the low concentration of AIBN would be used as optimised initiator concentration at 70 °C. in DMF. The optimised condition was carried out for conventional polymerisation of 4-ACPBAPE followed by RAFT. Both initiator concentrations AIBN (0.0029 M) (0.0015 M) were used in the presence of an internal standard. The low concentration of AIBN was not sufficient to start polymerisation. The first internal standard used was trioxane. However, it showed some interaction with the polymer components. Therefore, the internal standard was changed from trioxane to anisole where the methyl group was considered for a time vs conversion study.

4.28 Optimization of radical initiator concentration polymerization of 4-ACPBAPE using Anisole as internal standard

In this part of the project, we tried to optimize and calculate the monomer's conversion to the polymer after obtaining the monomer's limited livingness, adding to poly(DMA)macroRAFT. In this, the initiator was changed from VA-044 to AIBN due to the change in half-life. As half of AIBN is longer than VA-044. (Initiator efficacy was explained in the introduction of this chapter). The internal standard we chose was of 1,3,5-trioxane (0.13 mmol) in the reaction medium. The first observation was carried out to see the position of a trioxane peak in NMR in monomer presence.

Calculation of the (%) monomer conversion of 4-ACPBAPE by ^{1}HNMR and 1,3,5 trioxane as an internal standard

The remaining monomer vinyl peak has the chemical shift at δ = 5.76-5.79 ppm corresponding to the double bond. By comparing the integral area of their characteristic chemical shift, the monomer conversion can be calculated.

Conversion = I_M / 1 * $I_{(IS)}$ 6 /1* concentration of IS in the reaction medium (0.13 mmol)

% conversion = Mmol$_M$ and $_{IS}$ / mmol$_M$ * 100

1,3,5-Trioxane was added initially to the monomer to check the chemical shifts interaction of monomer and IS.

Figure 4. 19 ¹HNMR od 4-ACPBAPE Refer to monomer NMR.

Figure 4. 20 ¹HNMR od 4-ACPBAPE in presence of trioxane.

The monomer conversion of 4- ACPBAPE was obtained by adding the internal standard of 1,3,5-trioxane (0.13 mmol) in the reaction medium 2.6 mL DMF. A sample was taken by syringe in time intervals.

Trioxane (IS) has a single signal for 6 identical protons at δ = 5.11 - 5.17 ppm.

To understand better, the monomer conversion in presence of internal standard two different concentration of AIBN were used at 82 °C.

4.28.1 Conventional polymerization of N-(3-(4,4,5,5-tetramethyl-1,3,2-dioxaborolan-2-yl) phenyl) acrylamide pinacol ester at 82 °C

119.90 mg AIBN dissolved in DMF in 25 mL and diluted, 1 mL stock solution is added in 10 mL (250 times dilution). Trioxane 101.10 mg (1.122 mmol) as internal standard (IS) added to 10 mL flask (10 times dilution).
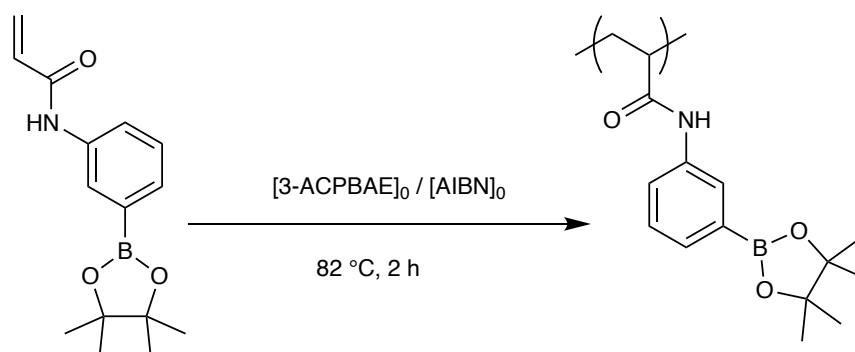
Scheme 4. 39 Conventional reaction of 3-ACPBAPE, for 2 h at 82 °C in DMF to optimize the condition for RAFT.
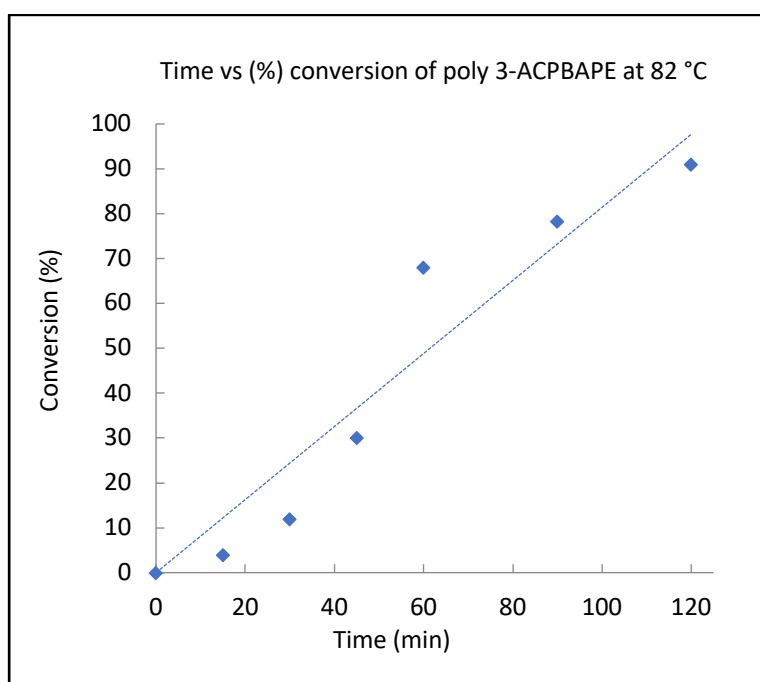
Figure 4. 21 monomer conversion (%)-time plot for the conventional polymerization of 3-ACPBAPE.

Polymerization conditions $[3\text{-ACPBAPE}]_0:[AIBN]_0= 345:1$, 82 °C. Monomer conversion up to 70 % at 82 °C in DMF is linear after that the conversion becomes slower (Figure 21). Samples taken at different times during the synthesis at 15, 30, 60, 90 and 120

min, and analysed by proton NMR (dots), straight dotted line, is the theoretical conversion vs time (figure 4.22) is the pseudo first order reaction.

Table 4. 16 Quantities used for the reaction carried out in DMF.

Entry 249	mg	MW	mmol	Volume (mL)	Concentration mmol / mL (M) in test-tube	Ratio
AIBN	119.90	164.21	0.7302	1a	0.0029	1
3-ACPBAE	273.30	273.15	1.0005	1	1.0005	345
Trioxane	101.10	90.08	1.1223	1c	0.1122	39
DMF at 82 °C						

Pseudo-first order kinetic plot of conventional polymerisation of 3-ACPBAPE at 82 °C

y-axis: $\ln[M_0]/[M]$
x-axis: Time (min)
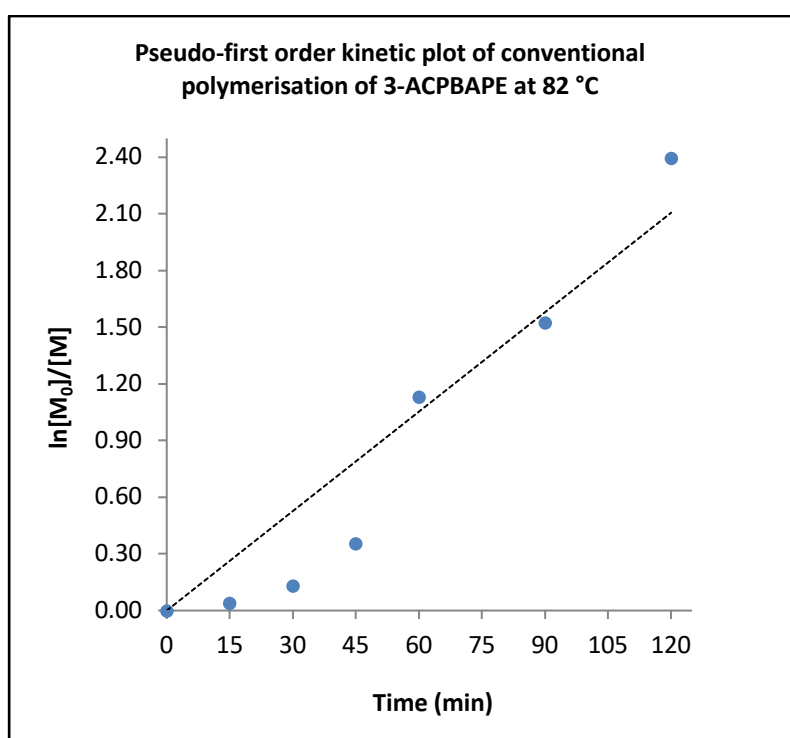
Figure 4. 22 Pseudo-first order kinetic plot of conventional polymerization of 3-ACPBAPE at 82 °C using high AIBN concentration.

Polymerization conditions [3-ACPBAPE]$_0$: [AIBN]$_0$= 345:1, 82 °C in DMF. Pseudo-first order kinetic plot is linear which is a good indication for adding RAFT agent to polymer to obtain macro-RAFT. Figure 4.22 shows that the MW conversion by NMR (dots) are not in line with theoretical Mw conversion (dotted theoretical line). This shows that

growing macroRAFT chain is slow up to 45 min and goes up at 60 min then plateaus as the macroRAFT chain stops growing.

GPC/SEC chromatograms (figure 4.23) of sample taken at different times during the synthesis of conventional polymerization at 15, 45, 60, 90 and 120 min. Polymerization conditions [3-ACPBAPE]0:[AIBN]0= 345:1, 82 °C in DMF. The polymerization results in high conversions of monomer which can be also proceeded with RAFT polymerization to obtain a macro-RAFT of 3-ACPBAPE. At 120 min the polymer shows a bimodal curve which shows three Mn (g mol^{-1}) values calculated from log M indicating high conversion of conventional polymerization.
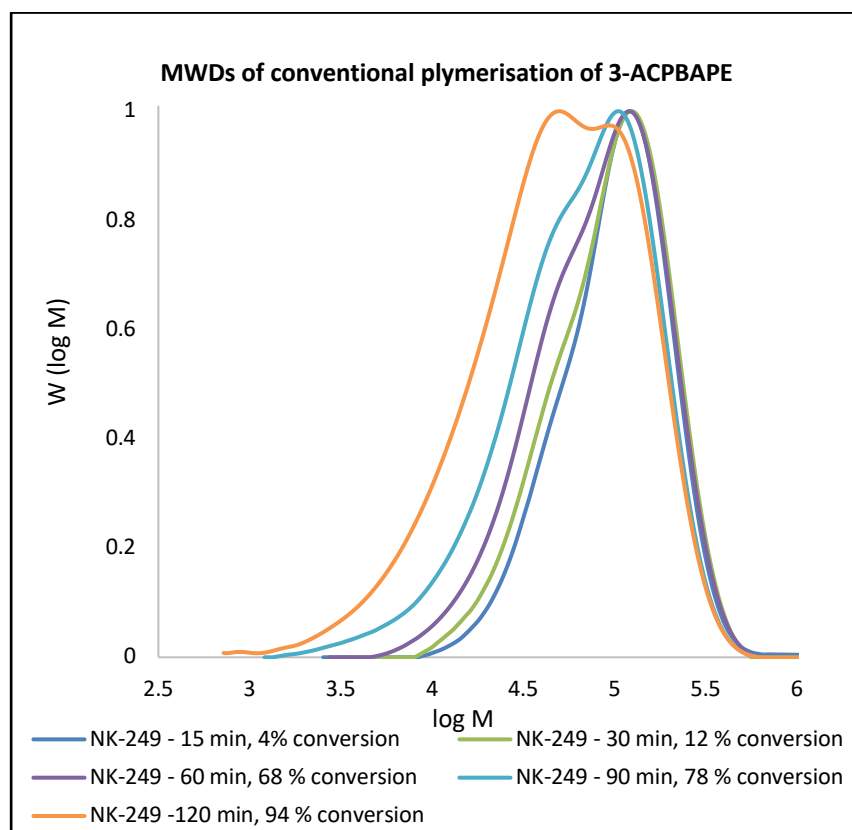
Figure 4. 23 Normalized MWDs plot for the conventional polymerization of 3-ACPBAPE.

MWDs of (figure 4.23) at 120 min conventional radical polymerization of *N*-(3-(4,4,5,5-tetramethyl-1,3,2-dioxaborolan-2-yl)phenyl)acrylamide pinacol ester for bimodal peak is evaluated for each peak from left to right is calculated separately as

peak a (Mn = 50119 g mol^{-1}), peaks b (Mn = 79433 g mol^{-1})and peak c (Mn = 125893 g mol^{-1}) respectively.
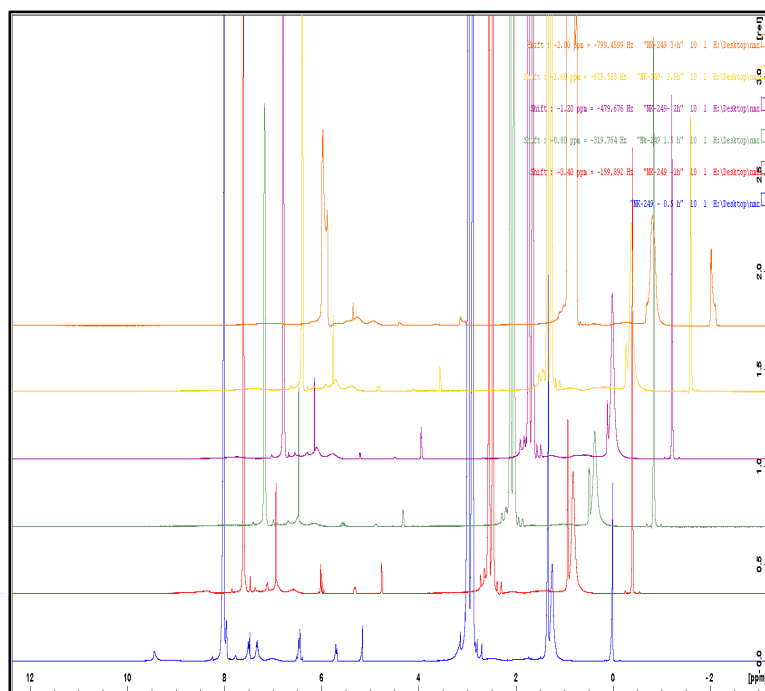
Figure 4. 24 ^{1}HNMR traces of the conventional radical polymerization of 1M N-(3-(4,4,5,5-tetramethyl-1,3,2-dioxaborolan-2-yl)phenyl)acrylamide pinacol ester at 82 °C using trioxane as internal standard and 0.0029 M AIBN in DMF. The specrum from bottom to top are the polymerisation fro m time 0 to 120 min.

The NMR shows disappearance of vinyl peaks at δ = 5.5 -5.7 ppm over time in CDCl$_3$ with reference to trioxane peak at δ = 5.1 ppm. GPC Mw (figure 4.23), PDI = 1.58 at 15 min and PDI = 3.00 at 2 (table 4.17) hours obtained by GPC analysis using 0.1 M LiBr in DMF as mobile phase at different time intervals. Indicates that the polymerisation is fast using (0.0029 M) AIBN. As the molecular weight increases drastically at 15 min (76350 gmol^{-1})

The NMR result are taken from integration value of vinyl peak to calculate the conversion of double bond. The spectra over time can also be removed.

Table 4. 17 ^{1}HNMR result of the conventional radical polymerization of 1M N-(3-(4,4,5,5-tetramethyl-1,3,2-dioxaborolan-2-yl)phenyl)acrylamide pinacol ester at 82 °C using trioxane as internal standard and 0.0029 M AIBN in DMF.

249 Polymer	Time (min) at 82 °C	Conversion Polymer by NMR %	Mn (g mol^{-1}) experimental by GPC	Mw/Mn
	15	4	76350	1.58
	30	12	69980	1.68
poly3-ACPBAPE	60	68	67300	1.87
	90	78	37350	2.38
	120	94	24500	3.00

4.28.2 Attempts to use AIBN (0.0029 M) and trioxane as an internal standard

RAFT polymerization of N-(3-(4,4,5,5-tetramethyl-1,3,2 dioxaborolan-2-yl) phenyl) acrylamide pinacol ester at 82 °C (50 block)

In order to study why the polymerisation undergoes conventional polymerisation and the RAFT agent we have increased the temperature to 82 °C and addition of trioxane as internal standard to calculate the conversion over time. AIBN (119.70 mg, 0.7289 mmol) dissolved in 25 mL of DMF and diluted 1 mL in 10 mL (250 times dilution). Trioxane (100.10 mg ,1.1112 mmol) as internal standard (IS) (10 times dilution) and DDMAT (75.00 mg, 0.0205 mmol) diluted 10 folds was added into 1 mL AIBN stock solution (0.0029 M) with monomer 3-ACPBAP (273.90, 1.0027 mmol).
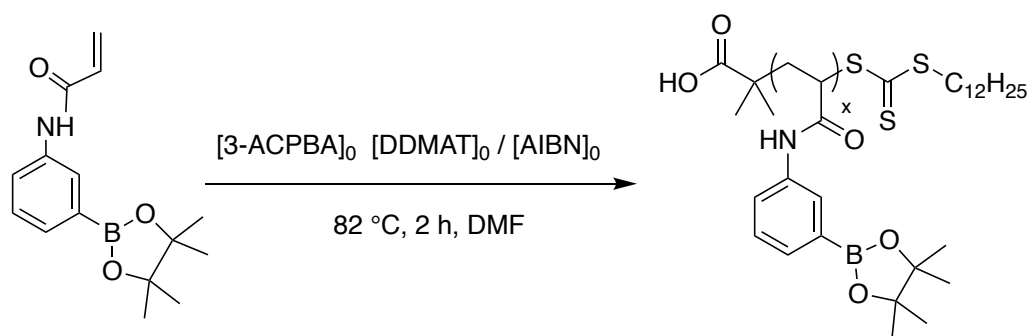
Scheme 4. 40 RAFT polymerization of N-(3-(4,4,5,5-tetramethyl-1,3,2-dioxaborolan-2-yl)phenyl)acrylamide pinacol ester at 82 °C (50 block).

Table 4. 18 Quantities used for RAFT polymerization of N-(3-(4,4,5,5-tetramethyl-1,3,2-dioxaborolan-2-yl)phenyl)acrylamide pinacol ester at 82 °C (50 block)

Chemical 251	mg	MW	Mmol	Volume (mL)	Concentration mmol / mL (M) in test-tube	Ratio
AIBN	119.70	164.21	0.7289	1a	0.0029	1
DDMAT	75.00	364.63	0.2057	1	0.0206	7
3-ACPBAE	273.90	273.15	1.0027	1	1.0027	346
Trioxane	100.10	90.08	1.1112	1c	0.1112	39

a diluted 250-fold, b diluted 10-fold, c diluted 10-fold
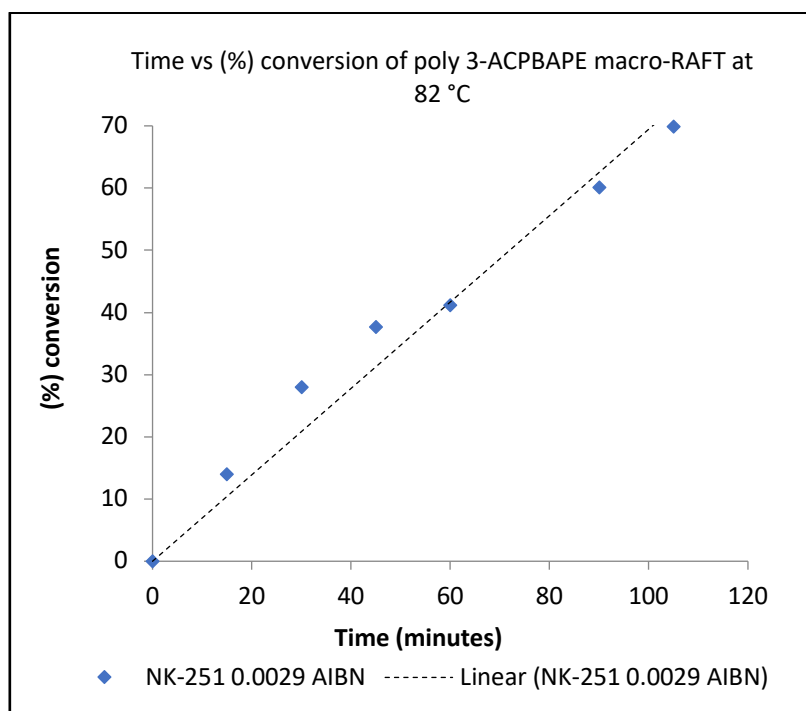
Figure 4. 25 Time vs (%) conversion of poly 3-ACPBAPE macro-RAFT at 82 °C

The monomer conversion (%) vs time plot for the RAFT polymerization of *N*-(3-(4,4,5,5-tetramethyl-1,3,2-dioxaborolan-2-yl) phenyl) acrylamide pinacol ester is fairly linear (blue dots) and in line with theoretical values (blue dotted line). Polymerization conditions were $[3\text{-ACPBAPE}]_0$: $[\text{DDMAT}]_0$: $[\text{AIBN}]_0 = 346: 7: 1$, 82 °C. This monomer conversion suggests that the conversion of monomer can be proceed 60 - 70 % using 0.0029 M AIBN at 60 min (figure 4.25).
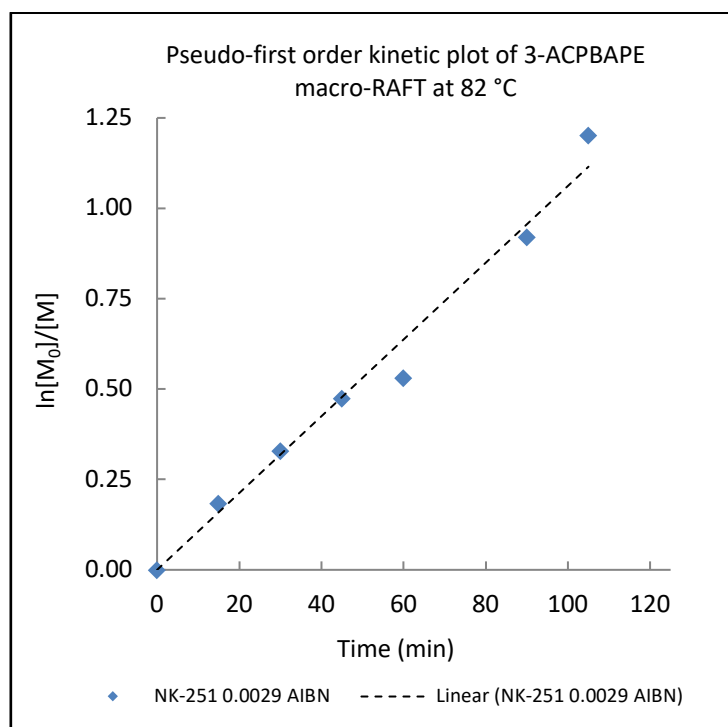
Figure 4. 26 Pseudo-first order kinetic plot of conventional polymerization of 3-ACPBAPE at 82 °C AIBN concentration (0.0029 M). Polymerization conditions [3-ACPBAPE]$_0$: [DDMAT]$_0$: [AIBN]$_0$= 346: 7: 1, 82 °C.

Pseudo-first order kinetic plot (figure 4.26) is linear after 60 min the conversion becomes slow and it indicated that if it is left longer dead chains or conventional polymerisation is happening, the livingness decreases.

Propagating constant is determined by rate initiation and termination in conventional radical polymerisation. Slow initiation suggests a decrease in Propagation because of termination reaction or side reaction.

Figure 4. 27 MWDs for polymerisation of for N-(3-(4,4,5,5-tetramethyl-1,3,2-dioxaborolan-2-yl) phenyl) acrylamide pinacol ester.

Where polymerization conditions $[\text{3-ACPBAPE}]_0$: $[\text{DDMAT}]_0$: $[\text{AIBN}]_0$ = 346: 7: 1, 82 °C. conversion of 14 % at 15 min, 27% at 30 min, 60% at 45 min and 70 % at one hour. The results (table 4.19) by GPC shows that the polymer polydispersity is PD = 1.14 and 24 % conversion by GPC it corelates with conversion by NMR = 14 % at 15 min, and at 1 hour the conversion by GPC reaches 50 % with a polydispersity PD = 1.25 which is broad for block co polymer.
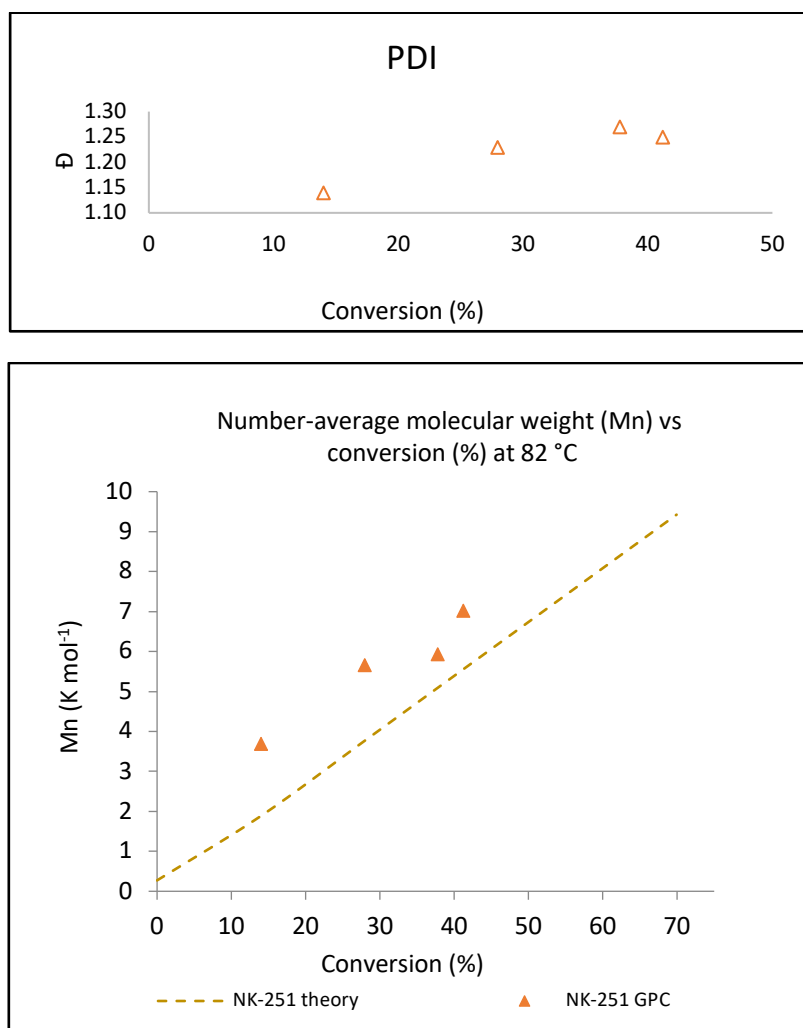
Figure 4. 28 Number-average molecular weight (Mn, K mol^{-1}) vs conversion (%) for N-(3-(4,4,5,5-tetramethyl-1,3,2-dioxaborolan-2-yl)phenyl)acrylamide pinacol ester

Macro-RAFT using DDMAT. Polymerization conditions [3-ACPBAPE]$_0$: [DDMAT]$_0$: [AIBN]$_0$= 346: 7: 1, (50 blocks) at 82 °C. The graph compares to predicted (Mn, g mol^{-1}) obtained from ^{1}HNMR conversion vs experimental data obtained by GPC (points, orange triangle). The open triangles show the PDI of the macro-RAFT vs conversion (%). Theoretical Mn is calculated as a product of M, nth and percent conversion using ^{1}HNMR.

^{1}HNMR and normalized GPC /SEC analysis of RAFT polymerization of *N*-(3-(4,4,5,5-tetramethyl-1,3,2-dioxaborolan-2-yl)phenyl)acrylamide pinacol ester at 82 °C using trioxane as internal standard and 0.0029 M AIBN in DMF after 15, 30, 45 and 60 min. The result shows a trend in conversion (%) and Mn (g mol^{-1}). ^{1}HNMR shows an

increase in conversion (%) from 14 % at 15 min to 70 % at 60 min. GPC/SEC shows a increase in Mn value and low PD over time.
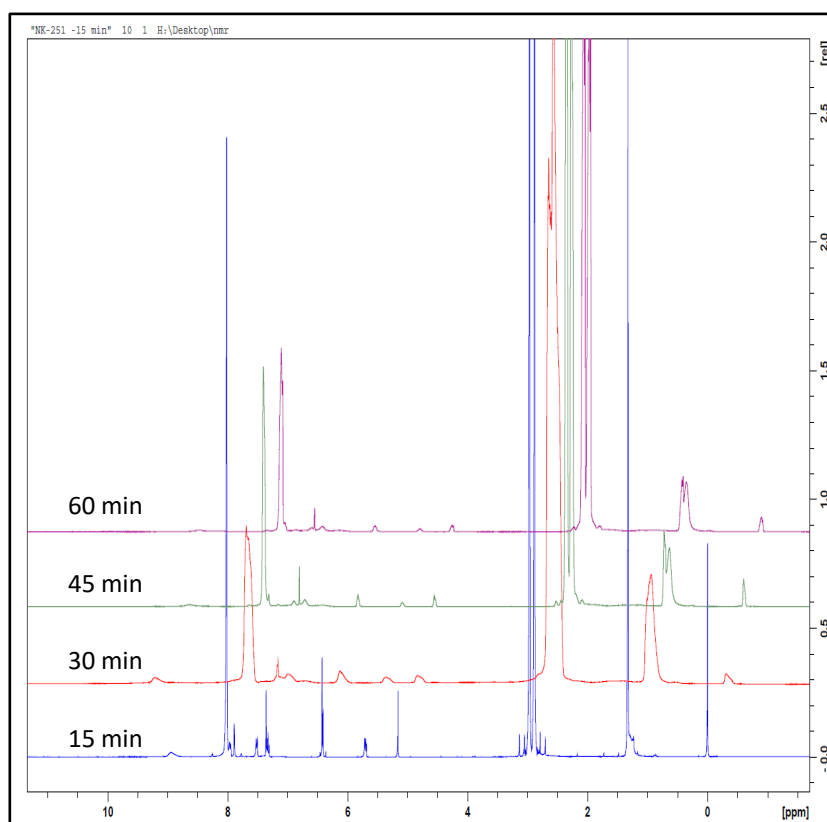
Figure 4. 29 ^{1}HNMR traces of the RAFT polymerization of 1M N-(3-(4,4,5,5-tetramethyl-1,3,2-dioxaborolan-2-yl)phenyl)acrylamide pinacol ester at 82 °C using trioxane as internal standard and 0.0029 M AIBN in DMF.

Calculation of the (%) monomer conversion of 3-ACPBAPE with reference to 1,3,5 trioxane as internal standard for RAFT radical polymerization from the integral of vinyl peak shows a trend increasing of polymer and disappearing of vinyl peak.

Table 4. 19 Conversion by ^{1}HNMR and GPC result over time for the RAF polymerization of 1M N-(3-(4,4,5,5-tetramethyl-1,3,2-dioxaborolan-2-yl)phenyl)acrylamide pinacol ester at 82 °C

251 Polymer	Time (min) at 82 °C.	Conversion Polymer by NMR %	M, nth at $(g\ mol^{-1})$	Conversion by GPC %	Mn $(g\ mol^{-1})$ experimental by GPC	Mw/Mn
	15	14	1915	24	3691	1.14
3-ACPBAPEmacro-RAFT	30	27	3694	39	5666	1.23
	45	60	8209	41	5938	1.27
	60	70	9577	50	7025	1.25

Using trioxane as internal standard and 0.0029 M AIBN in DMF (50 blocks) (Figure 4.28) is the conversion vs time. The result of using AIBN (0.0029 M) at 82 °C shows that the reaction proceeds very fast and causes degradation of the compound as well as the NMR shows some degradation peaks (at 3 ppm) near internal standard peak which may be caused by trioxane at 3 ppm and RAFT agent using high temperature (82 °C). In the next experiment the ratio of RAFT to AIBN is changed, to obtain 100 blocks.

4.28.3 RAFT polymerization of N-(3-(4,4,5,5-tetramethyl-1,3,2 dioxaborolan-2 yl) phenyl) acrylamide pinacol ester at 82 °C

Quantities used for RAFT polymerization of N-(3-(4,4,5,5-tetramethyl-1,3,2-dioxaborolan-2-yl) phenyl) acrylamide pinacol ester at 82 °C (100 block), is used to observed the rate of reaction at higher RAFT concentration.
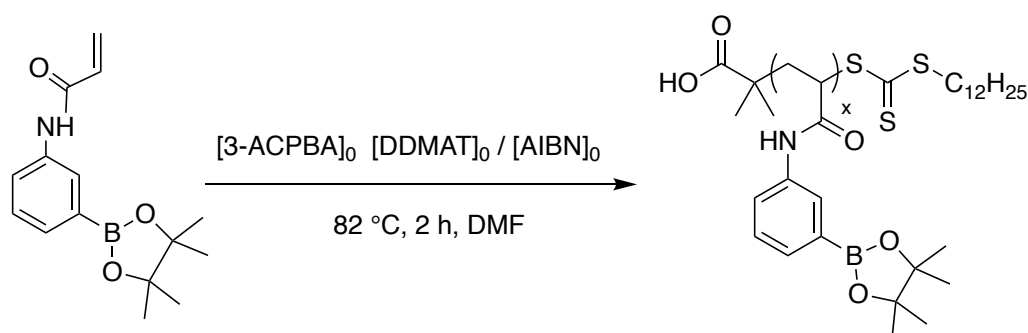
Scheme 4. 41 RAFT polymerization of N-(3-(4,4,5,5-tetramethyl-1,3,2 dioxaborolan-2 yl) phenyl) acrylamide pinacol ester at 82 °C, using DMF and AIBN (100 Blocks)

Table 4. 20 Quantities used for RAFT polymerization of N-(3-(4,4,5,5-tetramethyl-1,3,2-dioxaborolan-2-yl) phenyl) acrylamide pinacol ester at 82 °C (100 block)

Polymer ID 256	mg	MW	mmol	Volume (mL)	mmol / mL	Ratio
AIBN	119.40	164.21	0.7271	1a	0.0029	1
DDMAT	36.10	364.63	0.0990	1	0.0099	3.4
3-ACPBAE	273.21	273.15	1.0002	1	1.0002	346
Trioxane	102.00	90.08		1c	0.1132	

Time vs (%) conversion of poly 3-ACPBAPE macro-RAFT at 82 °C

Legend: □ NK-256 3ACPBAPE [AIBN] 0.0029   ------- Linear (NK-256 3ACPBAPE [AIBN] 0.0029)
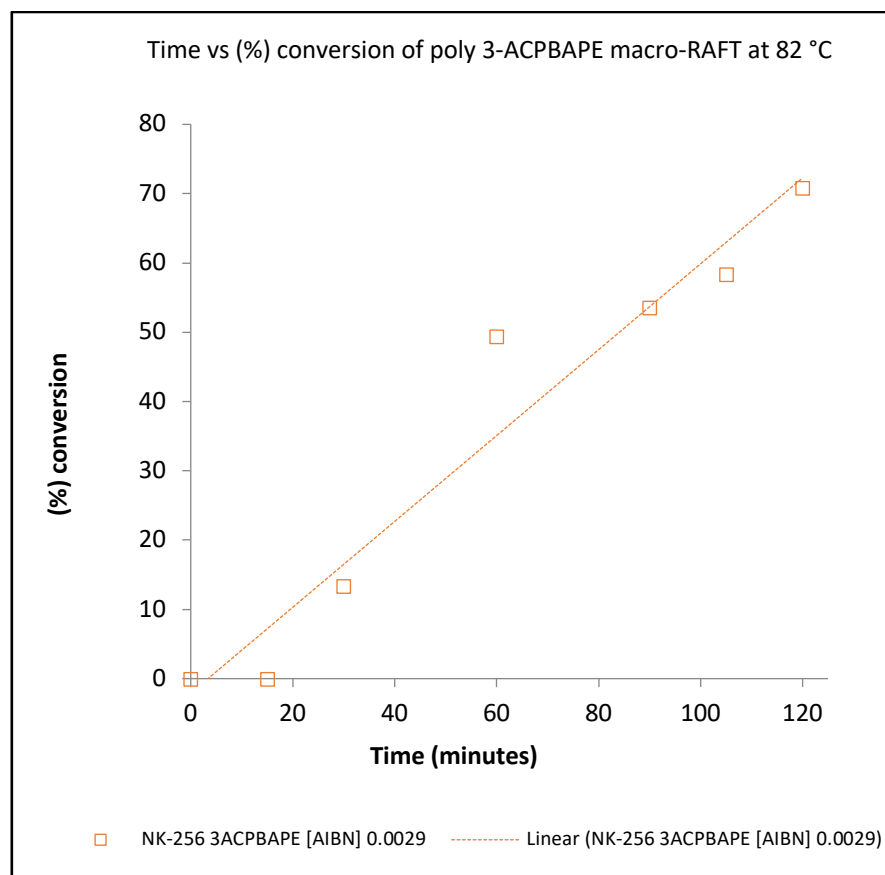
Figure 4. 30 The monomer conversion (%)-time plot for the RAFT polymerization of N-(3-(4,4,5,5-tetramethyl-1,3,2-dioxaborolan-2-yl)phenyl)acrylamide pinacol ester.

Polymerization conditions [3-ACPBAPE]0: [DDMAT]0: [AIBN]0= 346: 3.4: 1 at 82 °C. Monomer shows a slow conversion up to 50 % at 82 °C in DMF is fairly linear. This monomer conversion suggests that the conversion of monomer can be proceed using 0.0029 M AIBN however the reaction is slow (figure 4.30).
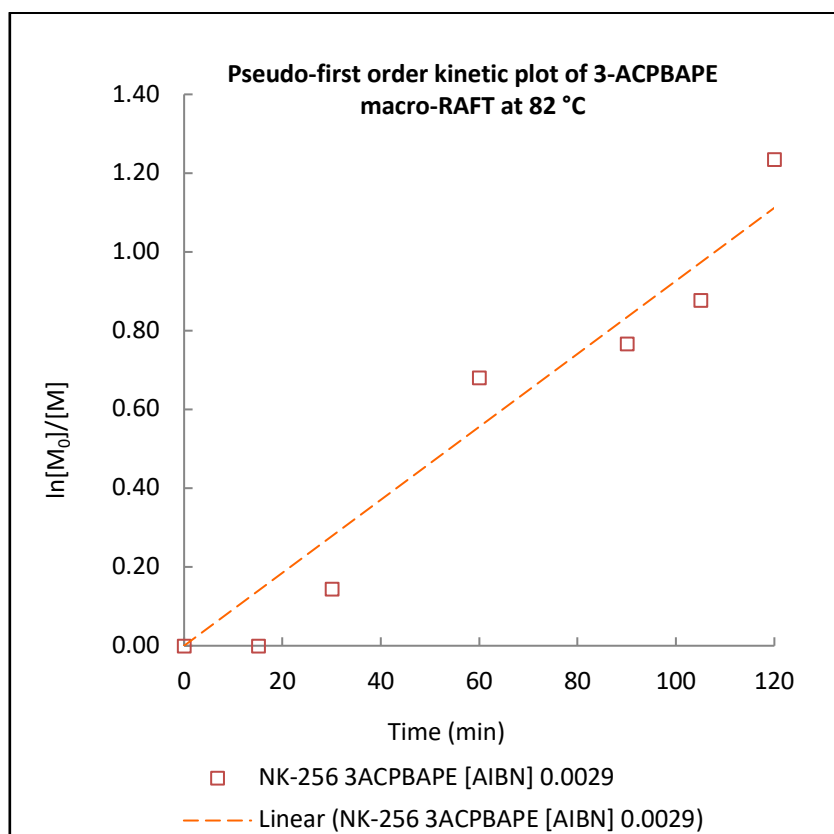
Figure 4. 31 Pseudo-first order kinetic plot of conventional polymerization of 3-ACPBAPEat 82 °C using high AIBN concentration. Polymerization conditions [3-ACPBAPE]$_0$: [DDMAT]$_0$: [AIBN]$_0$= 346 : 3.4 : 1, 82 °C in DMF.

Pseudo-first order kinetic plot (figure 4.31) shows a living polymerization with induction period and slow initiation. An inhibition period is often observed in RAFT mediated polymerization reaction even though the monomer has been purified enough. Methyl acrylate shows these effects strong. The literature suggested that this "inhibition" response is due to the slow fragmentation of formed intermediate radicals. Therefore, the slow rate at the start of the reaction is due to low propagation rate coefficients during the initiation period.
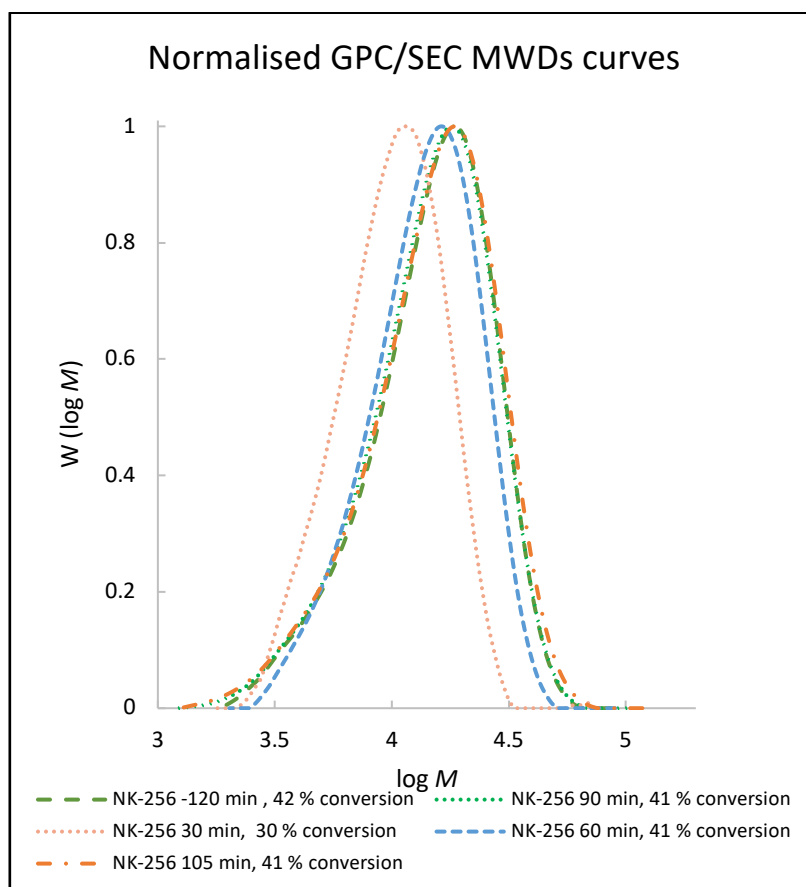
Figure 4. 32 Normalized GPC/SED MWDs curves of RAFT polymerization of N-(3-(4,4,5,5-tetramethyl-1,3,2-dioxaborolan-2-yl)phenyl)acrylamide pinacol ester at 82 °C using trioxane as internal standard and 0.0029 M AIBN in DMF after 120 min.

At 30 min the MWDs curve (figure 4.32) a peak with Mn value from 8691 g mol^{-1} which over time changes the peak at 60 min increases the Mn = 11686 with a PDI = 1.32 with 41 % conversion. The conversion remains at 42 % (table 4.21) which shows that the chain does not grow after one hour may be due to high amount of initiator (0.0029 M) as more initiator concentration more dead chains. .
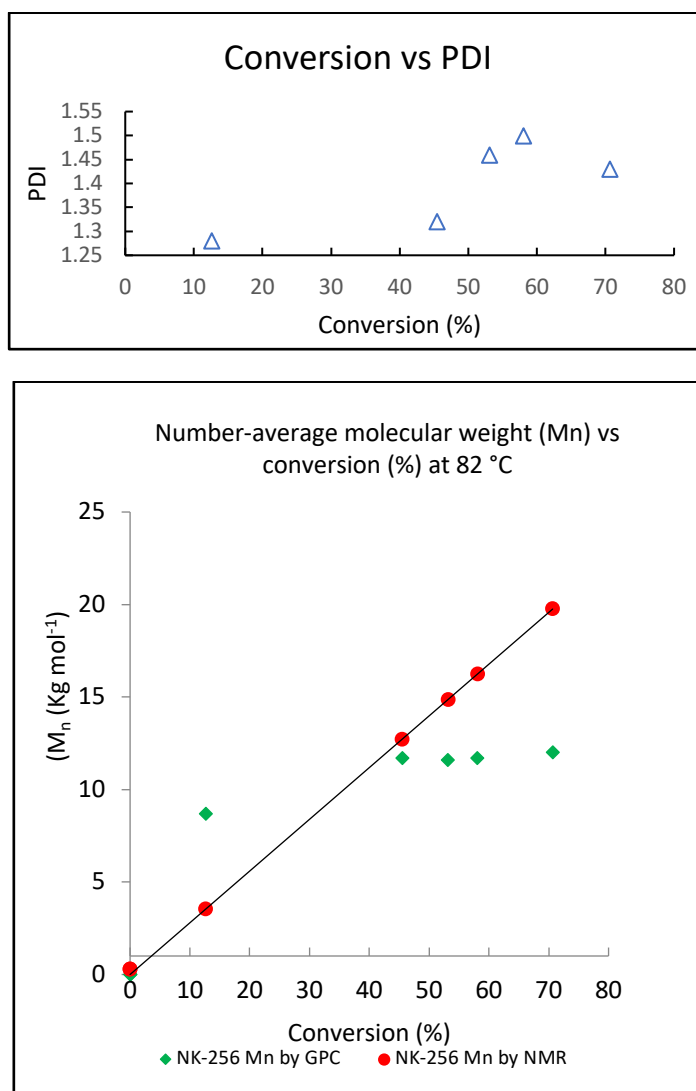
Figure 4. 33 Theoretical and experimental number-average molecular weight (Mn) vs conversion (%) and GPC/SEC normalized curve for N-(3-(4,4,5,5-tetramethyl-1,3,2-dioxaborolan-2-yl)phenyl)acrylamide pinacol ester.

 Polymerization conditions $[3\text{-ACPBAPE}]_0$: $[DDMAT]_0$: $[AIBN]_0$= 346: 3.4: 1. The graph compares to predicted (Mn, g mol^{-1}) obtained from ^1HNMR conversion (figure 4.33) (points, blue dots) vs experimental data obtained by GPC (points, orange square). The first order plot of monomer conversion is linear. The black triangle shows the PDI of the macro-RAFT vs conversion (%).

Table 4. 21 NMR and GPC results of RAFT radical polymerization of 1M N-(3-(4,4,5,5-tetramethyl-1,3,2-dioxaborolan-2-yl)phenyl)acrylamide pinacol ester and DDMAT at 82 °C using trioxane as internal standard and 0.0029 M AIBN in DMF.

256 Polymer	Time (min) at 82 °C.	Conversion Polymer by NMR %	Mn, th (g mol $^{-1}$)	Conversion by GPC %	Mn (g mol^{-1}) experimental by GPC	Mw/Mn
3 - ACPBAPEm acro-RAFT	30	13	3735	30	8691	1.28
	60	49	13813	41	11686	1.32
	90	54	14976	41	11593	1.46
	105	58	16333	41	11685	1.50
	120	71	19821	42	12002	1.43
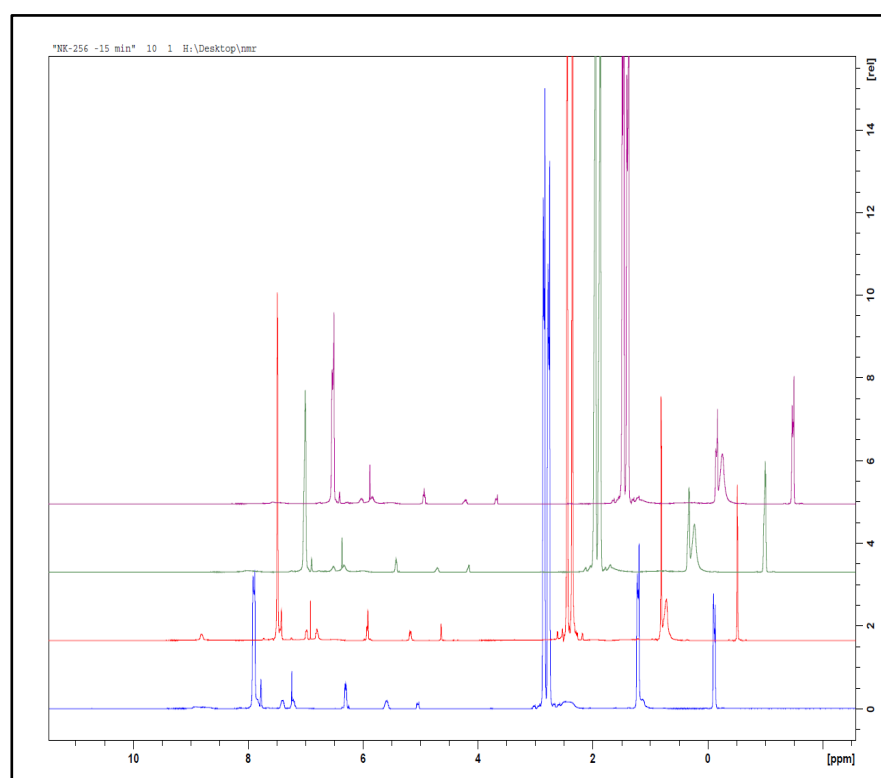
Figure 4. 34 ^{1}HNMR traces of the RAFT radical polymerization of 1M N-(3-(4,4,5,5-tetramethyl-1,3,2-dioxaborolan-2-yl)phenyl)acrylamide pinacol ester and DDMAT at 82 °C using trioxane as internal standard and 0.0029 M AIBN in DMF. Polymerization conditions [3-ACPBAPE]$_0$: [DDMAT]$_0$: [AIBN]$_0$= 346: 3.4: 1, 82 °C in DMF..

4.28.4 Attempts to use AIBN (0.0015 M) and trioxane internal standard RAFT polymerization of N-(3-(4,4,5,5-tetramethyl-1,3,2-dioxaborolan-2-yl) phenyl) acrylamide pinacol ester at 82 °C (50 block)

AIBN (60.30 mg, 0.3854 mmol) dissolved in 25 mL and diluted 1 mL in 10 mL (250 times dilution). Trioxane (101.20 mg ,1.00 mmol) as internal standard (IS) (10 times dilution) and DDMAT (75.00 mg, 0.0205 mmol) diluted 10 folds added into 1 mL AIBN stock solution (0.0015 M) with monomer 3-ACPBAPE (273.60, 1.0016 mmol), at 82 °C for 2 hours sample were taken periodically and analysed by NMR and GPC (table 4.23).

Table 4. 22 Quantities used in presence of trioxane internal standard.

258 Chemical	mg	MW	mmol	Volume (mL)	mmol / mL (M)	Ratio
AIBN	60.30	164.21	0.3854	1a	0.0015	1
DDMAT	75.00	364.63	0.2057	1b	0.0207	14
3-ACPBAE	273.60	273.15	1.0016	1	1.0016	669
Trioxane	101.20	90.08	1.	1c	0.1	

DMF at 82 °C, a diluted 250-fold, b diluted 10-fold, c diluted 10-fold.

Figure 4. 35 monomer conversion (%) vs time plot for the RAFT polymerization of N-(3-(4,4,5,5-tetramethyl-1,3,2-dioxaborolan-2-yl)phenyl)acrylamide pinacol ester is fairly linear (blue dots) up to 80 %.

Polymerization (figure 4.35) of 3-ACPBAPEmacro-RAFT [M]: [DDMAT]: [AIBN] = 669:14 :1, 82 °C. This monomer conversion suggests that the conversion of monomer can be proceed 60 - 70 % using 0.0015 M AIBN at 50 min time vs conversion plot shows slow growth up to 70 % and then a plateau in conversion. For formation of 50 block macro-RAFT of 3-ACPBAPE 0.0015 M AIBN gives higher conversion that same numbers of blocks with 0.0029 M AIBN. Higher conversion of polymer is due to initiation of most chains from the RAFT agent.

Figure 4. 36 Pseudo-first order kinetic plot of conventional polymerization of 3-ACPBAPE at 82 °C using high AIBN concentration. Polymerization conditions 3-ACPBAPEmacro-RAFT [M]: [DDMAT]: [AIBN] = 669:14:1, 82 °C.

Pseudo-first order kinetic plot is fairly linear after 60 min the conversion becomes slow. Propagating constant is determined by rate initiation and termination in conventional radical polymerisation. Slow initiation figure 4.36 dotted line suggests a decrease in Propagation because of termination reaction or side reactions at high temperature using 0.0015 M AIBN.

MWDs curve of 3-ACPBAPE macro-RAFT

Legend:
- NK-258 - 30 min 16% conversion
- NK-258 -60 min 19 % conversion
- NK-258 90 min, 40 % conversion
- NK-258 -105 min, 44 % conversion
- NK-258 - 120 min, 46 % conversion
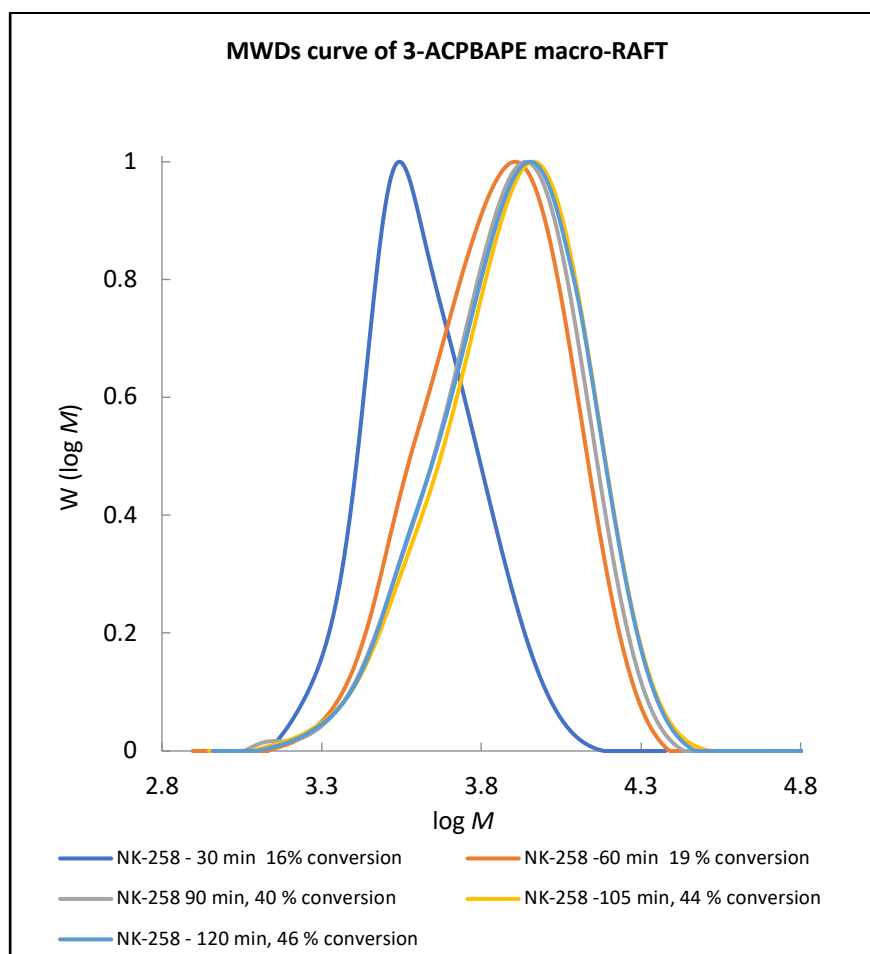
Figure 4. 37 MWDs for polymerization of for N-(3-(4,4,5,5-tetramethyl-1,3,2-dioxaborolan-2-yl)phenyl)acrylamide pinacol ester.

Polymerization conditions 3-ACPBAPEmacro-RAFT [M]: [DDMAT]: [AIBN] = 669:14:1, 82 °C. conversion of 16 % at 30 min, 19 % at 60 min, 40 % at 90 min and 44 % at 105 min and 46 % at 2 hours. At 82 °C the conversion is very rapid using 0.0015 M AIBN (figure 4.36), shows the rate is slow and then at 60 rapidly goes up. The MWDs by GPC (figure 4.37) shows dead chain tailing and the conversion is around 46 % in 2 hours. This means the temperature of the reaction should be lowered to optimise conversion.
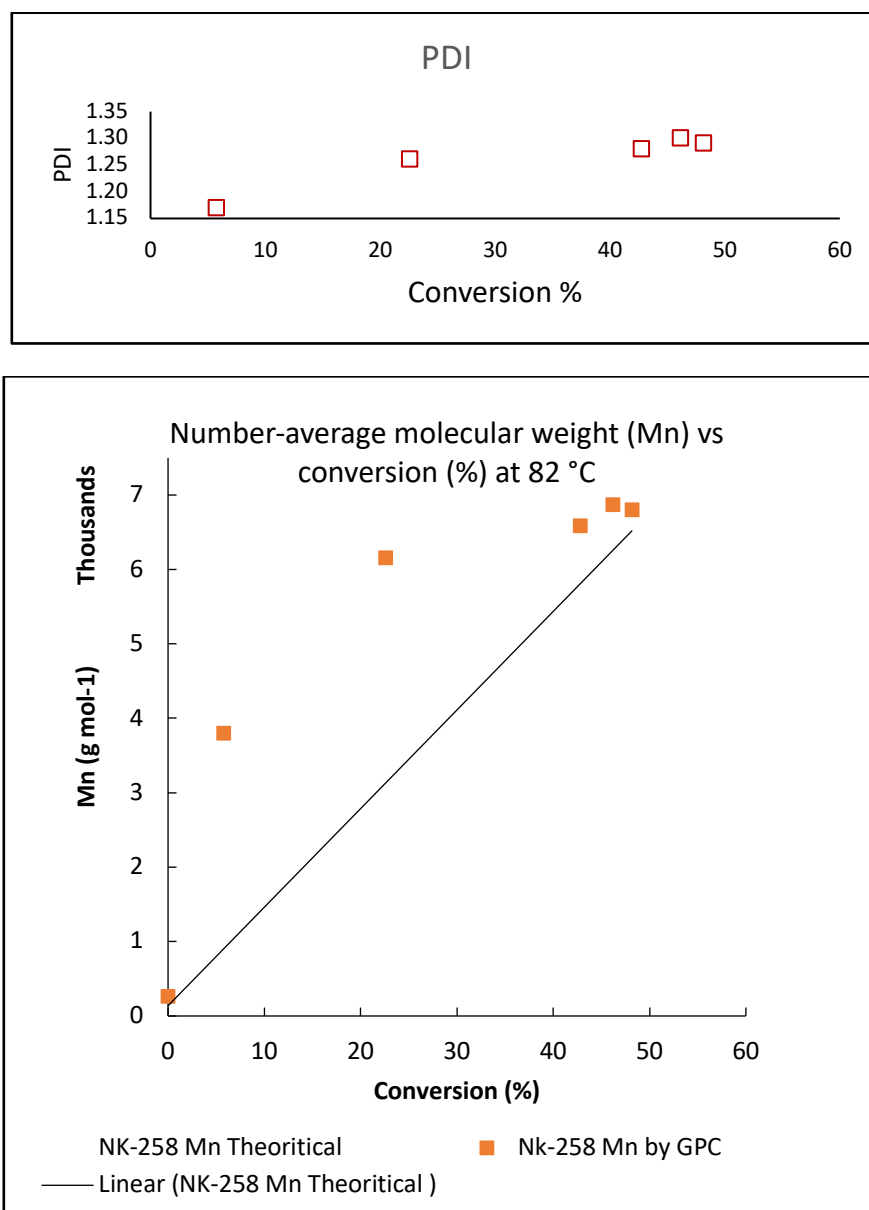
Figure 4. 38 Number-average molecular weight (Mn, g mol^{-1}) vs conversion (%) for N-(3-(4,4,5,5-tetramethyl-1,3,2-dioxaborolan-2-yl)phenyl)acrylamide pinacol ester Macro-RAFT using DDMAT. Polymerization 3-ACPBAPEmacro-RAFT [M]: [DDMAT]: [AIBN] = 669:14:1, 82 °C, (50 blocks).

The graph compares to predicted (Mn, g mol^{-1}) obtained from ^{1}HNMR conversion (points, blue square) vs experimental data obtained by GPC (points, red square). The open square shows the PDI of the macro-RAFT vs conversion (%). Theoretical Mn is calculated as a product of M, nth and percent conversion using ^{1}HNMR.
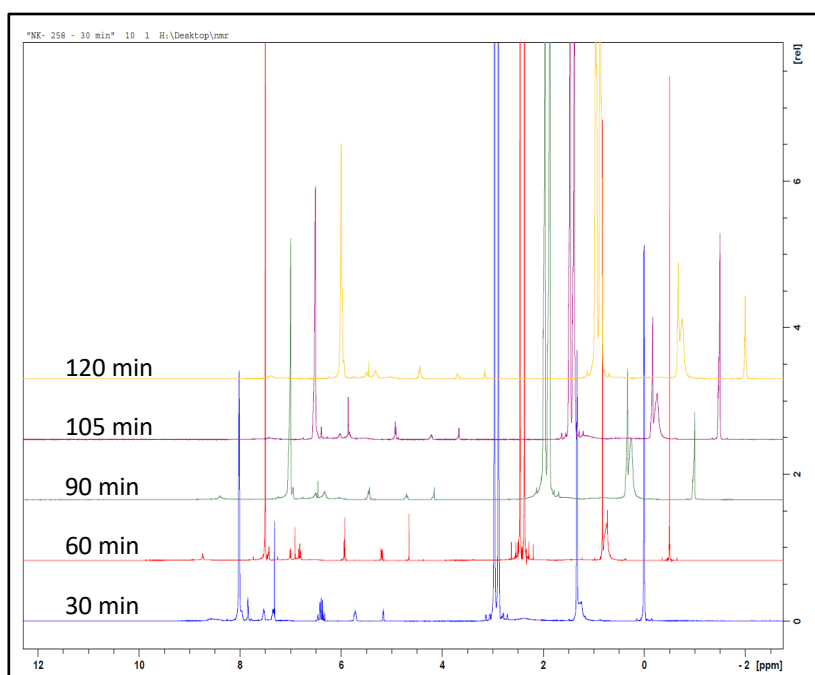
Figure 4. 39 ^{1}HNMR traces of the RAFT polymerization of 1M N-(3-(4,4,5,5-tetramethyl-1,3,2-dioxaborolan-2-yl)phenyl)acrylamide pinacol ester at 82 °C using trioxane as internal standard and 0.0015 M AIBN in DMF.

Calculation of the (%) monomer conversion of 3-ACPBAPE with reference to 1,3,5 trioxane as internal standard for RAFT radical polymerisation from the integral of vinyl peak shows a trend increasing of polymer and disappearing of vinyl peak. 3-ACPBAPEmacro-RAFT [M]: [DDMAT]: [AIBN] = 669:14:1, 82 °C

Table 4. 23 ^{1}HNMR conversion and GC/SEC molecular wight of the RAFT polymerization of 1M N-(3-(4,4,5,5-tetramethyl-1,3,2-dioxaborolan-2-yl)phenyl)acrylamide pinacol ester at 82 °C using trioxane as internal standard and 0.0015 M AIBN in DMF.

258 Polymer	Time (min) at 82 °C.	Polymer by NMR %	M, nth at (g mol^{-1})	GPC %	Mn GPC	Mw/Mn
3-ACPBAPEmacro-RAFT 669:14:1	30	16	2111	13	3804	1.17
	60	19	2633	21	6167	1.26
	90	40	5489	23	6590	1.28
	105	44	5965	52	6881	1.30
	120	46	6251	51	6810	1.29

119

The results of polymerisation of polymer 258 in table 4.23 shows that using 0.0015 M AIBN the polymer conversion is low (16 % by NMR and 13 % by GPC) at 30 min with molecular weight of around 3Kmol-1 and a broad polydispersity PD = 1.17 for a degree of polymerisation of DP = 47. After 90 min the conversion goes by 40 % but the chains are not growing and becomes shorter up to 2 hours. This is read from the average molecular weight (Mw) by GPC which shows in table 4.23 (polymer 258) from 90 -120 min.

4.28.5 Attempts of using AIBN (0.0015 M) and trioxane internal standard RAFT polymerization of N-(3-(4,4,5,5-tetramethyl-1,3,2-dioxaborolan-2-yl) phenyl) acrylamide pinacol ester at 82 °C (100 block)

AIBN (60.00mg) dissolved in 25 mL DMF and diluted 1 mL in 10 mL (250 times dilution). Trioxane 100.50 mg (1.1112 mmol) as internal standard (IS) (10 times dilution) and 36.00 mg DDMAT (0.0987 mmol) added to 10 mL flask.
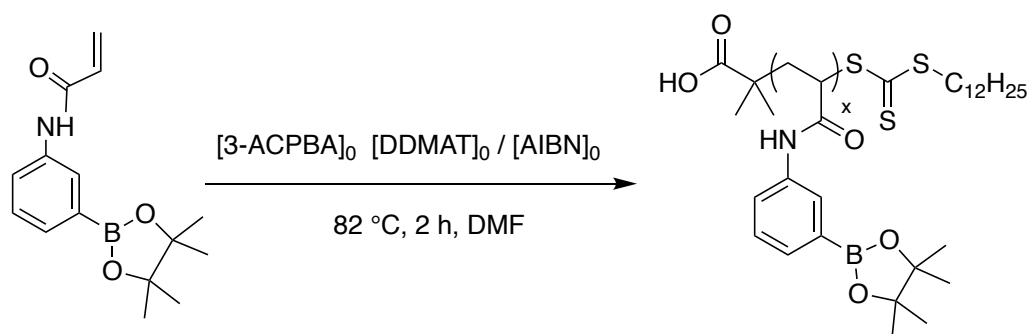
Scheme 4. 42 RAFT polymerization of N-(3-(4,4,5,5-tetramethyl-1,3,2-dioxaborolan-2-yl) phenyl) acrylamide pinacol ester at 82 °C (100 block) in DMF.

Table 4. 24 Quantities used in the 1 mL reaction with AIBN concentration of 0.0015 M and trioxane as internal standard.

252 Chemical	mg	MW	mmol	(mL)	mmol / mL (M)	Ratio
AIBN	60.00	164.21	0.365	1a	0.0015	1
DDMT	36.00	364.63	0.098	1b	0.0099	6.6
3-ACPBAE	273.91	273.15	1.002	1	1.0028	669
Trioxane	100.50	90.08	1.115	1c	0.1157	

DMF at 82 °C, a diluted 250-fold, b diluted 10-fold, c diluted 10-fold.

Time vs (%) conversion of poly 3-ACPBAPE macro-RAFT at 82 °C
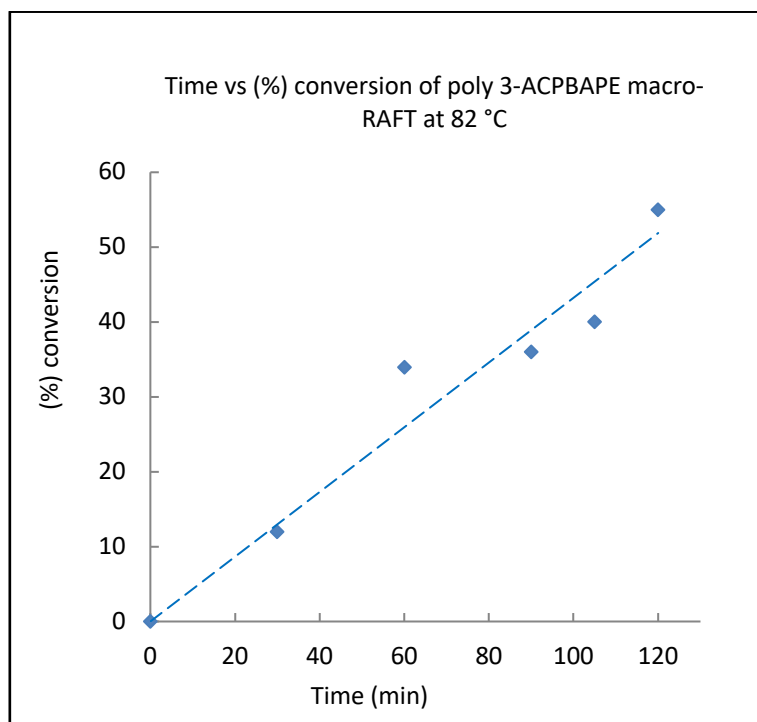
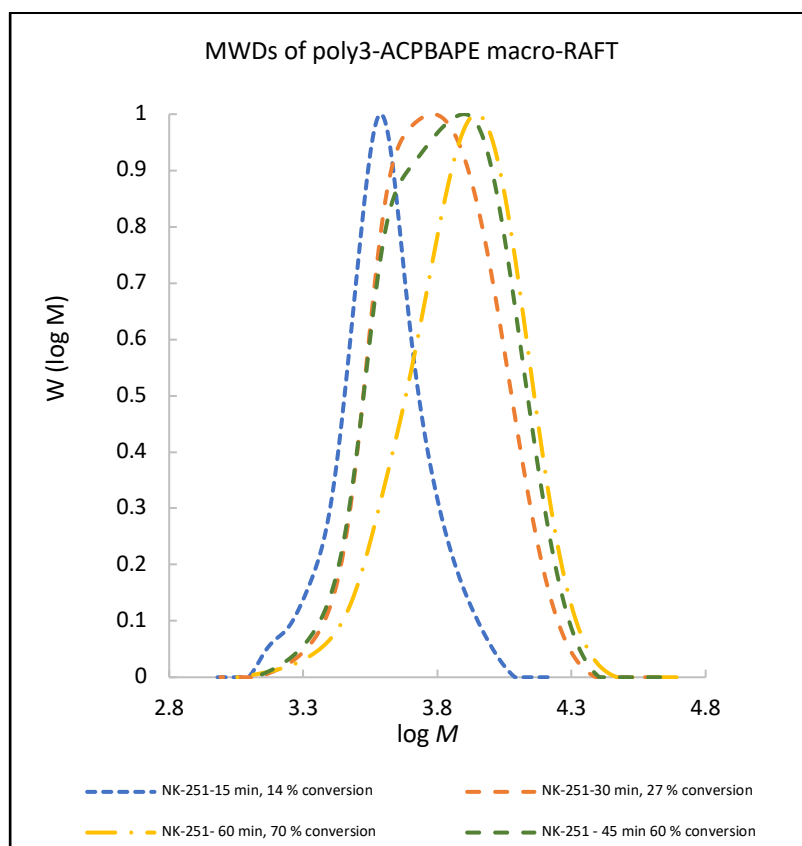Figure 4. 40 The monomer conversion (%)-time plot for the RAFT polymerization of N-(3-(4,4,5,5-tetramethyl-1,3,2-dioxaborolan-2-yl)phenyl)acrylamide pinacol ester.

Polymerization conditions $[3\text{-ACPBAPE}]_0$: $[DDMAT]_0$: $[AIBN]_0$= 669: 6.6: 1 at 82 °C. Monomer shows a slow conversion up to 50 % at 82 °C in DMF. This monomer conversion suggests that the conversion of monomer can proceed using 0.0015 M AIBN however the reaction is slow. Table 4.24 shows AIBN concentration of 0.0015 M and trioxane as internal standard, for 100 blocks of 3-ACPBAPE macroRAFT.
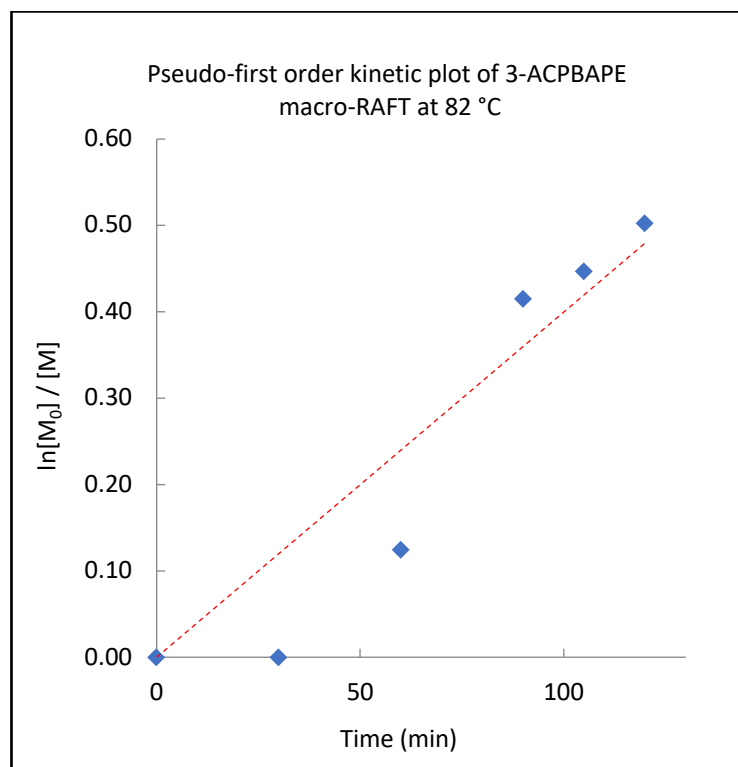
Figure 4. 41 Pseudo-first order kinetic plot of conventional polymerization of 3-ACPBAPE at 82 °C using high AIBN concentration. Polymerization conditions [3-ACPBAPE]$_0$: [DDMAT]$_0$: [AIBN]$_0$= 669: 6.6: 1, 82 °C in DMF. Pseudo-first order kinetic plot shows a living polymerisation with induction period and slow initiation.
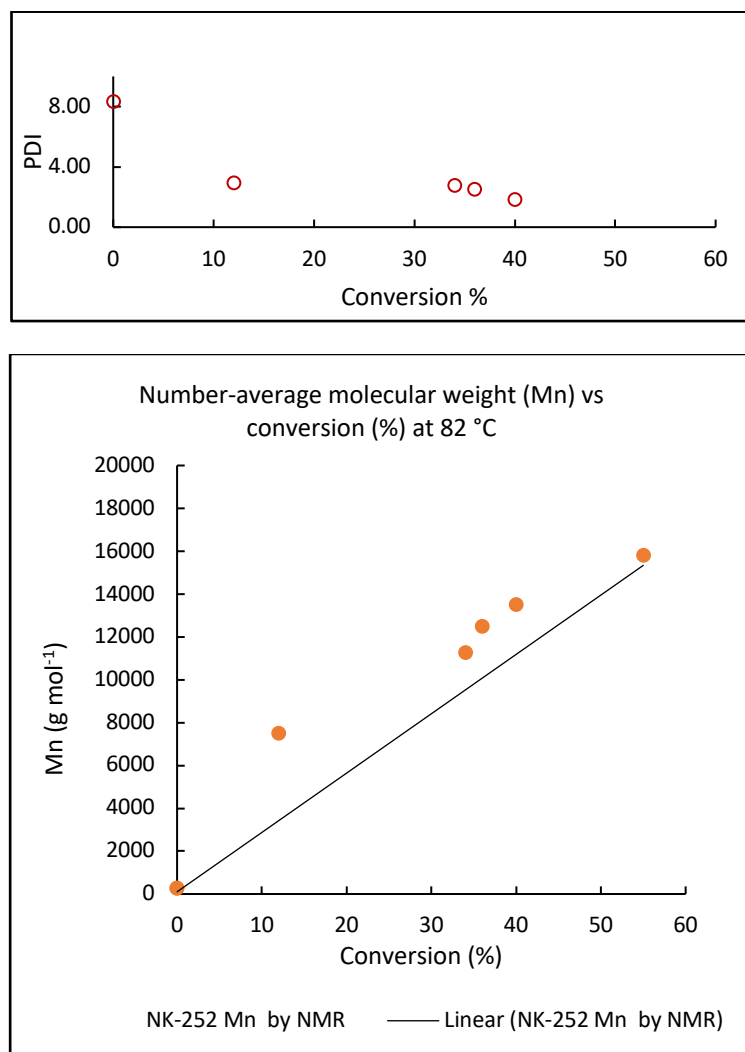
Figure 4. 42 Theoretical and experimental number-average molecular weight (Mn) vs conversion (%) and GPC/SEC normalized curve for N-(3-(4,4,5,5-tetramethyl-1,3,2-dioxaborolan-2-yl)phenyl)acrylamide pinacol ester.

Polymerization condition [3-ACPBAPE]0: [DDMAT]0: [AIBN]0= 669: 6.6: 1. The graph compares to predicted (Mn, g mol^{-1}) obtained from ^{1}HNMR conversion (points, blue dots) vs experimental data obtained by GPC (points, orange square). The first order plot of monomer conversion fitted linearly and forced through the origin (blue dotted line). The hole circles show the PDI of the macro-RAFT vs conversion (%).

Normalised GPC/SEC MWDs curves

Legend:
- NK-252 - 30 min, 12 % conversion
- NK-252 - 60 min 34 % conversion
- NK-252 - 90 min, 36 % conversion
- NK-252 -105 min, 40 % conversion
- NK- 252 120 min, 55 % conversion
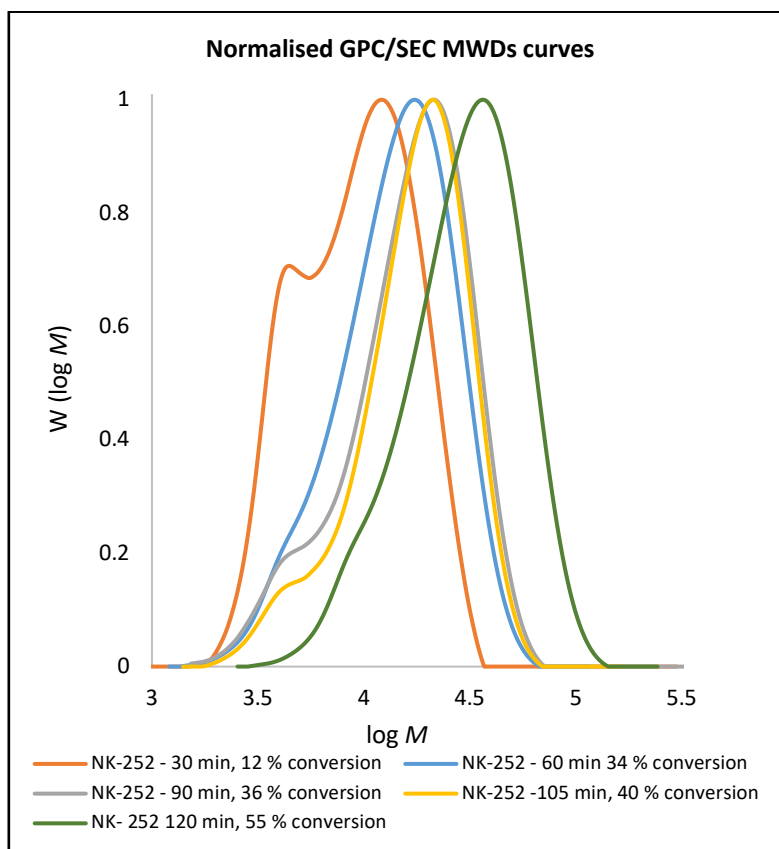
Figure 4. 43 Normalized GPC/SED MWDs curves of RAFT polymerization of N-(3-(4,4,5,5-tetramethyl-1,3,2-dioxaborolan-2-yl)phenyl)acrylamide pinacol ester at 82 °C using trioxane as internal standard and 0.0015 M AIBN in DMF after 120 min.

At 30 min the MWDs curve (figure 4.43) shows a bimodal peak with (Maximum point) Mp value from 3200 – 10000 g mol^{-1} which over time changes from bimodal to a monomodal peak at 60 min which is then observed at 90 – 105 min. At 120 min the MWDs curves give (55 % conversion) a reasonable value confirmed with ^{1}HNMR (55 %) conversion with Mn = 15800 and PDI = 1.82 (table 4.25) which is showing clearly picture of broad polydispersity and tailing of molecular weight. .

^{1}HNMR and normalized GPC /SEC analysis of RAFT polymerization [3-ACPBAPE]$_0$: [DDMAT]$_0$: [AIBN]$_0$= 669 : 6.6 : 1 of *N*-(3-(4,4,5,5-tetramethyl-1,3,2-dioxaborolan-2-yl)phenyl)acrylamide pinacol ester at 82 °C using trioxane as the internal standard and 0.0015 M AIBN in DMF after 30, 60, 90, 105, and 120 min. The result shows a

trend in conversion (%) and Mn (g mol^{-1}). ^{1}HNMR shows an increase in conversion (%) from 12 % at 30 min to 55 % at 120 min. GPC/SEC shows an increase in Mn over time

Table 4. 25 GPC/SED MWDs and NMR conversion of RAFT polymerization of 3-ACPBAPE at 82 °C using trioxane as internal standard and 0.0015 M AIBN in DMF after 120 min.

252 Polymer	Time (min) at 82 °C.	Conversion by NMR %	M, *nth* (g mol^{-1})	Conversion by GPC %	Mn (g mol^{-1}) by GPC	Mw/ Mn
3-ACPBAPE macro-RAFT	30	12	3354	26	7500	8.33
	60	34	9500	39	11250	2.94
	90	36	1007	44	12500	2.78
	105	40	1118	48	13500	2.50
	120	55	1540	56	15800	1.82
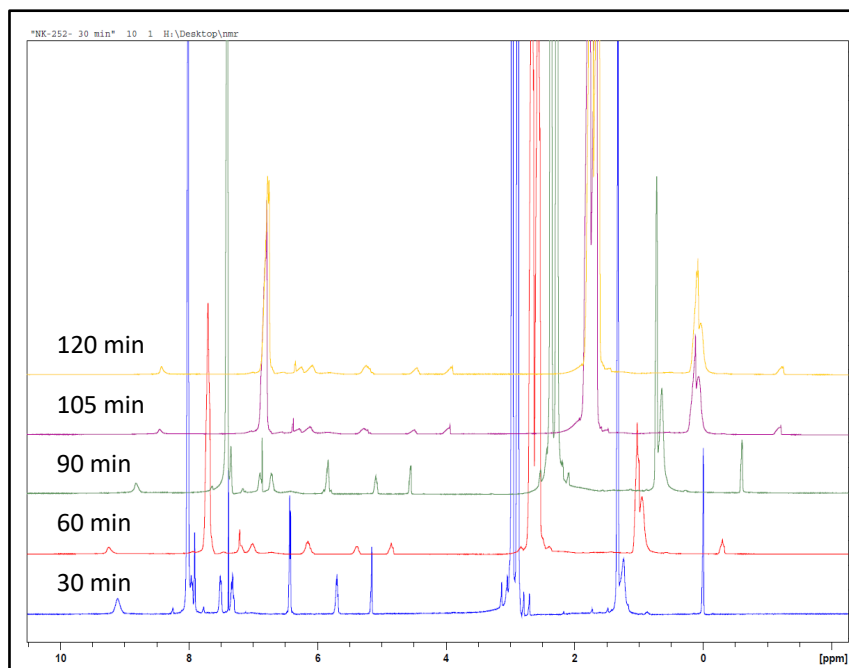
Figure 4. 44 ^{1}HNMR traces of the RAFT radical polymerization of 1M N-(3-(4,4,5,5-tetramethyl-1,3,2-dioxaborolan-2-yl)phenyl)acrylamide pinacol ester and DDMAT at 82 °C using trioxane as internal standard and 0.0015 M AIBN in DMF.

Polymerization conditions $[3\text{-ACPBAPE}]_0$: $[AIBN]_0$= 669: 7: 1, 82 °C in DMF. Conversion by NMR at 30 min = 12 % and reaches gradual increase at 120 min = 56 % (table 4.26)

4.28.6 RAFT polymerization of 4-ACPBAPE Using AIBN (0.0015 M) and Anisole as internal standard

RAFT polymerization of N-(4-(4,4,5,5-tetramethyl-1,3,2-dioxaborolan-2-yl) phenyl) acrylamide pinacol ester at 82 °C (50 block)

AIBN (63.00 mg, 0.387 mmol) dissolved in 25 mL DMF and diluted 1 mL in 10 mL (250 times dilution). Anisole (122.63 mg ,1.13 mmol) as internal standard (IS) (10 times dilution) and DDMAT (75.00 mg, 0.0218 mmol) diluted 10 folds added into 1 mL AIBN stock solution (0.0015 M) with monomer 4-ACPBAPE (273.75, 1.0022mmol), at 82 °C for 2 hours. Sample were taken periodically and analyzed by NMR and GPC.
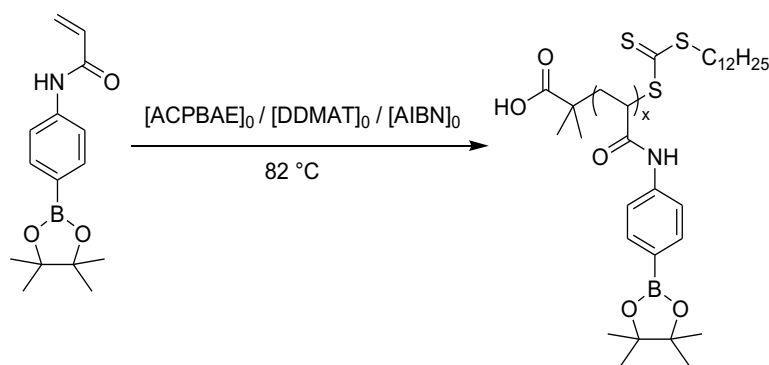
Scheme 4. 43 RAFT polymerization of N-(4-(4,4,5,5-tetramethyl-1,3,2-dioxaborolan-2-yl) phenyl) acrylamide pinacol ester at 82 °C (50 block)

Table 4. 26 Quantities used in the reaction to make 50 blocks. 4-ACPBAPE]$_0$: [DDMAT]$_0$: [AIBN]$_0$= 667 : 14 : 1 , 82 °C.

267 Chemical	mg	MW	mmol	(mL)	mmol / mL (M)	Ratio
4-ACPBAE	63.55	164.21	0.3870	1a	0.0015	1
AIBN	75.00	364.63	0.2108	1b	0.0218	14
Anisole	273.30	273.15	1.0005	1	1.0005	667
DDMAT	122.63	108.14	1.1340		0.1134	

DMF at 82 °C, a diluted 250-fold, b diluted 10-fold, c diluted 10-fold.
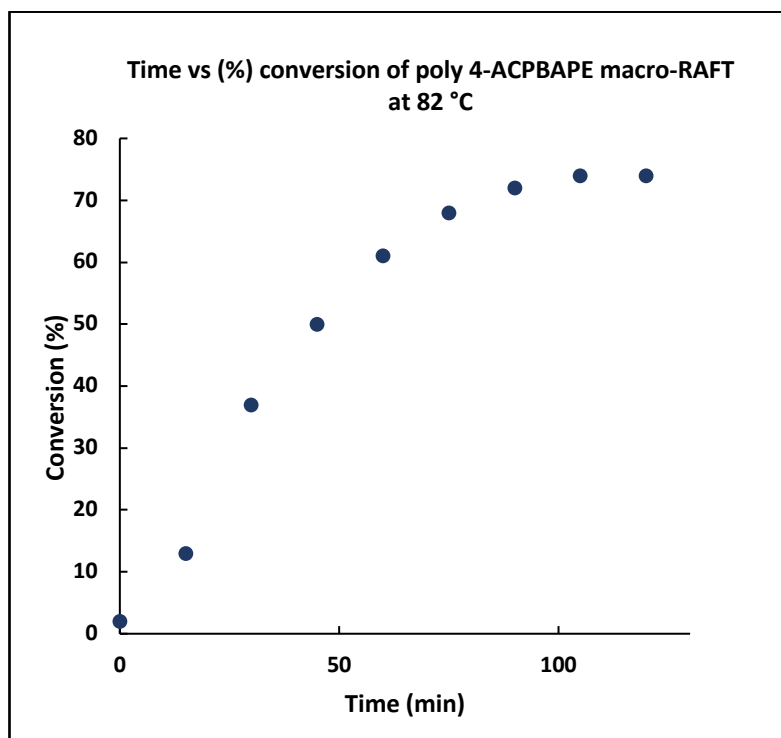
Figure 4. 45 The monomer conversion (%) vs time plot for the RAFT polymerization of N-(4-(4,4,5,5-tetramethyl-1,3,2-dioxaborolan-2-yl)phenyl)acrylamide pinacol ester is fairly linear (blue dots). Polymerization conditions [4-ACPBAPE]0: [DDMAT]0 : [AIBN]0= 667 : 14 : 1 , 82 °C.

This monomer conversion, suggests that the conversion of monomer can proceed 67 % using 0.0015 M AIBN at 120 min.
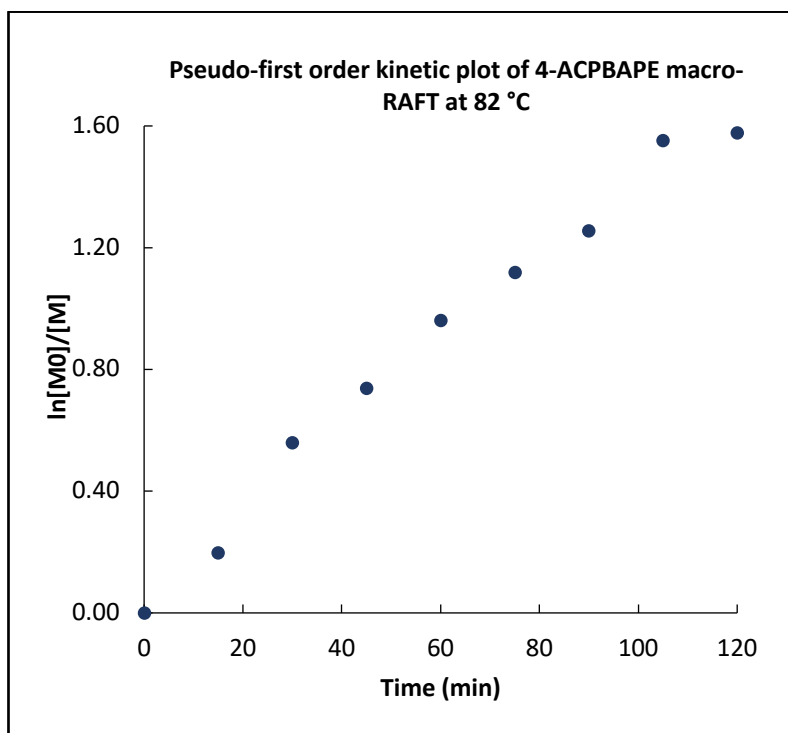
Figure 4. 46 Pseudo-first order kinetic plot of conventional polymerization of 4-ACPBAPE at 82 °C using high AIBN concentration. Polymerization conditions [4-ACPBAPE]$_0$: [DDMAT]$_0$: [AIBN]$_0$= 667 : 14 : 1 , 82 °C. Pseudo-first order kinetic plot is fairly linear.
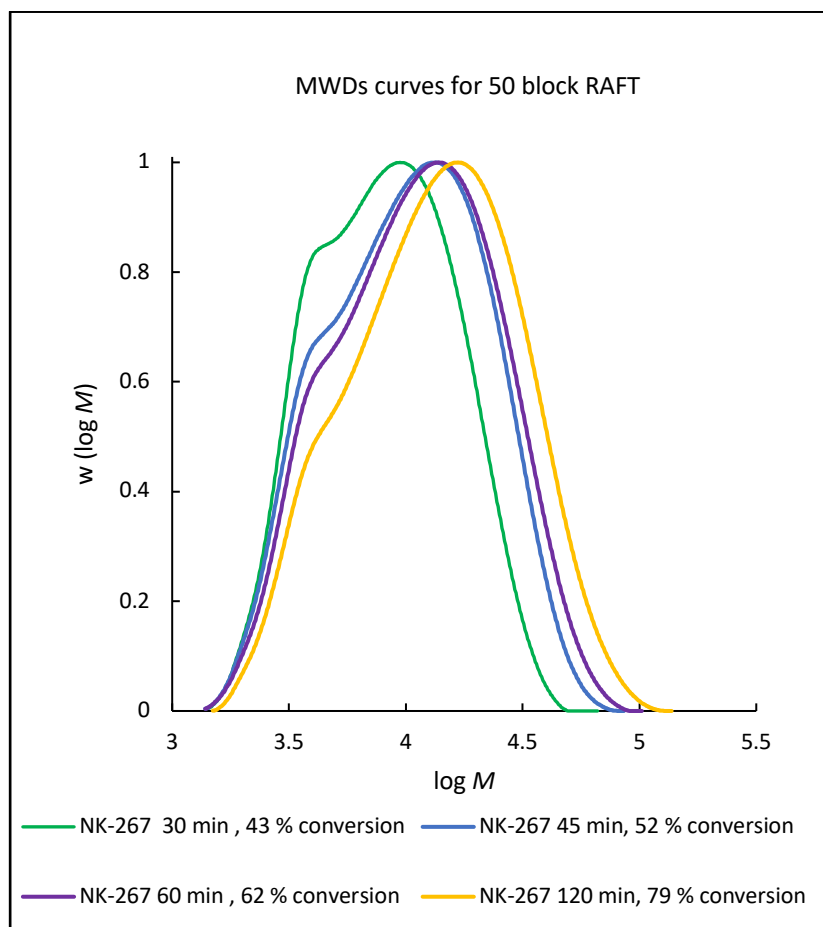
Figure 4. 47 GPC traces as function of monomer conversation for RAFT polymerization of for N-(4-(4,4,5,5-tetramethyl-1,3,2-dioxaborolan-2-yl) phenyl) acrylamide pinacol ester. Polymerization conditions [4-ACPBAPE]$_0$: [DDMAT]$_0$: [AIBN]$_0$= 667 : 14 : 1 , 82 °C.

Number-average molecular weight (Mn) vs conversion
(%) at 82 °C
for AIBN 0.0015 (NK-267)
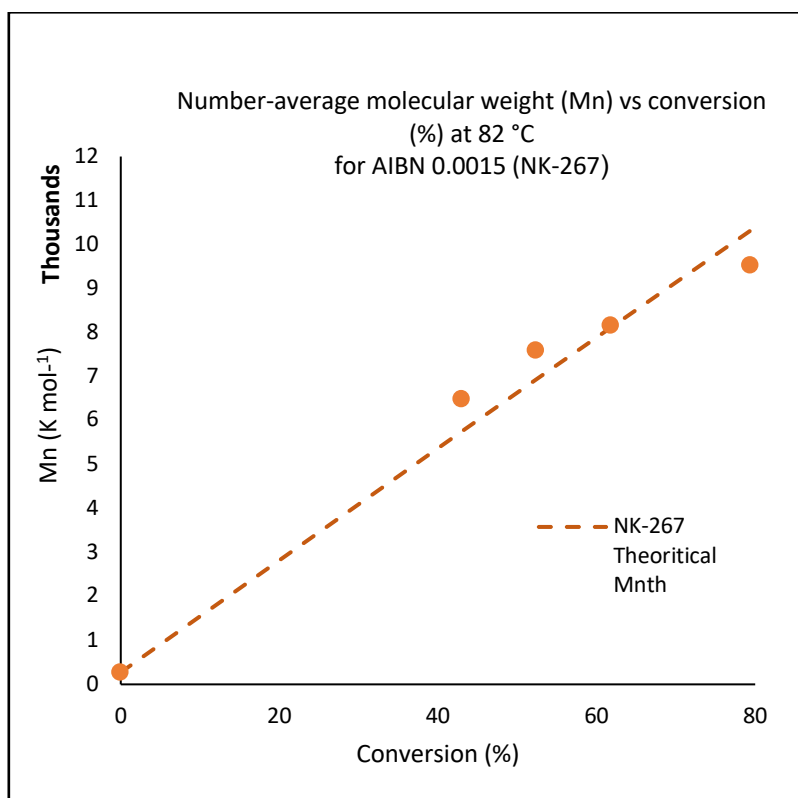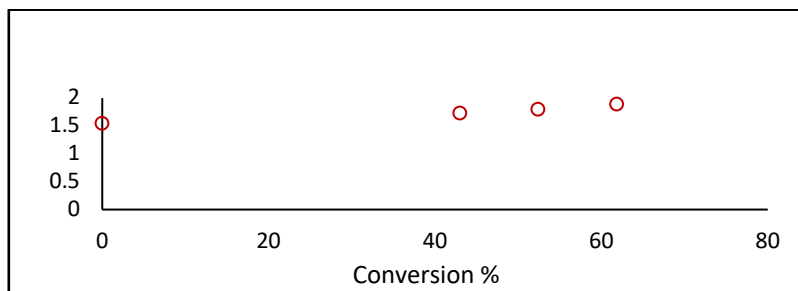
Figure 4. 48 Number-average molecular weight (Mn) vs conversion (%) at 82 °C for AIBN 0.0015 (NK-267), the clear triangle shows the PDI of polymer straight line the theoretical Mn,th line and the circle show the molecular weight obtained from GPC/SEC.

Table 4. 27[1]HNMR and normalized GPC /SEC analysis of RAFT polymerization of N-(4-(4,4,5,5-tetramethyl-1,3,2-dioxaborolan-2-yl)phenyl)acrylamide pinacol ester at 82 °C

267 Polymer	Time (min) at 82 °C.	Conversion Polymer by NMR %	M, nth at (g mol^{-1})	Conversion by GPC %	Mn (g mol^{-1}) experimental by GPC	Mw/Mn
4-ACPBAPEmacro-RAFT [M]$_0$: [DDMAT]$_0$: [AIBN]$_0$, 100: 1: 0.07	15	18	2620	-	-	-
	30	43	5753	45	6488	1.55
	45	52	6927	53	7590	1.74
	60	62	8118	57	8158	1.80
	75	67	8818	-	-	-
	90	72	9335	-	-	-
	120	79	10319	67	9519	1.89

Using anisole as internal standard and 0.0015 M AIBN in DMF after 15, 30, 45,60,90,105, and 120 min. The result shows (table 4.27) a trend in conversion (%) and Mn (g mol^{-1}). ^{1}HNMR shows an increase in conversion (%) from 43 % at 30, min to 79 % at 120 min. GPC/SEC shows an increase in Mn value and low (Mw /Mn or PDI = 1.55 to 1.89) over time.

4.28.7 RAFT polymerization of 4-ACPBAPE Using AIBN (0.0015 M) and Anisole as internal standard

RAFT polymerisation of N-(4-(4,4,5,5-tetramethyl-1,3,2-dioxaborolan-2-yl) phenyl) acrylamide pinacol ester at 82 °C (100 block)

60.30 mg AIBN dissolved in 25 mL and diluted 1 mL in 10 mL (250 times dilution). Anisole 123.00 mL (1.1340 mmol) as internal standard (IS) (10 times dilution) and 36.00 mg DDMAT (0.00987 mmol) diluted 10-fold with IS and added to 1 mL reaction volume. Theoretically, Mn (M, *nth*) is calculated as a function of the initial amount of monomer [M] and DDMAT multiplying by the Mw of monomer and addition of the molecular weight of DDMAT.

M, *nth* = [M] / [DMAT] · Mw M + Mw DDMA

Equation 4. 13 Mn is calculated as a product of M, nth and percent conversion.
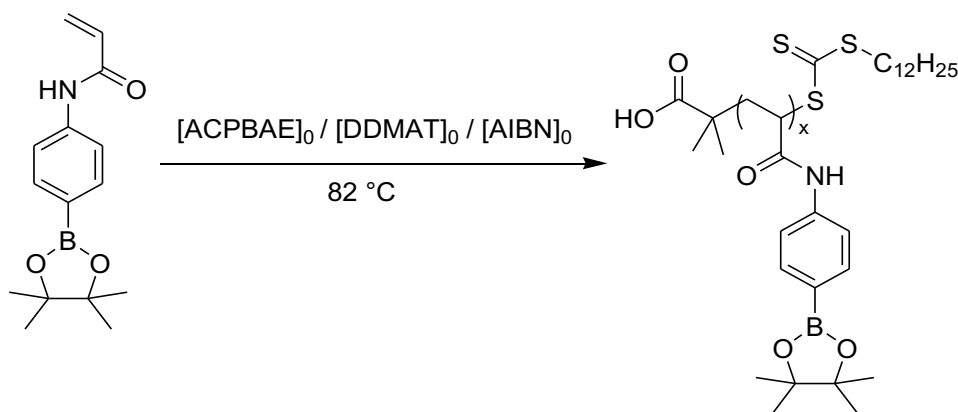
Scheme 4. 44 RAFT polymerization of N-(3-(4,4,5,5-tetramethyl-1,3,2-dioxaborolan-2-yl) phenyl) acrylamide pinacol ester at 82 °C (100 block).

Table 4. 28 Chemical quantities used for polymer 266.

Polymer 266	mg	MW	Mmol	Volume (mL)	mmol / mL (M)	Ratio
AIBN	60.30	164.21	0.3854	1a	0.0015	1
DDMAT	36.00	364.63	0.0987	1b	0.0099	6.6

| 4-ACPBAE | 273.60 | 273.15 | 1.0016 | 1 | 1.0016 | 669 |
| Anisole | 122.63 | 108.14 | 1.0111 | 1c | 0.1 | |

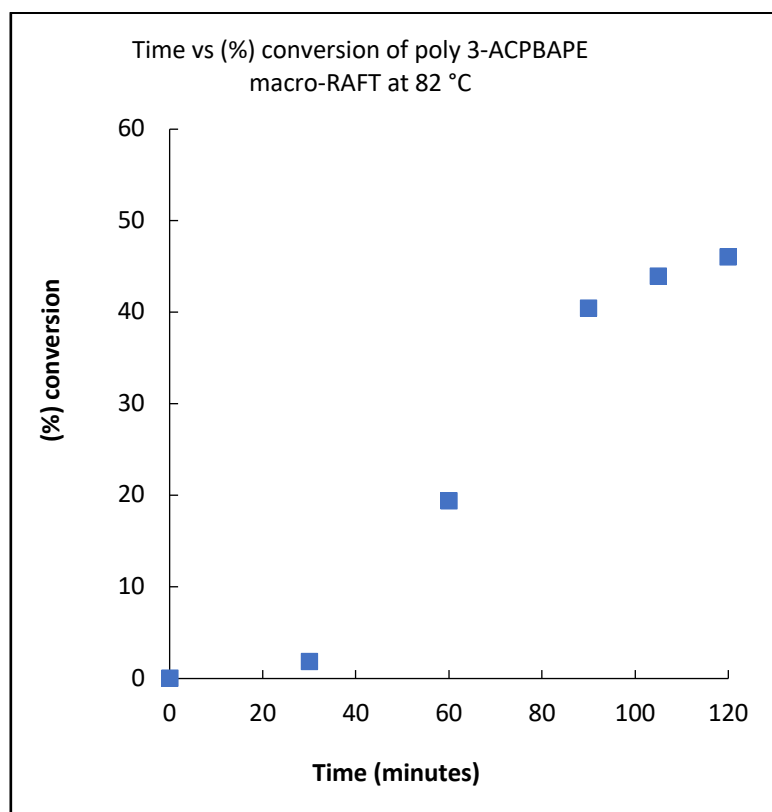DMF at 82 °C, a diluted 250-fold, b diluted 10-fold, c diluted 10-fold.
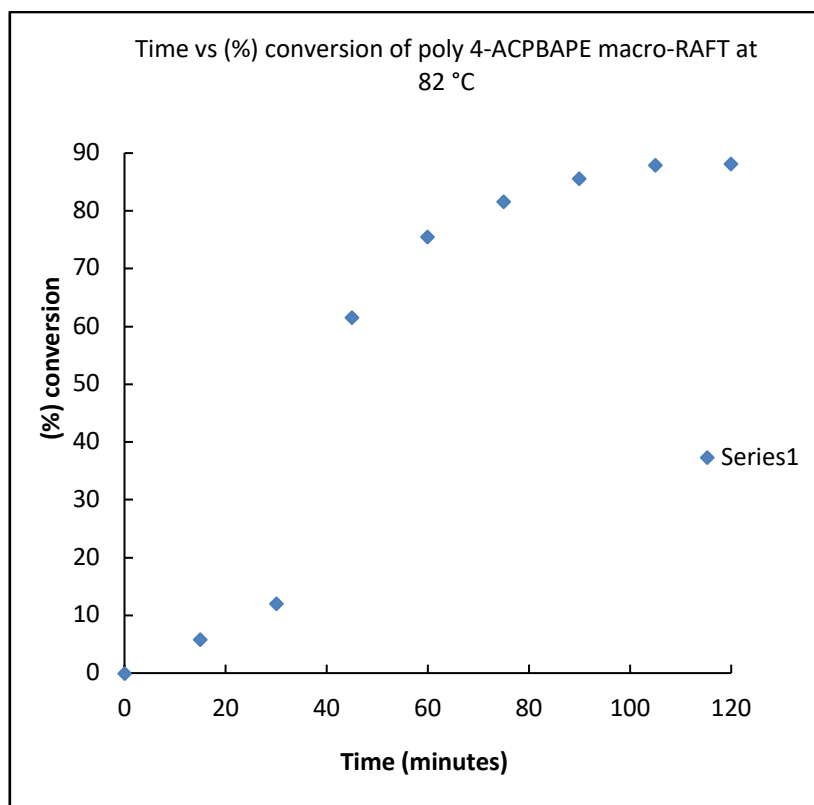
Figure 4. 49monomer conversion (%) vs time plot for the RAFT polymerization of N-(4-(4,4,5,5-tetramethyl-1,3,2-dioxaborolan-2-yl)phenyl)acrylamide pinacol ester is fairly linar (blue dots).

Polymerization conditions $[\text{4-ACPBAPE}]_0$: $[\text{DDMAT}]_0$: $[\text{AIBN}]_0$= 669 : 6.6 : 1, 82 °C. This monomer conversion, suggests that the conversion of monomer can be proceed   88 % using 0.0015 M AIBN at 120 min. After 60 min loss of linearity happened.
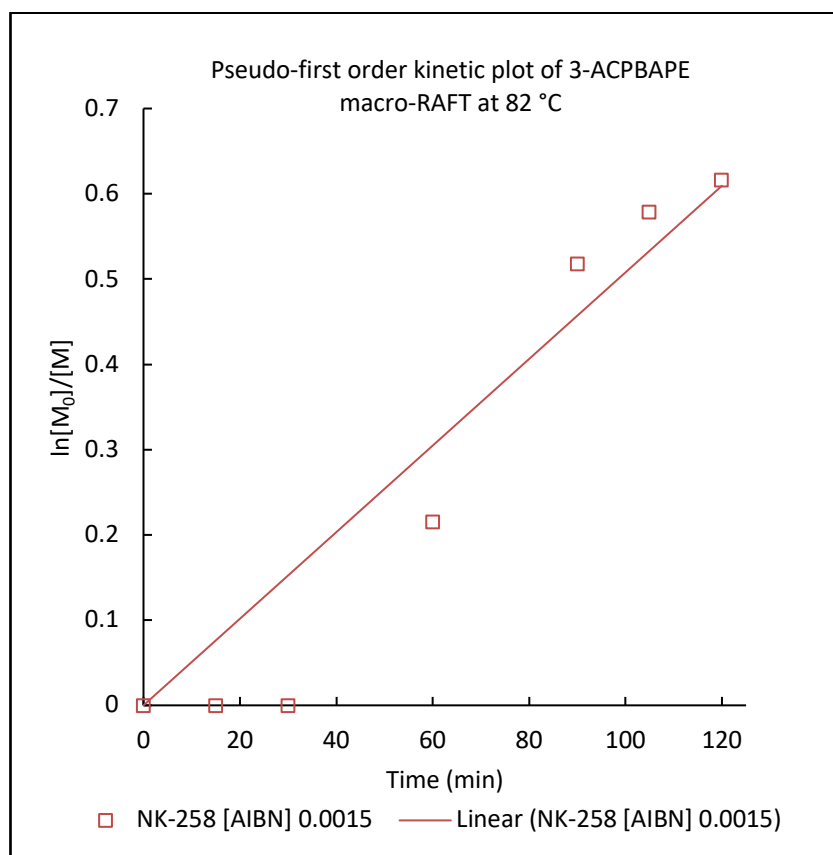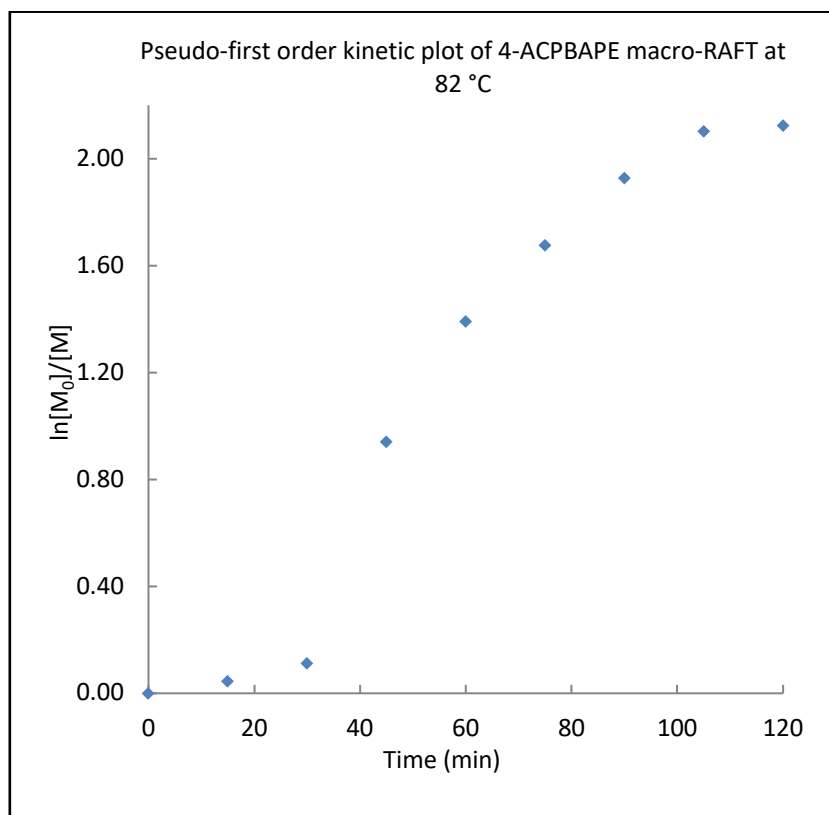
Figure 4. 50 Pseudo-first order kinetic plot of conventional polymerization of 4-ACPBAPE at 82 °C using high AIBN concentration. Polymerization conditions [4-ACPBAPE]$_0$: [DDMAT]$_0$: [AIBN]$_0$= 669 : 6.6 : 1, 82 °C. Pseudo-first order kinetic plot is fairly linear after 60 min the conversion becomes slow.

Slow initiation suggests a decrease in Propagation because of termination reaction or side reaction.
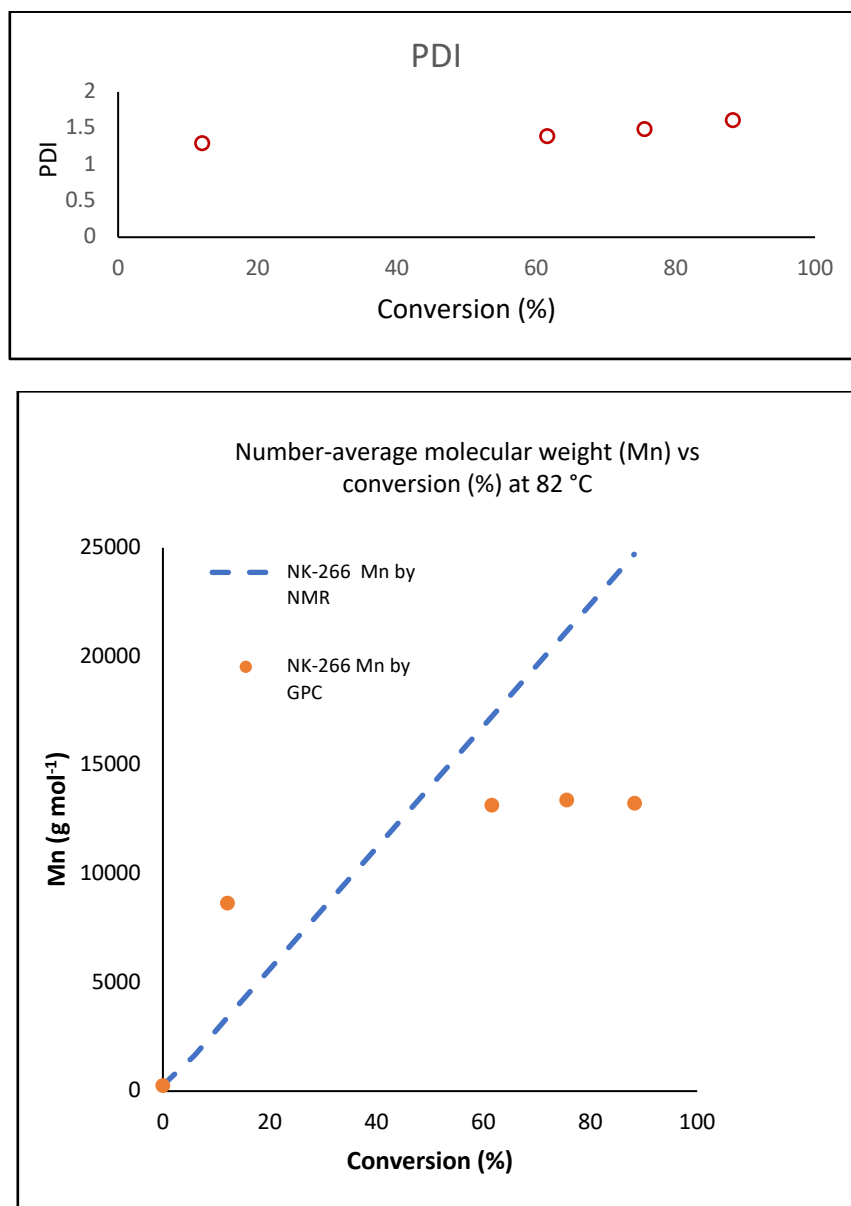
Figure 4. 51 Number-average molecular weight (Mn, g mol^{-1}) vs conversion (%) for N-(4-(4,5,5-tetramethyl-1,3,2-dioxaborolan-2-yl)phenyl)acrylamide pinacol ester.

Macro-RAFT using DDMAT. Polymerization conditions [4-ACPBAPE]$_0$: [DDMAT]$_0$: [AIBN]$_0$= 669 : 6.6 : 1, 82 °C. The graph compares to predicted (Mn, g mol^{-1}) obtained from ^{1}HNMR conversion (points, blue dotted line) vs experimental data obtained by GPC (orange dots). The orange hollow square shows the PDI of the macro-RAFT vs conversion (%).

Theoretical Mn is calculated as a product of M, *nth* and percent conversion using ^{1}HNMR.
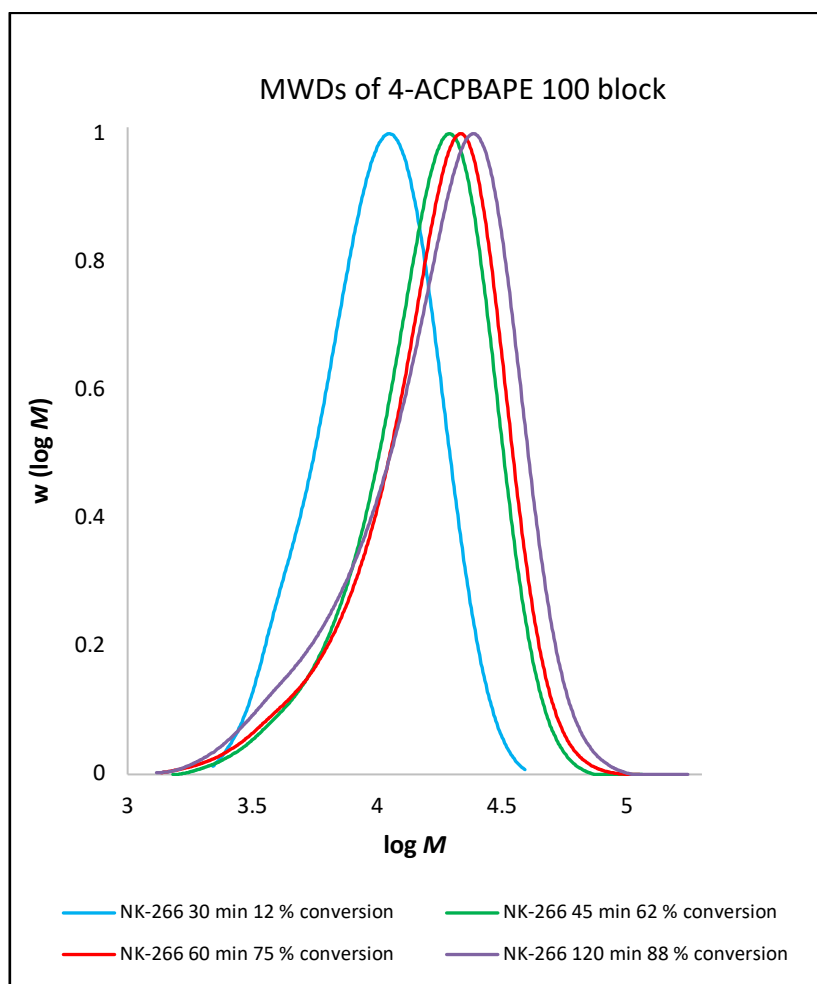
Figure 4. 52 GPC traces as function of monomer conversation for RAFT polymerization of for N-(4-(4,4,5,5-tetramethyl-1,3,2-dioxaborolan-2-yl *(* phenyl)acrylamide pinacol ester. Polymerization conditions [4-ACPBAPE]$_0$: [DDMAT]$_0$: [AIBN]$_0$= 100: 1: 0.15 at 82 °C.

^{1}HNMR and normalized GPC /SEC analysis of RAFT polymerization of *N*-(4-(4,4,5,5-tetramethyl-1,3,2-dioxaborolan-2-yl) phenyl) acrylamide pinacol ester at 82 °C using anisole as internal standard and 0.0015 M AIBN in DMF after 15, 30, 45, 60, 90, 105, and 120 min. The result shows a trend in conversion (%) and Mn (g mol^{-1}).

Table 4. 29 GPC and NMR results monomer conversation for RAFT polymerization of for N-(4-(4,4,5,5-tetramethyl-1,3,2-dioxaborolan-2-yl (phenyl)acrylamide pinacol ester. Polymerization conditions [4-ACPBAPE]$_0$: [DDMAT]$_0$: [AIBN]$_0$= 100: 1: 0.15 at 82 °C.

266 Polymer	Time (min) at 82 °C.	Conversion Polymer by NMR %	M, nth at (g mol^{-1})	Conversion by GPC %	Mn (g mol^{-1}) experimental by GPC	PDI
	15	0	1641	-	-	-
	30	6	3355	30	8639	1.30
	45	12	17235	47	13174	1.40
4- ACPBAPE	60	62	21138	48	13381	1.49
	75	75	22838	-	-	-
	90	82	23982	-	-	-
	105	86	24629	-	-	-
	120	88	24698	47	13249	1.62

The 100 blocks of 4-ACPBAPE shows a conversion of 6 % at 30 min by NMR and by GPC (table 4.25) it shows Mn = 8630 which is 30 % with a PDI = 1.30, growing this macroRAFT at 2 hours has a conversion of 88 % by NMR and Mn = 13249 with a broad PDI = 1.62 this means that the AIBN is consumed however dead chains appear and give average molecular weight smaller due to shorter chains which is visible by long tails of MWDs curves.

4.29 Discussion of section 5

An inhibition period is often observed in RAFT mediated polymerization reaction even though they have been purified. Methyl acrylate shows these effects strongly. The literature suggested that this "inhibition" response is due to the slow fragmentation of formed intermediate radicals. Therefore, the slow rate at the start of the reaction is due to low propagation rate coefficients during the initiation period. The continuation of this inhibition period is approximately equal to the RAFT agent concentration, considering the slow propagation lasts while the initial RAFT agent is

already propagating, after which the rate rises due to a move to a faster propagating radical. This behaviour can explain previous reports of inhibition appearances for long-chain target lengths in RAFT-mediated methyl acrylates (Stenzel, 2008).

The radical concentration is a significant part of the synthesis of well-defined block copolymers understanding that the RAFT agent employed has optimum addition-fragmentation rate constants. The synthesis of the homopolymer, which is the block copolymer's first block, can be affected by termination reactions. Therefore, the dead polymer will contaminate the subsequent block copolymer synthesis. The block copolymerization can then theoretically be generated as a homopolymer with RAFT end groups and dead di- or multiblock copolymer. The final product which was optimised for next section of this chapter can thus consist of the block copolymer with RAFT and functionality and a dead homopolymer. These side-products can become visible in size exclusion chromatography studies revealing low-molecular-weight tailing or high molecular weight shoulders. Consequently, the spectroscopic study can be used to quantify the number of active end groups (Graeme Moad, 2017).

Section 6 of chapter 4

In this part the RAFT polymerization of N-(4-(4,4,5,5-tetramethyl-1,3,2-dioxaborolan-2-yl) phenyl) acrylamide pinacol ester is polymerised using the optimised condition for initiator concentration (0.0015 M) at 70 °C in DMF. This condition is used to synthesis block copolymers using 150, 100, 50, 25 and 13 blocks to calculate livingness and the amount of initiator remaining.

The polymer's controlled/living character was studied at 82 °C, and it gives an idea that control for this monomer could be achieved by varying the ratio of RAFT agent. However, using a lower concentration of AIBN (0.0015 M) giver more livingness. Also, more livingness could be achieved using a lower temperature for polymerization. Therefore, we carried out the RAFT polymerization of 4-ACPBAE in DMF at 70 °C. Several attempts were made to optimize controlled/living character at the high molecular weight of 4-ACPBAE at 70 °C using different blocks of polymer from 150, 100, 50, 25, and 13 blocks.

4.30 RAFT polymerization of N-(4-(4,4,5,5-tetramethyl-1,3,2-dioxaborolan-2-yl) phenyl) acrylamide pinacol ester at 70 °C
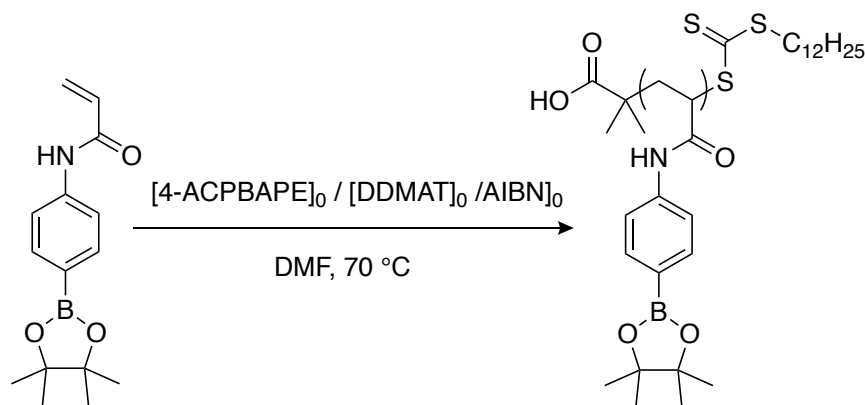
Scheme 4. 45 RAFT polymerization of 4-ACPBAE using $[AIBN]_0$ /$[DDMAT]_0$ / [4-APBAE]$_0$ = 0.2 / 1 / 141

4.30.1 RAFT polymerization of 4-ACPBAE using $[AIBN]_0$ / $[DDMAT]_0$ / $[4\text{-}ACPBAE]_0$ = 0.2 / 1 / 141

A 10 mL stock solution of initiator and RAFT agent in DMF was made by diluting AIBN (61.0 mg, 0.37 mmol) and DDMAT (25.8 mg, 0.07 mmol) 250 and 10 times respectively. The latter stock solution (1 mL) was transferred to 4-APBAE (0.2747 g, 1.0 mmol) and the 1 M monomer solution was heated at 70 °C with periodic sampling for conversion and molecular weight measurements. A 10 mL stock solution of external reference in DMF was made by diluting anisole (0.1255 g, 1.16 mmol) 10 times. Conversion was measured by combining in the NMR tube, 10 µL of the sampled polymerization with 10 µL of the anisole stock solution, and 480 µL of CDCl$_3$. ^{1}HNMR (400 MHz, CDCl$_3$) was used for estimating conversion by comparing the integral of the anisole peak at 3.78 ppm.

4.30.2 RAFT polymerization of 4-APBAE using $[AIBN]_0$ / $[DDMAT]_0$ / $[4\text{-}ACPBAE]_0$ = 0.15 / 1 / 102

A 10 mL stock solution of initiator and RAFT agent in DMF was made by diluting AIBN (61.0 mg, 0.37 mmol) and DDMAT (37.5 mg, 0.09 mmol) 250 , 10 times respectively. The latter stock solution (1 mL) was transferred to 4-APBAE (0.2732 g, 1.0 mmol) and

the 1 M monomer solution was heated at 70 °C with periodic sampling for conversion and molecular weight measurements. A 10 mL stock solution of external reference in DMF was made by diluting anisole (0.1224 g, 1.13 mmol) 10 times. Conversion was measured by combining in the NMR tube, 10 μL of the sampled polymerization with 10 μL of the anisole stock solution, and 480 μL of $CDCl_3$. ^{1}HNMR (400 MHz, $CDCl_3$) was used for estimating conversion by comparing the integral of the anisole peak at 3.78 ppm with the vinyl peak at 5.61 ppm.

4.30.3 RAFT polymerization of 4-APBAE using [AIBN]0 / [DDMAT]0 / [4-APBAE]0 = 0.07 / 1 / 49

A 10 mL stock solution of initiator and RAFT agent in DMF was made by diluting AIBN (61 mg, 0.37 mmol) and DDMAT (282.40 mg, 0.77 mmol) 250 and 10 times respectively. The latter stock solution (1 mL) was transferred to 4-APBAE (0.2735 g, 1.0 mmol) and the 1 M monomer solution was heated at 70 °C with periodic sampling for conversion and molecular weight measurements. A 10 mL stock solution of external reference in DMF was made by diluting anisole (0.1224 g, 1.13 mmol) 10 times. Conversion was measured by combining in the NMR tube, 10 μL of the sampled polymerization with 10 μL of the anisole stock solution, and 480 μL of $CDCl_3$. ^{1}HNMR (400 MHz, $CDCl_3$) was used for estimating conversion by comparing the integral of the anisole peak at 3.78 ppm with the vinyl peak at 5.61 ppm.

4.30.4 RAFT polymerization of 4-APBAE using [AIBN]0 / [DDMAT]0 / [4-APBAE]0 = 0.04 / 1 / 25

A 10 mL stock solution of initiator and RAFT agent in DMF was made by diluting AIBN (61 mg, 0.37 mmol) and DDMAT (142.10 mg, 0.38 mmol) 250 and 10 times respectively. The latter stock solution (1 mL) was transferred to 4-APBAE (0.2735 g, 1.0 mmol) and the 1 M monomer solution was heated at 70 °C with periodic sampling for conversion and molecular weight measurements. A 10 mL stock solution of

external reference in DMF was made by diluting anisole (0.1246 g, 1.11 mmol) 10 times. Conversion was measured by combining in the NMR tube, 10 µL of the sampled polymerization with 10 µL of the anisole stock solution, and 480 µL of CDCl$_3$. ^{1}HNMR (400 MHz, CDCl$_3$) was used for estimating conversion by comparing the integral of the anisole peak at 3.78 ppm with the vinyl peak at 5.61 ppm.

4.30.5 RAFT polymerization of 4-APBAE using [AIBN]0 / [DDMAT]0 / [4-APBAE]0 = 0.02 / 1 / 13

A 10 mL stock solution of initiator and RAFT agent in DMF was made by diluting AIBN (61 mg, 0.37 mmol) and DDMAT (142.10 mg, 0.38 mmol) 250 and 10 times respectively. The latter stock solution (1 mL) was transferred to 4-APBAE (0.2735 g, 1.0 mmol) and the 1 M monomer solution was heated at 70 °C with periodic sampling for conversion and molecular weight measurements. A 10 mL stock solution of external reference in DMF was made by diluting anisole (0.1246 g, 1.11 mmol) 10 times. Conversion was measured by combining in the NMR tube, 10 µL of the sampled polymerization with 10 µL of the anisole stock solution, and 480 µL of CDCl$_3$. ^{1}H NMR (400 MHz, CDCl$_3$) was used for estimating conversion by comparing the integral of the anisole peak at 3.78 ppm with the vinyl peak at 5.61 ppm. And the vinyl peak at 5.61 ppm.

Estimated using the integral of anisole at 3.78 ppm relative to the vinyl integral at 5.61 ppm.

$$Mn, \text{th} = \left[\left(\frac{[4-ACPBAPE]_0}{[DDMAT]_0} \right) \times MW_{4-ACPBAPE} \times conversion \right] + MW_{[DDMAT]}$$

Equation 4. 14 Avrage theoritical molecular weight of RAFT polymer (Mn,th) is calculated from the above equation.It is a ratio of monomer concentration and RAFT agent multiplied by molecular weight of monomer and percentage conversion (by NMR or gravity) added to the

Equation (4.14) represents the calculation of theoretical molecular weight of the polymer after obtaining the percentage conversion by NMR or gravimetry.

Equation (4.15) calculates the livingness of macroRAFT. It is calculated from the initial concentration of RAFT gent (DDMAT) divided by the sum of RAFT agent and initiator considering the initiator efficiency in the solvent used and temperature of the reaction.

$$L = \frac{[\text{CTA}]_0}{[\text{CTA}]_0 + 2 \times f \times [\text{I}]_0 \times (1 - e^{-k_d t}) \times \left(1 - \frac{f_c}{2}\right)}$$

Equation 4. 15 The fraction of living chains (L).

In this formula (equation 4.15) f is the radical effecicy and fc is is used for bimolecular termination of AIBN, as one AIBN gives two 3° carbon radical (Introduction to RAFT).

Initiator efficiency usually is depending on solvent and temperature of polymerisation. The rate is usually expressed as half life time ($t_{1/2}$) where $t_{½}$ is ln2 / k_d = 0.693 / k_d. The rate constant K_d (decomposition rate constant, s^{-1}) changes with temperature according to Arrhenius equation $Kd = (-Ae)^{Ea/RT}$. Equation (4.16) calculaes the amount of intiator remaning the polymerisation solution.

$$m_{\text{AIBN}_{remaining}} = m_{\text{AIBN}_{Total}} \times 2fe^{-k_d t} \times \left(1 - \frac{f_c}{2}\right)$$

Equation 4. 16 The total weight of AIBN at time t0 considering the weight of AIBN added (mAIBN added) + the weight of AIBN remaining (mAIBN remaining) from the previous block after 24h.

($m_{\text{AIBN remaining}}$ = $m_{\text{AIBN total}}$ x $2fe^{-kdt}$ x(1-f_c/2) with f=0.5 for 2 radicals, f_c=0, k_d = 1.92 10^{-5} s^{-1})

AIBN remaining (equation 4.16) is important in calculation for adding the next block as it shows how much initiator is consumed and how much is remaining.

Table 4. 30 Experiment list for 150. 100. 50. 25 and 13 blocks RAFT polymerization of 4-ACPBAPE, using RAFT agent DDMAT Constant, AIBN concentration. a diluted 250-fold, b diluted 10-fold, c diluted 500-fold

Experiment	[AIBN]$_0$ in DMF reaction		[DDMAT]$_0$ in DMF		[4-ACPBAPE]$_0$ in DMF		[Anisole] in DMF ext NMR	
	mg / mmol	M	mg / mmol	M	mg / mmol	M	mg / mmol	mmol 0.5 mL^{-1}
[AIBN]$_0$ / [DDMAT]$_0$ / [4-ACPBAPE]$_0$ = 0.2 / 1 / 141	61.50/0.3745^a	0.00150	**25.80/0.0708^b**	0.00708	274.5/1.0005	1.00049	125.6 / 1.1615^c	0.00232
[AIBN]$_0$ / [DDMAT]$_0$ / [4-ACPBAPE]$_0$ = 0.15 / 1 / 102	61.00/0.3715^a	0.00149	**35.70/0.0979^b**	0.00979	273.2/1.0002	1.00018	122.4 / 1.1319^c	0.00226
[AIBN]$_0$ / [DDMAT]$_0$ / [4-ACPBAPE]$_0$ = 0.07 / 1 / 49	59.98/0.3652^a	0.00146	**74.22/0.2035^b**	0.02035	273.9/1.0027	1.00275	120.6 / 1.1152^c	0.00223
[AIBN]$_0$ / [DDMAT]$_0$ / [4-ACPBAPE]$_0$ = 0.04 / 1 / 25	61.00/0.3715^a	0.00148	**142.10/0.3897^b**	0.03897	273.50/1.0012	1.00128	124.60/1.1152^c	0.00461
[AIBN]$_0$ / [DDMAT]$_0$ / [4-ACPBAPE]$_0$ = 0.02 / 1 / 13	61.00/0.3715^a	0.00148	**282.40/0.7745^b**	0.07745	273.50/1.0012	1.00128	122.40 /1.1319^c	0.11400
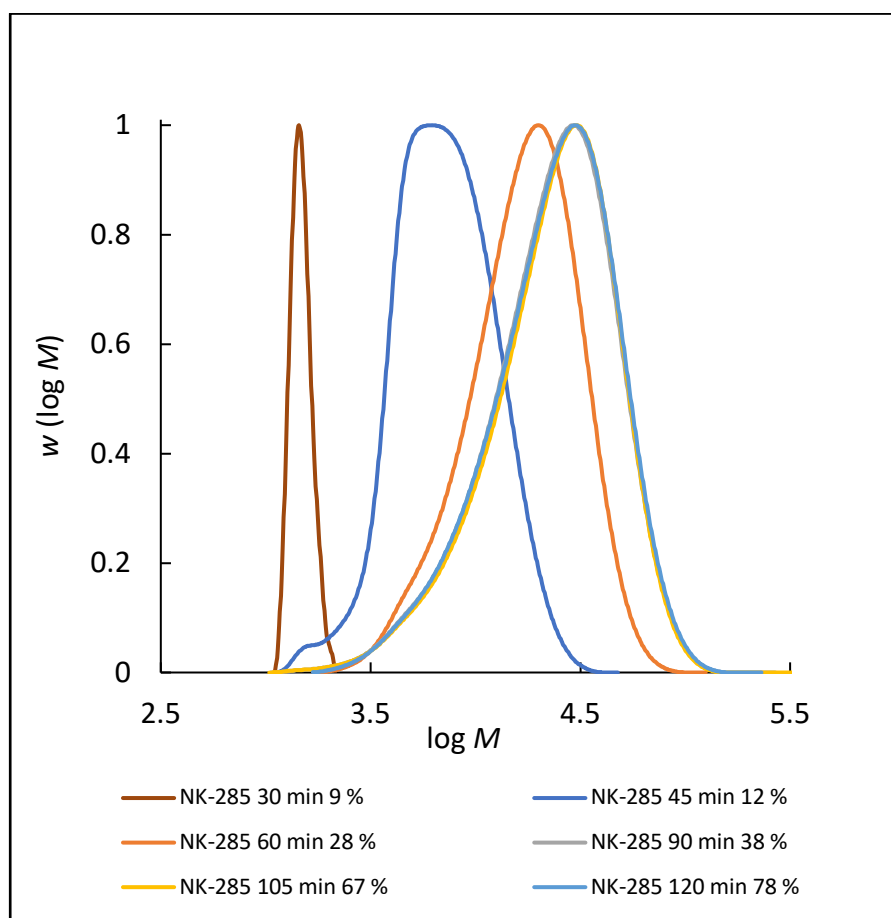
Figure 4. 53 MWDs curve of RAFT polymerization of 4-ACPBAPE using $[AIBN]_0$ / $[DDMAT]_0$ / $[4\text{-}ACPBAPE]_0$ = 0.2 / 1 / 141. Conversion is calculated using anisole as external standard by ^{1}HNMR.

GPC obtains the MWDs curves (Figure 4.53) for 141 blocks of macroRAFT show the conversion at 30 min up to two hours. As per results in table 4.31 and figure 4.53 (NMR) for the 141 blocks of the copolymer, it was observed that the conversion is fast the Mn,*th* = 1150 and Mn = 1450 at 30 min which correlates with each other. The living character of polymer (%) gradually decreases as the macroRAFT grows. Also, the AIBN is only 73 % consumed after 2 hours (calculated) which suggest that there is still a considerable amount of initiator remaining. As for RAFT, the amount of initiator must remain minimum, therefore at 2 hour the maximum Mn is not reached due to short chains initiated by AIBN.
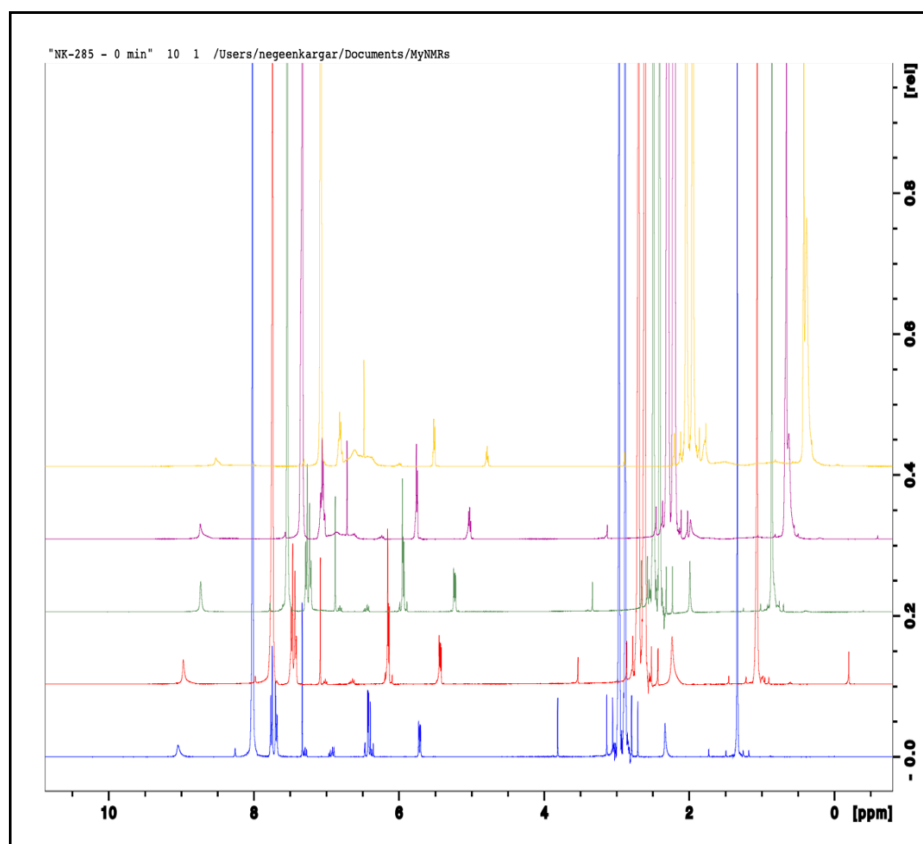
Figure 4. 54 ^{1}HNMR of the RAFT polymerization of 4-ACPBAPE using [AIBN]$_0$ / [DDMAT]$_0$ / [4-ACPBAPE]$_0$ = 0.2 / 1 / 141. Conversion is calculated using anisole as external standard.

For the RAFT polymerization of 44-ACPBAPE using [AIBN]$_0$ / [DDMAT]$_0$ / [4-ACPBAPE]$_0$ = 0.2 / 1 / 141. At 30 min (Table 4.31) the polymer start forming and after 90 min the chain does not grow which means the conversion is low and the other chains formed are not living. Chains by propagating radicals undergoing chain transfer to polymer fractions are observed as well as a degree of livingness. Nevertheless, polymerisation with 150 blocks leads to broadening of the molecular weight distribution and a *Đ* = 1.64. To prevent such side reactions, the polymerization conditions were optimized using a constant amount of AIBN, and monomer only variable amount of RAFT agent in presence of anisole added as external standard for conversion calculation by ^{1}H NMR.

Table 4. 31 RAFT polymerization of 1 M 4-ACPBAPE at 70 °C using DDMAT and 0.00146 M AIBN, $[AIBN]_0 / [DDMAT]_0 / [4\text{-}ACPBAPE]_0 = 0.2 / 1 / 141$

285 Polymer	Time (min) at 70 °C	Conversion by ^{1}H NMR (%)	Mn,th by ^{1}H NMR (g mol^{-1})	Mn by GPC (g mol^{-1})	Đ^c	L (%)	AIBN Remaining (%)
NK-285 -150	30	3	1150	1450	1.01	98.4	92.5
	45	5	2700	6200	1.33	97.7	88.9
[AIBN] / [DDMAT] / [4-ACPBAPE]	60	18	6550	13850	1.44	97.0	85.5
0.2 / 1 / 141	90	38	15400	17300	1.64	95.8	79.1
	105	67	26250	17550	1.63	95.2	76.1
	120	78	30500	17800	1.61	94.6	73.2

Monomer conversion was carried out with short (DP ≈ 150, 100, 50, 25 and 13) at high to very high monomer conversions and low fraction of dead chains. In the synthesis of with short (DP ≈ 13) and, at high to very high monomer conversions and low fraction of dead chains obtained.
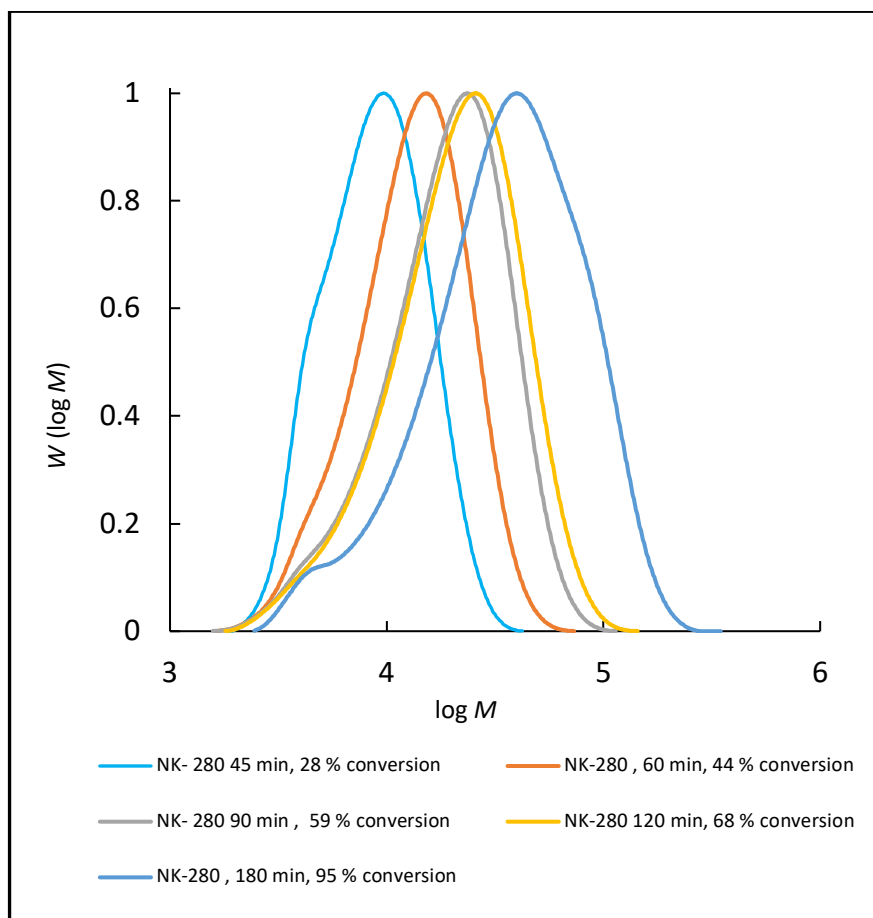
Figure 4. 55 Normalized GPC/SED MWDs curves of RAFT polymerization RAFT polymerisation of 4-ACPBAPE of N-(4-(4,4,5,5-tetramethyl-1,3,2-dioxaborolan-2-yl) phenyl) acrylamide pinacol ester RAFT polymerization of 1 M 4-ACPBAPE.

RAFT polymerization of N-(4-(4,4,5,5-tetramethyl-1,3,2-dioxaborolan-2-yl) phenyl) acrylamide pinacol ester.

RAFT polymerization of 1 M 4-ACPBAPE using DDMAT and 0.00146 M AIBN, $[AIBN]_0$ / $[DDMAT]_0$ / $[4\text{-}ACPBAPE]_0$ = 0.15 / 1 / 102 at 70 °C using Anisole as internal standard and 0.0015 M AIBN in DMF after overtime interval, at 45 min the polymer reaches 28 % conversion, as well 44 % and 59 % , 68 %, and 95 % conversion at 60, 90, 120 and 180 min (table 4.32) respectively. The GPC /SEC curves show a slightly bimodal peak, which is carried out to the last one; however, the degree of livingness is greater than DP = 150 (Figure 4.55). GPC

obtains the MWDs curves (Figure 4.54) for 100 blocks of macroRAFT show the conversion at 45 min up to three hours. The living character of polymer (%) remains better than the 141 blocks (95 %) macroRAFT grows. Also, the AIBN is 73 % consumed after 2 hours which suggest that there is still a considerable amount of initiator remaining.
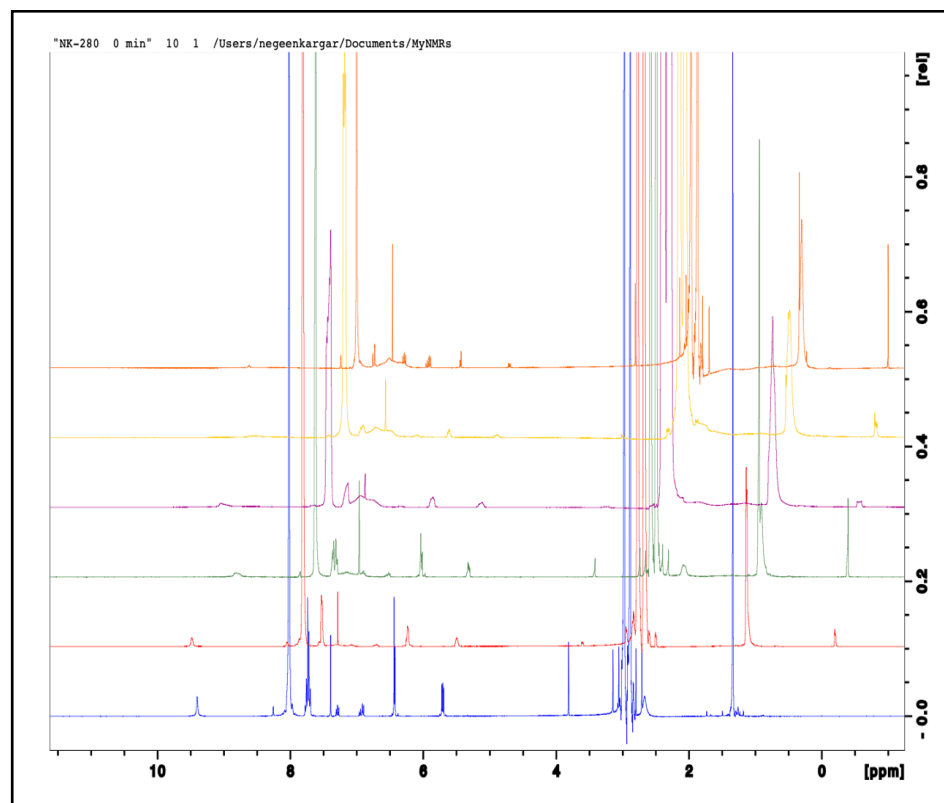
Figure 4. 56 ^{1}HNMR of the RAFT polymerization of 4-ACPBAPE using [AIBN]0 / [DDMAT]0 / [4-ACPBAPE]0 = 0.07 / 1 / 49. Conversion is calculated using anisole as external standard.

Table 4. 32 RAFT polymerization of 1 M 4-ACPBAPE at 70 °C using DDMAT and
0.00146 M AIBN, $[AIBN]_0$ / $[DDMAT]_0$ / $[4\text{-}ACPBAPE]_0$ = 0.15 / 1 / 102

280 Polymer	Time (min) at 70 °C	Conversion by ^{1}H NMR^a (%)	$M_{n,th}$ by ^{1}H NMR (g mol $^{-1}$)	M_n by GPC (g mol $^{-1}$)	Đ	L (%)	AIBN Remaining (%)
NK-280 -100	45	19	5650	7650	1.30	98.3	88.9
[AIBN] /	60	28	8200	10800	1.40	97.8	85.5
[DDMAT] / [4-	90	54	15450	14450	1.54	96.9	79.1
ACPBAPE]	120	68	19350	15700	1.61	96.1	73.2
0.15 / 1 / 102	180	96	27150	23750	1.97	94.6	62.6

Using Anisole as internal standard and 0.0015 M AIBN in DMF after over time
interval, reaching a conversion of 89 %. RAFT polymerization of 1 M 4-APBAE at
70 °C using DDMAT and 0.0015 M AIBN, [AIBN]0 / [DDMAT]0 / [4-APBAE]0 = 0.07
/ 1 / 49 , MWDs curves in figure 4.57 shows up that at 90 min the polymer grows
around 50%.
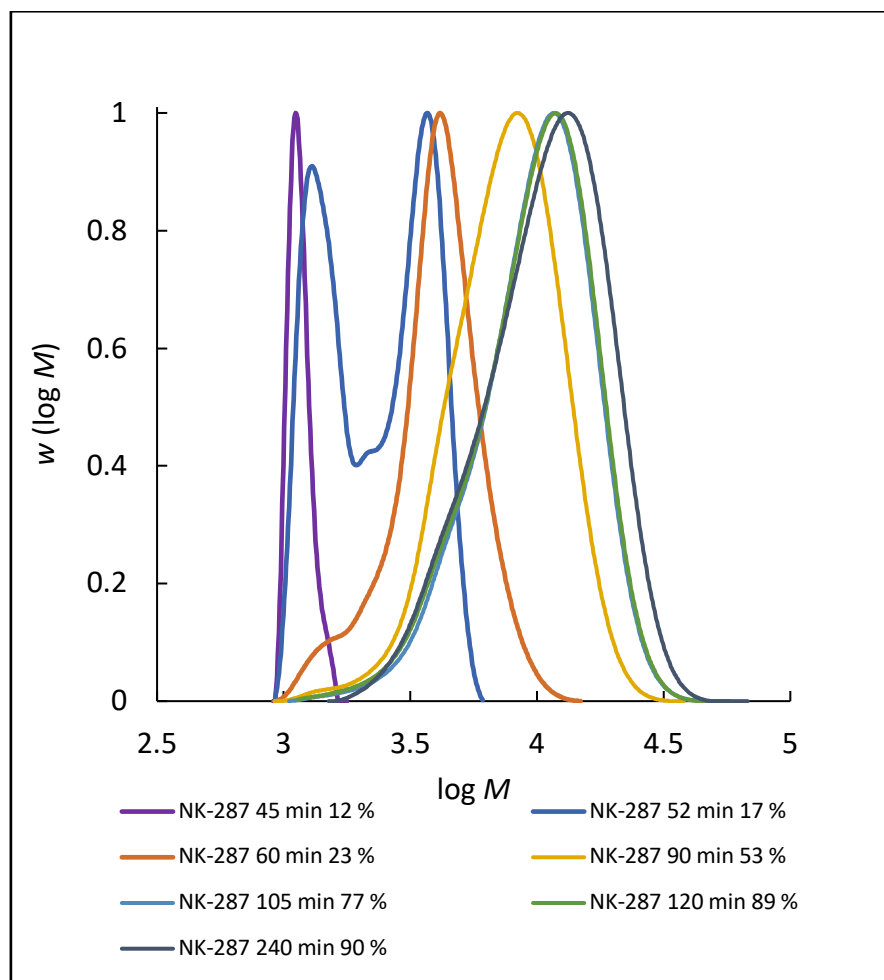
Figure 4. 57 Normalized GPC/SED MWDs curves of RAFT polymerization of N-(4-(4,4,5,5-tetramethyl-1,3,2-dioxaborolan-2-yl)phenyl)acrylamide pinacol ester at 70 °C.

Normalised MWDs curves of 50 blocks macroRAFT of 4-ACPBAPE shows that the chain starts growing slower at 45 min (12 %) conversion, and at 52 min it shows a bimodal peak which is part of growing the macroRAFT (Figure 4.57) At 2 hour the conversion is 89% with 98 % livingness, still AIBN (%) remaining is 73 % (Table 4.33).
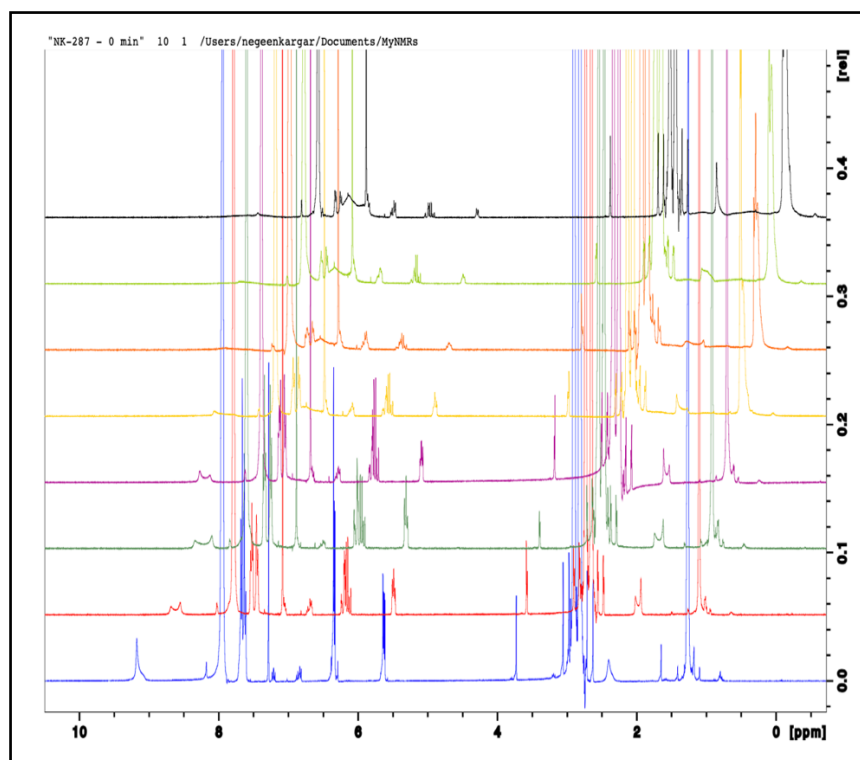
Figure 4. 58 ^{1}HNMR of RAFT polymerization of 1 M 4-APBAE at 70 °C using DDMAT and 0.0015 M AIBN, [AIBN]0 / [DDMAT]0 / [4-APBAE]0 = 0.07 / 1 / 49 , anisole used as external standard for conversion calculation over time from bottom to top at 45 min to 240 min).

The results of macroRAFT (50 blocks), (Table 4.29) shows that the longer the time of polymerisation the more AIBN is consumed (240 min, 53 %). The molecular weight by GPC correlates to conversion by NMR up to 60 min, this means the livingness is improved, however shorter DP would be more ideal for this large monomer (Figure 4.59, Table 4.33).

Table 4. 33 RAFT polymerization of 1 M 4-ACPBAPE at 70 °C using DDMAT and 0.00146 M AIBN, [AIBN]$_0$ / [DDMAT]$_0$ / [4-ACPBAPE]$_0$ = 0.07 / 1 / 49

287 Polymer	Time (min) at 70 °C	Conversion Polymer % by ^{1}H NMR	$M_{n,th}$ at (g mol^{-1})	M_n (g mol^{-1}) by GPC	Đ	L (%)	AIBN Remaining (%)
ACPBAPEmacro-RAFT	45	12	1720	1150	1.01	99.2	88.9
	52	17	2350	2050	1.25	99.0	87.3
	60	23	3200	3600	1.18	98.9	85.5

154

[AIBN] /	90	53	7300	6600	1.27	98.4	79.1
[DDMAT] / [4-ACPBAPE]	105	77	10650	8500	1.31	98.2	76.1
0.07 / 1 / 49	120	89	12220	8350	1.32	98.0	73.1
	240	90	12400	9100	1.35	96.7	53.5
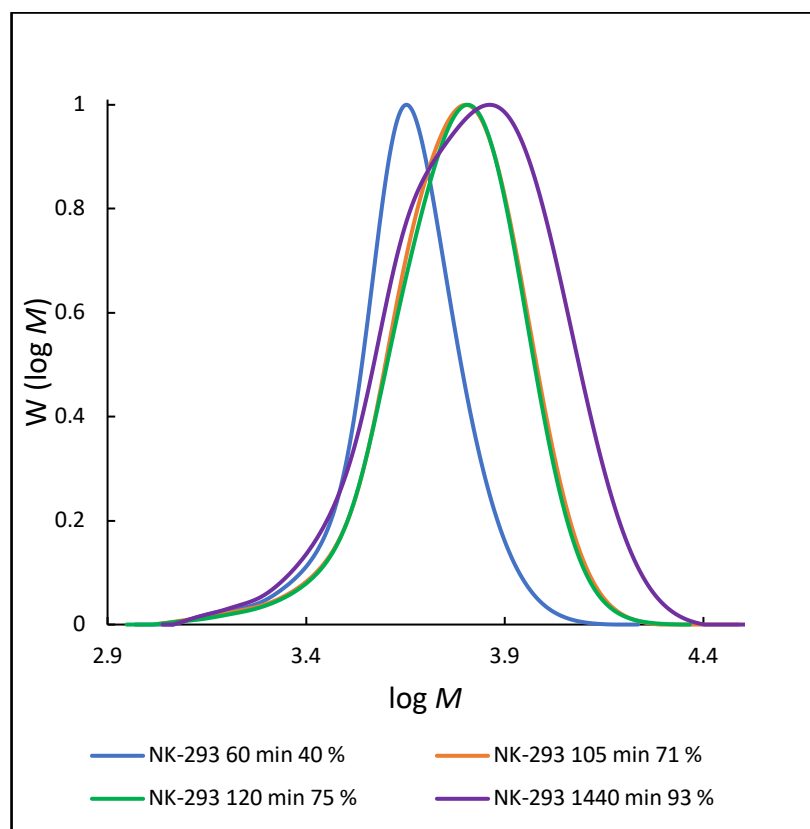
Figure 4. 59 Normalized GPC/SED MWDs curves of RAFT polymerization of N-(4-(4,4,5,5-tetramethyl-1,3,2-dioxaborolan-2-yl)phenyl)acrylamide pinacol ester at 70 °C using

Shorter DP for macroRAFT was carried out using the same condition with variable RAFT agent and anisole as internal standard and 0.0015 M AIBN for NMR in DMF after over time interval (Table 4.33). At 105 min the polymer reaches 75 % conversion, as well % and 76 % AIBN remaining and 99 % livingness. When the reaction was left for 24 hours to see the full AIBN consumption, it was observed that the AIBN remained only 2.3 % and the chain conversion by NMR (Mn,*th* = 6900) compared to GPC, Mn = 5800 with a PDI= 1.25 was achieved.
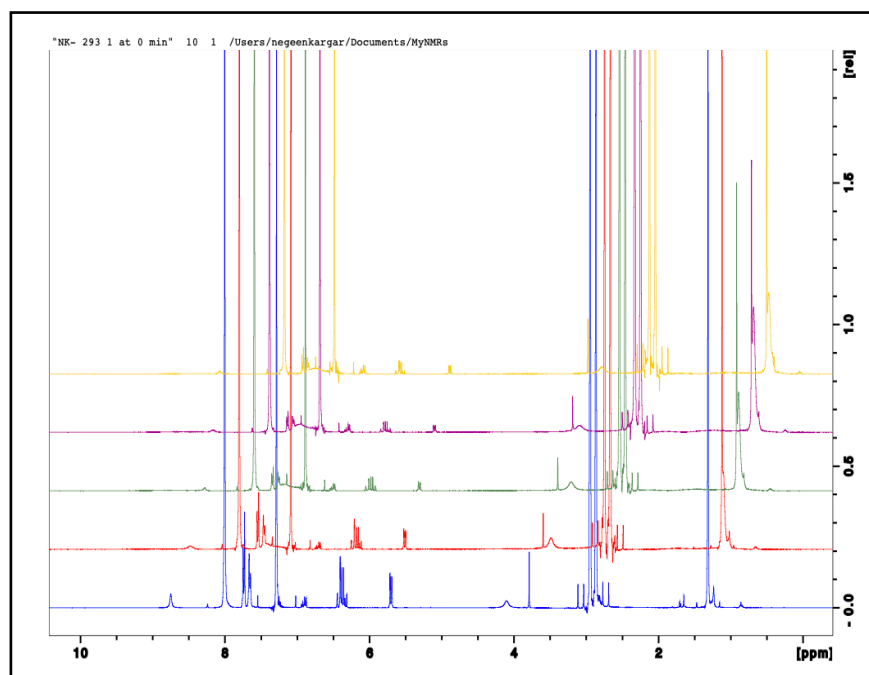
Figure 4. 60 ^{1}HNMR of RAFT polymerization of 1 M 4-APBAE at 70 °C using DDMAT and 0.0015 M AIBN, $[AIBN]_0 / [DDMAT]_0 / [4\text{-}ACPBAPE]_0 = 0.04 / 1 / 25$

Table 4. 34 RAFT polymerization of 1 M 4-ACPBAPE at 70 °C using DDMAT and 0.00146 M AIBN, $[AIBN]_0 / [DDMAT]_0 / [4\text{-}ACPBAPE]_0 = 0.04 / 1 / 25$

293 Polymer	Time (min) at 70 °C	Conversion by 1H NMRa (%)	Mn,th by ^{1}H NMRb (g mol $^{-1}$)	Mn by GPCc (g mol $^{-1}$)	Đc	Ld (%)	AIBN Remaining (%)
[AIBN] / [DDMAT] / [4-ACPBAPE] 0.04 / 1 / 25	60	40	3010	4300	1.11	99.4	85.5
	105	71	5300	5400	1.16	99.1	76.1
	120	75	5600	5500	1.16	98.8	73.1
	1440	93	6900	5800	1.25	96.4	2.3

The RAFT agent ratio was even further changed to obtain DP =13 (Table 4.35). By this, the amount of AIBN remaining a significant decrease (85 %) at one hour, and the conversion was high by NMR (46%). The reaction was left for 24 hours (Figures 4.60, 4.61 (NMR conversion) shows that at 24 hours with the total consumption of AIBN a polymer with Mn = 3300 (Mn,th =3900) is obtained with narrow PDI = 1.21

156

which is acceptable for RAFT polymerisation. Therefore, the macroRAFT of 4-ACPBAPE was successfully optimised and can be further chain extended with DMA or a short chain of 4-ACPBAPE.
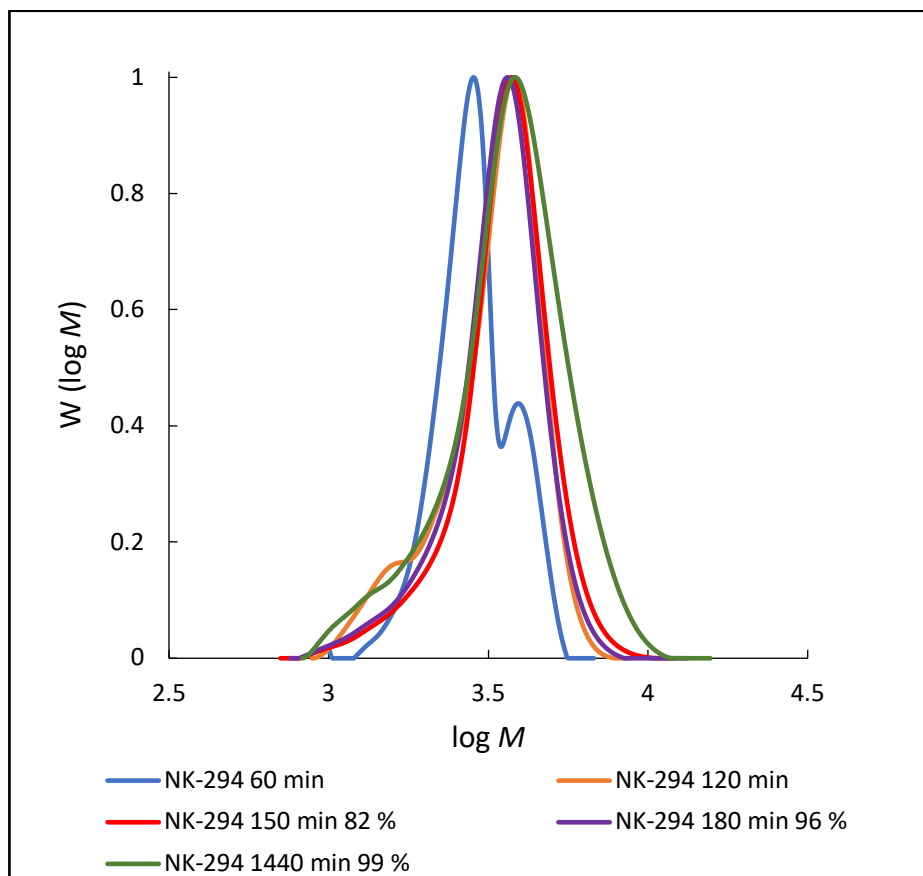
Figure 4. 61 Normalized GPC/SED MWDs curves of RAFT polymerization of N-(4-(4,4,5,5-tetramethyl-1,3,2-dioxaborolan-2-yl)phenyl)acrylamide pinacol ester at 70 °C using Anisole as internal standard and 0.0015 M AIBN in DMF after over time interval, full conversion of the polymer reached over 24 h.
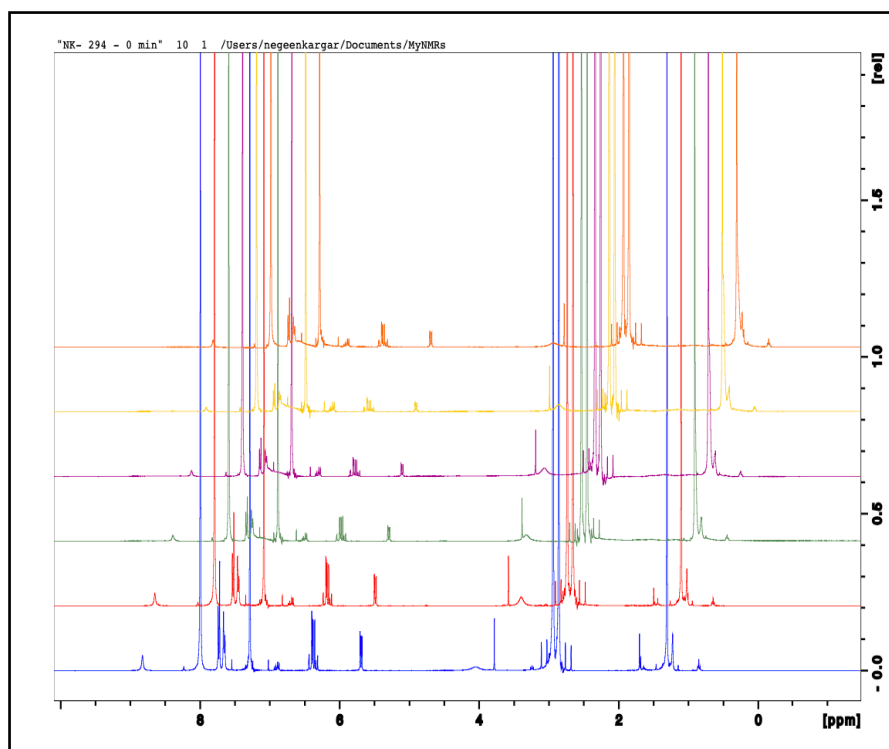
Figure 4. 62 ^{1}HNMR of RAFT polymerization of 1 M 4-APBAE at 70 °C using DDMAT and 0.0015 M AIBN, $[AIBN]_0 / [DDMAT]_0 / [4\text{-}ACPBAPE]_0 = 0.02 / 1 / 13$

The NMR conversion shows disappearance of vinyl peaks by growing chain f polymer at region of (6.5 -7.5 ppm)

Table 4. 35 RAFT polymerization of 1 M 4-ACPBAPE at 70 °C using DDMAT and 0.00146 M AIBN, $[AIBN]_0 / [DDMAT]_0 / [4\text{-}ACPBAPE]_0 = 0.02 / 1 / 13$

294 Polymer	Time (min) at 70 °C	Conversion by ^{1}H NMR (%)	$M_{n,th}$ by ^{1}H NMR (g mol^{-1})	M_n by GPC (g mol^{-1})	$Đ^c$	L (%)	AIBN Remaining (%)
P 294- 13	60	46	1800	2350	1.08	99.7	85.5
[AIBN] /	120	72	2800	2600	1.15	99.4	73.1
[DDMAT] / [4-	150	82	3250	3300	1.12	99.3	67.6
ACPBAPE]	180	96	3800	3100	1.12	99.2	62.6
0.02 / 1 / 13	1440	99	3900	3300	1.21	98.1	2.3
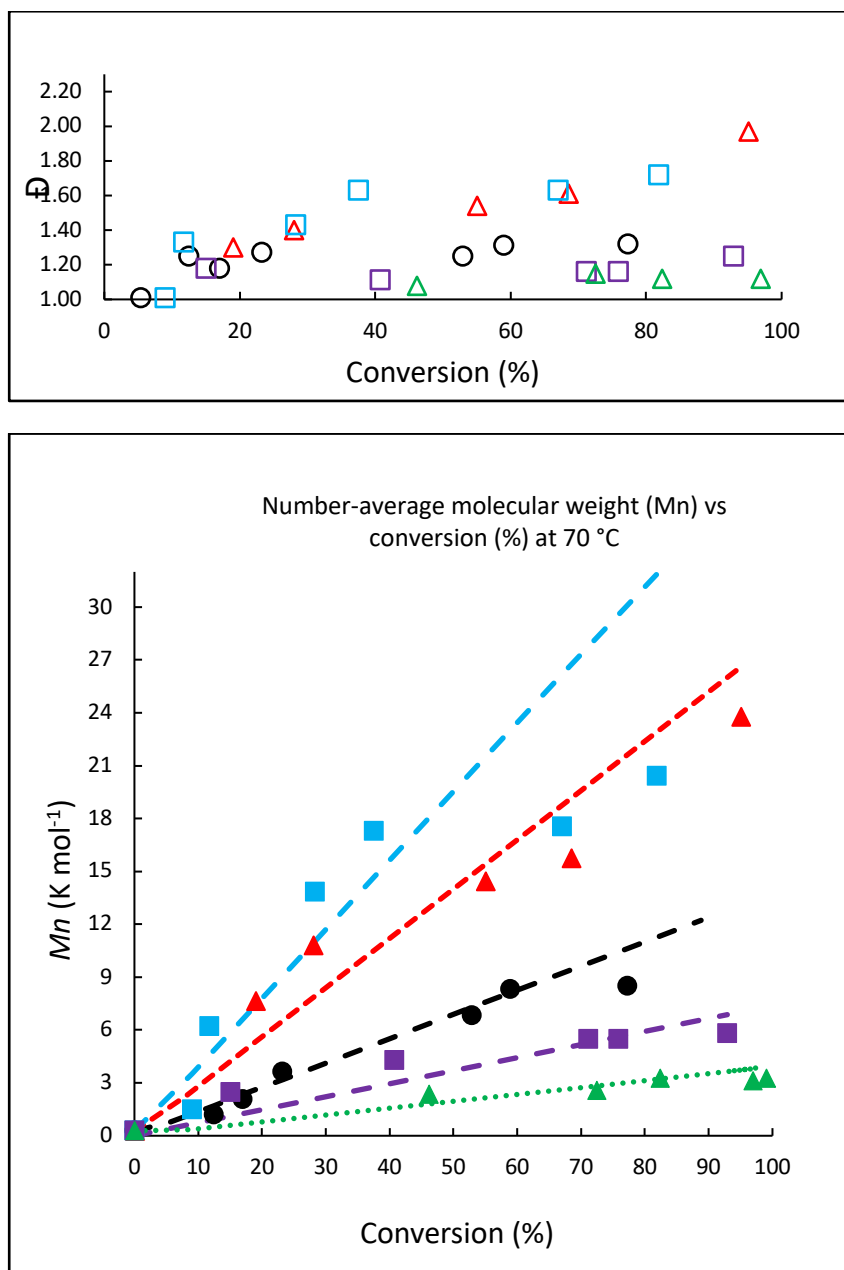
Figure 4. 63 a), PDI vs conversion (b)Number-average molecular weight (Mn) vs conversion (%) at 70 °C. Colour codeing are as follows: blue 150, red 100, black 50, purple 25 and green 13 blocks of polymers.

The monomer conversions determined by proton nuclear magnetic resonance (^{1}H NMR) spectroscopy in the presence of standard external anisole.

From the literature of the RAFT polymerization mechanism, the $[M]_0/[CTA]_0$ molar ratio has a significant influence on the chain and livingness of the polymer.

An ideal concentration of monomer or RAFT agent is required and is crucial to gain suitable molecular weight (Mw) and narrow molecular weight distributions (Mw/Mn) of polymers. Many different effects of the molar ratio of the AIBN, monomer to the RAFT agent, monomer concentration, and reaction time on the polymerization behaviours carried out to improve the controllability of the molecular weight and molecular weight distribution of the obtained for 4-ACPBAPE. The feature of the controlled polymerization proven by the first-order kinetics, a linear increase of the molecular weight with the monomer conversion, and a successful chain-extension experiment. This work provides a new way for chain extension and blocks copolymers of 4-ACPBAPE sugar sensitive polymer (Figure 4.64).
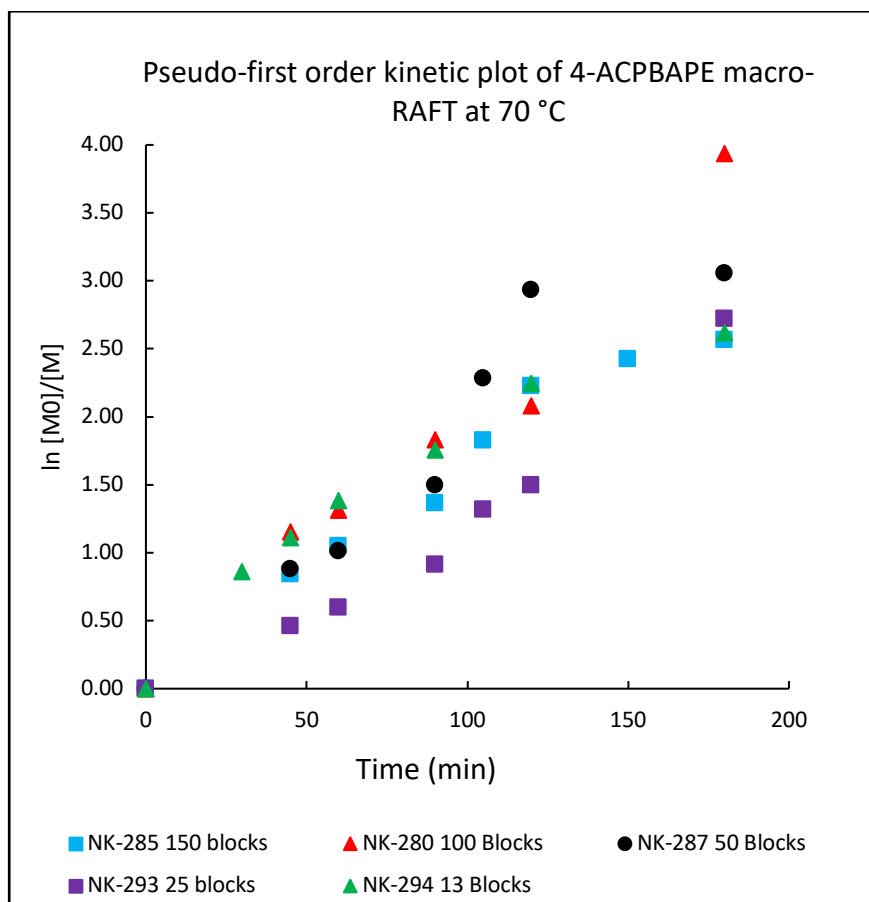
Figure 4. 64 Pseudo-first order kinetic plot of 4-ACPBAPE macro-RAFT at 70 °C

The first-order kinetics of $\ln([M]_0/[M])$ as a function of polymerization time for AIBN initiated RAFT polymerization under constant concentration of AIBN and monomer with different concentration of RAFT agent show that the polymerisation profiles of plots were approximately linear, indicating the stability of the number of the active centres during the polymerization process.

Rate measurements or the overall rate of polymerization provides information about the mechanism of polymerization. However, polymerization rate measurements can be very challenging, and even time-dependent monomer conversion carried out. Different parameters and coefficients are involved in the reaction; for example, the size of the equilibrium constant, which through time-dependent monomer conversion, the polymerization can estimate. The low RAFT agent and the high number of blocks lead to a period of the steady state,

which suggests that propagating radical concentration does not remain constant in the reaction. The reason for not having a constant propagating radical concentration can be few, for example, change of rate coefficient or a more extended steady-state condition, which can make the polymerization slow or other reason could be RAFT and initiator radical self-termination as well as other radical disproportionation.

4.31 Chapter 4 Discussion

Polymer with end functionality that response to different environments such as pH, temperature, oxidation and light is called a stimuli-responsive polymer. In RAFT polymerization, polymer modification can be carried out. The functional polymer can be synthesized with different choices that can be made; for instance, functionality can be include in the RAFT agent, monomer, or can be incorporated post-polymerization. Block copolymer such as di, tri, or multi-block polymers can be made by sequential addition. However, the process requires time and precession as it is similar to unique art with a delicate and precious product (Jiong Zou, 2012). To establish an experimental procedure condition of precise temperature, solvent, initiator concentration, and all factors must be considered carefully. During the RAFT reaction, some chains will be initiated from the initiator. As a chain of the polymer extends the impurity in the reaction also increases. However, using a smaller number of blocks makes it possible to achieve narrow PDI and a well-defined block copolymer because the initiator remaining in the reaction is a minimum of which the remaining can be calculated to add the minimum amount into the next step. The livingness (L) was also calculated. Preliminary experiments were performed to observe if the ACPBAPE, RAFT polymer is living after purification by precipitation.

The chains of the PBAPE macro-RAFT are living. However, it requires a better system with higher conversion and maximum livingness. After optimizing the condition of the polymerization, such as monomer solubility, choice of initiator, solvent, and temperature with different attempted RAFT preparation of Poly (N, N Dimethylacrylamide)$_{50-b-50}$ polymerization from Poly N, N-Dimethylacrylamide (DMA)$_{50}$ macro-RAFT in order to familiarise with the procedure of polymerisation polyDMA$_{50}$ blocks were chain extended successfully reproduced from literature. Consequently, attempted RAFT preparation of Poly N, N-Dimethylacrylamide (DMA)$_{50-b-50}$ macro-RAFT and Poly (N, N Dimethylacrylamide)$_{50-b-50-b-50}$ were

carried out. The second batch of experiments are the attempts of RAFT polymerization of N-(4-(4,4,5,5-tetramethyl-1,3,2-dioxaborolan-2-yl) phenyl) acrylamide pinacol ester with Poly DMA macroRAFT$_{28}$ which concluded that addition of acid can improve the RAFT character of the polymer. However, the addition of acids caused polymer precipitation and gelation during the reaction time while looking at physical appearance of the reaction, as it must be in solution all the time. Therefore, the condition was changed to optimise the amount of initiator and form a macro-RAFT of ACPBAPE. The polymerisation condition was further improved to increase the conversion and study the rate of polymerisation.

To find the accurate conversion of the monomer, addition of internal standard was employed. The monomer conversion of 4-ACPBAPE was obtained by adding the internal standard of 1,3,5-trioxane (0.13 mmol) in the reaction medium 2.6 mL DMF. A sample was taken by syringe in time intervals. Trioxane (IS) has a single signal for 6 identical protons at δ = 5.11 - 5.17 ppm.

The remained monomer vinyl peak has the chemical shift at δ = 5.76-5.79 ppm corresponding to the double bond. By comparing the integral area of their characteristic chemical shift, the monomer conversion was calculated. RAFT polymerization of 3-ACPBAPE and 4-ACPBPE using AIBN (0.0029 M) and trioxane internal standard was used from these two concentrations (0.0029 and 0.0015 M). The ideal temperature and concentration of AIBN was optimized for further improvement. RAFT polymerization of N-(3-(4,4,5,5-tetramethyl-1,3,2-dioxaborolan-2-yl) phenyl) acrylamide pinacol ester. Polymerization conditions [3-ACPBAPE]$_0$: [DDMAT]$_0$: [AIBN]$_0$= 669 : 6.6 : 1 at 82 °C. Monomer shows a slow conversion up to 50 % at 82 °C in DMF and is fairly linear. This monomer conversion suggests that the conversion of monomer proceed using 0.0015 M AIBN, however the reaction is slow.

Though, trioxane showed interaction with monomer and degradation while heating. The reason was that the conversion result was not as expected. When the trioxane was tested before the reaction, there was no degradation. However, trioxane was heated with a RAFT agent without a monomer, and there was an interaction observed.

AIBN concentration reduced to 0.0015 M, and the reaction was carried out at the ideal temperature of 70 degrees. Block copolymers were made starting from 150 blocks the same as stated in literature and reduced to 100, 50, 25, and 13 blocks, using new standard anisole added as external standard in NMR analysis from the stock solution. Anisole was added 10 μL to NMR tube with a specific amount of solvent and sample for conversion measurement. Anisole (1.1340 mmol) as external standard (IS) (10 times dilution) and 36.00 mg DDMAT (0.00987 mmol) diluted 10-fold with IS and added to 1 mL reaction volume. Theoretically, Mn (M, *nth*) is calculated as a function of the initial amount of monomer [M] and DDMAT multiplying by the Mw of monomer and the addition of the molecular weight of DDMAT.

M, nth = [M] / [DMAT] · Mw M + Mw DDMA

The result showed that the longer the chain (Figure 4.63), the more deviation occurred from the theoretical time vs. conversion line. The livingness also indicates that more dead chains are existing in the synthesis of a larger chain. Therefore, the chain length was reduced to 100. Similar behaviour with slight improvement was observed, and as the chain got smaller, the better livingness was obtained. Therefore, it can be concluded that the complicated sugar sensitive monomer of 4-ACPBA can polymerize by RAFT and give living chains.

RAFT polymerization of 4-APBAPE was carried out. Monomer conversion is carried out with short (DP ≈ 150, 100, 50, 25 and 13) at high to very high monomer conversions and low fraction of dead chains. In the synthesis of with short (DP ≈ 13) and, at high to very high monomer conversions a low fraction of

dead chains was obtained. For the RAFT polymerization of 44-APBAPE using [AIBN]$_0$ / [DDMAT]$_0$ / [4-APBAPE]$_0$ = 0.2 / 1 / 141. At 30 min the polymer start forming and after 90 min the chain did not grow which means the conversion was low and the other chains formed were not living. Chains by propagating radicals undergoing chain transfer to polymer were observed as well as a degree of livingness. Nevertheless, polymerisation with 150 blocks leads to broadening of the molecular weight distribution and a $Đ$ = 1.64. To prevent such side reactions, the polymerization conditions were optimized using a constant amount of AIBN, and monomer only variable amount of RAFT agent in presence of anisole added as external standard for conversion calculation by ^{1}H NMR.

This was a totally synthetic system that could possibly operate as glucose sensitive system at physiological pH. Previously glucose sensitive systems were incorporated with enzymes and protein that causes degradation of protein and enzyme. The toxicity of such system requires further investigation.

The literature suggests that the studies were using conventional radical polymerization and RAFT polymerization methods for boronic acid glucose sensing systems. However, many of these studies used unprotected phenylboronic acid, which is problematic during GPC/SEC analysis.

This synthetic system was prepared via free radical polymerization that operates as a glucose-sensitive system at physiological pH synthesized by (Kazunori Kataoka, 1998 , Matsumoto et al., 2004, Matsumoto et al., 2003, A. Matsumoto, 2010).

4.32 Future work

Further study is required to obtain the phenylboronic acid monomer's full (98%) conversion, as macro-RAFT of extension of polyDMA macro-RAFT. Control is achieved by protecting most propagating radicals from the bimolecular

termination process through their reversible trapping in a dormant thiocarbonyl compound (RAFT).

Dormant RAFT radical
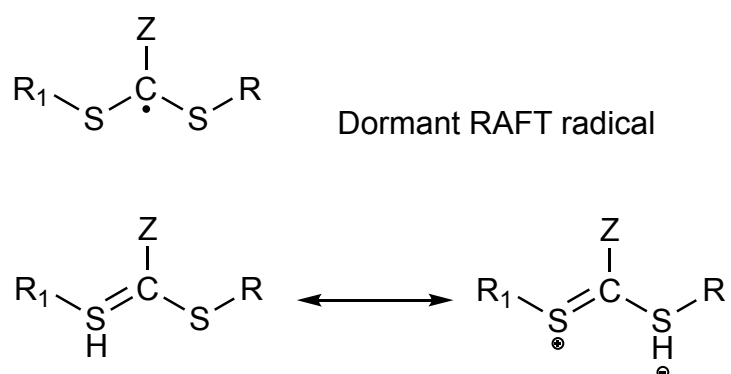
Scheme 4. 46 RAFT resonance stability

Resonance stabilization of the Thiocarbonyl bond and the chemical nature of attacking radicals from leaving group R affect the addition and fragmentation reaction's kinetics. In RAFT polymerization, the oligomeric radicals are formed in the early stages of the process, either can initiate with an initial leaving group of RAFT (R) or initiator fragment (I), and these end groups modify the reactivity of attacking radicals. The original chain comes from the reactivity of tertiary radicals (most stable radical). Further work requires using different acid such a trifluoroacetic acid (TFA) for the dioxane water (80: 20) system, as TFA is miscible with water, or benzoic acid for the DMF system, which is soluble in the organic solvent, also formic acid as an alternative acid to avoid RAFT agent reaction. The literature suggests that engineering a glucose-sensitive polymer with the ability to encapsulate insulin; there are many factors such as boronic acid pKa, diol pKa, the dihedral angle of diol, steric hindrance and stabilization of boronate center at neutral pH that need to be considered. In addition to synthesizes, the RAFT block copolymer of Boronic acid requires in-depth kinetic studies to obtain a living block copolymer with hydrophobic and hydrophilic properties. Possibly a

simulation studies using Predici to obtain in dept knowledge of such novel sugar sensing molecule (Per B. Zetterlund, 2014b).

Future work is required for sugar sensing and micelle formation. Test of release profile of insulin in presence of different glucose concentration (et.al, 2004 , Roy et al., 2009).

4.33 Conclusion and general discussion

To address the need for enhancement in delivering insulin more efficiently, this work focused on achieving and establishing a new polymeric end functionalised material for sugar sensing. A new efficient method was developed to synthesise an end functionalised polyglycerol based polymer using DL-1,2-isopropylideneglycerol with 4-carboxyphenylboronic acid pinacol ester, forming (2,2-dimethyl-1,3-dioxane-5-yl) methyl 4-(4,4,5,5-tetramethyl-1,3,2-dioxaborolan-2-yl)benzoate polymerising this with glycidol and glycerol. The first binding of DL-1,2-Isopropylideneglycerol to carboxyphenylboronic acid-forming of and then carrying out the second step of the reaction after confirmation of the product is the polymerisation step of glycerol and glycidol, which eventually lead to the deprotection of pinacol as well in same response during wash up. This is a novel polymer achieved and was confirmed by NMR and FTIR in good yield. Moreover, all results were analysed using NMR, MALDI-TOF and FTIR.

Three and four carboxy terminated phenylboronic acid monomers were successfully protected with pinacol achieving high yield by modifying two literature methods, which are examined to achieve a better yield. A standard method for the protection of boronic acid has been successfully developed. The yield of 91, 95 and 97% proposes the optimum conditions for the reaction to be the ratio of 1:0.95 for carboxyphenylboronic acid to pinacol, using approximately 4 g of molecular sieves instead of 8 g, and 24 h. The NMR peak for the last experiment at around 1.36 and the peaks for the other experiments around the same range confirms our product. The purity of the product confirmed by the melting point range also suggests that the experiment for the formation of carboxyphenylboronic acid pinacol ester has proceeded successfully. It can, therefore, be recommended that the experiment with the ideal conditions can be repeated with 2-carboxyphenylboronic acid or amino phenylboronic acid.

Amino phenylboronic acid pinacol ester (*ortho, meta and para*) reaction was carried out using maleic anhydride. This can be used as a derivative of carboxymethyl chitosan (Weith et al., 1970) for nanoparticle formation and insulin incorporation. The same condition was used for all three substituted monomers (Andrea Temperini 2009). In the analysis of the binding of various sugars and other polyols, it has become apparent that the most critical factor is the availability in the polyol of a glycol group containing the required configuration and conformation. Upon binding these monomers with the amine group of chitosan, it can be possible form nanoparticles followed by deprotection and study of the boronic acid for the sugar-binding property.

The low molecular weight (LMw) and high molecular weight (HMw), polyglycerol was used for the solubility study of antidiabetic drug hydrochlorothiazide in chapter three. The solubility was compared against commercial polymers such as PEG-400, commercial polyglycerine and glycerol. The result obtained from HPLC shows a good solubility of the drug and a potential liquid formulation of hydrochlorothiazide at room temperature using food additive (polyglycerine and small molecule glycerol). The polymers that showed higher solubility of hydrochlorothiazide were PEG-400 and polyglycerine. The small molecule also showed solubility of the drug. Conversely, the high molecular weight solid polyether made in the lab did not demonstrate a good solubility. Besides, it drastically showed a change of pH which can cause degradation of the drug.

Nevertheless, our findings suggest that PEG -400 and polyglycerine enhances both solubilities. However, the polyglycerol polymers synthesised in the lab are not suitable for such a purpose without improving the functionality.

The results show that the more favourable solubility cosolvents for a hydrophobic drug such as HCTZ are the mixture that matches the polarity of the hydrophobic drug. These experiments indicate that the solution is stable and

have not reached the pH at 12, which can cause hydrolysis at 24 hours at room temperature. However, stability test is carried out over period for day 1, day 3, week 2, week 4- and 6-months relative humidity (RH) at 25°C, RH-65 % and 40°C RH-75 %.

In Chapter 4, all the essential parameters were obtained, and the kinetics study and the ideal ratio (13 blocks of polymer suitable for chain extension) for RAFT polymerisation of 4-PBAPE monomer were achieved. The number of radicals remaining was calculated, and the perfect number of blocks (13) was decided to be used for further chain extension as this one give minimum dead chains and high livingness. High monomer purity is essential for maintaining the integrity of the polymerisation process. The monomer was obtained in high yield and pure form. Fortunately, nearly all products were synthesised in high purity at a 30 – 70 % yield.

A RAFT polymerisation system comprises a monomer, the minimum amount of a radical source, a RAFT agent, and a suitable solvent. A right RAFT agent with designed solubility of pure monomer ideal temperature and RAFT initiator ratios was essential to optimise such polymerisation. With the appropriate amount of radical balance, chain growth was initiated. The RAFT agent's radicals further carried out the reaction to maintain the RAFT equilibrium toward the active state compared with the dormant state. However, the polymerisation process is a powerful tool for the synthesis of a diversity of materials. The similarity to utilise the RAFT process for polymer synthesis is an intense mechanistic and kinetic understanding of the particular RAFT-specific reactions. This was sought from the very beginning of RAFT technology to establish structure-rate correlations for specific RAFT agents. Such information is compulsory for designing novel mediating compounds and modelling the polymerisation process, whereby costly and time-consuming investigations may be minimised.

Further work is required to chain extension the 4-ACPBAPE monomer and the transformation into nanostructures. Study the morphology of the di or triblock, synthesis of a different combination of RAFT copolymer block, determination of the pH and sugar sensing properties. Each step requires analytical procedures such as nuclear magnetic resonance (NMR), dynamic light scattering (DLS), transmission electron microscopy (TEM). Further to this optimisation, a mathematical model could be established from the kinetic data.

This synthetic system was prepared via free radical polymerisation that operates as a glucose-sensitive system at physiological pH synthesised by (Kazunori Kataoka, 1998 , Matsumoto et al., 2004, Matsumoto et al., 2003, A. Matsumoto, 2010).

The literature suggests that the studies were using conventional radical polymerisation and RAFT polymerisation methods for boronic acid glucose sensing systems. However, many of these studies used unprotected phenylboronic acid, which is problematic during gel permeation chromatography/size exclusion chromatography (GPC/SEC) analysis.

The literature suggests that engineering a glucose-sensitive polymer with the ability to encapsulate insulin; there are many factors such as boronic acid pKa, diol pKa, the dihedral angle of diol, steric hindrance and stabilisation of boronate centre at neutral pH need to be considered. In addition to synthesises, the RAFT block copolymer of boronic acid requires in-depth kinetic studies to obtain a living block copolymer with hydrophobic and hydrophilic properties. Possibly a simulation studies using Predici to get in-depth knowledge of such novel sugar sensing molecule (Per B. Zetterlund, 2014b). This is a synthetic system that operates as a glucose-sensitive system at physiological pH. Previously glucose-sensitive such systems were incorporated with enzymes and protein that causes degradation of protein and enzyme. The toxicity of such a system requires further investigation.

In conclusion, a new monomer and polymerisation method with *in situ* deprotection method was developed. The liquid formulation of HCTZ was developed with polyglycerine compared to PEG and small molecule.

RAFT polymerisation condition was optimised for the first time polymerisation of 4-ACPBAPE monomer. For end functionalised phenylboronic acid RAFT block copolymer.

4.34 List of publications from thesis

The impact of natural and synthetic polymers in formulating micro and nanoparticles for antidiabetic drugs, Current Drug Delivery., DOI: 10.2174/1567201817666200810111726

4.35 Conference proceedings and poster presentations:

Royal Society of Chemistry (RSC) Drug Discovery Symposium, Kingston University 2019

Reversible addition Fragmentation chain Transfer (RAFT) towards Sugar-responsive polymer

European Conference on Pharmaceutics Novel Dosage Forms and Innovative Technologies, April 2017, Kraków Poland

Glucose sensitive system for delivery of anti-diabetic drugs

Diabetes UK, March 2017, Manchester

Smart delivery system for antidiabetic drugs

Science Engineering and computing (SEC) Faculty conference at Kingston University 2017

Glucose sensitive system for delivery of anti-diabetic drugs

UK & Ireland Controlled Release Society, 2016, Cardiff wales

Smart delivery system for antidiabetic drugs

In preparation

Drug delivery of Insulin Literature review, Negeen Kargar, Ian Beadham, Raid Alany, Amr ElShaer., (Advanced Drug Delivery Review)

The development of liquid formulation of hydrochlorothiazide (HCTZ) using biodegradable polymers an HPLC study, Negeen Kargar and Amr ElShaer (Molecules)

Polymerization of end functionalized sugar sensitive polyglycerol with an in situ deprotection of pinacol. Negeen Kargar, Ian Beadham, Amr ElShaer (short communication)

4.36 References:

A. MATSUMOTO, E. A. 2012. A Synthetic Approach Toward a Self-Regulated Insulin Delivery System. Chem., Int. Ed, 2124 - 2128.

A. MATSUMOTO, K. Y., R. YOSHIDA, K. KATAOKA, T. AOYAGI AND Y. MIYAHARA 2010. A totally synthetic glucose responsive gel operating in physiological aqueous conditions. Chem. Commun, 46, 2203 - 2205

A.HUTTON, et.al, 2004 Deprotection of pinacolyl boronate esters by transesterification with polystyrene–boronic acid. Tetrahedron Letters, 45, 6657-6660.

ABRAHAM J. DOMB, N. K. 2011. Biodegradable Polymers in Clinical Use and Clinical Development.

ADAMS G, et.al, 2013. Drug delivery systems for the treatment of diabetes mellitus: State of the art. Current Pharmaceutical Design, 19, 7244 - 63.

ADDITIVES, E. P. O. F., NUTRIENT SOURCES ADDED TO, F., MORTENSEN, A., AGUILAR, F., CREBELLI, R., DI DOMENICO, A., DUSEMUND, B., FRUTOS, M. J., GALTIER, P., GOTT, D., GUNDERT-REMY, U., LEBLANC, J. C., LINDTNER, O., MOLDEUS, P., MOSESSO, P., PARENT-MASSIN, D., OSKARSSON, A., STANKOVIC, I., WAALKENS-BERENDSEN, I., WOUTERSEN, R. A., WRIGHT, M., YOUNES, M., BOON, P., CHRYSAFIDIS, D., GURTLER, R., TOBBACK, P., RINCON, A. M., TARD, A. & LAMBRE, C. 2017. Re-evaluation of polyglycerol polyricinoleate (E 476) as a food additive. EFSA J, 15, e04743.

AGRAWAL, A. 2014. Improved stability and antidiabetic potential of insulin containing folic acid functionalized polymer stabilized multilayered liposomes following oral administration. Biomacromolecules, 15, 350-60.

 Reiner. H. E. 2000. An Approach to Core-Shell-Type Architectures in Hyperbranched Polyglycerols by Selective Chemical Differentiation. Macromolecules, 33, 8158 -8166.

ALABRABA, V., FARNSWORTH, A., LEIGH, R., DODSON, P., GOUGH, S. C. & SMYTH, T. 2009. Exubera inhaled insulin in patients with type 1 and type 2 diabetes: the first 12 months. Diabetes Technol Ther, 11, 427-30.

ALEXANDER K L YUENA, C. A. H. 2005. Deprotection of pinacolyl boronate esters via hydrolysis of intermediate potassium trifluoroborates. Tetrahedron Letters 46, 7899 -7903.

ALEXANDER T FLORENCE, U. S. O. P., UNIVERSITY COLLEGE LONDON, UK & DAVID ATTWOOD, M. P. S. U. O. M., UK 2016. Physicochemical Principles of Pharmacy In Manufacture, Formulation and Clinical Use, Pharmaceutical Press.

ALTAMIMI, M. A., ELZAYAT, E. M., ALHOWYAN, A. A., ALSHEHRI, S., & SHAKEEL, F. 2018 Effect of β-cyclodextrin and different surfactants on solubility, stability, and permeability of hydrochlorothiazide Journal of Molecular Liquids, 250, 323–328.

ANDREA TEMPERINI , R. T., LORENZO TESTAFERRI & MARCELLO TIECCO 2009. Additive-Free Chemoselective Acylation of Amines. Synthetic Communications, 40 295 -302

AROURI, A. & MOURITSEN, O. G. 2013. Membrane-perturbing effect of fatty acids and lysolipids. Prog Lipid Res, 52, 130-40.

AVDEEF, A. 2012. Absorption and Drug Development Solubility, Permeability, and Charge State, Hoboken, New Jersey, John Wiley & Sons, Inc., .

AYOGU, I. E. A. 2009. Evaluation of the pharmacodynamic activity of insulin from bilosomal formulation. Curr Drug Deliv, 6, 415-8.

BAKSHI, P. S., SELVAKUMAR, D., KADIRVELU, K. & KUMAR, N. S. 2020. Chitosan as an environment friendly biomaterial - a review on recent modifications and applications. Int J Biol Macromol, 150, 1072-1083.

BALLY, L. & THABIT, H. 2017. Real-World Challenges of Controller Adaptation with the Artificial Pancreas. Diabetes Technol Ther, 19, 552-554.

BALLY, L., THABIT, H. & HOVORKA, R. 2017a. Closed-loop for type 1 diabetes - an introduction and appraisal for the generalist. BMC Med, 15, 14.

BALLY, L., THABIT, H. & HOVORKA, R. 2018. Glucose-responsive insulin delivery for type 1 diabetes: The artificial pancreas story. Int J Pharm, 544, 309-318.

BALLY, L., THABIT, H., KOJZAR, H., MADER, J. K., QERIMI-HYSENI, J., HARTNELL, S., TAUSCHMANN, M., ALLEN, J. M., WILINSKA, M. E., PIEBER, T. R., EVANS, M. L. & HOVORKA, R. 2017b. Day-and-night glycaemic control with closed-loop insulin delivery versus conventional insulin pump therapy in free-living adults with well controlled type 1 diabetes: an open-label, randomised, crossover study. Lancet Diabetes Endocrinol, 5, 261-270.

BANGA AK, C. Y. 1993. Characterization of in vitro transdermal iontophoretic delivery of insulin. Drug Dev. Ind. Pharm, 19, 2069–2087.

BERND ENSING, A. T., MARTIJN TROS, JOHANNES HUNGER, SÉRGIO R. DOMINGOS, CRISTÓBAL PÉREZ, GERTIEN SMITS, MISCHA BONN, DANIEL BONN & SANDER WOUTERSEN 2019. On the origin of the extremely different solubilities of polyethers in water. NATURE COMMUNICATIONS 10.

BI, R., SHAO, W., WANG, Q. & ZHANG, N. 2009. Solid lipid nanoparticles as insulin inhalation carriers for enhanced pulmonary delivery. J Biomed Nanotechnol, 5, 84-92.

BLANDAMER, M. J., FOX, M. F., POWELL, E., & STAFFORD, J. W. 1969. A Viscometric Study of Poly(Ethylene Oxide) in t-Butyl Alcohol / Water Mixtures. Die Makromolekulare Chemie,, 124, 222-231.

BLONDE, L., ROSENSTOCK, J., DEL PRATO, S., HENRY, R., SHEHADEH, N., FRIAS, J., NIEMOELLER, E., SOUHAMI, E., JI, C. & ARODA, V. R. 2019. Switching to iGlarLixi Versus Continuing Daily or Weekly GLP-1 RA in Type 2 Diabetes Inadequately Controlled by GLP-1 RA and Oral Antihyperglycemic Therapy: The LixiLan-G Randomized Clinical Trial. Diabetes Care, 42, 2108-2116.

BLONDE, L., ROSENSTOCK, J., FRIAS, J., BIRKENFELD, A. L., NIEMOELLER, E., SOUHAMI, E., JI, C., DEL PRATO, S. & ARODA, V. R. 2021. Durable Effects of iGlarLixi Up to 52 Weeks in Type 2 Diabetes: The LixiLan-G Extension Study. Diabetes Care, 44, 774-780.

BNF 2020. Joint Formulary Committee (2020) British National Formulary. . Pharmaceutical Press., September 2019-March 2020. London.

BRITTAIN, H. G. 2001. Analytical Profiles of Drug Substances and Excipients, Center for Pharmaceutical Physics 10 Charles Road Milford, New Jersey 08848, Elsevier, Academic Press.

BROOKS, W. L. A. & SUMERLIN, B. S. 2016. Synthesis and Applications of Boronic Acid-Containing Polymers: From Materials to Medicine. Chemical Reviews, 116, 1375-1397.

BURKE, M. J. & ROUGVIE, M. A. 1972. Cross- protein structures. I. Insulin fibrils. Biochemistry, 11, 2435-9.

C.MA´RQUEZ-ALVAREZ, E. S. A. J. P. R.-P. 2004. Solid catalysts for the synthesis of fatty esters of glycerol, polyglycerols and sorbitol from renewable resources. Topics in Catalysis, 27, 1-4.

CAMBRE, J. N., ROY, D., BROOKS, W. L. A. & SUMERLIN, B. S. 2013. Boronic acid block copolymers: Sugar-responsive materials for drug delivery. Abstracts of Papers of the American Chemical Society, 246.

CAMBRE, J. N., ROY, D., GONDI, S. R. & SUMERLIN, B. S. 2007a. Facile strategy to well-defined water-soluble boronic acid (co)polymers. Journal of the American Chemical Society, 129, 10348-+.

CAMBRE, J. N., ROY, D., GONDI, S. R. & SUMERLIN, B. S. 2007b. Facile strategy to well-defined water-soluble boronic acid (co)polymers. J Am Chem Soc, 129, 10348-9.

CAMBRE, J. N., ROY, D. & SUMERLIN, B. S. 2012. Tuning the sugar-response of boronic acid block copolymers. Journal of Polymer Science Part a-Polymer Chemistry, 50, 3373-3382.

CARDOSO, W. V. & LU, J. 2006. Regulation of early lung morphogenesis: questions, facts and controversies. Development, 133, 1611-24.

CAROLINA ARDILA-SUÁREZ, D. R.-A., AND GUSTAVO E. RAMIREZ-CABALLERO 2015. Effect of Temperature and Catalyst Concentration on Polyglycerol during Synthesis. International Journal of Polymer Science, 1-8.

CHALASANI, K. B., RUSSELL-JONES, G. J., JAIN, A. K., DIWAN, P. V. & JAIN, S. K. 2007a. Effective oral delivery of insulin in animal models using vitamin B12-coated dextran nanoparticles. J Control Release, 122, 141-50.

CHALASANI, K. B., RUSSELL-JONES, G. J., YANDRAPU, S. K., DIWAN, P. V. & JAIN, S. K. 2007b. A novel vitamin B12-nanosphere conjugate carrier system for peroral delivery of insulin. J Control Release, 117, 421-9.

CHALMERS, B. A. A., ABDULLAH; HAWKINS, GERARD; ET AL. 2017. Efficient synthesis and RAFT polymerization of the previously elusive N-[(cycloalkylamino)methyl]acrylamide monomer class. Journal of Polymer Science Part a-Polymer Chemistry 55, 2123-2128.

CHANTHAMATH, S., TAKAKI, S., SHIBATOMI, K. & IWASA, S. 2013. Highly stereoselective cyclopropanation of alpha,beta-unsaturated carbonyl compounds with methyl (diazoacetoxy)acetate catalyzed by a chiral ruthenium(II) complex. Angew Chem Int Ed Engl, 52, 5818-21.

CHEN, M. C., LING, M. H. & KUSUMA, S. J. 2015a. Poly-gamma-glutamic acid microneedles with a supporting structure design as a potential tool for transdermal delivery of insulin. Acta Biomater, 24, 106-16.

CHEN, Q. J., HILL, M. R., BROOKS, W. L. A., ZHU, A. Q., SUMERLIN, B. S.. 2015b. Boronic Acid Linear Homopolymers as Effective Emulsifiers and Gelators. Acs Applied Materials & Interfaces, 7, 21668-21672.

CHIKUKWA, M. T. R., WALKER, R. B. & KHAMANGA, S. M. M. 2020. Formulation and Characterisation of a Combination Captopril and Hydrochlorothiazide Microparticulate Dosage Form. Pharmaceutics, 12.

CHOW, A. H., TONG, H. H., CHATTOPADHYAY, P. & SHEKUNOV, B. Y. 2007. Particle engineering for pulmonary drug delivery. Pharm Res, 24, 411-37.

CHOWDHURY, T. A. & ESCUDIER, V. 2003. Poor glycaemic control caused by insulin induced lipohypertrophy. BMJ, 327, 383-4.

CHRISTIANE DAMGÉ, C. M., MARC APRAHAMIAN AND PATRICK COUVREUR 1998. New Approach for Oral Administration of Insulin With Polyalkylcyanoacrylate Nanocapsules as Drug Carrier. Diabetes, 37, 246-251.

CHU, K., LEE, E., JEONG, S. & PARK, E. 2012. Effect of particle size on the dissolution behaviors of poorly water-soluble drugs. Arch Pharm Res, 35, 1187-95.

CINTHYA MARIA PEREIRA DE SOUZA, J. A. B. D. S., AGNALDO LUIZ DO NASCIMENTO, JOSÉ VENÂNCIO CHAVES JÚNIOR, FERNANDO JOSÉ DE LIMA RAMOS JÚNIOR, SEVERINO ANTÔNIO DE LIMA NETO, FÁBIO SANTOS DE SOUZA & RUI OLIVEIRA MACÊDO 2017. Thermal analysis study of solid dispersions hydrochlorothiazide. Thermal Analysis and Calorimetry, 131, 681–689.

COURTS, A. 1955. The N-terminal amino acid residues of gelatin. 3. Enzymic degradation. Biochem J, 59, 382-6.

COUTTS, S. J., ADAMS, J., KROLIKOWSKI, D., & SNOW, R. J. 1994. Two efficient methods for the cleavage of pinanediol boronate esters yielding the free boronic acids. . Tetrahedron Letters, 35, 5109–5112.

CRAFT, S., BAKER, L. D., MONTINE, T. J., MINOSHIMA, S., WATSON, G. S., CLAXTON, A., ARBUCKLE, M., CALLAGHAN, M., TSAI, E., PLYMATE, S. R., GREEN, P. S., LEVERENZ, J., CROSS, D. & GERTON, B. 2012. Intranasal insulin therapy for Alzheimer disease and amnestic mild cognitive impairment: a pilot clinical trial. Arch Neurol, 69, 29-38.

CUI, M., WU, W., HOVGAARD, L., LU, Y., CHEN, D. & QI, J. 2015. Liposomes containing cholesterol analogues of botanical origin as drug delivery systems to enhance the oral absorption of insulin. Int J Pharm, 489, 277-84.

DAMGE, C., MAINCENT, P. & UBRICH, N. 2007. Oral delivery of insulin associated to polymeric nanoparticles in diabetic rats. J Control Release, 117, 163-70.

DAMGE, C., REIS, C. P. & MAINCENT, P. 2008. Nanoparticle strategies for the oral delivery of insulin. Expert Opin Drug Deliv, 5, 45-68.

DAMGE, C., VONDERSCHER, J., MARBACH, P. & PINGET, M. 1997. Poly(alkyl cyanoacrylate) nanocapsules as a delivery system in the rat for octreotide, a long-acting somatostatin analogue. J Pharm Pharmacol, 49, 949-54.

DANDEGAONKER, R. L. L. A. S. H. 1959. Organoboron Compounds. IX. 8-Quinolineboronic Acid, its Preparation and Influence on Reactions of Chlorohydrins. J. Am. Chem. Soc., 81, 498-501.

DANIEL WILIMS , S.-E. S., AND HOLGER FREY 2010. Hyperbranched Polyglycerols: From the Controlled Synthesis of Biocompatible Polyether Polyols to Multipurpose Applications. Accounts of chemical reaserch 43, 129 -141.

DE BOER, I. H., CARAMORI, M. L., CHAN, J. C. N., HEERSPINK, H. J. L., HURST, C., KHUNTI, K., LIEW, A., MICHOS, E. D., NAVANEETHAN, S. D., OLOWU, W. A., SADUSKY, T., TANDON, N., TUTTLE, K. R., WANNER, C., WILKENS, K. G., ZOUNGAS, S., LYTVYN, L., CRAIG, J. C., TUNNICLIFFE, D. J., HOWELL, M.,

TONELLI, M., CHEUNG, M., EARLEY, A. & ROSSING, P. 2020. Executive summary of the 2020 KDIGO Diabetes Management in CKD Guideline: evidence-based advances in monitoring and treatment. Kidney Int, 98, 839-848.

DE, P., GONDI, S. R., ROY, D. & SUMERLIN, B. S. 2009. Boronic Acid-Terminated Polymers: Synthesis by RAFT and Subsequent Supramolecular and Dynamic Covalent Self-Assembly. Macromolecules, 42, 5614-5621.

DEKEL, Y., GLUCKSAM, Y. & MARGALIT, R. 2010. Novel fibrillar insulin formulations for oral administration: Formulation and in vivo studies in diabetic mice. J Control Release, 143, 128-35.

DEMIRDJIAN, S., BARDIN, C., SAVIN, S., ZIRINIS, P., CHAST, F., SLAMA, G. & SELAM, J. L. 1998. Lispro insulin is suitable for external pumps but not for implantable pumps. Diabetes Care, 21, 867-8.

DEPPELER, H. P. 1981. Hydrochlorothiazide Analytical Profiles of Drug Substances, 405–441.

DONNA ZAZWORSKY, J. N. B. A. V. B. G. 2005. Handbook of Diabetes Management, New York, Springer Science Business Media Inc.

EHTERAMI, A., SALEHI, M., FARZAMFAR, S., VAEZ, A., SAMADIAN, H., SAHRAPEYMA, H., MIRZAII, M., GHORBANI, S. & GOODARZI, A. 2018. In vitro and in vivo study of PCL/COLL wound dressing loaded with insulin-chitosan nanoparticles on cutaneous wound healing in rats model. Int J Biol Macromol, 117, 601-609.

ELDOR, R., ARBIT, E., CORCOS, A. & KIDRON, M. 2013. Glucose-reducing effect of the ORMD-0801 oral insulin preparation in patients with uncontrolled type 1 diabetes: a pilot study. PLoS One, 8, e59524.

ELENA MATTEUCCI, E. A. 2015. Insulin administration: present strategies and future directions for a noninvasive (possibly more physiological) delivery. DovePress , Drug Design, Development and Therapy, 9, 3109 -3118.

ET.AL, B. M. 2004 Thermoresponsive Properties of Sugar Sensitive Copolymer of N-Isopropylacrylamide and 3-(Acrylamido)phenylboronic Acid. Maccromolecular Chemistry and Physics

205 27 - 34.

ET.AL., A. S. 1999. Controlled Synthesis of Hyperbranched Polyglycerols by Ring-Opening Multibranching Polymerization. Macromolecules, 32, 424- - 4246.

ET.AL., R. Y. 2011. Glucose and pH dual-responsive concanavalin A based microhydrogels for insulin delivery. International Journal of Biological Macromolecules, 49, 1137 - 1142.

FANG, X., BIBART, R. T., MAYR, S., YIN, W., HARMON, P. A., MCCAFFERTY, J. F., TYRRELL, R. J. & REED, R. A. 2001. Purification and identification of an impurity in bulk hydrochlorothiazide. J Pharm Sci, 90, 1800-9.

FERNÁNDEZ-URRUSUNO, R., CALVO, P., REMUÑÁN-LÓPEZ, C. ET AL. 1999. Enhancement of Nasal Absorption of Insulin Using Chitosan Nanoparticles. Pharm Res, 16, 1576–1581.

FERNANDO D.PITT , A. M. D., A.A. CHIVANG BARROS 2019 Purification of residual glycerol recovered from biodiesel production. South African Journal of Chemical Engineering, 29, 42 - 51.

FLAVIA LAFFLEUR, T. P., ANDREAS SAXER, MARLENE THALER, BRITTA DEUTEL, AND ANDREAS BERNKOP-SCHNÜRCH 2016. In vitro characterization of insulin containing thiomeric microparticles as nasal drug delivery system. European Journal of Pharmaceutical Sciences, 81, 157 -161.

FLAVIA SOUSA, P. C. P. F. & BRUNO, S. 2015. How to overcome the limitations of current insulin administration with new non-invasive delivery systems. Theraputic Delivery, 5, 83 - 94.

FORLENZA, G. P., CAMERON, F. M., LY, T. T., LAM, D., HOWSMON, D. P., BAYSAL, N., KULINA, G., MESSER, L., CLINTON, P., LEVISTER, C., PATEK, S. D., LEVY, C. J., WADWA, R. P., MAAHS, D. M., BEQUETTE, B. W. & BUCKINGHAM, B. A. 2018. Fully Closed-Loop Multiple Model Probabilistic Predictive Controller Artificial Pancreas Performance in Adolescents and Adults in a Supervised Hotel Setting. Diabetes Technol Ther, 20, 335-343.

FRANÇOIS D'HOOGE , D. R., MICHAEL J. THATCHER , SEMALI P. PERERA , JEAN M.H. VAN DEN ELSEN , A. TOBY A. JENKINS , TONY D. JAMES , JOHN S. FOSSEY 2008 Polymerisation resistant synthesis of methacrylamido phenylboronic acids. Polymer 49 3362–3365.

FUDE CUI, et.al, 2006. Biodegradable nanoparticles loaded with insulin–phospholipid complex for oral delivery: Preparation, in vitro characterization and in vivo evaluation. Journal of Controlled Release, 114, 242 -250.

FWU-LONG MI, et.al, 2008. Oral Delivery of Peptide Drugs Using Nanoparticles Self-Assembled by Poly(γ-glutamic acid) and a Chitosan Derivative Functionalized by Trimethylation. Bioconjugate Chem, 19, 1248 - 1255.

GARCIA-DIAZ, M., FOGED, C. & NIELSEN, H. M. 2015. Improved insulin loading in poly(lactic-co-glycolic) acid (PLGA) nanoparticles upon self-assembly with lipids. Int J Pharm, 482, 84-91.

GATTO, N. M., KORALEK, D. O., BRACKEN, M. B., DUGGAN, W. T., LEM, J., KLIOZE, S., KOCH, G. G., WISE, R. A., COHEN, R. B. & JACKSON, N. C. 2019. Lung Cancer-Related Mortality With Inhaled Insulin or a Comparator: Follow-Up Study of patients previously enrolled in Exubera Controlled Clinical Trials (FUSE) Final Results. Diabetes Care, 42, 1708-1715.

GILBERT S. BANKER, J. S., CHRISTOPHER RHODES 2007. Modern Pharmaceutics (Drugs and the Pharmaceutical Sciences)

, CRC Press (22 Jan 2007).

GODY, G., MASCHMEYER, T., ZETTERLUND, P. B. & PERRIER, S. 2013. Rapid and quantitative one-pot synthesis of sequence-controlled polymers by radical polymerization. Nat Commun, 4, 2505.

GRAEME MOAD, R. T. A. M., EZIO RIZZARDO, MELISSA SKIDMORE, AND SAN H. THANG 2003. Kinetics and Mechanism of RAFT Polymerization. The Chemistry of Radical Polymerization. American Chemical Society: CSIROMolecular Science and CRC for Polymers, CSIRO Molecular Science Bag 10, Clayton South, Victoria 3169, Australia.

GRAEME MOAD, R. T. A. M., EZIO RIZZARDO, MELISSA SKIDMORE, AND SAN H. THANG 2017. Mechanism and Kinetics of Dithiobenzoate-Mediated RAFT Polymerization – Status of the Dilemma. Macromolecular Chemistry and Physics, 218.

GRAF, A., RADES, T. & HOOK, S. M. 2009. Oral insulin delivery using nanoparticles based on microemulsions with different structure-types: optimisation and in vivo evaluation. Eur J Pharm Sci, 37, 53-61.

GUENTHER BODEN, M. D. 2011. 45 Obesity, Insulin Resistance and Free Fatty Acids. Curr Opin Endocrinol Diabetes Obes., 18, 139 -143.

GUILLAUME BINSON, K. B., VIRGINIE MIGEOT, LÉA MARCO, BARBARA TROUSSIER, NICOLAS VENISSE, AND ANTOINE DUPUIS 2019. Preparation and Physicochemical Stability of Liquid Oral Dosage Forms Free of Potentially Harmful Excipient Designed for Pediatric Patients. Pharmaceutics 190.

H. PATEL, et.al, 1976. Oral administration of insulin by encapsulation within liposomes. FEBS Letters, 62, 60 -63.

HAMISHEHKAR, H., EMAMI, J., NAJAFABADI, A. R., GILANI, K., MINAIYAN, M., HASSANZADEH, K., MAHDAVI, H., KOOHSOLTANI, M. & NOKHODCHI, A. 2010a. Pharmacokinetics and pharmacodynamics of controlled release insulin loaded PLGA microcapsules using dry powder inhaler in diabetic rats. Biopharm Drug Dispos, 31, 189-201.

HAMISHEHKAR, H., EMAMI, J., NAJAFABADI, A. R., GILANI, K., MINAIYAN, M., MAHDAVI, H. & NOKHODCHI, A. 2010b. Effect of carrier morphology and surface characteristics on the development of respirable PLGA microcapsules for sustained-release pulmonary delivery of insulin. Int J Pharm, 389, 74-85.

HANDELSMAN, Y., MUSKIET, M. H. A. & MENEILLY, G. S. 2019. Combining GLP-1 Receptor Agonists and Basal Insulin in Older Adults with Type 2 Diabetes: Focus on Lixisenatide and Insulin Glargine. Adv Ther, 36, 3321-3339.

HAO YANG, X. S., GAN LIU, RUJIANG MA, ZHONG LI, YINGLI AN AND LINQI SHI 2013. Glucose-responsive complex Micelles for self-regulated release of insulin under physiological condition. Soft matter, RSC Publishing 9.

HASHIDE, R., YOSHIDA, K., HASEBE, Y., SENO, M., TAKAHASHI, S., SATO, K. & ANZAI, J. 2014. Poly(lactic acid) microparticles coated with insulin-containing layer-by-layer films and their pH-dependent insulin release. J Nanosci Nanotechnol, 14, 3100-5.

HERRERO, E. P., ALONSO, M. J. & CSABA, N. 2012. Polymer-based oral peptide nanomedicines. Ther Deliv, 3, 657-68.

HILLENKAMP, F., KARAS, M., BEAVIS, R. C. & CHAIT, B. T. 1991. Matrix-assisted laser desorption/ionization mass spectrometry of biopolymers. Anal Chem, 63, 1193A-1203A.

HISAMITSU, I., KATAOKA, K., OKANO, T. & SAKURAI, Y. 1997. Glucose-responsive gel from phenylborate polymer and poly(vinyl alcohol): prompt response at physiological pH through the interaction of borate with amino group in the gel. Pharm Res, 14, 289-93.

HOFMANN, A. F. 2009. Bile acids: trying to understand their chemistry and biology with the hope of helping patients. Hepatology, 49, 1403-18.

HOMPESCH, M., KOLLMEIER, A., RAVE, K., HEINEMANN, L., MITNICK, M., DAVIES, S. & STRACK, T. 2009. Glycemic exposure is affected favorably by inhaled human insulin (Exubera) as compared with subcutaneous insulin glargine (Lantus) in patients with type 2 diabetes. Diabetes Technol Ther, 11, 307-13.

HONG, T. D., EDGINGTON, S., ELLIS, R. H., DE MURO, M. A. & MOORE, D. 2005. Saturated salt solutions for humidity control and the survival of dry powder and oil formulations of Beauveria bassiana conidia. J Invertebr Pathol, 89, 136-43.

HONGXIANG LI, Z. Z., XIAOYAN BAO GUANGRUI, XU PINGYAO 2018. Fatty acid and quaternary ammonium modified chitosan nanoparticles for insulin delivery, Colloids and Surfaces B: Biointerfaces, 170 136 - 143.

HUTTON. A, 2004. Deprotection of pinacolyl boronate esters by transesterification with polystyrene–boronic acid. Tetrahedron Letters, 45, 6657 - 6660.

ILLUM, L. 2003. Nasal drug delivery--possibilities, problems and solutions. J Control Release, 87, 187-98.

INOO, K., BANDO, H. & TABATA, Y. 2018a. Enhanced survival and insulin secretion of insulinoma cell aggregates by incorporating gelatin hydrogel microspheres. Regen Ther, 8, 29-37.

INOO, K., BANDO, H. & TABATA, Y. 2018b. Insulin secretion of mixed insulinoma aggregates-gelatin hydrogel microspheres after subcutaneous transplantation. Regen Ther, 8, 38-45.

IRIE, T. & UEKAMA, K. 1999. Cyclodextrins in peptide and protein delivery. Adv Drug Deliv Rev, 36, 101-123.

IWANAGA, K., ONO, S., NARIOKA, K., KAKEMI, M., MORIMOTO, K., YAMASHITA, S., NAMBA, Y. & OKU, N. 1999. Application of surface-coated liposomes for oral delivery of peptide: effects of coating the liposome's surface on the GI transit of insulin. J Pharm Sci, 88, 248-52.

J.N. CAMBRE, B. S. S. 2011. Biomedical applications of boronic acid polymers. Polymer, 52, 4631 -4643.

JAIN, A. K., CHALASANI, K. B., KHAR, R. K., AHMED, F. J. & DIWAN, P. V. 2007. Muco-adhesive multivesicular liposomes as an effective carrier for transmucosal insulin delivery. J Drug Target, 15, 417-27.

JAMES D GIFFORD et.al, 1984. Control of serum potassium during fasting in patients with end-stage renal disease. Nature, 35, 90 - 94.

JENKINS A, T. STEPTO AND U. W. SUTER 1996. Glossary of basic terms in polymer science (IUPAC Recommendations 1996).

JIN, X., ZHANG, X., WU, Z., TENG, D., ZHANG, X., WANG, Y., WANG, Z. & LI, C. 2009. Amphiphilic random glycopolymer based on phenylboronic acid: synthesis, characterization, and potential as glucose-sensitive matrix. Biomacromolecules, 10, 1337-45.

JIONG ZOU, S. Z., RITU SHRESTHA, KELLIE SEETHO, CARRIE L. DONLEY, AND KAREN L. WOOLEY 2012. pH-Triggered reversible morphological inversion of orthogonally-addressable poly(3-acrylamidophenylboronic acid)-block-poly(acrylamidoethylamine) micelles and their shell crosslinked nanoparticles. J Polym Sci A Polym Chem. , 3, 3146–3156.

JOHN CHIEFARI, Y. K. B. C., FRANCES ERCOLE, JULIA KRSTINA, JUSTINE JEFFERY, TAM P. T. LE, ROSHAN T. A. MAYADUNNE, GORDON F. MEIJS, CATHERINE L. MOAD, GRAEME MOAD*, EZIO RIZZARDO*, AND SAN H. THANG* 1998. Living Free-Radical Polymerization by Reversible Addition-Fragmentation Chain Transfer: The RAFT Process. Macromolecules, 31, 5559–5562.

K. IWANAGA, S. O., K. NARIOKA, K. MORIMOTO, M. KAKEMI, S. YAMASHITA, M. NANGO AND N. OKU, 1997. Oral delivery of insulin by using surface coating liposomes: Improvement of stability of insulin in GI tract. International Journal of Pharmaceutics, 157, 73 - 80

KALIA, Y. N., NAIK, A., GARRISON, J. & GUY, R. H. 2004. Iontophoretic drug delivery. Adv Drug Deliv Rev, 56, 619-58.

KAMYAR SHAMELI, M. B. A., SEYED DAVOUD JAZAYERI, SAJJAD SEDAGHAT, PARVANEH SHABANZADEH, HOSSEIN JAHANGIRIAN, MAHNAZ MAHDAVI AND YADOLLAH ABDOLLAHI 2012.

Synthesis and Characterization of Polyethylene Glycol Mediated Silver Nanoparticles by the Green Method. *International Journal ofnMolecular Sciences, 13, 6639-6650.*

KATAOKA, K., HISAMITSU, I., SAYAMA, N., OKANO, T. & SAKURAI, Y. 1995. Novel sensing system for glucose based on the complex formation between phenylborate and fluorescent diol compounds. *J Biochem, 117, 1145-7.*

KAWAI, P. D. F. 2005. Biodegradation of Polyethers (Polyethylene Glycol, Polypropylene Glycol, Polytetramethylene glycol, and Others).

KAZUNORI KATAOKA, H. M., MASAYUKI BUNYA, TERUO OKANO, AND YASUHISA SAKURAI 1998 Totally Synthetic Polymer Gels Responding to External Glucose Concentration: Their Preparation and Application to On–Off Regulation of Insulin Release. *J. Am. Chem. Soc., 120, 12694–12695.*

KE CAOA, et.al, 2013. Phenylboronic acid modified silver nanoparticles for colorimetric dynamic analysis of glucose. *Biosensors and Bioelectrocnics, 52, 188 - 195.*

K. A. GÜNAY, et.al, 2012. Synthesis and post-polymerization modification of poly(pentafluorophenyl methacrylate) brushes. *Polymer Chemistry 3, 2186 -2192.*

KENNETH A. CONNORS, G. L. A., VALENTINO J. STELLA 1996. Chemical Stability of Pharmaceuticals: A Handbook for Pharmacists, Canada

KENTARO YOSHIDA. 2015. pH-Dependent Release of Insulin from Layer-by-Layer-Deposited Polyelectrolyte Microcapsules. *Polymers, 7, 1269-1278.*

KHEDKAR, A., IYER, H., ANAND, A., VERMA, M., KRISHNAMURTHY, S., SAVALE, S. & ATIGNAL, A. 2010. A dose range finding study of novel oral insulin (IN-105) under fed conditions in type 2 diabetes mellitus subjects. *Diabetes Obes Metab, 12, 659-64.*

KIM, B. H., & KIM, J. K. 1984. Pharmaceutical studies on the polymorphism of hydrochlorothiazide. . *Archives of Pharmacal Research 7, 47 - 52.*

KIM K, C. J., NOLTE R, HEST J. 2009. Polymeric Monosaccharide Receptors Responsive at Neutral pH. . *Journal of the American Chemical Society, 131, 13908-13909.*

KIM, Y. C., PARK, J. H., LUDOVICE, P. J. & PRAUSNITZ, M. R. 2008. Synergistic enhancement of skin permeability by N-lauroylsarcosine and ethanol. *Int J Pharm, 352, 129-38.*

KISEL M. et.al, 2011. Liposomes with phosphatidylethanol as a carrier for oral delivery of insulin: studies in the rat. *International Journal of Pharmaceutics, 23, 105-114.*

KISEL MA1, K. L., TSYBOVSKY IS, VLASOV AP, VOROB'YOV MS, KHOLODOVA EA, ZABAROVSKAYA ZV. 2011. Liposomes with phosphatidylethanol as a carrier for oral delivery of insulin: studies in the rat. *International Journal of Pharmaceutics, 23, 105-114.*

KISEL, M. A., KULIK, L. N., TSYBOVSKY, I. S., VLASOV, A. P., VOROB'YOV, M. S., KHOLODOVA, E. A. & ZABAROVSKAYA, Z. V. 2001. Liposomes with phosphatidylethanol as a carrier for oral delivery of insulin: studies in the rat. *Int J Pharm, 216, 105-14.*

KO, K. S., LEE, M., KOH, J. J. & KIM, S. W. 2001. Combined administration of plasmids encoding IL-4 and IL-10 prevents the development of autoimmune diabetes in nonobese diabetic mice. *Mol Ther, 4, 313-6.*

KOSKELA, H. O., SALONEN, P. H., ROMPPANEN, J. & NISKANEN, L. 2015. A history of diabetes but not hyperglycaemia during exacerbation of obstructive lung disease has impact on long-term mortality: a prospective, observational cohort study. BMJ Open, 5, e006794.

KRATZ, F. 2008. Albumin as a drug carrier: design of prodrugs, drug conjugates and nanoparticles. J Control Release, 132, 171-83.

KRAULAND, A. H., GUGGI, D., BERNKOP-SCHNURCH, A. 2004. Oral insulin delivery: the potential of thiolated chitosan-insulin tablets on non-diabetic rats. J Control Release, 95, 547-55.

LAI, P., DAEAR, W., LOBENBERG, R. & PRENNER, E. J. 2014. Overview of the preparation of organic polymeric nanoparticles for drug delivery based on gelatine, chitosan, poly(d,l-lactide-co-glycolic acid) and polyalkylcyanoacrylate. Colloids Surf B Biointerfaces, 118, 154-63.

LAMPING, S., OTREMBA, T. & RAVOO, B. J. 2018. Carbohydrate-Responsive Surface Adhesion Based on the Dynamic Covalent Chemistry of Phenylboronic Acid- and Catechol-Containing Polymer Brushes. Angew Chem Int Ed Engl, 57, 2474-2478.

LANG, S., LANGGUTH, P., OSCHMANN, R., TRAVING, B. & MERKLE, H. P. 1996. Transport and metabolic pathway of thymocartin (TP4) in excised bovine nasal mucosa. J Pharm Pharmacol, 48, 1190-6.

LARISSA SAKIS BERNARDI, P. N. S. J., ISABELA FANELLI BARRETO BISCAIA, MAXIMILIANO DA SILVA SANGOI, VITOR TODESCHINI, CASSIANA MENDES, MARCOS ANTÔNIO SEGATTO SILVA, PAULO RENATO OLIVEIRA* 2020. Determination of Hydrochlorothiazide and Two Major Degradation Products by Stability Indicating High Performance Liquid Chromatography. Current Pharmaceutical Analysis, 16.

LENNARTSON, A. 2017. The Chemical Works of Carl Wilhelm Scheele, Gewerbestrasse 11, 6330 Cham, Switzerland, Springer International Publishing AG.

LI H., LIU J, LIU Z. 2011. A Wulff-type boronate for boronate affinity capture of cis-diol compounds at medium acidic pH condition. . Chemical Communications, 47, 8169.

LI, J., WANG, Y., HAN, L., SUN, X., YU, H. & YU, Y. 2012. Time-action profile of an oral enteric insulin formulation in healthy Chinese volunteers. Clin Ther, 34, 2333-8.

LI, L., JIANG, G., YU, W., LIU, D., CHEN, H., LIU, Y., HUANG, Q., TONG, Z., YAO, J. & KONG, X. 2016a. A composite hydrogel system containing glucose-responsive nanocarriers for oral delivery of insulin. Mater Sci Eng C Mater Biol Appl, 69, 37-45.

LI, L., JIANG, G., YU, W., LIU, D., CHEN, H., LIU, Y., TONG, Z., KONG, X. & YAO, J. 2017. Preparation of chitosan-based multifunctional nanocarriers overcoming multiple barriers for oral delivery of insulin. Mater Sci Eng C Mater Biol Appl, 70, 278-286.

LI, Y., LI, J., ZHANG, X., DING, J. & MAO, S. 2016b. Non-ionic surfactants as novel intranasal absorption enhancers: in vitro and in vivo characterization. Drug Deliv, 23, 2272-2279.

LI, Y., ZHANG, Z., LIU, B. & LIU, J. 2019. Adsorption of DNA Oligonucleotides by Boronic Acid-Functionalized Hydrogel Nanoparticles. Langmuir, 35, 13727-13734.

LIN, Y. 2011. Polyamidoamine dendrimers as novel potential absorption enhancers for improving the small intestinal absorption of poorly absorbable drugs in rats. Journal of Controlled Release, 149, 21 - 28.

LIN, Y. H., MI, F. L., CHEN, C. T., CHANG, W. C., PENG, S. F., LIANG, H. F. & SUNG, H. W. 2007. Preparation and characterization of nanoparticles shelled with chitosan for oral insulin delivery. Biomacromolecules, 8, 146-52.

LIPPMANN, M., YEATES, D. B. & ALBERT, R. E. 1980. Deposition, retention, and clearance of inhaled particles. Br J Ind Med, 37, 337-62.

LIU, S., JIN, M. N., QUAN, Y. S., KAMIYAMA, F., KATSUMI, H., SAKANE, T. & YAMAMOTO, A. 2012. The development and characteristics of novel microneedle arrays fabricated from hyaluronic acid, and their application in the transdermal delivery of insulin. J Control Release, 161, 933-41.

LOPES, M., SHRESTHA, N., CORREIA, A., SHAHBAZI, M. A., SARMENTO, B., HIRVONEN, J., VEIGA, F., SEICA, R., RIBEIRO, A. & SANTOS, H. A. 2016. Dual chitosan/albumin-coated alginate/dextran sulfate nanoparticles for enhanced oral delivery of insulin. J Control Release, 232, 29-41.

LORAND, J. P., & EDWARDS, J. O. 1959. Polyol Complexes and Structure of the Benzeneboronate Ion. T. he Journal of Organic Chemistry, 24, 769-774.

LORAND, J. P. & EDWARDS, J. O. 1959. Polyol complexes and structure of the benzeneboronate ion. Journal of Organic Chemistry, 24, 769 - 774.

LUCIA BABCOCK, R. P. 1980. Dynamics of boron acid complexation reactions. Formation of 1:1 boron acid-ligand complexes. Inorganic Chemistry, 19, 56 -61.

MAHOBIA, S., BAJPAI, J. & BAJPAI, A. K. 2016. An In-vitro Investigation of Swelling Controlled Delivery of Insulin from Egg Albumin Nanocarriers. Iran J Pharm Res, 15, 695-711.

MAJI, S., VANCOILLIE, G., VOORHAAR, L., ZHANG, Q. & HOOGENBOOM, R. 2014. RAFT polymerization of 4-vinylphenylboronic acid as the basis for micellar sugar sensors. Macromol Rapid Commun, 35, 214-220.

MAKHLOF, A., TOZUKA, Y. & TAKEUCHI, H. 2011. Design and evaluation of novel pH-sensitive chitosan nanoparticles for oral insulin delivery. Eur J Pharm Sci, 42, 445-51.

MANSOURPOUR, M., MAHJUB, R., AMINI, M., OSTAD, S. N., SHAMSA, E. S., RAFIEE-TEHRANI, M. & DORKOOSH, F. A. 2015. Development of acid-resistant alginate/trimethyl chitosan nanoparticles containing cationic beta-cyclodextrin polymers for insulin oral delivery. AAPS PharmSciTech, 16, 952-62.

MARTA RODRIGUEZ-ALLER, D., JEAN-LUCVEUTHEY, ROBERTGURNY 2015. Strategies for formulating and delivering poorly water-soluble drugs. Journal of Drug Delivery Science and Technology, 30, 342-351.

MARTTIN, E., VERHOEF, J. C., SPIES, F., VAN DER MEULEN, J., NAGELKERKE, J. F., KOERTEN, H. K. & MERKUS, F. W. 1999. The effect of methylated beta-cyclodextrins on the tight junctions of the rat nasal respiratory epithelium: electron microscopic and confocal laser scanning microscopic visualization studies. J Control Release, 57, 205-13.

MATSUMOTO, A., IKEDA, S., HARADA, A. & KATAOKA, K. 2003. Glucose-responsive polymer bearing a novel phenylborate derivative as a glucose-sensing moiety operating at physiological pH conditions. Biomacromolecules, 4, 1410-6.

MATSUMOTO, A., YOSHIDA, R. & KATAOKA, K. 2004. Glucose-responsive polymer gel bearing phenylborate derivative as a glucose-sensing moiety operating at the physiological pH. Biomacromolecules, 5, 1038-45.

MCMARTIN, C., HUTCHINSON, L. E., HYDE, R. & PETERS, G. E. 1987. Analysis of structural requirements for the absorption of drugs and macromolecules from the nasal cavity. J Pharm Sci, 76, 535-40.

MENGMENG NIU, Y. N. T., PEIPEI GUAN, LARS HOVGAARD, YI LU, JIANPING QI, RUYUE LIAN, XIAOYANG LI, WEI WU, 2014a. Enhanced oral absorption of insulin-loaded liposomes containing bile salts: A mechanistic study. International Journal of Pharmaceutics, 460 119 - 130

MENGMENG NIU et.a,. 2014b. Enhanced oral absorption of insulin-loaded liposomes containing bile salts: A mechanistic study. International Journal of Pharmaceutics, 460, 119 - 130.

MERKUS, F. W., VERHOEF, J. C., MARTTIN, E., ROMEIJN, S. G., VAN DER KUY, P. H., HERMENS, W. A. & SCHIPPER, N. G. 1999. Cyclodextrins in nasal drug delivery. Adv Drug Deliv Rev, 36, 41-57.

MIKHAIL, N. 2016. Place of technosphere inhaled insulin in treatment of diabetes. World J Diabetes, 7, 599-604.

MOAD, G., RIZZARDO, E. & THANG, S. H. 2008. Toward living radical polymerization. Acc Chem Res, 41, 1133-42.

MOHAMMAD EA, E. W., ELSAYED AA, ABD-ELGHANY AA 2016. Electroporation parameters for successful transdermal delivery of insulin. Am. J. Ther, 23, e1560–e1567.

MOHANRAJ, V. J., BARNES, T. J. & PRESTIDGE, C. A. 2010. Silica nanoparticle coated liposomes: a new type of hybrid nanocapsule for proteins. Int J Pharm, 392, 285-93.

MOKTA, J. K., MOKTA, K. K. & PANDA, P. 2013. Insulin lipodystrophy and lipohypertrophy. Indian J Endocrinol Metab, 17, 773-4.

MOLLICA, J. A., REHM, C. R., & SMITH, J. B. 1969. Hydrolysis of Hydrochlorothiazide. . Journal of Pharmaceutical Sciences, 58, 635 – 636.

MOMOH A.MUMUNIAM FRANKLIN C.KENECHUKWUA, K. C. O., ANTHONY A.ATTAMAA, DAVID DÍAZDÍAZBC 2020. Insulin-loaded mucoadhesive nanoparticles based on mucin-chitosan complexes for oral delivery and diabetes treatmen. Carbohydrate Polymers, 229.

MULLER, T. D., FINAN, B., BLOOM, S. R., D'ALESSIO, D., DRUCKER, D. J., FLATT, P. R., FRITSCHE, A., GRIBBLE, F., GRILL, H. J., HABENER, J. F., HOLST, J. J., LANGHANS, W., MEIER, J. J., NAUCK, M. A., PEREZ-TILVE, D., POCAI, A., REIMANN, F., SANDOVAL, D. A., SCHWARTZ, T. W., SEELEY, R. J., STEMMER, K., TANG-CHRISTENSEN, M., WOODS, S. C., DIMARCHI, R. D. & TSCHOP, M. H. 2019. Glucagon-like peptide 1 (GLP-1). Mol Metab, 30, 72-130.

N. ZHANG, Q. N. P., G. H. HUANG AND W. F. XU 2005a. Investigation of lectin-modified insulin liposomes as carriers for oral administration. International Journal of Pharmaceutics, 294, 247–259.

N. ZHANG, 2005b. Investigation of lectin-modified insulin liposomes as carriers for oral administration. International Journal of Pharmaceutics, 294, 247–259.

N. ZHANG, Q. P., G. HUANG, W. XU, Y. CHENG AND X. HAN 2006. Pharmaceutical Nanotechnology, Lectin-modified solid lipid nanoparticles as carriers for oral administration of insulin. International Journal of Pharmaceutics, 327, 153 -159

NAGPAL, K., SINGH, S. K. & MISHRA, D. N. 2010. Chitosan nanoparticles: a promising system in novel drug delivery. Chem Pharm Bull (Tokyo), 58, 1423-30.

NAKAMURA, T. 1965. A Methode for Preparing an Aqueous Colloidal Dispersion of Organic Materials by Using Water-Soluble Polymers: Dispersion of fl-Carotene by Polyvinylpyrrolidone. Kolloide und natiirliehe Makromolekiile, 1.

NARAYAN, R. J. 2014. Transdermal delivery of insulin via microneedles. J Biomed Nanotechnol, 10, 2244-60.

NAZAR, H. & TSIBOUKLIS, J. 2012. Towards the nasal delivery of insulin. Ther Deliv, 3, 1241-3.

NEENA WASHINGTON, C. W. C. G. W. 2001. Physiological Pharmaceutics Barrires to drug absorption, London, Taylor and Francis.

NIEDERHOFER, A. & MULLER, B. W. 2004. A method for direct preparation of chitosan with low molecular weight from fungi. Eur J Pharm Biopharm, 57, 101-5.

NIHAD AL-HASHIMI, M. B., MARIA SAAED, NEGEEN KARGAR, AMR ELSHAER 2020. The impact of natural and synthetic polymers in formulating micro and nanoparticles for antidiabetic drugs. Current Drug Delivry review

NIR, T., MELTON, D. A. & DOR, Y. 2007. Recovery from diabetes in mice by beta cell regeneration. J Clin Invest, 117, 2553-61.

NIU, M., LU, Y., HOVGAARD, L. & WU, W. 2011. Liposomes containing glycocholate as potential oral insulin delivery systems: preparation, in vitro characterization, and improved protection against enzymatic degradation. Int J Nanomedicine, 6, 1155-66.

NIU, M., TAN, Y., GUAN, P., HOVGAARD, L., LU, Y., QI, J., LIAN, R., LI, X. & WU, W. 2014. Enhanced oral absorption of insulin-loaded liposomes containing bile salts: a mechanistic study. Int J Pharm, 460, 119-30.

OH, S., LEE, M., KO, K. S., CHOI, S. & KIM, S. W. 2003. GLP-1 gene delivery for the treatment of type 2 diabetes. Mol Ther, 7, 478-83.

OKAFOR, I. S., OFOEFULE, S. I. & UDEALA, O. K. 2001. A comparative study of modified starches in direct compression of a poorly water soluble drug (hydrochlorothiazide). Boll Chim Farm, 140, 36-9.

P. MUKHOPADHYAY, S. C., S. BHATTACHARYA, ROSHNARA MISHRA, P. P. KUNDU 2015a. pH-sensitive chitosan/alginate core-shell nanoparticles for efficient and safe oral insulin delivery. International Journal of Biological Macromolecules, 72, 640 - 684.

P. MUKHOPADHYAY, 2015b. pH-sensitive chitosan/alginate core-shell nanoparticles for efficient and safe oral insulin delivery. International Journal of Biological Macromolecules, 72, 640 - 684.

PALERMO, A., NAPOLI, N., MANFRINI, S., LAURIA, A., STROLLO, R. & POZZILLI, P. 2011. Buccal spray insulin in subjects with impaired glucose tolerance: the prevoral study. Diabetes Obes Metab, 13, 42-6.

PANIGRAHI, A. 2012. Solubility Enhancement of Etoricoxib by Cosolvency Approach. International Scholarly Research Network ISRN Physical Chemistry, 2012, 1-5.

PER B. ZETTERLUND, F. A., MASYOSHI OKUBO 2009. Controlled/Living Heterogeneous Radical Polymerization in Supercritical Carbon Dioxide Polymer Chemistry, 47, 3711–3728

PER B. ZETTERLUND, G. G., SE BASTIEN PERRIER 2014a. Sequence-Controlled Multiblock Copolymers via RAFT Polymerization: Modeling and Simulations. Macromol. Theory Simul., 23, 331-339.

PER B. ZETTERLUND, G. G., SE BASTIEN PERRIER 2014b. Sequence-Controlled Multiblock Copolymers via RAFT Polymerization: Modeling and Simulationsa. Macromol. Theory Simul., 23, 331–339.

P. MUKHOPADHYAY, et.al. 2014. Efficient oral insulin delivery by dendronized chitosan: in vitro and in vivo studies. RSC Advances, 4, 43890-43902.

PROUD, D. 2008. The Pulmonary Epithelium in Health and Disease John Wiley & Sons Ltd.

QIU D, J. L., ZHENG Z, MENG H, MO F, WANG X ET AL. 2012. Synthesis of Pinacol Arylboronates from Aromatic Amines: A Metal-Free Transformation. . The Journal of Organic Chemistry. 2012, 78, 1923-1933.

R. WILSON, et.al, 1998. Overview of the Preparation, Use and Biological Studies on Polyglycerol Polyricinoleate (PGPR) Food and Chemical Toxicology 36, 711- 718.

RADZIUK, J. 2012. The Artificial Pancreas. Diabetes, 61, 2221 - 2224.

RAMIREZ-DOMINGUEZ, M. 2016. Historical Background of Pancreatic Islet Isolation. Adv Exp Med Biol, 938, 1-9.

REIS, C. P., RIBEIRO, A. J., NEUFELD, R. J. & VEIGA, F. 2007. Alginate microparticles as novel carrier for oral insulin delivery. Biotechnol Bioeng, 96, 977-89.

ROSARIA GRASSO, F. M., MARISA GULINO, AGATA SCORDINO 2018. Exploring the behaviour of water in glycerol solutions by using delayed luminescence. PLoS ONE, 13.

ROY, D., CAMBRE, J. N. & SUMERLIN, B. S. 2008a. Sugar-responsive block copolymers by direct RAFT polymerization of unprotected boronic acid monomers. Chemical Communications, 2477-2479.

ROY, D., CAMBRE, J. N. & SUMERLIN, B. S. 2008b. Sugar-responsive block copolymers by direct RAFT polymerization of unprotected boronic acid monomers. Chem Commun (Camb), 2477-9.

ROY, D., CAMBRE, J. N. & SUMERLIN, B. S. 2009. Triply-responsive boronic acid block copolymers: solution self-assembly induced by changes in temperature, pH, or sugar concentration. Chem Commun (Camb), 2106-8.

ROY, D. & SUMERLIN, B. S. 2012. Glucose-Sensitivity of Boronic Acid Block Copolymers at Physiological pH. Acs Macro Letters, 1, 529-532.

RUDY BILOUS, R. D. 2010. Handbook of Diabetes, 4th Edition, England, Wiley-Blackwell.

S. SAJEESH, E. A. 2010. Cyclodextrin complexed insulin encapsulated hydrogel microparticles: An oral delivery system for insulin. Journal of Controlled Release, 147, 377 - 384.

SAINI, A., CHADHA, R., GUPTA, A., SINGH, P., BHANDARI, S., KHULLAR, S., … JAIN, D. S. 2015. New conformational polymorph of hydrochlorothiazide with improved solubility. Pharmaceutical Development and Technology, 1.

SANGER, F. 1945. The free amino groups of insulin. Biochem J, 39, 507-15.

SARAH Y.EILLEIA, M. E. S., SAMAR MANSOUR, AHMED.S. GENEIDI 2018. Novel technique of insulin loading into porous carriers for oral delivery. Asian Journal of Pharmaceutical Sciences, 13, 297-309.

SARMENTO, B., RIBEIRO, A., VEIGA, F., FERREIRA, D. & NEUFELD, R. 2007a. Oral bioavailability of insulin contained in polysaccharide nanoparticles. Biomacromolecules, 8, 3054-60.

SARMENTO, B., RIBEIRO, A., VEIGA, F., SAMPAIO, P., NEUFELD, R. & FERREIRA, D. 2007b. Alginate/chitosan nanoparticles are effective for oral insulin delivery. Pharm Res, 24, 2198-206.

SCOTT, A. 1931. ACTION OF ACID ALCOHOL. J. Biol. Chem, May 6.

SEKI, T. 2012. [Basic studies on the nasal delivery of insulin]. Yakugaku Zasshi, 132, 1255-62.

SELAM, J. L. 2001. External and implantable insulin pumps: current place in the treatment of diabetes. Exp Clin Endocrinol Diabetes, 109 Suppl 2, S333-40.

SELAM, J. L., HAARDT, M. J., BERNE, C., DORANGE, C., LANOE, J. L., BETHOUX, J. P. & SLAMA, G. 1993. [Cost benefits of intensive insulin therapy using injections, external pumps and implantable pumps]. Diabete Metab, 19, 506-9.

SHAOYUN YU, Y. Z. F., WU XUAN, ZHANG WANLIANG, LÜ HUA ZHANG, QIANG ZHANG 2004. Nasal insulin delivery in the chitosan solution: in vitro and in vivo studies. International Journal of Pharmaceutics, 281, 11 - 23.

SHARMA, S., VERMA, A., TEJA, B. V., PANDEY, G., MITTAPELLY, N., TRIVEDI, R. & MISHRA, P. R. 2015. An insight into functionalized calcium based inorganic nanomaterials in biomedicine: Trends and transitions. Colloids Surf B Biointerfaces, 133, 120-39.

SHI, R. M. A. L. 2014. Phenylboronic acid-based glucose-responsive polymeric nanoparticles: synthesis and applications in drug delivery Polymer Chemistry 5, 1503 - 1518.

SHIOTSUKA, R. N., STUART, B. P., CHARLES, J. M., SIMON, G. S., MALICHKY, P. & MOSTOWY, J. M. 2010. Chronic inhalation exposures of Fischer 344 rats to 1,6-hexamethylene diisocyanate did not reveal a carcinogenic potential. Inhal Toxicol.

SHRESTHA, N., SHAHBAZI, M. A., ARAUJO, F., ZHANG, H., MAKILA, E. M., KAUPPILA, J., SARMENTO, B., SALONEN, J. J., HIRVONEN, J. T. & SANTOS, H. A. 2014. Chitosan-modified porous silicon microparticles for enhanced permeability of insulin across intestinal cell monolayers. Biomaterials, 35, 7172-9.

SHU LIU, M.-N., JIN YING-SHU, QUAN FUMIO KAMIYAMA, HIDEMASA KATSUMI, TOSHIYASU SAKANE, AKIRA YAMAMOTO 2012. The development and characteristics of novel microneedle arrays fabricated from hyaluronic acid, and their application in the transdermal delivery of insulin. Journal of Controlled Release, 161, 933 -941.

SIMON J.COUTTS, J., DALEKROLIKOWSKI, ROGER J.SNOW 1994. Two efficient methods for the cleavage of pinanediol boronate esters yielding the free boronic acids. tetrahedron Letters 35, 5109 -5112.

SLAMA, G. & SELAM, J. L. 1992. [External and implantable insulin pumps and other techniques in insulin therapy]. Journ Annu Diabetol Hotel Dieu, 113-22.

SNARSKI, E., TOROSIAN, T., PALUSZEWSKA, M., URBANOWSKA, E., MILCZARCZYK, A., JEDYNASTY, K., FRANEK, E. & JEDRZEJCZAK, W. W. 2009. Alleviation of exogenous insulin requirement in type 1 diabetes mellitus after immunoablation and transplantation of autologous hematopoietic stem cells. Pol Arch Med Wewn, 119, 422-6.

SONAJE, K., CHEN, Y. J., CHEN, H. L., WEY, S. P., JUANG, J. H., NGUYEN, H. N., HSU, C. W., LIN, K. J. & SUNG, H. W. 2010. Enteric-coated capsules filled with freeze-dried chitosan/poly(gamma-glutamic acid) nanoparticles for oral insulin delivery. Biomaterials, 31, 3384-94.

SONAJE, K., CHUANG, E. Y., LIN, K. J., YEN, T. C., SU, F. Y., TSENG, M. T. & SUNG, H. W. 2012. Opening of epithelial tight junctions and enhancement of paracellular permeation by chitosan: microscopic, ultrastructural, and computed-tomographic observations. Mol Pharm, 9, 1271-9.

SOSALE, B., SOSALE, A. & BHATTACHARYYA, A. 2016. Clinical Effectiveness and Impact on Insulin Therapy Cost After Addition of Dapagliflozin to Patients with Uncontrolled Type 2 Diabetes. Diabetes Ther, 7, 765-776.

STANDL, E. 2019. GLP-1 receptor agonists and cardiovascular outcomes: an updated synthesis. Lancet Diabetes Endocrinol, 7, 741-743.

STANDL, E., DEXEL, T., LANDER, T., ALBERT, E. D., SCHOLZ, S., GREITE, J. H., JANKA, H. U. & MEHNERT, H. 1981. Association of HLA antigens with severity of diabetic retinopathy in Southern Germany. Horm Metab Res Suppl, 11, 81-6.

STEIL, G., REBRIN, K. & MASTROTOTARO, J. J. 2006. Metabolic modelling and the closed-loop insulin delivery problem. Diabetes Res Clin Pract, 74 Suppl 2, S183-6.

STEIL, G. M., PANTELEON, A. E. & REBRIN, K. 2004. Closed-loop insulin delivery-the path to physiological glucose control. Adv Drug Deliv Rev, 56, 125-44.

STENZEL, M. H. 2008. RAFT polymerization: an avenue to functional polymeric micelles for drug delivery. Chem Commun (Camb), 3486-503.

SU, F. Y., LIN, K. J., SONAJE, K., WEY, S. P., YEN, T. C., HO, Y. C., PANDA, N., CHUANG, E. Y., MAITI, B. & SUNG, H. W. 2012. Protease inhibition and absorption enhancement by functional nanoparticles for effective oral insulin delivery. Biomaterials, 33, 2801-11.

SU, W.-F. 2013. Principles of Polymer Design and Synthesis, Berlin Heidelberg Springer-Verlag.

SUGNAUX, C. & KLOK, H. A. 2014. Glucose-sensitive QCM-sensors via direct surface RAFT polymerization. Macromol Rapid Commun, 35, 1402-7.

SUN, J., PERFETTI, M. T. & SANTOS, W. L. 2011. A method for the deprotection of alkylpinacolyl boronate esters. J Org Chem, 76, 3571-5.

SZWARC, M., LEVY, M., & MILKOVICH, R. 1956. POLYMERIZATION INITIATED BY ELECTRON TRANSFER TO MONOMER.A NEW METHOD OF FORMATION OF BLOCK POLYMERS. . Journal of the American Chemical Society, 78, 2656 - 2657.

T.AOKI, Y. N., K. SANUI, NAOYA OGATA, AKIHIKO KIKUCHI, YASUHISA SAKURAI, KAZUNORI KATAOKA & TERUO OKANO 1996 Glucose-Sensitive Lower Critical Solution Temperature Changes of Copolymers Composed of N-Isopropylacrylamide and Phenylboronic Acid Moieties. Polymer Journal 28 371 - 374

TAE KEUN OH, M. Z. L. S., TAIK KIM 2006. Gene therapy for diabetes mellitus in rats by intramuscular injection of lentivirus containing insulin gene. Diabetes Research and Clinical Practice, 71, 233–240.

TAKENOUCHI, K., SHRESTHA, B., YAMAKUCHI, M., YOSHINAGA, N., ARIMURA, N., KAWAGUCHI, H., NAGASATO, T., FEIL, R., KAWAHARA, K., SAKAMOTO, T., MARUYAMA, I. & HASHIGUCHI, T. 2014.

Upregulation of non-beta cell-derived vascular endothelial growth factor A increases small clusters of insulin-producing cells in the pancreas. Exp Clin Endocrinol Diabetes, 122, 308-15.

TAYLOR, L. J., BUHL, M., CHALMERS, B. A., RAY, M. J., WAWRZYNIAK, P., WALTON, J. C., CORDES, D. B., SLAWIN, A. M. Z., WOOLLINS, J. D. & KILIAN, P. 2017. Dealkanative Main Group Couplings across the peri-Gap. J Am Chem Soc, 139, 18545-18551.

THABIT, H., HARTNELL, S., ALLEN, J. M., LAKE, A., WILINSKA, M. E., RUAN, Y., EVANS, M. L., COLL, A. P. & HOVORKA, R. 2017. Closed-loop insulin delivery in inpatients with type 2 diabetes: a randomised, parallel-group trial. Lancet Diabetes Endocrinol, 5, 117-124.

TOLKSDORF, W., STRANG, C. M., SCHIPPERS, E., SIMON, H. B. & TRUONG, S. 1992. [The effects of the carbon dioxide pneumoperitoneum in laparoscopic cholecystectomy on postoperative spontaneous respiration]. Anaesthesist, 41, 199-203.

TOWEY, J. J., SOPER, A. K., & DOUGAN, L. 2011. The structure of glycerol in the liquid state: a neutron diffraction study. Physical Chemistry Chemical Physics, 13, 9397.

TSAI, L. C., CHEN, C. H., LIN, C. W., HO, Y. C. & MI, F. L. 2019. Development of mutlifunctional nanoparticles self-assembled from trimethyl chitosan and fucoidan for enhanced oral delivery of insulin. Int J Biol Macromol, 126, 141-150.

UNGARO, F., D'EMMANUELE DI VILLA BIANCA, R., GIOVINO, C., MIRO, A., SORRENTINO, R., QUAGLIA, F. & LA ROTONDA, M. I. 2009. Insulin-loaded PLGA/cyclodextrin large porous particles with improved aerosolization properties: in vivo deposition and hypoglycaemic activity after delivery to rat lungs. J Control Release, 135, 25-34.

UNGARO, P., MIRRA, P., ORIENTE, F., NIGRO, C., CICCARELLI, M., VASTOLO, V., LONGO, M., PERRUOLO, G., SPINELLI, R., FORMISANO, P., MIELE, C. & BEGUINOT, F. 2012. Peroxisome proliferator-activated receptor-gamma activation enhances insulin-stimulated glucose disposal by reducing ped/pea-15 gene expression in skeletal muscle cells: evidence for involvement of activator protein-1. J Biol Chem, 287, 42951-61.

VANCOILLIE, G. & HOOGENBOOM, R. 2016. Responsive Boronic Acid-Decorated (Co)polymers: From Glucose Sensors to Autonomous Drug Delivery. Sensors (Basel), 16.

VARSHOSAZ, J., SADRAI, H. & HEIDARI, A. 2006. Nasal delivery of insulin using bioadhesive chitosan gels. Drug Deliv, 13, 31-8.

VEISEH, O., TANG, B. C., WHITEHEAD, K. A., ANDERSON, D. G. & LANGER, R. 2015. Managing diabetes with nanomedicine: challenges and opportunities. Nat Rev Drug Discov, 14, 45-57.

VILLEMIN, D. A. T.-S., F., 1991. Domestic microwave ovens in the laboratory. . Journal of Chemical Education, 68, 346.

WANG, B., CHEN, L., SUN, Y., ZHU, Y., SUN, Z., AN, T., LI, Y., LIN, Y., FAN, D. & WANG, Q. 2015. Development of phenylboronic acid-functionalized nanoparticles for emodin delivery. J Mater Chem B, 3, 3840-3847.

WANG, J., TABATA, Y. & MORIMOTO, K. 2006. Aminated gelatin microspheres as a nasal delivery system for peptide drugs: evaluation of in vitro release and in vivo insulin absorption in rats. J Control Release, 113, 31-7.

WEITAI WU, S. Z. 2013. Responsive Materials for Self-Regulated Insulin Delivery. Macromolecular Bioscience, 64, 1464 - 1477.

WEITH, H. L., WIEBERS, J. L. & GILHAM, P. T. 1970. Synthesis of cellulose derivatives containing the dihydroxyboryl group and a study of their capacity to form specific complexes with sugars and nucleic acid components. Biochemistry, 9, 4396-401.

WOITISKI, C. B., NEUFELD, R. J., VEIGA, F., CARVALHO, R. A. & FIGUEIREDO, I. V. 2010. Pharmacological effect of orally delivered insulin facilitated by multilayered stable nanoparticles. Eur J Pharm Sci, 41, 556-63.

WOLFSON, A., DLUGY, C. & SHOTLAND, Y 2007. Glycerol as a green solvent for high product yields and selectivities. . Environ Chem Lett 5, 67 - 71.

WU, W. Q., HUANG, S. G., MA, Z., ZHANG, Y. Q. & SHI, J. B. 2005. [Effects of irrigating solution of Sihuang on morphology and function of nasal mucosa following surgery for chronic sinusitis and nasal polyps]. Di Yi Jun Yi Da Xue Xue Bao, 25, 424-7.

XU, S., HELD, I., KEMPF, B., MAYR, H., STEGLICH, W. & ZIPSE, H. 2005. The DMAP-catalyzed acetylation of alcohols--a mechanistic study (DMAP = 4-(dimethylamino)pyridine). Chemistry, 11, 4751-7.

XU S, H. I., KEMPF B, MAYR H, STEGLICH W, ZIPSE H. 2005. The DMAP-Catalyzed Acetylation of Alcohols—A Mechanistic Study (DMAP= 4-(Dimethylamino) pyridine). Chemistry–A European Journal, 5, 4751 - 7.

Y. DEKEL, Y. G. R. M. 2009. Novel fibrillar insulin formulations for oral administration: Formulation and in vivo studies in diabetic mice. Journal of Controlled Release, 143, 128–135.

YAN, M. E. A. 2016. Gel Point Suppression in RAFT Polymerization of Pure Acrylic Cross-Linker Derived from Soybean Oil. Biomacromolecules, 17, 2701-9.

YEH, T. H., HSU, L. W., TSENG, M. T., LEE, P. L., SONJAE, K., HO, Y. C. & SUNG, H. W. 2011. Mechanism and consequence of chitosan-mediated reversible epithelial tight junction opening. Biomaterials, 32, 6164-73.

YIHONG QIU, Y. C., GEOFF G.Z. ZHANG, LIRONG LIU, WILLIAM PORTER 2009. Developing Solid Oral Dosage Forms: Pharmaceutical Theory and Practice.

ZHANG, N., PING, Q. N., HUANG, G. H. & XU, W. F. 2005. Investigation of lectin-modified insulin liposomes as carriers for oral administration. Int J Pharm, 294, 247-59.

ZHANG, X., QI, J., LU, Y., HU, X., HE, W. & WU, W. 2014. Enhanced hypoglycemic effect of biotin-modified liposomes loading insulin: effect of formulation variables, intracellular trafficking, and cytotoxicity. Nanoscale Res Lett, 9, 185.

ZHANG, X., SUN, M., ZHENG, A., CAO, D., BI, Y. & SUN, J. 2012. Preparation and characterization of insulin-loaded bioadhesive PLGA nanoparticles for oral administration. Eur J Pharm Sci, 45, 632-8.

ZHANG, Y., WANG, F., QIAN, S., LIU, Z., WANG, Q., GU, Y., WU, Z., JING, Z., SUN, C. & PENG, W. 2017. A Novel Fiber Optic Surface Plasmon Resonance Biosensors with Special Boronic Acid Derivative to Detect Glycoprotein. Sensors (Basel), 17.

ZHONG, A., CHOUDHARY, P., MCMAHON, C., AGRAWAL, P., WELSH, J. B., CORDERO, T. L. & KAUFMAN, F. R. 2016. Effectiveness of Automated Insulin Management Features of the MiniMed(R) 640G Sensor-Augmented Insulin Pump. Diabetes Technol Ther, 18, 657-663.

ZHOU, Y., DONG, H., LIU, L., HAO, Y., CHANG, Z. & XU, M. 2015. Fabrication of electrochemical interface based on boronic acid-modified pyrroloquinoline quinine/reduced graphene oxide composites for voltammetric determination of glycated hemoglobin. Biosens Bioelectron, 64, 442-8.

ZIEGLER, A. G., STANDL, E., ALBERT, E. & MEHNERT, H. 1991. HLA-associated insulin autoantibody formation in newly diagnosed type I diabetic patients. Diabetes, 40, 1146-9.

ZIJLSTRA, E., HEINEMANN, L. & PLUM-MORSCHEL, L. 2014. Oral insulin reloaded: a structured approach. J Diabetes Sci Technol, 8, 458-65.